SYNTHÈSE ET CARACTÉRISATION DE POLYMÈRES ORGANOMÉTALLIQUES LUMINESCENTS DE CUIVRE(I) ET D'ARGENT(I) A BASE DE DIPHOSPHINES ET DIISOCYANURES

Par

Éric Fournier

mémoire présenté au Département de chimie en vue de
l'obtention du grade de maître ès sciences (M.Sc.)

FACULTÉ DES SCIENCES
UNIVERSITÉ DE SHERBROOKE

Sherbrooke, Québec, Canada, septembre 2003

Your file Votre référence
ISBN: 0-494-00254-9
Our file Notre référence
ISBN: 0-494-00254-9

Le 5 septembre 2003, le jury suivant a accepté ce mémoire dans sa version finale.
date

Président-rapporteur : M. Paul Rowntree
Département de chimie

Membre : M. Patrick Ayotte
Département de chimie

Membre : M. Pierre D. Harvey
Département de chimie

AVANT-PROPOS

Le contenu de ce mémoire rassemble trois publications soumises en langue anglaise dans des revues internationales de large diffusion avec comité de lectures.

I- Articles soumis

1 Preparation and Characterization of Small Mixed-Ligand Oligomers Containing Luminescent $M_2(dmpm)_x$ and $M_2(dmb)_y$ Building Blocks (M = Cu, Ag; x = 2, 3 ; y = 1, 2)
Éric Fournier and Pierre D. Harvey
Submitted as a full paper in Inorganic Chemistry

2 Luminescent 1-D and Zig-Zag Organometallic Polymers Built Upon Diphosphine and Diisocyanide Ligands, and Copper(I) and Silver(I)
Éric Fournier, Frédéric Lebrun and Pierre D. Harvey
Submitted to Chemical Communications

3 Organometallic Polymers Based on 1,8-Diisocyano-*p*-menthane(dmb); Synthesis and Characterization of the $\{[M(diphos)(dmb)]BF_4\}_n$ and $\{[Pd_2(diphos)_2(dmb)](BF_4)_2\}_n$ Materials (M = Cu, Ag; diphos = dppe, dppp)
Éric Fournier, Stéphanie Sicard and Pierre D. Harvey
Submitted as a full paper in Inorganic Chemistry

SOMMAIRE

Récemment, les travaux menés dans notre laboratoire sur les polymères organométalliques ont conduit à une nouvelle approche qui consiste à utiliser des ligands mixtes pour former des "co-polymères". Les ligands utilisés sont le (1,8-diisocyano-*p*-menthane) dmb et les bis(diphénylphosphine)alcanes (des ligands bidentates). Les métaux étudiés sont le cuivre(I) et l'argent(I), deux métaux de la rangée IB du tableau périodique et de configuration électronique d^{10}. Ces nouveaux matériaux présentent un potentiel dans la fabrication de matériaux conducteurs, semi-conducteurs, photoconducteurs ainsi que des dispositifs de diodes émissives ou d'optique non-linéaire. En effet, le mariage des propriétés du polymère et des métaux constitue une voie très prometteuse.

La première approche fût de synthétiser les unités de base et de les caractériser cristallographiquement afin de connaître l'arrangement spatial du polymère. Les unités de base étaient constituées du métal, d'une bis(diphénylphosphine)alcane et d'un ligand monodentate, le (*tert*-butylisonitrile) *t*-BuNC ayant approximativement le même encombrement stérique que le dmb. Étant donné que l'obtention de cristaux favorables à l'analyse cristallographique n'est pas toujours facile, d'autres analyses comme la RMN ^{31}P, l'ATG et la DRX de poudre ont dû être effectuées dans le but d'obtenir des informations sur la structure moléculaire du matériau.

À la suite de l'étude de la conformation des unités de base et des polymères, l'étude des propriétés photophysiques de ces nouveaux matériaux a été faite. Le but était de caractériser une série de composés polymériques pour approfondir les connaissances et même de développer une méthode de contrôle sur les propriétés luminescentes de ces polymères. En effet, ces polymères sont luminescents à température ambiante mais le contrôle des propriétés photophysiques reste encore plus complexe.

L'effet des groupements phényles sur les diphénylphosphines compliquait les données photophysiques. Nous avons donc décidé de remplacer les diphénylphosphines par des diméthylphosphines. Cette nouvelle approche à été étudiée en profondeur (structures cristallographiques, analyses photophysiques à l'état solide, en solution et à 77K). Cette étude a permis de réaliser qu'il était possible d'avoir un certain contrôle sur la dimension des oligomères et de sonder le phénomène excitonique intra-chaîne tout en évitant les transferts inter-chaînes causés par l'empilement π des groupements phényles mentionnés plus haut.

La liste des travaux de cet ouvrage a permis de composer trois publications et d'en entamer une quatrième. Cette chimie, reliée à celle des polymères organométalliques, est riche et prometteuse.

REMERCIEMENTS

Je remercie tout d'abord le professeur Pierre D. Harvey pour m'avoir accueilli dans son laboratoire et de m'avoir laissé beaucoup de responsabilités en parallèle du projet de recherche. Sa confiance m'a permis de me surpasser dans bien d'autres domaines que celui présenté dans le cadre de ce mémoire et je n'en suis pas moins reconnaissant.

J'aimerais aussi remercier David, Frédéric, Sébastien, François, Stéphanie, Pascal, Karine et Jean-François pour avoir été des amis en premier lieu et des compagnons de laboratoire en second.

J'aimerais spécialement remercier Katherine et toute ma famille pour m'avoir soutenu tout au long de mes études.

Je remercie les organismes (Fonds Québécois de la Recherche sur la Nature et les Technologies) (FQRNT) et (Conseil de Recherche en Sciences Naturelles et en Génie du Canada) (CRSNG) qui ont contribué financièrement à cette recherche.

TABLE DES MATIÈRES

LISTE DES ABRÉVIATIONS

diphos : diphénylphosphine

dmb : 1,8-diisocyano-*p*-menthane

dppm :bis(diphénylphosphino)méthane

dppe : 1,2-bis(diphénylphosphino)éthane

dppp : 1,3-bis(diphénylphosphino)propane

dppb : 1,4-bis(diphénylphosphino)butane

dpppen : 1,5-bis(diphénylphosphino)pentane

dpph : 1,6-bis(diphénylphosphino)hexane

dmpm : bis(diméthylphosphino)méthane

t-BuNC : *tert*-butylisonitrile

TCNQ : 7,7,8,8-tétracyano-*p*-quinodiméthanate

DSC : balayage calorimétrique différentiel (anglais) Differential Scanning Calorimery.

ε : absorptivité molaire

Φ_e : rendement quantique d'émission

τ_e : temps de vie

FAB : bombardement rapide d'atome (anglais) Fast Atom Bonbardment

IR : infra-rouge

U.V. : ultraviolet

RMN ou NMR (anglais) : résonance magnétique nucléaire

DRX ou XRD (anglais) : diffraction des rayons-X (de poudre)

ATG ou TGA (anglais) : analyse thermogravimétrique

Tg : température de transition vitreuse

HOMO : orbitale moléculaire occupée de plus haute énergie

LUMO : orbitale moléculaire vide de plus basse énergie

ORTEP : Oak Ridge Thermal Ellipsoid Plot Program

LISTE DES FIGURES

LISTE DES SCHÉMAS

INTRODUCTION

i. Généralités

Au cours de ces dernières années, la chimie des matériaux a connu un grand intérêt et s'est beaucoup diversifiée. Le simple fait de se tenir à l'affût des nouvelles découvertes et de la technologie reste un défi de taille. La compréhension fondamentale des propriétés structurales et physiques à l'échelle moléculaire d'un matériaux nous amène à une meilleure compréhension des propriétés à l'échelle macroscopiques de ce dernier. L'étude des propriétés photophysiques de composés caractérisés permet de sonder plus en détails les propriétés physiques du matériaux. La majorité des recherches effectuées dans ce domaine porte sur la forme solide de cristaux et de polymères organiques et sur des agrégats métalliques plus petits (1-12). Les études de ce type sur des polymères et des oligomères organométalliques sont très rares relativement à la chimie des polymères organiques. Peu de matériaux sont bien connus pour leurs propriétés de luminescence à température ambiante, mais les applications de tels systèmes sont tout de même nombreuses (13-20). Cette section portera sur une revue des travaux effectués sur ce sujet dans le laboratoire du professeur Harvey depuis les 10 dernières années. Une section théorique suivra pour aider à la compréhension des chapitres suivants.

L'intérêt porté aux polymères-métaux est vaste en plus d'être diverse. L'idée première de joindre des métaux aux polymères est de tirer avantage des propriétés du métal et de la chimie du carbone en même temps. L'insolubilité et la malléabilité des polymères jumelées aux propriétés catalytiques et optiques des métaux sont des sujets de grand intérêt pour les chercheurs. Le Schéma 1 présente deux approches pour fabriquer ces polymères. La première approche consiste à greffer des métaux sur des matrices polymériques (polymères branchés). Cette voie est surtout utilisée en catalyse où le catalyseur est le métal et le polymère est la matrice insoluble. Le principal problème de

cette méthode réside dans la difficulté d'obtenir des monocristaux pour déterminer la structure moléculaire étant donné que la section polymérique organique est souvent très amorphe. La deuxième méthode (polymères linéaires) consiste à utiliser le métal au centre de la chaîne polymérique. Cette méthode trouve ses applications dans des dispositifs photoniques, photoélectriques et plusieurs autres (21) et la probabilité d'obtenir des monocristaux semble plus prometteuse car cette approche donnera des polymères plus cristallins.

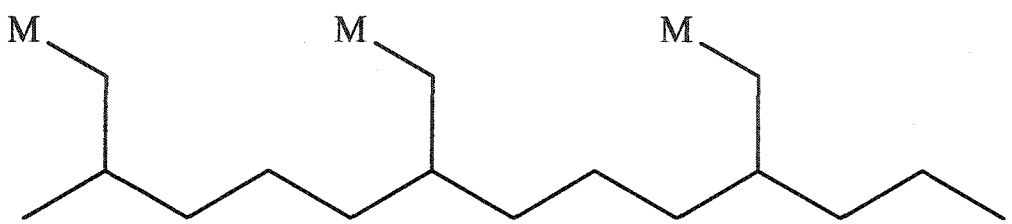

Branché

Linéaire

Schéma 1 : Représentation de deux stratégies pour incorporer un métal à une chaîne polymérique.

Notre groupe de recherche a misé sur cette dernière optique et une des stratégies de conception est présentée au Schéma 2. Cette approche consiste à utiliser deux ligands bidentates pontants pour lier les métaux comme le ferait une pince, de là l'expression "méthode double pince" .

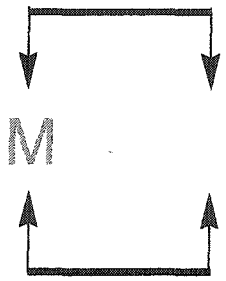

Schéma 2 : Stratégie d'assemblage des métaux pour obtenir des polymères linéaires à centres métalliques.

ii. Polymères de type $M(dmb)_2^+$

Un des premiers ligands utilisés à cette fin fut le dmb (1,8 diisocyano-*p*-menthane) (Figure 1). Celui-ci possède deux conformères possibles, le conformère U est majoritairement rencontré mais lorsqu'il y a un encombrement stérique, on peut observer le conformère Z (22). Ce ligand qui normalement préfère former des unités dimériques, (23) peut aussi former les polymères linéaires espérés (24, 25).

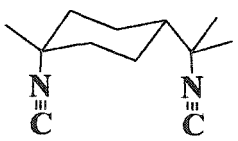

1,8 diisocyano-p-menthane

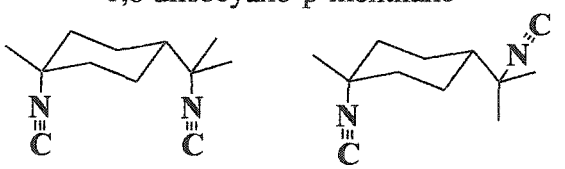

dmb, conformère-U (*anti-*)

dmb, conformère-Z (*gauche-*)

Figure 1 : Ligand assembleur dmb et ses deux conformères.

Ces polymères de type $\{[M(dmb)_2]Y\}_n$ (M = Cu(I), Ag(I); Y = PF_6^-, BF_4^-, NO_3^-, ClO_4^- et $CH_3CO_2^-$) sont représentés dans les Figures 2 et 3.

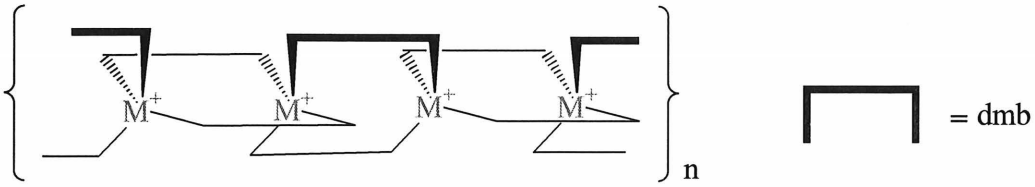

$\{M(dmb)_2^+\}_n$; M = Cu, Ag

Figure 2 : Représentation des polymères de type$\{[M(dmb)_2]Y\}_n$ (M = Cu(I), Ag(I); Y = PF_6^-, BF_4^-, NO_3^-, ClO_4^- et $CH_3CO_2^-$)

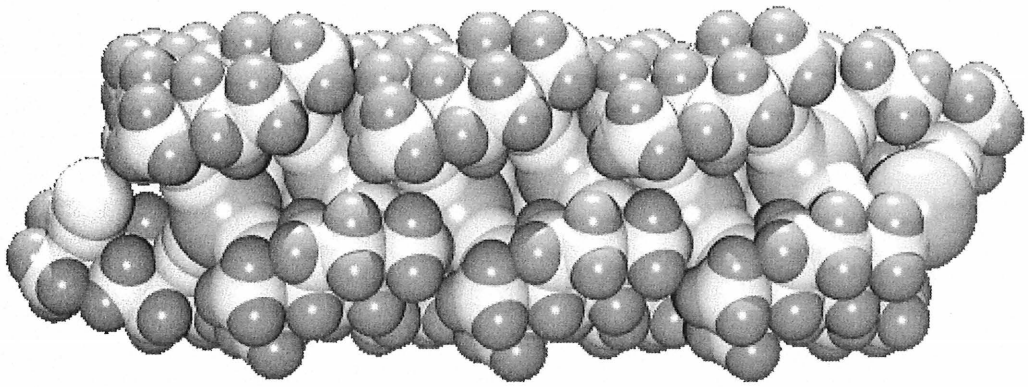

Figure 3 : Représentation CPK d'un segment du polymère $\{[Ag(dmb)_2]^+\}_n$.

La structure étant établie, la quasi linéarité de ce polymère a amené le groupe de recherche à utiliser ces polymères "rigides" polycationiques pour y insérer une composante semi-conductrice. Cette composante semi-conductrice fût obtenue en remplaçant par métathèse les contre-ions du polymère initial par un $TCNQ^-$ (7,7,8,8-tétracyano-*p*-quinodiméthanate) qui produit une chaîne conductrice grâce à l'empilement

π (26, 27) (Schema 3). Ces recherches plus poussées furent réalisées dans le cadre des mémoire et thèse de Daniel Fortin (1994-1998) M.Sc & Ph.D, Université de Sherbrooke.

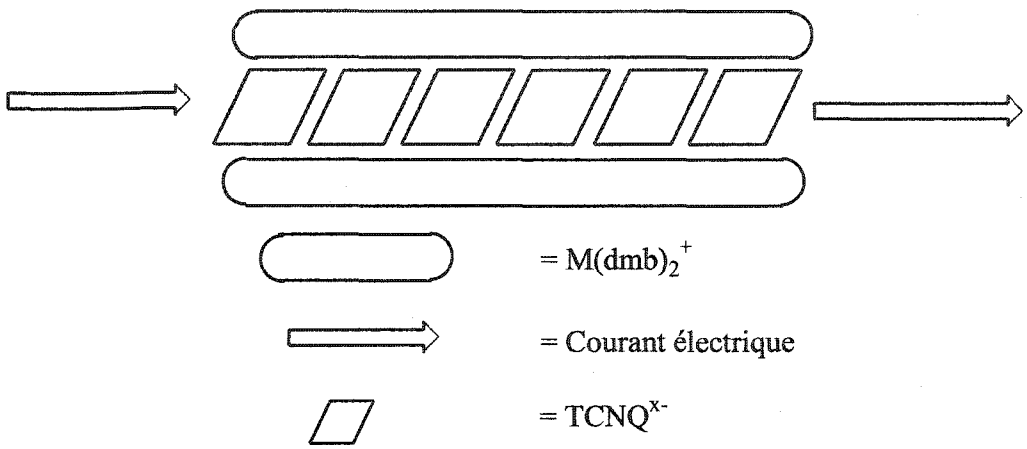

Schéma 3 : Conduction d'une chaîne de $\{TCNQ\}_n^{x-}$ provenant de l'alignement dirigé par les polymères rigides cationiques.

Un des résultats de cet ouvrage qui nous intéresse particulièrement est que les polymères de type $\{[Ag(dmb)_2]Y\}_n$ (Y = PF_6^-, BF_4^-, NO_3^-, ClO_4^- et $CH_3CO_2^-$) présentent de petites masses moléculaires (MW ≅ 10 000) tandis que l'analogue de cuivre montre des masses moléculaires beaucoup plus élevés (MW ≅ 160 000) (25, 28).

iii. Polymères de complexes

Toujours dans l'optique de faire des polymères organométalliques, d'autres métaux ont été introduits dans le cadre de ce vaste projet. Tout d'abord, le palladium sous forme de complexe linéaire tétranucléaire (Figure 4) fut envisagé dans une nouvelle approche.

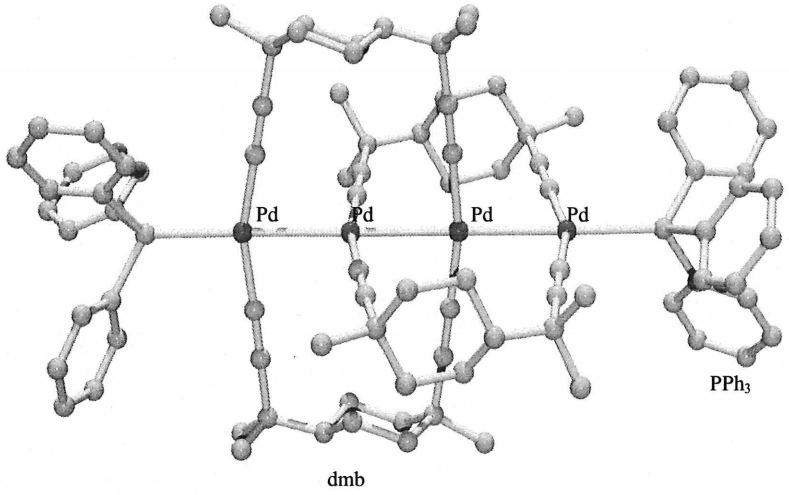

Figure 4 : Représentation « boules et bâtons » du complexe tétranucléaire $[Pd_4(dmb)_4(PPh_3)_2]^{2+}$.

Cette nouvelle approche n'est pas seulement originale par le fait d'utiliser un nouveau métal, elle remplace de plus l'unité monomérique métallique par une entité tétramérique ayant déjà ses propriétés uniques. L'obtention de monocristaux de l'unité de base devient un atout pour pouvoir caractériser comparativement l'unité de base versus le polymère. Cette innovation fût réalisée dans le cadre de la thèse de Tianle Zang (1995-1997) Ph.D, Université de Sherbrooke. La première particularité peut être observée à la Figure 5 où l'on observe le polymère bâti à partir du complexe tétranucléaire et assemblé par le ligand bidentate dmb. Il est très intéressant de remarquer la forme zig-zag du polymère due au conformère Z du dmb (22). Cette conformation est expliquée par l'effet stérique important qu'apporterait la forme U du ligand assembleur. Il est aussi intéressant de noter que la stratégie de double pince n'est pas appliquée dans ce cas.

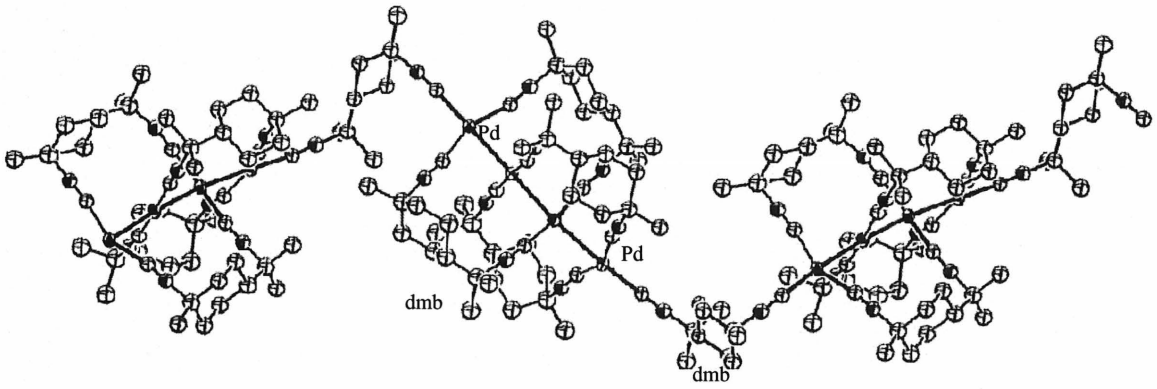

Figure 5 : Dessin ORTEP d'un fragment du polymère $\{[Pd_4(dmb)_4(dmb)]^{2+}\}_n$.

Par la suite, l'idée d'utiliser d'autres ligands assembleurs a conduit le groupe de recherche à se tourner vers les ligands de types "diphos". Ces ligands représentés à la Figure 6 sont similaires au dmb car ils sont également bidentates. La première étape serait de synthétiser des polymères du même type que le $\{[Pd_4(dmb)_4(dmb)]^{2+}\}_n$ en remplaçant le dmb assembleur par un ligand de type "diphos". Il serait ainsi possible de varier la longueur de la chaîne aliphatique entre les deux phosphores de façon à éviter la forme zig-zag due à l'encombrement stérique.

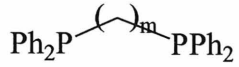

diphos; m = 1-6

Figure 6 : Représentation des ligands bis(diphénylphosphino)(méthane à hexane).

Les polymères de type $\{[Pt_4(dmb)_4(diphos)]^{2+}\}_n$ (29) furent conçus à partir de complexes tétranucléaires de platine analogues au complexe précédent et de "diphos" contenant une chaîne aliphatique de 4 à 6 unités (Figure 7).

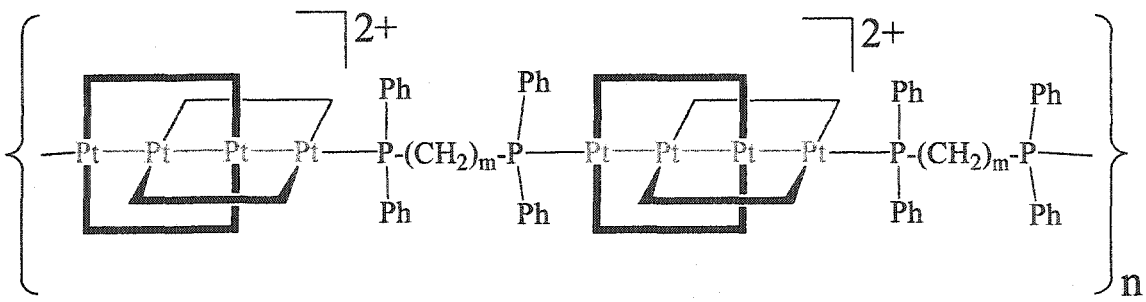

$\{[Pt_4(dmb)_4]^{2+}\text{-}PPh_2\text{-}(CH_2)_m\text{-}PPh_2\text{-}\}_n$; m = 4-6

Figure 7 : Dessin du polymère de type $\{[Pt_4(dmb)_4(diphos)]^{2+}\}_n$.

Cette nouvelle approche a conduit le laboratoire du Pr. Harvey à essayer d'autres polymères contenant des ligands mixtes. Frédéric Lebrun (1999-2001) M.Sc., Université de Sherbrooke, s'est quant à lui penché sur des complexes dimériques connus $M_2(dppm)_2^{2+}$ (M = Cu, Ag) (30, 31). Ces dimères peuvent être polymérisés avec l'ajout de 2 équivalents de dmb (Figure 8) pour donner le polymère $\{[M_2(dppm)_2(dmb)_2](Y)_2\}_n$ (M = Cu, Ag Y= BF_4, ClO_4).

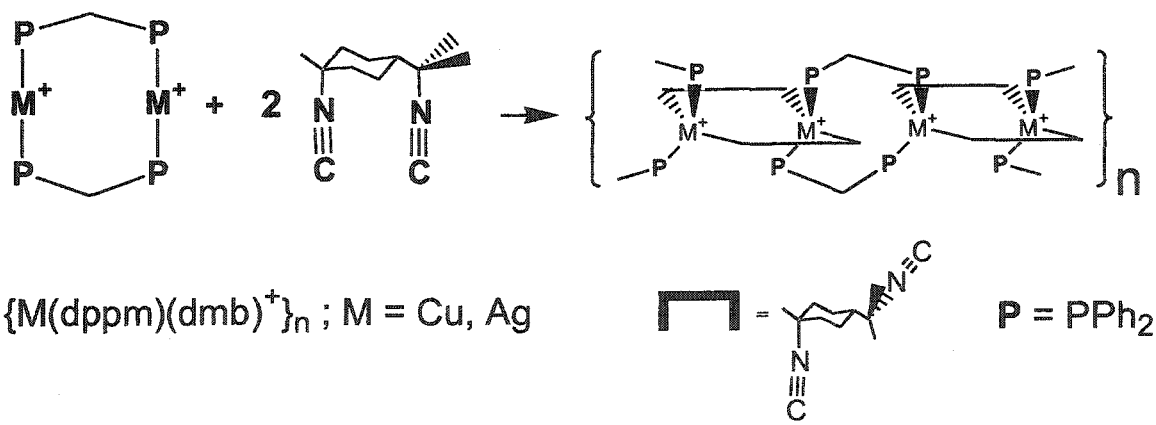

$\{M(dppm)(dmb)^+\}_n$; M = Cu, Ag

P = PPh_2

Figure 8 : Copolymères alternés $\{[M_2(dppm)_2(dmb)_2](Y)_2\}_n$ (M = Cu, Ag Y= BF_4, ClO_4).

Une structure cristallographique de ce type de polymères fût obtenue (Figure 9). Il est intéressant de noter que le dmb est sous sa forme Z à cause de l'encombrement stérique Ph···Ph interdimères et que dans cette conformation les métaux sont très éloignés l'un de l'autre.

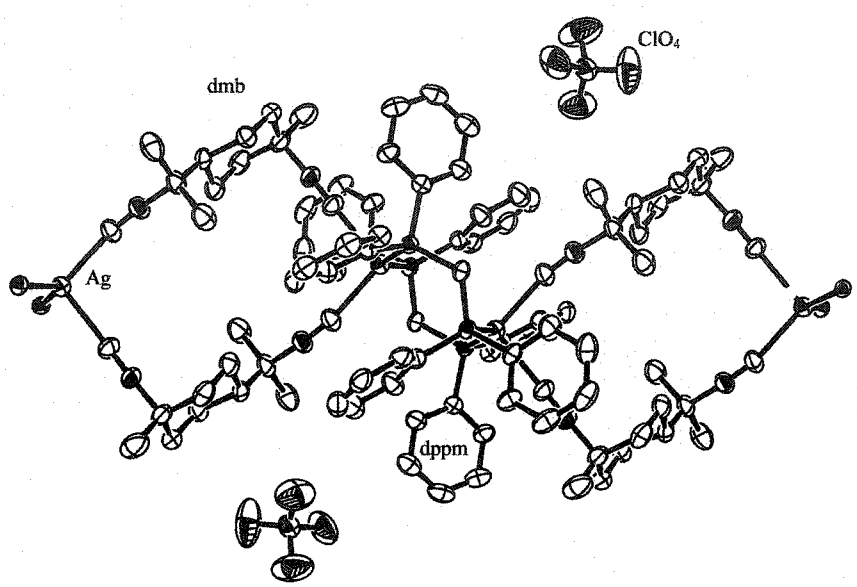

Figure 9 : Dessin ORTEP du polymère $\{[Ag_2(dppm)_2(dmb)_2](ClO_4)_2\}_n$.

iv. Projet initial

La suite logique de cette série est d'utiliser d'autres ligands "diphos" mais en changeant la longueur de la chaîne aliphatique. Les "diphos" contenant des chaînes de 1 à 6 carbones sont disponibles commercialement. Cette nouvelle étude se fera avec des métaux bien connus dans le laboratoire du Pr. Harvey : le cuivre(I) et l'argent(I). Il va de soit que l'allongement de la chaîne aliphatique des "diphos" créera une banque de composés ayant différentes distances métal-métal et la photophysique des transferts énergétiques devra être étudiée. La venue de nouveaux appareils, tel qu'un LASER à N_2 pulsé et un système de détection nanoseconde, dans le laboratoire aidera grandement la

caractérisation de ces nouveaux matériaux. Le Schéma 4 présente cette nouvelle approche qui consiste à éloigner les chromophores bimétalliques pour en étudier les transferts énergétiques. Ces transferts peuvent passer par deux chemins; l'énergie peut passer à travers l'espace ou bien par les liaisons chimiques (32).

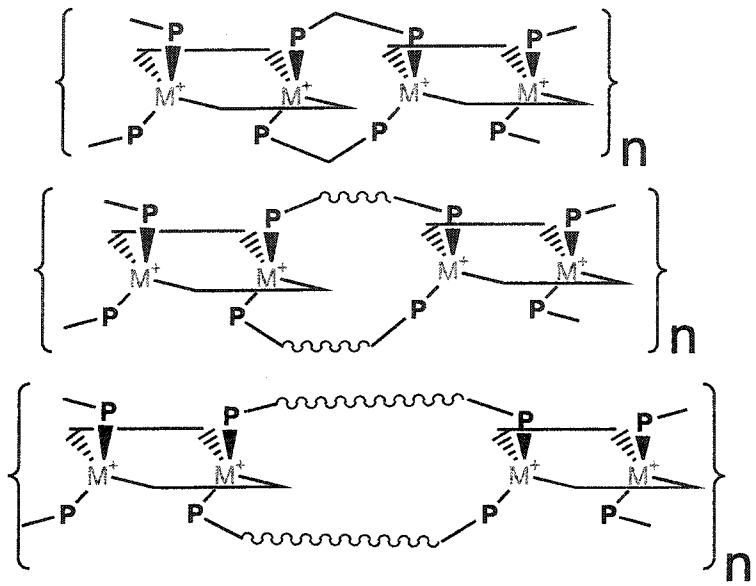

Schéma 4 : Stratégie pour éloigner les chromophores en allongeant la chaîne aliphatique des "diphos".

D'autres dimères de départ ont été synthétisés dans le but de compléter cette série. Ces dimères sont similaires hormis le ligand "diphos" qui est différent, il s'agit du bis(diméthylphosphino)méthane (dmpm). De ce fait, les polymères correspondants seront dépourvus de la possibilité d'empilements π intermoléculaires compliquant les données de transferts énergétiques.

v. Photophysique

La photophysique est une discipline qui étudie l'absorption et l'émission de photons. Une fois que ces photons ont été absorbés, plusieurs processus de relaxation du chromophore peuvent survenir. Si le complexe excité réagit avec le milieu, ce sera un processus photochimique, mais même s'il n'y a pas de réaction, peu importe par quelle voie la désactivation se produit, ce sera un processus photophysique. La Figure 10 présente quelques processus de transition possibles lors de l'absorption ou l'émission de photons. Les processus photophysiques radiatifs et non-radiatifs sont numérotés de 1 à 7. Aucun processus photochimique n'a été observé tels que numérotés 8 et 9 en ce qui concerne notre projet.

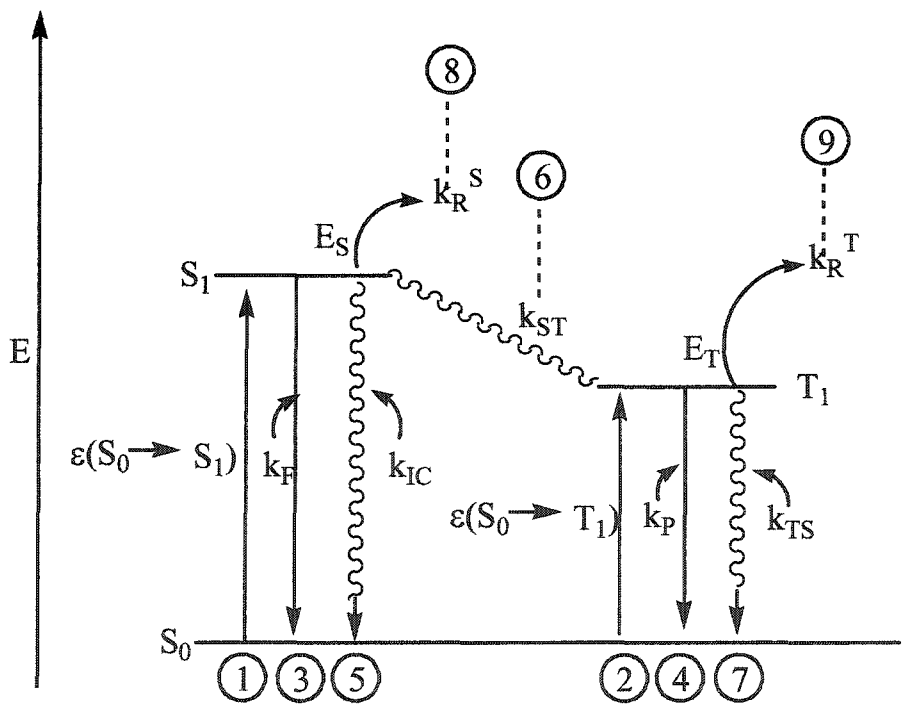

Figure 10 : Représentation de quelques processus photophysiques possibles lors de l'absorption de photons par une molécule.

S_0 = État singulet (spins antiparallèles) à l'état fondamental ($2S + 1 = 1 \rightarrow S = 0$)

S_1 = État singulet (spins antiparallèles) au premier niveau excité ($2S + 1 = 1 \rightarrow S = 0$)

T_1 = État triplet (spins parallèles) au premier niveau excité ($2S + 1 = 3 \rightarrow S = 1$)

1= transition permise d'absorption radiative singulet-singulet ($S_0 + h\nu \rightarrow S_1$)

2 = transition interdite d'absorption radiative singulet-triplet ($S_0 + h\nu \rightarrow T_1$)

3 = transition permise d'émission radiative singulet-singulet ($S_1 \rightarrow S_0 + h\nu$)

4 = transition interdite d'émission radiative triplet-singulet ($T_1 \rightarrow S_0 + h\nu$)

5 = transition permise non-radiative singulet-singulet ($S_1 \rightarrow S_0$+ chaleur)

6 = transition interdite entre les spins des états excités singulet-triplet ($S_1 \rightarrow T_1$+ chaleur)

7 = transition non-radiative triplet-singulet ($T_1 \rightarrow S_0$+ chaleur)

ε = coefficient d'extinction molaire

k_F = constante de vitesse de fluorescence

k_{IC} = constante de vitesse de relaxation non-radiative

k_R^S (8) = constante de vitesse d'une réaction à l'état singulet excité

k_{ST} = constante de vitesse de changement de spin entre les états excités

k_P = constante de vitesse de phosphorescence

k_R^T (9) = constante de vitesse d'une réaction à l'état triplet excité

k_{TS} = constante de vitesse de relaxation non-radiative

E_S = énergie relative de l'état singulet

E_T = énergie relative de l'état triplet

La luminescence observée est de la phosphorescence, facilement décelée grâce à la durée de vie qui est assez longue et au grand décalage entre la bande d'absorption et la bande d'émission. Normalement, les durées de vie de fluorescence se situent entre 10^{-12} et 10^{-6} s, tandis que les durées de vie de phosphorescence sont plutôt de l'ordre de 10^{-6} à 10 s. Les complexes étudiés ici respectent les durées de vie d'une phosphorescence. À la Figure 10, on peut voir que l'absorption d'un photon se fait de l'état singulet S_0 à l'état excité singulet S_1 où il y a un électron qui est promu de la HOMO à la LUMO (dans la

plupart des cas) sans changement de multiplicité. Cette transition dipôlaire électrique est permise selon la règle de multiplicité et l'intensité devrait être maximale. Pour une désactivation "radiative" de cet état excité, il n'y a que deux possibilités. La première est de relaxer directement à l'état fondamental et de réémettre un photon qui possède une énergie aussi grande que celle de l'absorption, de l'état singulet excité S_1 à l'état fondamental S_0 sans changement de multiplicité. Ce phénomène est de la fluorescence, et explique le fait que la bande d'émission est très près de la bande d'absorption. C'est aussi le chemin le plus "rapide" de désactivation, comme les durées de vie de fluorescence (processus permis par multiplicité) sont généralement plus courtes que les durées de vie de phosphorescence (processus interdit par multiplicité). Pour les complexes étudiés dans cet ouvrage, ces bandes d'émission de fluorescence n'ont pas été observées. Les seules bandes observées étaient celles de la phosphorescence. L'émission d'un photon se fait d'un état excité triplet T_1 où il y a deux spins non-pairés et parallèles, à un état fondamental singulet S_o où on a les deux électrons pairés et antiparallèles. Cette différence énergétique étant plus petite que la fluorescence, un déplacement vers le rouge (à plus faible énergie) de la bande d'émission par rapport à la bande d'absorption est observé. Il faut que la constante de vitesse de conversion interne (k_{ST}) de l'état excité (S_1) soit plus grande que la constante de vitesse de fluorescence (k_F). Pour une molécule isolée, la conversion interne est interdite par multiplicité car la molécule passe d'un état excité S_1 où les spins sont antiparallèles, à un état excité T_1 où les spins sont parallèles. Pour que ce processus soit observé plus facilement, il sera généralement nécessaire qu'il y ait des atomes lourds dans la molécule ou à proximité. Ce phénomène est causé par un couplage spin-orbitale qui est très faible pour les atomes légers mais croît rapidement dans les atomes lourds. C'est ce qui explique que très souvent, les molécules organiques (atomes légers) sont plus fluorescentes tendis que les molécules inorganiques et organométalliques (atomes lourds) sont presque toujours uniquement phosphorescentes.

L'approximation de Born-Oppenheimer en mécanique quantique indique que le mouvement des électrons dans les orbitales est beaucoup plus rapide que le mouvement

des noyaux, ce qui nous permet d'approximer les fonctions d'onde vibrationelle $|\chi>$ et électronique $|\Psi>$ comme étant séparables. La probabilité de transition électronique, P, est exprimée par l'intégrale de recouvrement représentant l'élément de matrice de l'Hamiltonien dipôlaire électrique, $H=\mu\cdot E$, couplant l'état initial, $|\Psi\chi\zeta>$, à l'état final, $|\Psi'\chi'\zeta'>$. Similairement, les fonctions d'onde spin-orbitale sont séparables pour les atomes légers, et beaucoup moins pour les atomes lourds, justement à cause du couplage spin-orbitale. Lorsque les fonctions d'onde vibroniques et spin-orbitales ne sont pas séparables, on détermine une fonction d'onde totale. La probabilité qu'une transition électronique se produise entre deux états (fondamental et excité par exemple), est déterminé par :

$$P \sim <\Psi\chi\zeta|H|\Psi'\chi'\zeta'> \qquad [1]$$

l'indice dénote l'état excité, Ψ est une fonction d'onde électronique, χ une fonction d'onde nucléaire (i.e. vibronique), ζ une fonction d'onde de spin.

L'absorption d'un photon pour une transition électronique peut être décrite comme le saut d'un état électronique inférieur représenté par un puits de potentiel à un état électronique supérieur (Figure 11). Ces puits de potentiel présentent des niveaux vibrationnels, dont la séparation énergétique peut parfois être observée en spectroscopie UV-visible. La différence d'énergie qui sépare deux pics d'une bande résolue vibrationnellement peut être utilisée pour extraire la valeur d'un quantum de vibration. Ceci est accomplie en remplaçant les valeurs de ν qui sont les fréquences de vibration en cm^{-1} et υ qui est le nombre quantique vibrationnel qui, dans l'approximation harmonique, prend une valeur entière (0, 1, 2...) dans l'équation [2].

$$E_\upsilon = \nu\,(\upsilon + \tfrac{1}{2}) \qquad [2]$$

La valeur trouvée ΔE par différence de l'énergie entre deux pics, sera l'énergie du mode vibrationnel du lien chimique en oscillation à l'état excité. Le même exercice avec le spectre d'émission nous donnerait cette énergie, mais à l'état fondamental.

Les spectres d'émission et d'absorption des complexes étudiés dans ce travail ne sont pas résolus. C'est-à-dire que l'on ne pourra distinguer l'énergie vibrationnelle quantifiée que contient l'enveloppe vibrationnelle de l'absorption et de l'émission (voir graphique au bas de la figure 11 pour un exemple de spectre).

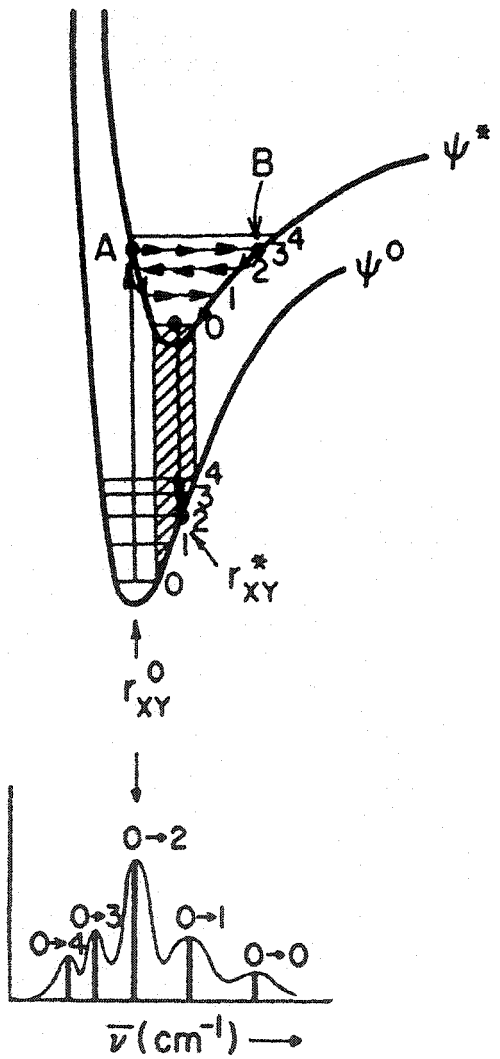

Figure 11 : Diagramme de puits de potentiels avec des sous-niveaux vibrationnels.

Discussion générale des propriétés des excitons :

La localisation complète d'une excitation sur une particule, dans un système de particules identiques, est en principe impossible car cette situation ne constitue pas un état stationnaire du système. Il y aura toujours une probabilité que l'excitation « transfère » d'une particule à l'autre. En effet, les particules ayant des niveaux d'excitation électronique égaux interagiront entre elles. Ces interactions ou couplages peuvent promouvoir des « transferts d'énergie » d'une particule à l'autre dû à la délocalisation de la fonction d'onde et, en effet, le quantum énergétique démontrera une certaine mobilité. Ce quantum d'énergie électronique a été comparé à une particule migrante et est appelé un exciton.

Imaginez une situation où une molécule de solvant excitée électroniquement est capable de transférer, d'une façon non-radiative, son énergie d'excitation à une autre molécule de solvant qui est à l'état fondamental. Ce processus peut continuer et les excitations électroniques peuvent migrer à travers le solvant jusqu'à ce qu'elles soient désactivées par un processus de relaxation (radiatif ou réactionnel par exemple). Cette situation est présentée dans le schéma 5 pour un mécanisme à courte distance. L'étape 1 est un transfert d'énergie par collision normale suivit par l'étape 2, l'étape 3, etc., jusqu'à ce que « n » sauts se produisent et que l'excitation se retrouve sur un site A*(A = accepteur) qui est soumit à une forme de désactivation. Remarquez que le résultat de la migration de l'excitation à travers le solvant M est le même que la diffusion du donneur M_1 (originellement excité) au site occupé par le site final dans lequel M_n est désactivé par le transfert de l'énergie à partir de M_n jusqu'à A. Par analogie, on réfèrera au processus de migration des excitons par le terme « diffusion ». La migration d'énergie peut survenir plusieurs fois dans des cas favorables et le mécanisme pour le processus $D^* \rightarrow A^*$ (D = donneur) peut être observé comme présenté au schéma 5. Une migration d'énergie est attendue lorsque le solvant peut servir d'agent de transfert énergétique et lorsque la vitesse de migration à travers le solvant est plus rapide que la diffusion moléculaire.

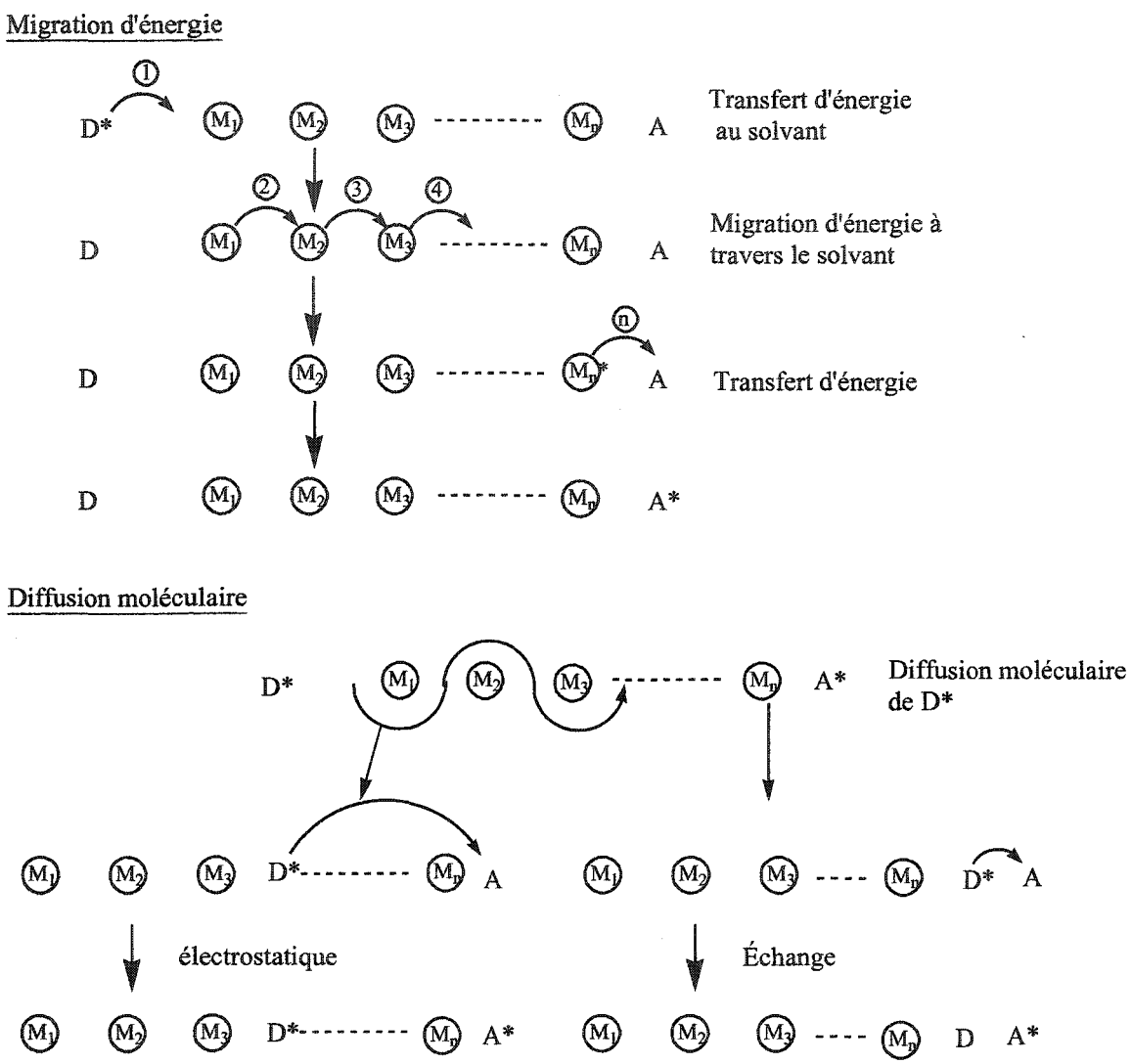

Schéma 5 : Comparaison de transfert d'énergie (D* + A → D + A*) via une migration d'énergie ou diffusion moléculaire.

Lorsque la migration d'énergie est rapide, la vitesse nette de transfert d'énergie va dépendre des vitesses de diffusion moléculaire et de migration d'énergie. Expérimentalement, la migration d'énergie peut être testée sous deux types de conditions :

1. Dans une phase fluide où la diffusion moléculaire est possible.

2. Dans une phase solide où la diffusion moléculaire n'est pas possible.

Dans le cas 1, la migration d'énergie sera seulement importante dans le transfert d'énergie globale à partir de D* vers A* si $k_m[M] > k^{DA}_{ET}[A]$ (k_m étant la constante de vitesse de migration et k^{DA}_{ET} la constante de vitesse de transfert d'énergie (D→A)). D'une façon figurative, on peut voir la situation en terme des contributions individuelles de la migration d'énergie par diffusion excitonique et de la migration moléculaire par la diffusion moléculaire (schéma 5) pour atteindre le même transfert d'énergie net. Dans le cas 2, si D* et A sont séparé dans l'espace par plus de quelques Å de plus que leur grandeur de collision, alors les seuls mécanismes possibles pour atteindre le transfert D*→A* doivent être de caractère « longue distance » Ex :

1. Migration d'énergie via les molécules intermédiaires entre D et A.
2. Au travers l'espace, interaction électrostatique entre D* et A.
3. L'émission de D* suivit par une absorption de A.

La migration d'énergie de singulet et de triplet est bien connue dans les cristaux moléculaires. Par exemple, dans les cristaux de benzène, à basse température, l'énergie du singulet « saute » ~ 10^5 fois pendant la période correspondant au temps de vie moyen τ_S d'une molécule de benzène isolée. L'excitation triplet subit ~ 10^{11} « sauts » pendant la période (τ_T) qui correspond au temps de vie moyen d'une molécule à l'état triplet. Ce qui veut dire que, traduit en distances, un « exciton » singulet peut voyager jusqu'à ~ 10^5 x 2Å = $2x10^5$Å pendant τ_S et le triplet $2x10^{11}$Å pendant τ_T. En fait, de telles longueur de diffusion ne sont pas vraiment accomplies car, au cours des processus de transfert d'énergie, l'excitation (molécule de benzène excitée) se propagera occasionnellement à un site du cristal qui servira à désactiver ce processus de transfert (tel qu'illustré dans le schéma 5).

Théorie de Förster :

Quels sont les facteurs qui déterminent la grandeur des interactions électrostatiques qui mènent au transfert d'énergie à partir de D* vers A, et comment la grandeur de cette interaction est reliée à k_{ET} (constante de vitesse de transfert d'énergie)? Selon le théories classiques décrites ci-bas, l'énergie d'interaction dipôle-dipôle, $E_{d\text{-}d}$, entre deux dipôles (μ_D et μ_A) et les distances entre eux (R_{DA}) équation [3]

$$\text{Énergie d'interaction } E_{d\text{-}d} \propto \frac{\mu_D \mu_A}{R_{DA}^3} \qquad [3]$$

Förster a identifié μ_D et μ_A avec la force de l'oscillateur pour une transition D*⇔ D et A⇔A* radiative. Il a pu quantifier l'interaction d'énergie dipôle-dipôle en terme de f_D et f_A, la force mesurée de l'oscillateur pour une transition radiative de D et A qui, étant des propriétés de systèmes réels, inclue les facteurs de vibration et de spin. Donc, un petit facteur de Franck-Condon vibrationnel ou un changement de multiplicité mènera à de petites valeurs de f et une petite énergie d'interaction associée. Förster a montré que, étant donné que la vitesse de transfert d'énergie k_{ET} est reliée, par un mécanisme dipôle-dipôle, à E^2. Aussi, E^2 est relié aux propriétés expérimentales, donc k_{ET} peut être relié à E^2 comme démontré dans l'équation [4]

$$k_{ET}(\text{électrostatique}) \rightarrow E^2 \sim \left(\frac{\mu_D \mu_A}{R_{DA}^3}\right)^2 = \frac{\mu_D^2 \mu_A^2}{R_{DA}^6} \qquad [4]$$

La théorie de Förster prédit que pour un transfert d'énergie via une interaction électrostatique du type dipôle-dipôle, k_{ET} sera proportionnel à :

1. Le carré de la transition du moment dipolaire μ_D.
2. Le carré de la transition d'un moment dipolaire μ_A.
3. L'inverse à la puissance six de la séparation de D* et A.

Dans les équations [5] et [6], les relations entre les transitions des moments dipolaires et quantités expérimentales ont été dérivés.

$$\mu_D^2(D^* \Leftrightarrow D) \rightarrow \int \varepsilon_D \, d\nu \text{ ou } k^0{}_D \qquad [5]$$

$$\mu_A^2(A^* \Leftrightarrow A) \rightarrow \int \varepsilon_A \, d\nu \text{ ou } k^0{}_A \qquad [6]$$

Où $\int \varepsilon$ est le coefficient d'extinction intégré d'une bande d'absorption et k^0 est la vitesse radiative pure.

Étant donné que l'on considère spécifiquement le processus D*→ D et A→ A* dans un transfert d'énergie, on choisit $k^0{}_D$ et $\int \varepsilon_A$ comme termes expérimentaux pour remplacer le carré de la transition du moment dipolaire [7]

$$k_{ET} \text{ (électrostatique)} \rightarrow \frac{k_D^0 \int \varepsilon_A}{R_{DA}^6} \qquad [7]$$

Finalement, on doit reconnaître les exigences de recouvrement spectral et considérer le recouvrement d'émission de D* avec l'absorption de A. Förster a montré que :

$$k_{ET} \text{ (électrostatique)} = k \frac{\kappa^2 k_D^0}{R_{DA}^6} J(\varepsilon_A) \qquad [8]$$

Le terme k est une constante déterminée par des conditions expérimentales comme l'indice de réfraction du solvant et la concentration. Le terme κ^2 tient compte du

fait que les interactions entre deux dipôles oscillants dépendent de l'orientation des dipôles dans l'espace. Le terme $J(\varepsilon_A)$ représente une intégrale de recouvrement spectral.

Réactions possibles :

La figure 12 représente une vue d'ensemble de la photochimie moléculaire et montre plusieurs processus rencontrés. La plupart des analyses effectuées dans notre laboratoire sont de nature qualitative et implique la partie de gauche de la figure 12. Il est bon de comprendre que la photophysique et la photochimie ne s'arrête pas simplement à ces analyses mais que plusieurs réactions et mécanismes peuvent être réalisés et interprétés dans cette optique.

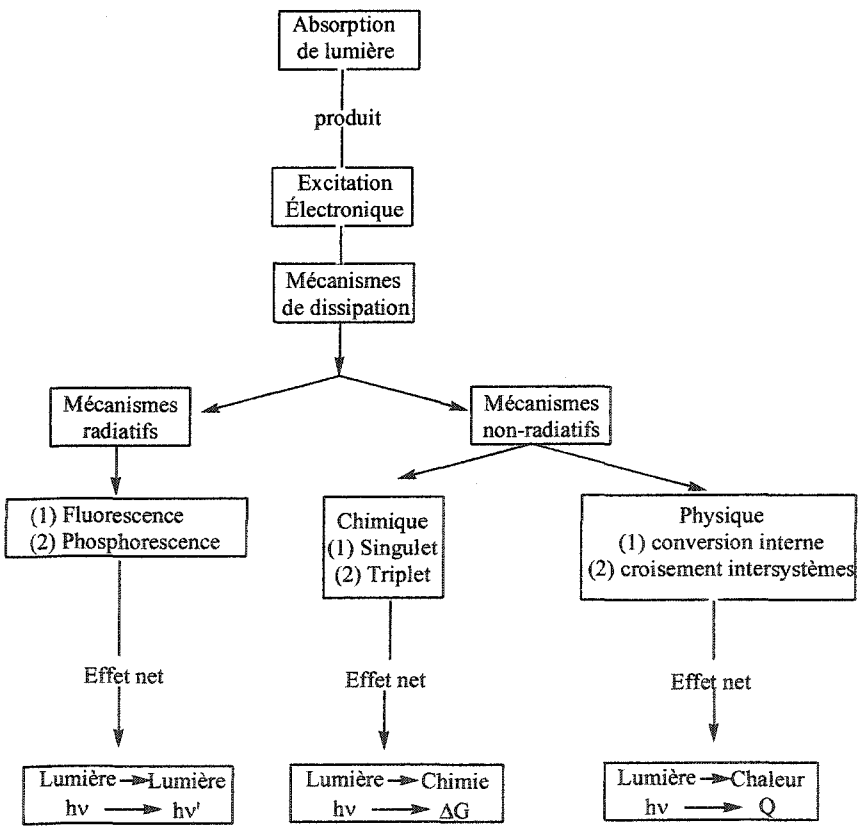

Figure 12 : Liste des processus d'intérêts pour un photochimiste moléculaire.

Cinétique :

En général, une combinaison de durées de vie d'émission τ_e et de rendements quantiques d'émission Φ_e expérimentaux sont de bons moyens de mesurer la constante de vitesse unimoléculaire de conversion interne et croisement inter-système. La connaissance de ces vitesses d'inter-conversions et de durées de vie des états excités sont d'une grande importance dans l'analyse de problèmes photochimiques. Cette section nous permettra d'estimer ces valeurs à partir des données spectrales. En absence de réactions photochimiques irréversibles et de désactivation bimoléculaire les étapes de réactions suivantes décrivent les chemins importants de désactivation d'une molécule qui est à son singulet de plus basse excitation S_1.

	Étape	Vitesse	
$h\nu + S_0 \rightarrow S_1$	Excitation	I	[9]
$S_1 \sim> S_0$ + chaleur	Conversion interne	$k_{IC}[S_1]$	[10]
$S_1 \sim> T_1$ + chaleur	Croisement inter-système	$k_{ST}[S_1]$	[11]
$T_1 \sim> S_0$ + chaleur	Croisement inter-système	$k_{TS}[T_1]$	[12]
$T_1 \rightarrow S_0 + h\nu'$	Phosphorescence	$k_P^0[T_1]$	[13]
$S_1 \rightarrow S_0 + h\nu'$	Fluorescence	$k_F^0[S_1]$	[14]

L'approximation de l'état stationnaire des singulets excités mène à:

$$I = (k_{ST} + k_F^0 + k_{IC})[S_1] \qquad [15]$$

où I est la vitesse d'absorption de la lumière en einsteins/litre / seconde, et $[S_1]$ est la concentration des singulets excités. Similairement, nous obtenons pour les triplets :

$$k_{ST}[S_1] = (k_{TS} + k_P^0)[T_1] \qquad [16]$$

d'où on obtient

$$[T_1] = \frac{k_{ST}[S_1]}{(k_P^0 + k_{TS})} \qquad [17]$$

La durée de vie de singulets τ_S est égale à l'inverse de la somme des vitesses qui désactivent S_1 et la durée de vie du triplet τ_T est égale à l'inverse de la somme des vitesses qui désactivent T_1

$\tau_S = 1/(k_F^0 + k_{ST} + k_{IC})$ durée de vie S_1 expérimentale [18]

$\tau_P = 1/(k_P^0 + k_{TS})$ durée de vie T_1 expérimentale [19]

Si on néglige le processus [12] (i.e. $k_{TS} \cong 0$), la valeur τ_P est extraite en mesurant l'intensité de l'émission (phosphorescence) en fonction du temps. Considérant une cinétique unimoléculaire de premier ordre, on a :

$$\frac{d[T]}{dt} = k_P^0[T] \qquad [20]$$

$$\int_0^t \frac{d[T]}{[T]} = -\int_0^t k_P^0 dt \qquad [21]$$

À t = 0, $[T] = [T^0]$ donc :

$$\ln[T] - \ln[T^0] = \ln([T]/[T^0]) = -k_P^0 t \qquad [22]$$

$$k_P^0 = -\, d\ln([T]/[T^0]) / dt \qquad [23]$$

d'où on obtient

$$\tau_P = 1/ k_P^0 \qquad [24]$$

Étant donné que [T] est directement proportionnel à l'intensité de phosphorescence, nous pouvons mesurer τ_P à partir de l'évolution de l'intensité de phosphorescence (I_P) en fonction du temps. Cette intensité est proportionnelle à la concentration (ou population) de l'espèce excitée qui varie avec le temps après une excitation à cause des processus de relaxation. Pour un processus uni-moléculaire, le graphe ln I_P vs temps donnera une droite où la durée de vie de l'état excité responsable de l'émission est le négatif de l'inverse de la pente. Si le graphique montre deux droites, il y a alors deux processus radiatifs de relaxation. Il faut comprendre que les intensités relatives de chacune de ces contributions peuvent être différentes, et par conséquent le calcul ajuste un paramètre de pondération (populations relatives et leur temps de relaxation respectifs) pour tenir compte de ce phénomène. S'il y plusieurs droites, le nombre de processus est proportionnel à ce nombre. S'il y a une courbe, soit que le mécanisme n'est pas du premier ordre (ce qui n'est pas le cas ici), soit que le nombre de processus est tellement grand que la courbe est poly-exponentielles. Ce dernier cas est couramment rencontré pour la relaxation des états excitoniques.

Expérimentale :

Les mesures des durées de vie de phosphorescences ont été effectuées à l'aide d'un laser à N_2 pulsé (durée des pulses = 1ns, modèle GL-3300) de PTI. La longueur d'onde d'excitation était de 311 nm. Le détecteur étant placé à la position du maximum de la bande d'émission, il pouvait prendre les intensités d'émission par intervalles de 10 µs en mode phosphorescence. Les données furent traitées à l'aide du logiciel Time Master™ de PTI et les spectres ont été normalisés (lorsque nécessaire) à l'aide d'un tableur (Sigma Plot). Les temps de vie d'émission ont été analysés de deux façons. La première était la méthode commune de déconvolution à partir des données brutes utilisant de une à quatre décroissances exponentielles pour un graphique ln I_P en fonction du

temps (où I_P est l'intensité de l'émission (phosphorescence) après un pulse lumineux excitateur). Le critère de qualité est basé sur la comparaison de la droite (lorsqu'il s'agit d'un processus photophysique uni-moléculaire) ou de la courbe calculée (lorsqu'il y a plusieurs composantes) avec les données expérimentales. Ce paramètre s'appelle en anglais « goodness of fit », χ, qui doit être près de 1,00. Ce paramètre tient compte du résiduel, de la soustraction de la courbe calculée des données expérimentales. Un tel calcul donne une droite à zéro avec des pics au-dessus et en dessous de cette dernière. Un « bon » résiduel est la situation où les pics au-dessus et en dessous sont distribués de façon homogène le long de cette droite, et que la hauteur de ces pics sont approximativement les mêmes. En gros, la décision pour affirmer ou infirmer de la qualité relative des déconvolutions reste une décision humaine. Lorsque le nombre de composantes est trop élevé, cette méthode devient inutile. La deuxième méthode était l'ESM (Exponential Series Method) (33-34) qui consiste à calculer une courbe théorique de décroissance en considérant plusieurs exponentielles calculées (jusqu'à 200) avec une fenêtre de durées de vie qui excède la fenêtre de temps des données ce qui assure la détection de composantes courtes ou longues. Ce logiciel fait le même travail que celui du haut mais deux fonctions supplémentaires sont ajoutées. Comme déjà mentionné, ce logiciel est capable de gérer jusqu'à 200 composantes, rendant les calculs plus longs, mais il est aussi conçu pour varier les paramètres de pondération et de durées de vie et de chercher la meilleure solution. Il trouve donc la meilleure solution possible selon les données expérimentales. Le point important est qu'il faut s'assurer que la réponse ne soit pas fonction des paramètres d'entrée, c'est-à-dire le nombre de durées de vie maximal à gérer et le début et la fin des données analysées. C'est pourquoi toute la longueur de la courbe était analysée dans tout les cas.

CHAPITRE 1

PRÉPARATION ET CARACTÉRISATION DE PETITS OLIGOMÈRES À LIGANDS MIXTES AYANT DES UNITÉS DE CONSTRUCTION LUMINESCENTES DE TYPE $M_2(dmpm)_x$ ET $M_2(dmb)_y$ (M = Cu, Ag; x = 2, 3 ; y = 1, 2)

Dans la chimie de l'état solide, l'étude des interactions entre les atomes ou les molécules à l'échelle microscopique devient fascinante pour la compréhension des propriétés physiques et optiques à l'échelle macroscopique. Une de ces propriétés est le phénomène de l'exciton (35). La mobilité (diffusion) des excitons est très étudiée (32, 36-37) dans la forme solide portant sur les cristaux, polymères organiques et sur des agrégats plus petits. Ces études mettent en évidence la dépendance de cette excitation délocalisée sur le nombre d'unités impliquées et de leur séparation. Les travaux sur la quantification de ces propriétés optiques dans les polymères en fonction du nombre d'unités sont plutôt rares. En terme d'oligomères ou de polymères organométalliques, seule l'équipe du professeur Harvey a fait ce type de travaux (24, 25). Dans l'article présenté dans ce chapitre, nous étudions la synthèse et la caractérisation de complexes binucléaires et d'oligomères hexanucléaires à partir de ligands pontants (dmb (1,8-diisocyano-*p*-menthane) et dmpm (bis(diméthylphosphino)méthane)) et les cations Cu(I) et Ag(I). En effet, l'utilisation de complexes de type $M_2(dmpm)_3^{2+}$ (M = Cu, Ag) et $Ag_2(dmpm)_2^{2+}$ avec le dmb a permis d'obtenir des oligomères (en phase solide). Ces oligomères ont fait l'objet d'une caractérisation rigoureuse en solution (RMN ^1H, ^{13}C et ^{31}P) mais la majorité des analyses furent faites à l'état solide (IR, Raman, DRX, DSC, ATG et analyse élémentaire). Au cours de l'élaboration de cet article, deux structures cristallographiques ont été obtenues, une troisième fut empruntée d'un mémoire (Frédéric Lebrun M.Sc. Université de Sherbrooke) afin de fournir des explications supplémentaires et une quatrième qui sera

placée en annexe de ce mémoire (le désordre de cette dernière était trop grand pour rencontrer les exigences du journal et n'a pas été publié.). Ces nouveaux complexes ont été comparés spectroscopiquement et photophysiquement avec le $\{Ag(dmb)_2^+\}_n$ (~8 unités) et le $\{Cu(dmb)_2^+\}_n$ cristallin (~45 unités) pour démontrer l'influence de la dimension de l'oligomère sur le phénomène excitonique. Ce dernier a pu être observé pour ces nouveaux oligomères et s'est même manifesté dans les espèces binucléaires. Les travaux présentés dans ce chapitre ont été soumis le 18 juin 2003 au "Inorganic Chemistry" et ma contribution à ces travaux sont sur le plan expérimental (toutes les synthèses, purification et préparation d'échantillons pour analyses), analytique (spectre RMN ^1H, ^{13}C et ^{31}P, DRX de poudre, ATG, DSC, IR, RAMAN, UV-visible, calculs théoriques pour les analyses élémentaires, et des spectres de masse, spectres d'excitation, d'émission, d'émission en fonction du temps et durée de vie de l'émission) et aussi que pour la rédaction du texte (protocoles expérimentaux, compilation de données sous forme de tableaux et graphiques, figures et mise en forme).

Preparation and Characterization of Small Mixed-Ligand Oligomers Containing Luminescent $M_2(dmpm)_x$ and $M_2(dmb)_y$ Building Blocks (M = Cu, Ag; x = 2, 3 ; y = 1, 2)

Eric Fournier and Pierre D. Harvey*

Contribution from the Département de chimie, Université de Sherbrooke, Sherbrooke, PQ., Canada J1K 2R1

Submitted as a full paper in Inorganic Chemistry

*To whom correspondence should be addressed :

Tel : (819) 821-7092

Fax : (819) 821-8017

Email : p.harvey@Usherbrooke.ca

Abstract

The luminescent binuclear complexes $M_2(dmpm)_3^{2+}$ (M = Cu, Ag; dmpm = bis(dimethylphosphino)methane), $Ag_2(dmpm)_2^{2+}$ and $Cu_2(dmpm)_3(CN\text{-}t\text{-}Bu)_2^{2+}$ (as BF_4^- salts), as well as the oligomers described as $\{Cu_2(dmpm)_3(dmb)_{1.33}^{2+}\}_3$ and $\{Ag_2(dmpm)_2(dmb)_{1.33}^{2+}\}_3$ (dmb = 1,8-diisocyano-p-menthane), have been prepared and characterized in the solid state. These compounds exhibit emission maxima ranging from 445 to 485 nm with emission lifetimes found in the μs regime. The time-resolved emission spectra for the oligomers and the known polymers $\{M(dmb)_2^+\}_n$ (M = Cu, Ag) exhibit blue-shifted emission bands at the early stage of the photophysical event after the light pulse, which red-shift with longer delay times. The decay traces are more or less exponential, and their analysis according to the Exponential Series Method (ESM) exhibits a distribution of lifetimes that is fairly broad. The extent of red-shift of the emission band with delay time and the fwhm (full-width-at-half-maximum) of the distribution of lifetimes increase as the number of M_2-units increases in the oligomers. This behavior is interpreted by an exciton process. During the course of this study, the X-ray structures for the $M_2(dmpm)_3^{2+}$ and $Cu_2(dmpm)_3(CN\text{-}t\text{-}Bu)_2^{2+}$ complexes as well as a related dimer $[Ag_2(dppm)_2(CN\text{-}t\text{-}Bu)_2](ClO_4)_2$, the XRD patterns (X-ray powder diffraction), DSC (differential scanning calorimetry), TGA (thermal gravimetric analysis), and the solid state IR spectra have been examined in order to characterize the complexes and oligomers.

Introduction

The crystal engineering and supramolecular coordination polymeric networks constructed from multifunctional ligands and transition metals are areas that have experienced a tremendous increase in interest in recent years.[1] Although the field is overwhelmingly dominated by the use of N-containing assembling ligands,[2] the use of P- or C≡NR-donor containing bridging ligands is far less extensive,[3] but many new 1-, 2- and 3-D networks have still been discovered. One of the most basic concepts in solid state chemistry is that the physical and optical properties of a material depend upon the interactions and "communications" between the components at the molecular or atomic level. In order to probe such interactions, the use of 1-D materials in the form of small oligomers of various lengths appears to be a effective strategy. This group has recently reported the synthesis and characterization of 1-D polymers of the type $\{M(dmb)_2^{+}\}_n$[4] and the mixed-ligand $\{M_2(dppm)_2(dmb)_2^{2+}\}_n$[5] (M = Cu, Ag; dmb = 1,8-diisocyano-p-menthane; *anti-* or *gauche-*; dppm = bis(diphenylphosphino)methane, Scheme 1). The chromophores are the $M(C{\equiv}NR)_4^{+}$ centers (M = Cu, Ag) which are separated by 5 Å (Ag···Ag distance) in $\{Ag(dmb)_2^{+}\}_n$,[4] and $M(C{\equiv}NR)_2(P)_2^{+}$ units which are separated by 4.03 and 9.61 Å in $\{Ag_2(dppm)_2(dmb)_2^{2+}\}_n$.[5]

The average polymer length for the $\{Ag(dmb)_2^{+}\}_n$ materials in solution was determined to be ~ 8 units from T_1/NOE mesurements,[6] while the amorphous Cu analogue was 300 units (light scattering).[5] This difference is explained by the greater lability of the dmb ligand onto Ag(I) which was convincingly verified by the reversibility of the isomerisation of the $\{Ag(dmb)_2^{+}\}_n$ polymers, but not observed for the Cu analogue.[7] Previous works from this group on the $\{Pd_4(dmb)_4(dmb)^{2+}\}_n$[8] and $\{Pt_4(dmb)_4(diphos)^{2+}\}_n$[9] polymers (diphos = $Ph_2P(CH_2)_mPPh_2$; m = 4-6; 84000 < MW_n < 307000) have also shown that there are some sensitive differences in the photophysical data between the polymers and the corresponding building blocks (here $M_4(dmb)_4^{2+}$ (M = Pd, Pt)). A literature survey shows that the occurrence of investigations on organometallic and coordination polymers and their luminescence properties, including

transition metals such as Cu(I), Ag(I) and Au(I), have become more and more frequent in recent years,[10] but the detailed comparison of the photophysical properties between the repetitive unit and the polymer has not been performed.

We now wish to report the syntheses and characterization of new binuclear complexes and hexanuclear oligomers using dmb and dmpm (bis(dimethylphosphino)-methane) as bridging ligands and Cu(I) and Ag(I) cations. By changing the nature of the assembling ligands and building blocks, one can hope not only to change the distance between the building blocks, but also to change the number of units. These oligomers are composed of the following $M_2(dmpm)_3^{2+}$,[11] $Ag_2(dmpm)_2^{2+}$,[11] $M_2(dmb)_2^{2+}$ (M = Ag, Cu),[12] and $Ag_2(dmb)^{2+}$ [7] building units (Scheme 3). The spectroscopic and photophysical properties are compared to $\{Ag(dmb)_2^+\}_n$ (~ 8 units) and crystalline $\{Cu(dmb)_2^+\}_n$ (~ 45 units), and it is shown that the extent of the perturbation of the photophysical properties is function of the oligomer size. The results are interpreted by an exciton phenomenum.

Experimental Section

Materials: 1,8-diisocyano-p-menthane[13] and the $\{[M(dmb)_2]BF_4\}_n$ polymers (M = Ag and Cu (highly crystalline prepared from method 3)[4a] were synthesized according to literature procedures. $[Cu(CH_3CN)_4]BF_4$ was freshly prepared before use, following the published procedure.[14] All solvents were purified according to standard procedures.[15] The following products were purchased from: acetone (Fisher), acetonitrile (Anachemia), petroleum ether (ACP), argon (Praxair), dichloromethane (ACP), ethanol (Les alcools de commerce inc.), dinitrogen (Praxair); $AgBF_4$, $Cu(BF_4)_2 \cdot xH_2O$ and *t*-butyl isocyanide (Aldrich Chemicals Co); bis(dimethylphosphino)methane (Strem Chemicals Co); Cu(m) (Anachemia). All air or moisture sensitive materials were handled using standard Schlenk techniques, high-vacuum manifolds and an inert-atmosphere glove box.

$[Cu_2(dmpm)_3](BF_4)_2$ (1). Under inert atmosphere, 370.0 mg (1.18 mmol) of $[Cu(NCMe)_4]BF_4$ was dissolved in 20 ml of acetone. 0.35 ml (2.21 mmol) of dmpm was

added drop wise using a micro-syringe. The reaction flask was stirred for 1 hr prior to addition of 80 ml of diethylether. A white precipitate appeared which was filtered and dried in a glove box, and provided 315 mg (yield 60%). ^{1}H NMR (CD_3CN) δ 2.02 (m, 6H, PCH_2P), 1.36 (s, 36H, PCH_3); ^{31}P NMR (CD_3CN), δ -25.36; ^{13}C NMR (CD_3CN), δ 32.12, 16.12; UV-vis (CH_3CN), 210 (39500), 248 nm (8500 $M^{-1}cm^{-1}$).

$[Ag_2(dmpm)_3](BF_4)_2$ (2). 259.6 mg of $AgBF_4$ (1.33 mmol) was dissolved in 15 ml of acetone under inert atmosphere. The resulting solution was filtered prior to use. 0.35 ml, (2.21 mmol) of dmpm was added drop wise with a micro-syringe. The solution was stirred for 1 hr. Then 70 ml of diethylether were added to precipitate the white product, which was filtered and dried *in vaccuo*. Yield 90% (478 mg). ^{1}H NMR (CD_3COCD_3), δ 2.45 (m, 6H, PCH_2P), 1.60 (s, 36H, PCH_3); ^{31}P NMR (CD_3COCD_3), δ -13.98, -15.39, -16.86; ^{13}C NMR (CD_3COCD_3), δ 31.63, 16.41; UV-vis (CH_3CN), 200 (47400), 224 (31400), 254 nm (4300 $M^{-1}cm^{-1}$).

$[Ag_2(dmpm)_2](BF_4)_2$ (3). 53.4 mg of $AgBF_4$ (0.274 mmol) were dissolved in 15 ml of acetone under inert atmosphere. 37.5 mg (0.275 mmol) of dmpm were added drop wise using a micro-syringe. The solution was stirred for 1 hr prior to adding 70 ml of diethylether. The white precipitate was filtered and dried under inert atmosphere, and provided 90.6 mg (yield 76%). ^{1}H NMR (CD_2Cl_2), δ 2.31 (m, 4H, PCH_2P), 1.61 (s, 24H, PCH_3); ^{31}P NMR (CD_2Cl_2), δ -12.99 (br d, J(AgP) = 560); ^{13}C NMR (CD_3CN), δ 30.01, 14.46; UV-vis (CH_3CN), 202 (48000), 256 nm (23400 $M^{-1}cm^{-1}$).

$[Cu_2(dmpm)_3(CN\text{-}t\text{-}Bu)_2](BF_4)_2$ (4). **1** (102.1 mg, 0.144 mmol) was dissolved in 30 ml of degassed acetone. 0.1 ml (0.88 mmol) of *t*-BuNC was added dropwise using a micro-syringe. The solution was stirred for 1 hr prior to concentrating it in vaccuo until a volume of 5 ml was obtained. 25 ml of dimethylether was added to the remaining solution to precipitate a white solid which was filtered and dried *in vaccuo*. Yield 86%

(108 mg). ^{1}H NMR (CD_3COCD_3), δ 2.26 (m, 6H, PCH_2P), 1.59 (s, 18H, $(CH_3)_3C$), 1.45 (s, 36H, PCH_3); ^{31}P NMR (CD_3COCD_3), δ -25.41; ^{13}C NMR (CD_3COCD_3), δ 58.38, 33.03, 30.20, 17.84; IR (KBr), ν 1052 (BF_4), 2177 cm^{-1} (C≡N); Raman (solid), ν 2176 cm^{-1} (C≡N); UV-vis (CH_3CN), 212 (39500), 236 sh. nm (22200 $M^{-1}cm^{-1}$).

$\{[Cu_2(dmpm)_3(dmb)_{1.33}](BF_4)_2\}_3$ (5). **1** (106.2 mg, 0.150 mmol) was dissolved in 20 ml of degassed acetone. 100.0 mg (0.525 mmol) of dmb were dissolved separately in a round flask containing 150 ml of degassed acetone. This solution was slowly added drop wise to the former solution. The mixture was stirred for 4 hrs prior to being reduced to 15 ml *in vaccuo*. 150 ml of diethylether were added to the solution. A white product precipitated, which was filtered and dried. Yield 52% (86.9 mg). ^{1}H NMR (CD_3CN), δ 2.08-2.02 (m, 8H, dmb), 2.01 (m, 18H, PCH_2P), 1.87-1.83 (m, 8H, dmb), 1.61-1.56 (m, 12H, dmb), 1.51 (s, 20H, dmb), 1.45 (s, 24H, dmb), 1.35 (s, 108H, CH_3P); ^{31}P NMR (CD_3CN), δ -25.55; ^{13}C NMR (CD_3CN), δ 60.45, 63.18, 45.32, 37.10, 32.55, 29.11, 26.05, 23.32, 7.18 ; IR (KBr), ν 2161 cm^{-1} (C≡N); Raman (solid), ν 1052 (BF_4), 2160 cm^{-1} (C≡N); UV-vis (CH_3CN), 210 (51100), 236 sh. nm (26500 $M^{-1}cm^{-1}$). Chem. Anal. (calcd.) for $Cu_6C_{93}H_{198}N_8P_{18}B_4F_{16}$ C 38.67; H 6.91; N 3.88%; (Found) C 38.64; H 6.79; N 4.02%.

$\{[Ag_2(dmpm)_2(dmb)_{1.33}](BF_4)_2\}_3$ (6). **3** (59.1 mg, 0.089 mmol) was dissolved in 45 ml of degassed acetone. 53 mg (0.279 mmol) of dmb were dissolved separately in a round flask containing 60 ml of degassed acetone. This solution was slowly added drop wise in the former solution, and the mixture was stirred for 3 hrs prior to being reduced to 15 ml *in vaccuo*. 120 ml of diethylether were added to precipitate the white product, which was filtered and dried *in vaccuo*. Yield 99% (76.1 mg). ^{1}H NMR (CD_2Cl_2), δ 2.16 (m, 12H, PCH_2P), 2.03-1.85 (m, 16H, dmb) 1.53 (s, 88H, CH_3P + dmb) 1.50-1.43 (m, 40H, dmb); ^{31}P NMR (CD_2Cl_2), δ -15.68 (m); ^{13}C NMR (CD_3COCD_3), δ 64.12, 61.21, 43.78, 36.92, 31.96, 28.25, 27.21, 22.88, 16.44, 15.56; IR (KBr), ν 1051 (BF_4), 2181 cm^{-1} (C≡N); Raman (solid), ν 2182 cm^{-1} (C≡N); UV-vis (CH_3CN), 198 (40300), 254 nm (10200 M^{-}

$^{1}cm^{-1}$); Chem. Anal. (calcd.) for $Ag_3C_{39}H_{78}N_4P_6B_3F_{12}$ C 33.82; H 5.68; N 4.05%; (Found) C 34.29; H 5.32; N 3.96%.

Apparatus: All NMR spectra were acquired using a Bruker AC-300 spectrometer (^{1}H 300.15 MHz, ^{13}C 75.48 MHz, ^{31}P 121.50 MHz) using the solvent as chemical shift standard, except for ^{31}P NMR, where the chemical shifts are relative to D_3PO_4 85% in D_2O. All chemical shifts (δ) and coupling constants (J) are given in ppm and Hz, respectively. The IR spectra were acquired on a Bomem FT-IR MB series spectrometer equipped with a baseline diffused reflectance. The UV-vis spectra were acquired using a Hewlett Packard diode array spectrophotometer 8452A model. The continuous wave emission and excitation spectra were obtained using a SPEX Fluorolog II spectrometer. The emission lifetimes were measured with a nanosecond N_2 laser system from PTI model GL-3300 pumping a dye laser model GL-302. The excitation wavelength was 311 nm for all the measurements. The time-resolved emission spectra were acquired on the same instrument used for the lifetime measurements, and the excitation wavelength was also 311 nm. The delay times were set using different time windows after the pulse. MALDI-TOF mass spectra were acquired from a Bruker Proflex III linear mode spectrometer with a nitrogen laser (337 nm) from the Université de Bourgogne in Dijon (France) with a dithranol matrix. The glass transition temperatures (Tg) was measured using a Perkin-Elmer 5A DSC7 equipped with a thermal controller 5B TAC 7/DS. Calibration standards were water and indium. FT-Raman were acquired on a Bruker RFS 100/S spectrometer. XRD were acquired on a Rigaku/USA Inc with a copper lamp operating under a 30 mA current and a 40 KV tension. TGA were acquired on a TGA 7 of Perkin Elmer between 50 et 650 °C at 3°/minute under nitrogen atmosphere.

Crystallography. Crystals of $[Ag_2(dmpm)_3](BF_4)_2$ **(2)** were grown by vapor diffusion using acetonitrile – *tert*-butylmethylether at 23 C°. Crystals of $[Cu_2(dmpm)_3](BF_4)_2$ **(1)** were grown by vapor diffusion using acetone – *tert*-butylmethylether at 23 C°. Single crystals were coated with Paratone-N oil, mounted using a glass fiber and frozen in the

cold nitrogen stream of the goniometer. A hemisphere of data was collected on a Bruker AXS P4/SMART 1000 diffractometer using ω and θ scans with a scan width of 0.3 ° and 10 s exposure times. The sample-detector distance was 5 cm. The data were reduced (SAINT)[16] and corrected for absorption (SADABS).[17] The structure was solved by direct methods and refined by full-matrix least squares on F^2 (SHELXTL).[17] All non-hydrogen atoms were refined anisotropically. Hydrogen atoms were found in Fourier difference maps and refined isotropically. Thermal ellipsoid plots are at the 30% probability level. In some plots, hydrogen atoms have been omitted for clarity.

Procedures. The emission quantum yields were measured using 9,10-diphenylantracene as the standard (Φ_F = 1.00 for degassed solutions).[18] The average molecular weight in number (M_n) of the highly crystalline $\{[Cu(dmb)_2]BF_4\}_n$ polymer was obtained from the measurements of the intrinsic viscosity using polymethyl methacrylate standards from Aldrich (M_n = 12000, 15000, 120000, and 320000). The evaluated M_n is 24000 (i.e. about 45 units). The emission lifetimes were analyzed in two ways. The first way was the common deconvolution method allowing for analysis of the raw data using models form 1 to up to 4 exponential decays. The second way was the ESM (Exponential Series Method),[19] and consisted of calculating a decay curve composed of many exponentials (up to 200) with a window of lifetimes well exceeding the time window of the data, insuring that any short or long components be detected. The results were checked to ensure that they did not depend on input parameters. Typically, the results were presented as a distribution of lifetimes. For single exponential decays, both methods gave the same results, and the distribution of lifetimes was narrow. For data giving a large distribution with ESM, the deconvolution method failed to find satisfactory fits with 2, 3, or 4 decays. The quality of the fit between the experimental and calculated curves was addressed using the parameter χ (goodness of fit), and from the analysis of the residual. A good fit is accompanied with a residual where the "noise" above and under the baseline is evenly distributed. In this work, best results were obtained using ESM, and for homogeneity, the data were presented as such.

Computer modeling. The calculations were performed using the commercially available PC-model from Serena Software (version 7.0), which uses the MMX empirical model. No constraint on bond distances and angles was applied to insure that deviations from normal geometry was depicted. Comparisons between literature X-ray structures and computed models are provided in the text. The R-N≡C groups are replaced by R-C≡C$^-$ because PC Model does not model C≡N$^+$- fragments, as strongly bent structures were calculated. Instead -C≡C- is used securing a more linear and realistic frame for the ligand.

Results and Discussion

The "$M_2(dmpm)_x^{2+}$" building blocks. The binuclear $M_2(dmpm)_3^{2+}$ complexes (M = Cu (**1**), Ag (**2**)) are synthesized from the direct reaction between dmpm and the desired metal cationic species in the appropriate stoichiometric amount. In 1 :1 stoichiometric amount, the dmpm ligand also reacts with $AgBF_4$ to form the dicoordinated $Ag_2(dmpm)_2^{2+}$ dimer (**3**) . **2** and **3** can be distinguished by their sensitivity to light where **3** turns gray with time, and from ^{31}P NMR.[10]

Compounds **1** and **2** provide crystals suitable for X-ray analysis (Figs. 1 and 2; Table 1 and 2). The complexes exhibit two nearly trigonal planar coordinated metal atoms placed face-to-face, and separated by 2.9265(3) and 2.9893(2) Å, for **1** and **2**, respectively. Such distances fall short in comparison with the isostructural $Au_2(dmpm)_3^{2+}$ analogue (3.040 and 3.050 Å),[20] and follow the trend for their relative ionic radii (Cu(I), 0.91 Å; Ag(I), 1.29 Å; Au, 1.51 Å).[21] While the Ag_2 and Au_2 distances are shorter than the sum of the van der Waals radii (3.4 Å)[21] indicating the presence of M_2 interactions, the Cu_2 distance is not (2.8 Å)[21]. The average PCuCu angle (91.7°) still suggests the presence of weak M_2 interactions in this case. Both **1** and **2** belong to the approximate C_s point group, but exhibit notable distortions. For instance, each triangular MP_3 fragment exhibits different sets of M-P distances (shorter and longer) averaging 2.237(4) and 2.249(3) Å for **1**, and 2.434(10) and 2.458(19) Å for **2**. While **1** exhibits two symmetric CuP_3 planes with PCuP angles being close to 120° (± 2°), two of these angles deviate

from 120° in **2**. In addition, the AgP distances (average 2.434 Å) are long compared to that of CuP and AuP (Table 3).

The neutral isoelectronic $M_2(dppm)_3$ dimers (M = Pd, Pt)[22,23] exhibit M_2 distances similar to their neighboring atoms in the periodic table (Pd ~ Ag^+; Pt ~ Au^+), but the cationic systems show slightly longer M_2 distances (Table 3), likely reflecting the internuclear electrostatic repulsion. Remarkably, the $d(Ag_2)$ value for $[Ag_2(dmpm)_2](PF_6)_2$ (3.041(1)Å)[24] is longer than that found in **2**, indicating that the third dmpm ligand applies some extra restoring force. This is further exemplified in the $Cu_2(dmpm)_2(O_2CMe)^+$ complex where the shorter bite distance of the acetate ligand forces the Cu atoms to lie closer from to other (2.7883(11)Å)[25] in comparison with **1**.

The model compound **4** is prepared from the direct reaction between **1** and 2 equivalents of *t*-BuNC , and the identity of this compound is readily made from ^1H and ^{31}P NMR. Despite the poor quality of the single crystal,[26] both the spectra and crystallographic data are consistent with the addition of 2 *t*-BuNC ligands at the axial position of the $M_2(dmpm)_3^{2+}$ skeleton (Scheme 4). The position of the Cu atoms have been located in the crystal ($d(Cu_2) > 4$Å), and no evidence for short contact is observed, consistent with the change in metal coordination change from triangular plane to tetrahedral.

No attempt was made to synthesize the $Ag_2(dmpm)_2(CN\text{-}t\text{-}Bu)_2^{2+}$ complex. However, the $[Ag_2(dppm)_2(CN\text{-}t\text{-}Bu)_2](ClO_4)_2$ dimer is known (Scheme 5),[27] and was characterized from X-ray crystallography. The structure consists of two face-to-face tricoordinated Ag(I) atoms bridged by two dppm ligands, where one CN-*t*-Bu ligand binds each of the metals, similar to that of $Ag_2(dmpm)_3^{2+}$ with the difference that one diphosphine ligand is replaced by two isocyanide groups. This structure preliminary is available in the Supporting Information.[28]

Syntheses and characterization of the oligomers. **1** reacts with dmb with ratios varying from 1:1 to 1:2 (dimer/dmb) which invariably form an oligomeric material best described as $[Cu_6(dmpm)_9(dmb)_4](BF_4)_6$ or $\{[Cu_2(dmpm)_3(dmb)_{1.33}](BF_4)_2\}_2$ (**5**). This formulation, $[Cu_2(dmpm)_3(dmb)]_x(dmb)$ where x = 3, is established from the reproducible chemical analyses, ^1H NMR (integration of the dmpm vs dmb ones), and TGA data. It is possible that traces of shorter and longer oligomers (x = 1, 2 and x > 3) exist, but the product distribution must be narrow since the oligomer is relatively small, and all three techniques above indicate the same results. The chemical yield is modest indicating some losses during the attempts to obtain pure samples. The short oligomeric nature of the materials is also depicted from the IR spectra where both the ν(N≡C) for coordinated (2161 cm^{-1}) and free isocyanide (2132 cm^{-1}) are observed (Fig. 3).

The corresponding $Ag_2(dmpm)_3^{2+}$ complex does not react with dmb even in excess. This result may reflect the fact that the Ag(I) atoms here are significantly electron rich, as the dmpm ligand is a strong electron donor, rich enough to render the monodentate RNC ligand very labile. Conversely, the $Ag_2(dmpm)_2^{2+}$ complex reacts with dmb in a 1:1 ratio to generate another oligomeric material, also best described as $[Ag_6(dmpm)_6(dmb)_4](BF_4)_6$ or $\{[Ag_2(dmpm)_2(dmb)_{1.33}](BF_4)_2\}_3$ (**6**) (again, evaluated from the chemical analysis, ^1H NMR and TGA).[29] Similar IR characteristics as described above are depicted in the spectra, where a weak absorption associated to free ν(N≡C) is observed (Fig. 3). It is interesting to note that both oligomers **5** and **6** (6 metal atoms) exhibit a dimension smaller than that reported for $\{[Ag(dmb)_2]BF_4\}_n$ in solution (n = 7-8).[6]

Thermal properties. The thermal stability of the oligomers has been investigated by TGA, and the traces have been interpretted using **1** and **4** as standards for comparison purposes (Table 4). The former exhibits only a single weight loss at ≈ 350°C (position of the maximum in the first derivative), but spreading over ~ 80°C (scan rate 3°/min). On

the basis of the residual weight (~15%) only metallic copper remains above 500°C, and so the weight loss (~ 85%) must be due to both the dmpm ligand and BF_4^- anion. **4** exhibits two weight loss events at ~190°C (19%) and ~375°C (66%) which correspond to the loss of *t*-BuCN and dmpm/BF_4^-, respectively (typical examples of TGA traces are provided in the Supporting Information). Again, these events are spread over a large temperature range (~70°C). **5** also exhibit the same two decomposition events; the first one is found at ~220°C (loss of dmb; ~30%), and the second one ranges from 300 to 390°C (loss of dmpm and BF_4). The notable differences are that the loss of the isocyanide ligand occurs within a much narrower temperature range (~10-20°C) and at a higher temperature with respect to *t*-BuNC. In addition, the first derivative shows trace clearly two distinct events (in the 300-350°C range), and on the basis of the corresponding weight loss, the first one is assigned to the BF_4^- anion, while the second one, the dmpm.

6 behaves similarly but exhibits slightly lower temperatures of weight loss, suggesting weaker M-L and M-BF_4^- interactions. It is interesting to note that the calculated weight losses do not differ significantly from the experimental results. Any deviation from the presented stoichiometry worsens the comparison between the theoretical and experimental data. No glass transition (nor other thermal phenomenon) is found between –20°C and 100°C in the DSC traces for all investigated compounds. The result is consistent with the non-polymeric nature of the materials.

Modeling. The molecular structures for the model compounds $Ag_2(dmpm)_2(CN\text{-}t\text{-}Bu)_2^{2+}$ and $Cu_4(dmpm)_6(dmb)_2(CN\text{-}t\text{-}Bu)^{4+}$ were computed to address two specific questions in the absence of X-ray data. First, is the Ag···Ag distance in $Ag_2(dmpm)_2(CN\text{-}t\text{-}Bu)_2^{2+}$ (model coumpound for **6**) comparable to $Ag_2(dmpm)_3^{2+}$ (explaining some similarities in the electronic spectra)? Second, what distance separates the different dimer units in **5** (and ultimately in **6** as well)?

The methodology has been tested on the X-ray data for **1**, **2** and the related dimer $[Ag_2(dppm)_2(CN\text{-}t\text{-}Bu)_2](ClO_4)_2$ (Table 5) in order to provide a degree of confidence in the results. The M···M and M···P distances are computed within a 0.05-0.06 Å inaccuracy which is acceptable in the context of this work. The Ag-C bond length gives the worst agreement with a difference of ~ 0.3 Å with the experimental value, and is taken into account.

The computed model structure for $Ag_2(dmpm)_2(CN\text{-}t\text{-}Bu)_2^{2+}$ (Supporting Information) exhibits a Ag···Ag separation of 2.94 Å, similar to that for **2** (2.9265 Å, X-ray), and a twisted angle of 18°. The greater twisted angle may be induced by small steric contacts in the *t*-butyl groups. The first conclusion is that if this structure is correct, as suggested by the $Ag_2(dppm)_2(CN\text{-}t\text{-}Bu)_2^{2+}$ X-ray data, the UV-vis $d\sigma^* \rightarrow p\sigma$ signature should be present at the same wavelength for both **2** and **6** (see section below). The second feature is that the replacement of CN-t-Bu by dmb should not induce great ring stress or angle torsion.

The computed structure for $Cu_4(dmpm)_6(dmb)_2(CN\text{-}t\text{-}Bu)^{4+}$ exhibits a central bridging dmb ligand adopting a *gauche*-conformation (Supporting Information). The *anti*-form is clearly unfavorable due to steric problems. The M···M distance in the M-dmb-M unit is 9.112 Å, which may be slightly over evaluated by 2 x 0.3 Å as indicated above. The calculated triply bridged Cu···Cu distance is 4.35 Å, predictably longer than that found in **1**, and more similar to the preliminary X-ray data for **4** (~ 4.011 Å).[26] Similarly, the computed NC···CN and N···N distances in the *gauche*-dmb are 7.064 and 5.755 Å, respectively, which provide an approximation about what the closest interchromophore distance is. These M···M, C···C and N···N distance compares favorably with that reported for the crystallographically characterized polymer $\{[Pd_4(dmb)_4(dmb)]\text{-}(MeCO_2)_2\}_n$ (i.e. 9.241, 6.801 and 5.549 Å, respectively).[8]

Electronic spectra. The absorption spectra for the compounds **1** and **2** (Fig. 4) exhibit an absorption band at ~ 250 nm. These unstructured bands are due to the $d\sigma^* \rightarrow p\sigma$ transition; an electronic transition that is well documented for cofacial d^{10}-d^{10} species such as $Au_2(dmpm)_3^{2+}$,[30] $Au_2(dcpm)_2^{2+}$ (dcpm = bis(dicyclohexylphosphino)methane),[31] $Au_2(dmpm)_2^{2+}$,[32] $M_2(dppm)_3$ (M=Pd, Pt),[33] and $Ag_2(dmpm)_2^{2+}$.[34] In order to confirm this assignment, the absorption spectra are also recorded at 77K using butyronitrile as solvent. At this temperature, the bandwidths decrease greatly, somewhat similar to that seen for $Pd_2(dppm)_3$[33] and $Ag_2(dmpm)_2^{2+}$[34] (see also Supporting Information for **4** as an example). This phenomenon has been fully described by Gray and collaborators and others.[35] In comparison with other related triply bridged d^{10}-d^{10} species (Table 6), the λ_{max} for the $d\sigma^* \rightarrow p\sigma$ bands compare favorably to that of $Au_2(dmpm)_3^{2+}$. No obvious trend is seen along the Cu, Ag, Au series, perhaps reflecting the two opposite effects, where the lengthening of the M···M distance disfavors the M···M interactions, while the increase in atomic radii favors them. The most striking results are certainly the absorbtivity data for the $M_2(dmpm)_3^{2+}$ (M = Cu, Ag) which are significantly lower than those for the Au analogues, as well as the $M_2(dppm)_3$ species (M = Pd, Pt). This is even more puzzling when one compares the $d\sigma^* \rightarrow p\sigma$ absorption data for $[Ag_2(dmpm)_2](BF_4)_2$ in acetonitrile (λ_{max} = 256 nm; ν_{max} = 39000 cm^{-1}; ε = 23400 $M^{-1}cm^{-1}$) which also compares favorably to the recently published data for $[Ag_2(dmpm)_2](PF_6)_2$ data in ethanol.[34] A possible explanation is that the weaker M···M interactions in **1** and **2** place the $d\sigma^*$ MO level close to the atomic $d_{x^2-y^2,xy}$ ones. This proximity induces orbital mixings so that a symmetry allowed $d\sigma^* \rightarrow p\sigma$ transition gets a strong forbidden component. This hypothesis can be verified from the measurements of the UV-vis spectra of single crystals using polarized light. The size of the needle-shape crystals prevented such experiments.

This low intensity anomaly is not as extensive for the oligomer **6** in acetonitrile as the absorptivity for the $d\sigma^* \rightarrow p\sigma$ band (λ_{max} = 254 nm) is 10200 $M^{-1}cm^{-1}$.[36] The presence of the RNC ligand in the triangular plane geometry about the metal breaks the symmetry

and renders the selection rules less rigorous. The position of the $d\sigma^* \rightarrow p\sigma$ band at 254 nm indicates that the amplitude of Ag···Ag interactions are similar for all three investigated Ag species.

The absorption spectra for **4** and **5** exhibit spectra that are almost identical to each other, where strong absorptions are observed at 212 and 236, and at 210 and 236 nm respectively (see Fig. 5 as an example). As anticipated for the non-interacting Cu···Cu systems, the $d\sigma^* \rightarrow p\sigma$ absorption is absent from the spectra. The lowest energy absorption is assigned to the spin-allowed t_2 ($d\sigma^*$) $\rightarrow$ t_2 (π^*, $p\sigma^*$) transition.[37]

Emission. The compounds are luminescent in solution at 298 and 77K (Figs. 4 and 5; Table 7), as well as in the solid state. The excitation spectra measured for solution confirm the authenticity of the emission, and the μs timescale for the lifetimes is consistent with a phosphorescence process. **1** and **2** exhibit modest intensity luminescence in solution at 298K at 500 and 471 nm, respectively. The energy gaps between the absorption and emission (18800, for **1** ; 17300 cm^{-1}, for **2**) are somewhat large. The phenomenon has also been observed by Che, Miskowski and collaborators for $Au_2(dmpm)_3^{2+}$,[30] and the authors have suggested that the emission arises from $^3(d_{(x^2-y^2),\,xy} \rightarrow p\sigma)$ excitation, in agreement with Mason's former proposal.[38] We agree with this proposal for **1** and **2** as well. The similarity in the λ_{max} and τ_e for **2** and **6** in the solid state strongly suggests that this assignment also applies for the oligomer **6**.

In solution, the emission bands for all compounds red-shift from ~ 446 nm up to 466-520 nm. This range falls is the same region as that found for the tetracoordinated Cu species (474-502 nm), and suggests that the emission arising from the tricoordinated Ag species in solution may be due to tetracoordinated solvent/anion exiplexes.[30] For the formally tetracoordinated **4** and **5** materials, the assignment of the emissive state is

$^3([t_2(d\sigma^*)]\ ^5[t_2(\pi^*,p\sigma^*)]^1)$ in agreement with that of $M(diphos)_2$ (M = Pd, Pt; diphos = bis(diphenylphosphino)propane)[37a] and that of $M(CN\text{-}t\text{-}Bu)_4^+$ (M = Cu, Ag).[4]

The τ_e data show two trends (Table 7). First, τ_e predictably increases with the rigidity of the medium, and decreases as the temperature increases. Second, τ_e and Φ_e decrease as the size of the molecule increases. The latter is due to the well known "loose bolt" effect,[39] where the number of vibrational levels favoring internal conversion increases with the presence of groups around the chromophores, as well as their sizes. It is interesting to note that the excited state lifetimes for the tricoordinated silver species **2** and **6** are significantly longer than those reported for solid $Ag_2(dcpm)_2^{2+}$ at 298 K (λ_{emi} = 420 nm; τ_e = 0.5 μs),[40] and for $Ag_2(dmpm)_2^{2+}$ in ethanol at 77K (λ_{emi} 371 nm; τ_e = 49 μs),[34] the latter's being dicoordinated.

The photophysical properties of the $\{M(dmb)_2^+\}_n$ polymers were previously reported by us, and were compared to the tetrahedral mononuclear model complexes $M(CN\text{-}t\text{-}Bu)_4^+$ (M = Cu, Ag).[4a] The spectroscopic and photophysical properties were found to be drastically different between the mononuclear species and polymers. The key features are as follows: the λ_{max} for the $M(CN\text{-}t\text{-}Bu)_4^+$ species are blue-shifted with respect to the corresponding polymers (up to 40-65 nm), and the fwhm of the emission bands are smaller as well. The decay traces are rigorously mono-exponential for the mononuclear complexes, while they are non-exponential in the polymers. Time-resolved emission spectra indicate that at the early event after the light pulse, both λ_{max} and slope of the emission decay traces (equivalent of a lifetime) compare favorably with those of the corresponding mononuclear chromophores $M(CN\text{-}t\text{-}Bu)_4^+$ (M = Cu, Ag). At longer delay times, the recorded emission bands are significantly red-shifted (up to 50 nm). Finally, another notable difference is that the emission arising from the polymers is depolarized. All these features are typical of energy transfer exciton phenomena (Scheme 6).[39] One of the interesting features is that the decay traces in the polymers are found to

be independent of the medium (solution vs solid), indicating that the process is primarily intramolecular.

This feature is related to the long intermolecular N···N distances (8.25 and 8.67 Å) which indicate that the chains are relatively isolated from one another in the solid state.[29] Despite the fact that no X-ray data is available for **5** and **6**, it is possible to anticipate what the approximate interchromophore distances in the solid state are, by examining the X-ray data for the building blocks **1** and **2**. For these species, the closest intermolecular P···P distances are 6.683 Å for **1**, and 6.328, 6.585 and 6.982 Å for **2**. These distances are greater than the intramolecular N···N separation in the linking *gauche*-dmb ligand in the computed model compound $Cu_6(dmpm)_9(dmb)_2(CN\text{-}t\text{-}Bu)_4^{6+}$ (~5.8 Å) and in the polymer $\{[Pd_4(dmb)_4(dmb)]^{2+}\}_n$ (5.549 Å; X-ray).[8] If one accepts that the rate for exciton hoping or energy transfer (k_{ET}) varies as $k_{ET} \propto 1/r^6$ (r = interchromophore distance; for a i.e. Förster mechanism),[39] then the contribution of the intermolecular process is minor.

Fig. 6 shows the time resolved emission spectra (20-2000 μs) for **5** and **6** in the solid state. The λ_{max} are also found to be time-dependent. At the early event after the light pulse, the recorded emission band is blue-shifted with respect to the emission band measured in continuous wave mode. As the delay time increases, the observed emission band red-shifts constantly and the intensity decreases. All in all, the emission bands measured with continuous wave light are composed of a number of blue- and red-shifted components. The maximum band shifts are ~10 and 34 nm for **5** and **6**, respectively, which are smaller than those observed for the longer $\{M(dmb)_2^+\}_n$ polymers (~50nm).[4a]

The decay traces can be analyzed using ESM providing a distribution of the lifetimes. When a decay trace is relatively linear, the distribution is relatively narrow. Conversely, the opposite is observed. For **4** (binuclear species), **5** (~ hexanuclear oligomers) and the $\{Cu(dmb)_2^+\}_n$ polymer (about 45 units), this trend is indeed observed.

Such distributions are characterized by a maximum (most probable lifetime as reported in Table 7) and a fwhm (a measurement proportional to the curving extent of the decay traces). The data are compared in Table 8, as well as for **2**, **6** and $\{Ag(dmb)_2^+\}_n$. It is noted that the fwhm of the distribution increases as the size of the oligomer increases. The most spectacular change is found for **4** and **5** (Supporting Information), for which the ligand environment is the same (i.e. 3 P + 1 CN). The fwhm also varies rapidly with the number of metal atoms in the oligomers, but not extensively for larger ones (see entries 2 and 3 of Table 8). From experience, the fwhm for a mononuclear complex in dilute solution, a situation where no interaction with other chromophores should occur, is rather narrow as well, similar to that of the binuclear complexes, here **2** and **4**. The overall experimental data are consistent with an exciton process. The fact that the fwhm is smaller for Ag vs Cu oligomers only indicates that the time scale for the Ag species is shorter than that of the Cu time scales due to spin-orbit coupling. This model can be improved by taking into account the fact that the exciton delocalisation spreads both ways along the chain, since the chromophores are all identical; there is a no formal donor-acceptor direction (Scheme 7).

Evidence for an extensive exciton process in **5**, as provided in Table 8, suggests that the energy hoping can proceed for distances in the order of ~ 9.1 Å or ~ 5.8 Å (taking into account the Cu···Cu or N···N separations) based upon modeling. This observation is perfectly consistent with the literature which shows that energy transfer and exciton coupling are clearly perceptible in this distance range.[41]

Acknowledgment. This research was supported by the Natural Sciences ad Engineering Research Council of Canada (NSERC).

Supporting Information. Absorption spectra of **4** at 298 and 77K; XRD spectra for **5** and **6**; computed structure for the model compound $Ag_2(dmpm)_2(CN\text{-}t\text{-}Bu)_2^{2+}$; computed structure for a model compound $Cu_4(dmpm)_6(dmb)_2(CN\text{-}t\text{-}Bu)^{4+}$; solid state decay traces

for the emission of **4** versus $\{Cu(dmb)_2^+\}_n$ at 298K; comparison of the distribution of lifetimes as a function of lifetime fitting the emission decay traces for **5** and $\{Cu(dmb)_2^+\}_n$ in the solid state at 298K; comparison of the population distribution of lifetimes as a function of lifetimes fitting emission decay traces for **1**, **6** and $\{Ag(dmb)_2^+\}_n$ in the solid state at 298K. X-ray crystallographic files are available for **1**, **2** and $[Ag_2(dppm)_2(CN\text{-}t\text{-}Bu)_2](ClO_4)_2$ in CIF format. This material is available free of charge via the Internet at http://pubs.acs.org.

References.

(1) (a) Holloday, B. J.; Mirkin, C. A. Angew. *Chem., Int. Ed. Engl.* **2001**, *40*, 2023. (b) Seidel, R. S.; Stang, P. J. *Acc. Chem. Res.* **2002**, *35*, 972. (c) Eddaoui, M.; Moler, D. B.; Li, H.; Chen, B.; Reineke, T. M.; O`Keefe, M.; Yaghi, O. M. *Acc. Chem. Res.* **2001**, *34*, 319. (d) Moulton, B.; Zawortko, M. J. *Chem. Rev.* **2001**, *101*, 1629. (e) Khlobystov, A. N.; Blake, A. J.; Champness, N. R.; Lemenovskii, D. A.; Majouga, A. G.; Zyk, N.V.; Schröder, M. *Coord. Chem. Rev.* **2001**, *222*, 155. (f) Biradha, K.; Fujita, M. *Adv. Supramol. Chem.* **2000**, *6*, 1. (g) Braga, D. *Acc. Chem. Res.* **2000**, **33**, 601. (h) Leininger, S.; Olenyuk, B.; Stang, P. J. *Chem. Rev.* **2000**, *100*, 853. (i) Swiegers, G. F.; Melefetse, T. J. *Chem. Rev.* **2000**, *100*, 3483.

(2) See for recent examples (a) Abrahams, B. F.; Batten, S. R.; Hoskins, B. F.; Robson, R. *Inorg. Chem.* **2003**, *42*, 2654. (b) Wang, Q.-M.; Mak, T. C. W. *Inorg. Chem.* **2003**, *42*, 1637. (c) Shin, D. M.; Lee, I. S.; Lee, Y.-A.; Chung, Y. K. *Inorg. Chem.* **2003**, *42*, 2977. (d) Effendy; Marchetti, F.; Pettinari, C.; Pettinari, R.; Skelton, B. W.; White, A. H. *Inorg. Chem.* **2003**, *42*, 112. (e) Tong, M.-M.; Wu, Y-M.; Ru, J.; Chen, X.-M.; Chang, H.-C.; Kitagawa, S. *Inorg. Chem.* **2002**, *41*, 4846. (f) Konaka, H.; Wu, L. P.; Munakata, M.; Kuroda-Sowa, T.; Maekawa, M.; Suenaga, Y. *Inorg. Chem.* **2002**, *41*, 1928. (g) Dong, Y.-B.; Ma, R.-P.; Huang, R.-Q. *Inorg. Chem.* **2003**, *42*, 294. (h) Reger, D. L.; Semeniue, R. F.; Smith, M. D. *Inorg. Chem.* **2001**, *40*, 6545. (i) Bu, X-H.; Liu, H.; Du, M.; Wong, K. M.-C.; Yam, V. W.-W.; Shionoya, M. *Inorg. Chem.* **2001**, *40*, 4143. (j) Carlucci, L.; Ciani, G.; Proserpio, D. M.; Rizzato, S. *New J. Chem.* **2003**, *27*, 483. (k)

Muthu, S.; Yip, J. H. K.; Vittal, J. J. *J. Chem. Soc., Dalton Trans.* **2002**, 4561. (l) Hamilton, B. H.; Ziegler, C. J. *Chem. Comm.* **2002**, 842. (m) Carlucci, L.; Ciani, G.; Proserpio, D. M.; Rizzato, S. *Cryst. Eng. Comm.* **2002**, *4*, 121. (n) Ferlay, S.; Koenig, S.; Hosseini, M. W.; Pansanel, J.; De Cian, A.; Kyritsakas, N. *Chem. Comm.* **2002**, 218. (o) Patra, G. K.; Goldberg, I. *J. Chem. Soc., Dalton Trans.* **2002**, 1051. (p) Horikoshi, R.; Mochida, T.; Maki, N.; Yamada, S.; Morivana, H. *J. Chem. Soc., Dalton Trans.* **2002**, 28. (p) Caradoc-Davies, P. L.; Hanton, L. R. *Chem. Comm.* **2001**, 1098. (q) Blake, A. J.; Champness, N. R.; Cooke, P. A.; Nicolson, J. E. B. *Chem. Comm.* **2000**, 665. (s) Bu, W-M.; Ye, L.; Fan, Y.-G. *Chem. Letters* **2000**, 152.

(3) See for recent examples (a) Brandys, M.-C.; Puddephatt, R. J. *J. Am. Chem. Soc.* **2002**, *124*, 3946. (b) Adolf, A.; Gonsior, M.; Krossing, I. *J. Am. Chem. Soc.* **2002**, *124*, 7111. (c) Kuang, S.-M.; Zhang, Z.-Z.; Wang, Q.-G.; Mak, T. C. W. *Chem. Comm.* **1998**, 581. (d) Ino, I.; Zhong, J. C.; Manukata, M.; Kudora-Sowa, T.; Maekawa, M.; Suenaga, Kitamori, Y. *Inorg. Chem.* **2000**, *39*, 4273.

(4) (a) Fortin, D.; Drouin, M.; Turcotte, M.; Harvey, P.D. *J. Am. Chem. Soc.* **1997**, *119*, 531. (b) Perreault, D.; Drouin, M.: Michel, A.; Harvey, P.D. *Inorg. Chem.*, **1992**, *31*, 3688.

(5) Fournier, É.; Lebrun, F.; Harvey, P. D., submitted for publication, 2003.

(6) Turcotte, M.; Harvey, P.D. *Inorg. Chem.* **2002**, *41*, 1739.

(7) Fortin, D.; Drouin, M.; Harvey, P.D. *J. Am. Chem. Soc.* **1998**, *120*, 5351.

(8) Zhang, T.; Drouin, M.; Harvey, P.D. *Inorg. Chem.* **1999**, *38*, 1305.

(9) Zhang, T.; Drouin, M.; Harvey, P.D. *Inorg. Chem.* **1999**, *38*, 957.

(10) (a) Liu, Q.-X.; Uu, F.-B.; Li, Q.-S.; Zeng, X.-S.; Leng, X.-B.; Chou, Y.L.; Zang, Z.-Z. *Organometallics*, **2003**, *22*, 309. (b) Colacio, E.; Kivekas, R.; Lloret, F.; Sunberg, M.; Suarez-Varela, J.; Bardaji, M.; Laguna, A. *Inorg. Chem..*, **2002**, *41*, 5141. (c) Zang, H.; Cai, J.; Feng, X.-L.; Li, T.; Li, X.-Y.; Ji, L.-N., *Inorg. Chem. Commun.*, **2002**, *5*, 637. (d) Sun, D.; Cao, R.; Weng, J.; Hong, M.; Liang, Y., *J. Chem. Soc., Dalton Trans.*, **2002**, 291. (e) Tong, M.-L.; Shi, J.-X.; Chen, X.-M., *New J. Chem.*, **2002**, *26*, 814. (f) Zheng, S.-L.; Tong, M.-L.; Tan, S.-D.; Wang, Y. Shi, J.-X.; Tong, Y.-X.; Lee, H. K.; Chen, X.-

M., *Organometallics* **2001**, *20*, 5319. (g) Zhang, J.; Xiong, R.-G.; Chen, X.-T.; Xue, Z.; Peng, S.-M.; You, X.-Z., *Organometallics*, **2002**, *21*, 235. (h) Heyduk, A.F.; Krodel, D.J.; Meyer, E. E.; Nocera, D.G., *Inorg. Chem.*, **2002**, *41*, 634. (i) Zhang, J.; Xiong, R.-G.; Chen, X.-T.; Che, C.-M.; Xue, Z.; You, X.-Z., *Organometallics*, **2001**, *20*, 4118. (j) Tong, M.-L.; Yu, X.-L.; Chen, X.-M., Inorg. *Chem. Commun.*, **2000**, *3*, 694. (k) Tong, M.-L.; Chen, X.-M.; Ye, B.-L.; Ji, L.-N., *Angew. Chem. Int. Ed.*, **1999**, *38*, 2237. (l) Henary, M.; Wootton, J.L;. Khan, S.I.; Zink, J.I., *Inorg. Chem.*, **1997**, *36*, 796. (m) Seward, C.; Chan, J.; Song, D.; Wang, S. *Inorg. Chem.*, **2003**, *42*, 1112.

(11) (a) Dean, P.A.; Vittal, J.J.; Srivastava, R. S. *Can. J. Chem.* **1987**, *65*, 2628. (b) Perreault, D.; Drouin, Michel, A.; Miskowski, V. M.; Schaefer, W.P.; Harvey, P.D. *Inorg. Chem.*, **1992**, *31*, 695.

(12) (a) Harvey, P.D. *Coord. Chem. Rev.* **2001**, *219-221*, 17. (b) Fortin, D.; Drouin, M.; Harvey, P.D.; Herring, F.G.; Summers, D.A.; Thompson, R.C. *Inorg. Chem.* **1999**, *38*, 1253. (c) Perreault, D.; Drouin, M.; Michel, A.; Harvey, P.D. *Inorg. Chem.* **1993**, *32*, 1903.

(13) Weber, W.D.; Gokel, G.W.; UGI, I.K. *Angew. Chem. Int. Ed. Engl.* **1972**,*11*, 530.

(14) Hathaway, B. J.; Holah, D. G.; Postlethwaite, J. D. *J. Chem. Soc.* **1961**, 3215.

(15) (a) Perrin, D. D.; Armarego, W. L. F.; Perrin, D.R. *Purifications of laboratory chemicals*; Pergamon: Oxford, U.K. **1966**. (b) Gordon, A. J.; Ford, R. A. *The Chemist's companion, a handbook of practical data, techniques, and references*; Wiley: New York, **1972**; p436.

(16) SAINT 6.02, Bruker AXS, Inc., Madison, Wisconsin, **1997-1999,** USA.

(17) (a) SADABS George Sheldrick, Bruker AXS, Inc., Madison, Wisconsin, **1999**,USA. (b) SHELXTL 5.1, George Sheldrick, Bruker AXS, Inc., Madison, Wisconsin, 1997, USA.

(18) Lim, E.C.; Laposa, J. D.; Yu, J. M. H. *J. Mol. Spectrosc.* **1966**, *19*, 412.

(19) (a) Siemiarczuk, A.; Wagner, B. D.; Ware, W. R. *J. Phys. Chem.* **1990**, *94*, 1661. (b) Siemiarczuk, A.; Ware, W. R. *Chem. Phys. Lett.* **1989**, *160*, 285.

(20) Bensch, W.; Prelati, M.; Ludwig, W. *J. Chem. Soc., Chem. Commun.* **1986**, 1162

(21) Cotton, F.A.; Wilkinson, G.; Gaus, P. *Basic Inorganic Chemistry* Wiley, New York, **1995**, p.61.

(22) Kirss, R.V.; Eisenberg, R. *Inorg. Chem.* **1989**, *28*, 3372.

(23) (a) Manojlovic-Muir, L.J.; Muir, K.W. *J. Chem. Soc., Chem. Commun.* **1982**, 1155. (b) Manojlovic-Muir, L.J.; Muir, K.W,; Grossel, M.C.; Brown, M.P.; Nelson, C.D.; Yavari, A.; Kallas, E.; Moulding, R.P.; Seddon, K.R. *J. Chem. Soc., Dalton Trans.* **1986**, 1955.

(24) Karsch, H.H.; Schubert, *U. Z. Naturforsch.* **1982**, *37b*, 186.

(25) Harvey, P.D.; Drouin, M.; Zhang, T. *Inorg. Chem.* **1997**, *36*, 4998.

(26) (a) Poor quality data were collected for **4**; monoclinic; a = 24.935 (4), b = 10.5070 (15), c= 19.266 (3) Å, β = 111.034(2)°, V = 4711.2(12) $Å^3$, Z = 8, d = 2.061 Mg/m^3, R_1 = 0.22; wR_2 = 0.55. The Cu···Cu distance is found to be 4.011 Å, and two *t*-BuNC ligands are found at the axial positions of the $Cu_2(dppm)_3^{2+}$ unit. The structure exhibits similarities with the complexes $Pt_2(dppm)_3(PPh_3)$[26b] where one Pt atom adopts a tetracoordinated geometry causing an increase in Pt···Pt distance. (b) Ling, S. S. M.; Jobe, I. R.; McLennan, A. J.; Manojlovic-Muir, L.; Muir, K.W.; Puddephatt, R.J. *J. Chem. Soc., Chem. Commun.* **1985**, 566

(27) Lebrun, F.; *M.Sc. Dissertation*, Université de Sherbrooke, **2001**

(28) (a) Although the $[Ag_2(dppm)_2(CN\text{-}t\text{-}Bu)_2](ClO_4)_2$ complex has been investigated from a structural point of view, the photophysical properties are not reported. In this case, the nature of the excited state involved a HOMO and a LUMO that are composed with a certain degree of Ph- components.[25] In the solid state, efficient intermolecular exciton processes occurs through the close Ph···Ph contacts.

(29) Attempts were made to characterize the oligomers further using MALDI-TOF and size-exclusion chromatography. The MALDI-TOF spectra for **5** and **6** were very complex where fragment peaks showed evidence for M-P, P-C and C-N bond cleavages. In both cases, the molecular ion was not observed. The size-exclusion chromatography

was also inadequate as the compounds tended to stay trapped in the column, despite the use of different columns. Both oligomeric materials crystallize to form long needle-shaped crystals, a shape that is common for dmb-containing polymers,[5] but the thickness of these needles was inadequate for X-ray analysis. However, both materials exhibit a good degree of crystallinity as shown in the XRD patterns (Supporting Information).

(30) Leung K.H.; Phillips, D.L.; Mao, Z.; Che, C.-M.; Miskowski, V.M., Chan, C.-M.; *Inorg. Chem.* **2002**, *41*, 2054.

(31) Zhang, H.-X.; Che, C.-M. *Chem. Eur. J.* **2001**, *7*, 4887.

(32) (a) Fu, W.-F.; Chan, K.-C.; Cheung, K.-K.; Che, C.M. *Chem. Eur. J.* **2001**, *7*, 4656. (b) Leung, K.H.; Phillips, D.L.; Tse, M.-C.; Che, C.-M.; Miskowski, V.M. *J. Am. Chem. Soc.* **1999**, *121*, 4799. (c) Fu, W.-Fu; Chan, K.-C.; Miskowski, V.M.; Che, C.-M. *Angew. Chem. Int. Ed.* **1999**, *38*, 2783.

(33) (a) Harvey, P.D.; Gray, H.B. *J. Am. Chem. Soc.* **1988**, *110* , 2145. (b) Harvey, P.D. ; Dallinger, R.F. ; Woodruff, W. H. ; Gray, H.B. *Inorg. Chem.* **1989**, *28* , 3057.

(34) Piché, D. ; Harvey, P.D. *Can. J. Chem.* **1994**, *72* , 705.

(35) (a) Miskowski, V. M.; Smith, T. P.; Loehr, T. M.; Gray, H. B. *J. Am. Chem. Soc.* **1985**, 107, 7925. (b) Levenson, R. A.; Gray, H. B. *J. Am. Chem. Soc.* **1975**, *97*, 6042. (c) Wrighton, M. S.; Ginley, D. S. *J. Am. Chem. Soc.* **1975**, *97*, 4246. (d) Abrahamson, H. B.; Frazier, C. C.; Ginley, D. S.; Gray, H. B.; Lilienthal, J.; Tyler, D. R.; Wrighton M. S. *Inorg. Chem.* **1977**, *16*, 1554. (e) Tyler, D. R.; Levenson, R. A.; Gray, H. B. *J. Am. Chem. Soc.* **1978**, *100*, 7888. (f) Markham, J. *J. Rev. Mod. Phys.* **1959**, *31*, 956. (g) Ballhausen, C. *J. Molecular Electronic Structures of Transition Metal Complexes*; McGraw-Hill: New York, **1979**: pp 132-135. (h) Harvey, P. D.; Murtaza, Z. *Inorg. Chem.* **1993**, *32*, 4721.

(36) This absorptivity is calculated using the molecular weight of the presented repetitive unit, and not the oligomer weight. By doing so, the calculated absorptivity would be three times greater and would not reflect the number of chromophores.

(37) (a) Harvey, P.D.; Schaefer, W.P.; Gray, H.B. *Inorg. Chem.* **1988**, *27*, 1101. (b) Orio, A. A.; Chastain, B.B. ; Gray, H.B. *Inorg. Chim. Acta* **1969**, *3* , 8.

(38) Savas, M.M.; Mason, W.R. *Inorg. Chem.* **1987**, *26*, 301.

(39) Turro, N. J. *Modern Molecular Photochemistry* Benjamen / Cummings Pub. Co., Menlo Park, **1978**, p.235.

(40) Che, C.-M.; Tse, M.-C.; Chan, M. C. W.; Cheung, K.-K.; Phillips, D. L.; Leung, K. H. *J. Am. Chem. Soc.* **2000**, *122*, 2464

(41) See for example Harvey, P. D. *Porphyrin and Phthalocyanine Handbook*, Editors: Kadish, K. M.; Smith, K. M.; Guilard, R., Elsevier **2003**, *18*, 63.

Table 1. Crystal data for **1** and **2**

	$[Cu_2(dmpm)_3](BF_4)_2$	$[Ag_2(dmpm)_3](BF_4)_2$
Empirical formula	$C_{15}H_{42}B_2Cu_2F_8P_6$	$C_{15}H_{42}Ag_2B_2F_8P_6$
Formula weight	709.01	797.67
Temperature (K)	198(1)	198(1)
Wavelength (Å)	0.71073	0.71073
Crystal system	Monoclinic	Orthorhombic
Space group	P2(1)/c	Pbca
a (Å)	16.9960(9)	13.9467(7)
b (Å)	11.0485(5)	14.6460(8)
c (Å)	16.9515(9)	31.6720(17)
β (°)	99.258(1)	90
V ($Å^3$)	3141.7(3)	6469.4(6)
Z	4	8
Density calc. (Mg/m^3)	1.499	1.638
Reflection collected	22019	43787
Independent reflections	7131 [R(int) = 0.0187]	7391
Goodness-of-fit	1.085	1.037
R_1	0.0299	0.0202
R_2	0.0824	0.0499

$R_1 = \Sigma | |F_o| - |F_c| | / \Sigma |F_o|$; $R_2 = (\Sigma[w(F_o^2-F_c^2)^2]/\Sigma[F_o^4])^{1/2}$; Weight = $1 / [\sigma^2(F_o^2) + (0.0463 * P)^2 + (1.7267 * P)]$ where $P = (\max(F_o^2, 0) + 2 * F_c^2)/3$

Table 2. Selected bond distances (Å) and angle (°) for **1** (left) and **2** (right).

Cu(1)-Cu(2)	2.9265(3)	Ag(1)-Ag(2)	2.9893(2)
Cu(1)-P(1)	2.2484(5)	Ag(1)-P(1)	2.4415(5)
Cu(1)-P(3)	2.2519(5)	Ag(1)-P(3)	2.4537(5)
Cu(1)-P(5)	2.2463(5)	Ag(1)-P(5)	2.4774(5)
Cu(2)-P(2)	2.2329(5)	Ag(2)-P(2)	2.4403(5)
Cu(2)-P(4)	2.2392(5)	Ag(2)-P(4)	2.4246(5)
Cu(2)-P(6)	2.2378(5)	Ag(2)-P(6)	2.4378(5)
P(5)-Cu(1)-P(1)	120.12(2)	P(1)-Ag(1)-P(5)	120.298(18)
P(5)-Cu(1)-P(3)	118.11(2)	P(3)-Ag(1)-P(5)	113.530(18)
P(1)-Cu(1)-P(3)	121.67(2)	P(1)-Ag(1)-P(3)	126.122(18)
P(2)-Cu(2)-P(6)	118.74(2)	P(2)-Ag(2)-P(6)	117.882(18)
P(2)-Cu(2)-P(4)	121.19(2)	P(4)-Ag(2)-P(2)	119.69(2)
P(6)-Cu(2)-P(4)	119.53(2)	P(4)-Ag(2)-P(6)	122.16(2)
P(5)-Cu(1)-Cu(2)	92.475(15)	P(5)-Ag(1)-Ag(2)	89.931(13)
P(1)-Cu(1)-Cu(2)	89.760(16)	P(1)-Ag(1)-Ag(2)	92.317(13)
P(3)-Cu(1)-Cu(2)	90.888(15)	P(3)-Ag(1)-Ag(2)	85.399(14)
P(2)-Cu(2)-Cu(1)	93.963(16)	P(2)-Ag(1)-Ag(2)	88.852(13)
P(6)-Cu(2)-Cu(1)	90.983(15)	P(6)-Ag(1)-Ag(2)	91.912(13)
P(4)-Cu(2)-Cu(1)	92.386(15)	P(4)-Ag(1)-Ag(2)	94.312(14)

Table 3. Comparison of selected structural data for d^{10}-d^{10} $M_2(dmpm)_3^{2+}$ and $M'_2(dppm)_3$ dimers

	$d(M_2)$/ Å	$2r_{vdw}$/ Å	$d(MP)_{av}$/ Å	Approx. point group	references
$Cu_2(dmpm)_3^{2+}$	2.9265 (3)	2.80	2.243 (10)	C_s	This work
$Ag_2(dmpm)_3^{2+}$	2.9893 (2)	3.40	2.434 (31)	C_s	This work
$Au_2(dmpm)_3^{2+}$	3.040 (1), 3.050 (1)	3.40	2.358	C_s	20
$Pd_2(dppm)_3$	2.956 (1)	3.20	2.310 (10)	C_3	22
$Pt_2(dppm)_3$	3.022 (3)	3.50	2.265 (3)	C_3	23

Table 4. TGA data for 1, 4, 5 and 6 [a]

	Compounds	Weight loss 1			Weight loss 2			Residue	
		Temp. Range (°C)	Exp. %	(Theor. %)	Temp. Range (°C)	Exp. %	(Theor. %)	Exp. %	(Theor. %)
1	$[Cu_2(dmpm)_3](BF_4)_2$				320-390	86	81	14	19
4	$[Cu_2(dmpm)_3(CN\text{-}t\text{-}Bu)_2](BF_4)_2$	120-190	19	19	320-390	66	66	15	15
5	$\{[Cu_2(dmpm)_3(dmb)_{1.67}](BF_4)_2\}_3$	210-230	27	26	300-390	60	61	13	13
6	$\{[Ag_2(dmpm)_2(dmb)_{1.33}](BF_4)_2\}_3$	180-210	28	29	290-345	46	48	26	23

[a]Weight loss 1 is due to the loss of *t*-BuNC or dmb. Weight loss 2 is due to the loss of dmpm and BF_4. The uncertainties are ± 2% based on the small drift of the baseline

Table 5. Comparison between X-ray data and MMX computations[a]

	X-ray			MMX		
	d(M···M)	d(M-P)	d(M-C)	d(M···M)	d(M-P)	d(M-C)
1	2.9265	2.243	-	2.978	2.267	-
2	2.9893	2.434	-	2.974	2.463	-
$Ag_2(dppm)_2(CN\text{-}t\text{-}Bu)_2^{2+}$	3.223	2.428	2.334	3.216	2.473	2.024

[a] All the distances are in Å

Table 6. Comparison of the $d\sigma^* \rightarrow p\sigma$ absorption data at 298K for various "$M_2(diphos)_3$" complexes

	λ ($\pm$ 1 nm)	$\bar{\nu}$ (cm^{-1})	ε ($M^{-1}cm^{-1}$)	Refs
$[Cu_2(dmpm)_3](BF_4)_2$ / CH_3CN/ 298K	258	38800	8500	This work
$[Ag_2(dmpm)_3](BF_4)_2$ / CH_3CN/ 298K	254	39400	4300	This work
$[Au_2(dmpm)_3](ClO_4)_2$ / H_2O/ 298K	256	39000	18500	30
$Pd_2(dppm)_3$ / 2MeTHF/ 77K	440	22700	33800	33a
$Pt_2(dppm)_3$ / 2MeTHF/ 77K	488	20500	27400	33a

Table 7. Comparison of the emission spectroscopy and photophysical data.

	Compounds	Solid, 298K		Solution, [b] 298K			Solution, [c] 77K	
		λ_{emi} (nm)	τ_{em} (μs)[a]	λ_{emi} (nm)	τ_e (μs)[d]	Φ_e	λ_{emi} (nm)	τ_e (μs)
1	$[Cu_2(dmpm)_3](BF_4)_2$	Not mesured		500	16.5[a]	0.020	505	840
4	$[Cu_2(dmpm)_3(CN\text{-}t\text{-}Bu)_2](BF_4)_2$	476	291	501	3.8	0.0043	502	712
5	$\{[Cu_2(dmpm)_3(dmb)_{1.33}](BF_4)_2\}_3$	482	257	500	< 2[e]	0.0013	474	523
2	$[Ag_2(dmpm)_3](BF_4)_2$	445	41	466	3.0	0.0031	482	6300
6	$\{[Ag_2(dmpm)_2(dmb)_{1.33}](BF_4)_2\}_3$	447	31	520	~ 2[e]	0.0014	500	542

[a] The reported lifetimes are those obtained from a calculation of the lifetime distribution. The lifetime is the one obtained at the maximum of the distribution. [b] In acetonitrile. [c] In butyronitrile. [d] The lifetimes are approximated (since the lifetime distribution analysis could be performed from a curve fitting calculation)[40]. [e] The limit of the instrument is 2 μs, so the accuracy is poor near this limit.

Table 8. Comparison of the fwhm of the population distribution of lifetimes

Entries	Compounds	n. of metals	fwhm (± 10%)
1	$Cu_2(dmpm)_3(CN\text{-}t\text{-}Bu)_2^{2+}$(**4**)	2	13
2	$\{Cu_2(dmpm)_3(dmb)_{1.33}\}_3^{2+}$(**5**)	~6	50
3	$\{Cu(dmb)_2^{+}\}_n$[a]	~45[b]	70
4	$Ag_2(dmpm)_3^{2+}$(**2**)	2	3
5	$\{Ag_2(dmpm)_2(dmb)_{1.33}\}_3^{2+}$(**6**)	~6	7
6	$\{Ag(dmb)_2^{+}\}_n$	~8	25

[a]Highly crystalline material prepared according to method 3 in reference 4a.

[b]Evaluated using the measurements of the intrinsic viscosity.

Figure Captions

1. ORTEP drawing for **1**. The ellipsoids are shown with 30% probability. The H-atoms and BF_4^- ions are not shown for clarity.
2. ORTEP drawing for **2**. The ellipsoids are shown with 30% probability. The H-atoms and BF_4^- ions are not shown for clarity.
3. Solid state FT-IR spectra of **5** (top) and **6** (bottom) in the ν (N≡C) region (—) in comparison with free dmb stressing evidence of non-coordinated -N≡C groups in the oligomers.
4. Comparison of the UV-vis (left) and emission spectra (right) for **1** (top) and **2** (bottom) in acetonitrile at 298K, the broken line is an example of an excitation spectrum, here for **1**.
5. Absorption (left) and emission spectra (right) for **4** in acetonitrile at 298K.
6. Time resolved emission spectra for **5** and **6** in the solid state at room temperature. The measurements have been made in the following time frames: for **5**: 474 nm, 20-70; 478, 500-600; 481, 1000-1300; 484; 2000-2500μs; for **6**: 444 nm, 20-70; 453, 300-400; 472, 500-600; 478, 1000-1300 μs.

Fig. 1

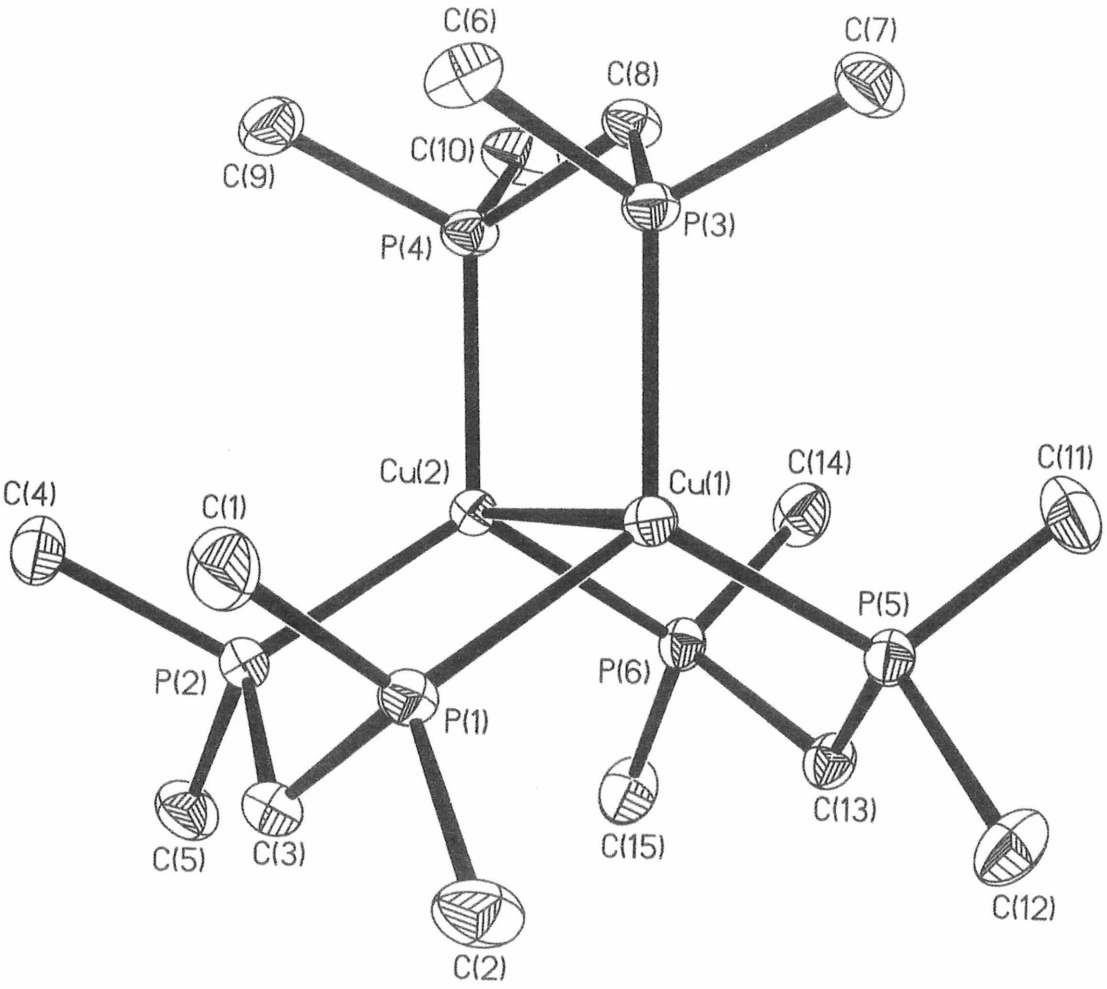
C(6)
C(7)
C(8)
C(10)
C(9)
P(4)
P(3)
Cu(2)
Cu(1)
C(14)
C(11)
C(4)
C(1)
P(5)
P(2)
P(6)
P(1)
C(13)
C(5)
C(3)
C(15)
C(12)
C(2)

Fig. 2

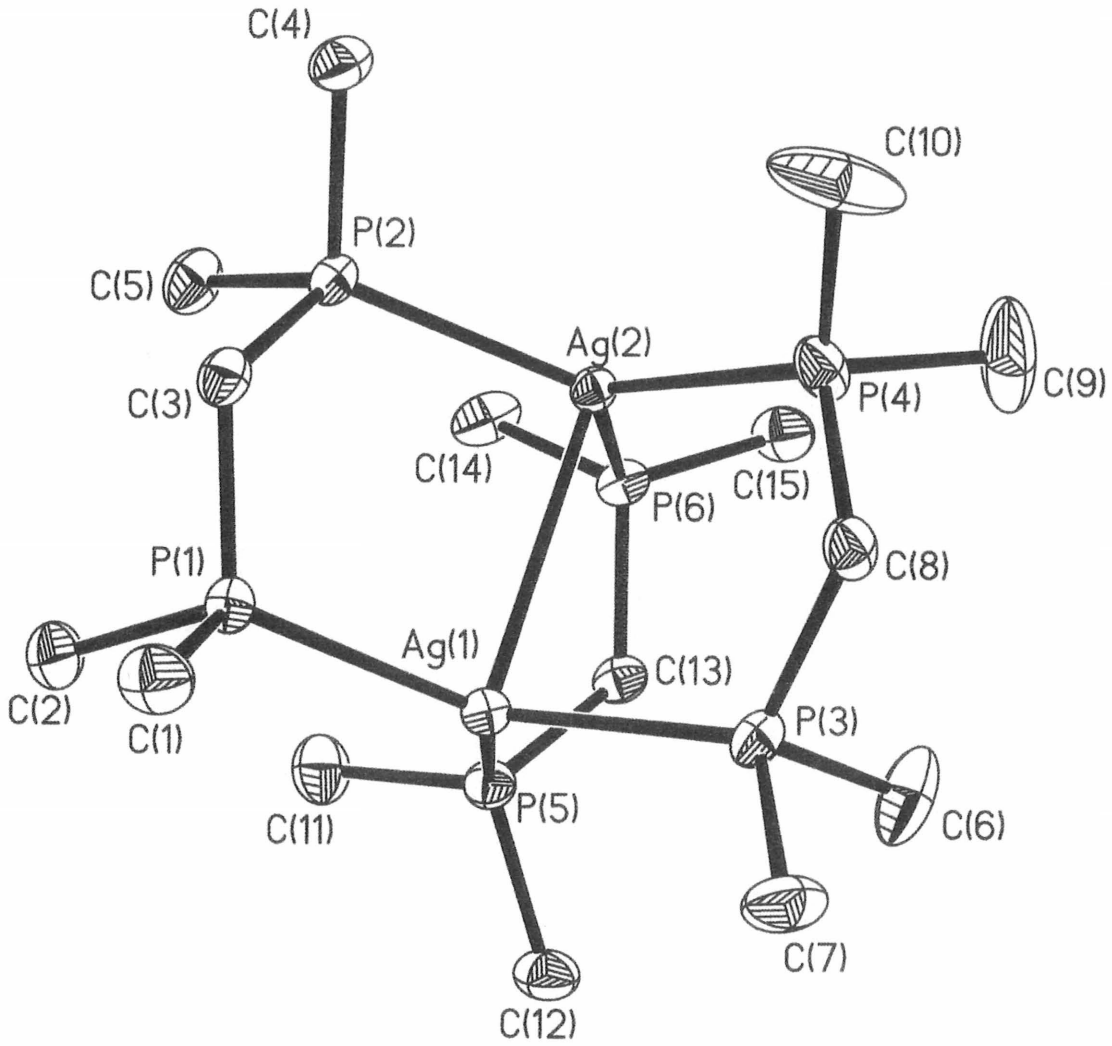
C(4)
C(10)
P(2)
C(5)
Ag(2)
C(3)
P(4)
C(9)
C(14)
C(15)
P(6)
P(1)
C(8)
Ag(1)
C(13)
C(2)
C(1)
P(3)
C(11)
P(5)
C(6)
C(7)
C(12)

Figure 3.

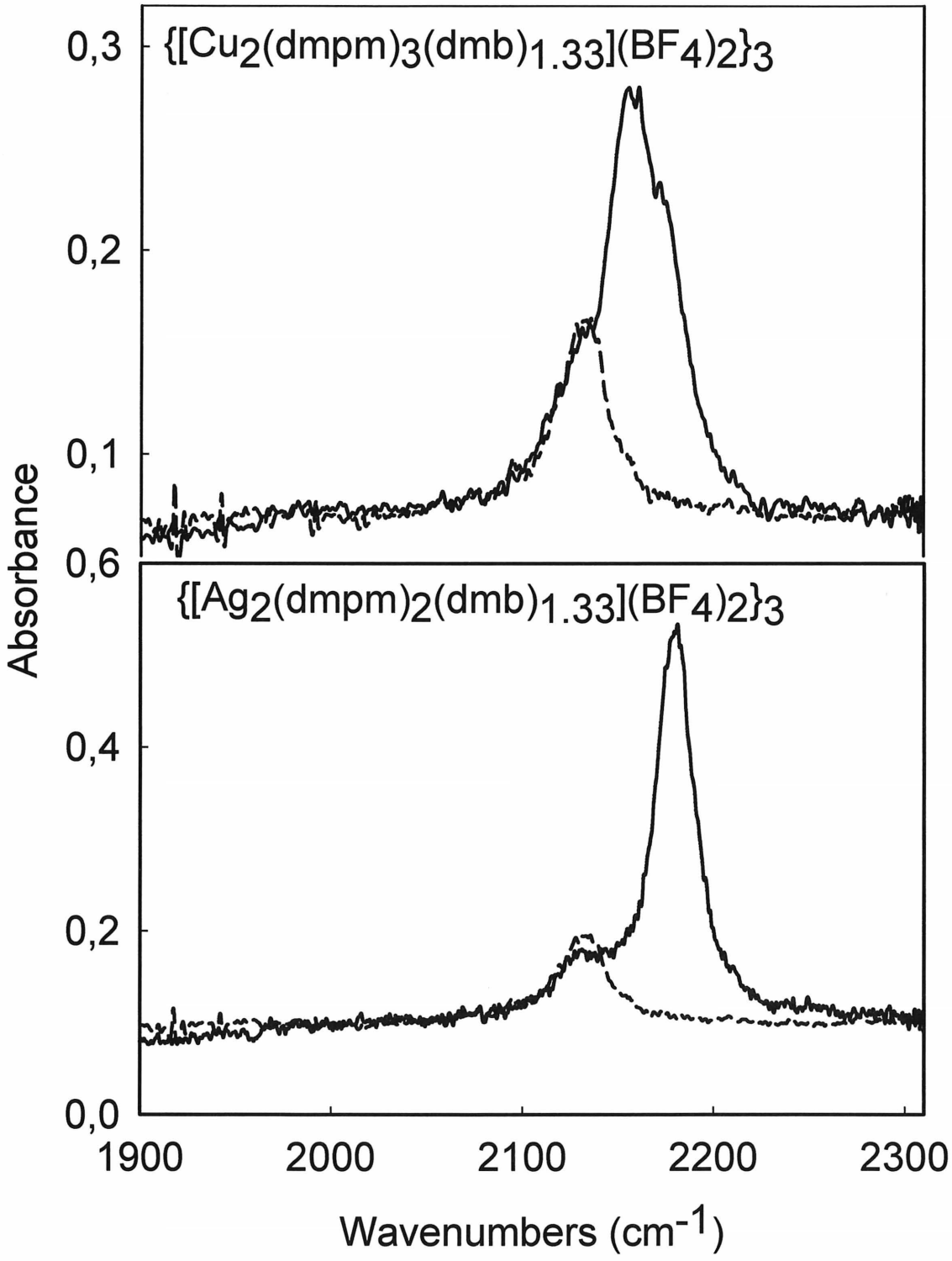
{[Cu2(dmpm)3(dmb)1.33](BF4)2}3
{[Ag2(dmpm)2(dmb)1.33](BF4)2}3
Absorbance
0,3
0,2
0,1
0,6
0,4
0,2
0,0
1900
2000
2100
2200
2300
Wavenumbers (cm-1)

Figure 4

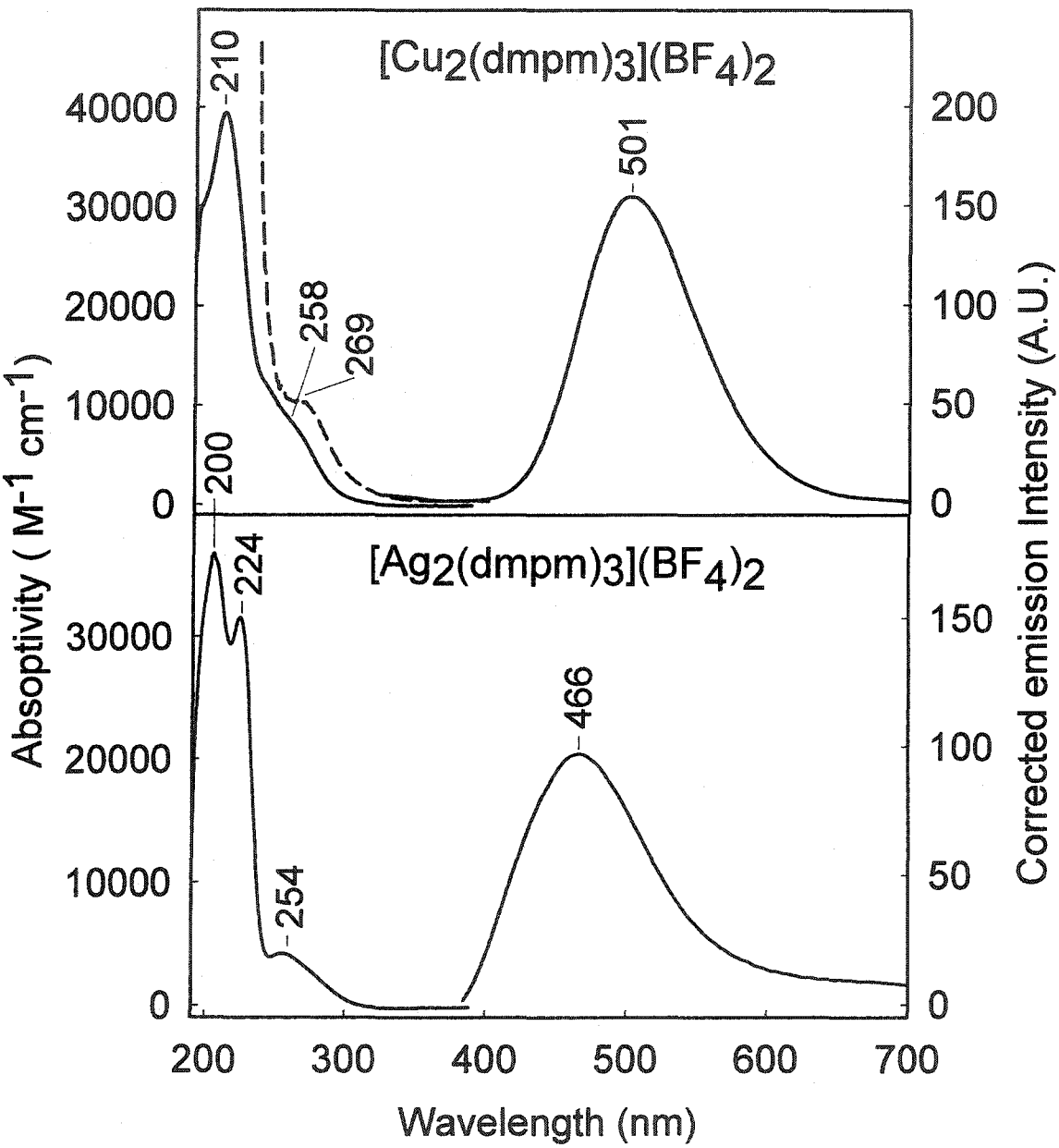
[Cu2(dmpm)3](BF4)2
210
200
258
269
501
[Ag2(dmpm)3](BF4)2
224
254
466
Absoptivity (M-1 cm-1)
Corrected emission Intensity (A.U.)
Wavelength (nm)
0
10000
20000
30000
40000
50
100
150
200
300
400
500
600
700

Figure 5.

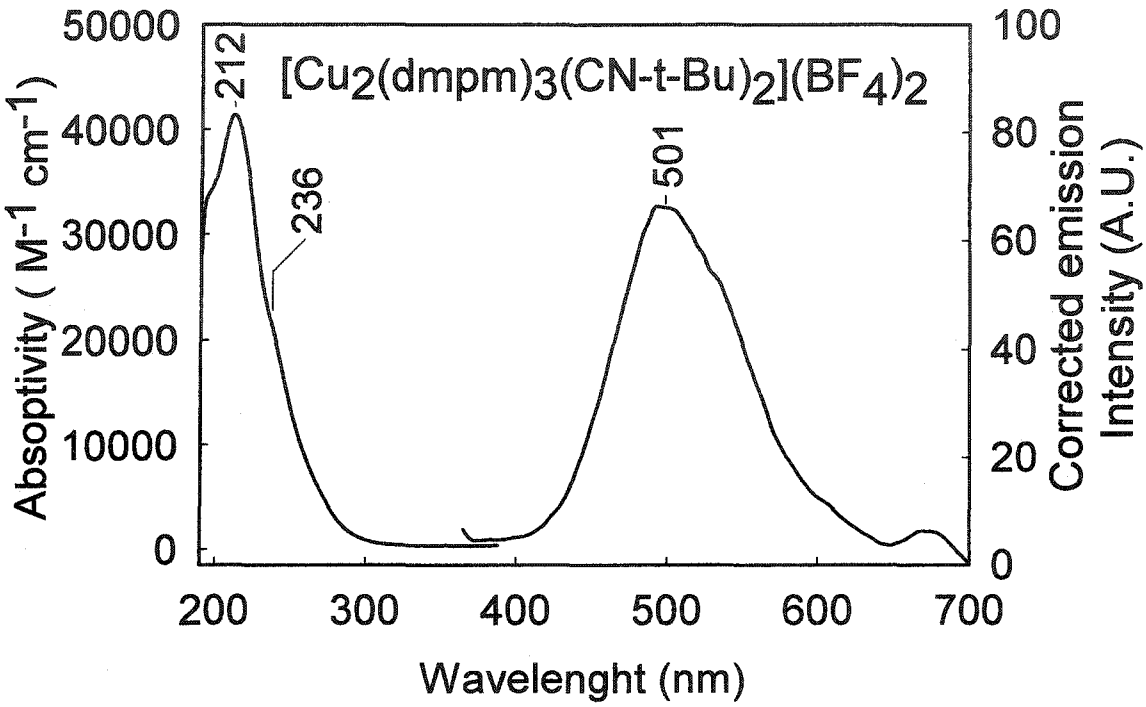
[Cu2(dmpm)3(CN-t-Bu)2](BF4)2
212
236
501
Absoptivity (M-1 cm-1)
Corrected emission Intensity (A.U.)
Wavelenght (nm)
50000
40000
30000
20000
10000
0
100
80
60
40
20
0
200
300
400
500
600
700

Figure 6.

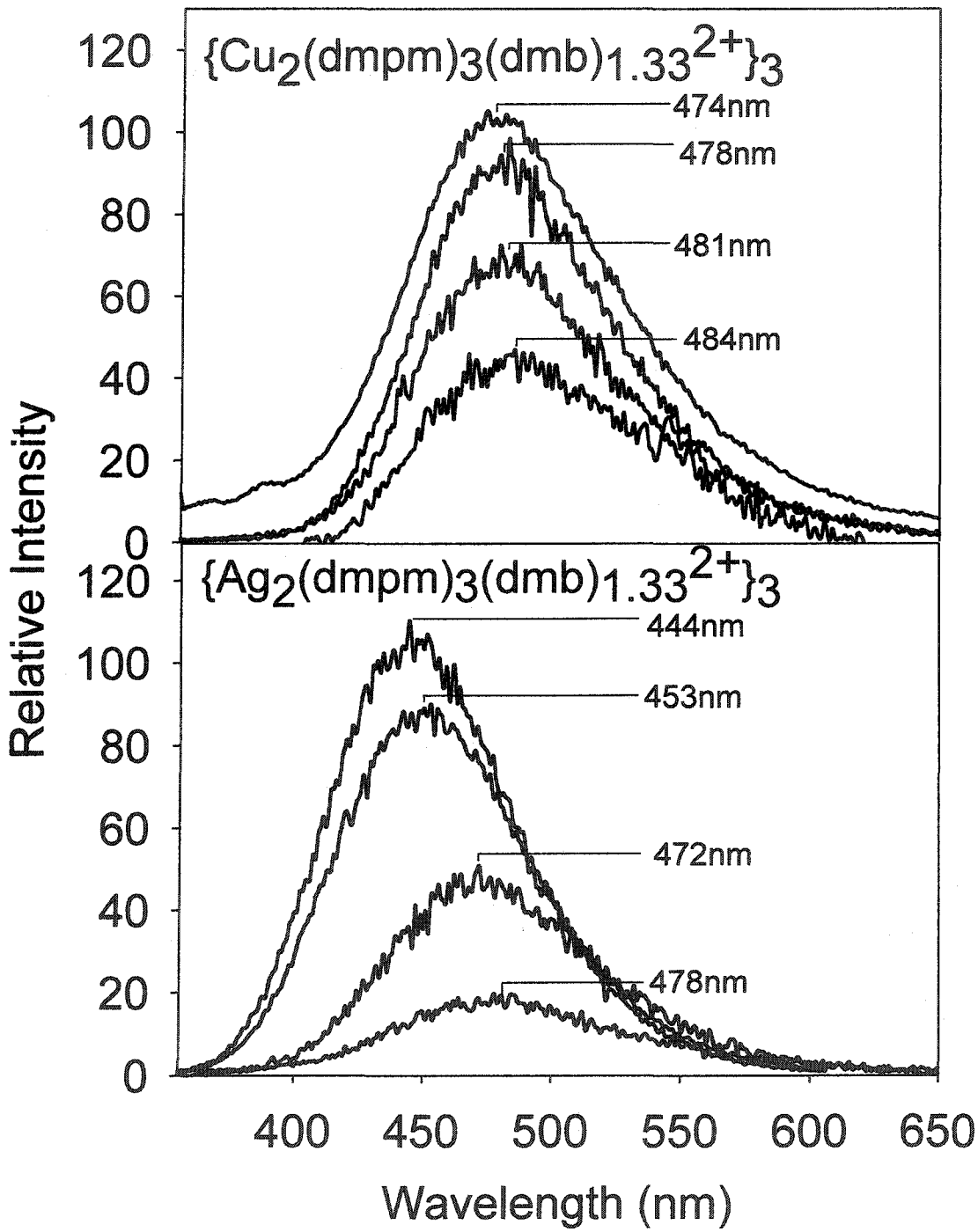
{Cu2(dmpm)3(dmb)1.33 2+}3
474nm
478nm
481nm
484nm
{Ag2(dmpm)3(dmb)1.33 2+}3
444nm
453nm
472nm
478nm
Relative Intensity
Wavelength (nm)
0
20
40
60
80
100
120
400
450
500
550
600
650

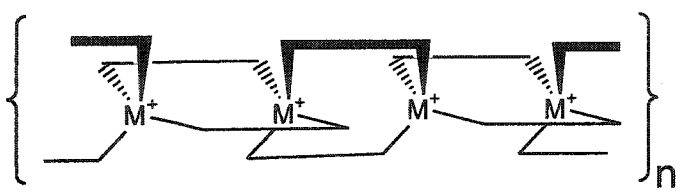

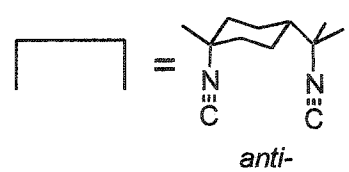

$\{M(dmb)_2^+\}_n$; M = Cu, Ag

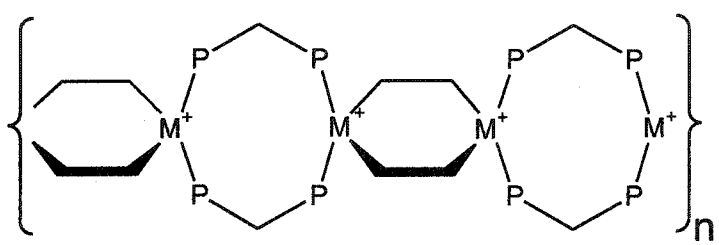

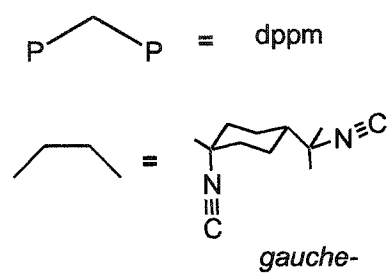

$\{M_2(dppm)_2(dmb)_2^{2+}\}_n$; M = Cu, Ag

Scheme 1

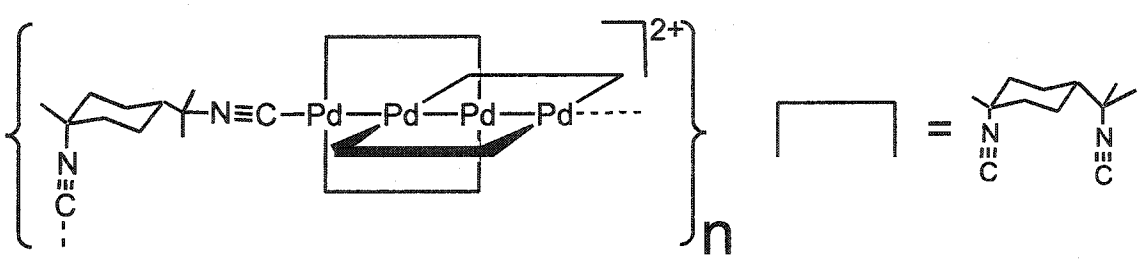

$\{Pd_4(dmb)_4(dmb)^{2+}\}_n$

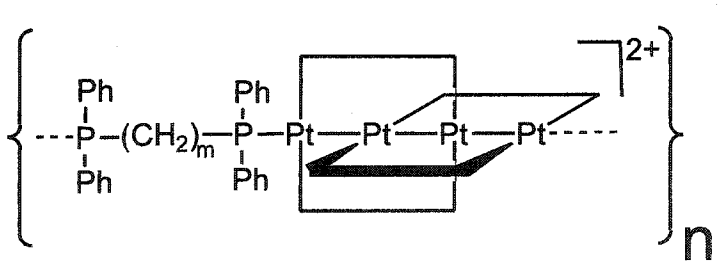

$\{Pt_4(dmb)_4(diphos)^{2+}\}_n$

diphos	
dppb	(m = 4),
dpppen	(m = 5),
dpph	(m = 6)

Scheme 2

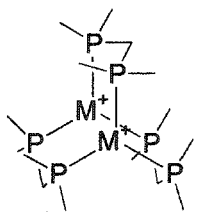

$M_2(dmpm)_3^{2+}$

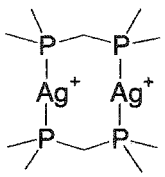

$Ag_2(dmpm)_2^{2+}$

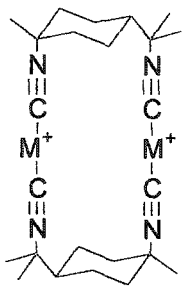

$M_2(dmb)_2^{2+}$

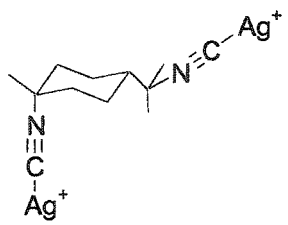

$Ag_2(dmb)^{2+}$

Scheme 3

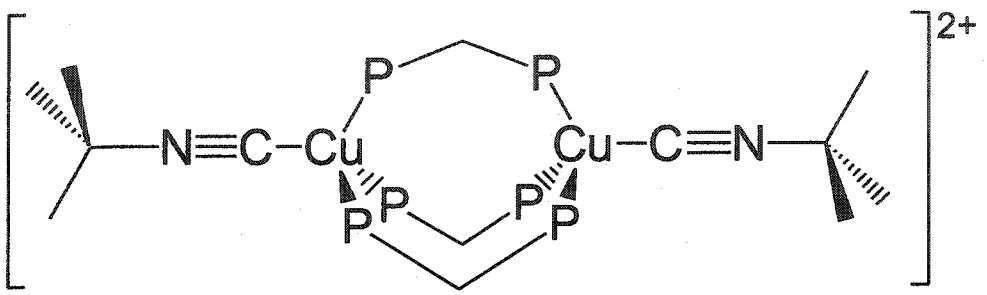

$Cu_2(dmpm)_3(CN\text{-}t\text{-}Bu)_2^{2+}$

Scheme 4

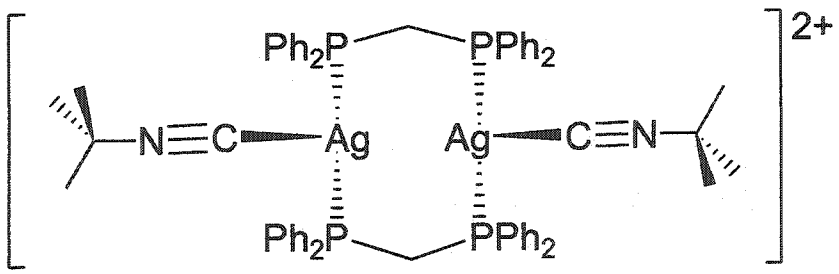

Scheme 5

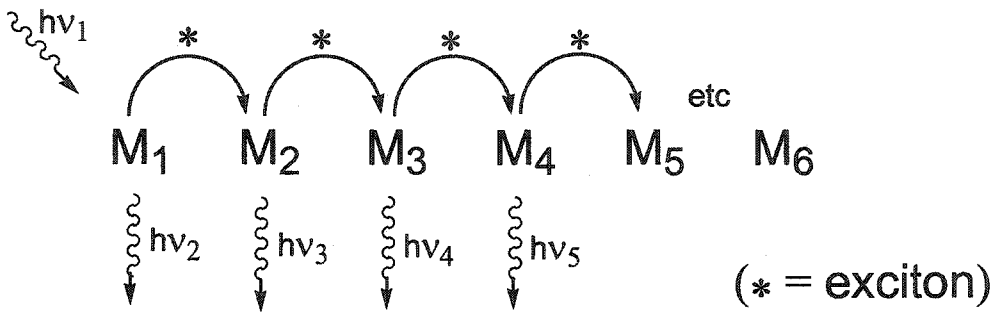

Scheme 6

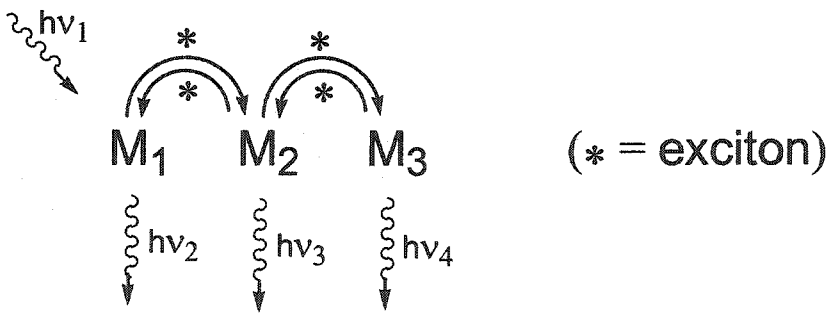

Scheme 7

Preparation and Characterization of Small Mixed-Ligand Oligomers Containing Luminescent $M_2(dmpm)_x$ and $M_2(dmb)_y$ Building Blocks (M = Cu, Ag; x = 2, 3 ; y = 1, 2)

Éric Fournier and Pierre D. Harvey*

Supporting Information

Table of contents

Table 1. Crystal data and structure refinement for $[Cu_2(dmpm)_3](BF_4)_2$

Identification code	PH020872	
Empirical formula	C15 H42 B2 Cu2 F8 P6	
Formula weight	709.01	
Temperature	198(1) K	
Wavelength	0.71073 Å	
Diffractometer used	Bruker AXS P4/SMART 1000	
Detector distance	5 cm	
Monochrometer used	Graphite	
Crystal size	0.125 x 0.325 x 0.35 mm^3	
Colour and habit	Colourless, prism	
Crystal system	Monoclinic	
Space group	P2(1)/c	
Unit cell dimensions	a = 16.9960(9) Å	$\alpha = 90°$
	b = 11.0485(5) Å	$\beta = 99.2580(10)°$
	c = 16.9515(9) Å	$\gamma = 90°$
Volume	3141.7(3) $Å^3$	
Z	4	
Density (calculated)	1.499 Mg/m^3	
Absorption coefficient	1.712 mm^{-1}	
F(000)	1448	
Theta range for data collection	2.21 to 27.50°	
Completeness to theta = 27.50°	98.7 %	
Scan type	ω and ϕ	
Scan range	0.3°	
Exposure time	30s	

Index ranges	$-22 \leq h \leq 21, -12 \leq k \leq 14, -21 \leq l \leq 22$
Standard reflections	50 frames at beginning and end of data
collection	
Crystal stability	no decay
Reflections collected	22019
Independent reflections	7131 [R(int) = 0.0187]
System used	SHELXL 5.1
Solution	Direct methods
Hydrogen atoms	Found, refined isotropically
Absorption correction	SADABS
Min./Max. transmission ratio	0.830
Refinement method	Full-matrix least-squares on F^2
Data / restraints / parameters	7131 / 0 / 466
Goodness-of-fit on F^2	1.085
Final R indices [I>2sigma(I)]	R1 = 0.0299, wR2 = 0.0824
R indices (all data)	R1 = 0.0361, wR2 = 0.0862
Largest/mean shift/esd	0.001/0.000
Largest diff. peak and hole	0.902 and -0.508 e.$Å^{-3}$

$wR2 = (\Sigma[w(F_o^2-F_c^2)^2]/\Sigma[F_o^4])^{1/2}$

$R1 = \Sigma \, | \, |F_o| - |F_c| \, | \, / \Sigma \, |F_o|$

$Weight = 1 / [\sigma^2(F_o^2) + (0.0528 * P)^2 + (0.919 * P)]$

where $P = (\max(F_o^2, 0) + 2 * F_c^2)/3$

Table 2. Atomic coordinates (x 10^4) and equivalent isotropic displacement parameters ($Å^2$x 10^3) for $[Cu_2(dmpm)_3](BF_4)_2$. U(eq) is defined as one third of the trace of the orthogonalized U^{ij} tensor.

	x	y	z	U(eq)
Cu(1)	2176(1)	5930(1)	3170(1)	27(1)
Cu(2)	2831(1)	3907(1)	2368(1)	27(1)
P(1)	1469(1)	4617(1)	3789(1)	32(1)
P(2)	2146(1)	2509(1)	2925(1)	31(1)
P(3)	1672(1)	6762(1)	1983(1)	28(1)
P(4)	2374(1)	4659(1)	1154(1)	31(1)
P(5)	3391(1)	6529(1)	3765(1)	30(1)
P(6)	4067(1)	4365(1)	2965(1)	30(1)
C(1)	415(1)	4524(3)	3387(2)	52(1)
C(2)	1437(2)	4972(3)	4828(2)	50(1)
C(3)	1815(1)	3043(2)	3841(1)	36(1)
C(4)	1265(2)	1853(2)	2334(2)	46(1)
C(5)	2720(2)	1155(2)	3245(2)	46(1)
C(6)	631(1)	6490(2)	1593(1)	41(1)
C(7)	1744(2)	8404(2)	1922(2)	42(1)
C(8)	2190(1)	6291(2)	1171(1)	32(1)
C(9)	1460(2)	4009(2)	623(2)	48(1)
C(10)	3034(2)	4562(3)	416(2)	51(1)
C(11)	3835(2)	7778(2)	3300(2)	52(1)
C(12)	3483(2)	7041(3)	4792(2)	50(1)
C(13)	4144(1)	5341(2)	3843(1)	33(1)
C(14)	4662(2)	5101(3)	2303(2)	47(1)

C(15)	4700(2)	3112(2)	3346(2)	49(1)
B(1)	9016(2)	3377(2)	1071(2)	41(1)
B(2)	3514(2)	3656(3)	6044(2)	50(1)
F(1)	9301(1)	3168(2)	377(1)	82(1)
F(2)	9376(2)	2656(3)	1663(1)	126(1)
F(3)	8230(1)	3144(3)	975(1)	118(1)
F(4)	9120(2)	4527(2)	1293(2)	146(1)
F(5)	4064(1)	2913(2)	6470(1)	91(1)
F(6)	3542(2)	3577(2)	5247(1)	103(1)
F(7)	3645(1)	4835(2)	6299(1)	94(1)
F(8)	2770(1)	3284(2)	6155(1)	83(1)

Table 3. Bond lengths [Å] and angles [°] for $[Cu_2(dmpm)_3](BF_4)_2$.

Cu(1)-P(5)	2.2463(5)	C(2)-P(1)-Cu(1)	114.56(10)
Cu(1)-P(1)	2.2484(5)	C(1)-P(1)-Cu(1)	115.53(10)
Cu(1)-P(3)	2.2519(5)	C(3)-P(1)-Cu(1)	116.32(7)
Cu(1)-Cu(2)	2.9265(3)	C(4)-P(2)-C(5)	101.06(13)
Cu(2)-P(2)	2.2329(5)	C(4)-P(2)-C(3)	104.97(12)
Cu(2)-P(6)	2.2378(5)	C(5)-P(2)-C(3)	103.59(12)
Cu(2)-P(4)	2.2392(5)	C(4)-P(2)-Cu(2)	118.90(9)
P(1)-C(2)	1.814(2)	C(5)-P(2)-Cu(2)	113.78(9)
P(1)-C(1)	1.815(2)	C(3)-P(2)-Cu(2)	112.79(7)
P(1)-C(3)	1.833(2)	C(6)-P(3)-C(7)	102.41(12)
P(2)-C(4)	1.813(2)	C(6)-P(3)-C(8)	103.86(11)
P(2)-C(5)	1.821(2)	C(7)-P(3)-C(8)	101.31(11)
P(2)-C(3)	1.833(2)	C(6)-P(3)-Cu(1)	117.86(8)
P(3)-C(6)	1.811(2)	C(7)-P(3)-Cu(1)	115.94(8)
P(3)-C(7)	1.822(2)	C(8)-P(3)-Cu(1)	113.37(7)
P(3)-C(8)	1.826(2)	C(9)-P(4)-C(10)	102.07(15)
P(4)-C(9)	1.813(3)	C(9)-P(4)-C(8)	105.28(11)
P(4)-C(10)	1.814(2)	C(10)-P(4)-C(8)	101.24(11)
P(4)-C(8)	1.830(2)	C(9)-P(4)-Cu(2)	116.87(9)
P(5)-C(11)	1.813(2)	C(10)-P(4)-Cu(2)	116.77(10)
P(5)-C(12)	1.813(3)	C(8)-P(4)-Cu(2)	112.72(7)
P(5)-C(13)	1.824(2)	C(11)-P(5)-C(12)	101.63(15)
P(6)-C(15)	1.808(2)	C(11)-P(5)-C(13)	104.06(12)
P(6)-C(14)	1.819(2)	C(12)-P(5)-C(13)	101.73(12)
P(6)-C(13)	1.826(2)	C(11)-P(5)-Cu(1)	116.48(10)
B(1)-F(4)	1.329(3)	C(12)-P(5)-Cu(1)	117.07(10)
B(1)-F(3)	1.343(3)	C(13)-P(5)-Cu(1)	113.84(7)

B(1)-F(2)	1.349(3)	C(15)-P(6)-C(14)	101.84(14)
B(1)-F(1)	1.362(3)	C(15)-P(6)-C(13)	101.53(11)
B(2)-F(5)	1.361(3)	C(14)-P(6)-C(13)	105.33(11)
B(2)-F(6)	1.362(4)	C(15)-P(6)-Cu(2)	116.74(9)
B(2)-F(8)	1.370(3)	C(14)-P(6)-Cu(2)	113.42(9)
B(2)-F(7)	1.379(3)	C(13)-P(6)-Cu(2)	116.17(7)
P(5)-Cu(1)-P(1)	120.12(2)	P(2)-C(3)-P(1)	113.84(11)
P(5)-Cu(1)-P(3)	118.11(2)	P(3)-C(8)-P(4)	113.35(10)
P(1)-Cu(1)-P(3)	121.67(2)	P(5)-C(13)-P(6)	114.08(11)
P(5)-Cu(1)-Cu(2)	92.475(15)	F(4)-B(1)-F(3)	107.5(3)
P(1)-Cu(1)-Cu(2)	89.760(16)	F(4)-B(1)-F(2)	109.2(3)
P(3)-Cu(1)-Cu(2)	90.888(15)	F(3)-B(1)-F(2)	107.5(2)
P(2)-Cu(2)-P(6)	118.74(2)	F(4)-B(1)-F(1)	110.9(2)
P(2)-Cu(2)-P(4)	121.19(2)	F(3)-B(1)-F(1)	110.4(2)
P(6)-Cu(2)-P(4)	119.53(2)	F(2)-B(1)-F(1)	111.1(2)
P(2)-Cu(2)-Cu(1)	93.963(16)	F(5)-B(2)-F(6)	110.9(3)
P(6)-Cu(2)-Cu(1)	90.983(15)	F(5)-B(2)-F(8)	108.5(2)
P(4)-Cu(2)-Cu(1)	92.386(15)	F(6)-B(2)-F(8)	107.3(2)
C(2)-P(1)-C(1)	101.27(15)	F(5)-B(2)-F(7)	109.9(2)
C(2)-P(1)-C(3)	102.55(11)	F(6)-B(2)-F(7)	110.0(2)
C(1)-P(1)-C(3)	104.68(12)	F(8)-B(2)-F(7)	110.2(3)

Symmetry transformations used to generate equivalent atoms:

Table 4. Anisotropic displacement parameters ($Å^2 x\ 10^3$) for $[Cu_2(dmpm)_3](BF_4)_2$. The anisotropic displacement factor exponent takes the form: $-2\pi^2[\ h^2\ a^{*2}U^{11} + ... + 2\ h\ k\ a^*\ b^*\ U^{12}\ ]$

	U^{11}	U^{22}	U^{33}	U^{23}	U^{13}	U^{12}
Cu(1)	28(1)	28(1)	24(1)	1(1)	3(1)	0(1)
Cu(2)	28(1)	25(1)	26(1)	0(1)	3(1)	-1(1)
P(1)	32(1)	34(1)	29(1)	4(1)	5(1)	-3(1)
P(2)	34(1)	28(1)	31(1)	3(1)	3(1)	-5(1)
P(3)	32(1)	28(1)	23(1)	1(1)	3(1)	2(1)
P(4)	40(1)	31(1)	23(1)	0(1)	5(1)	4(1)
P(5)	29(1)	27(1)	32(1)	-2(1)	2(1)	0(1)
P(6)	27(1)	28(1)	35(1)	-2(1)	3(1)	1(1)
C(1)	32(1)	56(1)	66(2)	11(1)	2(1)	-6(1)
C(2)	67(2)	53(1)	33(1)	3(1)	18(1)	5(1)
C(3)	43(1)	35(1)	31(1)	6(1)	5(1)	-4(1)
C(4)	44(1)	47(1)	45(1)	-5(1)	4(1)	-15(1)
C(5)	59(2)	32(1)	48(1)	9(1)	8(1)	2(1)
C(6)	34(1)	55(1)	32(1)	-2(1)	3(1)	5(1)
C(7)	59(2)	29(1)	38(1)	3(1)	9(1)	5(1)
C(8)	40(1)	32(1)	25(1)	4(1)	8(1)	3(1)
C(9)	59(2)	41(1)	39(1)	-5(1)	-9(1)	0(1)
C(10)	71(2)	51(1)	34(1)	3(1)	22(1)	17(1)
C(11)	46(1)	36(1)	74(2)	11(1)	9(1)	-7(1)
C(12)	50(2)	54(1)	42(1)	-17(1)	-2(1)	7(1)
C(13)	28(1)	33(1)	36(1)	-2(1)	0(1)	2(1)
C(14)	37(1)	60(1)	44(1)	-6(1)	11(1)	-11(1)

C(15)	41(1)	38(1)	62(2)	-8(1)	-7(1)	12(1)
B(1)	42(1)	47(1)	31(1)	9(1)	-2(1)	-8(1)
B(2)	44(1)	50(1)	51(2)	15(1)	-7(1)	-16(1)
F(1)	88(1)	120(2)	41(1)	10(1)	22(1)	11(1)
F(2)	131(2)	189(3)	65(1)	67(2)	34(1)	93(2)
F(3)	56(1)	212(3)	81(2)	-12(2)	1(1)	-42(2)
F(4)	230(4)	88(2)	138(2)	-43(2)	81(2)	-84(2)
F(5)	86(1)	70(1)	99(2)	15(1)	-38(1)	7(1)
F(6)	133(2)	119(2)	60(1)	24(1)	24(1)	-30(2)
F(7)	94(1)	50(1)	124(2)	10(1)	-26(1)	-21(1)
F(8)	58(1)	75(1)	117(2)	4(1)	22(1)	-18(1)

Table 5. Hydrogen coordinates (x 10^4) and isotropic displacement parameters ($Å^2$x 10 ^{3}) for $[Cu_2(dmpm)_3](BF_4)_2$.

	x	y	z	U(eq)
H(1A)	367(18)	4230(30)	2850(20)	58(8)
H(1B)	140(20)	4030(30)	3710(20)	87(11)
H(1C)	243(18)	5380(30)	3384(19)	69(9)
H(2A)	1970(20)	4950(30)	5140(20)	79(10)
H(2B)	1149(18)	4460(30)	5054(18)	57(8)
H(2C)	1223(19)	5770(30)	4839(19)	65(9)
H(3A)	2224(16)	3030(20)	4201(17)	45(7)
H(3B)	1423(17)	2510(30)	4004(17)	55(8)
H(4A)	1439(19)	1540(30)	1910(20)	69(9)
H(4B)	897(14)	2420(20)	2164(14)	33(6)
H(4C)	1077(18)	1260(30)	2676(19)	64(9)
H(5A)	3181(17)	1390(20)	3675(17)	52(7)
H(5B)	2906(17)	860(30)	2808(19)	56(8)
H(5C)	2455(19)	550(30)	3457(19)	69(9)
H(6A)	518(14)	6750(20)	1118(16)	34(6)
H(6B)	345(15)	6860(20)	1957(16)	49(7)
H(6C)	529(14)	5660(20)	1599(15)	40(6)
H(7A)	2291(19)	8620(30)	2020(18)	60(8)
H(7B)	1530(17)	8760(20)	2310(18)	51(7)
H(7C)	1512(16)	8670(20)	1405(17)	47(7)
H(8A)	2695(14)	6660(20)	1275(14)	36(6)
H(8B)	1942(15)	6530(20)	715(17)	42(6)
H(9A)	1554(17)	3190(30)	567(17)	58(8)
H(9B)	1083(18)	4070(20)	941(19)	52(8)

H(9C)	1303(17)	4380(30)	156(19)	55(8)
H(10A)	3497(17)	4960(30)	605(17)	53(8)
H(10B)	2808(19)	4910(30)	-10(20)	67(9)
H(10C)	3161(18)	3800(30)	332(18)	59(8)
H(11A)	3799(16)	7620(30)	2758(19)	54(8)
H(11B)	4340(20)	7900(30)	3532(18)	63(9)
H(11C)	3548(17)	8480(30)	3384(18)	58(8)
H(12A)	3992(19)	7330(30)	4938(18)	60(8)
H(12B)	3140(20)	7620(30)	4835(19)	70(9)
H(12C)	3361(16)	6460(30)	5119(18)	51(8)
H(13A)	4039(14)	4820(20)	4264(14)	36(6)
H(13B)	4625(16)	5630(20)	3974(15)	42(6)
H(14A)	4698(17)	4490(30)	1883(18)	60(8)
H(14B)	5210(17)	5230(30)	2592(17)	59(8)
H(14C)	4371(19)	5750(30)	2100(19)	63(9)
H(15A)	4496(15)	2750(20)	3797(16)	44(7)
H(15B)	4712(17)	2560(30)	2957(18)	62(9)
H(15C)	5203(18)	3360(20)	3561(17)	51(7)

Table 6. Crystal data and structure refinement for $[Ag_2(dmpm)_3](BF_4)_2$

Identification code	PH021109	
Empirical formula	C15 H42 Ag2 B2 F8 P6	
Formula weight	797.67	
Temperature	198(1) K	
Wavelength	0.71073 Å	
Diffractometer used	Bruker AXS P4/SMART 1000	
Detector distance	5 cm	
Monochrometer used	Graphite	
Crystal size	0.3 x 0.45 x 0.6 mm^3	
Colour and habit	Colourless, parallelepiped	
Crystal system	Orthorhombic	
Space group	Pbca	
Unit cell dimensions	a = 13.9467(7) Å	$\alpha = 90°$
	b = 14.6460(8) Å	$\beta = 90°$
	c = 31.6720(17) Å	$\gamma = 90°$
Volume	6469.4(6) $Å^3$	
Z	8	
Density (calculated)	1.638 Mg/m^3	
Absorption coefficient	1.559 mm^{-1}	
F(000)	3184	
Theta range for data collection	1.29 to 27.50°	
Completeness to theta = 27.50°	99.6 %	
Scan type	ω and ϕ	
Scan range	0.3°	
Exposure time	10s	

Index ranges	$-18 \leq h \leq 18, -18 \leq k \leq 17, -41 \leq l \leq 38$
Standard reflections	50 frames at beginning and end of data
collection	
Crystal stability	no decay
Reflections collected	43787
Independent reflections	7391 [R(int) = 0.0295]
System used	SHELXL 5.1
Solution	Direct methods
Hydrogen atoms	Found, refined isotropically
Absorption correction	SADABS
Min./Max. transmission ratio	0.841
Refinement method	Full-matrix least-squares on F^2
Data / restraints / parameters	7391 / 0 / 466
Goodness-of-fit on F^2	1.037
Final R indices [I>2sigma(I)]	R1 = 0.0202, wR2 = 0.0499
R indices (all data)	R1 = 0.0253, wR2 = 0.0520
Largest/mean shift/esd	0.006/0.000
Largest diff. peak and hole	0.507 and -0.348 e.$Å^{-3}$

$wR2 = (\sum [w(F_o^2 - F_c^2)^2] / \sum [F_o^4])^{1/2}$

$R1 = \sum | |F_o| - |F_c| | / \sum |F_o|$

$Weight = 1 / [\sigma^2(F_o^2) + (0.0239 * P)^2 + (3.3001 * P)]$

where $P = (\max(F_o^2, 0) + 2 * F_c^2)/3$

Table 7. Atomic coordinates (x 10^4) and equivalent isotropic displacement parameters ($Å^2$x 10^3) for $[Ag_2(dmpm)_3](BF_4)_2$. U(eq) is defined as one third of the trace of the orthogonalized U^{ij} tensor.

	x	y	z	U(eq)
Ag(1)	5852(1)	8170(1)	9056(1)	30(1)
Ag(2)	4595(1)	6883(1)	8576(1)	27(1)
P(1)	7280(1)	7682(1)	8672(1)	32(1)
P(2)	5936(1)	6578(1)	8102(1)	31(1)
P(3)	5185(1)	7443(1)	9690(1)	36(1)
P(4)	4316(1)	5888(1)	9176(1)	43(1)
P(5)	4885(1)	9474(1)	8797(1)	35(1)
P(6)	3489(1)	8105(1)	8387(1)	33(1)
C(1)	8336(2)	7404(2)	8979(1)	50(1)
C(2)	7750(2)	8531(2)	8313(1)	51(1)
C(3)	7116(1)	6658(1)	8352(1)	35(1)
C(4)	5920(2)	5419(2)	7898(1)	45(1)
C(5)	6050(2)	7255(2)	7624(1)	47(1)
C(6)	4034(3)	7919(3)	9848(1)	75(1)
C(7)	5906(3)	7529(2)	10166(1)	58(1)
C(8)	4943(2)	6224(2)	9661(1)	39(1)
C(9)	3065(3)	5812(5)	9321(1)	115(2)
C(10)	4644(6)	4701(2)	9119(2)	114(2)
C(11)	5296(2)	10074(2)	8329(1)	58(1)
C(12)	4724(2)	10409(2)	9169(1)	52(1)
C(13)	3639(1)	9173(1)	8680(1)	36(1)
C(14)	3584(2)	8429(2)	7835(1)	51(1)

C(15)	2215(2)	7891(2)	8446(1)	51(1)
B(1)	3227(2)	5468(2)	7850(1)	42(1)
B(2)	7444(2)	9909(2)	9547(1)	48(1)
F(1)	3691(1)	5186(1)	8210(1)	72(1)
F(2)	3238(1)	4793(1)	7554(1)	68(1)
F(3)	2284(1)	5673(1)	7956(1)	66(1)
F(4)	3679(1)	6232(1)	7692(1)	75(1)
F(5)	7274(2)	10061(1)	9126(1)	86(1)
F(6)	6618(1)	9577(2)	9721(1)	101(1)
F(7)	8166(2)	9300(2)	9601(1)	105(1)
F(8)	7673(1)	10695(1)	9749(1)	90(1)

Table 8. Bond lengths [Å] and angles [°] for $[Ag_2(dmpm)_3](BF_4)_2$.

Ag(1)-P(1)	2.4415(5)	C(12)-P(5)-C(13)	101.31(11)
Ag(1)-P(3)	2.4537(5)	C(11)-P(5)-Ag(1)	118.14(10)
Ag(1)-P(5)	2.4774(5)	C(12)-P(5)-Ag(1)	115.62(10)
Ag(1)-Ag(2)	2.9893(2)	C(13)-P(5)-Ag(1)	113.44(7)
Ag(2)-P(4)	2.4246(5)	C(15)-P(6)-C(14)	102.50(14)
Ag(2)-P(6)	2.4378(5)	C(15)-P(6)-C(13)	101.94(11)
Ag(2)-P(2)	2.4403(5)	C(14)-P(6)-C(13)	104.82(12)
P(1)-C(2)	1.809(2)	C(15)-P(6)-Ag(2)	117.90(10)
P(1)-C(1)	1.810(2)	C(14)-P(6)-Ag(2)	112.49(8)
P(1)-C(3)	1.825(2)	C(13)-P(6)-Ag(2)	115.48(7)
P(2)-C(5)	1.815(2)	P(1)-C(1)-H(1A)	110(2)
P(2)-C(4)	1.815(2)	P(1)-C(1)-H(1B)	106.7(19)
P(2)-C(3)	1.831(2)	H(1A)-C(1)-H(1B)	108(3)
P(3)-C(7)	1.817(3)	P(1)-C(1)-H(1C)	108.8(18)
P(3)-C(8)	1.820(2)	H(1A)-C(1)-H(1C)	113(3)
P(3)-C(6)	1.820(3)	H(1B)-C(1)-H(1C)	109(3)
P(4)-C(10)	1.807(5)	P(1)-C(2)-H(2A)	107.2(16)
P(4)-C(9)	1.808(4)	P(1)-C(2)-H(2B)	110.8(18)
P(4)-C(8)	1.835(2)	H(2A)-C(2)-H(2B)	111(2)
P(5)-C(11)	1.817(3)	P(1)-C(2)-H(2C)	109.2(18)
P(5)-C(12)	1.819(2)	H(2A)-C(2)-H(2C)	113(2)
P(5)-C(13)	1.832(2)	H(2B)-C(2)-H(2C)	105(2)
P(6)-C(15)	1.814(2)	P(1)-C(3)-P(2)	113.98(10)
P(6)-C(14)	1.815(2)	P(1)-C(3)-H(3A)	107.8(13)
P(6)-C(13)	1.830(2)	P(2)-C(3)-H(3A)	106.3(13)

C(1)-H(1A)	0.85(3)	P(1)-C(3)-H(3B)	113.3(14)
C(1)-H(1B)	0.94(3)	P(2)-C(3)-H(3B)	108.4(13)
C(1)-H(1C)	0.94(3)	H(3A)-C(3)-H(3B)	106.6(18)
C(2)-H(2A)	0.98(3)	P(2)-C(4)-H(4A)	112.5(15)
C(2)-H(2B)	0.93(3)	P(2)-C(4)-H(4B)	108.1(18)
C(2)-H(2C)	0.90(3)	H(4A)-C(4)-H(4B)	112(2)
C(3)-H(3A)	0.93(2)	P(2)-C(4)-H(4C)	105.9(18)
C(3)-H(3B)	0.93(2)	H(4A)-C(4)-H(4C)	108(2)
C(4)-H(4A)	0.96(3)	H(4B)-C(4)-H(4C)	110(2)
C(4)-H(4B)	0.91(3)	P(2)-C(5)-H(5A)	108.3(17)
C(4)-H(4C)	0.98(3)	P(2)-C(5)-H(5B)	113.1(16)
C(5)-H(5A)	0.90(3)	H(5A)-C(5)-H(5B)	107(2)
C(5)-H(5B)	0.97(3)	P(2)-C(5)-H(5C)	107.9(18)
C(5)-H(5C)	0.92(3)	H(5A)-C(5)-H(5C)	115(2)
C(6)-H(6A)	0.97(3)	H(5B)-C(5)-H(5C)	106(2)
C(6)-H(6B)	0.90(3)	P(3)-C(6)-H(6A)	110(2)
C(6)-H(6C)	1.01(4)	P(3)-C(6)-H(6B)	102(2)
C(7)-H(7A)	0.89(3)	H(6A)-C(6)-H(6B)	111(3)
C(7)-H(7B)	0.96(3)	P(3)-C(6)-H(6C)	108(2)
C(7)-H(7C)	0.99(3)	H(6A)-C(6)-H(6C)	112(3)
C(8)-H(8A)	0.93(2)	H(6B)-C(6)-H(6C)	113(3)
C(8)-H(8B)	0.90(3)	P(3)-C(7)-H(7A)	107.5(18)
C(9)-H(9B)	1.01(3)	P(3)-C(7)-H(7B)	108.1(19)
C(9)-H(9C)	0.91(4)	H(7A)-C(7)-H(7B)	112(3)
C(9)-H(9A)	0.86(4)	P(3)-C(7)-H(7C)	110.7(17)
C(10)-H(10A)	0.92(4)	H(7A)-C(7)-H(7C)	109(3)
C(10)-H(10B)	0.73(4)	H(7B)-C(7)-H(7C)	109(3)
C(10)-H(10C)	0.88(4)	P(3)-C(8)-P(4)	113.14(11)
C(11)-H(11A)	0.96(3)	P(3)-C(8)-H(8A)	106.4(14)

C(11)-H(11B)	0.93(3)	P(4)-C(8)-H(8A)	106.7(14)
C(11)-H(11C)	0.92(3)	P(3)-C(8)-H(8B)	111.0(17)
C(12)-H(12A)	0.90(3)	P(4)-C(8)-H(8B)	111.5(17)
C(12)-H(12B)	0.96(3)	H(8A)-C(8)-H(8B)	108(2)
C(12)-H(12C)	0.97(3)	P(4)-C(9)-H(9B)	104.9(19)
C(13)-H(13A)	0.91(2)	P(4)-C(9)-H(9C)	104(3)
C(13)-H(13B)	0.94(3)	H(9B)-C(9)-H(9C)	113(3)
C(14)-H(14A)	1.05(3)	P(4)-C(9)-H(9A)	105(3)
C(14)-H(14B)	0.92(3)	H(9B)-C(9)-H(9A)	115(4)
C(14)-H(14C)	0.95(3)	H(9C)-C(9)-H(9A)	113(4)
C(15)-H(15A)	0.98(3)	P(4)-C(10)-H(10A)	109(2)
C(15)-H(15B)	0.96(3)	P(4)-C(10)-H(10B)	108(4)
C(15)-H(15C)	0.91(3)	H(10A)-C(10)-H(10B)	115(5)
B(1)-F(2)	1.363(3)	P(4)-C(10)-H(10C)	111(3)
B(1)-F(1)	1.377(3)	H(10A)-C(10)-H(10C)	108(3)
B(1)-F(4)	1.377(3)	H(10B)-C(10)-H(10C)	106(4)
B(1)-F(3)	1.391(3)	P(5)-C(11)-H(11A)	105.2(19)
B(2)-F(8)	1.355(3)	P(5)-C(11)-H(11B)	109.0(18)
B(2)-F(7)	1.356(3)	H(11A)-C(11)-H(11B)	108(3)
B(2)-F(6)	1.367(3)	P(5)-C(11)-H(11C)	109.2(17)
B(2)-F(5)	1.372(3)	H(11A)-C(11)-H(11C)	113(3)
P(1)-Ag(1)-P(3)	126.122(18)	H(11B)-C(11)-H(11C)	112(3)
P(1)-Ag(1)-P(5)	120.298(18)	P(5)-C(12)-H(12A)	108(2)
P(3)-Ag(1)-P(5)	113.530(18)	P(5)-C(12)-H(12B)	110.5(17)
P(1)-Ag(1)-Ag(2)	92.317(13)	H(12A)-C(12)-H(12B)	111(3)
P(3)-Ag(1)-Ag(2)	85.399(14)	P(5)-C(12)-H(12C)	108.4(17)
P(5)-Ag(1)-Ag(2)	89.931(13)	H(12A)-C(12)-H(12C)	112(3)
P(4)-Ag(2)-P(6)	122.16(2)	H(12B)-C(12)-H(12C)	106(2)
P(4)-Ag(2)-P(2)	119.69(2)	P(6)-C(13)-P(5)	114.68(10)

P(6)-Ag(2)-P(2)	117.880(18)	P(6)-C(13)-H(13A)	104.4(15)
P(4)-Ag(2)-Ag(1)	94.312(14)	P(5)-C(13)-H(13A)	106.8(15)
P(6)-Ag(2)-Ag(1)	91.912(13)	P(6)-C(13)-H(13B)	109.1(15)
P(2)-Ag(2)-Ag(1)	88.852(13)	P(5)-C(13)-H(13B)	111.0(15)
C(2)-P(1)-C(1)	101.40(14)	H(13A)-C(13)-H(13B)	111(2)
C(2)-P(1)-C(3)	105.07(11)	P(6)-C(14)-H(14A)	108.3(17)
C(1)-P(1)-C(3)	102.43(11)	P(6)-C(14)-H(14B)	108.7(18)
C(2)-P(1)-Ag(1)	114.09(10)	H(14A)-C(14)-H(14B)	111(2)
C(1)-P(1)-Ag(1)	117.56(10)	P(6)-C(14)-H(14C)	109.7(16)
C(3)-P(1)-Ag(1)	114.52(7)	H(14A)-C(14)-H(14C)	109(2)
C(5)-P(2)-C(4)	102.43(13)	H(14B)-C(14)-H(14C)	110(2)
C(5)-P(2)-C(3)	104.25(12)	P(6)-C(15)-H(15A)	111.4(16)
C(4)-P(2)-C(3)	103.04(10)	P(6)-C(15)-H(15B)	109.3(15)
C(5)-P(2)-Ag(2)	118.70(9)	H(15A)-C(15)-H(15B)	110(2)
C(4)-P(2)-Ag(2)	112.41(8)	P(6)-C(15)-H(15C)	110.1(15)
C(3)-P(2)-Ag(2)	114.22(7)	H(15A)-C(15)-H(15C)	113(2)
C(7)-P(3)-C(8)	102.22(12)	H(15B)-C(15)-H(15C)	103(2)
C(7)-P(3)-C(6)	103.51(18)	F(2)-B(1)-F(1)	110.4(2)
C(8)-P(3)-C(6)	103.07(17)	F(2)-B(1)-F(4)	109.6(2)
C(7)-P(3)-Ag(1)	116.01(11)	F(1)-B(1)-F(4)	109.22(18)
C(8)-P(3)-Ag(1)	117.08(7)	F(2)-B(1)-F(3)	109.50(18)
C(6)-P(3)-Ag(1)	113.14(11)	F(1)-B(1)-F(3)	108.0(2)
C(10)-P(4)-C(9)	102.2(4)	F(4)-B(1)-F(3)	110.2(2)
C(10)-P(4)-C(8)	102.72(15)	F(8)-B(2)-F(7)	108.9(2)
C(9)-P(4)-C(8)	105.27(15)	F(8)-B(2)-F(6)	108.1(2)
C(10)-P(4)-Ag(2)	117.3(2)	F(7)-B(2)-F(6)	110.0(2)
C(9)-P(4)-Ag(2)	113.07(19)	F(8)-B(2)-F(5)	111.3(2)
C(8)-P(4)-Ag(2)	114.69(7)	F(7)-B(2)-F(5)	110.9(2)
C(11)-P(5)-C(12)	101.77(15)	F(6)-B(2)-F(5)	107.7(2)

C(11)-P(5)-C(13)	104.46(13)

Symmetry transformations used to generate equivalent atoms:

Table 9. Anisotropic displacement parameters ($Å^2 x\ 10^3$) for $[Ag_2(dmpm)_3](BF_4)_2$. The anisotropic displacement factor exponent takes the form: $-2\pi^2[\ h^2\ a^{*2}U^{11} + ...\ + 2\ h\ k\ a^*\ b^*\ U^{12}\ ]$

	U^{11}	U^{22}	U^{33}	U^{23}	U^{13}	U^{12}
Ag(1)	31(1)	31(1)	30(1)	-3(1)	1(1)	-2(1)
Ag(2)	29(1)	27(1)	24(1)	0(1)	-1(1)	1(1)
P(1)	31(1)	34(1)	31(1)	2(1)	4(1)	1(1)
P(2)	34(1)	32(1)	26(1)	-1(1)	4(1)	5(1)
P(3)	42(1)	40(1)	25(1)	0(1)	4(1)	4(1)
P(4)	50(1)	51(1)	29(1)	12(1)	-9(1)	-21(1)
P(5)	37(1)	30(1)	38(1)	-1(1)	1(1)	3(1)
P(6)	35(1)	33(1)	31(1)	-2(1)	-5(1)	8(1)
C(1)	43(1)	53(2)	55(2)	-4(1)	-9(1)	4(1)
C(2)	58(2)	48(1)	47(1)	6(1)	14(1)	-10(1)
C(3)	33(1)	36(1)	36(1)	0(1)	5(1)	7(1)
C(4)	46(1)	40(1)	49(1)	-11(1)	5(1)	5(1)
C(5)	57(1)	52(1)	33(1)	7(1)	6(1)	8(1)
C(6)	72(2)	93(3)	60(2)	17(2)	33(2)	35(2)
C(7)	89(2)	49(1)	36(1)	-7(1)	-15(1)	-7(1)
C(8)	42(1)	49(1)	27(1)	8(1)	-3(1)	-11(1)
C(9)	67(2)	230(7)	49(2)	15(3)	-4(2)	-82(3)
C(10)	228(7)	37(2)	77(3)	14(2)	-88(4)	-29(3)
C(11)	59(2)	56(2)	58(2)	15(1)	6(1)	0(1)
C(12)	52(1)	40(1)	63(2)	-15(1)	-3(1)	2(1)
C(13)	36(1)	36(1)	38(1)	-5(1)	-3(1)	9(1)
C(14)	75(2)	44(1)	33(1)	2(1)	-10(1)	21(1)

C(15)	36(1)	56(2)	61(2)	-11(1)	-8(1)	4(1)
B(1)	47(1)	39(1)	40(1)	1(1)	-10(1)	-10(1)
B(2)	51(1)	45(1)	48(2)	0(1)	-13(1)	-4(1)
F(1)	74(1)	86(1)	57(1)	16(1)	-27(1)	-7(1)
F(2)	74(1)	70(1)	61(1)	-26(1)	11(1)	-24(1)
F(3)	57(1)	68(1)	71(1)	3(1)	-1(1)	7(1)
F(4)	82(1)	49(1)	93(1)	20(1)	-9(1)	-26(1)
F(5)	111(2)	92(1)	55(1)	16(1)	-11(1)	-3(1)
F(6)	84(1)	128(2)	91(1)	31(1)	-9(1)	-45(1)
F(7)	117(2)	104(2)	94(1)	-18(1)	-29(1)	61(1)
F(8)	86(1)	69(1)	116(2)	-38(1)	-6(1)	-13(1)

Table 10. Hydrogen coordinates (x 10^4) and isotropic displacement parameters ($Å^2$x 10^3) for$[Ag_2(dmpm)_3](BF_4)_2$.

	x	y	z	U(eq)
H(1A)	8210(20)	6980(20)	9155(10)	74(10)
H(1B)	8500(20)	7930(20)	9131(10)	74(9)
H(1C)	8840(20)	7257(19)	8793(9)	63(8)
H(2A)	7917(19)	9070(20)	8482(9)	63(8)
H(2B)	8280(20)	8307(19)	8169(9)	69(9)
H(2C)	7310(19)	8647(18)	8111(9)	59(8)
H(3A)	7168(15)	6153(16)	8530(7)	37(6)
H(3B)	7583(16)	6589(15)	8144(7)	37(5)
H(4A)	5824(17)	4973(18)	8115(9)	54(7)
H(4B)	6470(20)	5326(19)	7753(9)	68(8)
H(4C)	5370(20)	5390(20)	7706(10)	80(10)
H(5A)	6590(20)	7086(18)	7492(8)	59(8)
H(5B)	6107(19)	7900(20)	7680(8)	59(7)
H(5C)	5500(20)	7182(19)	7469(9)	63(8)
H(6A)	3770(20)	7570(20)	10080(11)	87(10)
H(6B)	4200(20)	8480(20)	9930(10)	76(11)
H(6C)	3590(30)	7910(20)	9594(12)	94(12)
H(7A)	6440(20)	7200(20)	10125(9)	63(9)
H(7B)	6050(20)	8160(20)	10212(10)	75(9)
H(7C)	5550(20)	7290(20)	10413(10)	67(8)
H(8A)	5539(17)	5935(16)	9655(7)	43(6)
H(8B)	4631(19)	6031(18)	9891(9)	62(8)
H(9B)	2900(20)	6440(20)	9431(10)	70(11)

H(9C)	3050(30)	5370(30)	9524(13)	109(14)
H(9A)	2770(30)	5650(30)	9095(13)	109(13)
H(10A)	4340(20)	4470(20)	8883(11)	85(10)
H(10B)	5170(30)	4670(30)	9116(16)	104(19)
H(10C)	4460(30)	4380(30)	9340(13)	110(13)
H(11A)	5890(20)	10360(20)	8410(10)	76(9)
H(11B)	4860(20)	10530(20)	8262(9)	69(9)
H(11C)	5371(19)	9661(19)	8111(9)	61(8)
H(12A)	4420(20)	10190(20)	9399(10)	75(10)
H(12B)	5330(20)	10674(19)	9242(9)	69(8)
H(12C)	4360(20)	10890(20)	9031(9)	67(8)
H(13A)	3347(17)	9067(16)	8931(8)	44(6)
H(13B)	3330(18)	9645(17)	8533(8)	51(7)
H(14A)	4280(20)	8670(20)	7780(10)	80(9)
H(14B)	3140(20)	8880(20)	7780(9)	73(9)
H(14C)	3466(19)	7911(19)	7661(9)	59(8)
H(15A)	1834(19)	8388(19)	8328(9)	62(8)
H(15B)	2054(18)	7323(19)	8311(8)	56(7)
H(15C)	2073(17)	7778(16)	8722(8)	45(7)

Table 11. Crystal data and structure refinement for $[Ag_2(dppm)_2(CN\text{-}t\text{-}Bu)_2](ClO_4)_2$.

Identification code	shelx	
Empirical formula	C70 H80 Ag2 Cl2 N4 O8 P2	
Formula weight	1453.96	
Temperature	293(2) K	
Wavelength	0.70930 Å	
Crystal system	Monoclinic	
Space group	P $2_1/n$	
Unit cell dimensions	a = 21.650(1) Å	α= 90°.
	b = 13.315(1) Å	β= 115.96(2)°.
	c = 23.352(2) Å	γ = 90°.
Volume	6052.4 $Å^3$	
Z	4	
Density (calculated)	1.596 Mg/m^3	
Absorption coefficient	0.852 mm^{-1}	
F(000)	3000	
Crystal size	.2 x .2 x .2 mm^3	
Theta range for data collection	1.71 to 24.94°.	
Index ranges	-25<=h<=23, 0<=k<=15, 0<=l<=27	
Reflections collected	10585	
Independent reflections	10585 [R(int) = 0.0000]	
Completeness to theta = 24.94°	99.4 %	
Refinement method	Full-matrix least-squares on F^2	
Data / restraints / parameters	10585 / 50 / 617	
Goodness-of-fit on F^2	0.903	
Final R indices [I>2sigma(I)]	R1 = 0.0918, wR2 = 0.1989	

R indices (all data)	R1 = 0.2167, wR2 = 0.2478
Largest diff. peak and hole	0.808 and -0.850 e.Å^{-3}

Table 12. Atomic coordinates (x 10^4) and equivalent isotropic displacement parameters ($Å^2$x 10^3) for $[Ag_2(dppm)_2(CN\text{-}t\text{-}Bu)_2](ClO_4)_2$. U(eq) is defined as one third of the trace of the orthogonalized U^{ij} tensor.

	x	y	z	U(eq)
C(1)	3682(6)	4485(10)	702(6)	60(3)
C(2)	3738(9)	5358(12)	1022(8)	93(5)
C(3)	4134(9)	5460(14)	1663(10)	104(6)
C(4)	4477(9)	4649(16)	2020(8)	97(5)
C(5)	4473(8)	3773(14)	1715(8)	95(5)
C(6)	4071(8)	3670(10)	1079(7)	74(4)
C(13)	2351(5)	4941(8)	-367(5)	46(3)
C(14)	1939(6)	4415(9)	615(6)	60(3)
C(15)	1880(6)	3646(10)	960(6)	63(4)
C(16)	2022(7)	3710(12)	1594(7)	77(4)
C(17)	2226(8)	4623(14)	1893(7)	79(4)
C(18)	2307(8)	5401(13)	1567(8)	93(5)
C(19)	2159(7)	5316(9)	929(6)	62(4)
C(20)	934(6)	4973(8)	-664(6)	47(3)
C(21)	672(6)	5013(10)	-1320(6)	62(4)
C(22)	73(8)	5516(11)	-1676(7)	80(4)
C(23)	-263(6)	6012(11)	-1366(9)	80(5)
C(24)	-18(8)	5949(11)	-726(8)	82(4)
C(25)	577(7)	5441(10)	-371(6)	64(4)
C(32)	1534(6)	-290(9)	-391(6)	49(3)
C(33)	1618(7)	-1211(10)	-94(6)	68(4)
C(34)	1395(10)	-2078(12)	-405(13)	107(7)

C(35)	1073(9)	-2030(15)	-1078(12)	104(7)
C(36)	1012(9)	-1164(16)	-1384(9)	110(7)
C(37)	1228(7)	-283(10)	-1037(7)	73(4)
C(26)	1436(6)	851(9)	603(6)	51(3)
C(27)	1808(6)	829(12)	1243(6)	74(4)
C(28)	1475(9)	951(13)	1642(7)	98(5)
C(29)	795(8)	1079(12)	1378(8)	87(5)
C(30)	425(7)	1078(14)	722(8)	95(5)
C(31)	752(6)	1013(12)	335(6)	73(4)
C(38)	2751(5)	662(8)	532(5)	48(3)
C(45)	4124(6)	790(8)	672(6)	50(3)
C(46)	4347(6)	746(12)	1321(5)	69(4)
C(47)	5031(7)	830(12)	1712(6)	79(4)
C(48)	5528(6)	865(12)	1506(8)	88(5)
C(49)	5309(7)	889(14)	859(7)	89(5)
C(50)	4644(6)	854(11)	451(6)	68(4)
C(39)	3097(6)	-219(8)	-432(6)	47(3)
C(40)	3234(7)	-1179(9)	-150(7)	70(4)
C(41)	3102(9)	-1966(11)	-611(12)	103(6)
C(43)	2900(10)	-1779(17)	-1234(11)	108(7)
C(42)	2762(8)	-890(15)	-1478(7)	86(5)
C(44)	2860(6)	-83(10)	-1069(7)	66(4)
C(7)	3595(7)	5059(9)	-525(7)	61(4)
C(8)	3269(8)	5079(12)	-1192(7)	88(5)
C(9)	3551(10)	5654(14)	-1510(8)	106(6)
C(10)	4134(11)	6188(14)	-1169(11)	110(7)
C(11)	4458(8)	6149(13)	-525(10)	100(6)
C(12)	4171(7)	5624(11)	-199(7)	77(4)
Ag(2)	1560(1)	2462(1)	-536(1)	61(1)

Ag(1)	3102(1)	2521(1)	-412(1)	60(1)
P(2)	1716(2)	4231(2)	-226(2)	49(1)
P(1)	3184(2)	4283(2)	-138(2)	54(1)
P(4)	3246(2)	881(2)	84(1)	42(1)
P(3)	1833(2)	871(2)	43(1)	43(1)
Cl(2)	3301(2)	8190(3)	1753(2)	82(1)
O(5)	2921(12)	7680(16)	1187(8)	137(5)
O(6)	3109(12)	9138(12)	1783(12)	137(5)
O(7)	3978(8)	8220(17)	1830(11)	137(5)
O(8)	3278(13)	7600(16)	2232(10)	137(5)
O(5')	3490(13)	9193(12)	1903(12)	137(5)
O(6')	3345(14)	7906(17)	1217(9)	137(5)
O(7')	2637(8)	8115(17)	1685(11)	137(5)
O(8')	3720(12)	7625(17)	2275(9)	137(5)
Cl(1)	1714(2)	2669(3)	-1972(2)	92(1)
O(1)	2134(7)	2559(10)	-2285(6)	162(3)
O(2)	1082(6)	2323(9)	-2389(6)	162(3)
O(3)	1676(7)	3668(8)	-1851(6)	162(3)
O(4)	1966(7)	2117(9)	-1421(5)	162(3)
C(51)	381(12)	2365(15)	-1187(10)	132(7)
N(1)	-191(14)	2410(20)	-1420(14)	267(14)
C(52)	-923(15)	2514(18)	-1696(13)	500(50)
C(53)	-1096(18)	2940(30)	-1269(17)	337(13)
C(54)	-1231(17)	1630(20)	-1834(18)	337(13)
C(55)	-1186(18)	3060(30)	-2231(15)	337(13)
C(56)	3865(10)	2434(14)	-920(9)	116(6)
N(2)	4031(15)	2320(20)	-1310(13)	263(13)
C(57)	4269(13)	2317(17)	-1817(12)	353(13)
C(58)	3882(19)	1760(30)	-2317(15)	353(13)

C(59)	4902(15)	1980(30)	-1569(18)	353(13)
C(60)	4260(20)	3260(20)	-1999(17)	353(13)

Table 13. Bond lengths [Å] and angles [°] for $[Ag_2(dppm)_2(CN\text{-}t\text{-}Bu)_2](ClO_4)_2$.

C(1)-C(2)	1.359(18)	C(1)-C(6)	1.419(17)
C(1)-P(1)	1.797(14)	C(2)-C(3)	1.37(2)
C(2)-H(2)	0.9300	C(3)-C(4)	1.37(2)
C(3)-H(3)	0.9300	C(4)-C(5)	1.36(2)
C(4)-H(4)	0.9300	C(5)-C(6)	1.361(19)
C(5)-H(5)	0.9300	C(6)-H(6)	0.9300
C(13)-P(2)	1.814(11)	C(13)-P(1)	1.862(11)
C(13)-H(13A)	0.9700	C(13)-H(13B)	0.9700
C(14)-C(15)	1.344(16)	C(14)-C(19)	1.379(16)
C(14)-P(2)	1.821(13)	C(15)-C(16)	1.377(17)
C(15)-H(15)	0.9300	C(16)-C(17)	1.374(19)
C(16)-H(16)	0.9300	C(17)-C(18)	1.34(2)
C(17)-H(17)	0.9300	C(18)-C(19)	1.384(18)
C(18)-H(18)	0.9300	C(19)-H(19)	0.9300
C(20)-C(21)	1.382(15)	C(20)-C(25)	1.383(16)
C(20)-P(2)	1.836(12)	C(21)-C(22)	1.371(17)
C(21)-H(21)	0.9300	C(22)-C(23)	1.39(2)
C(22)-H(22)	0.9300	C(23)-C(24)	1.35(2)
C(23)-H(23)	0.9300	C(24)-C(25)	1.368(17)
C(24)-H(24)	0.9300	C(25)-H(25)	0.9300
C(32)-C(37)	1.357(16)	C(32)-C(33)	1.382(16)
C(32)-P(3)	1.806(12)	C(33)-C(34)	1.34(2)
C(33)-H(33)	0.9300	C(34)-C(35)	1.41(3)
C(34)-H(34)	0.9300	C(35)-C(36)	1.33(3)
C(35)-H(35)	0.9300	C(36)-C(37)	1.39(2)
C(36)-H(36)	0.9300	C(37)-H(37)	0.9300
C(26)-C(27)	1.352(15)	C(26)-C(31)	1.350(15)

C(26)-P(3)	1.851(11)	C(27)-C(28)	1.416(18)
C(27)-H(27)	0.9300	C(28)-C(29)	1.335(19)
C(28)-H(28)	0.9300	C(29)-C(30)	1.38(2)
C(29)-H(29)	0.9300	C(30)-C(31)	1.372(18)
C(30)-H(30)	0.9300	C(31)-H(31)	0.9300
C(38)-P(4)	1.819(11)	C(38)-P(3)	1.829(11)
C(38)-H(38A)	0.9700	C(38)-H(38B)	0.9700
C(45)-C(46)	1.375(15)	C(45)-C(50)	1.430(15)
C(45)-P(4)	1.798(12)	C(46)-C(47)	1.361(17)
C(46)-H(46)	0.9300	C(47)-C(48)	1.361(19)
C(47)-H(47)	0.9300	C(48)-C(49)	1.371(19)
C(48)-H(48)	0.9300	C(49)-C(50)	1.336(17)
C(49)-H(49)	0.9300	C(50)-H(50)	0.9300
C(39)-C(44)	1.357(16)	C(39)-C(40)	1.409(15)
C(39)-P(4)	1.834(11)	C(40)-C(41)	1.44(2)
C(40)-H(40)	0.9300	C(41)-C(43)	1.35(2)
C(41)-H(41)	0.9300	C(43)-C(42)	1.29(2)
C(43)-H(43)	0.9300	C(42)-C(44)	1.391(18)
C(42)-H(42)	0.9300	C(44)-H(44)	0.9300
C(7)-C(12)	1.369(17)	C(7)-C(8)	1.400(18)
C(7)-P(1)	1.837(12)	C(8)-C(9)	1.382(19)
C(8)-H(8)	0.9300	C(9)-C(10)	1.36(2)
C(9)-H(9)	0.9300	C(10)-C(11)	1.35(2)
C(10)-H(10)	0.9300	C(11)-C(12)	1.367(19)
C(11)-H(11)	0.9300	C(12)-H(12)	0.9300
Ag(2)-C(51)	2.33(2)	Ag(2)-P(3)	2.443(3)
Ag(2)-P(2)	2.444(3)	Ag(2)-O(4)	2.615(14)
Ag(2)-Ag(1)	3.2227(13)	Ag(1)-P(1)	2.418(3)
Ag(1)-P(4)	2.427(3)	Ag(1)-C(56)	2.42(2)

Ag(1)-O(4)	2.610(13)	Cl(2)-O(6')	1.352(14)
Cl(2)-O(6)	1.340(14)	Cl(2)-O(8')	1.381(15)
Cl(2)-O(7)	1.396(14)	Cl(2)-O(5)	1.392(15)
Cl(2)-O(8)	1.386(14)	Cl(2)-O(5')	1.395(15)
Cl(2)-O(7')	1.379(14)	O(5)-O(6')	0.94(3)
O(5)-O(7')	1.64(3)	O(6)-O(5')	0.75(3)
O(6)-O(7')	1.66(3)	O(7)-O(8')	1.59(3)
O(7)-O(6')	1.54(3)	O(7)-O(5')	1.73(3)
O(8)-O(8')	0.92(3)	O(8)-O(7')	1.57(3)
Cl(1)-O(2)	1.367(11)	Cl(1)-O(4)	1.371(11)
Cl(1)-O(3)	1.369(11)	Cl(1)-O(1)	1.402(12)
C(51)-N(1)	1.11(3)	N(1)-C(52)	1.432(18)
C(52)-C(54)	1.32(3)	C(52)-C(53)	1.33(3)
C(52)-C(55)	1.34(3)	C(53)-H(53A)	0.9600
C(53)-H(53B)	0.9600	C(53)-H(53C)	0.9600
C(54)-H(54A)	0.9600	C(54)-H(54B)	0.9600
C(54)-H(54C)	0.9600	C(55)-H(55A)	0.9600
C(55)-H(55B)	0.9600	C(55)-H(55C)	0.9600
C(56)-N(2)	1.12(3)	N(2)-C(57)	1.483(18)
C(57)-C(59)	1.31(3)	C(57)-C(58)	1.32(3)
C(57)-C(60)	1.32(3)	C(58)-H(58A)	0.9600
C(58)-H(58B)	0.9600	C(58)-H(58C)	0.9600
C(59)-H(59A)	0.9600	C(59)-H(59B)	0.9600
C(59)-H(59C)	0.9600	C(60)-H(60A)	0.9600
C(60)-H(60B)	0.9600	C(60)-H(60C)	0.9600
C(2)-C(1)-C(6)	115.2(13)	C(2)-C(1)-P(1)	126.5(12)
C(6)-C(1)-P(1)	118.2(10)	C(3)-C(2)-C(1)	123.3(16)
C(3)-C(2)-H(2)	118.3	C(1)-C(2)-H(2)	118.3
C(2)-C(3)-C(4)	120.2(16)	C(2)-C(3)-H(3)	119.9

C(4)-C(3)-H(3)	119.9	C(5)-C(4)-C(3)	118.6(15)
C(5)-C(4)-H(4)	120.7	C(3)-C(4)-H(4)	120.7
C(6)-C(5)-C(4)	120.7(17)	C(6)-C(5)-H(5)	119.6
C(4)-C(5)-H(5)	119.6	C(5)-C(6)-C(1)	121.5(14)
C(5)-C(6)-H(6)	119.2	C(1)-C(6)-H(6)	119.2
P(2)-C(13)-P(1)	114.7(6)	P(2)-C(13)-H(13A)	108.6
P(1)-C(13)-H(13A)	108.6	P(2)-C(13)-H(13B)	108.6
P(1)-C(13)-H(13B)	108.6	H(13A)-C(13)-H(13B)	107.6
C(15)-C(14)-C(19)	116.4(12)	C(15)-C(14)-P(2)	119.6(10)
C(19)-C(14)-P(2)	123.9(10)	C(14)-C(15)-C(16)	124.3(13)
C(14)-C(15)-H(15)	117.9	C(16)-C(15)-H(15)	117.9
C(15)-C(16)-C(17)	118.2(13)	C(15)-C(16)-H(16)	120.9
C(17)-C(16)-H(16)	120.9	C(18)-C(17)-C(16)	119.1(14)
C(18)-C(17)-H(17)	120.4	C(16)-C(17)-H(17)	120.4
C(19)-C(18)-C(17)	121.4(15)	C(19)-C(18)-H(18)	119.3
C(17)-C(18)-H(18)	119.3	C(18)-C(19)-C(14)	120.5(13)
C(18)-C(19)-H(19)	119.7	C(14)-C(19)-H(19)	119.7
C(21)-C(20)-C(25)	118.9(11)	C(21)-C(20)-P(2)	118.0(9)
C(25)-C(20)-P(2)	123.0(9)	C(22)-C(21)-C(20)	120.8(12)
C(22)-C(21)-H(21)	119.6	C(20)-C(21)-H(21)	119.6
C(23)-C(22)-C(21)	119.1(13)	C(23)-C(22)-H(22)	120.5
C(21)-C(22)-H(22)	120.5	C(24)-C(23)-C(22)	120.2(12)
C(24)-C(23)-H(23)	119.9	C(22)-C(23)-H(23)	119.9
C(23)-C(24)-C(25)	120.6(14)	C(23)-C(24)-H(24)	119.7
C(25)-C(24)-H(24)	119.7	C(24)-C(25)-C(20)	120.4(13)
C(24)-C(25)-H(25)	119.8	C(20)-C(25)-H(25)	119.8
C(37)-C(32)-C(33)	117.2(12)	C(37)-C(32)-P(3)	119.9(10)
C(33)-C(32)-P(3)	122.8(10)	C(34)-C(33)-C(32)	123.9(15)
C(34)-C(33)-H(33)	118.1	C(32)-C(33)-H(33)	118.1

C(33)-C(34)-C(35)	116.8(17)	C(33)-C(34)-H(34)	121.6
C(35)-C(34)-H(34)	121.6	C(36)-C(35)-C(34)	121.3(17)
C(36)-C(35)-H(35)	119.4	C(34)-C(35)-H(35)	119.4
C(35)-C(36)-C(37)	119.3(17)	C(35)-C(36)-H(36)	120.3
C(37)-C(36)-H(36)	120.3	C(32)-C(37)-C(36)	121.4(15)
C(32)-C(37)-H(37)	119.3	C(36)-C(37)-H(37)	119.3
C(27)-C(26)-C(31)	121.1(11)	C(27)-C(26)-P(3)	122.9(9)
C(31)-C(26)-P(3)	115.2(9)	C(26)-C(27)-C(28)	119.8(12)
C(26)-C(27)-H(27)	120.1	C(28)-C(27)-H(27)	120.1
C(29)-C(28)-C(27)	119.2(14)	C(29)-C(28)-H(28)	120.4
C(27)-C(28)-H(28)	120.4	C(28)-C(29)-C(30)	119.9(14)
C(28)-C(29)-H(29)	120.1	C(30)-C(29)-H(29)	120.1
C(31)-C(30)-C(29)	120.9(13)	C(31)-C(30)-H(30)	119.6
C(29)-C(30)-H(30)	119.6	C(26)-C(31)-C(30)	118.9(12)
C(26)-C(31)-H(31)	120.6	C(30)-C(31)-H(31)	120.6
P(4)-C(38)-P(3)	111.7(6)	P(4)-C(38)-H(38A)	109.3
P(3)-C(38)-H(38A)	109.3	P(4)-C(38)-H(38B)	109.3
P(3)-C(38)-H(38B)	109.3	H(38A)-C(38)-H(38B)	107.9
C(46)-C(45)-C(50)	116.6(11)	C(46)-C(45)-P(4)	126.0(9)
C(50)-C(45)-P(4)	117.2(9)	C(47)-C(46)-C(45)	119.4(12)
C(47)-C(46)-H(46)	120.3	C(45)-C(46)-H(46)	120.3
C(46)-C(47)-C(48)	124.1(13)	C(46)-C(47)-H(47)	117.9
C(48)-C(47)-H(47)	117.9	C(47)-C(48)-C(49)	116.5(12)
C(47)-C(48)-H(48)	121.8	C(49)-C(48)-H(48)	121.8
C(50)-C(49)-C(48)	122.0(13)	C(50)-C(49)-H(49)	119.0
C(48)-C(49)-H(49)	119.0	C(49)-C(50)-C(45)	121.2(12)
C(49)-C(50)-H(50)	119.4	C(45)-C(50)-H(50)	119.4
C(44)-C(39)-C(40)	122.4(11)	C(44)-C(39)-P(4)	119.1(9)
C(40)-C(39)-P(4)	118.4(9)	C(39)-C(40)-C(41)	112.2(14)

C(39)-C(40)-H(40)	123.9	C(41)-C(40)-H(40)	123.9
C(43)-C(41)-C(40)	122.6(16)	C(43)-C(41)-H(41)	118.7
C(40)-C(41)-H(41)	118.7	C(42)-C(43)-C(41)	123.3(19)
C(42)-C(43)-H(43)	118.3	C(41)-C(43)-H(43)	118.3
C(43)-C(42)-C(44)	118.0(16)	C(43)-C(42)-H(42)	121.0
C(44)-C(42)-H(42)	121.0	C(39)-C(44)-C(42)	121.3(14)
C(39)-C(44)-H(44)	119.4	C(42)-C(44)-H(44)	119.4
C(12)-C(7)-C(8)	120.1(13)	C(12)-C(7)-P(1)	123.7(11)
C(8)-C(7)-P(1)	116.2(11)	C(9)-C(8)-C(7)	118.9(15)
C(9)-C(8)-H(8)	120.6	C(7)-C(8)-H(8)	120.6
C(10)-C(9)-C(8)	119.3(16)	C(10)-C(9)-H(9)	120.4
C(8)-C(9)-H(9)	120.4	C(11)-C(10)-C(9)	121.8(15)
C(11)-C(10)-H(10)	119.1	C(9)-C(10)-H(10)	119.1
C(10)-C(11)-C(12)	119.8(17)	C(10)-C(11)-H(11)	120.1
C(12)-C(11)-H(11)	120.1	C(7)-C(12)-C(11)	119.8(15)
C(7)-C(12)-H(12)	120.1	C(11)-C(12)-H(12)	120.1
C(51)-Ag(2)-P(3)	104.1(5)	C(51)-Ag(2)-P(2)	102.5(5)
P(3)-Ag(2)-P(2)	134.62(11)	C(51)-Ag(2)-O(4)	97.3(6)
P(3)-Ag(2)-O(4)	101.7(3)	P(2)-Ag(2)-O(4)	110.7(3)
C(51)-Ag(2)-Ag(1)	148.7(5)	P(3)-Ag(2)-Ag(1)	88.96(7)
P(2)-Ag(2)-Ag(1)	86.96(8)	O(4)-Ag(2)-Ag(1)	51.8(3)
P(1)-Ag(1)-P(4)	140.10(12)	P(1)-Ag(1)-C(56)	100.9(5)
P(4)-Ag(1)-C(56)	102.6(4)	P(1)-Ag(1)-O(4)	111.7(3)
P(4)-Ag(1)-O(4)	96.8(3)	C(56)-Ag(1)-O(4)	97.1(5)
P(1)-Ag(1)-Ag(2)	90.05(8)	P(4)-Ag(1)-Ag(2)	86.11(7)
C(56)-Ag(1)-Ag(2)	148.9(5)	O(4)-Ag(1)-Ag(2)	52.0(3)
C(13)-P(2)-C(14)	105.2(6)	C(13)-P(2)-C(20)	101.8(5)
C(14)-P(2)-C(20)	105.9(6)	C(13)-P(2)-Ag(2)	117.7(4)
C(14)-P(2)-Ag(2)	112.8(4)	C(20)-P(2)-Ag(2)	112.3(4)

C(1)-P(1)-C(7)	105.4(6)	C(1)-P(1)-C(13)	106.6(5)
C(7)-P(1)-C(13)	102.2(5)	C(1)-P(1)-Ag(1)	111.9(4)
C(7)-P(1)-Ag(1)	114.2(4)	C(13)-P(1)-Ag(1)	115.5(4)
C(45)-P(4)-C(38)	104.1(5)	C(45)-P(4)-C(39)	105.7(5)
C(38)-P(4)-C(39)	105.8(5)	C(45)-P(4)-Ag(1)	107.3(4)
C(38)-P(4)-Ag(1)	115.7(4)	C(39)-P(4)-Ag(1)	117.1(4)
C(32)-P(3)-C(38)	104.1(5)	C(32)-P(3)-C(26)	102.8(5)
C(38)-P(3)-C(26)	105.7(5)	C(32)-P(3)-Ag(2)	119.4(4)
C(38)-P(3)-Ag(2)	114.3(4)	C(26)-P(3)-Ag(2)	109.2(4)
O(6')-Cl(2)-O(6)	117.5(16)	O(6')-Cl(2)-O(8')	112.3(12)
O(6)-Cl(2)-O(8')	124.5(15)	O(6')-Cl(2)-O(7)	68.4(13)
O(6)-Cl(2)-O(7)	107.4(12)	O(8')-Cl(2)-O(7)	69.9(13)
O(6')-Cl(2)-O(5)	40.1(13)	O(6)-Cl(2)-O(5)	116.2(13)
O(8')-Cl(2)-O(5)	117.3(14)	O(7)-Cl(2)-O(5)	106.7(12)
O(6')-Cl(2)-O(8)	129.1(14)	O(6)-Cl(2)-O(8)	111.7(13)
O(8')-Cl(2)-O(8)	38.8(12)	O(7)-Cl(2)-O(8)	108.6(12)
O(5)-Cl(2)-O(8)	105.9(12)	O(6')-Cl(2)-O(5')	111.6(12)
O(6)-Cl(2)-O(5')	31.7(14)	O(8')-Cl(2)-O(5')	107.1(12)
O(7)-Cl(2)-O(5')	76.4(13)	O(5)-Cl(2)-O(5')	133.8(14)
O(8)-Cl(2)-O(5')	116.8(15)	O(6')-Cl(2)-O(7')	111.4(12)
O(6)-Cl(2)-O(7')	75.1(14)	O(8')-Cl(2)-O(7')	108.0(12)
O(7)-Cl(2)-O(7')	177.3(13)	O(5)-Cl(2)-O(7')	72.6(13)
O(8)-Cl(2)-O(7')	69.3(13)	O(5')-Cl(2)-O(7')	105.9(12)
O(6')-O(5)-Cl(2)	67.7(13)	O(6')-O(5)-O(7')	119.4(18)
Cl(2)-O(5)-O(7')	53.3(9)	O(5')-O(6)-Cl(2)	78.2(18)
O(5')-O(6)-O(7')	130(2)	Cl(2)-O(6)-O(7')	53.6(9)
Cl(2)-O(7)-O(8')	54.6(8)	Cl(2)-O(7)-O(6')	54.5(8)
O(8')-O(7)-O(6')	92.8(13)	Cl(2)-O(7)-O(5')	51.8(8)
O(8')-O(7)-O(5')	84.5(12)	O(6')-O(7)-O(5')	87.8(13)

O(8')-O(8)-Cl(2)	70.4(14)	O(8')-O(8)-O(7')	125.5(18)
Cl(2)-O(8)-O(7')	55.2(9)	O(6)-O(5')-Cl(2)	70.1(16)
O(6)-O(5')-O(7)	121(2)	Cl(2)-O(5')-O(7)	51.8(8)
O(5)-O(6')-Cl(2)	72.3(14)	O(5)-O(6')-O(7)	126.6(19)
Cl(2)-O(6')-O(7)	57.2(9)	Cl(2)-O(7')-O(5)	54.0(8)
Cl(2)-O(7')-O(6)	51.4(8)	O(5)-O(7')-O(6)	89.4(12)
Cl(2)-O(7')-O(8)	55.5(8)	O(5)-O(7')-O(8)	87.2(13)
O(6)-O(7')-O(8)	88.6(13)	O(8)-O(8')-Cl(2)	70.9(14)
O(8)-O(8')-O(7)	126.4(18)	Cl(2)-O(8')-O(7)	55.5(9)
O(2)-Cl(1)-O(4)	110.6(8)	O(2)-Cl(1)-O(3)	110.1(8)
O(4)-Cl(1)-O(3)	111.2(8)	O(2)-Cl(1)-O(1)	105.6(8)
O(4)-Cl(1)-O(1)	110.6(8)	O(3)-Cl(1)-O(1)	108.7(9)
Cl(1)-O(4)-Ag(2)	120.9(8)	Cl(1)-O(4)-Ag(1)	124.5(8)
Ag(2)-O(4)-Ag(1)	76.2(3)	N(1)-C(51)-Ag(2)	169(2)
C(51)-N(1)-C(52)	176(3)	C(54)-C(52)-C(53)	106.5(19)
C(54)-C(52)-C(55)	107.0(19)	C(53)-C(52)-C(55)	109(2)
C(54)-C(52)-N(1)	111.2(19)	C(53)-C(52)-N(1)	108.8(18)
C(55)-C(52)-N(1)	114.2(19)	C(52)-C(53)-H(53A)	109.5
C(52)-C(53)-H(53B)	109.5	H(53A)-C(53)-H(53B)	109.5
C(52)-C(53)-H(53C)	109.5	H(53A)-C(53)-H(53C)	109.5
H(53B)-C(53)-H(53C)	109.5	C(52)-C(54)-H(54A)	109.5
C(52)-C(54)-H(54B)	109.5	H(54A)-C(54)-H(54B)	109.5
C(52)-C(54)-H(54C)	109.5	H(54A)-C(54)-H(54C)	109.5
H(54B)-C(54)-H(54C)	109.5	C(52)-C(55)-H(55A)	109.5
C(52)-C(55)-H(55B)	109.5	H(55A)-C(55)-H(55B)	109.5
C(52)-C(55)-H(55C)	109.5	H(55A)-C(55)-H(55C)	109.5
H(55B)-C(55)-H(55C)	109.5	N(2)-C(56)-Ag(1)	159(2)
C(56)-N(2)-C(57)	173(3)	C(59)-C(57)-C(58)	109.6(19)
C(59)-C(57)-C(60)	109(2)	C(58)-C(57)-C(60)	109.4(19)

C(59)-C(57)-N(2)	108.0(18)	C(58)-C(57)-N(2)	113.7(19)
C(60)-C(57)-N(2)	106.8(18)	C(57)-C(58)-H(58A)	109.5
C(57)-C(58)-H(58B)	109.5	H(58A)-C(58)-H(58B)	109.5
C(57)-C(58)-H(58C)	109.5	H(58A)-C(58)-H(58C)	109.5
H(58B)-C(58)-H(58C)	109.5	C(57)-C(59)-H(59A)	109.5
C(57)-C(59)-H(59B)	109.5	H(59A)-C(59)-H(59B)	109.5
C(57)-C(59)-H(59C)	109.5	H(59A)-C(59)-H(59C)	109.5
H(59B)-C(59)-H(59C)	109.5	C(57)-C(60)-H(60A)	109.5
C(57)-C(60)-H(60B)	109.5	H(60A)-C(60)-H(60B)	109.5
C(57)-C(60)-H(60C)	109.5	H(60A)-C(60)-H(60C)	109.5
H(60B)-C(60)-H(60C)	109.5		

Symmetry transformations used to generate equivalent atoms:

Table 14. Anisotropic displacement parameters ($Å^2 x\ 10^3$) for $[Ag_2(dppm)_2(CN\text{-}t\text{-}Bu)_2](ClO_4)_2$. The anisotropic displacement factor exponent takes the form: $-2\pi^2[\ h^2\ a^{*2}U^{11} + \ldots + 2\ h\ k\ a^*\ b^*\ U^{12}\ ]$

	U^{11}	U^{22}	U^{33}	U^{23}	U^{13}	U^{12}
C(1)	53(8)	53(8)	84(9)	-2(7)	39(8)	-4(7)
C(2)	96(13)	74(11)	104(13)	-18(10)	40(11)	-6(9)
C(3)	93(14)	93(13)	118(15)	-34(12)	38(12)	-5(11)
C(4)	96(13)	119(15)	72(11)	-32(11)	32(10)	-19(12)
C(5)	87(12)	126(15)	67(11)	-11(10)	29(9)	-13(11)
C(6)	81(11)	64(9)	84(11)	8(8)	42(9)	-1(8)
C(13)	39(6)	43(6)	57(7)	-3(5)	21(6)	4(6)
C(14)	60(9)	54(8)	73(9)	0(7)	34(7)	5(7)
C(15)	52(8)	72(9)	73(9)	14(8)	34(7)	-4(7)
C(16)	71(10)	87(11)	83(11)	28(9)	43(9)	19(9)
C(17)	69(10)	104(13)	63(10)	-2(9)	26(8)	-12(9)
C(18)	77(11)	111(14)	87(12)	-23(10)	32(10)	-18(10)
C(19)	74(10)	54(8)	63(9)	-9(7)	35(8)	-9(7)
C(20)	43(7)	40(6)	62(8)	2(6)	26(6)	-3(5)
C(21)	36(7)	72(9)	68(9)	5(7)	14(7)	19(7)
C(22)	77(11)	78(10)	73(10)	3(8)	23(9)	5(9)
C(23)	39(8)	65(9)	121(13)	50(9)	21(9)	25(7)
C(24)	63(10)	81(11)	109(12)	30(10)	44(10)	20(9)
C(25)	61(9)	58(8)	79(9)	10(7)	36(8)	7(7)
C(32)	34(7)	51(7)	67(9)	-10(6)	27(7)	-2(6)
C(33)	75(10)	56(9)	78(9)	14(7)	36(8)	-12(7)
C(34)	104(15)	50(9)	210(20)	-13(13)	112(17)	-8(10)

C(35)	56(11)	94(13)	180(20)	-67(15)	73(13)	-41(10)
C(36)	87(13)	132(16)	124(15)	-78(14)	58(12)	-64(13)
C(37)	68(10)	69(10)	78(10)	-15(8)	27(8)	-15(8)
C(26)	49(8)	50(7)	68(8)	8(6)	38(7)	5(6)
C(27)	47(8)	120(12)	53(8)	30(9)	21(7)	24(8)
C(28)	107(14)	130(15)	78(10)	34(10)	61(10)	26(12)
C(29)	52(10)	108(13)	117(13)	-13(11)	53(10)	12(9)
C(30)	50(9)	136(15)	98(12)	-20(11)	33(9)	-5(10)
C(31)	34(7)	122(12)	61(8)	-2(8)	19(7)	-7(8)
C(38)	41(7)	51(7)	60(7)	-8(6)	28(6)	1(6)
C(45)	53(8)	35(6)	74(8)	6(6)	40(7)	4(6)
C(46)	37(7)	122(12)	39(7)	10(8)	7(6)	-5(8)
C(47)	65(10)	100(12)	65(9)	11(8)	22(8)	11(9)
C(48)	28(7)	112(13)	98(12)	-17(10)	5(8)	-9(8)
C(49)	44(9)	146(15)	79(10)	-38(11)	29(8)	-27(10)
C(50)	48(8)	110(11)	53(8)	8(8)	27(7)	-4(8)
C(39)	50(8)	37(6)	59(8)	-12(6)	30(7)	11(6)
C(40)	77(10)	37(7)	109(11)	3(7)	53(9)	7(7)
C(41)	81(12)	32(8)	210(20)	-10(12)	79(15)	1(8)
C(43)	89(14)	115(17)	134(18)	-28(15)	61(14)	12(13)
C(42)	66(10)	110(13)	71(10)	-28(10)	19(8)	6(10)
C(44)	41(8)	64(9)	76(10)	-21(8)	10(7)	8(7)
C(7)	61(9)	48(7)	91(10)	8(7)	48(8)	8(7)
C(8)	103(13)	93(11)	73(10)	8(9)	42(10)	1(10)
C(9)	111(14)	122(15)	110(14)	47(12)	73(12)	-4(12)
C(10)	114(16)	101(14)	170(20)	72(14)	116(16)	34(12)
C(11)	75(11)	99(13)	163(17)	46(13)	86(13)	13(10)
C(12)	54(9)	73(10)	101(11)	16(9)	30(8)	-2(8)
Ag(2)	65(1)	45(1)	73(1)	8(1)	31(1)	4(1)

Ag(1)	76(1)	45(1)	67(1)	7(1)	40(1)	8(1)
P(2)	53(2)	42(2)	54(2)	6(2)	25(2)	3(2)
P(1)	59(2)	43(2)	70(2)	7(2)	39(2)	6(2)
P(4)	41(2)	41(2)	49(2)	2(1)	25(2)	4(1)
P(3)	40(2)	39(2)	55(2)	0(2)	24(2)	2(1)
O(5)	178(14)	112(6)	125(7)	16(5)	70(8)	10(8)
O(6)	178(14)	112(6)	125(7)	16(5)	70(8)	10(8)
O(7)	178(14)	112(6)	125(7)	16(5)	70(8)	10(8)
O(8)	178(14)	112(6)	125(7)	16(5)	70(8)	10(8)
O(5')	178(14)	112(6)	125(7)	16(5)	70(8)	10(8)
O(6')	178(14)	112(6)	125(7)	16(5)	70(8)	10(8)
O(7')	178(14)	112(6)	125(7)	16(5)	70(8)	10(8)
O(8')	178(14)	112(6)	125(7)	16(5)	70(8)	10(8)
Cl(1)	114(3)	97(3)	48(2)	2(2)	20(2)	15(3)
O(1)	194(7)	145(6)	116(5)	12(5)	40(5)	21(6)
O(2)	194(7)	145(6)	116(5)	12(5)	40(5)	21(6)
O(3)	194(7)	145(6)	116(5)	12(5)	40(5)	21(6)
O(4)	194(7)	145(6)	116(5)	12(5)	40(5)	21(6)

Table 15. Hydrogen coordinates (x 10^4) and isotropic displacement parameters ($Å^2$x 10 ^{3}) for $[Ag_2(dppm)_2(CN\text{-}t\text{-}Bu)_2](ClO_4)_2$.

	x	y	z	U(eq)
H(2)	3494	5915	794	111
H(3)	4170	6082	1856	124
H(4)	4708	4694	2462	117
H(5)	4748	3241	1945	114
H(6)	4051	3051	887	89
H(13A)	2437	5567	-132	55
H(13B)	2160	5108	-817	55
H(15)	1733	3030	758	75
H(16)	1981	3151	1815	92
H(17)	2306	4700	2316	95
H(18)	2467	6010	1774	112
H(19)	2208	5872	711	74
H(21)	905	4695	-1522	74
H(22)	-108	5527	-2118	96
H(23)	-656	6386	-1601	96
H(24)	-257	6255	-525	99
H(25)	743	5409	69	77
H(33)	1844	-1230	348	82
H(34)	1448	-2683	-190	128
H(35)	900	-2615	-1311	124
H(36)	827	-1151	-1826	132
H(37)	1162	326	-1251	88
H(27)	2281	735	1420	88
H(28)	1727	941	2083	118

H(29)	571	1169	1635	104
H(30)	-52	1122	541	113
H(31)	506	1079	-104	88
H(38A)	2913	1109	897	58
H(38B)	2823	-23	689	58
H(46)	4034	660	1490	83
H(47)	5166	866	2148	95
H(48)	5993	872	1788	105
H(49)	5634	932	699	107
H(50)	4516	872	15	82
H(40)	3392	-1291	285	84
H(41)	3159	-2630	-473	124
H(43)	2858	-2318	-1502	130
H(42)	2602	-793	-1914	104
H(44)	2761	564	-1236	79
H(8)	2870	4711	-1416	106
H(9)	3345	5676	-1953	127
H(10)	4315	6590	-1384	132
H(11)	4874	6480	-305	120
H(12)	4368	5650	244	92
H(53A)	-790	3488	-1066	506
H(53B)	-1063	2451	-954	506
H(53C)	-1559	3185	-1479	506
H(54A)	-1230	1375	-2219	506
H(54B)	-1696	1698	-1892	506
H(54C)	-990	1168	-1492	506
H(55A)	-1011	2814	-2518	506
H(55B)	-1058	3749	-2131	506
H(55C)	-1677	3001	-2427	506

H(58A)	3443	2079	-2545	529
H(58B)	3819	1109	-2176	529
H(58C)	4104	1695	-2592	529
H(59A)	5175	2364	-1193	529
H(59B)	5087	2057	-1872	529
H(59C)	4907	1288	-1459	529
H(60A)	4597	3641	-1655	529
H(60B)	3813	3542	-2116	529
H(60C)	4365	3281	-2358	529

Table 16. Torsion angles [°] for $[Ag_2(dppm)_2(CN\text{-}t\text{-}Bu)_2](ClO_4)_2$.

C(6)-C(1)-C(2)-C(3)	0(2)	P(1)-C(1)-C(2)-C(3)	-179.2(13)
C(1)-C(2)-C(3)-C(4)	-3(3)	C(2)-C(3)-C(4)-C(5)	7(3)
C(3)-C(4)-C(5)-C(6)	-8(3)	C(4)-C(5)-C(6)-C(1)	5(2)
C(2)-C(1)-C(6)-C(5)	0(2)	P(1)-C(1)-C(6)-C(5)	178.4(12)
C(19)-C(14)-C(15)-C(16)	0(2)	P(2)-C(14)-C(15)-C(16)	-178.7(11)
C(14)-C(15)-C(16)-C(17)	1(2)	C(15)-C(16)-C(17)-C(18)	-3(2)
C(16)-C(17)-C(18)-C(19)	3(2)	C(17)-C(18)-C(19)-C(14)	-2(2)
C(15)-C(14)-C(19)-C(18)	0(2)	P(2)-C(14)-C(19)-C(18)	178.8(11)
C(25)-C(20)-C(21)-C(22)	0.7(19)	P(2)-C(20)-C(21)-C(22)	177.0(11)
C(20)-C(21)-C(22)-C(23)	2(2)	C(21)-C(22)-C(23)-C(24)	-3(2)
C(22)-C(23)-C(24)-C(25)	3(2)	C(23)-C(24)-C(25)-C(20)	-1(2)
C(21)-C(20)-C(25)-C(24)	-1.2(19)	P(2)-C(20)-C(25)-C(24)	-177.3(11)
C(37)-C(32)-C(33)-C(34)	-3(2)	P(3)-C(32)-C(33)-C(34)	179.2(12)
C(32)-C(33)-C(34)-C(35)	2(2)	C(33)-C(34)-C(35)-C(36)	2(3)
C(34)-C(35)-C(36)-C(37)	-4(3)	C(33)-C(32)-C(37)-C(36)	0(2)
P(3)-C(32)-C(37)-C(36)	178.0(12)	C(35)-C(36)-C(37)-C(32)	4(2)
C(31)-C(26)-C(27)-C(28)	2(2)	P(3)-C(26)-C(27)-C(28)	171.5(12)
C(26)-C(27)-C(28)-C(29)	0(3)	C(27)-C(28)-C(29)-C(30)	1(3)
C(28)-C(29)-C(30)-C(31)	-4(3)	C(27)-C(26)-C(31)-C(30)	-5(2)
P(3)-C(26)-C(31)-C(30)	-175.6(13)	C(29)-C(30)-C(31)-C(26)	6(3)
C(50)-C(45)-C(46)-C(47)	4(2)	P(4)-C(45)-C(46)-C(47)	-170.1(12)
C(45)-C(46)-C(47)-C(48)	-6(3)	C(46)-C(47)-C(48)-C(49)	5(3)
C(47)-C(48)-C(49)-C(50)	-2(3)	C(48)-C(49)-C(50)-C(45)	0(3)
C(46)-C(45)-C(50)-C(49)	-1(2)	P(4)-C(45)-C(50)-C(49)	173.6(13)
C(44)-C(39)-C(40)-C(41)	0.7(18)	P(4)-C(39)-C(40)-C(41)	-179.3(10)
C(39)-C(40)-C(41)-C(43)	3(2)	C(40)-C(41)-C(43)-C(42)	-5(3)
C(41)-C(43)-C(42)-C(44)	3(3)	C(40)-C(39)-C(44)-C(42)	-2(2)

P(4)-C(39)-C(44)-C(42)	177.7(11)	C(43)-C(42)-C(44)-C(39)	0(2)
C(12)-C(7)-C(8)-C(9)	2(2)	P(1)-C(7)-C(8)-C(9)	179.6(12)
C(7)-C(8)-C(9)-C(10)	0(3)	C(8)-C(9)-C(10)-C(11)	2(3)
C(9)-C(10)-C(11)-C(12)	-5(3)	C(8)-C(7)-C(12)-C(11)	-5(2)
P(1)-C(7)-C(12)-C(11)	177.5(11)	C(10)-C(11)-C(12)-C(7)	6(2)
C(51)-Ag(2)-Ag(1)-P(1)	107.7(10)	P(3)-Ag(2)-Ag(1)-P(1)	-136.28(11)
P(2)-Ag(2)-Ag(1)-P(1)	-1.49(11)	O(4)-Ag(2)-Ag(1)-P(1)	118.0(3)
C(51)-Ag(2)-Ag(1)-P(4)	-112.0(10)	P(3)-Ag(2)-Ag(1)-P(4)	3.98(11)
P(2)-Ag(2)-Ag(1)-P(4)	138.77(10)	O(4)-Ag(2)-Ag(1)-P(4)	-101.8(3)
C(51)-Ag(2)-Ag(1)-C(56)	-3.9(13)	P(3)-Ag(2)-Ag(1)-C(56)	112.1(9)
P(2)-Ag(2)-Ag(1)-C(56)	-113.1(9)	O(4)-Ag(2)-Ag(1)-C(56)	6.4(9)
C(51)-Ag(2)-Ag(1)-O(4)	-10.2(10)	P(3)-Ag(2)-Ag(1)-O(4)	105.8(3)
P(2)-Ag(2)-Ag(1)-O(4)	-119.5(3)	P(1)-C(13)-P(2)-C(14)	82.0(7)
P(1)-C(13)-P(2)-C(20)	-167.8(6)	P(1)-C(13)-P(2)-Ag(2)	-44.6(7)
C(15)-C(14)-P(2)-C(13)	-141.5(10)	C(19)-C(14)-P(2)-C(13)	39.7(13)
C(15)-C(14)-P(2)-C(20)	111.2(11)	C(19)-C(14)-P(2)-C(20)	-67.6(12)
C(15)-C(14)-P(2)-Ag(2)	-11.9(12)	C(19)-C(14)-P(2)-Ag(2)	169.3(10)
C(21)-C(20)-P(2)-C(13)	66.7(10)	C(25)-C(20)-P(2)-C(13)	-117.2(10)
C(21)-C(20)-P(2)-C(14)	176.4(10)	C(25)-C(20)-P(2)-C(14)	-7.5(12)
C(21)-C(20)-P(2)-Ag(2)	-60.1(10)	C(25)-C(20)-P(2)-Ag(2)	116.0(10)
C(51)-Ag(2)-P(2)-C(13)	-126.1(7)	P(3)-Ag(2)-P(2)-C(13)	109.2(4)
O(4)-Ag(2)-P(2)-C(13)	-23.3(5)	Ag(1)-Ag(2)-P(2)-C(13)	23.7(4)
C(51)-Ag(2)-P(2)-C(14)	111.1(7)	P(3)-Ag(2)-P(2)-C(14)	-13.5(5)
O(4)-Ag(2)-P(2)-C(14)	-146.1(5)	Ag(1)-Ag(2)-P(2)-C(14)	-99.1(4)
C(51)-Ag(2)-P(2)-C(20)	-8.4(7)	P(3)-Ag(2)-P(2)-C(20)	-133.0(4)
O(4)-Ag(2)-P(2)-C(20)	94.4(5)	Ag(1)-Ag(2)-P(2)-C(20)	141.4(4)
C(2)-C(1)-P(1)-C(7)	66.1(14)	C(6)-C(1)-P(1)-C(7)	-112.6(11)
C(2)-C(1)-P(1)-C(13)	-41.9(14)	C(6)-C(1)-P(1)-C(13)	139.4(10)
C(2)-C(1)-P(1)-Ag(1)	-169.1(12)	C(6)-C(1)-P(1)-Ag(1)	12.2(11)

C(12)-C(7)-P(1)-C(1)	1.7(13)	C(8)-C(7)-P(1)-C(1)	-176.0(11)
C(12)-C(7)-P(1)-C(13)	113.0(11)	C(8)-C(7)-P(1)-C(13)	-64.8(11)
C(12)-C(7)-P(1)-Ag(1)	-121.5(11)	C(8)-C(7)-P(1)-Ag(1)	60.7(11)
P(2)-C(13)-P(1)-C(1)	-83.3(7)	P(2)-C(13)-P(1)-C(7)	166.3(6)
P(2)-C(13)-P(1)-Ag(1)	41.7(7)	P(4)-Ag(1)-P(1)-C(1)	18.7(5)
C(56)-Ag(1)-P(1)-C(1)	-106.5(6)	O(4)-Ag(1)-P(1)-C(1)	151.2(5)
Ag(2)-Ag(1)-P(1)-C(1)	102.7(4)	P(4)-Ag(1)-P(1)-C(7)	138.3(5)
C(56)-Ag(1)-P(1)-C(7)	13.1(7)	O(4)-Ag(1)-P(1)-C(7)	-89.2(6)
Ag(2)-Ag(1)-P(1)-C(7)	-137.7(5)	P(4)-Ag(1)-P(1)-C(13)	-103.6(4)
C(56)-Ag(1)-P(1)-C(13)	131.2(6)	O(4)-Ag(1)-P(1)-C(13)	28.9(5)
Ag(2)-Ag(1)-P(1)-C(13)	-19.6(4)	C(46)-C(45)-P(4)-C(38)	-10.4(13)
C(50)-C(45)-P(4)-C(38)	175.4(10)	C(46)-C(45)-P(4)-C(39)	-121.6(12)
C(50)-C(45)-P(4)-C(39)	64.2(11)	C(46)-C(45)-P(4)-Ag(1)	112.8(11)
C(50)-C(45)-P(4)-Ag(1)	-61.5(10)	P(3)-C(38)-P(4)-C(45)	173.1(6)
P(3)-C(38)-P(4)-C(39)	-75.8(7)	P(3)-C(38)-P(4)-Ag(1)	55.6(6)
C(44)-C(39)-P(4)-C(45)	-124.8(10)	C(40)-C(39)-P(4)-C(45)	55.2(11)
C(44)-C(39)-P(4)-C(38)	125.2(10)	C(40)-C(39)-P(4)-C(38)	-54.8(11)
C(44)-C(39)-P(4)-Ag(1)	-5.4(11)	C(40)-C(39)-P(4)-Ag(1)	174.5(8)
P(1)-Ag(1)-P(4)-C(45)	-61.2(4)	C(56)-Ag(1)-P(4)-C(45)	63.5(6)
O(4)-Ag(1)-P(4)-C(45)	162.4(5)	Ag(2)-Ag(1)-P(4)-C(45)	-146.6(4)
P(1)-Ag(1)-P(4)-C(38)	54.4(4)	C(56)-Ag(1)-P(4)-C(38)	179.1(6)
O(4)-Ag(1)-P(4)-C(38)	-82.0(5)	Ag(2)-Ag(1)-P(4)-C(38)	-31.0(4)
P(1)-Ag(1)-P(4)-C(39)	-179.7(4)	C(56)-Ag(1)-P(4)-C(39)	-55.0(6)
O(4)-Ag(1)-P(4)-C(39)	43.9(5)	Ag(2)-Ag(1)-P(4)-C(39)	94.9(4)
C(37)-C(32)-P(3)-C(38)	-121.7(11)	C(33)-C(32)-P(3)-C(38)	56.6(11)
C(37)-C(32)-P(3)-C(26)	128.2(11)	C(33)-C(32)-P(3)-C(26)	-53.5(11)
C(37)-C(32)-P(3)-Ag(2)	7.2(12)	C(33)-C(32)-P(3)-Ag(2)	-174.5(9)
P(4)-C(38)-P(3)-C(32)	82.3(7)	P(4)-C(38)-P(3)-C(26)	-169.7(6)
P(4)-C(38)-P(3)-Ag(2)	-49.6(6)	C(27)-C(26)-P(3)-C(32)	117.3(12)

C(31)-C(26)-P(3)-C(32)	-72.3(12)	C(27)-C(26)-P(3)-C(38)	8.4(13)
C(31)-C(26)-P(3)-C(38)	178.8(11)	C(27)-C(26)-P(3)-Ag(2)	-114.9(11)
C(31)-C(26)-P(3)-Ag(2)	55.4(11)	C(51)-Ag(2)-P(3)-C(32)	49.2(7)
P(2)-Ag(2)-P(3)-C(32)	173.2(4)	O(4)-Ag(2)-P(3)-C(32)	-51.5(5)
Ag(1)-Ag(2)-P(3)-C(32)	-102.1(4)	C(51)-Ag(2)-P(3)-C(38)	173.3(7)
P(2)-Ag(2)-P(3)-C(38)	-62.6(4)	O(4)-Ag(2)-P(3)-C(38)	72.7(5)
Ag(1)-Ag(2)-P(3)-C(38)	22.0(4)	C(51)-Ag(2)-P(3)-C(26)	-68.5(7)
P(2)-Ag(2)-P(3)-C(26)	55.5(4)	O(4)-Ag(2)-P(3)-C(26)	-169.2(5)
Ag(1)-Ag(2)-P(3)-C(26)	140.2(4)	O(6)-Cl(2)-O(5)-O(6')	102(3)
O(8')-Cl(2)-O(5)-O(6')	-93(2)	O(7)-Cl(2)-O(5)-O(6')	-17(3)
O(8)-Cl(2)-O(5)-O(6')	-133(2)	O(5')-Cl(2)-O(5)-O(6')	70(3)
O(7')-Cl(2)-O(5)-O(6')	165(3)	O(6')-Cl(2)-O(5)-O(7')	-165(3)
O(6)-Cl(2)-O(5)-O(7')	-63.0(17)	O(8')-Cl(2)-O(5)-O(7')	101.7(14)
O(7)-Cl(2)-O(5)-O(7')	177.3(13)	O(8)-Cl(2)-O(5)-O(7')	61.7(15)
O(5')-Cl(2)-O(5)-O(7')	-95.7(18)	O(6')-Cl(2)-O(6)-O(5')	-87(3)
O(8')-Cl(2)-O(6)-O(5')	64(4)	O(7)-Cl(2)-O(6)-O(5')	-13(4)
O(5)-Cl(2)-O(6)-O(5')	-132(3)	O(8)-Cl(2)-O(6)-O(5')	106(3)
O(7')-Cl(2)-O(6)-O(5')	166(4)	O(6')-Cl(2)-O(6)-O(7')	106.7(15)
O(8')-Cl(2)-O(6)-O(7')	-101.9(15)	O(7)-Cl(2)-O(6)-O(7')	-179.1(13)
O(5)-Cl(2)-O(6)-O(7')	61.6(16)	O(8)-Cl(2)-O(6)-O(7')	-60.0(16)
O(5')-Cl(2)-O(6)-O(7')	-166(4)	O(6')-Cl(2)-O(7)-O(8')	-125.5(15)
O(6)-Cl(2)-O(7)-O(8')	121.1(17)	O(5)-Cl(2)-O(7)-O(8')	-113.6(16)
O(8)-Cl(2)-O(7)-O(8')	0.1(19)	O(5')-Cl(2)-O(7)-O(8')	114.3(14)
O(7')-Cl(2)-O(7)-O(8')	-39(28)	O(6)-Cl(2)-O(7)-O(6')	-113.3(17)
O(8')-Cl(2)-O(7)-O(6')	125.5(15)	O(5)-Cl(2)-O(7)-O(6')	11.9(18)
O(8)-Cl(2)-O(7)-O(6')	125.7(16)	O(5')-Cl(2)-O(7)-O(6')	-120.2(14)
O(7')-Cl(2)-O(7)-O(6')	87(28)	O(6')-Cl(2)-O(7)-O(5')	120.2(14)
O(6)-Cl(2)-O(7)-O(5')	7(2)	O(8')-Cl(2)-O(7)-O(5')	-114.3(14)
O(5)-Cl(2)-O(7)-O(5')	132.1(15)	O(8)-Cl(2)-O(7)-O(5')	-114.1(16)

O(7')-Cl(2)-O(7)-O(5')	-153(27)	O(6')-Cl(2)-O(8)-O(8')	77(3)
O(6)-Cl(2)-O(8)-O(8')	-119(3)	O(7)-Cl(2)-O(8)-O(8')	0(3)
O(5)-Cl(2)-O(8)-O(8')	114(3)	O(5')-Cl(2)-O(8)-O(8')	-84(3)
O(7')-Cl(2)-O(8)-O(8')	178(3)	O(6')-Cl(2)-O(8)-O(7')	-101.3(17)
O(6)-Cl(2)-O(8)-O(7')	63.5(17)	O(8')-Cl(2)-O(8)-O(7')	-178(3)
O(7)-Cl(2)-O(8)-O(7')	-178.2(14)	O(5)-Cl(2)-O(8)-O(7')	-63.9(16)
O(5')-Cl(2)-O(8)-O(7')	97.9(15)	O(7')-O(6)-O(5')-Cl(2)	14(4)
Cl(2)-O(6)-O(5')-O(7)	11(3)	O(7')-O(6)-O(5')-O(7)	26(7)
O(6')-Cl(2)-O(5')-O(6)	108(3)	O(8')-Cl(2)-O(5')-O(6)	-129(3)
O(7)-Cl(2)-O(5')-O(6)	167(4)	O(5)-Cl(2)-O(5')-O(6)	67(4)
O(8)-Cl(2)-O(5')-O(6)	-88(3)	O(7')-Cl(2)-O(5')-O(6)	-14(4)
O(6')-Cl(2)-O(5')-O(7)	-59.8(16)	O(6)-Cl(2)-O(5')-O(7)	-167(4)
O(8')-Cl(2)-O(5')-O(7)	63.6(15)	O(5)-Cl(2)-O(5')-O(7)	-100.3(18)
O(8)-Cl(2)-O(5')-O(7)	104.2(14)	O(7')-Cl(2)-O(5')-O(7)	178.7(13)
Cl(2)-O(7)-O(5')-O(6)	-14(4)	O(8')-O(7)-O(5')-O(6)	-62(4)
O(6')-O(7)-O(5')-O(6)	31(4)	O(8')-O(7)-O(5')-Cl(2)	-48.3(10)
O(6')-O(7)-O(5')-Cl(2)	44.7(10)	O(7')-O(5)-O(6')-Cl(2)	13(2)
Cl(2)-O(5)-O(6')-O(7)	19(3)	O(7')-O(5)-O(6')-O(7)	32(5)
O(6)-Cl(2)-O(6')-O(5)	-99(2)	O(8')-Cl(2)-O(6')-O(5)	106(2)
O(7)-Cl(2)-O(6')-O(5)	162(3)	O(8)-Cl(2)-O(6')-O(5)	65(3)
O(5')-Cl(2)-O(6')-O(5)	-133(2)	O(7')-Cl(2)-O(6')-O(5)	-15(3)
O(6)-Cl(2)-O(6')-O(7)	99.0(15)	O(8')-Cl(2)-O(6')-O(7)	-55.7(16)
O(5)-Cl(2)-O(6')-O(7)	-162(3)	O(8)-Cl(2)-O(6')-O(7)	-96.9(17)
O(5')-Cl(2)-O(6')-O(7)	64.6(16)	O(7')-Cl(2)-O(6')-O(7)	-177.1(14)
Cl(2)-O(7)-O(6')-O(5)	-21(3)	O(8')-O(7)-O(6')-O(5)	20(4)
O(5')-O(7)-O(6')-O(5)	-64(4)	O(8')-O(7)-O(6')-Cl(2)	41.6(11)
O(5')-O(7)-O(6')-Cl(2)	-42.8(10)	O(6')-Cl(2)-O(7')-O(5)	10.0(18)
O(6)-Cl(2)-O(7')-O(5)	124.2(15)	O(8')-Cl(2)-O(7')-O(5)	-113.8(16)
O(7)-Cl(2)-O(7')-O(5)	-76(28)	O(8)-Cl(2)-O(7')-O(5)	-115.2(14)

O(5')-Cl(2)-O(7')-O(5)	131.7(15)	O(6')-Cl(2)-O(7')-O(6)	-114.1(17)
O(8')-Cl(2)-O(7')-O(6)	122.0(17)	O(7)-Cl(2)-O(7')-O(6)	160(28)
O(5)-Cl(2)-O(7')-O(6)	-124.2(15)	O(8)-Cl(2)-O(7')-O(6)	120.7(15)
O(5')-Cl(2)-O(7')-O(6)	7(2)	O(6')-Cl(2)-O(7')-O(8)	125.2(16)
O(6)-Cl(2)-O(7')-O(8)	-120.7(15)	O(8')-Cl(2)-O(7')-O(8)	1(2)
O(7)-Cl(2)-O(7')-O(8)	40(28)	O(5)-Cl(2)-O(7')-O(8)	115.2(14)
O(5')-Cl(2)-O(7')-O(8)	-113.2(17)	O(6')-O(5)-O(7')-Cl(2)	-16(3)
O(6')-O(5)-O(7')-O(6)	25(3)	Cl(2)-O(5)-O(7')-O(6)	40.3(10)
O(6')-O(5)-O(7')-O(8)	-64(3)	Cl(2)-O(5)-O(7')-O(8)	-48.3(10)
O(5')-O(6)-O(7')-Cl(2)	-18(4)	O(5')-O(6)-O(7')-O(5)	-60(5)
Cl(2)-O(6)-O(7')-O(5)	-42.0(11)	O(5')-O(6)-O(7')-O(8)	28(5)
Cl(2)-O(6)-O(7')-O(8)	45.2(11)	O(8')-O(8)-O(7')-Cl(2)	-2(3)
O(8')-O(8)-O(7')-O(5)	45(4)	Cl(2)-O(8)-O(7')-O(5)	47.2(9)
O(8')-O(8)-O(7')-O(6)	-45(4)	Cl(2)-O(8)-O(7')-O(6)	-42.2(10)
O(7')-O(8)-O(8')-Cl(2)	2(3)	Cl(2)-O(8)-O(8')-O(7)	0(3)
O(7')-O(8)-O(8')-O(7)	2(6)	O(6')-Cl(2)-O(8')-O(8)	-125(2)
O(6)-Cl(2)-O(8')-O(8)	82(3)	O(7)-Cl(2)-O(8')-O(8)	180(3)
O(5)-Cl(2)-O(8')-O(8)	-81(3)	O(5')-Cl(2)-O(8')-O(8)	112(3)
O(7')-Cl(2)-O(8')-O(8)	-2(3)	O(6')-Cl(2)-O(8')-O(7)	54.9(16)
O(6)-Cl(2)-O(8')-O(7)	-97.8(16)	O(5)-Cl(2)-O(8')-O(7)	98.9(14)
O(8)-Cl(2)-O(8')-O(7)	-180(3)	O(5')-Cl(2)-O(8')-O(7)	-68.0(16)
O(7')-Cl(2)-O(8')-O(7)	178.2(14)	Cl(2)-O(7)-O(8')-O(8)	0(3)
O(6')-O(7)-O(8')-O(8)	-42(4)	O(5')-O(7)-O(8')-O(8)	46(4)
O(6')-O(7)-O(8')-Cl(2)	-41.5(11)	O(5')-O(7)-O(8')-Cl(2)	46.0(9)
O(2)-Cl(1)-O(4)-Ag(2)	-80.2(11)	O(3)-Cl(1)-O(4)-Ag(2)	42.4(12)
O(1)-Cl(1)-O(4)-Ag(2)	163.2(8)	O(2)-Cl(1)-O(4)-Ag(1)	-174.5(8)
O(3)-Cl(1)-O(4)-Ag(1)	-51.9(12)	O(1)-Cl(1)-O(4)-Ag(1)	69.0(11)
C(51)-Ag(2)-O(4)-Cl(1)	52.4(11)	P(3)-Ag(2)-O(4)-Cl(1)	158.5(9)
P(2)-Ag(2)-O(4)-Cl(1)	-53.9(10)	Ag(1)-Ag(2)-O(4)-Cl(1)	-122.2(10)

C(51)-Ag(2)-O(4)-Ag(1)	174.7(5)	P(3)-Ag(2)-O(4)-Ag(1)	-79.3(2)
P(2)-Ag(2)-O(4)-Ag(1)	68.4(3)	P(1)-Ag(1)-O(4)-Cl(1)	46.3(10)
P(4)-Ag(1)-O(4)-Cl(1)	-162.1(9)	C(56)-Ag(1)-O(4)-Cl(1)	-58.5(11)
Ag(2)-Ag(1)-O(4)-Cl(1)	118.2(11)	P(1)-Ag(1)-O(4)-Ag(2)	-71.9(3)
P(4)-Ag(1)-O(4)-Ag(2)	79.6(2)	C(56)-Ag(1)-O(4)-Ag(2)	-176.7(5)
P(3)-Ag(2)-C(51)-N(1)	97(12)	P(2)-Ag(2)-C(51)-N(1)	-46(12)
O(4)-Ag(2)-C(51)-N(1)	-159(12)	Ag(1)-Ag(2)-C(51)-N(1)	-151(12)
Ag(2)-C(51)-N(1)-C(52)	23(63)	C(51)-N(1)-C(52)-C(54)	-146(53)
C(51)-N(1)-C(52)-C(53)	-29(54)	C(51)-N(1)-C(52)-C(55)	92(53)
P(1)-Ag(1)-C(56)-N(2)	-115(6)	P(4)-Ag(1)-C(56)-N(2)	98(6)
O(4)-Ag(1)-C(56)-N(2)	-1(6)	Ag(2)-Ag(1)-C(56)-N(2)	-6(7)
Ag(1)-C(56)-N(2)-C(57)	112(23)	C(56)-N(2)-C(57)-C(59)	101(24)
C(56)-N(2)-C(57)-C(58)	-137(24)	C(56)-N(2)-C(57)-C(60)	-17(25)

Symmetry transformations used to generate equivalent atoms:

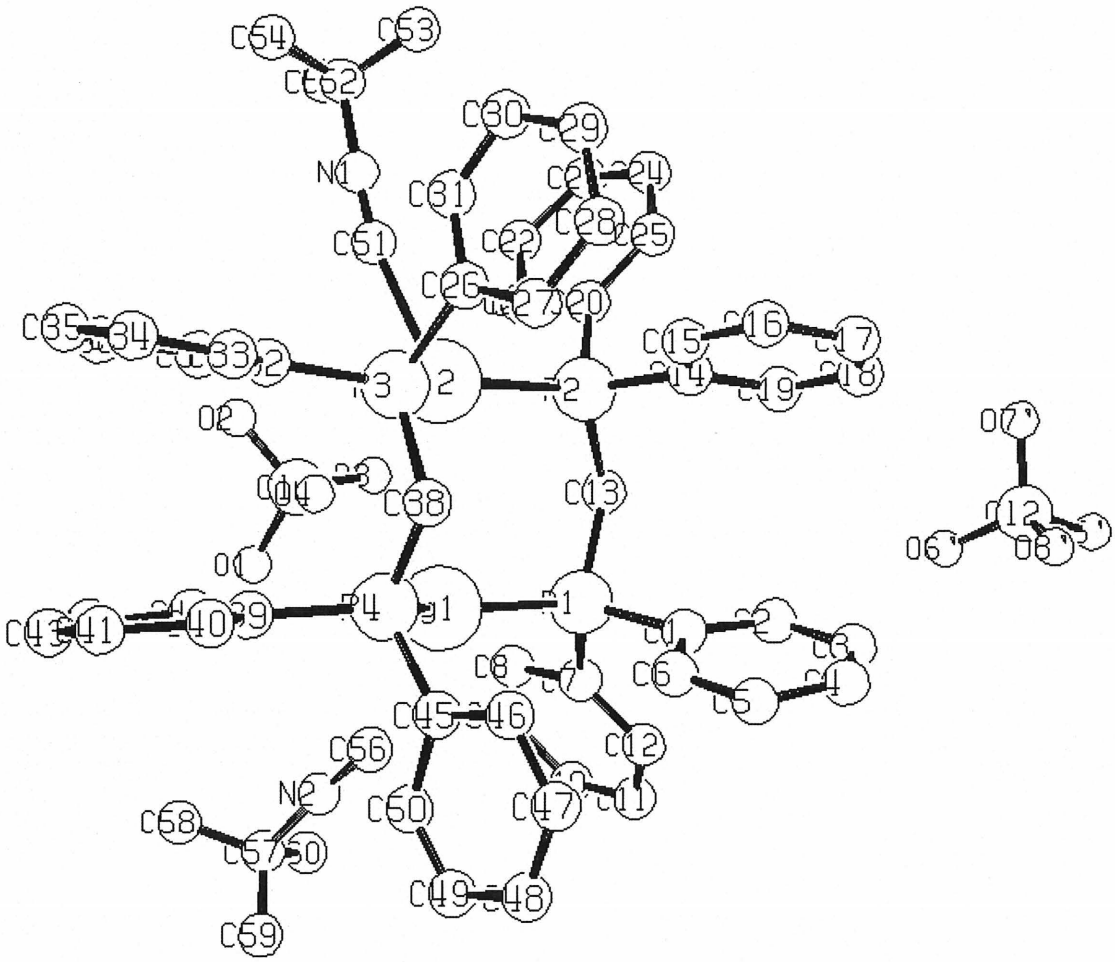

Figure S1: Numbering scheme for $[Ag_2(dppm)_2(CN\text{-}t\text{-}Bu)_2](ClO_4)_2$

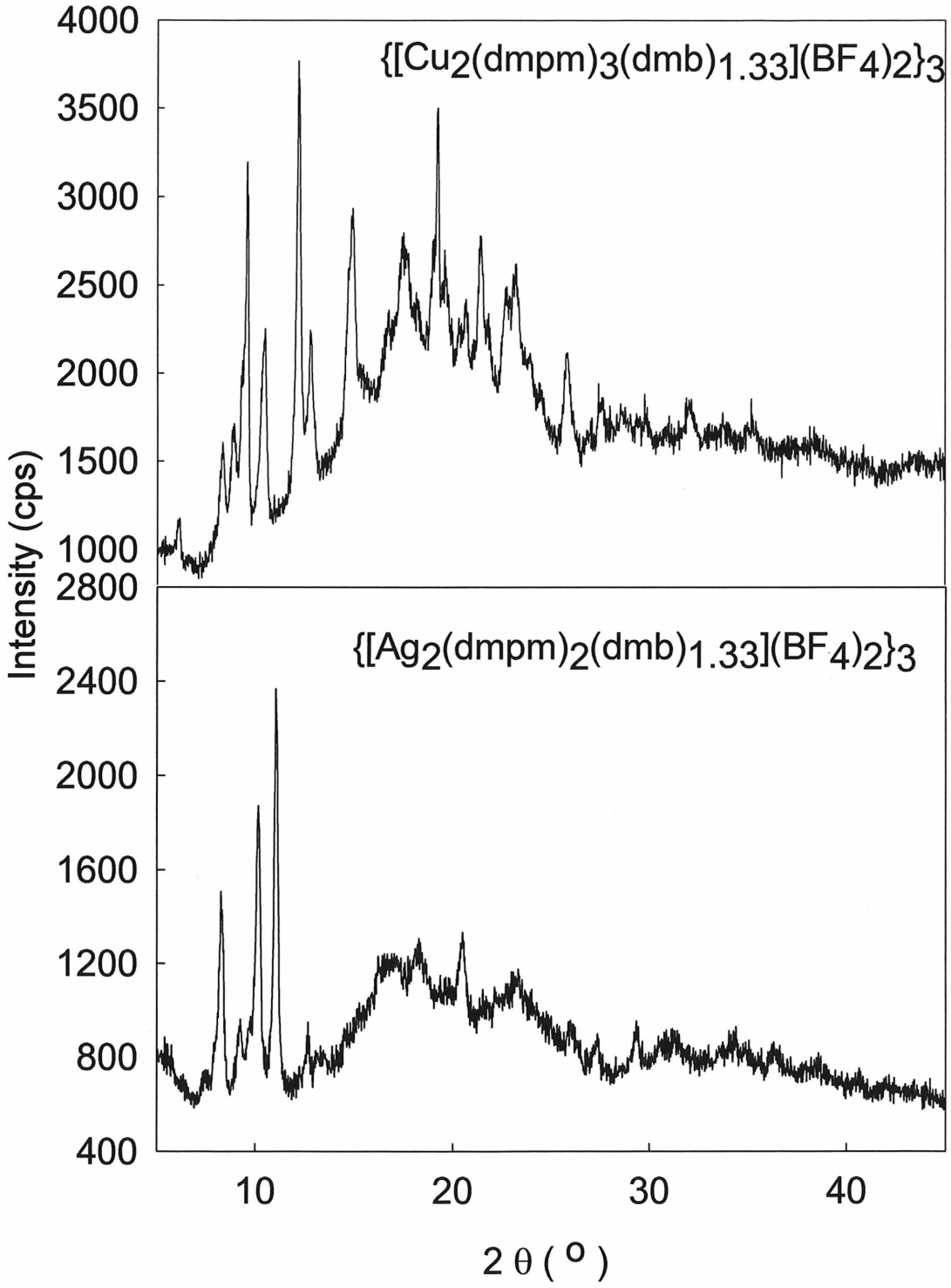

Figure S2: XRD patterns for 5 (top) and 6 (bottom).

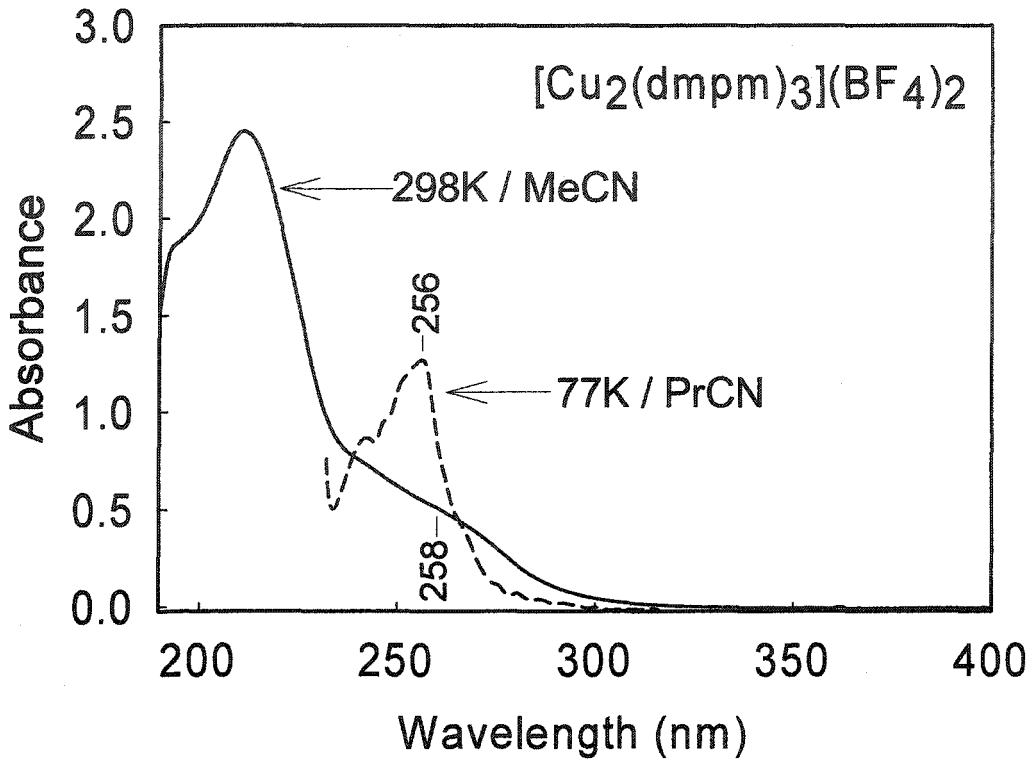

Fig. S3 : Comparison of the UV-vis spectra of **1** at 298K (—) and 77K (---). The lowest wavelength possible is 240 nm, due to the absorption caused by the 77K quartz employed.

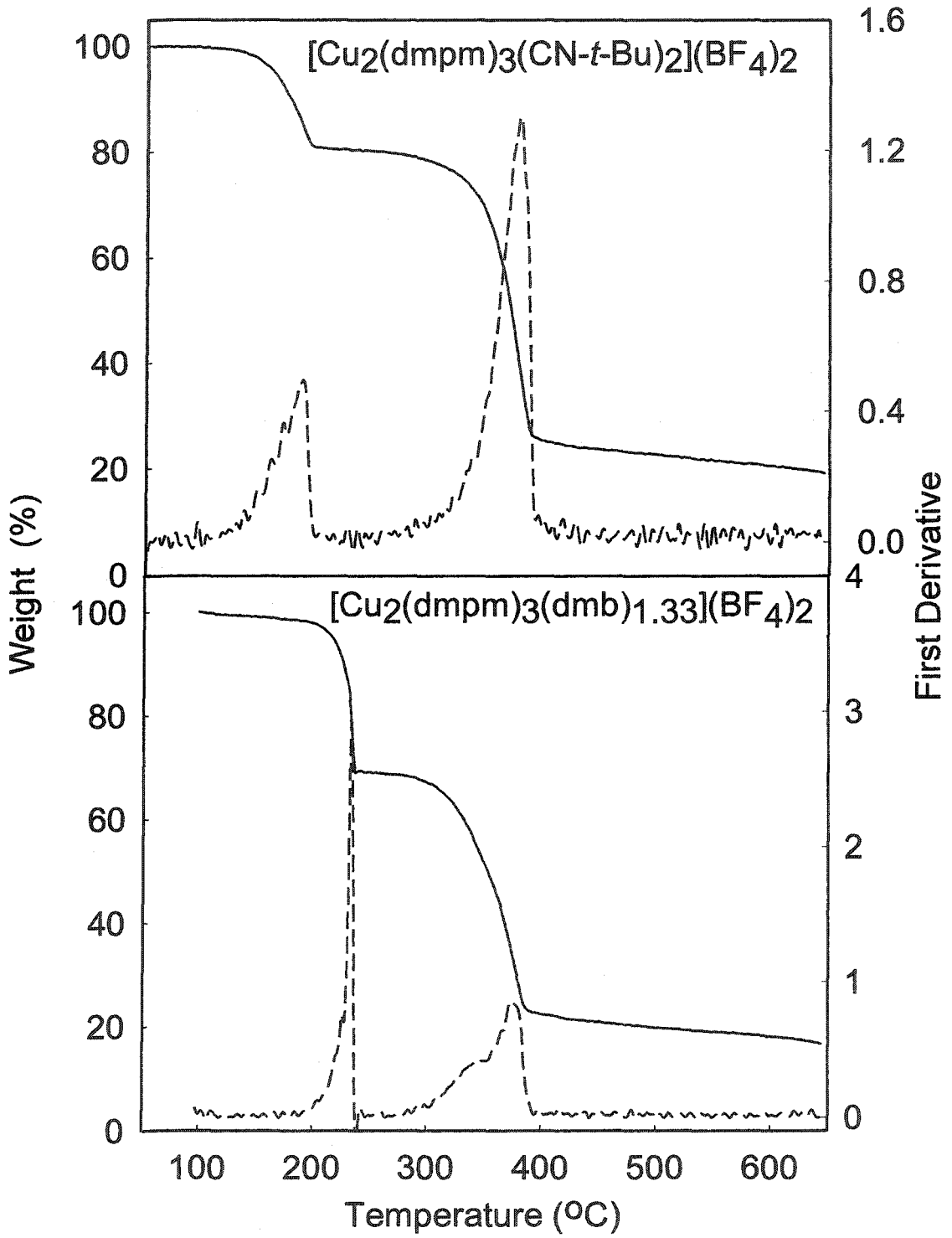

Fig. S4. Comparison of the TGA traces for **4** (top) and **5** (bottom).

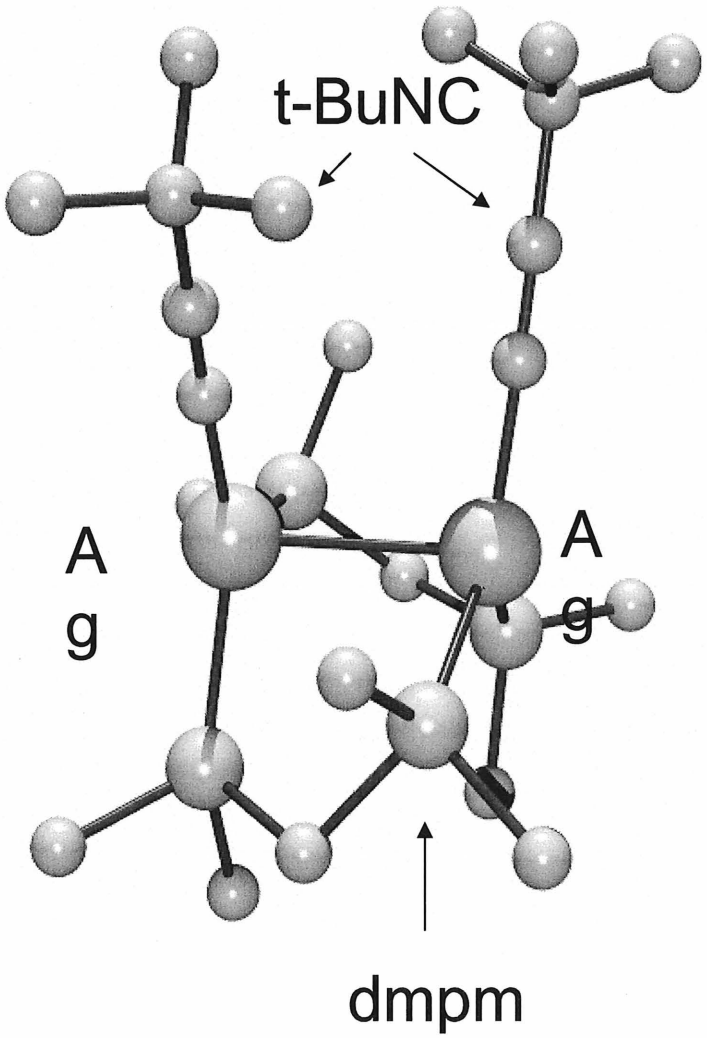

Fig. S5. Computed structure for the model compound $Ag_2(dmpm)_2(CN\text{-}t\text{-}Bu)_2^{2+}$. The calculated distances are 2.94, 2.02, 1.20, and 2.47 Å, for the Ag···Ag separation, as AgC, C≡N and AgP bond lengths, respectively.

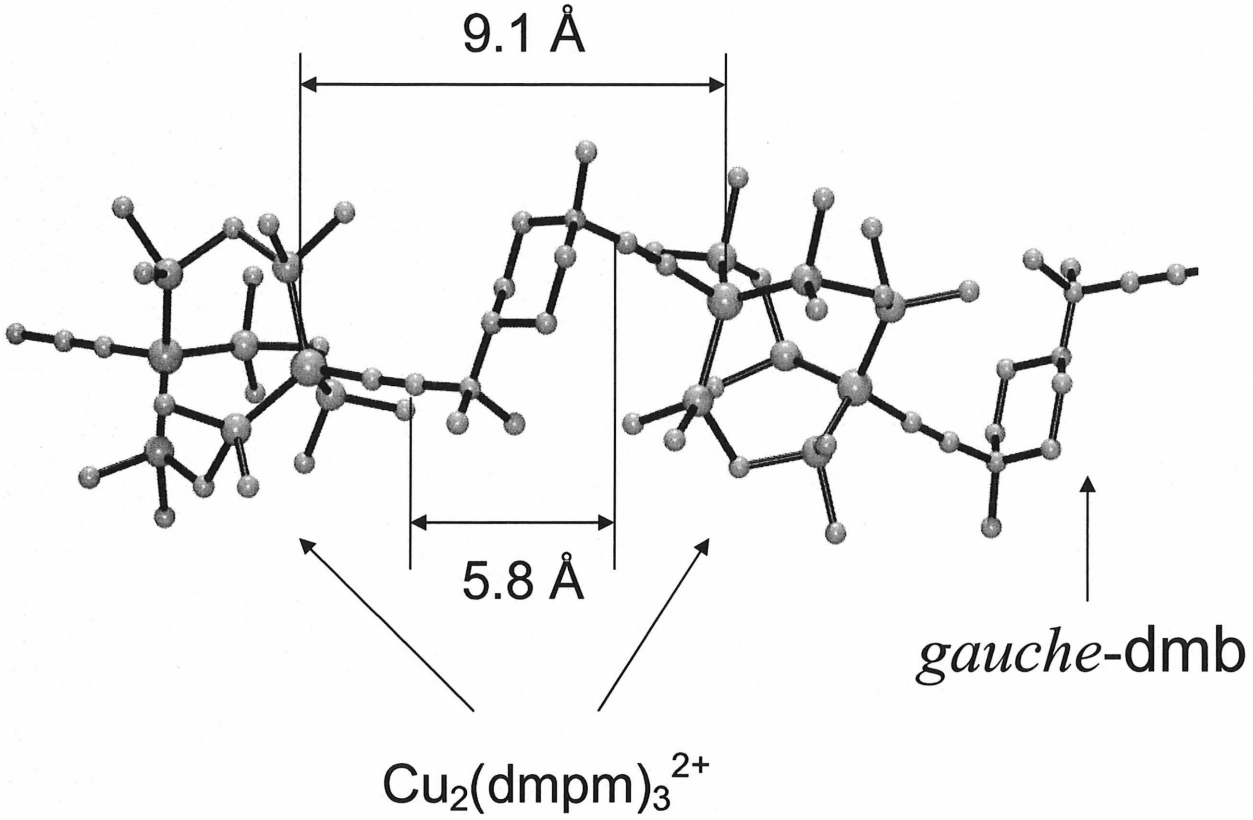

Fig. S6. Computed structure for a model compound $Cu_4(dmpm)_6(dmb)_2(CN\text{-}t\text{-}Bu)^{4+}$. The calculated distances are 4.35, 1.83, 1.20, and 2.36 Å, for the Cu···Cu separation, and CuC, C≡N and CuP bond lengths, respectively.

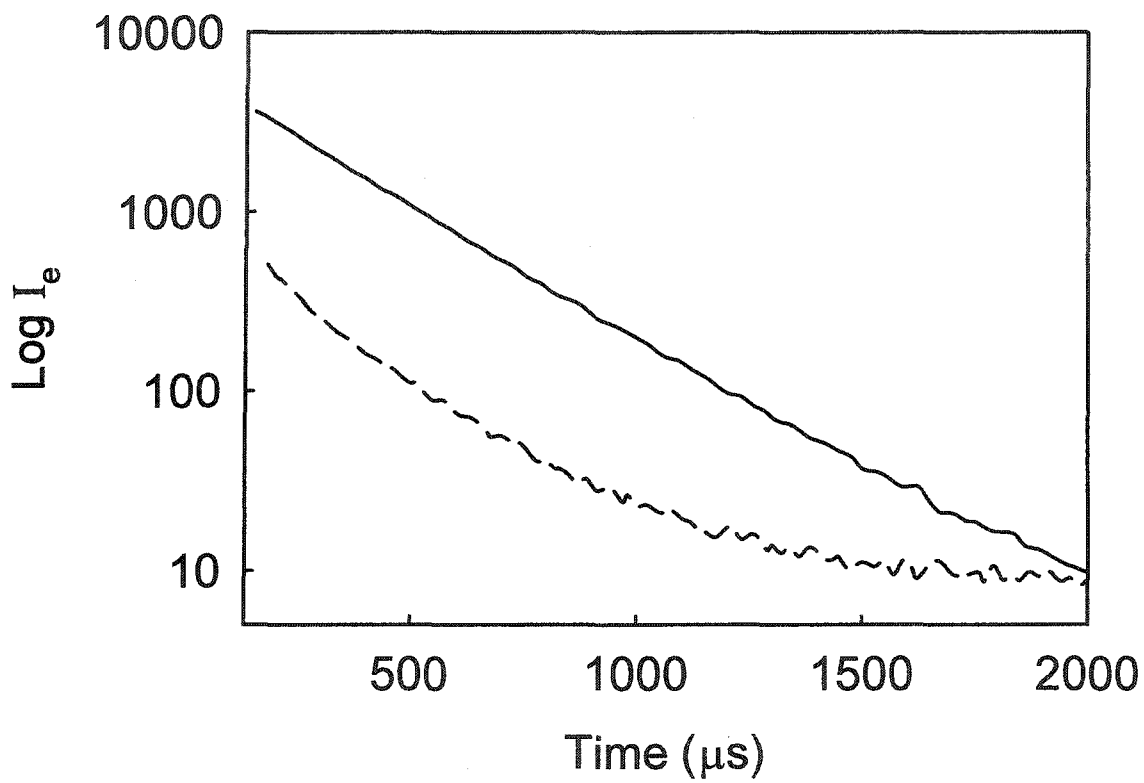

Fig. S7. Solid state decay trace for the emission of **4** (—) versus $\{Cu(dmb)_2^+\}_n$ (----) at 298K.

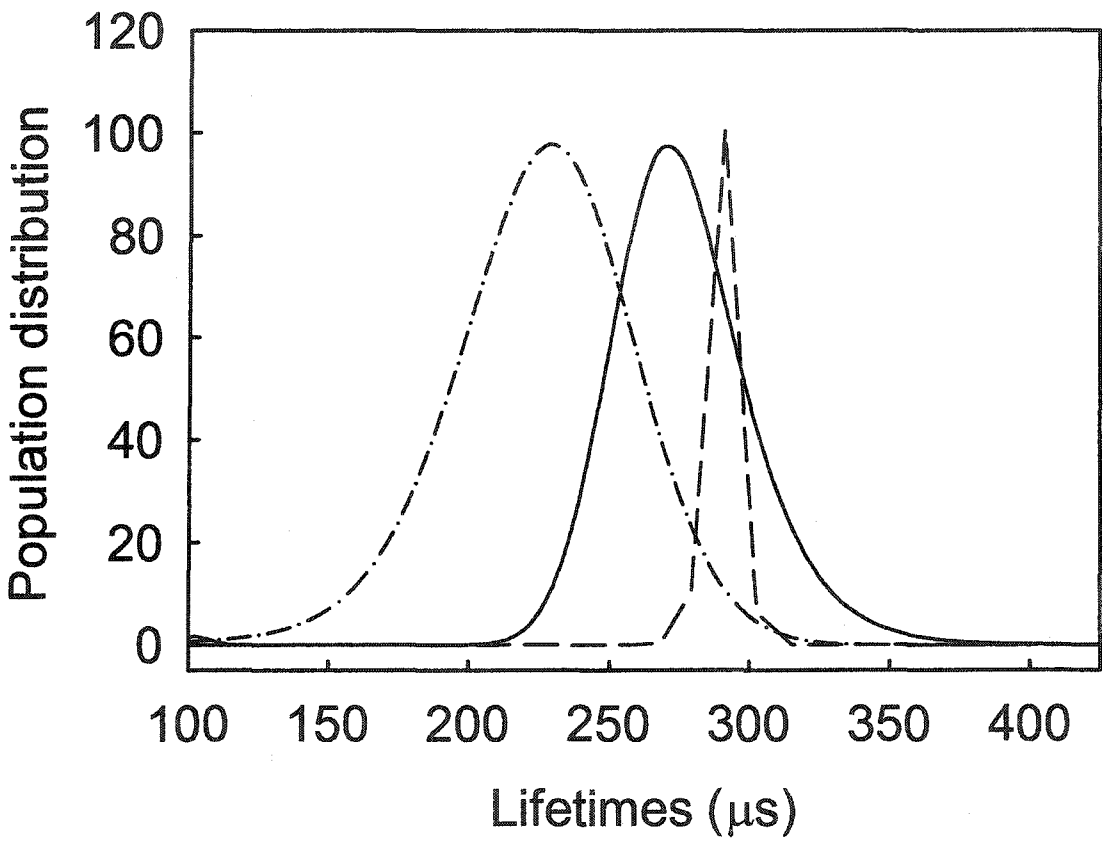

Fig. S8. Comparison of the distribution of lifetimes as a function of lifetime fitting the emission decay traces for **1** (---), **5** (—) and $\{Cu(dmb)_2^+\}_n$ (-·-·-) in the solid state at 298K.

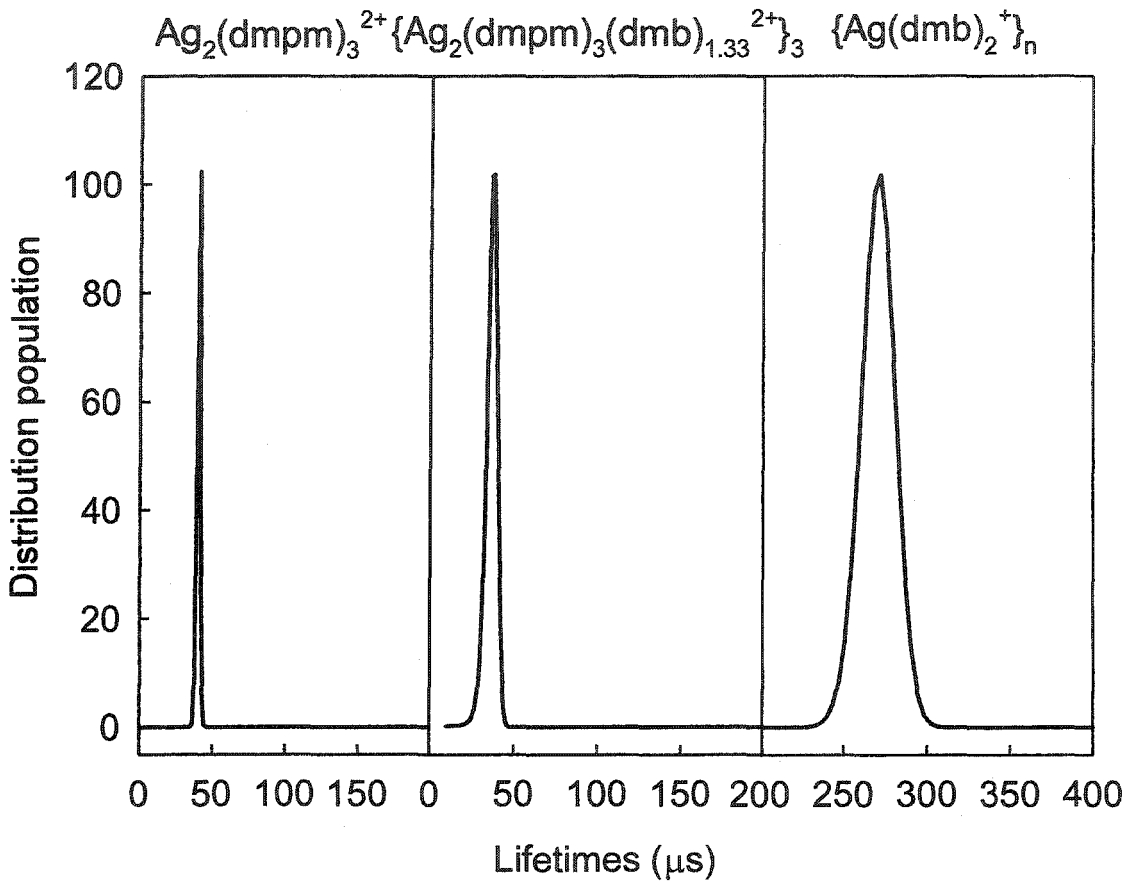

Fig. S9. Comparison of the distribution of lifetimes as a function of lifetimes fitting emission decay traces for **2**, **6** and $\{Ag(dmb)_2^{+}\}_n$ in the solid state at 298K.

CHAPITRE 2

POLYMÈRES ORGANOMÉTALLIQUES 1-D ET ZIG-ZAG LUMINESCENTS CONSTRUITS À PARTIR DE LIGANDS DIPHOSPHINES ET DIISONITRILES AVEC DU CUIVRE(I) OU DE L'ARGENT(I)

La synthèse de polymères organométalliques de coordination luminescents est devenue un sujet de recherche intéressant dans le but de découvrir les propriétés optiques fascinantes de ces nouveaux matériaux (24-25, 28, 38-44). Dernièrement, des ligands diphosphinés $Ph_2P(CH_2)_nPPh_2$ n = 4-6 ont été utilisés dans la fabrication de tels composés (22, 29, 45-47). Ce chapitre portera sur la synthèse et la caractérisation de quatorze nouveaux polymères organométalliques mixtes isonitrile/diphosphine luminescents ayant le cuivre(I) ou l'argent(I) comme centres métalliques. Au cours de cette étude, deux structures cristallographiques ont été obtenues. Deux de ces polymères étant insolubles, ils ont dû être caractérisés sous forme solide seulement. Cette insolubilité est attribuée hypothétiquement à une structure 2- ou 3-D d'un polymère réticulé. Cependant, à partir des onze autres polymères analogues, qui eux sont solubles, nous avons une très bonne idée de leur arrangement moléculaire. Des analyses de diffraction des rayons X de poudre soutiennent le caractère amorphe ou cristallin des produits. De plus, d'autres analyses comme la DSC, l'ATG et l'analyse élémentaire nous permettent de consolider les modèles. L'analyse spectrale à l'état solide fût réalisée pour treize de ces nouveaux polymères au cours de ce travail. Cet article a été soumis le 6 mai 2003 comme une communication dans le journal "Chemical Communication". Le rôle de Frédéric Lebrun a été d'obtenir la structure cristallographique du composé **11b** alors que mon rôle à été de réaliser la synthèse des treize autres polymères, d'en faire la caractérisation complète

(spectres RMN ^{1}H, ^{13}C et ^{31}P, DRX de poudre, ATG, DSC, IR, RAMAN, calculs théoriques des analyses élémentaires, spectres d'excitation, d'émission et mesures des durée de vie d'émission) et de rédiger l'article (protocoles expérimentaux, tableaux graphiques, figures et mise en forme du format de communication). La contribution de mon directeur de recherche, M. Harvey, a été dans la formulation des résultats en fonction d'une communication (faire ressortir les résultats importants pour le lecteur).

Luminescent 1-D and Zig-Zag Organometallic Polymers Built Upon Diphosphine and Diisocyanide Ligands, and Copper(I) and Silver(I)

Eric Fournier, Frédéric Lebrun and Pierre D. Harvey*

Contribution from the Département de chimie, Université de Sherbrooke, Sherbrooke, PQ., Canada J1K 2R1

Submitted to Chemical Communications

*To whom correspondence should be addressed :

Email : p.harvey@USherbrooke.ca

Abstract

This work reports the synthesis and characterization of 14 luminescent mixed ligand diphosphine/isocyanide organometallic polymers (M = Cu(I), Ag(I)), along with two X-ray structures. This field is still in its infancy as a very few number of published works exist. This manuscript contains practically all the references in this area (see references 1 and 2). This work is significant for two reasons. First, it reports the structure of the first mixed-ligand doubly bridged 1-D polymer (see compound **11b** as scheme below). The closest related polymers are the doubly bridged $\{M(dmb)_2^+\}_n$ (M = Cu, Ag) reported by us over the past few years. This polymer (**11b**) is unique since it is essentially a polymer of dimers. Attempts to expand this family with other diphosphines failed as demonstrated by this work, in fact, weakly soluble or insoluble materials are obtained, suggesting that the materials may be reticulated. Second, its reports a new strategy to obtain information on insoluble materials by synthesizing model polymers which are soluble and for which one can extract valuable information. The accumulated data for 11 soluble polymers in this work allowed one to get a fairly good idea what the insoluble (amorphous and crystalline) materials look like at the molecular level. To our knowledge, this approach is unprecedented in the field, and we believe that should attract attention among coordination, organometallic and polymer chemists, as well as some material scientists interested in optical properties.

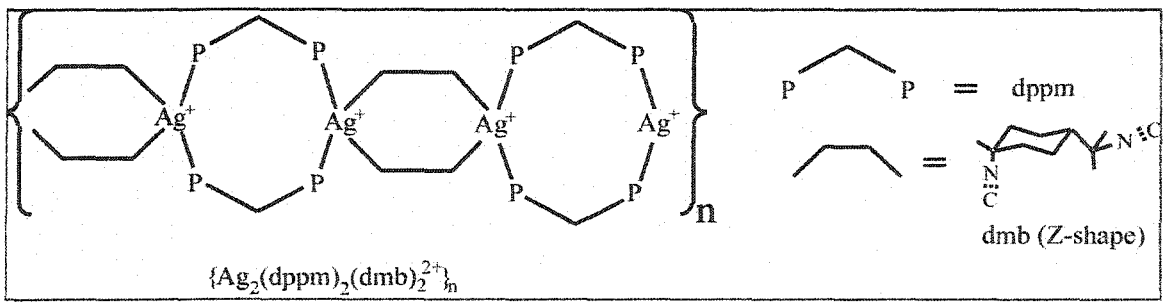

Introduction

The $[M_2(diphos)_2](BF_4)_2$ dimers ($M^+ = Cu^+$, Ag^+; diphos = dppm, dppb, dpppen, dpph) react with t-BuNC (dppm excluded) and 1,8-diisocyano-*p*-menthane (dmb) to form luminescent polymers of the type $\{[M(diphos)(CN\text{-}t\text{-}Bu)_2]\text{-}(BF_4)\}_n$ and $\{[M(diphos)(dmb)_2](BF_4)\}_n$, among which an unprecedented 1-D structure is reported.

Results and discussion

The synthesis of luminescent coordination and organometallic polymers has become a field of increasing interest,[1,2] with the hope of discovering new materials exhibiting interesting optical properties. Recently, the use of diphosphine $Ph_2P(CH_2)_nPPh_2$ ligands (n = 4-6) have been made for such purposes.[3,4] These organometallic polymers are usually soluble in common solvents allowing their characterization, and a chance of getting crystals suitable for X-ray analysis. On the other hand, the insolubility of other polymers renders the characterization very difficult. One possible strategy to overcome this problem is to synthesize closely related model polymers, which can reliably be analysed, allowing one to extract valuable information. We now wish to report the syntheses and properties of 14 luminescent polymeric materials of the type $\{[M(diphos)(CN\text{-}t\text{-}Bu)_2](BF_4)\}_n$ (M = Cu; dppb (**1**), dpppen (**2**), dpph (**3**); M = Ag; dppb (**8**), dpppen (**9**), dpph (**10**)) and $\{[M(diphos)(dmb)](BF_4)\}_n$.(M = Cu; dppm (**4**), dppb (**5**), dpppen (**6**), dpph (**7**); M = Ag; dppm (**11a**, BF_4^-; **11b**, ClO_4^-), dppb (**12**), dpppen (**13**), dpph (**14**)), two of which (**9** and **11b**) have been characterized from X-ray crystallography. In one case, **11b**, an unprecedented 1-D structure has been revealed.

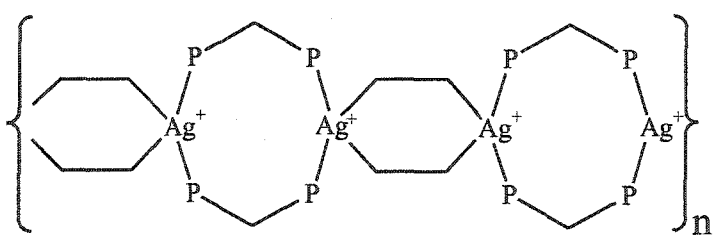

$\{Ag_2(dppm)_2(dmb)_2^{2+}\}_n$

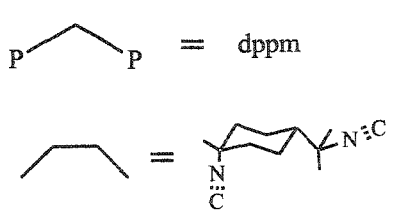

These new polymers are obtained from the reactions between the $[M_2(diphos)_2](BF_4)_2$ materials ($M^+ = Cu^+$, Ag^+)[6] and t-BuNC or dmb[7] (diphos = dppb, dpppen, dpph; Supporting Information). Similarly, both $Ag_2(dppm)_2^{2+}$ [8] and $Cu_2(dppm)_2(NCMe)^{2+}$ [9] react with dmb to form the corresponding $\{[M_2(dppm)_2(dmb)_2]^{2+}\}_n$ polymers (**4**, **11**). The colourless polymers are weakly soluble or insoluble in common organic solvents (the dmb materials being more insoluble), and the materials prove to be relatively stable towards heat (as most start losing weight at T > 150°C; TGA) and sun light (over months as they did not change colour, nor were the spectroscopic results modified). **6** and **7** exhibit T_g (glass transition; DSC) at 47.4 (ΔC_p = 0.55) and 39.4 (ΔC_p = 0.45 J/g·deg), respectively, while no T_g was observed from -20 to 150°C for the other materials. The soluble materials make brittle (M = Ag) , and stand alone films (M = Cu) from spin-coating or simple evaporation, revealing the polymeric nature of the latter polymers. The insoluble materials (**6**, **7**, **13**) just swelled in the solvents. These mechanic properties, "brittle" vs "amorphous", are consistent with the XRD patterns which reveal the crystalline (M = Ag) and semi-crystalline or amorphous morphology of the materials (M = Cu) (see Table 1 and Supporting Information). This property is well known for the $\{M(dmb)_2^+\}_n$ polymers,[2a,c] where for M = Ag and Cu shorter (n~8)[2c] and longer chains (n~300) are observed.[2a] Concurrently, **8**-**11** exhibit strong and weak ν(NC) IR peaks associated to coordinated and free RNC groups (end-of-chain), indicating that these materials may be oligomers. This feature is consistent with the high degree of crystalline morphology. Conversely, **4**-**7** do not.

11b is soluble, and crystals suitable for X-ray analyses were obtained[†] (Fig. 1). The data reveal an unprecedented 1-D structure of a mixed-ligand chain, best described as a polymer of $Ag_2(dppm)_2^{2+}$ dimers, which are doubly bridged by dmb ligands.

The d(Ag···Ag) between the tetrahedral Ag atoms, are 4.028(1)Å and 9.609(1)Å for the dppm and dmb bridged units, respectively. The dmb ligand adopts the rarely encountered Z-shape (*anti*-conformation),[10] to avoid inter $Ag_2(dppm)_2^{2+}$ unit Ph···Ph

steric interactions, otherwise obtained in the *syn*-form. Ring stresses are seen, as ∠PAgP, ∠PAgC, and ∠CAgC deviate from the ideal tetrahedral angle, and the AgC bond lengths are different from each other. The $Ag_2C_4P_2$ ring does not exhibit the typical S_8 crown structure, but rather the 4 P-atoms describe a plane where one Ag and one C atoms are above, and below the plane, describing a local point group C_i.

The X-ray structure for **9** reveals two crystallographically independent zig-zag $\{Ag(dpppen)^+\}_n$ chains (Fig. 2),[†] where the $\angle P_3$ is 87.5°. These chains differ from slight Ph orientations. The Ag atoms describe a plane where the P and C (CNR) atoms are located above and below the Ag_n plane, respectively. The d(Ag···Ag) is 8.757(1)Å. This structure is not unprecedented as a similar polymer has been reported for $\{Hg(dpppen)I_2\}_n$.[11] The smaller deviations in ∠PAgP, ∠PAgC, ∠CAgC in comparison with **11b** indicate a lesser stress is seen in the polymer chain, but there is still a longer AgC bond. This polymer can certainly give information about the polymer structures for the dppb and dpph analogues, but cannot be transferred to the $\{M(diphos)(dmb)^+\}_n$ ones. The replacement of dmb by two t-BuNC certainly mimic the electronic density and local steric hindrance about the metal, but the similarity stops there. For instance, the $Me_3C\cdots CMe_3$ distances between two adjacent t-BuNC ligands located on the same chain, are 5.227 and 5.986Å for the two independent chains. This distance falls short compared to the one seen within dmb ($MeC\cdots CMe_2$: 4.429Å). So, the replacement of the t-BuNC ligands by dmb will not lead to 1-D polymers similar to **11b**, but to reticulated materials,[12] consistent with the observed poor solubility. The similarity in XRD patterns between **1** and **8**, **2** and **9**, and **3** and **10**, indicate these materials are isostructural.

The luminescence properties for these 14 polymers in the solid state have been investigated at room temperature (Fig. 3 and Table 1). The similarity in λ_{max} (491±8nm), τ_e (emission lifetime; 6 to 56μs) is obvious, and indicates that the nature of the excited state is the same. The observation is consistent with the similarity in structure about the chromophore (i.e. $MP_2(CNR)_2$). On the basis of recent spectroscopic findings and

theorical DFT calculations on the related compounds $M(CN\text{-}t\text{-}Bu)_4^+$ (M = Cu, Ag),[2a] and $[Cu_2(dppm)_2(O_2CMe)]^+$,[13] the excited state responsible for the luminescence is assigned to a metal-to-ligand-charge-transfer (MLCT), where the ligand manifold is both the π-system of the CNR and PPh groups. The photophysical properties for these polymers in solution are not investigated as strong RNC ligand dissociation are noticed for the Ag materials.

Conclusion.

In conclusion, the similarities in the physical and optical properties indicate that the structures for this series of polymers must be strongly related to that of **11b** and **9**.

Acknowledgment.

This research is supported by NSERC (Natural Sciences and Engineering Council of Canada).

Notes and references:

† Crystal data for **11b**. $C_{74}H_{80}Ag_2Cl_2N_4O_8P_4$, M = 1563.94, triclinic, a = 13.1321(19), b = 13.3093(18), c = 13.4611(16)Å; α = 103.780(12), β = 107.349(11), γ = 115.764(11)°, V = 1828.0(4)Å^3, T = 293K, space group P-1, Z = 1, d = 1.421Mg/m^3, μ (CuK_α) = 6.25mm^{-1}, 6931 reflections measured, 5990 unique (R_{int} = 0.0178). The final R_1, wR_2 and GOF are 0.0415, 0.1068 and 1.036 (all data). Crystal data for **9**. $C_{39}H_{48}AgBF_4N_2P_2$, M = 801.41, triclinic, a = 8.7574(9), b = 14.8390(16), c = 16.7222(18)Å; α = 86.462(2), β = 77.099(2), γ = 73.170(2)°, V = 2027.5(4)Å^3, T = 198K, space group P-1, Z = 2, d = 1.313Mg/m^3, μ (MoK_α) = 0.622mm^{-1}, 10516 reflections measured, 9001 unique (R_{int} = 0.0125). The final R_1, wR_2 and GOF are 0.0625, 0.2051 and 1.062 (all data).

1 (a) J. Zhang, R.-G. Xiong, X.-T. Chen, C.-M. Che, Z. Xue, X.-Z. You,*Organometallics*, 2001, **20**, 4118. (b) Q.-X. Liu, F.-B. Xu, Q.-S. Li, X.-S. Zang, X.-B. Leng, Y. L. Chou, Z.-Z. Zhang, *Organometallics*, 2003, **22**, 309. (c) J. Zhang, R.-G. Xiong, X.-T. Chen, Z. Xue, S.-M. Peng, X.-Z. You, *Organometallics*, 2002, **21**, 235. (d) D. Sun, R. Cao, J. Weng, M. Hong, Y. Liang, *Dalton*, 2002, 291. (e) M.-L. Tong, J.-X. Shi, X.-M. Chen, *New. J. Chem.*, 2002, **26**, 814. (f) S.-L. Zheng, M.-L. Tong, S.-D. Tan, Y. Wang, J.-X. Shi, Y.-X. Tong, H. K. Lee, X.-M. Chen, *Organometallics*, 2001, **20**, 5319. (g) M. Henary, J. L. Wootton, S. I. Khan, J. I. Zink, *Inorg. Chem.*, 1997, **36**, 796.

2 (a) D. Fortin, M. Drouin, M. Turcotte, P. D. Harvey, *J. Am. Chem. Soc.*, 1997, **119**, 531. (b) D. Perreault, M. Drouin, A. Michel, P. D. Harvey, *Inorg. Chem.*, 1992, **31**, 3688. (c) M. Turcotte, P. D. Harvey, *Inorg. Chem.*, 2002, **41**, 1739.

3 (a) M.-C. Brandys, R. J. Puddephatt, *Chem. Commun.*, 2001, 1508. (b) M.-C. Brandys, R. J. Puddephatt, *J. Am. of Chem. Soc.*, 2001, **123**, 4839. (c) M.-C. Brandys, R. J. Puddephatt, *Chem. Commun.*, 2001, 1280.

4 (a) T. Zhang, M. Drouin, P. D. Harvey, *Inorg. Chem.*, 1999, **38**, 957. (b) T. Zhang, M. Drouin, P. D. Harvey, *Inorg. Chem.*, 1999, **38**, 1305.

5 D. Fortin, M. Drouin, P. D. Harvey, *J. Am. Chem. Soc.*, 1998, **120**, 5351.

6 S. Kitawaga, M. Kondo, S. Kawata, S. Wada, M. Maekawa, M. Munakata, *Inorg. Chem.*, 1995, **34**, 1455.

7 W.D. Weber, G.W. Gokel, I.K. Ugi. *Angew. Chem. Int. Ed. Engl.* 1972, *11*, 530.

8 (a) A. Birte and P.G. Jones. *Acta Cryst.* 1998, **C54**, 16. (b) A.F.M.J. Van Der Ploeg and G. Van Koten. *Inorg. Chim. Acta.* 1981 **51**, 225 .

9 J. Diez, M.P. Gamasa, J. Gimeno, A. Tiripicchio, M. Tiripicchio Camellini, *J. Chem. Soc., Dalton Trans* 1987, 1275.

10 P. D. Harvey, Coord. *Chem. Rev.*, 2002, **233-234**, 289.

11 K. Aurivillius, K. Wendel, *Acta Cryst., Sect. B.; Struct. Crystallogr. Cryst. Chem.*, 1976, **32**, 2941.

12 (a) M. Dartiguenave, Y. Dartiguenave, A. Mari, A. Guitard, M.J. Olivier, A.L. Beauchamp, *Can. J. Chem.*, 1988, **66**, 2386. (b) A. Guitard, A. Mari, A.L. Beauchamp, Y. Dartiguenave, M. Dartiguenave, *Inorg. Chem.*, 1983, **22**, 1603.

13 P. D. Harvey, M. Drouin, T. Zhang, *Inorg. Chem.*, 1997, **36**, 4998.

Table 1 Solid state spectroscopic and emission lifetime data for **1** to **14**.[a]

Pol#	Morp	λ_{max} nm	τ_e / μs	Pol#	Morp	λ_{max} / nm	τ_e / μs
1	**SC**	475	22 ±5	**8**	C	481	14 ±3
2	**SC**	483	31 ±5	**9**	C	491	55 ±4
3	**SC**	485	12 ±3	**10**	C	486	56 ±4
4	**A**	495	42 ±7	**11a**	C	499	27 ±3
5	**A**	490	15 ±5	**12**	C	487	26 ±5
6	**A**	492	24 ±5	**13**	C	483	48 ±4
7	**A**	485	18 ±3	**14**	C	487	6 ±1

[a] C = crystalline, SC = semi-crystalline, A = amorphous.

Figure Captions

1. ORTEP drawing for **11b**. The thermal ellipsoids are shown with 50% probability.

2. ORTEP drawing for **7**. The thermal ellipsoids are 50 shown with % probability.

3. Comparison of the solid state emission spectra for(**2**, **4**, **6**, **9**, **11** and **13**) at room temperature.

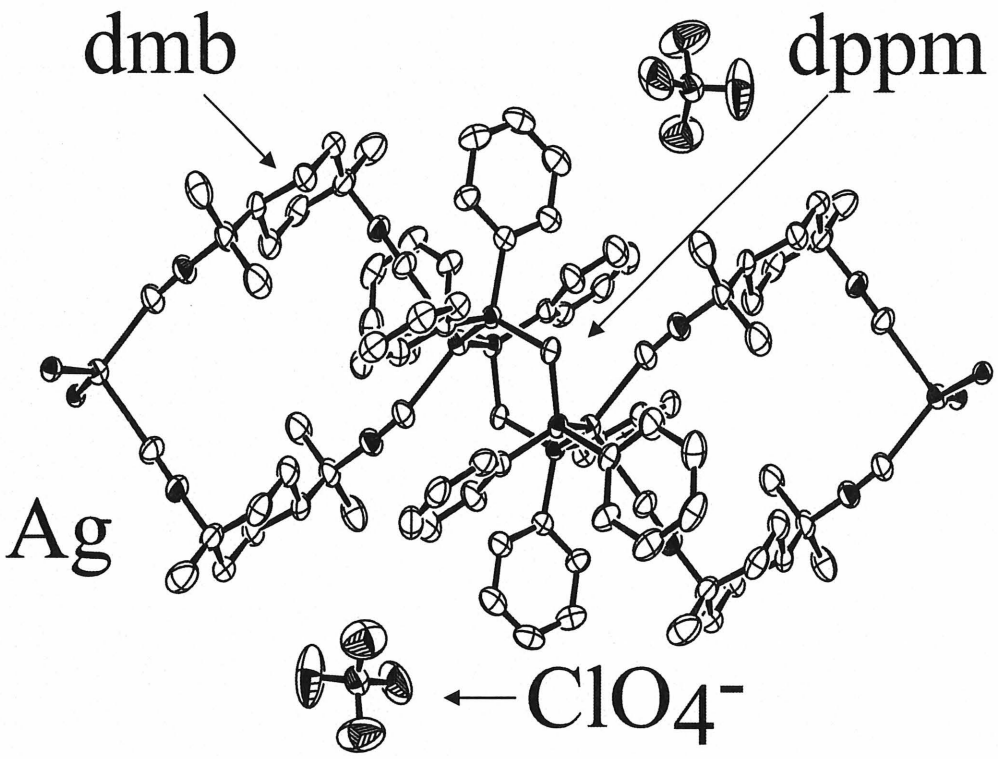

Fig. 1 ORTEP drawing for **11b**. The thermal ellipsoids are shown with 50% probability. Only a segment of the polymer chain is shown. The H-atoms are not shown for clarity. (d(AgP) = 2.4672(14), 2.4921(15); d(AgC) = 2.251(6), 2.331(6); d(CN) = 1.133(7), 1.142(8) Å; ∠PAgP = 136.48(4); ∠CAgC = 99.0(2); ∠PAgC = 118.58(17), 97.57(18), 98.14 (18), 98.90(18)°).

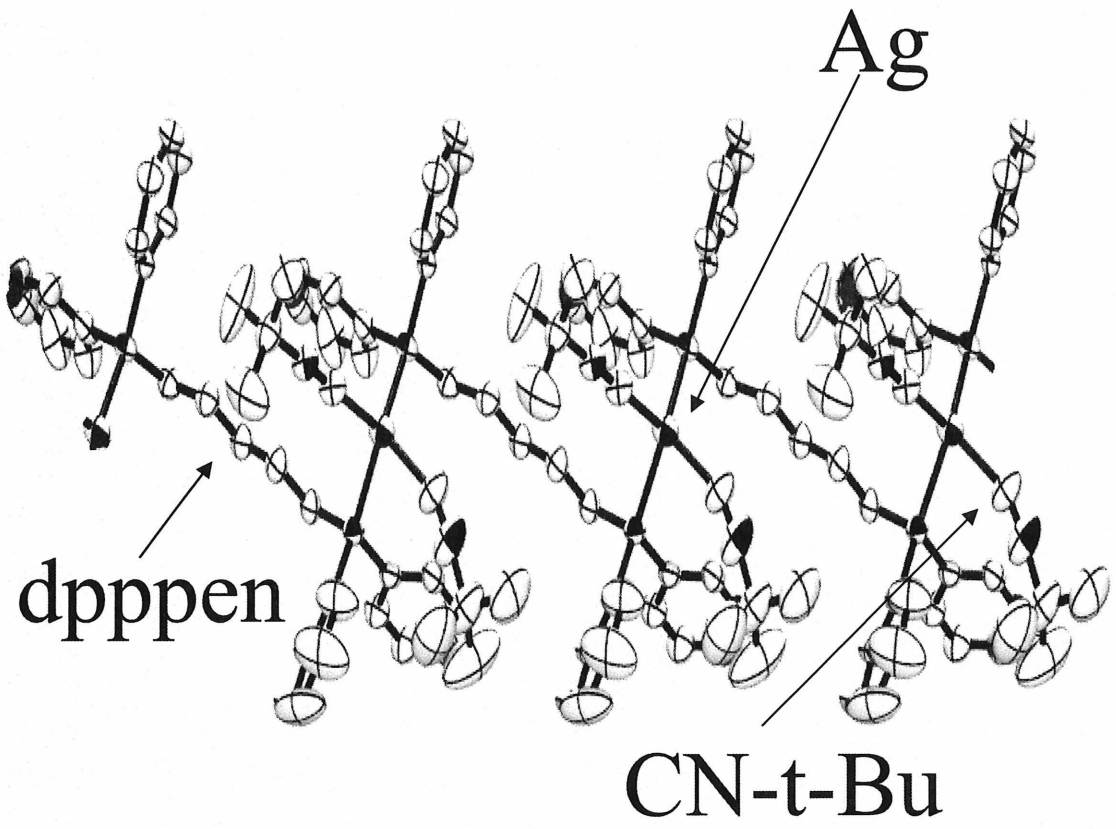

Fig. 2 ORTEP drawing for **7**. The thermal ellipsoids are shown with 50% probability. Only a segment of the polymer chain is shown. The H-atoms and the BF_4^- ions are not shown for clarity. (d(AgP) = 2.4706(15), 2.5136(16), 2.5132(14), 2.5213(14); d(AgC) = 2.189(7), 2.335(8), 2.214(6), 2.228(6); d(CN) = 1.141(10), 1.141(7), 1.127(8), 1.154(8) Å; ∠PAgP = 105.56(5), 101.49(5); ∠CAgC = 109.0(3), 111.3(2); ∠PAgC = 114.30(17), 117.6(2), 112.69(19), 115.65(15), 105.58(16), 108.20(17), 114.43(16), 96.2(2)°)

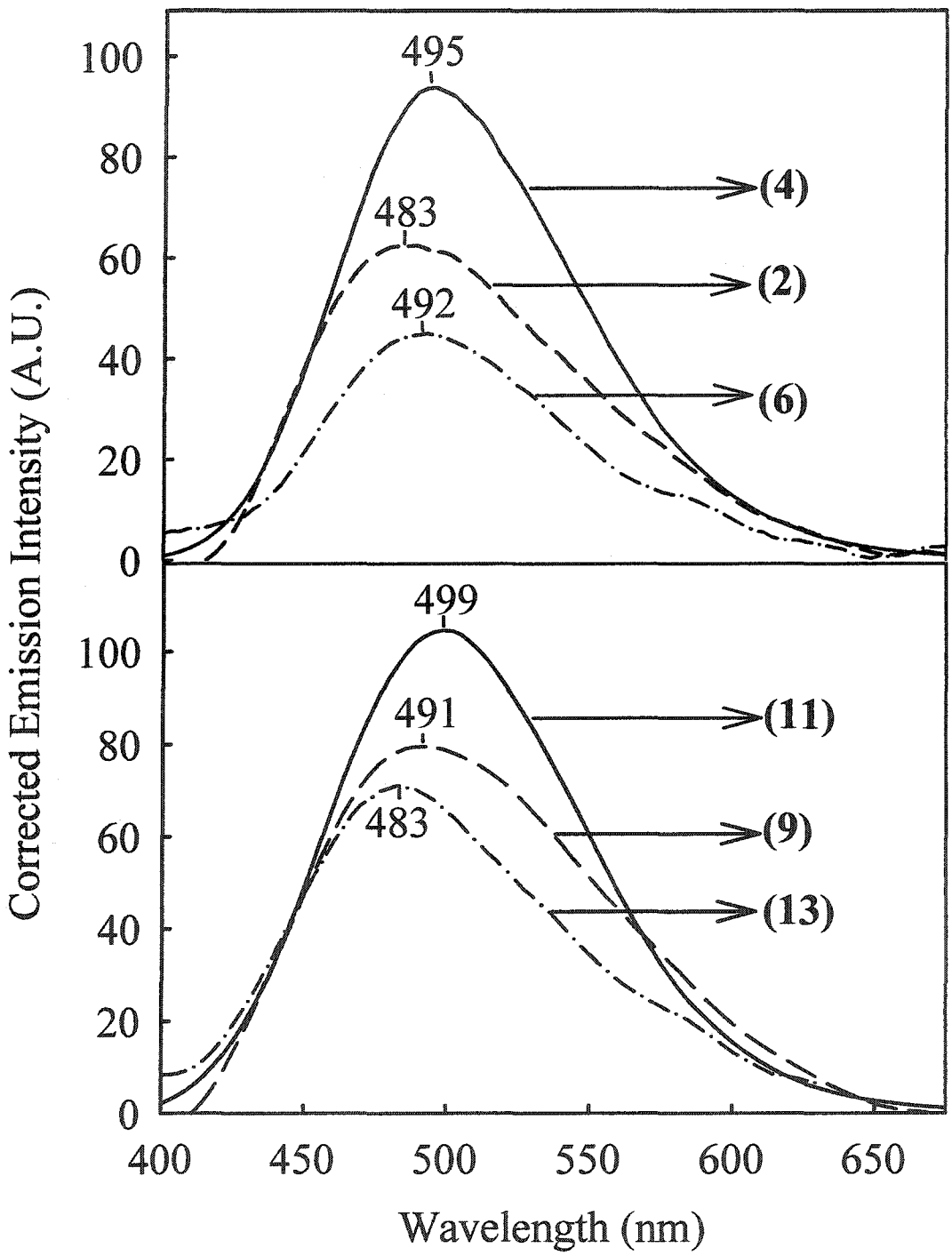

Fig. 3 Comparison of the solid state emission spectra for(**2, 4, 6, 9, 11** and **13**) at room temperature. The intensity has not been normalized so the bands could be distinguished.

Luminescent 1-D and Zig-Zag Organometallic Polymers Built Upon Diphosphine and Diisocyanide Ligands, and Copper(I) and Silver(I)

Eric Fournier, Frédéric Lebrun and Pierre D. Harvey*

Supporting Information

Table of contents

Table S1. Crystal data and structure refinement for $\{[Ag(dpppen)(CN\text{-}t\text{-}Bu)_2](BF_4)\}_n$.

Empirical formula	C39 H48 Ag B F4 N2 P2	
Formula weight	801.41	
Temperature	198(1) K	
Wavelength	0.71073 Å	
Diffractometer used	Bruker AXS P4/SMART 1000	
Detector distance	6 cm	
Monochrometer used	Graphite	
Crystal size	0.175 x 0.175 x 0.325 mm^3	
Colour and habit	Colourless, irregular	
Crystal system	Triclinic	
Space group	P1	
Unit cell dimensions	a = 8.7574(9) Å	α = 86.462(2)°
	b = 14.8390(16) Å	β = 77.099(2)°
	c = 16.7222(18) Å	γ = 73.170(2)°
Volume	2027.5(4) $Å^3$	
Z	2	
Density (calculated)	1.313 Mg/m^3	
Absorption coefficient	0.622 mm^{-1}	
F(000)	828	
Theta range for data collection	1.25 to 25.00°	
Completeness to theta = 25.00°	93.7 %	
Scan type	ω and ϕ	
Scan range	0.3°	
Exposure time	30s	
Index ranges	$-10 \leq h \leq 10$, $-15 \leq k \leq 17$, $-19 \leq l \leq 19$	

Standard reflections collection	50 frames at beginning and end of data
Crystal stability	no decay
Reflections collected	10516
Independent reflections	9001 [R(int) = 0.0125]
System used	SHELXL 5.1
Solution	Direct methods
Hydrogen atoms	Calculated positions, riding model
Absorption correction	SADABS
Min./Max. transmission ratio	0.936
Refinement method	Full-matrix least-squares on F^2
Data / restraints / parameters	9001 / 3 / 922
Goodness-of-fit on F^2	1.036
Final R indices [I>2sigma(I)]	R1 = 0.0402, wR2 = 0.1053
R indices (all data)	R1 = 0.0415, wR2 = 0.1068
Largest/mean shift/esd	0.000/0.000
Absolute structure parameter	0.01(2)
Largest diff. peak and hole[1]	1.906 and -0.458 e.Å^{-3}

$wR2 = (\Sigma[w(F_o^2-F_c^2)^2]/\Sigma[F_o^4])^{1/2}$

$R1 = \Sigma \| |F_o| - |F_c| | / \Sigma |F_o|$

$Weight = 1 / [\sigma^2(F_o^2) + (0.0657 * P)^2 + (1.6 * P)]$

where $P = (\max(F_o^2, 0) + 2 * F_c^2)/3$

1: near Ag(2)

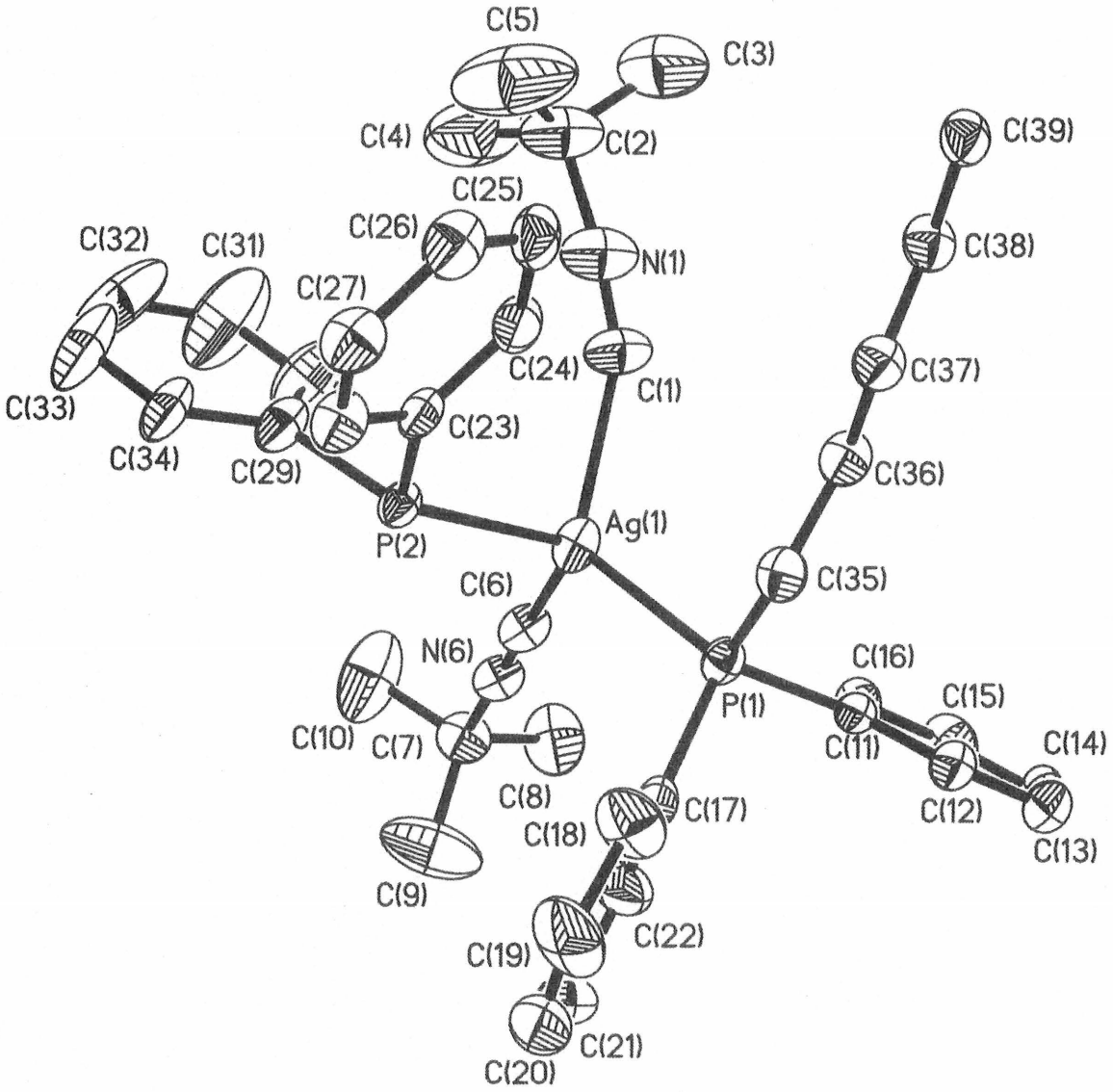

Figure S1. Numbering scheme for $\{[Ag(dpppen)(CN\text{-}t\text{-}Bu)_2](BF_4)\}_n$.

Table S2. Atomic coordinates (x 10^4) and equivalent isotropic displacement parameters ($Å^2$x 10^3) for{[Ag(dpppen)(CN-*t*-Bu)$_2$](BF$_4$)}$_n$. U(eq) is defined as one third of the trace of the orthogonalized U^{ij} tensor.

	x	y	z	U(eq)
Ag(1)	10188(1)	6481(1)	4784(1)	55(1)
P(1)	8636(2)	6566(1)	6219(1)	44(1)
P(2)	12067(2)	4833(1)	4596(1)	45(1)
C(1)	8820(11)	6402(6)	3752(5)	78(2)
N(1)	8648(11)	6099(6)	3179(5)	95(2)
C(2)	8626(17)	5657(9)	2424(7)	114(4)
C(3)	6990(20)	6099(11)	2238(9)	149(5)
C(4)	9920(20)	5950(15)	1701(8)	184(8)
C(5)	8900(30)	4595(9)	2550(11)	212(11)
C(6)	11488(9)	7553(5)	4460(4)	57(2)
N(6)	12210(7)	8104(4)	4360(3)	55(1)
C(7)	13171(10)	8781(5)	4221(5)	67(2)
C(8)	12029(13)	9747(6)	4216(8)	109(3)
C(9)	14070(20)	8651(11)	4889(9)	154(6)
C(10)	14352(17)	8519(8)	3391(8)	143(5)
C(11)	7188(7)	7669(4)	6640(4)	44(1)
C(12)	6125(8)	7710(5)	7398(4)	57(2)
C(13)	5083(9)	8557(6)	7712(5)	71(2)
C(14)	5091(9)	9358(6)	7281(6)	75(2)
C(15)	6114(10)	9340(5)	6521(6)	76(2)
C(16)	7164(8)	8488(4)	6197(5)	54(2)
C(17)	10004(8)	6241(5)	6940(4)	57(2)

C(18)	10245(11)	5398(7)	7357(5)	86(3)
C(19)	11380(13)	5164(10)	7851(6)	114(4)
C(20)	12220(13)	5770(11)	7957(6)	109(4)
C(21)	12009(13)	6583(9)	7556(7)	104(4)
C(22)	10901(10)	6836(6)	7019(6)	79(2)
C(23)	11183(7)	3845(4)	4750(4)	49(2)
C(24)	9649(8)	3973(5)	4588(5)	62(2)
C(25)	8971(9)	3209(5)	4650(5)	67(2)
C(26)	9824(10)	2355(6)	4880(5)	70(2)
C(27)	11347(10)	2204(5)	5056(5)	69(2)
C(28)	12016(9)	2948(5)	4976(5)	60(2)
C(29)	13402(8)	4616(5)	3571(5)	65(2)
C(30)	13097(16)	5249(8)	2961(6)	110(4)
C(31)	14040(20)	5101(12)	2174(8)	173(7)
C(32)	15270(20)	4301(13)	2005(8)	163(8)
C(33)	15650(15)	3674(8)	2595(8)	127(5)
C(34)	14688(10)	3817(6)	3391(5)	79(2)
C(35)	7443(8)	5737(4)	6399(4)	52(1)
C(36)	6182(8)	5962(4)	5874(4)	56(2)
C(37)	5370(8)	5199(5)	5868(4)	55(2)
C(38)	4261(8)	5372(5)	5285(4)	57(2)
C(39)	3456(8)	4578(5)	5291(4)	55(2)
Ag(2)	2690(1)	718(1)	9654(1)	41(1)
P(3)	2951(2)	2367(1)	9424(1)	37(1)
P(4)	1189(2)	802(1)	11128(1)	35(1)
C(40)	1378(7)	436(4)	8752(4)	46(1)
N(40)	732(6)	402(4)	8237(3)	50(1)
C(41)	-106(9)	371(6)	7570(4)	69(2)
C(42)	260(20)	1108(18)	6978(9)	231(13)

C(43)	-1907(9)	611(7)	7912(6)	89(3)
C(44)	552(16)	-599(11)	7207(9)	168(8)
C(45)	5051(7)	-392(4)	9607(4)	48(1)
N(45)	6144(7)	-980(4)	9702(3)	55(1)
C(46)	7556(9)	-1746(5)	9847(5)	71(2)
C(47)	7969(15)	-2491(7)	9228(9)	138(5)
C(48)	6960(20)	-2217(11)	10636(11)	195(8)
C(49)	8882(16)	-1356(8)	9873(14)	197(10)
C(50)	4073(6)	2602(4)	8409(3)	40(1)
C(51)	4927(8)	3267(5)	8262(4)	54(2)
C(52)	5763(9)	3378(5)	7468(5)	67(2)
C(53)	5706(9)	2853(6)	6829(4)	69(2)
C(54)	4816(10)	2226(5)	6961(4)	65(2)
C(55)	4016(8)	2091(4)	7746(4)	53(2)
C(56)	1037(7)	3305(5)	9529(4)	49(2)
C(57)	758(12)	4145(7)	9880(7)	95(3)
C(58)	-712(15)	4840(8)	9902(8)	127(5)
C(59)	-1895(12)	4700(9)	9607(8)	115(4)
C(60)	-1679(10)	3881(9)	9292(9)	118(5)
C(61)	-186(9)	3157(6)	9220(7)	86(3)
C(62)	779(6)	-255(4)	11640(3)	39(1)
C(63)	-254(8)	-204(5)	12405(4)	53(1)
C(64)	-474(10)	-1034(6)	12790(5)	70(2)
C(65)	377(13)	-1877(6)	12421(5)	83(2)
C(66)	1415(11)	-1933(5)	11663(5)	78(2)
C(67)	1595(8)	-1119(4)	11266(4)	53(2)
C(68)	2237(7)	1170(4)	11822(3)	40(1)
C(69)	3806(7)	602(4)	11840(4)	49(1)
C(70)	4675(9)	820(6)	12363(4)	59(2)

C(71)	4016(9)	1608(5)	12856(4)	60(2)
C(72)	2488(9)	2177(6)	12826(4)	66(2)
C(73)	1590(8)	1958(5)	12313(4)	56(2)
C(74)	4013(7)	2676(4)	10142(3)	41(1)
C(75)	5663(6)	1968(4)	10118(3)	40(1)
C(76)	6560(6)	2177(4)	10729(4)	40(1)
C(77)	8168(7)	1424(4)	10714(3)	43(1)
C(78)	9190(7)	1672(4)	11270(3)	41(1)
B(1)	3630(12)	6170(9)	9811(6)	81(3)
B(2)	6631(13)	1071(10)	4622(9)	93(3)
F(1)	4339(7)	6325(4)	10423(4)	111(2)
F(2)	4356(12)	6499(9)	9123(5)	182(4)
F(3)	2031(7)	6491(5)	9973(5)	135(2)
F(4)	4042(8)	5222(5)	9688(6)	144(3)
F(5)	7793(8)	673(6)	5025(7)	167(4)
F(6)	6085(14)	2008(12)	4927(8)	124(5)
F(7)	5380(30)	753(17)	4690(30)	257(16)
F(8)	7240(20)	1281(18)	3809(10)	173(9)
F(6A)	6550(40)	350(30)	4139(18)	167(14)
F(7A)	6620(70)	1770(40)	4180(50)	280(30)
F(8A)	5160(30)	1130(20)	5125(13)	136(15)

Table S3. Bond lengths [Å] and angles [°] for $\{[Ag(dpppen)(CN\text{-}t\text{-}Bu)_2](BF_4)\}_n$.

Ag(1)-C(6)	2.189(7)	Ag(1)-C(1)	2.335(8)
Ag(1)-P(1)	2.4706(15)	Ag(1)-P(2)	2.5136(16)
P(1)-C(35)	1.804(6)	P(1)-C(11)	1.823(6)
P(1)-C(17)	1.833(7)	P(2)-C(39)#1	1.813(7)
P(2)-C(23)	1.826(6)	P(2)-C(29)	1.833(7)
C(1)-N(1)	1.141(10)	N(1)-C(2)	1.463(12)
C(2)-C(3)	1.489(18)	C(2)-C(5)	1.532(18)
C(2)-C(4)	1.597(18)	C(3)-H(3A)	0.9600
C(3)-H(3B)	0.9600	C(3)-H(3C)	0.9600
C(4)-H(4A)	0.9600	C(4)-H(4B)	0.9600
C(4)-H(4C)	0.9600	C(5)-H(5A)	0.9600
C(5)-H(5B)	0.9600	C(5)-H(5C)	0.9600
C(6)-N(6)	1.154(8)	N(6)-C(7)	1.465(9)
C(7)-C(9)	1.479(14)	C(7)-C(8)	1.492(12)
C(7)-C(10)	1.529(13)	C(8)-H(8A)	0.9600
C(8)-H(8B)	0.9600	C(8)-H(8C)	0.9600
C(9)-H(9A)	0.9600	C(9)-H(9B)	0.9600
C(9)-H(9C)	0.9600	C(10)-H(10A)	0.9600
C(10)-H(10B)	0.9600	C(10)-H(10C)	0.9600
C(11)-C(16)	1.381(9)	C(11)-C(12)	1.388(9)
C(12)-C(13)	1.376(10)	C(12)-H(12)	0.9300
C(13)-C(14)	1.352(11)	C(13)-H(13)	0.9300
C(14)-C(15)	1.378(12)	C(14)-H(14)	0.9300
C(15)-C(16)	1.387(10)	C(15)-H(15)	0.9300
C(16)-H(16)	0.9300	C(17)-C(22)	1.370(11)
C(17)-C(18)	1.377(10)	C(18)-C(19)	1.387(13)
C(18)-H(18)	0.9300	C(19)-C(20)	1.358(17)

C(19)-H(19)	0.9300	C(20)-C(21)	1.328(17)
C(20)-H(20)	0.9300	C(21)-C(22)	1.423(13)
C(21)-H(21)	0.9300	C(22)-H(22)	0.9300
C(23)-C(24)	1.387(10)	C(23)-C(28)	1.394(10)
C(24)-C(25)	1.413(9)	C(24)-H(24)	0.9300
C(25)-C(26)	1.354(12)	C(25)-H(25)	0.9300
C(26)-C(27)	1.382(11)	C(26)-H(26)	0.9300
C(27)-C(28)	1.379(10)	C(27)-H(27)	0.9300
C(28)-H(28)	0.9300	C(29)-C(30)	1.361(13)
C(29)-C(34)	1.373(11)	C(30)-C(31)	1.381(15)
C(30)-H(30)	0.9300	C(31)-C(32)	1.35(2)
C(31)-H(31)	0.9300	C(32)-C(33)	1.34(2)
C(32)-H(32)	0.9300	C(33)-C(34)	1.399(13)
C(33)-H(33)	0.9300	C(34)-H(34)	0.9300
C(35)-C(36)	1.512(9)	C(35)-H(35A)	0.9700
C(35)-H(35B)	0.9700	C(36)-C(37)	1.503(8)
C(36)-H(36A)	0.9700	C(36)-H(36B)	0.9700
C(37)-C(38)	1.485(9)	C(37)-H(37A)	0.9700
C(37)-H(37B)	0.9700	C(38)-C(39)	1.537(8)
C(38)-H(38A)	0.9700	C(38)-H(38B)	0.9700
C(39)-P(2)#2	1.813(7)	C(39)-H(39A)	0.9700
C(39)-H(39B)	0.9700	Ag(2)-C(40)	2.214(6)
Ag(2)-C(45)	2.228(6)	Ag(2)-P(4)	2.5132(14)
Ag(2)-P(3)	2.5213(14)	P(3)-C(56)	1.824(6)
P(3)-C(74)	1.824(6)	P(3)-C(50)	1.829(6)
P(4)-C(68)	1.825(5)	P(4)-C(78)#2	1.826(5)
P(4)-C(62)	1.827(5)	C(40)-N(40)	1.141(7)
N(40)-C(41)	1.476(8)	C(41)-C(42)	1.486(17)
C(41)-C(43)	1.497(11)	C(41)-C(44)	1.498(14)

C(42)-H(42A)	0.9600	C(42)-H(42B)	0.9600
C(42)-H(42C)	0.9600	C(43)-H(43A)	0.9600
C(43)-H(43B)	0.9600	C(43)-H(43C)	0.9600
C(44)-H(44A)	0.9600	C(44)-H(44B)	0.9600
C(44)-H(44C)	0.9600	C(45)-N(45)	1.127(8)
N(45)-C(46)	1.472(8)	C(46)-C(49)	1.449(15)
C(46)-C(47)	1.471(13)	C(46)-C(48)	1.513(18)
C(47)-H(47A)	0.9600	C(47)-H(47B)	0.9600
C(47)-H(47C)	0.9600	C(48)-H(48A)	0.9600
C(48)-H(48B)	0.9600	C(48)-H(48C)	0.9600
C(49)-H(49A)	0.9600	C(49)-H(49B)	0.9600
C(49)-H(49C)	0.9600	C(50)-C(51)	1.381(8)
C(50)-C(55)	1.400(9)	C(51)-C(52)	1.391(9)
C(51)-H(51)	0.9300	C(52)-C(53)	1.379(11)
C(52)-H(52)	0.9300	C(53)-C(54)	1.357(11)
C(53)-H(53)	0.9300	C(54)-C(55)	1.375(9)
C(54)-H(54)	0.9300	C(55)-H(55)	0.9300
C(56)-C(57)	1.344(12)	C(56)-C(61)	1.364(10)
C(57)-C(58)	1.392(12)	C(57)-H(57)	0.9300
C(58)-C(59)	1.313(17)	C(58)-H(58)	0.9300
C(59)-C(60)	1.301(17)	C(59)-H(59)	0.9300
C(60)-C(61)	1.418(13)	C(60)-H(60)	0.9300
C(61)-H(61)	0.9300	C(62)-C(63)	1.384(8)
C(62)-C(67)	1.385(8)	C(63)-C(64)	1.398(9)
C(63)-H(63)	0.9300	C(64)-C(65)	1.360(12)
C(64)-H(64)	0.9300	C(65)-C(66)	1.377(12)
C(65)-H(65)	0.9300	C(66)-C(67)	1.374(10)
C(66)-H(66)	0.9300	C(67)-H(67)	0.9300
C(68)-C(73)	1.375(8)	C(68)-C(69)	1.394(8)

C(69)-C(70)	1.386(9)	C(69)-H(69)	0.9300
C(70)-C(71)	1.376(10)	C(70)-H(70)	0.9300
C(71)-C(72)	1.370(11)	C(71)-H(71)	0.9300
C(72)-C(73)	1.394(9)	C(72)-H(72)	0.9300
C(73)-H(73)	0.9300	C(74)-C(75)	1.514(7)
C(74)-H(74A)	0.9700	C(74)-H(74B)	0.9700
C(75)-C(76)	1.515(7)	C(75)-H(75A)	0.9700
C(75)-H(75B)	0.9700	C(76)-C(77)	1.520(7)
C(76)-H(76A)	0.9700	C(76)-H(76B)	0.9700
C(77)-C(78)	1.551(7)	C(77)-H(77A)	0.9700
C(77)-H(77B)	0.9700	C(78)-P(4)#1	1.826(5)
C(78)-H(78A)	0.9700	C(78)-H(78B)	0.9700
B(1)-F(3)	1.312(11)	B(1)-F(2)	1.323(13)
B(1)-F(4)	1.364(13)	B(1)-F(1)	1.371(11)
B(2)-F(7A)	1.23(2)	B(2)-F(7)	1.291(16)
B(2)-F(5)	1.322(13)	B(2)-F(8A)	1.36(3)
B(2)-F(8)	1.40(2)	B(2)-F(6A)	1.41(3)
B(2)-F(6)	1.420(19)	F(6)-F(7A)	1.26(9)
F(6)-F(8A)	1.70(4)	F(7)-F(8A)	0.90(4)
F(7)-F(6A)	1.25(4)	F(8)-F(7A)	0.94(9)
F(8)-F(6A)	1.68(4)		
C(6)-Ag(1)-C(1)	109.0(3)	C(6)-Ag(1)-P(1)	114.30(17)
C(1)-Ag(1)-P(1)	117.6(2)	C(6)-Ag(1)-P(2)	112.69(19)
C(1)-Ag(1)-P(2)	96.2(2)	P(1)-Ag(1)-P(2)	105.56(5)
C(35)-P(1)-C(11)	103.9(3)	C(35)-P(1)-C(17)	105.4(3)
C(11)-P(1)-C(17)	103.3(3)	C(35)-P(1)-Ag(1)	111.0(2)
C(11)-P(1)-Ag(1)	120.5(2)	C(17)-P(1)-Ag(1)	111.4(2)
C(39)#1-P(2)-C(23)	103.3(3)	C(39)#1-P(2)-C(29)	104.5(3)
C(23)-P(2)-C(29)	103.6(3)	C(39)#1-P(2)-Ag(1)	111.8(2)

C(23)-P(2)-Ag(1)	118.9(2)	C(29)-P(2)-Ag(1)	113.3(3)
N(1)-C(1)-Ag(1)	155.2(9)	C(1)-N(1)-C(2)	173.5(11)
N(1)-C(2)-C(3)	106.7(11)	N(1)-C(2)-C(5)	110.2(10)
C(3)-C(2)-C(5)	110.1(12)	N(1)-C(2)-C(4)	107.4(9)
C(3)-C(2)-C(4)	106.7(12)	C(5)-C(2)-C(4)	115.2(15)
C(2)-C(3)-H(3A)	109.5	C(2)-C(3)-H(3B)	109.5
H(3A)-C(3)-H(3B)	109.5	C(2)-C(3)-H(3C)	109.5
H(3A)-C(3)-H(3C)	109.5	H(3B)-C(3)-H(3C)	109.5
C(2)-C(4)-H(4A)	109.5	C(2)-C(4)-H(4B)	109.5
H(4A)-C(4)-H(4B)	109.5	C(2)-C(4)-H(4C)	109.5
H(4A)-C(4)-H(4C)	109.5	H(4B)-C(4)-H(4C)	109.5
C(2)-C(5)-H(5A)	109.5	C(2)-C(5)-H(5B)	109.5
H(5A)-C(5)-H(5B)	109.5	C(2)-C(5)-H(5C)	109.5
H(5A)-C(5)-H(5C)	109.5	H(5B)-C(5)-H(5C)	109.5
N(6)-C(6)-Ag(1)	173.6(6)	C(6)-N(6)-C(7)	178.2(7)
N(6)-C(7)-C(9)	106.9(7)	N(6)-C(7)-C(8)	108.3(7)
C(9)-C(7)-C(8)	112.5(10)	N(6)-C(7)-C(10)	105.9(7)
C(9)-C(7)-C(10)	110.8(11)	C(8)-C(7)-C(10)	112.0(9)
C(7)-C(8)-H(8A)	109.5	C(7)-C(8)-H(8B)	109.5
H(8A)-C(8)-H(8B)	109.5	C(7)-C(8)-H(8C)	109.5
H(8A)-C(8)-H(8C)	109.5	H(8B)-C(8)-H(8C)	109.5
C(7)-C(9)-H(9A)	109.5	C(7)-C(9)-H(9B)	109.5
H(9A)-C(9)-H(9B)	109.5	C(7)-C(9)-H(9C)	109.5
H(9A)-C(9)-H(9C)	109.5	H(9B)-C(9)-H(9C)	109.5
C(7)-C(10)-H(10A)	109.5	C(7)-C(10)-H(10B)	109.5
H(10A)-C(10)-H(10B)	109.5	C(7)-C(10)-H(10C)	109.5
H(10A)-C(10)-H(10C)	109.5	H(10B)-C(10)-H(10C)	109.5
C(16)-C(11)-C(12)	119.1(6)	C(16)-C(11)-P(1)	119.1(5)
C(12)-C(11)-P(1)	121.8(5)	C(13)-C(12)-C(11)	120.5(7)

C(13)-C(12)-H(12)	119.8	C(11)-C(12)-H(12)	119.8
C(14)-C(13)-C(12)	120.0(7)	C(14)-C(13)-H(13)	120.0
C(12)-C(13)-H(13)	120.0	C(13)-C(14)-C(15)	121.0(7)
C(13)-C(14)-H(14)	119.5	C(15)-C(14)-H(14)	119.5
C(14)-C(15)-C(16)	119.5(7)	C(14)-C(15)-H(15)	120.2
C(16)-C(15)-H(15)	120.2	C(11)-C(16)-C(15)	119.9(7)
C(11)-C(16)-H(16)	120.0	C(15)-C(16)-H(16)	120.0
C(22)-C(17)-C(18)	119.2(7)	C(22)-C(17)-P(1)	118.0(6)
C(18)-C(17)-P(1)	122.6(6)	C(17)-C(18)-C(19)	119.9(10)
C(17)-C(18)-H(18)	120.0	C(19)-C(18)-H(18)	120.0
C(20)-C(19)-C(18)	120.9(11)	C(20)-C(19)-H(19)	119.5
C(18)-C(19)-H(19)	119.5	C(21)-C(20)-C(19)	119.8(10)
C(21)-C(20)-H(20)	120.1	C(19)-C(20)-H(20)	120.1
C(20)-C(21)-C(22)	121.0(11)	C(20)-C(21)-H(21)	119.5
C(22)-C(21)-H(21)	119.5	C(17)-C(22)-C(21)	119.0(10)
C(17)-C(22)-H(22)	120.5	C(21)-C(22)-H(22)	120.5
C(24)-C(23)-C(28)	118.0(6)	C(24)-C(23)-P(2)	118.7(5)
C(28)-C(23)-P(2)	123.2(5)	C(23)-C(24)-C(25)	120.3(7)
C(23)-C(24)-H(24)	119.9	C(25)-C(24)-H(24)	119.9
C(26)-C(25)-C(24)	119.3(7)	C(26)-C(25)-H(25)	120.3
C(24)-C(25)-H(25)	120.3	C(25)-C(26)-C(27)	122.0(7)
C(25)-C(26)-H(26)	119.0	C(27)-C(26)-H(26)	119.0
C(28)-C(27)-C(26)	118.3(7)	C(28)-C(27)-H(27)	120.9
C(26)-C(27)-H(27)	120.9	C(27)-C(28)-C(23)	122.1(7)
C(27)-C(28)-H(28)	118.9	C(23)-C(28)-H(28)	118.9
C(30)-C(29)-C(34)	118.4(8)	C(30)-C(29)-P(2)	119.6(7)
C(34)-C(29)-P(2)	121.9(7)	C(29)-C(30)-C(31)	121.6(12)
C(29)-C(30)-H(30)	119.2	C(31)-C(30)-H(30)	119.2
C(32)-C(31)-C(30)	119.0(14)	C(32)-C(31)-H(31)	120.5

C(30)-C(31)-H(31)	120.5	C(33)-C(32)-C(31)	121.4(11)
C(33)-C(32)-H(32)	119.3	C(31)-C(32)-H(32)	119.3
C(32)-C(33)-C(34)	119.7(11)	C(32)-C(33)-H(33)	120.1
C(34)-C(33)-H(33)	120.1	C(29)-C(34)-C(33)	119.8(10)
C(29)-C(34)-H(34)	120.1	C(33)-C(34)-H(34)	120.1
C(36)-C(35)-P(1)	111.0(4)	C(36)-C(35)-H(35A)	109.4
P(1)-C(35)-H(35A)	109.4	C(36)-C(35)-H(35B)	109.4
P(1)-C(35)-H(35B)	109.4	H(35A)-C(35)-H(35B)	108.0
C(37)-C(36)-C(35)	113.6(5)	C(37)-C(36)-H(36A)	108.8
C(35)-C(36)-H(36A)	108.8	C(37)-C(36)-H(36B)	108.8
C(35)-C(36)-H(36B)	108.8	H(36A)-C(36)-H(36B)	107.7
C(38)-C(37)-C(36)	113.7(5)	C(38)-C(37)-H(37A)	108.8
C(36)-C(37)-H(37A)	108.8	C(38)-C(37)-H(37B)	108.8
C(36)-C(37)-H(37B)	108.8	H(37A)-C(37)-H(37B)	107.7
C(37)-C(38)-C(39)	112.5(6)	C(37)-C(38)-H(38A)	109.1
C(39)-C(38)-H(38A)	109.1	C(37)-C(38)-H(38B)	109.1
C(39)-C(38)-H(38B)	109.1	H(38A)-C(38)-H(38B)	107.8
C(38)-C(39)-P(2)#2	111.1(5)	C(38)-C(39)-H(39A)	109.4
P(2)#2-C(39)-H(39A)	109.4	C(38)-C(39)-H(39B)	109.4
P(2)#2-C(39)-H(39B)	109.4	H(39A)-C(39)-H(39B)	108.0
C(40)-Ag(2)-C(45)	111.3(2)	C(40)-Ag(2)-P(4)	115.65(15)
C(45)-Ag(2)-P(4)	105.58(16)	C(40)-Ag(2)-P(3)	108.20(17)
C(45)-Ag(2)-P(3)	114.43(16)	P(4)-Ag(2)-P(3)	101.49(5)
C(56)-P(3)-C(74)	105.0(3)	C(56)-P(3)-C(50)	102.1(3)
C(74)-P(3)-C(50)	104.8(3)	C(56)-P(3)-Ag(2)	115.9(2)
C(74)-P(3)-Ag(2)	111.85(18)	C(50)-P(3)-Ag(2)	115.92(19)
C(68)-P(4)-C(78)#2	105.0(3)	C(68)-P(4)-C(62)	101.5(2)
C(78)#2-P(4)-C(62)	104.6(3)	C(68)-P(4)-Ag(2)	113.14(18)
C(78)#2-P(4)-Ag(2)	111.17(19)	C(62)-P(4)-Ag(2)	119.91(18)

N(40)-C(40)-Ag(2)	170.7(6)	C(40)-N(40)-C(41)	179.2(7)
N(40)-C(41)-C(42)	105.7(8)	N(40)-C(41)-C(43)	109.0(6)
C(42)-C(41)-C(43)	109.5(11)	N(40)-C(41)-C(44)	107.8(7)
C(42)-C(41)-C(44)	112.9(13)	C(43)-C(41)-C(44)	111.7(9)
C(41)-C(42)-H(42A)	109.5	C(41)-C(42)-H(42B)	109.5
H(42A)-C(42)-H(42B)	109.5	C(41)-C(42)-H(42C)	109.5
H(42A)-C(42)-H(42C)	109.5	H(42B)-C(42)-H(42C)	109.5
C(41)-C(43)-H(43A)	109.5	C(41)-C(43)-H(43B)	109.5
H(43A)-C(43)-H(43B)	109.5	C(41)-C(43)-H(43C)	109.5
H(43A)-C(43)-H(43C)	109.5	H(43B)-C(43)-H(43C)	109.5
C(41)-C(44)-H(44A)	109.5	C(41)-C(44)-H(44B)	109.5
H(44A)-C(44)-H(44B)	109.5	C(41)-C(44)-H(44C)	109.5
H(44A)-C(44)-H(44C)	109.5	H(44B)-C(44)-H(44C)	109.5
N(45)-C(45)-Ag(2)	169.6(6)	C(45)-N(45)-C(46)	178.6(7)
C(49)-C(46)-C(47)	114.4(11)	C(49)-C(46)-N(45)	109.0(7)
C(47)-C(46)-N(45)	109.6(7)	C(49)-C(46)-C(48)	114.0(13)
C(47)-C(46)-C(48)	103.2(11)	N(45)-C(46)-C(48)	106.3(8)
C(46)-C(47)-H(47A)	109.5	C(46)-C(47)-H(47B)	109.5
H(47A)-C(47)-H(47B)	109.5	C(46)-C(47)-H(47C)	109.5
H(47A)-C(47)-H(47C)	109.5	H(47B)-C(47)-H(47C)	109.5
C(46)-C(48)-H(48A)	109.5	C(46)-C(48)-H(48B)	109.5
H(48A)-C(48)-H(48B)	109.5	C(46)-C(48)-H(48C)	109.5
H(48A)-C(48)-H(48C)	109.5	H(48B)-C(48)-H(48C)	109.5
C(46)-C(49)-H(49A)	109.5	C(46)-C(49)-H(49B)	109.5
H(49A)-C(49)-H(49B)	109.5	C(46)-C(49)-H(49C)	109.5
H(49A)-C(49)-H(49C)	109.5	H(49B)-C(49)-H(49C)	109.5
C(51)-C(50)-C(55)	118.7(5)	C(51)-C(50)-P(3)	123.9(5)
C(55)-C(50)-P(3)	117.4(4)	C(50)-C(51)-C(52)	119.2(6)
C(50)-C(51)-H(51)	120.4	C(52)-C(51)-H(51)	120.4

C(53)-C(52)-C(51)	120.7(7)	C(53)-C(52)-H(52)	119.6
C(51)-C(52)-H(52)	119.6	C(54)-C(53)-C(52)	120.5(7)
C(54)-C(53)-H(53)	119.7	C(52)-C(53)-H(53)	119.7
C(53)-C(54)-C(55)	119.4(7)	C(53)-C(54)-H(54)	120.3
C(55)-C(54)-H(54)	120.3	C(54)-C(55)-C(50)	121.3(6)
C(54)-C(55)-H(55)	119.3	C(50)-C(55)-H(55)	119.3
C(57)-C(56)-C(61)	117.5(7)	C(57)-C(56)-P(3)	124.2(6)
C(61)-C(56)-P(3)	118.3(6)	C(56)-C(57)-C(58)	120.7(10)
C(56)-C(57)-H(57)	119.7	C(58)-C(57)-H(57)	119.7
C(59)-C(58)-C(57)	122.0(12)	C(59)-C(58)-H(58)	119.0
C(57)-C(58)-H(58)	119.0	C(60)-C(59)-C(58)	118.5(9)
C(60)-C(59)-H(59)	120.8	C(58)-C(59)-H(59)	120.8
C(59)-C(60)-C(61)	122.2(10)	C(59)-C(60)-H(60)	118.9
C(61)-C(60)-H(60)	118.9	C(56)-C(61)-C(60)	119.0(10)
C(56)-C(61)-H(61)	120.5	C(60)-C(61)-H(61)	120.5
C(63)-C(62)-C(67)	120.2(5)	C(63)-C(62)-P(4)	121.2(4)
C(67)-C(62)-P(4)	118.5(4)	C(62)-C(63)-C(64)	119.3(6)
C(62)-C(63)-H(63)	120.4	C(64)-C(63)-H(63)	120.4
C(65)-C(64)-C(63)	119.4(7)	C(65)-C(64)-H(64)	120.3
C(63)-C(64)-H(64)	120.3	C(64)-C(65)-C(66)	121.6(7)
C(64)-C(65)-H(65)	119.2	C(66)-C(65)-H(65)	119.2
C(67)-C(66)-C(65)	119.4(7)	C(67)-C(66)-H(66)	120.3
C(65)-C(66)-H(66)	120.3	C(66)-C(67)-C(62)	120.0(6)
C(66)-C(67)-H(67)	120.0	C(62)-C(67)-H(67)	120.0
C(73)-C(68)-C(69)	118.9(5)	C(73)-C(68)-P(4)	124.6(5)
C(69)-C(68)-P(4)	116.5(4)	C(70)-C(69)-C(68)	120.2(6)
C(70)-C(69)-H(69)	119.9	C(68)-C(69)-H(69)	119.9
C(71)-C(70)-C(69)	120.5(7)	C(71)-C(70)-H(70)	119.7
C(69)-C(70)-H(70)	119.7	C(72)-C(71)-C(70)	119.4(6)

C(72)-C(71)-H(71)	120.3	C(70)-C(71)-H(71)	120.3
C(71)-C(72)-C(73)	120.7(7)	C(71)-C(72)-H(72)	119.7
C(73)-C(72)-H(72)	119.7	C(68)-C(73)-C(72)	120.3(6)
C(68)-C(73)-H(73)	119.9	C(72)-C(73)-H(73)	119.9
C(75)-C(74)-P(3)	111.8(4)	C(75)-C(74)-H(74A)	109.3
P(3)-C(74)-H(74A)	109.3	C(75)-C(74)-H(74B)	109.3
P(3)-C(74)-H(74B)	109.3	H(74A)-C(74)-H(74B)	107.9
C(74)-C(75)-C(76)	113.5(4)	C(74)-C(75)-H(75A)	108.9
C(76)-C(75)-H(75A)	108.9	C(74)-C(75)-H(75B)	108.9
C(76)-C(75)-H(75B)	108.9	H(75A)-C(75)-H(75B)	107.7
C(75)-C(76)-C(77)	111.7(4)	C(75)-C(76)-H(76A)	109.3
C(77)-C(76)-H(76A)	109.3	C(75)-C(76)-H(76B)	109.3
C(77)-C(76)-H(76B)	109.3	H(76A)-C(76)-H(76B)	107.9
C(76)-C(77)-C(78)	112.7(4)	C(76)-C(77)-H(77A)	109.1
C(78)-C(77)-H(77A)	109.1	C(76)-C(77)-H(77B)	109.1
C(78)-C(77)-H(77B)	109.1	H(77A)-C(77)-H(77B)	107.8
C(77)-C(78)-P(4)#1	109.8(4)	C(77)-C(78)-H(78A)	109.7
P(4)#1-C(78)-H(78A)	109.7	C(77)-C(78)-H(78B)	109.7
P(4)#1-C(78)-H(78B)	109.7	H(78A)-C(78)-H(78B)	108.2
F(3)-B(1)-F(2)	114.0(10)	F(3)-B(1)-F(4)	108.1(10)
F(2)-B(1)-F(4)	104.7(9)	F(3)-B(1)-F(1)	114.2(8)
F(2)-B(1)-F(1)	107.3(9)	F(4)-B(1)-F(1)	107.9(8)
F(7A)-B(2)-F(7)	115.6(18)	F(7A)-B(2)-F(5)	123.6(14)
F(7)-B(2)-F(5)	120.7(15)	F(7A)-B(2)-F(8A)	113(4)
F(7)-B(2)-F(8A)	39.5(18)	F(5)-B(2)-F(8A)	109.0(15)
F(7A)-B(2)-F(8)	41(4)	F(7)-B(2)-F(8)	112(2)
F(5)-B(2)-F(8)	113.2(12)	F(8A)-B(2)-F(8)	137.8(15)
F(7A)-B(2)-F(6A)	108(4)	F(7)-B(2)-F(6A)	54.7(17)
F(5)-B(2)-F(6A)	105.5(17)	F(8A)-B(2)-F(6A)	93.9(18)

F(8)-B(2)-F(6A)	73.6(17)	F(7A)-B(2)-F(6)	56(4)
F(7)-B(2)-F(6)	108.8(19)	F(5)-B(2)-F(6)	102.0(11)
F(8A)-B(2)-F(6)	75.6(16)	F(8)-B(2)-F(6)	97.0(14)
F(6A)-B(2)-F(6)	152.5(17)	F(7A)-F(6)-B(2)	54.4(19)
F(7A)-F(6)-F(8A)	92.1(16)	B(2)-F(6)-F(8A)	50.5(10)
F(8A)-F(7)-F(6A)	140(3)	F(8A)-F(7)-B(2)	74(2)
F(6A)-F(7)-B(2)	67.5(18)	F(7A)-F(8)-B(2)	60(2)
F(7A)-F(8)-F(6A)	106(3)	B(2)-F(8)-F(6A)	53.6(13)
F(7)-F(6A)-B(2)	57.8(13)	F(7)-F(6A)-F(8)	98(2)
B(2)-F(6A)-F(8)	52.8(16)	F(8)-F(7A)-B(2)	79(3)
F(8)-F(7A)-F(6)	146(3)	B(2)-F(7A)-F(6)	69(3)
F(7)-F(8A)-B(2)	66(2)	F(7)-F(8A)-F(6)	112(3)
B(2)-F(8A)-F(6)	53.9(15)		

Symmetry transformations used to generate equivalent atoms:

#1 x+1,y,z #2 x-1,y,z

Table S4. Anisotropic displacement parameters ($Å^2 x\ 10^3$) for {[Ag(dpppen)(CN-*t*-Bu)$_2$](BF$_4$)}$_n$. The anisotropic displacement factor exponent takes the form: $-2\pi^2[\ h^2 a^{*2} U^{11} + ... + 2\ h\ k\ a^*\ b^*\ U^{12}\ ]$

	U^{11}	U^{22}	U^{33}	U^{23}	U^{13}	U^{12}
Ag(1)	62(1)	43(1)	52(1)	1(1)	3(1)	-13(1)
P(1)	47(1)	38(1)	41(1)	-1(1)	-6(1)	-5(1)
P(2)	46(1)	40(1)	46(1)	-9(1)	1(1)	-17(1)
C(1)	105(6)	89(6)	55(5)	1(4)	-27(4)	-45(5)
N(1)	132(7)	107(6)	73(5)	13(4)	-37(4)	-67(5)
C(2)	157(11)	130(10)	85(7)	-2(6)	-47(7)	-71(9)
C(3)	190(15)	156(13)	126(11)	-5(9)	-73(11)	-58(11)
C(4)	226(19)	270(20)	93(9)	-28(11)	-21(11)	-123(17)
C(5)	370(30)	87(9)	222(19)	-1(10)	-190(20)	-35(13)
C(6)	73(4)	49(4)	48(4)	1(3)	-9(3)	-19(3)
N(6)	70(3)	48(3)	48(3)	4(2)	-12(3)	-19(3)
C(7)	76(5)	54(4)	78(5)	6(4)	-17(4)	-31(4)
C(8)	104(7)	56(5)	168(11)	-4(6)	-16(7)	-34(5)
C(9)	207(15)	173(13)	167(12)	72(10)	-115(12)	-142(12)
C(10)	153(11)	91(7)	152(11)	-3(7)	60(9)	-50(7)
C(11)	39(3)	46(3)	45(3)	-10(3)	-12(2)	-5(2)
C(12)	51(3)	60(4)	54(4)	-10(3)	-11(3)	-6(3)
C(13)	58(4)	80(6)	71(5)	-30(4)	-6(4)	-11(4)
C(14)	51(4)	59(5)	103(6)	-36(5)	-5(4)	1(3)
C(15)	72(5)	46(4)	110(7)	-3(4)	-29(5)	-8(3)
C(16)	51(3)	37(3)	71(4)	-9(3)	-13(3)	-6(3)
C(17)	46(3)	68(4)	43(3)	-5(3)	-5(3)	4(3)

C(18)	83(5)	97(6)	79(5)	40(5)	-36(5)	-21(5)
C(19)	84(6)	155(11)	91(7)	52(7)	-41(6)	-7(7)
C(20)	80(6)	155(11)	74(6)	-10(7)	-36(5)	13(7)
C(21)	80(6)	130(9)	102(8)	-52(7)	-42(6)	-2(6)
C(22)	72(5)	64(5)	106(6)	-21(4)	-41(5)	-5(4)
C(23)	49(3)	46(3)	47(3)	-15(3)	8(3)	-17(3)
C(24)	52(4)	57(4)	71(4)	-18(3)	5(3)	-17(3)
C(25)	47(4)	69(5)	79(5)	-15(4)	12(3)	-23(3)
C(26)	72(5)	65(5)	72(5)	-4(4)	9(4)	-34(4)
C(27)	81(5)	52(4)	74(5)	0(3)	-7(4)	-27(4)
C(28)	67(4)	46(4)	63(4)	2(3)	0(3)	-23(3)
C(29)	65(4)	62(4)	65(4)	-22(4)	18(3)	-37(4)
C(30)	155(10)	89(7)	63(5)	-2(5)	21(6)	-33(7)
C(31)	246(18)	144(12)	78(8)	4(8)	68(10)	-53(12)
C(32)	254(19)	143(12)	84(8)	-58(9)	79(10)	-119(13)
C(33)	129(9)	85(7)	141(11)	-61(8)	68(8)	-50(7)
C(34)	76(5)	62(5)	88(6)	-39(4)	25(4)	-27(4)
C(35)	55(3)	41(3)	56(4)	2(3)	-10(3)	-11(3)
C(36)	62(4)	47(4)	58(4)	-1(3)	-3(3)	-22(3)
C(37)	56(4)	53(4)	55(4)	1(3)	-6(3)	-19(3)
C(38)	56(4)	52(4)	63(4)	4(3)	-7(3)	-22(3)
C(39)	48(3)	52(4)	64(4)	-5(3)	-2(3)	-20(3)
Ag(2)	39(1)	43(1)	40(1)	0(1)	-11(1)	-9(1)
P(3)	32(1)	37(1)	41(1)	3(1)	-9(1)	-6(1)
P(4)	35(1)	38(1)	33(1)	-4(1)	-11(1)	-7(1)
C(40)	40(3)	57(4)	41(3)	-4(3)	-11(3)	-11(3)
N(40)	41(3)	56(3)	53(3)	-9(2)	-9(2)	-11(2)
C(41)	68(4)	96(6)	47(4)	-10(4)	-23(3)	-15(4)
C(42)	188(15)	460(40)	125(11)	172(18)	-111(11)	-200(20)

C(43)	58(4)	120(7)	94(6)	-13(5)	-43(4)	-11(4)
C(44)	131(10)	200(15)	170(12)	-131(12)	-86(10)	25(10)
C(45)	44(3)	48(3)	53(4)	-3(3)	-14(3)	-9(3)
N(45)	52(3)	50(3)	61(3)	0(3)	-20(3)	-5(3)
C(46)	65(4)	52(4)	86(5)	-6(4)	-33(4)	12(3)
C(47)	116(8)	76(7)	209(14)	-44(8)	-76(10)	32(6)
C(48)	187(15)	147(13)	191(16)	66(12)	-55(13)	43(12)
C(49)	128(10)	66(7)	440(30)	-22(11)	-188(16)	10(6)
C(50)	36(3)	38(3)	41(3)	7(2)	-9(2)	-3(2)
C(51)	58(4)	56(4)	52(4)	8(3)	-14(3)	-19(3)
C(52)	66(4)	68(5)	69(5)	21(4)	-9(4)	-29(4)
C(53)	75(5)	69(5)	48(4)	19(4)	-3(3)	-6(4)
C(54)	81(5)	54(4)	50(4)	-2(3)	-10(3)	-6(4)
C(55)	66(4)	45(3)	45(3)	4(3)	-11(3)	-14(3)
C(56)	31(3)	49(4)	55(4)	18(3)	-4(3)	-2(3)
C(57)	75(5)	75(6)	109(8)	-23(5)	-33(5)	31(5)
C(58)	104(8)	101(8)	140(10)	-34(7)	-60(8)	58(7)
C(59)	54(5)	107(9)	141(10)	44(8)	-6(6)	23(6)
C(60)	46(4)	111(8)	198(12)	92(9)	-47(6)	-27(5)
C(61)	57(4)	62(5)	144(8)	29(5)	-46(5)	-9(4)
C(62)	40(3)	40(3)	38(3)	0(2)	-12(2)	-11(2)
C(63)	60(4)	47(3)	50(3)	0(3)	-8(3)	-18(3)
C(64)	94(5)	71(5)	50(4)	16(4)	-12(4)	-35(4)
C(65)	128(7)	64(5)	69(5)	25(4)	-27(5)	-48(5)
C(66)	113(7)	40(4)	82(5)	3(4)	-29(5)	-18(4)
C(67)	65(4)	38(3)	54(4)	4(3)	-12(3)	-14(3)
C(68)	45(3)	48(3)	31(3)	3(2)	-10(2)	-19(2)
C(69)	48(3)	49(3)	52(3)	5(3)	-17(3)	-15(3)
C(70)	58(4)	81(5)	54(4)	19(4)	-29(3)	-38(4)

C(71)	73(5)	81(5)	47(4)	2(3)	-22(3)	-49(4)
C(72)	74(5)	77(5)	57(4)	-20(4)	-10(3)	-35(4)
C(73)	53(3)	62(4)	51(4)	-17(3)	-8(3)	-12(3)
C(74)	43(3)	34(3)	41(3)	0(2)	-11(2)	-3(2)
C(75)	36(3)	41(3)	42(3)	-6(2)	-11(2)	-4(2)
C(76)	38(3)	38(3)	45(3)	-5(2)	-12(2)	-8(2)
C(77)	42(3)	41(3)	43(3)	-10(2)	-11(2)	-5(2)
C(78)	43(3)	43(3)	36(3)	-5(2)	-14(2)	-4(2)
B(1)	62(5)	104(8)	65(6)	-17(5)	-12(4)	0(5)
B(2)	62(6)	107(9)	114(9)	-9(8)	-26(6)	-23(6)
F(1)	100(4)	125(5)	107(4)	-34(4)	-40(3)	-11(3)
F(2)	184(8)	298(13)	112(6)	65(7)	-52(5)	-142(9)
F(3)	65(3)	152(6)	166(6)	-32(5)	-20(4)	4(3)
F(4)	108(4)	97(4)	232(8)	-45(5)	-59(5)	-12(4)
F(5)	104(5)	167(7)	270(10)	110(7)	-104(6)	-72(5)
F(6)	84(6)	147(10)	128(9)	-51(8)	-7(6)	-13(7)
F(7)	168(19)	167(17)	540(40)	180(20)	-230(30)	-136(16)
F(8)	111(9)	260(20)	118(10)	-94(13)	26(8)	-20(11)
F(6A)	130(20)	220(30)	139(19)	-110(20)	-20(16)	-10(20)
F(7A)	280(50)	260(40)	470(70)	290(50)	-300(50)	-230(40)
F(8A)	97(17)	190(30)	84(11)	-38(15)	-36(11)	43(19)

Table S5. Hydrogen coordinates (x 10^4) and isotropic displacement parameters ($Å^2$x 10^3) for $\{[Ag(dpppen)(CN\text{-}t\text{-}Bu)_2](BF_4)\}_n$.

	x	y	z	U(eq)
H(3A)	6180	5882	2624	223
H(3B)	6993	5929	1693	223
H(3C)	6731	6771	2278	223
H(4A)	9683	6623	1680	276
H(4B)	9869	5718	1188	276
H(4C)	11003	5684	1801	276
H(5A)	10020	4301	2570	317
H(5B)	8640	4336	2102	317
H(5C)	8205	4484	3055	317
H(8A)	11570	9822	3737	163
H(8B)	12614	10205	4209	163
H(8C)	11168	9836	4699	163
H(9A)	13306	8769	5408	231
H(9B)	14722	9082	4818	231
H(9C)	14766	8017	4877	231
H(10A)	14754	7846	3341	215
H(10B)	15252	8777	3354	215
H(10C)	13793	8769	2958	215
H(12)	6118	7160	7696	68
H(13)	4373	8580	8220	86
H(14)	4396	9930	7500	90
H(15)	6100	9894	6227	92
H(16)	7852	8469	5683	65
H(18)	9647	4987	7306	104

H(19)	11567	4584	8114	137
H(20)	12942	5617	8309	131
H(21)	12595	6993	7627	125
H(22)	10788	7396	6727	95
H(24)	9065	4564	4437	74
H(25)	7949	3292	4533	81
H(26)	9371	1854	4921	84
H(27)	11907	1615	5224	82
H(28)	13055	2849	5075	72
H(30)	12232	5794	3077	132
H(31)	13827	5546	1767	208
H(32)	15864	4180	1469	196
H(33)	16551	3147	2474	152
H(34)	14919	3372	3796	95
H(35A)	8161	5105	6273	62
H(35B)	6900	5756	6973	62
H(36A)	5351	6540	6073	67
H(36B)	6704	6071	5315	67
H(37A)	6207	4606	5726	66
H(37B)	4749	5137	6416	66
H(38A)	4878	5434	4735	68
H(38B)	3417	5962	5427	68
H(39A)	2861	4503	5843	66
H(39B)	4295	3991	5131	66
H(42A)	-202	1715	7237	347
H(42B)	-204	1097	6511	347
H(42C)	1422	990	6802	347
H(43A)	-2140	143	8305	134
H(43B)	-2465	628	7476	134

H(43C)	-2272	1216	8175	134
H(44A)	1710	-734	7002	252
H(44B)	35	-636	6766	252
H(44C)	332	-1050	7621	252
H(47A)	8484	-2283	8711	207
H(47B)	6989	-2626	9173	207
H(47C)	8701	-3049	9397	207
H(48A)	7705	-2830	10669	293
H(48B)	5896	-2275	10646	293
H(48C)	6911	-1842	11095	293
H(49A)	8990	-924	9427	295
H(49B)	9881	-1856	9825	295
H(49C)	8653	-1031	10383	295
H(51)	4943	3635	8689	65
H(52)	6366	3812	7367	81
H(53)	6283	2930	6302	83
H(54)	4747	1890	6525	78
H(55)	3424	1651	7838	64
H(57)	1556	4262	10110	114
H(58)	-861	5422	10133	152
H(59)	-2865	5176	9623	138
H(60)	-2533	3766	9109	141
H(61)	-43	2590	8966	104
H(63)	-795	375	12660	63
H(64)	-1196	-1011	13294	84
H(65)	254	-2429	12687	100
H(66)	1989	-2516	11422	94
H(67)	2264	-1149	10745	64
H(69)	4272	76	11501	58

H(70)	5711	431	12380	70
H(71)	4602	1752	13205	72
H(72)	2045	2716	13152	79
H(73)	549	2346	12303	67
H(74A)	4161	3294	10007	49
H(74B)	3348	2704	10693	49
H(75A)	6334	1957	9570	48
H(75B)	5511	1347	10229	48
H(76A)	5875	2217	11276	48
H(76B)	6771	2782	10601	48
H(77A)	8802	1340	10155	51
H(77B)	7945	832	10894	51
H(78A)	8623	1681	11840	50
H(78B)	9325	2293	11132	50

Table S6. Crystal data and structure refinement for $\{[Ag_2(dppm)_2(dmb)_2](ClO_4)_2\}_n$.

Empirical formula	C74 H80 Ag2 Cl2 N4 O8 P4	
Formula weight	1563.94	
Temperature	293(2) K	
avelength	1.54060 Å	
Crystal system	Triclinic	
Space group	P-1	
Unit cell dimensions	a = 13.1321(19) Å	α= 103.780(12)°.
	b = 13.3093(18) Å	β= 107.349(11)°.
	c = 13.4611(16) Å	γ = 115.764(11)°.
Volume	1828.0(4) $Å^3$	
Z	1	
Density (calculated)	1.421 Mg/m^3	
Absorption coefficient	6.249 mm^{-1}	
F(000)	804	
Crystal size	0.2 x 0.2 x 0.2 mm^3	
Theta range for data collection	3.80 to 69.93°.	
Index ranges	-16<=h<=13, 0<=k<=16, -16<=l<=15	
Reflections collected	6931	
Independent reflections	6931 [R(int) = 0.0178]	
Completeness to theta = 69.93°	100.0 %	
Refinement method	Full-matrix least-squares on F^2	
Data / restraints / parameters	6931 / 0 / 425	
Goodness-of-fit on F^2	1.062	
Final R indices [I>2sigma(I)]	R1 = 0.0484, wR2 = 0.1542	
R indices (all data)	R1 = 0.0625, wR2 = 0.2051	

Extinction coefficient	0.0010(3)
Largest diff. peak and hole	1.017 and -1.210 e.Å^{-3}

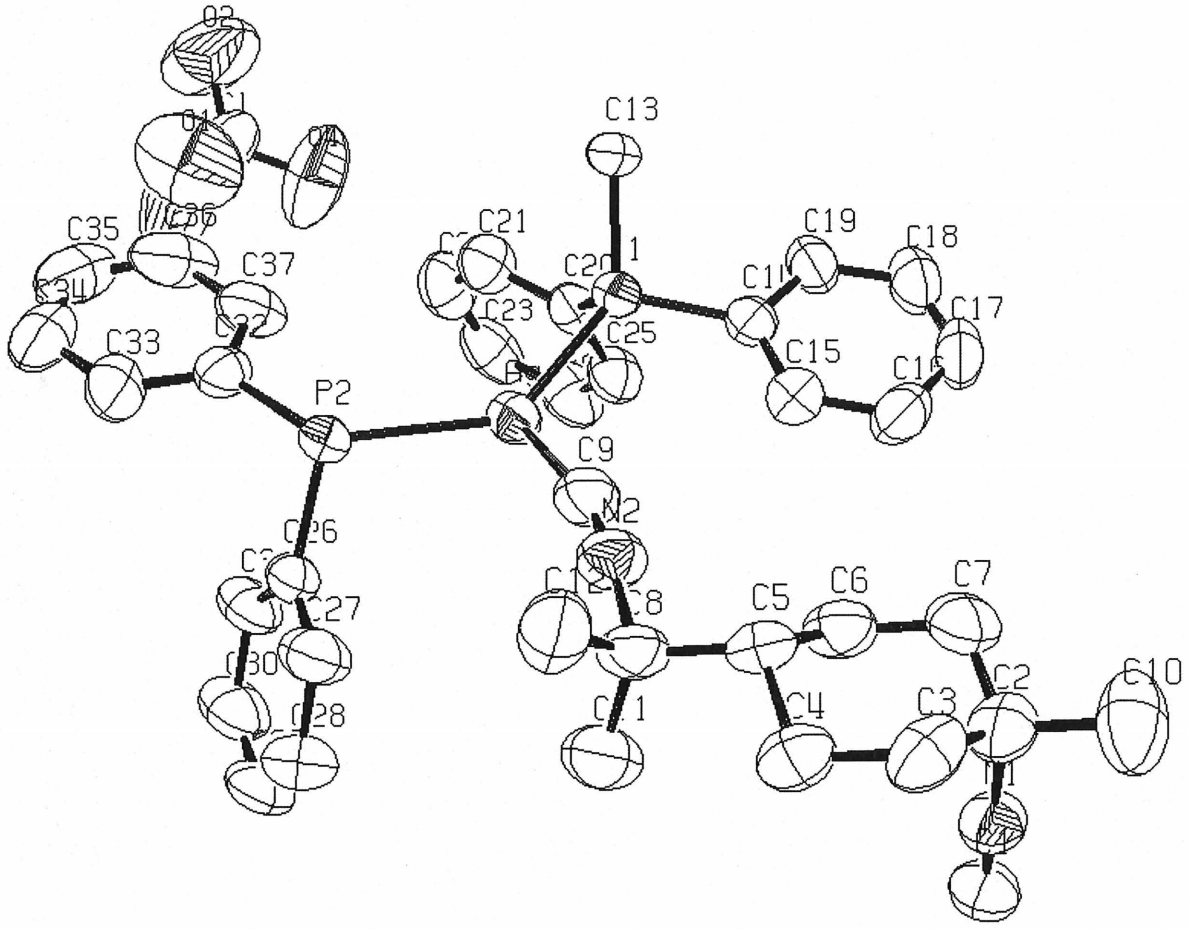

Figure S2. Numbering scheme for $\{[Ag_2(dppm)_2(dmb)_2](ClO_4)_2\}_n$

Table S7. Atomic coordinates (x 10^4) and equivalent isotropic displacement parameters ($Å^2$x 10^3) for $\{[Ag_2(dppm)_2(dmb)_2](ClO_4)_2\}_n$. U(eq) is defined as one third of the trace of the orthogonalized U^{ij} tensor.

	x	y	z	U(eq)
Ag	6342(1)	238(1)	4480(1)	52(1)
P(1)	7230(1)	2385(1)	5775(1)	45(1)
P(2)	4227(1)	-1545(1)	2901(1)	46(1)
Cl	2715(2)	3618(2)	1607(2)	90(1)
O(1)	2188(14)	2442(10)	1511(11)	186(5)
O(2)	2095(11)	4076(10)	1959(13)	215(6)
O(3)	2482(10)	3545(16)	496(10)	239(8)
O(4)	4034(8)	4326(10)	2195(9)	164(4)
N(1)	12132(5)	-810(6)	7209(5)	68(1)
N(2)	7385(6)	-1490(6)	5265(5)	70(1)
C(1)	12575(7)	-680(7)	6608(6)	69(2)
C(2)	11547(6)	-934(7)	7988(6)	73(2)
C(3)	10503(7)	-2269(8)	7516(7)	79(2)
C(4)	9406(7)	-2719(7)	6345(7)	71(2)
C(5)	8886(6)	-1883(6)	6408(5)	59(1)
C(6)	9962(7)	-541(6)	6850(7)	71(2)
C(7)	11036(7)	-119(8)	8016(6)	81(2)
C(8)	7738(7)	-2392(6)	5231(6)	66(2)
C(9)	7064(7)	-832(6)	5170(5)	68(2)
C(10)	12605(9)	-527(12)	9159(8)	115(4)
C(11)	8019(10)	-2602(9)	4203(7)	93(2)
C(12)	6560(8)	-3557(7)	5051(8)	93(2)

C(13)	6494(5)	2761(5)	6651(4)	51(1)
C(14)	8909(5)	3259(5)	6813(4)	51(1)
C(15)	9526(6)	2656(6)	6936(5)	62(1)
C(16)	10780(7)	3271(8)	7778(6)	76(2)
C(17)	11401(6)	4498(7)	8503(5)	75(2)
C(18)	10801(6)	5122(7)	8372(6)	73(2)
C(19)	9556(6)	4501(6)	7525(5)	60(1)
C(20)	7156(5)	3169(5)	4846(4)	50(1)
C(21)	6026(7)	3043(6)	4216(5)	67(2)
C(22)	5878(8)	3457(7)	3365(6)	81(2)
C(23)	6906(9)	4024(7)	3157(6)	82(2)
C(24)	8020(8)	4154(7)	3752(6)	82(2)
C(25)	8168(6)	3736(6)	4614(5)	64(1)
C(26)	4500(5)	-2277(5)	1764(4)	55(1)
C(27)	4903(8)	-3060(7)	1849(6)	79(2)
C(28)	5235(9)	-3498(9)	1032(8)	96(3)
C(29)	5124(8)	-3189(8)	107(6)	92(3)
C(30)	4658(9)	-2455(8)	-3(6)	88(2)
C(31)	4338(7)	-1996(6)	823(5)	71(2)
C(32)	2934(6)	-1418(6)	2123(5)	57(1)
C(33)	1760(7)	-2471(8)	1225(5)	73(2)
C(34)	794(7)	-2350(11)	654(7)	92(3)
C(35)	984(10)	-1213(14)	954(8)	106(3)
C(36)	2093(12)	-178(11)	1783(8)	103(3)
C(37)	3124(8)	-265(8)	2395(6)	79(2)

Table S8. Bond lengths [Å] and angles [°] for $\{[Ag_2(dppm)_2(dmb)_2](ClO_4)_2\}_n$.

Ag-C(9)	2.251(6)	Ag-C(1)	2.331(6)
Ag-P(1)	2.4672(14)	Ag-P(2)	2.4921(15)
P(1)-C(20)	1.816(5)	P(1)-C(14)	1.824(5)
P(1)-C(13)	1.842(5)	P(2)-C(32)	1.812(6)
P(2)-C(26)	1.827(5)	P(2)-C(13)	1.831(6)
Cl-O(2)	1.334(9)	Cl-O(1)	1.362(10)
Cl-O(4)	1.387(8)	Cl-O(3)	1.404(10)
N(1)-C(1)	1.133(7)	N(1)-C(2)	1.474(7)
N(2)-C(9)	1.142(8)	N(2)-C(8)	1.459(7)
C(1)-Ag	2.331(6)	C(2)-C(7)	1.502(11)
C(2)-C(3)	1.505(12)	C(2)-C(10)	1.530(11)
C(3)-C(4)	1.537(11)	C(3)-H(3A)	0.9700
C(3)-H(3B)	0.9700	C(4)-C(5)	1.537(8)
C(4)-H(4A)	0.9700	C(4)-H(4B)	0.9700
C(5)-C(6)	1.529(9)	C(5)-C(8)	1.555(9)
C(5)-H(5)	0.9800	C(6)-C(7)	1.529(11)
C(6)-H(6A)	0.9700	C(6)-H(6B)	0.9700
C(7)-H(7A)	0.9700	C(7)-H(7B)	0.9700
C(8)-C(11)	1.530(10)	C(8)-C(12)	1.538(11)
C(10)-H(10A)	0.9600	C(10)-H(10B)	0.9600
C(10)-H(10C)	0.9600	C(11)-H(11A)	0.9600
C(11)-H(11B)	0.9600	C(11)-H(11C)	0.9600
C(12)-H(12A)	0.9600	C(12)-H(12B)	0.9600
C(12)-H(12C)	0.9600	C(13)-P(2)	1.831(6)
C(13)-H(13A)	0.9700	C(13)-H(13B)	0.9700
C(14)-C(15)	1.370(8)	C(14)-C(19)	1.382(8)
C(15)-C(16)	1.393(9)	C(15)-H(15)	0.9300

C(16)-C(17)	1.376(11)	C(16)-H(16)	0.9300
C(17)-C(18)	1.377(11)	C(17)-H(17)	0.9300
C(18)-C(19)	1.386(9)	C(18)-H(18)	0.9300
C(19)-H(19)	0.9300	C(20)-C(21)	1.385(8)
C(20)-C(25)	1.386(8)	C(21)-C(22)	1.384(10)
C(21)-H(21)	0.9300	C(22)-C(23)	1.383(12)
C(22)-H(22)	0.9300	C(23)-C(24)	1.353(12)
C(23)-H(23)	0.9300	C(24)-C(25)	1.399(9)
C(24)-H(24)	0.9300	C(25)-H(25)	0.9300
C(26)-C(27)	1.372(9)	C(26)-C(31)	1.387(8)
C(27)-C(28)	1.393(10)	C(27)-H(27)	0.9300
C(28)-C(29)	1.388(14)	C(28)-H(28)	0.9300
C(29)-C(30)	1.373(14)	C(29)-H(29)	0.9300
C(30)-C(31)	1.400(9)	C(30)-H(30)	0.9300
C(31)-H(31)	0.9300	C(32)-C(37)	1.376(9)
C(32)-C(33)	1.416(9)	C(33)-C(34)	1.372(11)
C(33)-H(33)	0.9300	C(34)-C(35)	1.356(15)
C(34)-H(34)	0.9300	C(35)-C(36)	1.348(16)
C(35)-H(35)	0.9300	C(36)-C(37)	1.429(12)
C(36)-H(36)	0.9300	C(37)-H(37)	0.9300

C(9)-Ag-C(1)	99.0(2)	C(9)-Ag-P(1)	118.58(17)
C(1)-Ag-P(1)	97.57(18)	C(9)-Ag-P(2)	98.14(18)
C(1)-Ag-P(2)	98.90(18)	P(1)-Ag-P(2)	136.48(4)
C(20)-P(1)-C(14)	104.6(2)	C(20)-P(1)-C(13)	105.1(2)
C(14)-P(1)-C(13)	103.1(2)	C(20)-P(1)-Ag	105.28(16)
C(14)-P(1)-Ag	115.49(18)	C(13)-P(1)-Ag	121.71(18)
C(32)-P(2)-C(26)	103.3(3)	C(32)-P(2)-C(13)	104.7(3)
C(26)-P(2)-C(13)	103.5(2)	C(32)-P(2)-Ag	124.3(2)

C(26)-P(2)-Ag	107.42(18)	C(13)-P(2)-Ag	111.60(17)
O(2)-Cl-O(1)	107.9(8)	O(2)-Cl-O(4)	117.7(7)
O(1)-Cl-O(4)	113.7(7)	O(2)-Cl-O(3)	107.5(9)
O(1)-Cl-O(3)	107.1(9)	O(4)-Cl-O(3)	102.1(6)
C(1)-N(1)-C(2)	177.4(7)	C(9)-N(2)-C(8)	172.9(6)
N(1)-C(1)-Ag	174.5(6)	N(1)-C(2)-C(7)	106.8(6)
N(1)-C(2)-C(3)	108.1(6)	C(7)-C(2)-C(3)	111.7(6)
N(1)-C(2)-C(10)	106.2(6)	C(7)-C(2)-C(10)	112.9(8)
C(3)-C(2)-C(10)	110.8(7)	C(2)-C(3)-C(4)	112.8(6)
C(2)-C(3)-H(3A)	109.0	C(4)-C(3)-H(3A)	109.0
C(2)-C(3)-H(3B)	109.0	C(4)-C(3)-H(3B)	109.0
H(3A)-C(3)-H(3B)	107.8	C(5)-C(4)-C(3)	111.0(6)
C(5)-C(4)-H(4A)	109.4	C(3)-C(4)-H(4A)	109.4
C(5)-C(4)-H(4B)	109.4	C(3)-C(4)-H(4B)	109.4
H(4A)-C(4)-H(4B)	108.0	C(6)-C(5)-C(4)	110.2(5)
C(6)-C(5)-C(8)	114.7(5)	C(4)-C(5)-C(8)	110.0(5)
C(6)-C(5)-H(5)	107.2	C(4)-C(5)-H(5)	107.2
C(8)-C(5)-H(5)	107.2	C(7)-C(6)-C(5)	110.8(6)
C(7)-C(6)-H(6A)	109.5	C(5)-C(6)-H(6A)	109.5
C(7)-C(6)-H(6B)	109.5	C(5)-C(6)-H(6B)	109.5
H(6A)-C(6)-H(6B)	108.1	C(2)-C(7)-C(6)	112.8(6)
C(2)-C(7)-H(7A)	109.0	C(6)-C(7)-H(7A)	109.0
C(2)-C(7)-H(7B)	109.0	C(6)-C(7)-H(7B)	109.0
H(7A)-C(7)-H(7B)	107.8	N(2)-C(8)-C(11)	106.0(6)
N(2)-C(8)-C(12)	105.1(5)	C(11)-C(8)-C(12)	112.0(7)
N(2)-C(8)-C(5)	108.7(5)	C(11)-C(8)-C(5)	114.1(6)
C(12)-C(8)-C(5)	110.4(6)	N(2)-C(9)-Ag	164.1(6)
C(2)-C(10)-H(10A)	109.5	C(2)-C(10)-H(10B)	109.5
H(10A)-C(10)-H(10B)	109.5	C(2)-C(10)-H(10C)	109.5

H(10A)-C(10)-H(10C)	109.5	H(10B)-C(10)-H(10C)	109.5
C(8)-C(11)-H(11A)	109.5	C(8)-C(11)-H(11B)	109.5
H(11A)-C(11)-H(11B)	109.5	C(8)-C(11)-H(11C)	109.5
H(11A)-C(11)-H(11C)	109.5	H(11B)-C(11)-H(11C)	109.5
C(8)-C(12)-H(12A)	109.5	C(8)-C(12)-H(12B)	109.5
H(12A)-C(12)-H(12B)	109.5	C(8)-C(12)-H(12C)	109.5
H(12A)-C(12)-H(12C)	109.5	H(12B)-C(12)-H(12C)	109.5
P(2)-C(13)-P(1)	111.4(3)	P(2)-C(13)-H(13A)	109.3
P(1)-C(13)-H(13A)	109.3	P(2)-C(13)-H(13B)	109.3
P(1)-C(13)-H(13B)	109.3	H(13A)-C(13)-H(13B)	108.0
C(15)-C(14)-C(19)	119.1(5)	C(15)-C(14)-P(1)	119.2(4)
C(19)-C(14)-P(1)	121.6(4)	C(14)-C(15)-C(16)	120.9(6)
C(14)-C(15)-H(15)	119.5	C(16)-C(15)-H(15)	119.5
C(17)-C(16)-C(15)	119.4(6)	C(17)-C(16)-H(16)	120.3
C(15)-C(16)-H(16)	120.3	C(16)-C(17)-C(18)	120.2(6)
C(16)-C(17)-H(17)	119.9	C(18)-C(17)-H(17)	119.9
C(17)-C(18)-C(19)	119.8(6)	C(17)-C(18)-H(18)	120.1
C(19)-C(18)-H(18)	120.1	C(14)-C(19)-C(18)	120.5(6)
C(14)-C(19)-H(19)	119.7	C(18)-C(19)-H(19)	119.7
C(21)-C(20)-C(25)	118.4(5)	C(21)-C(20)-P(1)	120.5(4)
C(25)-C(20)-P(1)	120.3(4)	C(22)-C(21)-C(20)	122.1(7)
C(22)-C(21)-H(21)	119.0	C(20)-C(21)-H(21)	119.0
C(23)-C(22)-C(21)	118.1(7)	C(23)-C(22)-H(22)	120.9
C(21)-C(22)-H(22)	120.9	C(24)-C(23)-C(22)	121.2(6)
C(24)-C(23)-H(23)	119.4	C(22)-C(23)-H(23)	119.4
C(23)-C(24)-C(25)	120.6(7)	C(23)-C(24)-H(24)	119.7
C(25)-C(24)-H(24)	119.7	C(20)-C(25)-C(24)	119.6(6)
C(20)-C(25)-H(25)	120.2	C(24)-C(25)-H(25)	120.2
C(27)-C(26)-C(31)	119.8(5)	C(27)-C(26)-P(2)	121.1(5)

C(31)-C(26)-P(2)	119.1(5)	C(26)-C(27)-C(28)	119.7(7)
C(26)-C(27)-H(27)	120.2	C(28)-C(27)-H(27)	120.2
C(29)-C(28)-C(27)	121.1(8)	C(29)-C(28)-H(28)	119.4
C(27)-C(28)-H(28)	119.4	C(30)-C(29)-C(28)	118.8(6)
C(30)-C(29)-H(29)	120.6	C(28)-C(29)-H(29)	120.6
C(29)-C(30)-C(31)	120.5(7)	C(29)-C(30)-H(30)	119.7
C(31)-C(30)-H(30)	119.7	C(26)-C(31)-C(30)	119.9(7)
C(26)-C(31)-H(31)	120.0	C(30)-C(31)-H(31)	120.0
C(37)-C(32)-C(33)	120.1(6)	C(37)-C(32)-P(2)	118.7(5)
C(33)-C(32)-P(2)	121.2(5)	C(34)-C(33)-C(32)	120.0(8)
C(34)-C(33)-H(33)	120.0	C(32)-C(33)-H(33)	120.0
C(35)-C(34)-C(33)	119.2(9)	C(35)-C(34)-H(34)	120.4
C(33)-C(34)-H(34)	120.4	C(36)-C(35)-C(34)	123.1(8)
C(36)-C(35)-H(35)	118.5	C(34)-C(35)-H(35)	118.5
C(35)-C(36)-C(37)	119.5(9)	C(35)-C(36)-H(36)	120.3
C(37)-C(36)-H(36)	120.3	C(32)-C(37)-C(36)	118.1(8)
C(32)-C(37)-H(37)	120.9	C(36)-C(37)-H(37)	120.9

Symmetry transformations used to generate equivalent atoms:

Table S9. Anisotropic displacement parameters ($Å^2 x\ 10^3$) for $\{[Ag_2(dppm)_2(dmb)_2](ClO_4)_2\}_n$. The anisotropic displacement factor exponent takes the form: $-2\pi^2[\ h^2\ a^{*2}U^{11} + \ldots + 2\ h\ k\ a^*\ b^*\ U^{12}\ ]$

	U^{11}	U^{22}	U^{33}	U^{23}	U^{13}	U^{12}
Ag	55(1)	49(1)	46(1)	14(1)	21(1)	29(1)
P(1)	48(1)	46(1)	41(1)	17(1)	22(1)	27(1)
P(2)	48(1)	49(1)	40(1)	14(1)	22(1)	27(1)
Cl	77(1)	108(1)	109(1)	65(1)	44(1)	59(1)
O(1)	258(13)	117(7)	207(11)	85(7)	130(11)	96(8)
O(2)	157(9)	134(7)	336(17)	31(9)	126(11)	92(7)
O(3)	118(7)	370(19)	183(10)	198(13)	46(7)	74(10)
O(4)	89(5)	176(9)	198(9)	95(7)	23(5)	70(5)
N(1)	68(3)	91(4)	62(3)	38(3)	40(3)	48(3)
N(2)	86(4)	78(3)	67(3)	34(3)	37(3)	59(3)
C(1)	78(4)	85(4)	61(3)	33(3)	45(3)	47(4)
C(2)	63(3)	99(5)	71(4)	45(4)	43(3)	43(4)
C(3)	75(4)	110(6)	94(5)	70(5)	54(4)	61(4)
C(4)	75(4)	69(4)	92(5)	42(4)	45(4)	48(3)
C(5)	63(3)	64(3)	72(3)	30(3)	41(3)	44(3)
C(6)	76(4)	60(3)	89(4)	27(3)	44(4)	44(3)
C(7)	80(4)	92(5)	69(4)	23(4)	47(4)	44(4)
C(8)	81(4)	64(3)	75(4)	27(3)	40(3)	54(3)
C(9)	81(4)	74(4)	62(3)	26(3)	30(3)	55(4)
C(10)	76(5)	168(10)	75(5)	61(6)	32(4)	43(6)
C(11)	124(7)	111(6)	73(4)	35(4)	46(5)	87(6)
C(12)	76(5)	67(4)	112(6)	25(4)	22(4)	41(4)

C(13)	54(3)	53(3)	49(3)	15(2)	29(2)	32(2)
C(14)	54(3)	62(3)	42(2)	24(2)	25(2)	33(2)
C(15)	58(3)	66(3)	60(3)	24(3)	26(3)	35(3)
C(16)	62(4)	108(6)	77(4)	46(4)	36(3)	56(4)
C(17)	47(3)	93(5)	51(3)	26(3)	12(2)	22(3)
C(18)	56(3)	68(4)	58(3)	16(3)	17(3)	17(3)
C(19)	58(3)	58(3)	46(3)	14(2)	19(2)	25(3)
C(20)	53(3)	47(2)	42(2)	15(2)	17(2)	26(2)
C(21)	75(4)	70(4)	61(3)	31(3)	29(3)	44(3)
C(22)	91(5)	81(5)	64(4)	30(3)	20(3)	52(4)
C(23)	121(6)	68(4)	51(3)	28(3)	29(4)	54(4)
C(24)	96(5)	77(4)	61(4)	33(3)	41(4)	33(4)
C(25)	64(3)	71(4)	50(3)	27(3)	28(3)	31(3)
C(26)	51(3)	57(3)	45(2)	11(2)	25(2)	24(2)
C(27)	97(5)	84(5)	64(4)	22(3)	41(4)	59(4)
C(28)	99(6)	102(6)	89(5)	17(4)	48(5)	66(5)
C(29)	90(5)	98(5)	63(4)	1(4)	49(4)	40(4)
C(30)	100(6)	85(5)	63(4)	20(3)	50(4)	37(4)
C(31)	86(4)	74(4)	48(3)	19(3)	38(3)	39(3)
C(32)	61(3)	76(4)	47(3)	28(3)	28(2)	44(3)
C(33)	68(4)	100(5)	47(3)	35(3)	26(3)	42(4)
C(34)	67(4)	157(9)	66(4)	58(5)	37(3)	62(5)
C(35)	112(7)	203(12)	74(5)	78(7)	58(5)	120(8)
C(36)	161(9)	145(8)	81(5)	58(6)	73(6)	125(8)
C(37)	112(6)	93(5)	59(3)	30(3)	39(4)	78(5)

Table S10. Hydrogen coordinates (x 10^4) and isotropic displacement parameters ($Å^2$x 10^3) for $\{[Ag_2(dppm)_2(dmb)_2](ClO_4)_2\}_n$.

	x	y	z	U(eq)
H(3A)	10169	-2381	8061	94
H(3B)	10857	-2771	7432	94
H(4A)	9707	-2723	5768	85
H(4B)	8728	-3558	6114	85
H(5)	8564	-1924	6976	71
H(6A)	10294	-463	6299	85
H(6B)	9633	-17	6926	85
H(7A)	11723	718	8255	97
H(7B)	10722	-110	8584	97
H(10A)	13257	327	9448	173
H(10B)	12962	-1017	9075	173
H(10C)	12259	-636	9689	173
H(11A)	8749	-1853	4342	140
H(11B)	7297	-2843	3521	140
H(11C)	8188	-3243	4101	140
H(12A)	6416	-3389	5713	140
H(12B)	6699	-4217	4947	140
H(12C)	5830	-3790	4380	140
H(13A)	7136	3534	7328	61
H(13B)	5846	2867	6208	61
H(15)	9102	1825	6449	74
H(16)	11194	2856	7850	91
H(17)	12229	4908	9083	89
H(18)	11229	5956	8850	88

H(19)	9152	4923	7434	72
H(21)	5344	2669	4370	80
H(22)	5108	3357	2945	97
H(23)	6830	4322	2598	98
H(24)	8694	4524	3588	99
H(25)	8941	3839	5028	77
H(27)	4955	-3298	2449	94
H(28)	5536	-4006	1107	115
H(29)	5361	-3474	-427	110
H(30)	4553	-2262	-630	105
H(31)	4019	-1504	740	85
H(33)	1644	-3246	1023	88
H(34)	19	-3040	68	110
H(35)	317	-1143	571	127
H(36)	2187	586	1954	124
H(37)	3902	437	2961	95

Table S11. Torsion angles [°] for $\{[Ag_2(dppm)_2(dmb)_2](ClO_4)_2\}_n$.

C(9)-Ag-P(1)-C(20)	149.6(3)	C(1)-Ag-P(1)-C(20)	45.0(3)
P(2)-Ag-P(1)-C(20)	-66.49(19)	C(9)-Ag-P(1)-C(14)	34.8(3)
C(1)-Ag-P(1)-C(14)	-69.8(2)	P(2)-Ag-P(1)-C(14)	178.68(18)
C(9)-Ag-P(1)-C(13)	-91.3(3)	C(1)-Ag-P(1)-C(13)	164.1(3)
P(2)-Ag-P(1)-C(13)	52.6(2)	C(9)-Ag-P(2)-C(32)	166.6(3)
C(1)-Ag-P(2)-C(32)	-92.9(3)	P(1)-Ag-P(2)-C(32)	18.1(2)
C(9)-Ag-P(2)-C(26)	-73.1(3)	C(1)-Ag-P(2)-C(26)	27.4(3)
P(1)-Ag-P(2)-C(26)	138.4(2)	C(9)-Ag-P(2)-C(13)	39.7(2)
C(1)-Ag-P(2)-C(13)	140.2(2)	P(1)-Ag-P(2)-C(13)	-108.77(17)
C(2)-N(1)-C(1)-Ag	72(18)	C(1)-N(1)-C(2)-C(7)	9(16)
C(1)-N(1)-C(2)-C(3)	129(16)	C(1)-N(1)-C(2)-C(10)	-112(16)
N(1)-C(2)-C(3)-C(4)	-64.8(7)	C(7)-C(2)-C(3)-C(4)	52.4(8)
C(10)-C(2)-C(3)-C(4)	179.2(6)	C(2)-C(3)-C(4)-C(5)	-53.9(8)
C(3)-C(4)-C(5)-C(6)	55.3(7)	C(3)-C(4)-C(5)-C(8)	-177.3(5)
C(4)-C(5)-C(6)-C(7)	-56.1(7)	C(8)-C(5)-C(6)-C(7)	179.1(5)
N(1)-C(2)-C(7)-C(6)	64.6(8)	C(3)-C(2)-C(7)-C(6)	-53.3(8)
C(10)-C(2)-C(7)-C(6)	-179.0(6)	C(5)-C(6)-C(7)-C(2)	55.7(7)
C(9)-N(2)-C(8)-C(11)	29(6)	C(9)-N(2)-C(8)-C(12)	-90(6)
C(9)-N(2)-C(8)-C(5)	152(6)	C(6)-C(5)-C(8)-N(2)	-47.0(7)
C(4)-C(5)-C(8)-N(2)	-171.9(5)	C(6)-C(5)-C(8)-C(11)	71.1(7)
C(4)-C(5)-C(8)-C(11)	-53.8(7)	C(6)-C(5)-C(8)-C(12)	-161.8(5)
C(4)-C(5)-C(8)-C(12)	73.3(6)	C(8)-N(2)-C(9)-Ag	-8(8)
C(1)-Ag-C(9)-N(2)	-42(2)	P(1)-Ag-C(9)-N(2)	-145(2)
P(2)-Ag-C(9)-N(2)	59(2)	C(20)-P(1)-C(13)-P(2)	152.1(3)
C(14)-P(1)-C(13)-P(2)	-98.6(3)	Ag-P(1)-C(13)-P(2)	32.9(3)
C(20)-P(1)-C(14)-C(15)	-124.5(5)	C(13)-P(1)-C(14)-C(15)	125.8(5)
Ag-P(1)-C(14)-C(15)	-9.3(5)	C(20)-P(1)-C(14)-C(19)	59.3(5)

C(13)-P(1)-C(14)-C(19)	-50.4(5)	Ag-P(1)-C(14)-C(19)	174.5(4)
C(19)-C(14)-C(15)-C(16)	1.2(9)	P(1)-C(14)-C(15)-C(16)	-175.1(5)
C(14)-C(15)-C(16)-C(17)	0.6(10)	C(15)-C(16)-C(17)-C(18)	-2.0(11)
C(16)-C(17)-C(18)-C(19)	1.6(11)	C(15)-C(14)-C(19)-C(18)	-1.7(9)
P(1)-C(14)-C(19)-C(18)	174.6(5)	C(17)-C(18)-C(19)-C(14)	0.3(10)
C(14)-P(1)-C(20)-C(21)	-158.0(5)	C(13)-P(1)-C(20)-C(21)	-49.8(5)
Ag-P(1)-C(20)-C(21)	79.8(5)	C(14)-P(1)-C(20)-C(25)	32.3(5)
C(13)-P(1)-C(20)-C(25)	140.5(5)	Ag-P(1)-C(20)-C(25)	-89.8(4)
C(25)-C(20)-C(21)-C(22)	0.4(9)	P(1)-C(20)-C(21)-C(22)	-169.4(5)
C(20)-C(21)-C(22)-C(23)	-0.7(11)	C(21)-C(22)-C(23)-C(24)	1.1(11)
C(22)-C(23)-C(24)-C(25)	-1.3(12)	C(21)-C(20)-C(25)-C(24)	-0.5(9)
P(1)-C(20)-C(25)-C(24)	169.3(5)	C(23)-C(24)-C(25)-C(20)	0.9(11)
C(32)-P(2)-C(26)-C(27)	-147.7(6)	C(13)-P(2)-C(26)-C(27)	-38.8(6)
Ag-P(2)-C(26)-C(27)	79.4(6)	C(32)-P(2)-C(26)-C(31)	34.6(6)
C(13)-P(2)-C(26)-C(31)	143.6(5)	Ag-P(2)-C(26)-C(31)	-98.2(5)
C(31)-C(26)-C(27)-C(28)	4.6(11)	P(2)-C(26)-C(27)-C(28)	-173.1(6)
C(26)-C(27)-C(28)-C(29)	-2.2(13)	C(27)-C(28)-C(29)-C(30)	-1.1(14)
C(28)-C(29)-C(30)-C(31)	2.0(13)	C(27)-C(26)-C(31)-C(30)	-3.7(10)
P(2)-C(26)-C(31)-C(30)	174.0(6)	C(29)-C(30)-C(31)-C(26)	0.4(12)
C(26)-P(2)-C(32)-C(37)	-120.9(5)	C(13)-P(2)-C(32)-C(37)	131.1(5)
Ag-P(2)-C(32)-C(37)	1.3(6)	C(26)-P(2)-C(32)-C(33)	57.1(5)
C(13)-P(2)-C(32)-C(33)	-50.9(5)	Ag-P(2)-C(32)-C(33)	179.3(4)
C(37)-C(32)-C(33)-C(34)	-2.4(9)	P(2)-C(32)-C(33)-C(34)	179.6(5)
C(32)-C(33)-C(34)-C(35)	0.5(10)	C(33)-C(34)-C(35)-C(36)	1.2(12)
C(34)-C(35)-C(36)-C(37)	-0.9(13)	C(33)-C(32)-C(37)-C(36)	2.6(10)
P(2)-C(32)-C(37)-C(36)	-179.4(5)	C(35)-C(36)-C(37)-C(32)	-1.0(12)

Experimental Section

Materials: 1,8-diisocyano-p-menthane (dmb) and $[Ag_2(dppm)_2](ClO_4)_2$ has been prepared according to a procedure outlined in references 7 and 8, respectively. The dimeric starting materials $[Ag_2(dppm)_2](BF_4)_2$[8] and $[Cu_2(dppm)_2(NCMe)_4](BF_4)_2$[9] were prepared using procedure outlined for their corresponding ClO_4^- salt with the exception that $AgBF_4$ and $[Cu(NCMe)_4]BF_4$ were used as starting materials. The $[M_2(diphos)_2](BF_4)_2$ dimers (M = Cu, Ag; diphos = dppb, dpppen and dpph) were also prepared according to published methods for the corresponding $[M_2(diphos)_2](ClO_4)_2$, except again $AgBF_4$ and $[Cu(NCMe)_4]BF_4$ were used. Their identity was verified by ^1H, ^{31}P NMR and IR spectroscopy. The solvents used in the syntheses (acetone (Fisher), dichloromethane (ACP) and diethyl ether (ACP)) were purified according to procedures outlined in (a) D.D. Perrin, W.L.F. Armarego, D.R. Perrin, *Purifications of laboratory chemicals*; Pergamon: Oxford, U.K. 1966. (b) A.J. Gordon; R.A. Ford. *The Chemist's companion, a handbook of practical data, techniques, and references*; Wiley: New York, 1972; p436. $AgBF_4$, $Cu(BF_4)_2 \cdot xH_2O$, *tert*-butyl isocyanide, bis(diphenylphosphino)methane(dppm), 1,5-bis(diphenylphosphino) pentane, (dpppen) and 1,6-bis(diphenylphosphino)hexane were purchased from Aldrich Chemicals Co; while Cu(m) was purchased from Anachemia and used as received. All reactions were performed using standard Schlenk techniques to minimize phosphine oxidation.

$\{[Cu(dppb)(CN\text{-}t\text{-}Bu)_2](BF_4)\}_n$ (1). $[Cu_2(dppb)_2](BF_4)_2$ (165.1mg, 0.143mmol) was dissolved in 70 ml of degassed acetone. 100μl (0.884mmol) of *t*-BuNC was added dropwise using a micro-seringe. The solution was stirred for 2 hrs prior to concentrating it *in vaccuo* until dry. The white powder was dissolved in a minimum amount of methylene chloride prior to adding 100 ml of diethyl ether in order to precipitate a white solid, which was filtered and dried *in vaccuo*. Yield 55% (117.2mg). ^1H NMR (CD_2Cl_2), δ 7.50-7.42 (m, 20H, Ph), 2.36 (m, 4H, $\underline{CH_2}P$), 1.81 (m, 4H, $\underline{CH_2}CH_2P$), 1.29 (s, 18H,

CH_3); $^{31}P\{^1H\}$ NMR (CD_2Cl_2), δ -0.63; $^{13}C\{^1H\}$ NMR (CD_2Cl_2), δ 134.83, 132.55, 130.53, 129.25, 57.48, 30.05, 25.27, 23.97; IR (KBr) ν 1061 (BF_4), 2174cm^{-1} (C≡N); Raman (neat solid) ν 2178cm^{-1} (C≡N). Chem. Anal. (calcd.) for $CuC_{38}H_{46}N_2P_2BF_4$ C 61.42; H 6.24; N 3.77%; (Found) C 61.03; H 6.37; N 3.81%.

{[Cu(dpppen)(CN-*t*-Bu)$_2$](BF$_4$)}$_n$ (2). [Cu_2(dpppen)$_2$](BF_4)$_2$ (204.0 mg, 0.173 mmol) was dissolved in 70 ml of degassed acetone. 0.1 ml (0.884 mmol) of *t*-buNC was added dropwise using a micro-syringe. The solution was stirred for 2 hrs prior to concentrating it *in vaccuo* until it was dry. The white powder was then dissolved in a minimum amount of methylene chloride prior to add 100 ml of diethyl ether to precipitate a white solid, which was filtered and dried *in vaccuo*. Yield 89% (233.4 mg). ^1H RMN (CD_2Cl_2), δ 7.48-7.33 (m, 20H, Ph), 2.31 (m, 4H, $\underline{CH_2}P$), 1.36 (m, 4H, $\underline{CH_2}CH_2P$), 1.29 (s, 18H, CH_3), 1.23 (m, 2H, $\underline{CH_2}CH_2CH_2P$); $^{31}P\{^1H\}$ RMN (CD_2Cl_2), δ -3.69; $^{13}C\{^1H\}$ RMN (CD_2Cl_2), δ 134.71, 132.65, 130.47, 129.18, 57.43, 30.00, 26.30, 29.97, 25.72, 21.82; IR (KBr) ν 1059 (BF_4), 2172cm^{-1} (C≡N); Raman (neat solid) ν 2173cm^{-1} (C≡N). Chem. Anal. (calcd.) for $CuC_{39}H_{48}N_2P_2BF_4$ C 61.87; H 6.39; N 3.70%; (Found) C 61.72; H 6.52; N 3.70%.

{[Cu(dpph)(CN-*t*-Bu)$_2$](BF$_4$)}$_n$ (3). [Cu_2(dpph)$_2$](BF_4)$_2$ (275.6mg, 0.228mmol) was dissolved in 80ml of degassed acetone. 100μl (0.884mmol) of *t*-BuNC was added dropwise using a micro-syringe. The solution was stirred for 3 hrs prior to concentrating it *in vaccuo* until dry. The white powder was dissolved in a minimum of methylene chloride prior to adding 100 ml of diethyl ether to precipitate a white solid which was filtered and dried *in vaccuo*. Yield 73% (257.1mg). ^1H NMR (CD_2Cl_2), δ 7.50-7.29 (m, 20H, Ph), 2.18 (m, 4H, $\underline{CH_2}P$), 1.75 (m, 4H, $\underline{CH_2}CH_2P$), 1.41 (m, 4H, $\underline{CH_2}CH_2CH_2P$), 1.34 (s, 18H, CH_3); $^{31}P\{^1H\}$ NMR (CD_2Cl_2), δ -1.61; $^{13}C\{^1H\}$ NMR (CD_2Cl_2), δ 140.22, 134.03, 132.49, 130.47, 129.16, 57.60, 32.66, 30.06, 28.24, 26.09; IR (KBr) ν 1060 (BF_4), 2174cm^{-1} (C≡N); Raman (neat solid) ν 2178cm^{-1} (C≡N). Chem. Anal.

(calcd.) for $CuC_{40}H_{50}N_2P_2BF_4$ C 62.30; H 6.54; N 3.63%; (Found) C 62.18; H 6.64; N 3.60%.

$\{[Cu_2(dppm)_2(dmb)_2](BF_4)_2\}_n$ (4) $[Cu_2(dppm)_2(NCMe)_4](BF_4)_2$ (222.1 mg, 0.18 mmol) was dissolved in 30 ml of distilled acetonitrile. 69.0 mg, 0.36 mmol of dmb was dissolved separately in a round flask containing 60 ml of distilled acetonitrile. This solution was slowly added dropwise in the former solution. The mixture was stirred for 2 hrs prior to being reduced to 15 ml *in vaccuo*. Then 150 ml of diethyl ether were added to precipitate the white product, which was filtered and dried. Yield 74% (260.2 mg). ^1H NMR (CD_2Cl_2) δ 7.31-7.14 (m, 40H, Ph), 3.26 (m, 4H, $\underline{CH_2}P$), 1.96-0.93 (m, 36H dmb); $^{31}P\{^1H\}$ NMR (CD_2Cl_2) δ -4.50; $^{13}C\{^1H\}$ NMR (CD_2Cl_2) δ 140.58, 132.60, 131.20, 129.41, 66.00, 60.54, 44.20, 36.23, 28.45, 27.41, 22.72, 15.43; IR (KBr) ν 1103 (BF_4), 2181cm^{-1} (C≡N); Raman (neat solid) ν 2171cm^{-1} (C≡N). Chem. Anal. (calcd.) for $CuC_{37}H_{40}N_2P_2BF_4$ C 61.29; H 5.56; N 3.86%; (Found) C 60.31; H 5.61; N 3.96%.

$\{[Cu(dppb)(dmb)](BF_4)\}_n$ (5) The dimer $[Cu_2(dppb)_2](BF_4)_2$ (342.6 mg, 0.297 mmol) was dissolved in 100ml of degassed acetone. 118.4 mg (0.622 mmol) of dmb was dissolved in 150 ml of degassed acetone in another flask. Both solutions were cooled to 0°C, and the dmb solution was added dropwise to the dimer solution. The mixture was stirred for 2 hrs prior to being reduced to 25mL *in vaccuo*. Then 150ml of diethyl ether were added to precipitate the product which was filtered and dried. Yield 70% (318.8mg). ^1H NMR (CD_2Cl_2) δ 7.43 (m, 20H, Ph), 2,35 (m, 4H, $\underline{CH_2}P$), 2.10-1.07 (m, 22H, $\underline{CH_2}CH_2P$ + dmb); $^{31}P\{^1H\}$ NMR (CD_2Cl_2) δ -0.38, -2.78; $^{13}C\{^1H\}$ NMR (CD_2Cl_2) δ 134.60, 132.50, 130.67, 129.35, 63.18, 61.14, 43.90, 37.11, 29.34, 28.04, 26.06, 22.91; IR (KBr) ν 2170 (C≡N), 1061cm^{-1} (BF_4); Raman (neat solid) ν 2171cm^{-1} (C≡N).

$\{[Cu(dpppen)(dmb)](BF_4)\}_n$ (6). $[Cu_2(dpppen)_2](BF_4)_2$ (358.9 mg, 0.304 mmol) was dissolved in 30 ml of degassed acetone. 121.5 mg, (0.639 mmol) of dmb was dissolved

separately in a round flask containing 120 ml of distilled acetonitrile. This solution was slowly added dropwise in the former solution at 0°C. The mixture was stirred for 12 hrs while the product precipitated. The white powder was filtered and dried. Yield 67% (319.4 mg). IR (KBr) ν 2168 (C≡N), 1061cm^{-1} (BF_4); Raman (neat solid) ν 2173cm^{-1} (C≡N). Chem. Anal. (calcd.) for $CuC_{41}H_{48}N_2P_2BF_4$ C 63.04; H 6.19; N 3.59%; (Found) C 62.27; H 6.30; N 3.61%.

{[Cu(dpph)(dmb)](BF$_4$)}$_n$ (7) The dimer $[Cu_2(dpph)_2](BF_4)_2$ (350 mg, 0,289 mmol) was dissolved in 30ml of degassed acetone. 120.2 mg (0.631 mmol) of dmb was dissolved in 120 ml of degassed acetone in another flask. Both solutions were cooled to 0°C and the dmb solution was added dropwise to the dimer one. The mixture was stirred for 12 hrs while the product precipitated. The insoluble white product was filtred and dried. Yield 85% (392.5mg). IR (KBr) ν 2170 (C≡N), 1057cm^{-1} (BF_4); Raman (neat solid) ν 2172cm^{-1} (C≡N).

{[Ag(dppb)(CN-*t*-Bu)$_2$](BF$_4$)}$_n$ (8) $[Ag_2(dppb)_2](BF_4)_2$ (838.9mg, 0.675mmol) was dissolve in 100ml of degassed acetone. 305µl (2.70mmol) of *t*-BuNC was added dropwise using a micro-syringe. The solution was stirred for 2 hrs prior to concentrating it *in vaccuo* until dry. The resulting powder was dissolved in a minimum amount of methylene chloride prior to adding 100ml of diethyl ether to precipitate a white solid which was dried *in vaccuo*. Yield 91% (0.965g) ^{1}H NMR (CD_2Cl_2), δ 7.42-7.35 (m, 20H, Ph), 2.05 (m, 4H, $\underline{CH_2}$P), 1.42 (m, 4H, $\underline{CH_2}CH_2P$) 1.38 (s, 18H, CH_3); ^{31}P{^{1}H} NMR (CD_2Cl_2), δ 3.24; ^{13}C{^{1}H} NMR (CD_2Cl_2) δ 142.64, 132.61, 130.53, 129.14, 57.03, 29.98, 27.03, 26.56; IR (KBr) ν 2184 (C≡N), 1057 cm^{-1} (BF_4); Raman (neat solid) ν 2187 cm^{-1} (C≡N). Chem. Anal. (calcd.) for $AgC_{38}H_{46}N_2P_2BF_4$ C 57.96; H 5.89; N 3.56%; (Found) C 58.06; H 5.88; N 3.47%.

{[Ag(dpppen)(CN-*t*-Bu)$_2$](BF$_4$)}$_n$ (9). [Ag$_2$(dpppen)$_2$](BF$_4$)$_2$ (279.9 mg, 0.220 mmol) was dissolved in 50 ml of degassed acetone. 0.1 ml 0,884 mmol of *t*-buNC was added dropwise using a micro-syringe. The solution was stirred for 2 hrs prior to concentrating it *in vaccuo* until it was dry. The white powder was then dissolved in a minimum amount of methylene chloride prior to add 100 ml of diethyl ether to precipitate a white solid which was filtered and dried *in vaccuo*. Yield 72% (228.0 mg). ^{1}H NMR (CD_2Cl_2) δ 7.47-7.35 (m, 20H, Ph), 2.22 (m, 4H, $\underline{CH_2}$P), 1.62 (m, 2H, $\underline{CH_2}CH_2CH_2P$) 1.49 (m, 4H, $\underline{CH_2}CH_2P$) 1.34 (s, 18H, CH_3); $^{31}P\{^1H\}$ NMR (CD_2Cl_2) δ 2.45; $^{13}C\{^1H\}$ NMR (CD_2Cl_2) δ 142.25, 132.73, 130.71, 129.28, 57.29, 30.01, 26.82, 24.38; IR (KBr) ν 1056 (BF$_4$), 2178cm^{-1} (C≡N); Raman (neat solid) ν 2178cm^{-1} (C≡N). Chem. Anal. (calcd.) for $CuC_{39}H_{48}N_2P_2BF_4$ C 58.45; H 6.04; N 3.50%; (Found) C 58.11; H 5.85; N 4.07%.

{[Ag(dpph)(CN-*t*-Bu)$_2$](BF$_4$)}$_n$ (10) The dimer [Ag$_2$(dpph)$_2$](BF$_4$)$_2$ (554.5mg, 0.427mmol) was dissolved in 60ml of degassed acetone. 193μl (1.70mmol) of *t*-BuNC was added dropwise using a micro-syringe. The solution was stirred for 2 hrs prior to concentrating it *in vaccuo* until dry. The resulting powder was dissolved in a minimum amount of methylene chloride prior to adding 100ml of diethyl ether in order to precipitate a white solid which was dried in vacuum. Yield 84% (582.6mg) ^{1}H NMR (CD_2Cl_2) δ 7.42-7.33 (m, 20H, Ph), 2.10 (m, 4H, $\underline{CH_2}$P), 1.40 (s, 18H, CH_3) 1.26-1.25 (m, 8H, $\underline{CH_2}CH_2P$ + $\underline{CH_2}CH_2CH_2P$); $^{31}P\{^1H\}$ NMR (CD_2Cl_2) δ 2.80; $^{13}C\{^1H\}$ NMR (CD_2Cl_2) δ 143.15, 132.60, 130.53, 129.13, 57.0, 30.78, 30.12, 27.68, 25.68; IR (KBr) ν 2174, 2135 (C≡N), 1055cm^{-1} (BF$_4$); Raman (neat solid) ν 2181cm^{-1} (C≡N). Chem. Anal. (calcd.) for $CuC_{40}H_{50}N_2P_2BF_4$ C 58.92; H 6.18; N 3.44%; (Found) C 59.27; H 6.18; N 3.48%.

{[Ag$_2$(dppm)$_2$(dmb)$_2$](BF$_4$)$_2$}$_n$ (11a) [Ag$_2$(dppm)$_2$(NCMe)$_4$](BF$_4$)$_2$ (445.8 mg, 0.337 mmol) was dissolved in 20 ml of distilled acetonitrile. 146.5 mg, 0.770 mmol of dmb was dissolved separately in a round flask containing 60 ml of distilled acetonitrile. This

solution was slowly added dropwise in the former solution. The mixture was stirred for 12 hrs prior to being reduced to 25 ml *in vaccuo*. Then 150 ml of diethyl ether were added to precipitate the white product, which was filtered and dried. Yield 54% (282.4 mg). ^{1}H NMR (CD_2Cl_2) δ 7.42-7.21 (m, 40H, Ph), 3.36 (m, 4H, $\underline{CH_2}P$), 1.84 (m, 8H, dmb) 1.48-1.34 (m, 28H, dmb); $^{31}P\{^{1}H\}$ NMR (CD_2Cl_2) δ 5.71; $^{13}C\{^{1}H\}$ RMN (CD_2Cl_2) δ 146.59, 144.95, 132.78, 131.51, 129.56, 63.90, 60.72, 43.19, 36.50, 28.34, 26.76, 22.39; IR (KBr) ν 1059 (BF_4), 2180, 2134cm^{-1} (C≡N); Raman (neat solid) ν 2178cm^{-1} (C≡N). Chem. Anal. (calcd.) for $AgC_{37}H_{40}N_2P_2BF_4$ C 57.76; H 5.24; N 3.64%; (Found) C 57.23; H 5.28; N 3.64%. HRMS-FAB m/z 1071 for $[Ag_2(dppm)_2](BF_4)]$.

$\{[Ag_2(dppm)_2(dmb)_2](ClO_4)_2\}_n$ (11b) same procedure that the one used for **4** with $[Ag_2(dppm)_2(NCMe)_4](ClO_4)_2$ as starting material (yield 93%). ^{1}H NMR (CD_3CN) δ 7.45-7.10 (m, 40H, Ph), 3.55 (s, 4H, $\underline{CH_2}P$), 2.20-1.97 (m, 12H, dmb) 1.64-1.40 (m, 24H, dmb); $^{31}P\{^{1}H\}$ NMR (CD_3CN) δ 9.85; $^{13}C\{^{1}H\}$ RMN (CD_3CN) δ 145.8, 144.3, 133.1, 131.6, 129.4, 65.8, 65.0, 61.6, 42.3, 36.0, 27.4, 26.6, 25.4, 22.4, 15.1; IR (KBr) ν 1090 (ClO_4), 2178cm^{-1} (C≡N).

$\{[Ag(dppb)(dmb)](BF_4)\}_n$ (12) The dimer $[Ag_2(dppb)_2](BF_4)_2$ (449.9 mg, 0.358 mmol) was dissolved in 100ml of degassed acetone. 170.6mg (0.897 mmol) of dmb was dissolved in 250 ml of degassed acetone in another flask. Both solutions were cooled to 0°C and the dmb solution was added dropwise to the dimer one. The mixture was stirred for 2 hrs while the product precipitated. The white product was filtred and dried. Yield 85% (494mg). ^{1}H NMR (CD_2Cl_2) δ 7.40-7.28 (m, 20H, Ph), 2.22 (m, 4H, $\underline{CH_2}P$), 1.88-1.81 (m, 4H, dmb) 1.61-1.42 (m, 18H, dmb + $\underline{CH_2}CH_2P$); $^{31}P\{^{1}H\}$ NMR (CD_2Cl_2) δ 4.42 ; $^{31}P\{^{1}H\}$ NMR (DMF-d_7) δ 7.62; $^{13}C\{^{1}H\}$ NMR (DMF-d_7) δ 151.47, 137.15, 134.86, 133.42, 66.8, 64.12, 48.14, 40.82, 32.68, 30.67, 29.51, 26.79; $^{13}C\{^{1}H\}$ NMR (DMSO-d_6) δ 147.29, 146.75, 132.49, 130.36, 128.87, 61.76, 59.29, 43.25, 36.07, 28.44, 26.30,24.91, 22.03; IR (KBr) ν 2167, 2132 (C≡N), 1060cm^{-1} (BF_4); Raman (neat solid) ν 2172cm^{-1}

(C≡N); Anal. Cald. for $C_{40}H_{46}N_2P_2BF_4Ag$: C 59.21; H 5.71; N 3.45. Found : C 57.95; H 6.10; N 3.31. MS-FAB m/z 1238 for $[Ag(dppb)_2(dmb)](BF_4)]$.

$\{[Ag(dpppen)(dmb)](BF_4)\}_n$ (13) $[Ag_2(dpppen)_2](BF_4)_2$ (373.4 mg, 0.294 mmol) was dissolved in 30 ml of degassed acetone. 111.9 mg, 0.588 mmol of dmb was dissolved separately in a round flask containing 120 ml of degassed acetone. This solution was slowly added dropwise in the former solution at 0°C. The mixture was stirred for 12 hrs while the product precipitate. The white powder was filtered and dried. Yield 64% (310.0 mg). IR (KBr) ν 1056 (BF_4), 2176, 2130cm^{-1} (C≡N); Raman (neat solid) ν 2178cm^{-1} (C≡N); Chem. Anal. (calcd.) for $AgC_{41}H_{48}N_2P_2BF_4$ C 59.66; H 5.86; N 3.39%; (Found) C 59.18; H 6.25; N 3.43%. HRMS-FAB m/z 1183.1 for $[Ag_2(dpppen)_2](BF_4)]$.

$\{[Ag(dpph)(dmb)](BF_4)\}_n$ (14) The dimer ($[Ag_2(dpph)_2](BF_4)_2$) (362.2mg, 0.279mmol) was dissolved in 30ml of degassed acetone. 106.7mg (0.558mmol) of dmb was dissolved in 120 ml of degassed acetone in an other flask. Both solutions were cooled to 0°C and the dmb solution was added dropwise to the dimer one. The mixture was stirred for 12 hrs while the product precipitated. The white product was filtred and dried. Yield 65% (303.6mg). ^1H NMR (CD_2Cl_2) δ 7.41-7.33 (m, 20H, Ph), 2.18 (m, 4H, $\underline{CH_2}P$), 1.88-1.73 (m, 4H, dmb) 1.51-1.23 (m, 24H, dmb + $\underline{CH_2}CH_2P$); $^{31}P\{^1H\}$ NMR (CD_2Cl_2) δ 3.63; $^{13}C\{^1H\}$ NMR (CD_2Cl_2) δ 146.26, 145.55, 132.74, 130.72, 129.32, 63.31, 60.60, 44.17, 36.98, 30.47, 28.95, 27.61, 26.55, 25.45, 22.77; IR (KBr) ν 2169, 2130 (C≡N), 1057cm^{-1} (BF_4); Raman (neat solid) ν 2172cm^{-1} (C≡N); Anal. Cald. for $C_{42}H_{50}N_2P_2BF_4Ag$: C 60.09; H 6.00; N 3.34. Found : C 59.39; H 6.20; N 3.36. MS-FAB m/z 1277.2 for $[Ag_2(dpph)(dmb)_2(CN)_2](BF_4)_2]$.

Apparatus: All NMR spectra were acquired with a Bruker AC-300 spectrometer (^1H 300.15 MHz, ^{13}C 75.48 MHz, ^{31}P 121.50 MHz) using the solvent as chemical shift standard, except in ^{31}P NMR, where the chemical shift are relative to D_3PO_4 85% in D_2O.

All chemical shifts (δ) and coupling constants (J) are given in ppm and Hertz, respectively. The IR spectra were acquired on a Bomem FT-IR MB series spectrometer equiped with a baseline diffused reflectance. The emission spectra and the emission lifetime were measured with a nanosecond N_2 laser system from PTI model GL-3300 pumping a dye laser model GL-302. The excitation wavelength was 311nm. The emission spectra were also measured on a SPEX Fluorolog II spectrofluorometer. MALDI-TOF mass spectra were acquired from a Bruker proflex III linear mode spectrometer with a nitrogen laser (337nm) from the Université de Bourgogne in Dijon (France) with a dithranol matrix. The glass transition temperature (Tg) were measured using a Perkin-Elmer 5A DSC7 equipped with a thermal controller 5B TAC 7/DS. Calibration standards were water and indium. FT-Raman were acquired on a Bruker RFS 100/S spectrometer. XRD were acquired on a Rigaku/USA Inc with a copper lamp operating under a 30mA current and a 40KV tension. TGA were acquired on a TGA 7 of Perkin Elmer between 50 et 650 °C at 3°/minute under nitrogen atmosphere.

Crystallography. Crystal for **11b** were obtain from the slow evaporation of a concentrated acetonitrile solution. Intensity data from the long white needle-shape crystals were collected at 293(2)K on an Enrof-Nonius CAD-4 automatic diffractometer. Cell constants and an orientation matrix for data collection were obtained from a least-squares refinement using the setting angles of 24 centered reflections in the range $4°\leq 2\theta \leq 70°$. Space group determination was based upon systematic absences, packing considerations, a statistical analysis of intensity distribution, and the successful solution and refinement of the structure. The NRCCAD program(Le Page, Y.; White, P.S.; Gabe, *E. J. Proc. Am. Crystallogr.* Hamilton Meet. **1986**, Abstract PA23.) was used for centering, indexing, and data collection. Two-standard reflections were measured every 60 minutes. The NRCVAX programs(Gabe, E. J.; Le Page, Y.; Charland, J.-P.; Lee, F. L.; White, P. S. *J. Appl. Crystallogr.* **1989**, 22, 384.) were used for crystal structure solution by application of direct methods. The SHELX-97 program(Sheldrick, G. M. SHELX-97; University of Gottingen: Gottingen, Germany, 1997.) was used for

refinement by full-matrix least squares of F^2 Psi scan based on empirical absorption corrections were made. No significant decay was observed during data collection. Isotropic extinction coefficients were included in the refinement to account for secondary extinction effects(Larson, A. C. Crystallographic Computing, Munksgaard: Copenhagen, Denmark, 1970: p 291.). Hydrogen atoms were all geometrically placed and the respective final refinements included anisotropic thermal parameters for non-hydrogen atoms, and isotropic thermal parameters for the non-hydrogen atoms, and isotropic thermal parameter for the hydrogen atoms. The R_1 = 0.0484 and wR_2 = 0.1542 final discrepancy indices at convergence for the $I_{net} \geq 2.0\sigma$ (I_{net}) significant reflections.

Crystals of **9** were grown by vapour diffusion using acetonitrile– *tert*-butylmethylether at 23 C°. Single crystals were coated with Paratone-N oil, mounted using a glass fibre and frozen in the cold nitrogen stream of the goniometer. A hemisphere of data was collected on a Bruker AXS P4/SMART 1000 diffractometer using ω and θ scans with a scan width of 0.3 ° and 30 s exposure times. The detector distance was 6 cm. The data were reduced (SAINT 6.02, 1997-1999, Bruker AXS, Inc., Madison, Wisconsin, USA.) and corrected for absorption (SADABS George Sheldrick, 1999, Bruker AXS, Inc., Madison, Wisconsin, USA.). The structure was solved by direct methods and refined by full-matrix least squares on F (SHELXTL 5.1, George Sheldrick, 1997, Bruker AXS, Inc., Madison, Wisconsin, USA). One of the BF_4 anions was disordered and the site occupancy determined using an isotropic model as 0.65 (F(6) – F(8)) and 0.35 (F(6a) – F(8a)) and fixed in subsequent refinement cycles. All non-hydrogen atoms were refined anisotropically. Hydrogen atoms were included in calculated positions and refined using a riding model. Thermal ellipsoid plots are at the 30% probability level. In some plots, hydrogen atoms have been omitted for clarity.

Figure S3 XRD patterns for **11a** and **13**

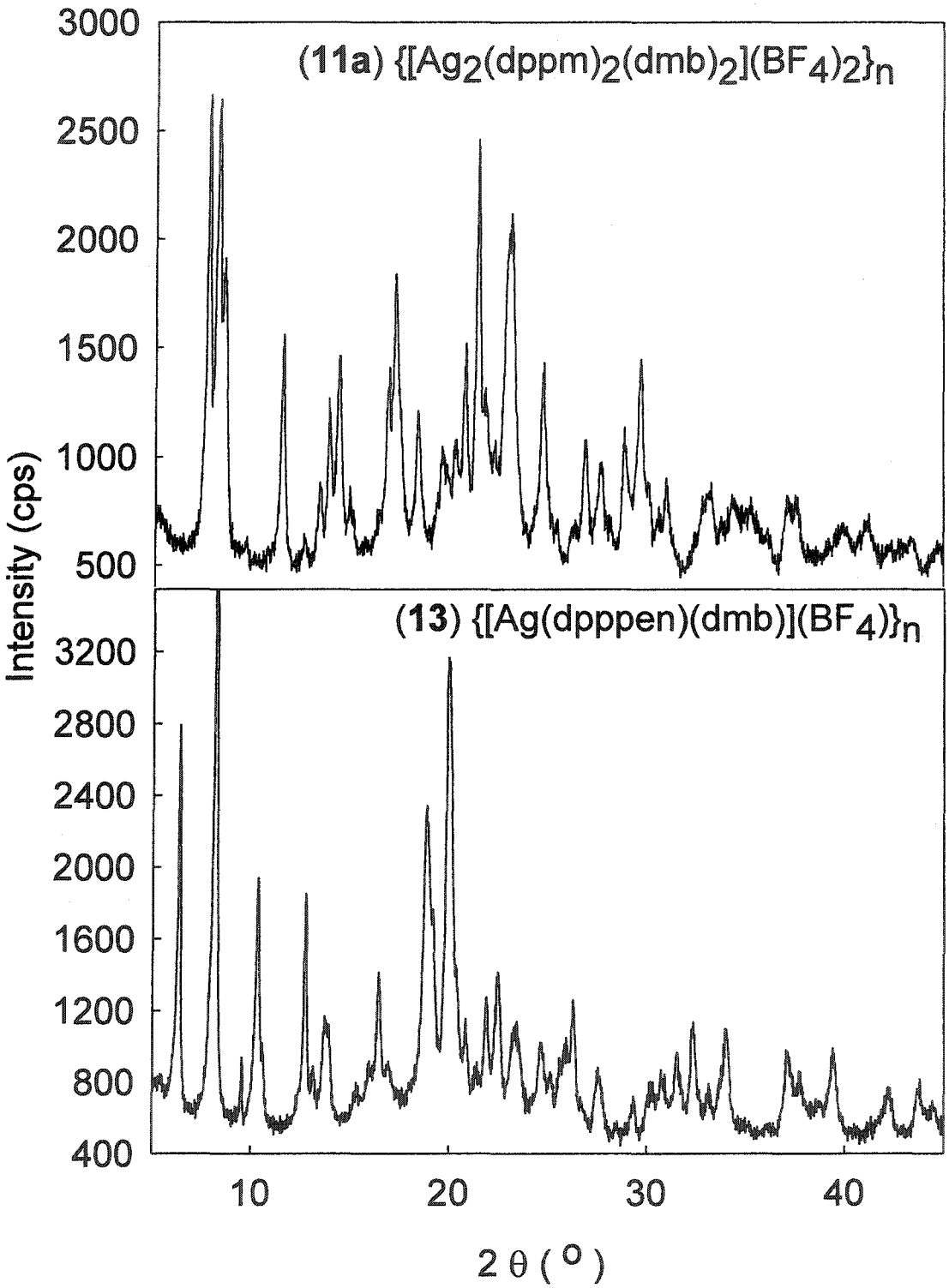

Figure S4 XRD patterns for **12** and **14**

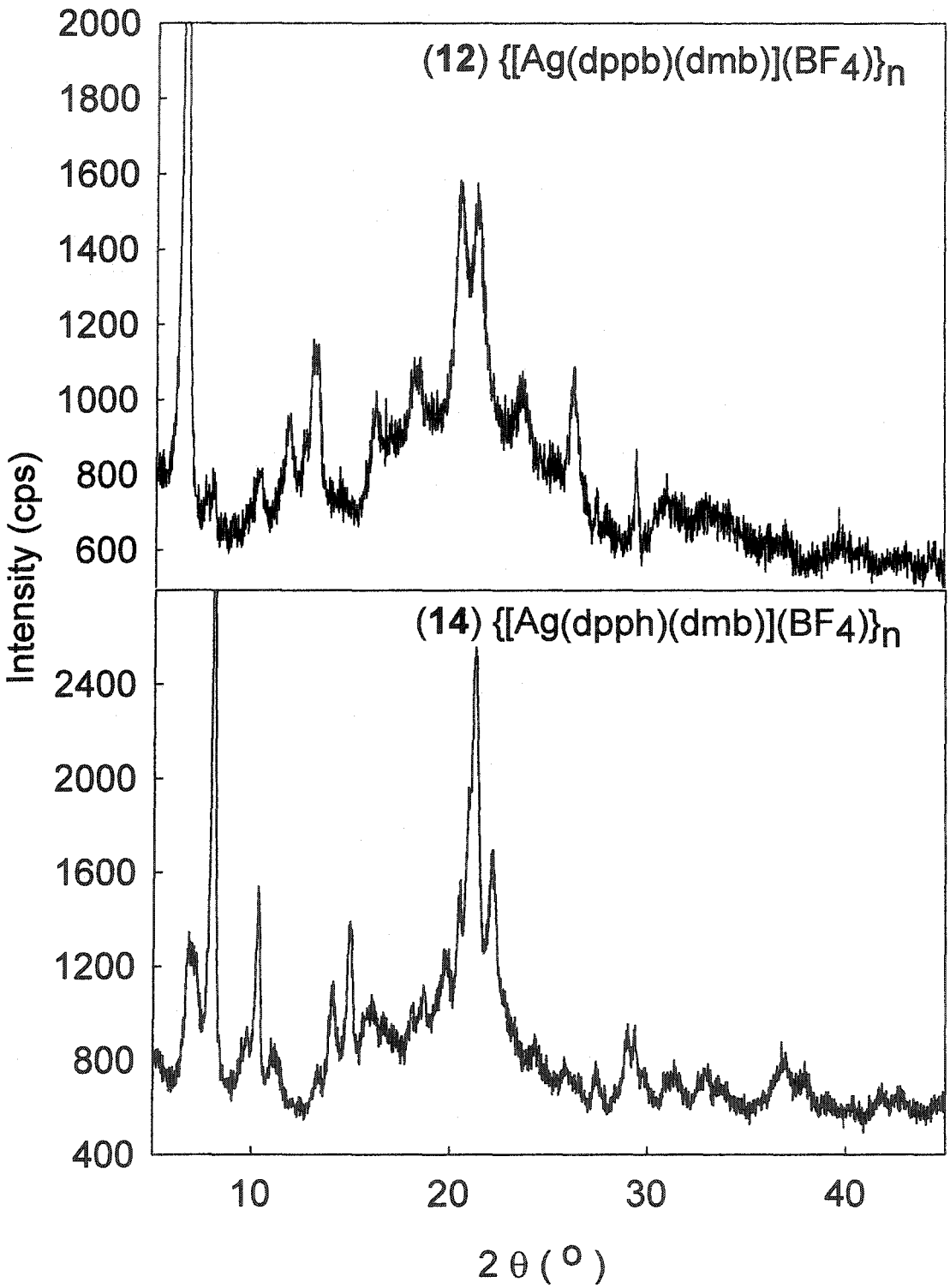

Figure S5 XRD patterns for **5**

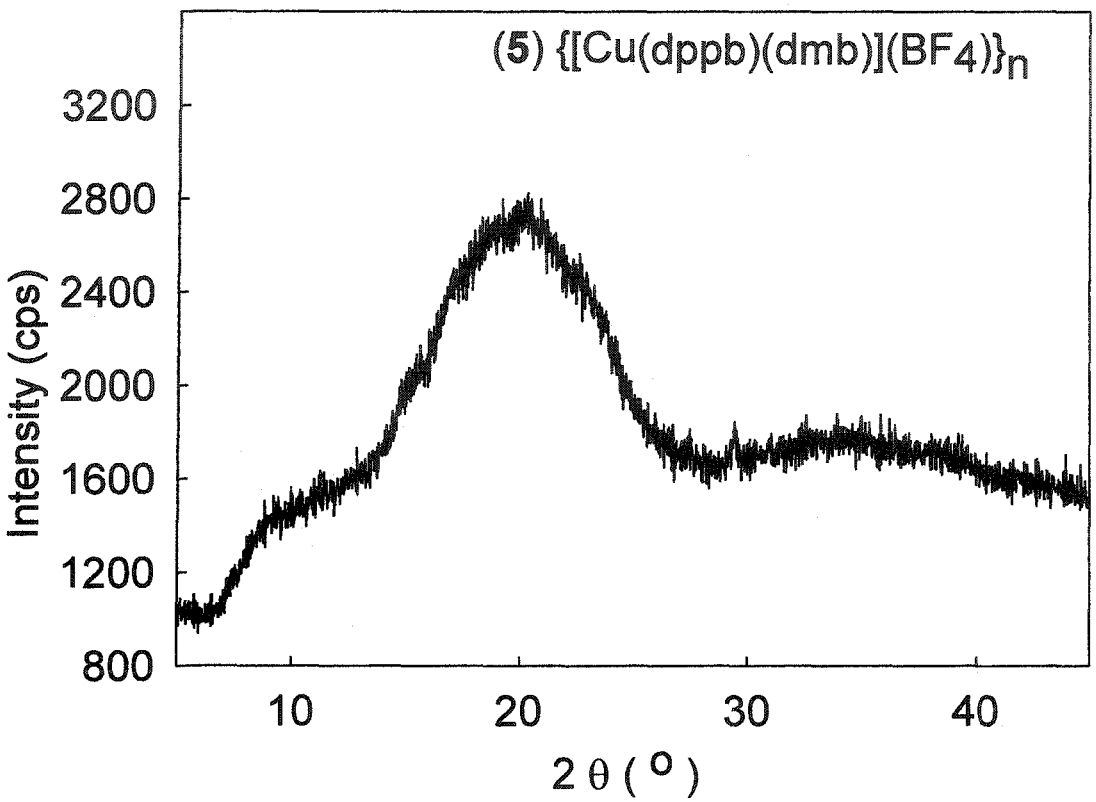

Figure S6 XRD patterns for **2** and **9**

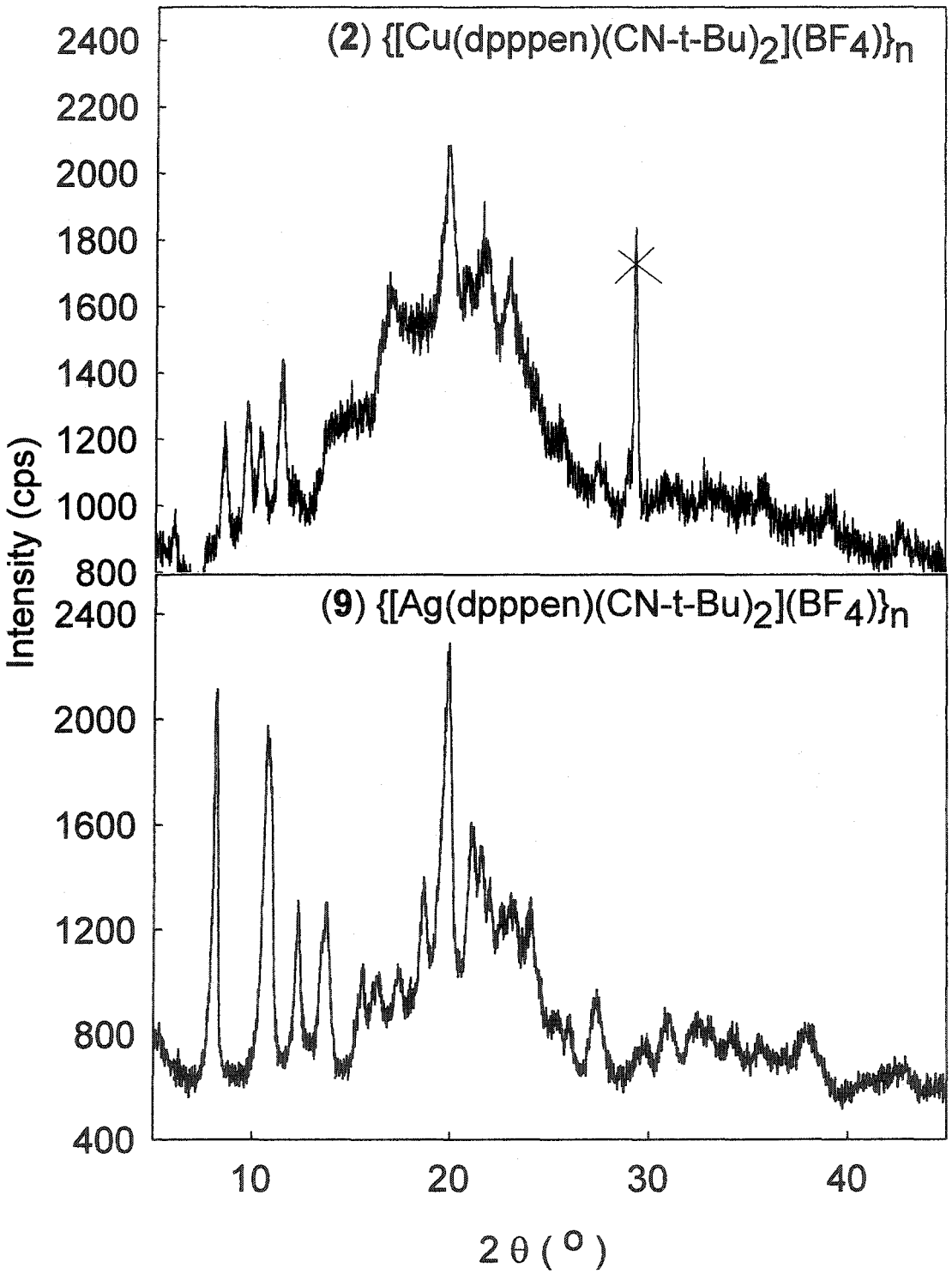

Figure S7 XRD patterns for **1** and **8**

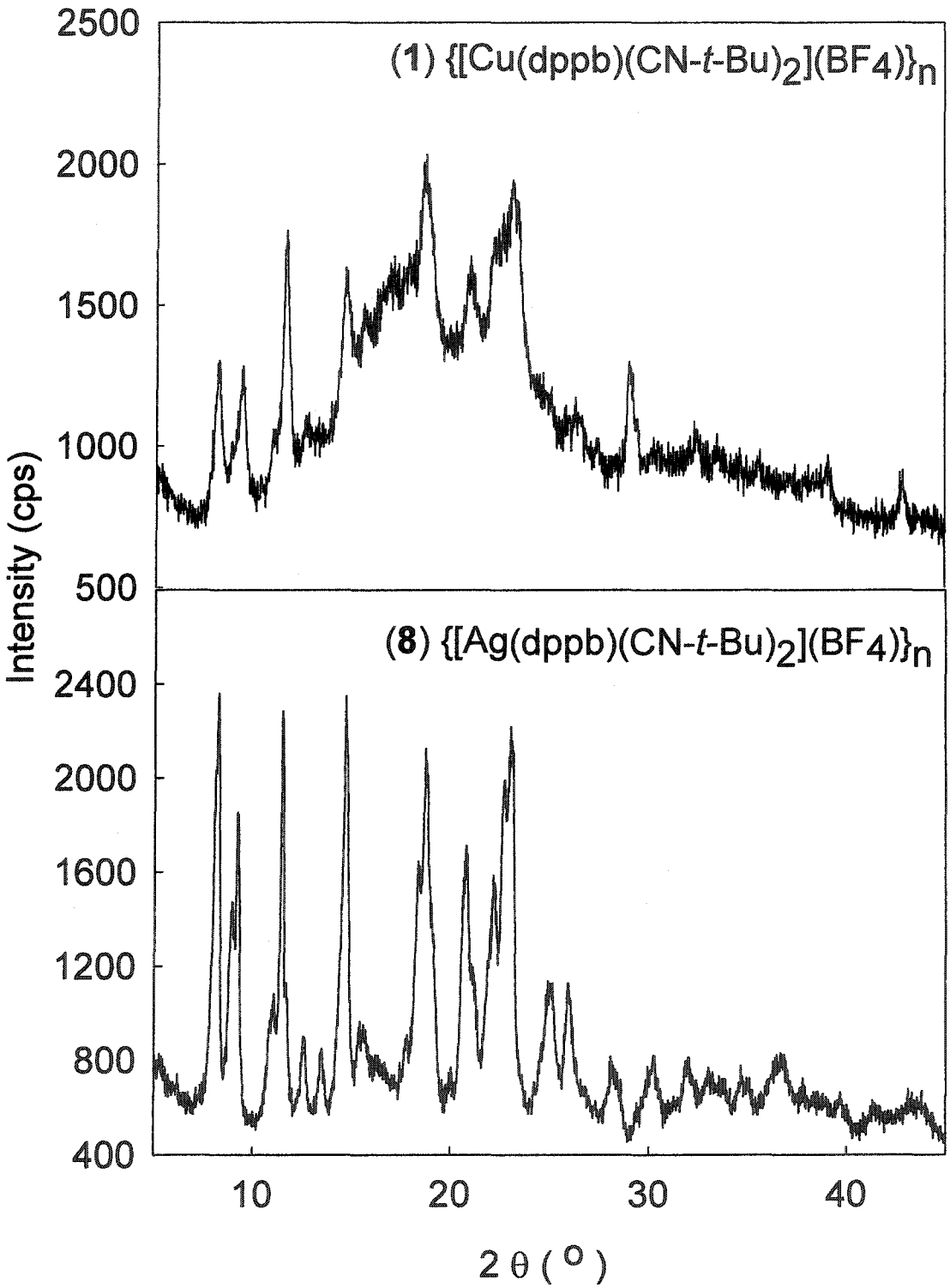

Figure S8 XRD patterns for **3** and **10**

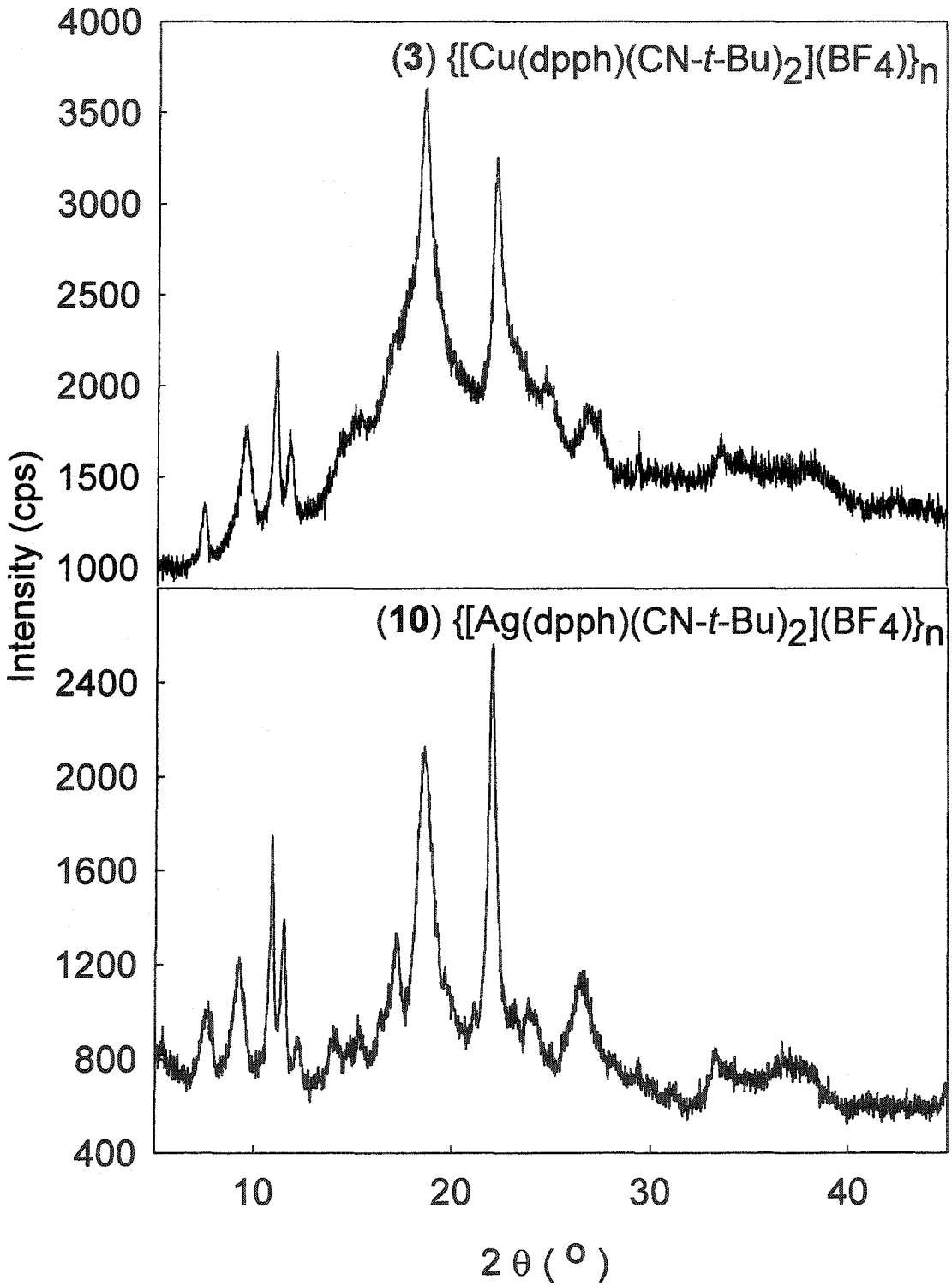

Table S12. TGA data for **1** - **14**[a]

	Weight loss 1[b] (loss of isocyanides)			Weight Loss 2[b] (loss of diphos)			Residue (metal alone)	
	Temp. Range(°C)	Exp. %	(Theor. %)	Temp. Range(°C)	Exp. %	(Theor. %)	Exp. %	(Theor. %)
1	171-229	22	23	305-445	68	68	10	9
2	180-220	23	22	310-420	66	69	11	9
3	162-224	21	21	297-458	70	70	9	8
4	150-330	36	38	330-400	55	53	9	9
5	178-340	36	36	340-442	54	56	10	8
6	195-340	34	35	350-420	58	57	8	8
7	180-249	36	35	333-455	56	57	8	8
8	144-176	21	21	300-420	65	65	14	14
9	150-200	20	21	290-385	67	65	13	14
10	110-190	21	21	288-424	66	66	13	13
11a	170-220	22	25	280-400	63	61	15	14
12	176-231	23	23	300-415	64	63	13	14
13	190-210	26	23	270-410	61	64	13	13
14	173-226	24	23	300-395	64	64	12	13

[a] The uncertainty is estimated to be ~ 2-3% because of a small drift in the baseline.

[b] For compounds **1-7** (the Cu-polymers), the TGA traces exhibit two thermal events during the first weight loss wich can spread between 150 to 340°C. The first derivative curve of the TGA traces exhibit a narrow peak at lower temperature dure to isocyanide losses, and an overlapping broader and weaker signal spreading in the higher temperature range, a process due to BF_4^- losses. The second weight loss is due to the diphosphine losses. For compounds **8-14** (the Ag-polymers), the weight loss events associated with BF_4^- move to higher temperatures, high enough that the signal overlaps with the second large weight losses (diphosphine). For accuracy, the experimental and theorical weight losses are presented as follow: for **1-7**, weight loss 1 = losses of isocyanide and BF_4^-, and weight loss 2 = losses of diphosphines; for **8-14**, weight loss 1 = losses of isocyanide and weight loss 2 = losses of diphosphines and BF_4^-.

CHAPITRE 3

POLYMÈRES ORGANOMÉTALLIQUES BASÉS SUR LE 1,8-DIISOCYANO-*P*-MENTHANE; SYNTHÈSES ET CARACTÉRISATIONS DES MATÉRIAUX DE TYPE $\{[M(diphos)(dmb)]BF_4\}_n$ ET $\{[Pd_2(diphos)_2(dmb)](BF_4)_2\}_n$ (M = Cu, Ag; diphos = dppe, dppp)

L'utilisation du dmb s'est beaucoup accrue depuis une trentaine d'années car c'est un ligand assembleur très versatile (48). Dernièrement, l'utilisation de ce ligand a permis de synthétiser des polymères organométalliques de type $\{[M(dmb)_2]^+\}_n$ (22, 24, 29) qui trouvent leur application dans le domaine de la semi- et photoconductivité ainsi que dans la fabrication de cellules photovoltaïques (27). La particularité de ces nouveaux matériaux vient du fait que ces derniers gardent leur nature polymérique en solution (25, 28). Les deux stratégies pour synthétiser des matériaux en une dimension (1-D) ou de forme zig-zag qui conservent une nature oligomérique en solution sont : l'utilisation de deux dmb pontants entre les fragments métalliques (fragment M^+ (24-28) et $M_2(dppm)_2^{2+}$ avec M = Cu, Ag); l'autre méthode est de fonctionnaliser un fragment métallique axialement. Dans ce dernier cas, le métal doit avoir une liaison $M\text{-}L_{axiale}$ très forte; on utilise donc un ligand qui est peu labile (22, 29). Ce chapitre portera sur la synthèse et la caractérisation d'une nouvelle série de polymères construits à partir de fragments métalliques ayant des diphosphines chélatées et des ligands dmb. Les polymères ont été caractérisés à partir de leurs viscosités intrinsèques, DSC, ATG, DRX et la spectroscopie de luminescence. Les composés modèles comme les complexes $[M(diphos)(CN\text{-}t\text{-}Bu)_2]BF_4$ (M = Cu, Ag; diphos = dppe, dppp) ont également été étudiés. Les travaux de ce chapitre ont été soumis au journal "Inorganic Chemistry" le 17 août 2003 et mon rôle

fût de synthétiser et de caractériser les sept composés d'argent et de cuivre (spectre RMN ^{1}H, ^{13}C et ^{31}P, DRX de poudre, ATG, DSC, IR, RAMAN, UV-visible, calculs théoriques des analyses élémentaires, et des analyses de spectres de masse, spectres d'excitation, d'émission et mesures des durée de vie d'émission) ainsi que d'obtenir les quatre structures cristallographiques présentées dans ce chapitre. De plus, l'informatique de la publication fût également ma responsabilité (texte, graphiques organisation des tableaux et images). Le rôle de Stéphanie Sicard a été la synthèse et la caractérisation des quatre composés à base de palladium. La contribution de mon directeur de recherche, Pr. Harvey a été dans l'agencement des résultats du manuscrit.

Organometallic Polymers Based on 1,8-Diisocyano-*p*-menthane (dmb); Syntheses and Characterization of the $\{[M(diphos)(dmb)]BF_4\}_n$ and $\{[Pd_2(diphos)_2(dmb)](ClO_4)_2\}_n$ Materials (M= Cu, Ag; diphos =dppe, dppp)

Eric Fournier, Stéphanie Sicard and Pierre D. Harvey*

Contribution from the Département de chimie, Université de Sherbrooke, Sherbrooke, PQ., Canada J1K 2R1

Submitted as a full paper in Inorganic Chemistry

*To whom correspondence should be addressed :
Tel : (819) 821-7092, or (819) 821-8000 ext 2005
Fax : (819) 821-8017
Email : p.harvey@USherbrooke.ca

Abstract

A new strategy to synthesize organometallic oligomers and polymers is presented, and consists of using the title diisocyanide and chelated metal fragments with bis(diphenylphosphine)alkanes. The title materials are synthesized by reacting the $[M(dppe)(BF_4)]$ and $[M_2(dppp)_2](BF_4)_2$ complexes (M = Cu, Ag; dppe = bis(diphenylphosphino)ethane, dppp = bis(diphenylphosphino)propane) with dmb, and the Pd_2-bonded d^9-d^9 $Pd_2(dmb)_2Cl_2$ dimer with dppe or dppp. The model compounds $[M(diphos)(CN\text{-}t\text{-}Bu)_2]BF_4$ (M = Cu, Ag) and $[Pd_2(diphos)_2(CN\text{-}t\text{-}Bu)_2](ClO_4)_2$ (diphos = dppe, dppp) have been prepared and characterized as well, for comparison purposes. Three of the model compounds were also characterized from X-ray crystallography to establish the diphosphine chelating behavior. The polymers are all amorphous and have been characterized from the measurements of the intrinsic viscosity, DSC, TGA and XRD, as well as their capacity for making stand alone films. The intrinsic viscosity data indicate that the Cu- and Pd_2- materials are oligomeric in solution (~8-9 units), while the Ag-materials are smaller. For $\{[Cu(dppe)(dmb)]BF_4\}_n$, a glass transition is reproducibly observed at 81.5°C (ΔC_p = 0.43J/g°). The Cu- and Ag-species are luminescent in the solid state at room temperature exhibiting λ_{max} and τ_e (emission lifetime) around 480 to 550 nm and 18 to 48 μs, respectively, while the Pd_2 species are not luminescent under these conditions. During the course of this study, the unsaturated $[M_2(dppp)_2](BF_4)_2$ starting materials (M = Cu, Ag) were prepared, one of which (M = Ag) was characterized from crystallography. The bridging behavior of the dppp ligand in this case contrasts with the chelating behavior seen for the saturated $[Cu(dppp)(CN\text{-}t\text{-}Bu)_2]BF_4$ complex.

Introduction

The title bridging ligand (Scheme 1) has become a highly versatile assembling building block over the past 30 years,[1] and is notorious for the synthesis of binuclear complexes, although some examples of tri-[2] and tetranuclear dmb-containing species[3] were also reported.

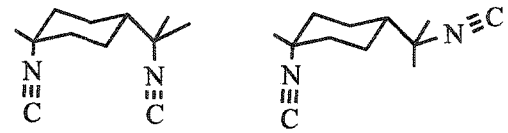

dmb (*anti*-) dmb (*gauche*-)

Scheme 1

Recently, the use of this ligand was made for the first time in the synthesis of the organometallic polymers $\{M(dmb)_2^+\}_n$ (M = Cu, Ag; Scheme 2),[4] which have been fully characterized from X-ray diffraction techniques, molecular weight measurements (M_n and M_w), and applications in the area of semi- and photoconductivity, and photovoltaic cells were reported as well.[4d]

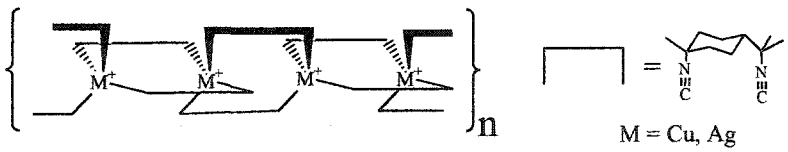

$\{M(dmb)_2^+\}_n$ M = Cu, Ag

Scheme 2

The uniqueness of these new materials is that they keep their polymeric, or at least oligomeric nature in solution,[4b,e] and can use both the *anti*- and *gauche*-conformations for dmb to form various isomeric 1-D polymers.[4c] On the other hand, the related and more flexible diisocyanide ligand tmb (2,5-dimethyl-2',5'-diisocyanohexane), produces 2- or 3-D polymer structures, as reported for polymers of the type $\{Ag(tmb)^+\}_n$ and $\{Ag_2(tmb)_3^{2+}\}_n$.[5] The two strategies for the synthsesis of 1-D materials that retain their oligomeric or polymeric nature in solution are the use of two dmb bridges between the metallic fragments (such as fragment = M^+ [4] and $M_2(dppm)_2^{2+}$ [6] with M = Cu, Ag; dppm = bis(diphenylphosphino)methane; Scheme 3):

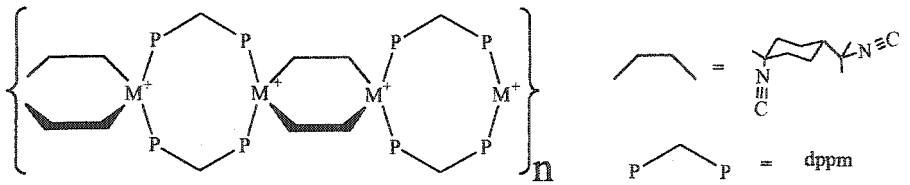

$\{M_2(dppm)_2(dmb)_2^{2+}\}_n$; M = Cu, Ag

Scheme 3

and of axially functionalizable metallic fragments exhibiting strong (and not so labile) M-L_{axial} bonding (such as Pd-CNR and Pd-P; Scheme 4).[3a,b] In the examples illustrated below, M_4 species are bridged together by the dmb (*gauche*-shape), or by flexible diphosphine ligands, leading to crystalline and amorphous materials, respectively.

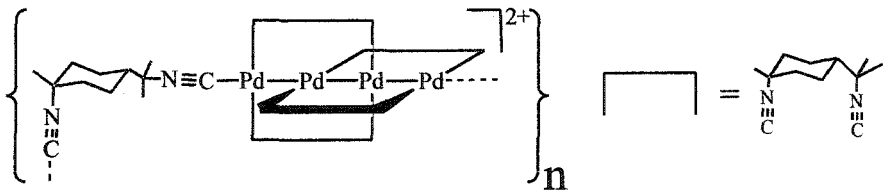

$\{Pd_4(dmb)_4(dmb)^{2+}\}_n$

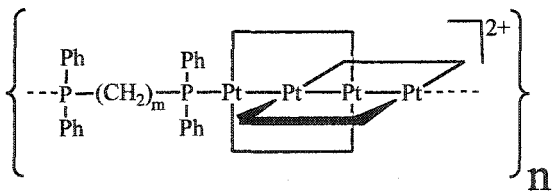

diphos

dppb (m = 4),
dpppen (m = 5),
dpph (m = 6)

$\{Pt_4(dmb)_4(diphos)^{2+}\}_n$

Scheme 4

We now wish to report the synthesis and characterization of a series of new polymers built upon chelated diphosphine metallic fragments, such as "$M(diphos)^{+}$" and "$Pd_2(diphos)_2^{2+}$" (M=Cu, Ag; diphos = dppe, dppp), and the bridging dmb ligands. This approach is novel, and is based on the intramolecular steric hindrance and ring stress that prevent the dimer formation. The polymers were characterized from the measurements of the intrinsic viscosity, DSC, TGA, XRD, and luminescence spectroscopy, and compared

to model compounds such as the mononuclear complexes $[M(dppe)(CN\text{-}t\text{-}Bu)_2]BF_4$ (M = Cu, Ag) and $[M(dppp)(CN\text{-}t\text{-}Bu)_2]BF_4$, and Pd_2-bonded dimers $[Pd_2(diphos)_2(CN\text{-}t\text{-}Bu)_2](ClO_4)_2$ (diphos = dppe, dppp). In the area of coordination polymers of Cu(I) and Ag(I) exhibiting luminescence, only a few examples have been reported so far.[7,8]

Experimental Section

Materials: Dmb, $Pd_2(CN\text{-}t\text{-}Bu)_4Cl_2$, $Pd_2(dmb)_2Cl_2$, and $[Cu(NCMe)_4]BF_4$ were synthesized according to literature procedures.[9] The $[M(dppe)(BF_4)]$ starting materials (M = Cu, Ag) were prepared in the same way as $[Ag(dppe)(ClO_4)]$,[10] except that $AgClO_4$ was replaced by with either $AgBF_4$ or $[Cu(CNMe)_4]BF_4$. The $[M_2(dppp)_2](BF_4)_2$ dimers were synthesized in the same manner as the complexes $[Cu_2(dppp)_2](ClO_4)_2$ [11] and $[Ag_2(dppb)_2](NO_3)_2$[12] (dppb = bis(diphenylphosphino)butane), except that dppp was used instead of dppb, $[Cu(NCMe)_4]BF_4$ instead of $[Cu(NCMe)_4]ClO_4$, and $AgBF_4$ instead of $AgNO_3$. The indentity of the $[M_2(dppp)_2](BF_4)_2$ starting materials were confirmed by X-ray structure determination methods for M = Ag (below and in the Supporting Information). $Cu(BF_4)_2{\cdot}H_2O$, $AgBF_4$, *t*-BuNC, dppe and dppp were purchased from Aldrich, and were used as received. The solvents, acetone (Fisher), acetonitrile (Anachemia), dichloromethane (ACP), diethyl ether (ACP) and butyronitrile (Aldrich) were purified according to published procedures.[13] The Cu and Ag compounds, and Pd_2 species were prepared as BF_4^- and ClO_4^- salts, respectively. The Pd_2-species were originally prepared as BF_4^- salt, but the use of ClO_4^- ion gave better chemical analysis.

$[Cu(dppe)(CN\text{-}t\text{-}Bu)_2]BF_4$. $[Cu(dppe)(BF_4)]$ (601.3 mg, 1.09 mmol) was dissolved in 150 ml of degassed acetone. 496 μl (4.38 mmol) of *t*-BuNC was added drop wise using a micro-syringe. The solution was stirred for 1 hr prior to drying it *in vaccuo*. The white powder was dissolved in a minimum amount of dichloromethane prior to adding 100 ml of diethyl ether to precipitate a white solid which was filtered and dried *in vaccuo*. Yield 60% (470 mg). ^1H NMR (CD_2Cl_2), δ 7.57-7.42 (m, 20H, Ph), 2.43 (m, 4H, CH_2), 1.38 (s, 18H, CH_3); $^{31}P\{^1H\}$ NMR (CD_2Cl_2), δ -7.58; $^{13}C\{^1H\}$ NMR (CD_2Cl_2), δ 132.7, 132.6,

131.0, 57.7, 30.1, 26.0; IR (KBr) ν 1059 (BF_4), 2170 cm^{-1} (C≡N); Raman (neat solid) ν 2172 cm^{-1} (C≡N); UV-vis (CH_3CN), 222 (44500), 272 nm (27500 $M^{-1}cm^{-1}$).

[Ag(dppe)(CN-*t*-Bu)$_2$]BF_4. [Ag(dppe)(BF_4)] (1.16 g, 1.96 mmol) was dissolved in 100 ml of degassed acetone. 442 μL (3.91 mmol) of *t*-BuNC was added drop wise using a micro-syringe. The solution was stirred for 2 hrs prior to being reduced to 20 ml *in vaccuo*. 150 ml of diethyl ether were added to precipitate the product, which was filtered and dried. Yield 88% (1.49 g). ^1H NMR (CD_2Cl_2) δ 7.49-7.36 (m, 20H, Ph), 2.43 (m, 4H, $\underline{CH_2}P$), 1.48 (s, 18H, CH_3); $^{31}P\{^1H\}$ NMR (CD_2Cl_2) δ 3.38; $^{13}C\{^1H\}$ NMR (CD_2Cl_2) δ 141.2, 132.7, 130.8, 129.3, 57.4, 30.0, 24.9; IR (KBr) ν 2183 (C≡N), 1057 cm^{-1} (BF_4); Raman (neat solid) ν 2184 cm^{-1} (C≡N); UV-vis (CH_3CN), 222 (44500), 270 nm (30300 $M^{-1}cm^{-1}$).

[Cu(dppp)(CN-*t*-Bu)$_2$]BF_4. [Cu_2(dppp)$_2$](BF_4)$_2$ (301 mg, 0.263 mmol) was dissolved in 100 ml of degassed acetone. 150 μl (1.33 mmol) of *t*-BuNC was added drop wise using a micro-syringe. The solution was stirred for 1 hr prior to concentrating it *in vaccuo* until dry. The white powder was dissolved in a minimum amount of dichloromethane prior to addition of 100 ml of diethyl ether to precipitate a white solid, which was filtered and dried *in vaccuo*. Yield 77% (301.6 mg). ^1H NMR (CD_2Cl_2), δ 7.49-7.36 (m, 20H, Ph), 2.40 (m, 4H, $\underline{CH_2}P$), 1.93 (m, 2H, $C\underline{CH_2}C$) 1.35 (s, 18H, CH_3); $^{31}P\{^1H\}$ NMR (CD_2Cl_2), δ -8.21; $^{13}C\{^1H\}$ NMR (CD_2Cl_2), δ 132.6, 130.8, 129.1, 30.1, 27.8, 19.1, 18.0; IR (KBr) ν 1061 (BF_4), 2172 cm^{-1} (C≡N); Raman (neat solid) ν 2171 cm^{-1} (C≡N); UV-vis (CH_3CN), 222 (43900), 274 nm (27200 $M^{-1}cm^{-1}$).

{[Cu(dppe)(dmb)]BF_4}$_n$. [Cu(dppe)(BF_4)] (609 mg, 1.11 mmol) was dissolved in 70 ml of degassed acetone. 425 mg (2.22 mmol) of dmb was dissolved in 200 ml of degassed acetone in another flask. Both solutions were cooled to 0°C and the dmb solution was added drop wise to the dimer solution. The mixture was stirred for 2 hrs prior to being

reduced to 15 ml *in vaccuo*. 150 ml of diethyl ether were added to precipitate the product, which was filtered and dried. Yield 57.5% (472 mg). ^{1}H NMR (CD_2Cl_2) δ 7.50-7.40 (m, 20H, Ph), 2.42 (m, 4H, $\underline{CH_2}P$), 1.83-1.11 (m, 18H, for 1.04 dmb); $^{31}P\{^{1}H\}$ NMR (CD_2Cl_2) δ 7.68; $^{13}C\{^{1}H\}$ NMR (CD_2Cl_2) δ 141.5, 132.6, 131.0, 129.5, 62.8, 60.5, 44.9, 37.3, 29.3, 26.5, 25.6, 22.8; IR (KBr) ν 2174 (C≡N), 1070 cm^{-1} (BF_4); Raman (neat solid) ν 2173 cm^{-1} (C≡N); Chem. Anal. (calcd.) for $C_{38}H_{42}N_2P_2BF_4Cu$ + 0.04 dmb : C, 62.53; H, 5.82; N, 3.94. (Found): C, 62.70; H, 6.19; N, 3.92; UV-vis (CH_3CN), 222 (43600), 270 nm (27900 $M^{-1}cm^{-1}$).

{[Ag(dppe)(dmb)]BF_4}$_n$. [Ag(dppe)(BF_4)] (272 mg, 0.230 mmol) was dissolved in 70 ml of degassed acetone. 86.8 mg (4.56 mmol) of dmb was dissolved in 200 ml of degassed acetone in another flask. Both solutions were cooled to 0°C, and the dmb solution was added drop wise to the dimer solution. The mixture was stirred for 2 hrs prior to being reduced to 15 ml *in vaccuo*. 150 ml of diethyl ether were added to precipitate the product which was filtered and dried. Yield 90% (323 mg). ^{1}H NMR (CD_2Cl_2) δ 7.47-7.32 (m, 20H, Ph), 2.41 (m, 4H, $\underline{CH_2}P$), 2.00-1.81 (m, 6H, dmb) 1.54-1.28 (m, 12H, for 1.21 dmb); $^{31}P\{^{1}H\}$ NMR (CD_2Cl_2) δ 4.49; $^{13}C\{^{1}H\}$ (CD_2Cl_2) δ 143.8, 143.3, 132.7, 131.0, 129.5, 63.2, 60.7, 44.1, 36.91, 29.0, 27.0, 25.1, 22.7 ; IR (KBr) ν 2180, 2133 (C≡N), 1058 cm^{-1} (BF_4); Raman (neat solid) ν 2178 cm^{-1} (C≡N); Chem. Anal. (calcd.) for $C_{38}H_{42}N_2P_2BF_4Ag$ + 0.21 dmb: C, 59.11; H, 5.60; N, 4.12. (Found): C, 59.14; H, 5.61; N, 4.08; UV-vis (CH_3CN), 222 (38600), 270 nm (32200 $M^{-1}cm^{-1}$).

{[Cu(dppp)(dmb)]BF_4}$_n$. ([Cu_2(dppp)$_2$](BF_4)$_2$) (312 mg, 0.227 mmol) was dissolved in 70 ml of degassed acetone. 109.3 mg (5.68 mmol) of dmb was dissolved in 150 ml of degassed acetone in an other flask. Both solutions were cooled to 0°C and the dmb solution was added drop wise to the dimer solution. The mixture was stirred for 1 hr prior to being reduced to 20 ml *in vaccuo*. Then 150 ml of diethyl ether were added to precipitate the product which was filtered and dried. Yield 92% (385 mg). ^{1}H NMR

(CD_2Cl_2) δ 7.40-7.40 (m, 20H, Ph), 2.41 (m, 4H, $\underline{CH_2}P$), 1.86-1.81 (m, 4H, dmb + CCH_2C dppp) 1.63-1.05 (m, 16H, for 1.13 dmb); $^{31}P\{^1H\}$ NMR (CD_2Cl_2) δ -8.17; $^{13}C\{^1H\}$ NMR (CD_2Cl_2) δ 133.8, 132.5, 130.7, 129.2, 63.4, 61.0, 45.5, 37.2, 29.2, 27.8, 22.8, 18.9; IR (KBr) ν 2168 (C≡N), 1057 cm^{-1} (BF_4); Raman (neat solid) ν 2171 cm^{-1} (C≡N); Chem. Anal. (calcd) for $C_{39}H_{44}N_2P_2BF_4Cu$ + 0.13 dmb: C, 62.20; H, 6.29; N, 3.72. Found : C, 62.65; H, 6.29; N, 3.67; UV-vis (CH_3CN), 222 (38900), 270 nm (23400 $M^{-1}cm^{-1}$).

{[Ag(dppp)(dmb)]BF_4}$_n$. The dimer [Ag_2(dppp)$_2$](BF_4)$_2$ (572 mg, 0.492 mmol) was dissolved in 100 ml of degassed acetone. 280 mg (1.48 mmol) of dmb was dissolved in 200 ml of degassed acetone in another flask. Both solutions were cooled to 0°C, and the dmb solution was added drop wise to the dimer solution. The mixture was stirred for 2 hrs prior to being reduced to 30 ml *in vaccuo*. 150 ml of diethyl ether were added to precipitate the product which was filtered and dried. Yield 96% (758 mg). ^1H NMR (CD_2Cl_2) δ 7.39-7.23 (m, 20H, Ph), 2.41 (m, 4H, $\underline{CH_2}P$), 2.03-1.91 (m, 4H, for 1.1 dmb) 1.68-1.48 (m, 18H, dmb + $C\underline{CH_2}C$ dppp); $^{31}P\{^1H\}$ NMR (CD_2Cl_2) δ -1.30; $^{13}C\{^1H\}$ NMR (CD_2Cl_2) δ 144.2, 143.5, 133.5, 132.6, 130.7, 129.3, 63.3, 60.6, 43.9, 36.9, 28.8, 27.1, 22.6, 18.9; IR (KBr) ν 2185, 2130 (C≡N), 1055 cm^{-1} (BF_4); Raman (neat solid) ν 2188 cm^{-1} (C≡N); Chem. Anal. (calcd) for $C_{39}H_{44}N_2P_2BF_4Ag$ + 0.1 dmb: C, 59.14; H, 5.65; N, 3.77, Found: C, 59.14; H, 5.61; N, 4.08; UV-vis (CH_3CN), 222 (40300), 272 nm (33700 $M^{-1}cm^{-1}$).

{[Pd_2(dppe)$_2$(CN-*t*-Bu)$_2$](ClO_4)$_2$}$_n$. Under inert atmosphere in the dark, {[Pd_2(CN-*t*-Bu)$_4Cl_2$] (37 mg, 0.06 mmol) was dissolved in 50 ml of acetonitrile, and 13 mg (0.13 mmol) of $LiClO_4$ was added to the mixture. 48 mg (0.12 mmol) of dppe was dissolved in 50 ml of acetonitrile in another flask. The dppe solution was added drop wise to the dimer solution. The mixture was stirred for 2 hrs prior to being reduced to 10 ml *in vaccuo*. 100 ml of diethyl ether were added to precipitate the product which was filtered

and dried. N.B. This compound must be prepared fresh prior to each analysis; it is unstable, even under inert atmosphere in the dark. Yield 78% (64.2 mg). ^{1}H NMR (CD_3CN) δ 7.59-7.16 (m, 40H, Ph), 2.53 (m, 8H, $\underline{CH_2}P$), 1.68 (s, 18H, CH_3); $^{13}C\{^{1}H\}$ NMR (CD_2Cl_2) δ 148.2, 131.7, 130.7, 129.2, 56.4, 30.0, 23.9; $^{31}P\{^{1}H\}$ 44,6 (d, J= ~0 Hz) 57.0 (d, J= ~0 Hz); IR (KBr) ν 2179 cm^{-1} (C≡N); Mass spec. FAB 1010 ($Pd_2(dppe)_2$; 1009.7), 1093 ($Pd_2(dppe)_2$(CN-*t*-Bu); 1092.8); UV-vis (CH_3CN) 420 nm (28600 $M^{-1}cm^{-1}$).

{[Pd_2(dppp)$_2$(CN-*t*-Bu)$_2$](ClO$_4$)$_2$}$_n$. Under inert atmosphere in the dark, {[Pd_2(CN-*t*-Bu)$_4Cl_2$] (15 mg, 0.024 mmol) were dissolved in 50 ml of acetonitrile and 5.4 mg (0.051 mmol) of $LiClO_4$. 21.1 mg (0.051 mmol) of dppp was dissolved in 50 ml of acetonitrile in another flask. The dppp solution was added drop wise to the dimer solution. The mixture was stirred for 2 hrs prior to being reduced to 10 ml *in vaccuo*. 100 ml of diethyl ether were added to precipitate the product which was filtered and dried. N.B. This compound must be prepared fresh prior to each analysis; it is unstable, even under inert atmosphere in the dark. Yield 92% (32.3 mg). ^{1}H NMR (CD_3CN) δ7.85-7,01 (m, 40H, Ph), 2,55(m, 8H, $\underline{CH_2}P$), 1,77 (m, 4H, $\underline{CH_2}CH_2P$), 1,61 (s, 18H, CH_3); ^{31}P $\{^{1}H\}$ NMR (CD_3CN) δ -5.62 (d, J = ~28 Hz), 10.25 (d, J = ~28 Hz) ^{13}C $\{^{1}H\}$ NMR (CD_3CN) δ 141.8, 131.5, 129.5, 128.9, 57.5, 28.9, 27.6, 18.3; IR (KBr) ν 2179 cm^{-1} (C≡N); Mass spec. FAB 1038 ($Pd_2(dppp)_2$; 1037.7), 1120 ($Pd_2(dppp)_2$(CN-*t*-Bu); 1120.9), 1303 (($Pd_2(dppp)_2$(CN-*t*-Bu)(ClO_4); 1303.4); UV-vis (CH_3CN) 414 nm (26000 $M^{-1}cm^{-1}$).

{[Pd_2(dppe)$_2$(dmb)](ClO$_4$)$_2$}$_n$. Under inert atmosphere in the dark, [$Pd_2(dmb)_2Cl_2$] (19 mg, 0.029 mmol) and 9.8 mg (0.092 mmol) of $LiClO_4$ were dissolved in 50 ml of acetonitrile. The solution was stirred for 1 hr. 22.8 mg (0.057 mmol) of dppe was dissolved in 50 ml of acetonitrile in another flask. The dppe solution was added drop wise to the dimer solution. The mixture was stirred for 2 hrs prior to being reduced to 10 ml *in vaccuo*. 100 ml of diethyl ether were added to precipitate the product which was

filtered and dried. Yield 79% (32.0 mg). ^{1}H NMR (CD_3CN) δ 7.56-6.98 (m, 40H, Ph), 2.65 (m, 8H, $\underline{CH_2}P$), 2.05-1.15 (m, 18H, dmb); $^{31}P\{^{1}H\}$ NMR (CD_3CN) δ -5 (d) 10 (d); $^{13}C\{^{1}H\}$ NMR (CD_3CN) δ 148.5, 142.2, 131.5, 131.8, 128.5, 65.2, 63.7, 44.2, 35.3, 27.8, 26.5, 24.9, 21.6; IR (KBr) ν 2170 cm^{-1} (C≡N); Mass spec. FAB 1010 ($Pd_2(dppe)_2$; 1009.7), 1199 ($Pd_2(dppp)_2(dmb)$; 1199.9); Chem. Anal. (calcd.) for $C_{64}H_{66}N_2Pd_2P_4Cl_2O_8$: C, 54.95; H 4.76; N 2.00. (Found) C, 52.67; H 4.76; N 2.06. UV-vis (CH_3CN), 412 nm (28000 $M^{-1}cm^{-1}$).

$\{[Pd_2(dppp)_2(dmb)](ClO_4)_2\}_n$. Under inert atmosphere in the dark, $[Pd_2(dmb)_2Cl_2]$ (29 mg, 0.044 mmol) and 6.3 mg (0.059 mmol) of $LiClO_4$ were dissolved in 50 ml of acetonitrile. The solution was stirred 1 hr. 36.0 mg (0.087 mmol) of dppp was dissolved in 50 ml of acetonitrile in another flask. The dppp solution was added drop wise to the dimer solution. The mixture was stirred for 2 hrs prior to being reduced to 10 ml *in vaccuo*. 100 ml of diethyl ether were added to precipitate the product which was filtered and dried, always in the dark. Yield 86% (53.6 mg). ^{1}H NMR (CD_3CN) δ 7,53-7,03 (m, 40H, Ph), 2,58 (m, 8H, $\underline{CH_2}P$), 2,10 (m, 4H, $\underline{CH_2}CH_2P$), 201-0.98 (m, 18H, dmb); $^{31}P\{^{1}H\}$ –5,72 (d, J = ~25 Hz), 10.38 (d, J = ~25 Hz); $^{13}C\{^{1}H\}$ NMR (CD_3CN) δ148.5, 142.2, 131.5, 131.8, 128.5, 65.2, 63.7, 61.9, 44.9, 37.6, 28.2, 27.7, 23.8, 17.9; IR (KBr) ν 2170 cm^{-1} (C≡N); Mass spec. FAB 1038 ($Pd_2(dppp)_2$; 1037.9), 1227.3 ($Pd_2(dppp)_2(dmb)$; 1227.2); Chem. Anal. (calcd.) for $C_{66}H_{70}N_2Pd_2Cl_2O_8$: C, 55.56; H 4.94; N 1.96. (Found) C, 52.12; H 5.14; N 2.08; UV-vis (CH_3CN) 414 nm (25700 $M^{-1}cm^{-1}$).

Apparatus: All NMR spectra were acquired with a Bruker AC-300 spectrometer (^{1}H 300.15 MHz, ^{13}C 75.48 MHz, ^{31}P 121.50 MHz) using the solvent as chemical shift standard, except in ^{31}P NMR, where the chemical shifts are relative to D_3PO_4 85% in D_2O. All chemical shifts (δ) and coupling constants (J) are given in ppm and Hertz, respectively. The IR spectra were acquired on a Bomem FT-IR MB series spectrometer equipped with a baseline diffused reflectance. The emission spectra were measured on a

Spex Fluorolog II spectrofluorometer using a HgXe excitation lamp. The emission lifetimes were measured with a nanosecond N_2 laser system from PTI model GL-3300 pumping a dye laser model GL-302. The glass transition temperatures (Tg) were measured using a Perkin-Elmer 5A DSC7 equipped with a thermal controller 5B TAC 7/DS. Calibration standards were water and indium. FT-Raman were acquired on a Bruker RFS 100/S spectrometer. XRD were acquired on a Rigaku/USA Inc with a copper lamp operating under a 30 mA current and a 40 KV tension. TGA were acquired on a TGA 7 of Perkin Elmer between 50 et 650 °C at 3°/minute under nitrogen atmosphere.

Crystallography. All three crystals were grown by vapor diffusion using acetone – *tert*-butylmethylether at 23 C°. Single crystals were coated with Paratone-N oil, mounted using a glass fiber and frozen in the cold nitrogen stream of the goniometer. A hemisphere of data was collected on a Bruker AXS P4/SMART 1000 diffractometer using ω and θ scans with a scan width of 0.3 ° and 30 for $[Cu(dppe)(CN\text{-}t\text{-}Bu)_2]BF_4$, 10 for $[Ag(dppe)(CN\text{-}t\text{-}Bu)_2]BF_4$, and $[Cu(dppp)(CN\text{-}t\text{-}Bu)_2]BF_4$, and 25s for $[Ag_2(dppp)_2](BF_4)_2$ exposure times. The detector distance was 5 cm. The data were reduced (SAINT)[14] and corrected for absorption (SADABS).[15] The structure was solved by direct methods and refined by full-matrix least squares on F[15] (SHELXTL).[16] For $[Cu(dppe)(CN\text{-}t\text{-}Bu)_2]BF_4$, one of the *t*-butyl groups was disordered and the site occupancy determined using an isotropic model as 0.75 (C(34) – C(36)) and 0.25 (C(34A) – C(36A)) and fixed in subsequent refinement cycles. All non-hydrogen atoms were refined anisotropically. Hydrogen atoms were found in Fourier difference maps and refined isotropically. Hydrogen atoms at C(34) – C(36) were included in calculated positions and refined using a riding model. Hydrogen atoms at C(34A) – C(36A) were omitted. For $[Ag(dppe)(CN\text{-}t\text{-}Bu)_2]BF_4$, one of the *t*-Bu groups was disordered and the site occupancy determined using an isotropic model as 0.33 (C(8)-C(10)), 0.33 (C(8A)-C(10A) and 0.33 (C(8B)-C(10B)) and fixed in subsequent refinement cycles. All non-hydrogen atoms were refined anisotropically with the exception of the disordered *t*-Bu group. Hydrogen atoms were located in Fourier difference maps and refined isotropically

with the exception of the methyl hydrogens at C(8)-C(10) which were omitted. For $[Cu(dppp)(CN\text{-}t\text{-}Bu)_2]BF_4$, the BF_4 anion and one *t*-Bu group was disordered and the site occupancy determined using an isotropic model as 0.75 (F(1)-F(3)), 0.25 (F(1A)-F(3A), 0.7 (C(10)-C(12)) and 0.3 (C(10A)-C(12A)) and fixed in subsequent refinement cycles. All non-hydrogen atoms were refined anisotropically. Hydrogen atoms were located in Fourier difference maps and refined isotropically with the exception of the methyl hydrogens at C(6) which were included in calculated positions and refined using a riding model. For $[Ag_2(dppp)_2](BF_4)_2$, the BF_4 anion was disordered and the site occupancy determined using an isotropic model as 0.75 (F(2)-F(4)) and 0.25 (F(2A)-F(4A) and fixed in subsequent refinement cycles. All non-hydrogen atoms were refined anisotropically. Hydrogen atoms were located in Fourier difference maps and refined isotropically. Thermal ellipsoid plots are at the 30% probability level. In some plots, hydrogen atoms were omitted for clarity.

Intrinsic viscosity. The oligomeric nature of the materials in solution were qualitatively established from the measurements of the intrinsic viscosity using the universal standard polymethyl methacrylate from Aldrich (M_n = 12000, 15000, 120000, and 320000). All measurements were reproduced 5 times for greater accuracy. Although the results were checked against the known oligomer $\{[Ag(dmb)_2]BF_4\}_n$ (M_n = 4000),[4e] the results are still at the lower end of the method's accuracy. Only an approximate value of number of units can be obtained.

Computer modeling. The calculations were performed using the commercially available PC-model from Serena Software (version 7.0), which uses the MMX empirical model. No constraint on bond distances and angles was applied to insure that deviations from normal geometry was depicted. The R-N≡C groups were replaced by R-C≡C$^-$ because PC Model does not model C≡N$^+$- appropriately as strongly bent structures were calculated. Instead -C≡C- was used securing a more linear and realistic frame for the ligand.

Results and discussion

The model compounds. The dppe[17] and dppp[11,18] ligands can act either as chelates or bridging species on both Cu(I) and Ag(I) ions based on the literature. Because no crystal suitable for X-ray diffraction studies has been obtained for the reported polymers in this work and no data on complexes of the type $[M(diphos)(CNR)]^+$ are reported in the Cambridge Databank, the "chelate vs bridging" behavior has been addressed by synthesizing and characterizing the model mononuclear compounds $[M(dppe)(CN\text{-}t\text{-}Bu)_2]BF_4$ (M = Cu, Ag) and $[Cu(dppp)(CN\text{-}t\text{-}Bu)_2]BF_4$. This monodentate CNR ligand can adequately mimic both the electronic density and steric behavior of dmb.

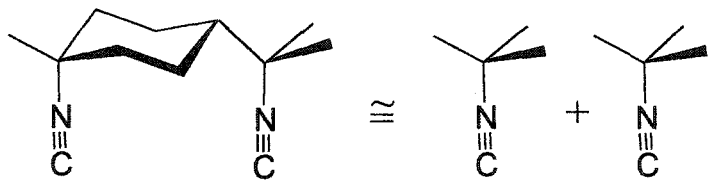

Scheme 5

The syntheses proceed from a 1:2 (M / *t*-BuNC) stoichiometric reaction between the starting materials $[M(dppe)(BF_4)]$ or $[M_2(dppp)_2](BF_4)_2$ [19] and the isocyanide. These compounds crystallize easily and have been characterized from X-ray crystallography (Tables 1 and 2; Figures 1 and 2). The chelate form for these diphosphines is observed, where the 5- and 6- membered rings for the dppe and dppp species exhibit puckered and chair structures, respectively. The *t*-BuCN ligands coordinate the two remainder tetrahedral positions of the M atoms and the M-P, M-C, and C≡N distances are normal (Table 2). Some deviations from linearity of the MCN angles averaging 173 and 169° for M = Cu and Ag in the $[M(dppe)(CN\text{-}t\text{-}Bu)_2]BF_4$ and 172° for $[Cu(dppp)(CN\text{-}t\text{-}Bu)_2]BF_4$, are observed. The PMP and CMC angles are smaller and greater than the ideal tetrahedral angle, due to the smaller bite angle of the chelating diphos ligand.

The model compounds $[Pd_2(diphos)_2(CN\text{-}t\text{-}Bu)_2](ClO_4)_2$ (diphos = dppe, dppp) were prepared in one step from the starting $Pd_2(CN\text{-}t\text{-}Bu)_4Cl_2$ (Scheme 6).

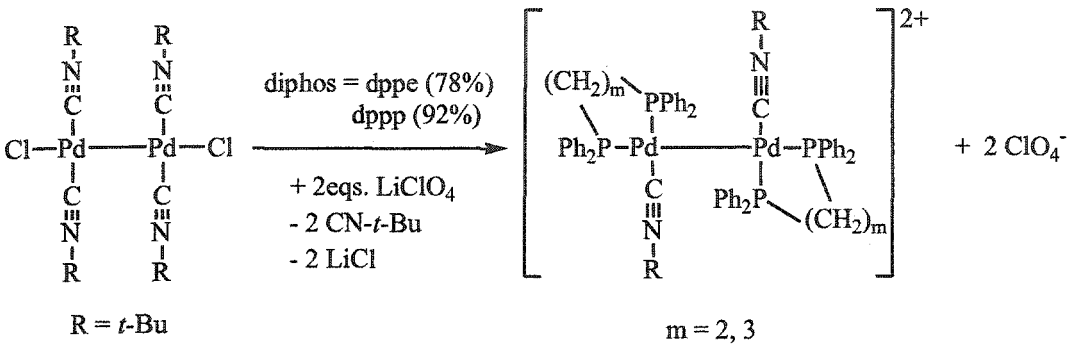

Scheme 6

Other related d^9-d^9 Pd_2 dimers were reported in the literature including the $M_2(diphos)_2(CNR)_2^{2+}$ complexes and the $Pd_2(dppp)_2^{2+}$ species where M = Pd or Pt, R = Me, 2,4,6-$Me_3C_6H_2$, and 2,6-$Me_2C_6H_3$ (Scheme 7).[20] These dimers can be prepared either from a 1 + 1 addition of a d^8 and a d^{10} Pd (or Pt) mononuclear or binuclear species,[20d] or from the electrochemical reduction of a d^8 Pd (or Pt) compound. For instance, the related d^9-d^9 $M_2(diphos)_2(CNR)_2^{2+}$ (M = Pd, Pt; diphos = dppe, dppp; R = 2,4,6-$Me_3C_6H_2$, and 2,6-$Me_2C_6H_3$) are synthesized from the electrochemical reduction of the corresponding d^8 $M(diphos)(CNR)_2^{2+}$.[20a,b] The second route is the ligand substitution of labile CNR groups[20c] and Cl^- ions as shown in Scheme 6.

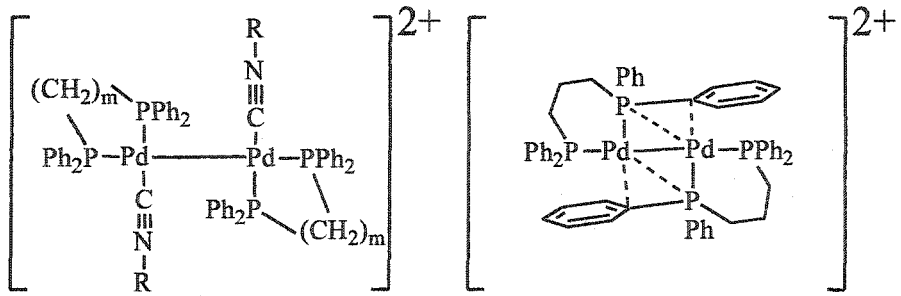

m = 2, 3
R = Me
2,4,6-$Me_3C_6H_2$
2,6-$Me_2C_6H_3$

$Pd_2(dppp)_2^{2+}$

Scheme 7

Their structures consist of an unsupported M-M bond with two square planar M-fragments forming angles of 84 to 88°.[20] The two diphosphine ligands are chelating each of the M atoms via one of the equatorial and the axial positions. The remaining equatorial coordination site is occupied by the isocyanide ligands. No crystal suitable for X-ray analysis was obtained for these dimers in this work. The ^{31}P NMR signature shows two δ,s for the equatorial and axial positions with very small $^{2}J(P, P)$ values, consistent with the approximate right PPdP angle. The UV-visible spectra also exhibit a strong absorption at ~414 nm, characteristic of the presence of a Pd-Pd bond (discussed below).

The dmb polymers. The colorless Cu and Ag materials are obtained by reacting the corresponding starting $[M(dppe)(BF_4)]$ or $[M_2(dppp)_2](BF_4)_2$ materials with dmb in excess. The yellow Pd_2 polymers are obtained differently by reacting the d^9-d^9 dimer $Pd_2(dmb)_2Cl_2$ with 2 equivalents of dppe or dppp according to:

$$Pd_2(dppm)_2Cl_2 + 2\ diphos \rightarrow 1/n\{Pd_2(diphos)_2(dmb)^{2+}\}_n + dmb + 2\ Cl^- \qquad (1)$$

where diphos is dppe (79% yield) or dppp (86% yield). The close similarity in the ^{31}P NMR, IR and UV-vis spectra between the model compounds and the polymers indicate

that the "$Pd_2(diphos)_2(CNR)_2^{2+}$" unit is present in the polymers, including the chelate structure of the "Pd(diphos)" fragment.

All investigated polymers exhibit an amorphous morphology based on the XRD patterns as exemplified in Figure 3, so no crystal suitable for X-ray studies was obtained despite numerous attempts. The chemical analysis and the integration of the ^1H NMR signals are consistent with the 1:1.x diphos / dmb stoichiometries for the $\{M(diphos)(dmb)^+\}_n$ (M = Cu, Ag) polymers, where x is a small number (~1-2) and is due to the presence of dmb acting as end-of-chain units. The presence of weak IR peaks associated with free C≡NR groups (~2130cm^{-1}) are noted for some solid samples, confirming their presence, but also indicating the presence of oligomers in the solid state. For the $\{Pd_2(diphos)_2(dmb)^{2+}\}_n$ materials, there is no evidence for such a peak, suggesting that the oligomers are of greater dimension.

The intrinsic viscosity measurements indicate that the Cu and Pd_2 materials are at least oligomeric in solution, where a number of units is evaluated to be ~8-9. Conversely, the Ag materials which dissolve far more rapidly than those of Cu and Pd_2 species, and exhibit no time difference between the pure solvent and the Ag material-containing solutions. This result indicates the presence of extensively dissociated materials in solution. All in all, these spectroscopic data along with the intrinsic viscosity measurements indicate that the dissolution of these materials is accompanied by a polymer or oligomer dissociation, and the data are indeed consistent with the formulation shown in Scheme 8 for these new materials.

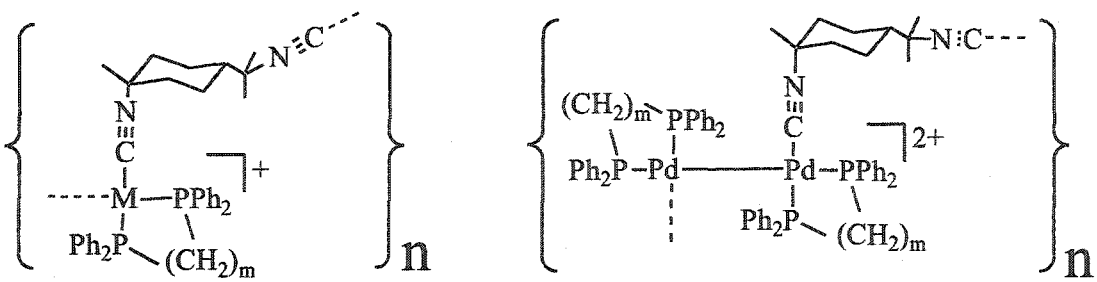

M = Cu, Ag; m = 2, 3 m = 2, 3

Scheme 8

The comparison of the TGA traces between the model compounds and polymers indicate that the *t*-BuNC ligand is lost at a lower temperature with respect to the dmb analogues (see Figure 4 as an example, Supporting Information). Using the spin-coating technique, or by simply evaporating an acetonitrile solution, these 6 materials form clear films with no sign of heterogeneous area under the microscope. While the films formed by the Ag polymers are found to be brittle, stand alone films are obtained for the Cu and Pd_2 materials. These observations are consistent with the fact that the Ag materials are of a smaller dimension with respect to the Cu and Pd_2 polymers. In one case, $\{[Cu(dppe)(dmb)]BF_4\}_n$, a glass transition at T_g = 81.5°C (ΔC_p = 0.43 J/g°) is reproducibly observed in the DSC traces. These Pd_2-polymers belong to a broader family of organometallic polymers which contains unsupported M_2 bonds in the backbone. The number of examples is still somewhat limited,[21] but the incorporation of a Pd_2-bond is to our knowledge, unprecedented.

Computer modeling. Modeling is used to address qualitatively two issues. The first one concerns why polymer structures are favored in this work, while in other related complexes, dimer species are observed. The second one concerns what we can extract from the computed structures in terms of predicted properties. The first series of computations deals with the comparison between computed and X-ray structures of related Cu, Ag and Pd_2 complexes, providing a degree of reliability of the method

employed. These complexes are the three model Cu and Ag complexes described above, and the X-ray characterized $Pd_2(dmb)_2Cl_4$[22] and $[Pd(dppe)(dmb)]_2^{4+}$ (Scheme 9).[23]

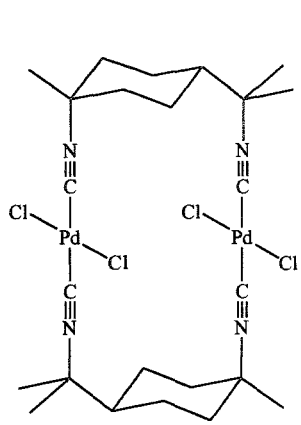

$Pd_2(dmb)_2Cl_4$

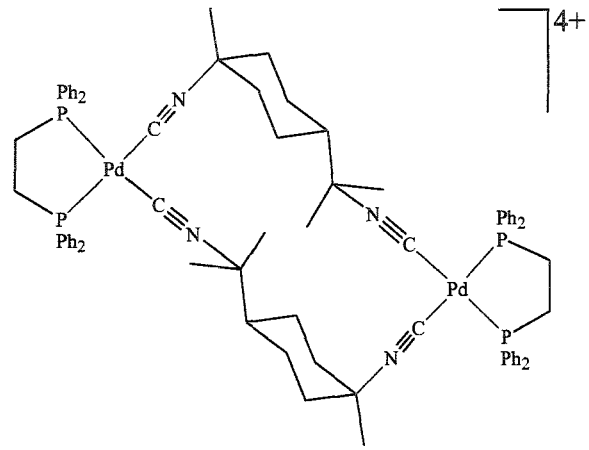

$[Pd(dppe)(dmb)]_2^{4+}$

Scheme 9

The comparison between MMX and X-ray data for the $M(diphos)(CN\text{-}t\text{-}Bu)_2^+$ complexes are presented in Table 3. The computations give satisfactory results in M-P distances (the largest difference is 0.3 Å, 1.3%) and skeleton angles (the largest difference is ~5°, but usually it is ~1°) for the Cu complexes, but worse comparisons are noticed for the Ag species. The M-C and C≡N are respectively under and over estimated. Their sums, however, provide a better comparison. Similar observations are made for the $Pd_2(dmb)_2Cl_4$[22] and $[Pd_2(dppe)(dmb)]_2^{4+}$ complexes,[23] where bond lengths and angles are well reproduced in the calculations, except that the Pd-P distance is somewhat off.

The structures for the chiral $Pd_2(diphos)_2(CN\text{-}t\text{-}Bu)_2^{2+}$ complexes (diphos = dppe, dppp) have modeled as well (see Figure 5 for example). The computed Pd-Pd (2.66), Pd-P_{ax} (2.36), Pd-P_{eq} (2.36), and Pd-C (1.89 Å) distances compare reasonably well with those found experimentally for the corresponding aryls species (2.60-2.62, 2.32-2.36, 2.30-2.33, 1.96-1.97 Å, respectively)[20] shown in Scheme 7. The structures exhibit a twisted geometry where the dihedral angle (CPdPdC) is about 77-78°; an angle that is greater than those seen for the above compounds (86°),[20] which reflects the presence of greater

steric hindrance between the *t*-butyl groups and the diphos-phenyl fragments. Full rotation about the Pd-Pd bond is severely hindered, so inversion of configuration is impossible.

The replacement of the two *t*-BuNC groups in these computed models by one dmb bridging ligand generates the dinuclear "$Pd_2(diphos)_2(dmb)^{2+}$" complex, where the Pd-Pd bond is now supported by a dmb ligand (a picture is provided in the Supporting Information). While most distances remained unchanged, significant changes have been noted in PdCN (158-169°), and dihedral angles (~73°), witnessing significant ring stress. In addition, the PPdPdP axis now exhibits a pronounced arch where the PPdPd angles are in the range of 160°. This structure is not favored.

Similarly, the tetranuclear structure for "$[Pd_2(diphos)_2(dmb)]_2^{4+}$" exhibits a macrocycle composed of two Pd-Pd-(*gauche*-dmb) units where the two Pd-Pd axes are placed parallel to each other (Supporting Information). Although no major distortions are noted in the structure, the dmb ligand is found quasi-encapsulated between the four diphos chelates pressed in between the phenyl groups. Numerous C-H···C contacts are obvious indicating the presence of some steric interactions. These interactions are felt by a small increase in calculated Pd-P_{ax} distances (from 2.38 to 2.39-2.40 Å), and a small deviation of the $PdPdP_{ax}$ angles (~169° in comparison with ~174° calculated for the model compounds $Pd_2(diphos)_2(CN\text{-}t\text{-}Bu)_2^{2+}$; Figure 5).

On the other hand, the computed models for the $\{Pd_2(diphos)_2(dmb)^{2+}\}_n$ polymers (see Figure 6 as an example) exhibit dmb ligands in their *gauche*-conformation that are significantly less encapsulated than the above dimer, and phenyl groups with no or only little close C-H···C contacts. The computed PdCN angles are ~176.5°. In addition, multiple conformations (relative orientation of Pd_2 units with respect to each other) are possible, where the Pd-Pd bond is never found parallel to each other. Computations performed on three identical (same stereoisomer) or different units (both enantiomers)

show that stereoregularity seems impossible at least for short fragments. This result may explain the amorphous morphology observed (XRD) for the solid material.

The structure of a cyclic "$Cu_2(diphos)_2(dmb)_2^{2+}$" dimer has also been examined and consists of a similar geometry to the $[Pd(dppe)(dmb)]_2^{4+}$ discussed above. The difference is that the CMC angle is tetrahedral instead of 90°. This macrocycle exhibits some ring stress (see Supporting Information). For instance, the computed PdCN angles range from 165 to 171° in comparison with computed angles of 172.5° for the mononuclear $Cu(dppp)(CN\text{-}t\text{-}Bu)_2^+$ (Table 4). This result contrasts greatly with the comparative d^8-d^8 compound $[Pd(dppe)(dmb)]_2^{4+}$ and suggests that a simple increase in CMC angle from 90 to 109.5° is enough to drive the polymer formation.[24]

Electronic spectra. The $\{[M(diphos)(dmb)]BF_4\}_n$ and $[M(diphos)(CN\text{-}t\text{-}Bu)_2]BF_4$ species (M = Cu, Ag; diphos = dppe, dppp) exhibit a structureless low-energy absorption at 272 ± 2 nm, with absorptivities ranging from 23000 to 34000 $M^{-1}cm^{-1}$(see Experimental section for data, and Figure 7 as an example). This electronic band is assigned to a metal-to-ligand-charge-transfer (MLCT), where the ligand manifold comprises both the π-systems of the C≡NR and PPh_2 groups. This assignment is based on the recent theoretical findings (EHMO and DFT) and spectroscopic experimental data for the mixed-ligand related dimer complex $[Cu_2(dppm)_2(O_2CMe)]^+$,[25] and the monomer $[M(CN\text{-}t\text{-}Bu)_4]^+$.[4b]

The electronic absorption spectra for the $Pd_2(diphos)_2(CN\text{-}t\text{-}Bu)_2^{2+}$ model compounds and the $\{Pd_2(diphos)_2(dmb)^{2+}\}_n$ polymers in PrCN exhibit narrow featureless absorptions at 293 K at 420 and 414 nm for the dimers and at 428 and 416 nm for the polymers with diphos = dppe and dppp, respectively (see Figure 8 as an example). These values are slightly blue-shifted with respect to the starting material $Pd_2(dmb)_2Cl_2$ (444 nm), but compare favorably with that of the related d^9-d^9 dimer $Pd_2(dppm)_2Cl_2$ (418 nm).[26] This absorption is easily assigned to $d\sigma \rightarrow d\sigma^*$ as previously demonstrated by Sourisseau and co-workers for $Pd_2(dppm)_2Cl_2$ (by resonance Raman spectroscopy),[26] and

by this group for $Pd_2(dmb)_2Cl_2$ (EHMO,[27] DFT,[28] and FT-Raman spectroscopy second moment band analysis[27]). The electronic bands associated with $d\sigma \rightarrow d\sigma^*$ electronic transitions for M_2-bonded species generally exhibit low energy, high intensity ($\varepsilon > 25\ 000\ M^{-1}cm^{-1}$; Table 4), and small FWHM (full-width-at-half-maximum; $2200 < FWHM < 2700\ cm^{-1}$ at 293 K), as seen for these two materials (2540 and 2670 cm^{-1} for the dppe and dppp species, respectively). Upon cooling the $\{Pd_2(diphos)_2(dmb)^{2+}\}_n$-containing solution from 293 to 77 K, the λ_{max} and FWHM of the $d\sigma \rightarrow d\sigma^*$ bands decrease slightly down to 424 and 406 nm, and 2500 and 2300 cm^{-1}, for dppe and dppp, respectively.

Solid state luminescence. The $M(diphos)(CN\text{-}t\text{-}Bu)_2^+$ model compounds and $\{M(diphos)(dmb)^+\}_n$ polymers (M = Cu, Ag; diphos = dppe, dppp) exhibit broad luminescence found between ~480-550 nm in the solid state (Figure 7). The Stoke shift is very large (> 17000 cm^{-1}), and the emission lifetimes range in the μs time scale ($18 < \tau_e < 48$ μs; see detail in Table 5). This experimental evidence indicate that the emission is a phosphorescence. These emission maxima and lifetimes compare favorably to other tetravalent mononuclear,[4b,29] dinuclear,[30,31] trinuclear,[30,32] and polynuclear species.[30,33] The emissive excited state responsible for the emission in these cases is assigned to a ^{3}MLCT as described above.

Conversely, the $Pd_2(diphos)_2(CN\text{-}t\text{-}Bu)_2^{2+}$ and $\{Pd_2(diphos)_2(dmb)^{2+}\}_n$ species are found to be non luminescent at 293K in the solid state. This lack of luminescence has also been observed for other d^9-d^9 dimers such as $Pd_2(dppm)_2Cl_2$ and $Pd_2(dmb)_2Cl_2$ for example.[34] This behavior has been discussed previously in terms of an efficient photoinduced homolytic Pd-Pd bond cleavage, followed by a diradical recombination.[27]

Concluding remarks. The bridging ligand dmb exhibits a very strong tendency to assemble metallic fragments to provide organometallic polymeric materials. This observation greatly conflicts with most works reported on this ligand in the literature,

where dimeric species are numerously observed.[1] The absence of crystals suitable for X-ray analysis certainly plays a role in this phenomena. This paper reports another strategy for the synthesize of dmb-based organometallic polymers, which consists of using bulky metallic fragments such as the $Pd_2(diphos)_2$ units. The steric hindrance prevents dmb from bridging the Pd_2-bond (presumably due to a large unfavorable twist CPdPdC angle), and also from making the unobserved dimer $[Pd_2(diphos)_2(dmb)^{+2}]_2$.

Acknowledgment. This research was supported by the Natural Sciences and Engineering Research Council of Canada (NSERC).

Supporting Information. Pictures showing numerous computed structures for model Cu and Pd_2 compounds, table gathering TGA data. X-ray crystallographic files are available for $[M(dppe)(CN\text{-}t\text{-}Bu)_2]BF_4$ (M = Cu, Ag) and $[Cu(dppp)(CN\text{-}t\text{-}Bu)_2]BF_4$ in CIF format. This material is available free of charge via the Internet at http://pubs.acs.org.

References:

(1) Harvey, P. D. *Coord. Chem. Rev.* **2001**, *219*, 17, and the references therein.

(2) (a) Sykes, A. G.; Mann, K. R. *Inorg, Chem.* **1990**, *29*, 4449. (b) Sykes, A. G.; Mann, K. R. *J. Am. Chem. Soc.* **1988**, *110,* 8252. (c) Sykes, A. G.; Mann, K. R. *J. Am. Chem. Soc.* **1990**, *112,* 7247. (d) Harvey, P. D.; Drouin, M.; Michel, A.; Perreault, D. *J. Chem. Soc. Dalton Trans.* **1993**, 1365.

(3) (a) Zhang, T.; Drouin, M.; Harvey, P. D. *Inorg. Chem.* **1999**, *38*, 1305. (b) Zhang, T.; Drouin, M.; Harvey, P. D. *Inorg. Chem.* **1999**, *38*, 957. (c) Fortin, D.; Drouin, M.; Harvey, P. D.; Herring, F. G.; Summers, D. A.; Thompson, R. C. *Inorg. Chem.* **1999**, *38*, 1253. (d) Zhang, T.; Drouin, M.; Harvey, P. D. *Inorg. Chem.* **1999**, *38*, 4928.

(4) (a) Perreault, D. ; Drouin, M.; Michel, A.; Harvey, P. D. *Inorg. Chem.* **1992**, *31,* 3688. (b) Fortin, D.; Drouin, M.; Turcotte, M. ; Harvey, P. D. *J. Am. Chem. Soc.* **1997**, *119*, 531. (c) Fortin, D.; Drouin, M.; Harvey, P. D. *J. Am. Chem. Soc.* **1998**, *120*, 5351.

(d) Fortin, D.; Drouin, M.; Harvey, P. D. *Inorg. Chem.* **2000**, *39*, 2758. (e) Turcotte, M.; Harvey, P. D. *Inorg. Chem.* **2002**, *41*, 1739.

(5) (a) Guitard, A.; Mari, A.; Beauchamp, A. L. ; Dartiguenave, Y. ; Dartiguenave, M. *Inorg. Chem.* **1983**, *22*, 1603. (b) Dartiguenave, M. ; Dartiguenave, A.; Mari, A. ; Guitard, A. ; Olivier, M.-J. ; Beauchamp, A. L. *Can. J. Chem.* **1988**, *66*, 2386.

(6) (a) Fournier, E. ; Lebrun, F.; Harvey, P. D. submitted for publication. (b) Lebrun, F., M.Sc. Dissertation, Université de Sherbrooke, 2001.

(7) (a) Zhang, J.; Xiong, R. G.; Chen, X. T.; Che, C.-M.; Xue, Z.; You, X.-Z. *Organometallics* **2001**, *20*, 4118. (b) Liu, Q.-X.; Xu, F.-B.; Li, Q.-S.; Zang, X.-B.; Leng, Y. L.; Chou, Z.-Z. Zhang, *Organometallics* **2003**, *22*, 309. (c) Zhang, J.; Xiong, R.-G.; Chen, X.-T.; Xue, Z.; Peng, S.-M; You, X.-Z. *Organometallics* **2002**, *21*, 235.

(8) Sun, D.; Cao, R.; Weng, J.; Hong, M.; Liang, Y. *Dalton* **2002**, 291. (e) Tong, M.-L.; Shi, X.-M. Chen, *New. J. Chem.* **2002**, *26*, 814. (f) Zheng, S.-L.; Tong, M.-L.; Tan, S.-D.; Wang, Y.; Shi, J.-X.; Tong, Y.-X.; Lee, H. K.; Chen, X.-M. *Organometallics* **2001**, *20*, 5319. (g) Henary, M.; Wootton, J. L.; Khan, S. I.; Zink, J. I. *Inorg. Chem.* **1997**, *36*, 796.

(9) (a) For $Pd(COD)Cl_2$ see: Chatt, J.; Vallarino; L. M.; Venanzi, L. M. *J. Chem. Soc.* **1957**, 3413. (b) For dmb see: Weber, W. D. ; Gokel, G. W.; Ugi, I. K. *Angew. Chem. Int. Ed. Engl.* **1972**, *11*, 530. (c) For $Pd_2(dmb)_2Cl_2$ see: Perreault, D.; Drouin, M.; Michel, A.; Harvey, P. D. *Inorg. Chem.* **1992**, *31*, 2740. (d) For $[Cu(NCMe)_4]BF_4$ see: Diez, J.; Gamasa, M. P.; Gimeno, J.; Tiripichio, A.; Tiripicchio Camellini, M. *J. Chem. Soc. Dalton Trans.* **1987**, 1275.

(10) Coronas, J. M.; Rossel, O.; Sales, J. *J. Organomet. Chem.* **1976**, *121*, 265.

(11) Kitagawa, S.; Kondo, M.; Katawa, S.; Wada, S.; Mackawa, M.; Munakata, M. *Inorg. Chem.* **1995**, *34*, 1455.

(12) Ruina, Y.; Yimin, H.; Baoyu, X.; Dongmei, W.; Douman, *J. Transition Met. Chem.* **1996**, *21*, 28.

(13) (a) Perrin, D. D.; Armarego, W. L. F.; Perrin, D. R. *Purification of laboratory Chemicals*; Pergamon: Oxford, U.K. 1966. (b) Gordon, A. J.; Ford, R. A. *The Chemist's*

Companion, a Handbook of Practical Data, Techniques, and References; Wiley: New York, 1972; p.436.

(14) SAINT 6.02, 1997-1999, Bruker AXS, Inc., Madison, Wisconsin, USA.

(15) SADABS George Sheldrick, 1999, Bruker AXS, Inc., Madison, Wisconsin, USA.

(16) SHELXTL 5.1, George Sheldrick, 1997, Bruker AXS, Inc., Madison, Wisconsin, USA.

(17) (a) Albano, V. C.; Bellon, P. L.; Ciani, G. *J. Chem. Soc., Dalton Trans.* **1972**, 1938. (b) Chi-Chang, L.; Yong-Shou, L.; Li, L. *Jiegou Huaxue* **1993**, *12*, 286 (also Cambridge Structural Database). (c) Saravanabharathi, D.; Monika ; Venugopalan, P. ; Samuelson, A. G. *Polyhedron* **2002**, *21*, 2433. (d) Semmelmann, M., Ph. D. Dissertation, Universität Karlsruhe, 1997, p.35.

(18) (a) Affandi, D.; Berners-Price, S. J.; Effendy, Harvey, P. J.; Healy, P. C.; Ruch, B. E.; White, A. H. *J. Chem. Soc., Dalton Trans.* **1997**, 1411. (b) Tiekink, E. R. T. Acta Cryst. 1990, 46c, 1933. (c) Brandys, M.-C.; Puddephatt, R. J. *Chem. Commun.* **2001**, 1508. (d) Xie, W.-G. ; Wang, R.-W. ; Xiong, Y.-F. ; Yang, R.-N. ; Wang, D.-M. ; Jin, D.-M. ; Chen, L.-R. ; Luo, B.-S. *Jiegou Huaxue*, **1997**, *16*, 293, see also the Cambridge Databank. (e) Ferrer, M. ; Rossel, O.; Seco, M.; Soler, M.; Font-Bardia, M.; Solans, X. ; de Montauzon, D. *J. Organomet. Chem.* **2000**, *598*, 215.

(19) The dication is isostructural to that of $Au_2(dppp)_2^{2+}$; Brandys, M.-C.; Puddephatt, R. J. *Chem. Commun.* **2001**, 1280. Moreover, a distinctive difference is noticed in Ag-P distances (2.3797(4) and 2.3890(4) Å) between the unsaturated $Ag_2(dppp)_2^{2+}$ cation (shorter than 0.1 Å) and the saturated $Ag(dppe)(CN\text{-}t\text{-}Bu)_2^+$ species. Electronic effect is likely to be at the origin for this difference. In addition, the PAgP angle (159°) strongly deviates from linearity, witnessing the important $Ag^{+}\cdots F\text{-}BF_3^-$ interactions.

(20) (a) Tanase, T.; Kawahara, Ukaji, H.; Kobayashi, K.; Yamazaki, H.; Yamamoto, Y. *Inorg. Chem.* **1993**, *32*, 3682. (b) Tanase, T.; Ukaji, H.; Kudo, Y.; Ohno, M.; Kobayashi, K.; Yamamoto, Y. *Organometallics*, **1994**, *13*, 1374. (c) Lindsay, C. H.;

Benner, L. S.; Balch, A. L. *Inorg. Chem.* **1980**, *19*, 3503. (d) Budzelaar, P. H. M.; van Leeuwen, P. W. N. M.; Roobeek, C. F. *Organometallics* **1992**, *11*, 23.

(21) (a) Tenhaeff, S. C.; Tyler, D.R. *Organometallics* **1991**, *10*, 473. (b) Tenhaeff, S. C.; Tyler, D.R. *J. Chem. Soc., Chem. Commun.* **1989**, 1459. (c) Tenhaeff, S. C.; Tyler, D.R. *Organometallics* **1992**, **11**, 1466. (d) Tenhaeff, S. C.; Tyler, D.R. *Organometallics* **1991**, *10*, 1116. (e) Male, J. L.; Lindsfors, B. E.; Covert, J.; Tyler, D. R. *Macromolecules* **1997**, *30*, 6404. (f) Nieckarz, G. F.; Tyler, D. R. *Inorg. Chim. Acta* **1996**, *242*, 303. (g) Male, J. L.; Yoon, M.; Glenn, A, G.; Weakly, T. J. R.; Tyler, D. R. Macromolecules 1999, 32, 3898. (h) Nieckarz, G. F.; Litty, J. J.; Tyler, D. R. *J. Organomet. Chem.* **1998**, *554*, 19.

(22) Perreault, D.; Drouin, M.; Michel, A.; Harvey, P.D. *Inorg. Chem.*, **1992**, *31*, 2740.

(23) The X-ray structure for $[Pd(dppe)(dmb)]_2(PF_6)_4$ will be reported elsewhere. Fortin, J.-F.; Harvey, P.D., to be published.

(24) The computed segments for $\{Cu(dppp)(dmb)^+\}_n$ exhibit PdCN angles of 175° indicating the absence of stress in the chain.

(25) Harvey, P.D.; Drouin, M.; Zhang, T. *Inorg. Chem.* **1997**, *36*, 4998.

(26) Alves, O.L.; Virtoge, M.-C.; Sourisseau, C. *Nouv. J. Chim.* **1983**, *7*, 231.

(27) Harvey, P.D.; Murtaza, Z. *Inorg. Chem.*, **1993**, *32* , 4721.

(28) Provencher, R.; Harvey, P.D. *Inorg. Chem.*, **1996**, *35*, 2113.

(29) (a) Simon, J. A.; Palke, W. E.; Ford, P. C. *Inorg. Chem.*. **1996**, *35*, 6413. (b) Crane, D. R. ; DiBenedetto, J.; Palmer, C. E. A.; McMillin, D. R.; Ford, P. C. *Inorg. Chem.*. **1988**, *27*, 3698.

(30) Ford, P. C.; Cariati, E.; Bourassa, *J. Chem. Rev.* **1999**, *99*, 3625, and the references therein.

(31) Piché, D. ; Harvey, P.D. *Can J. Chem.* **1994**, *72*, 705.

(32) Wang, C. –F.; Peng, S.-M.; Chan, C.-K.; Che, C.-M. *Polyhedron* **1996**, *15*, 1853.

(33) (a) Cariati, E.; Roberto, D.; Ugo, R.; Ford, P.C.; Galli, S.; Sironi, A. *Chem. Mater.* **2002**, *14*, 5116. (b) Herary, M.; Wootton, J. L.; Khan, S. I.; Zink, J. I. *Inorg.*

Chem. **1997**, *36*, 796. (c) Lai, D.C.; Zink, J. I. Inorg. Chem. **1993**, *32*, 2594. (d) Henary, M.; Zink, J.I. *Inorg. Chem.* **1991**, *30*, 3111.

(34) The $Pd_2(dmb)_2Cl_2$ complex weakly luminesces in solution at 77K (λ_{max} = 625 nm; $\tau_e = 71 \pm 6$ ns.[23] The $Pd_2(diphos)_2(CN\text{-}t\text{-}Bu)^{2+}$ and $\{Pd_2(diphos)_2(dmb)^{2+}\}_n$ species also show some luminescence in solution at 77K between 510-560 nm with τ_e in the ns time scale as well.

Table 1. Crystallographic data for [Cu(dppe)(CN-*t*-Bu)$_2$](BF$_4$), [Cu(dppp)(CN-*t*-Bu)$_2$](BF$_4$), and [Ag(dppe)(CN-*t*-Bu)$_2$](BF$_4$).

	[Cu(dppe)(CN-*t*-Bu)$_2$](BF$_4$)	[Cu(dppp)(CN-*t*-Bu)$_2$](BF$_4$)	[Ag(dppe)(CN-*t*-Bu)$_2$](BF$_4$)
Formula	$C_{36}H_{42}BCuF_4N_2P_2$	$C_{37}H_{44}BCuF_4N_2P_2$	$C_{36}H_{42}AgBF_4N_2P_2$
Fw	715.01	729.03	759.34
Crystal size	0.275 x 0.45 x 0.5	0.25 x 0.3 x 0.4	0.40 x 0.45 x 0.45
Lattice	Monoclinic	Monoclinic	Monoclinic
Space group	P2(1)/n	P2(1)/c	P2(1)/n
a, Å	14.0252(15)	15.5433(9)	14.1130(8)
b, Å	10.2034(11)	11.2094(6)	10.2075(6)
c, Å	25.515(2)	21.4362(12)	25.8175(16)
α,°	90	90	90
β,°	103.765(2)	92.4830(10)	103.3810(10)
γ,°	90	90	90
V, Å^3	3546.4(6)	3731.3(4)	3618.3(4)
Z	4	4	4
ρ(calcd.),gcm^{-3}	1.339	1.298	1.394
F(000)	1488	1520	1560
μ(M_oK_α), mm^{-1}	0.755	0.719	0.693
Diffractometer	Bruker	Bruker	Bruker
Temp,K	198(1)	173(1)	173(1)
R[a]	0.0289	0.0327	0.0292
R_w[b]	0.0785	0.0905	0.0828
No. of observns. (I > 2.00σ(I))	6101	8479	8217
No. of variables	577	642	556

$R = \Sigma \| |F_o| - |F_c| \| / \Sigma |F_o|$

$Rw = (\Sigma[w(F_o^2-F_c^2)^2]/\Sigma[F_o^4])^{1/2}$

$Weight = 1 / [\sigma^2(F_o^2) + (0.0463 * P)^2 + (1.7267 * P)]$

where $P = (\max (F_o^2, 0) + 2 * F_c^2)/3$

Table 2. Selected bond distances (Å) and angles (°) for $[Ag_2(dppp)_2](BF_4)_2$, $[Cu(dppe)(CN\text{-}t\text{-}Bu)_2]BF_4$, $[Ag(dppe)(CN\text{-}t\text{-}Bu)_2]BF_4$ and $[Cu(dppp)(CN\text{-}t\text{-}Bu)_2]BF_4$.

	[Cu(dppe)-(CN-*t*-Bu)$_2$]BF_4	[Ag(dppe)-(CN-*t*-Bu)$_2$]BF_4	[Cu(dppp)-(CN-*t*-Bu)$_2$]BF_4
d(MP)	2.2979(5)	2.4939(5)	2.2636(4)
	2.3038(5)	2.4982(5)	2.2898(5)
d(MC)	1.9245(18)	2.145(2)	1.9176(18)
	1.9306(18)	2.1719(19)	1.935(2)
d(C≡N)	1.144(2)	1.141(3)	1.142(2)
	1.145(2)	1.139(3)	1.132(3)
∠PMP	89.088(17)	84.504(16)	98.737(17)
∠CMC	120.19(1)	119.67(8)	113.54(8)
∠CMP	112.39(5)	114.21(6)	118.98(5)
	108.35(5)	108.57(6)	110.63(6)
	116.61(5)	118.28(5)	108.61(5)
	105.69(5)	106.01(6)	104.22(6)
∠MCN	175.55(16)	174.96(18)	170.86(15)
	170.33(16)	163.54(18)	172.85(18)

Table 3. Comparison of MMX and X-ray data for the M(diphos)(CN-t-Bu)$_2^+$ (M = Cu, Ag), $Pd_2(dmb)_2Cl_4$, and [Pd(diphos)(dmb)]$_2^{4+}$complexes.[a]

	Cu(dppe)(CN-t-Bu)$_2^+$	Cu(dppp)(CN-t-Bu)$_2^+$	Ag(dppe)(CN-t-Bu)$_2^+$
d(M-P) / Å	2.27 (2.30)	2.27 (2.28)	2.43 (2.50)
d(M-C) / Å	1.82 (1.93)	1.82 (1.92)	1.99 (2.16)
d(C≡N) / Å	1.19 (1.15)	1.19 (1.14)	1.18 (1.14)
∠(PMP) / °	85.2 (89.1)	93.7 (98.7)	79.4 (84.5)
∠(CMC) / °	121.4 (120.2)	118.6 (119.7)	122.0 (119.7)
∠(MCN) / °	171.6 (172.8)	172.5 (171.9)	171.7 (169.3)
∠(PMC) / °	110.7 (110.8)	110.9 (110.9)	108.0 (118.8)

	$Pd_2(dmb)_2Cl_4$[b]	[Pd(dppe)(dmb)]$_2^{4+}$[c]	[Pd(dppp)(dmb)]$_2^{4+}$
d(Pd-P) / Å	-----	2.38 (2.27)	2.38
d(Pd-C) / Å	1.93 (1.97)	1.93 (2.02)	1.93
d(C≡N) / Å	1.14 (1.13)	1.20 (1.13)	1.20
∠(PPdP) / °	-----	78.9 (82.7)	82.7
∠(CPdC) / °	178.0 (178.6)	92.5 (90.6)	94.2
∠(PdCN) / °	177.5 (178.6)	174.3 (176.0)	174.0
∠(PPdC) / °[d]	-----	94.3 (93.4)	91.6

[a] The X-ray data are placed in parentheses, and are from this work unless stated otherwise. [b] From ref. a. [c] From ref. b. [d] Only the angles approaching 90° of the square planar geometry are provided

Table 4. UV-vis data for the $Pd_2(diphos)_2(CN\text{-}t\text{-}Bu)_2^{2+}$ and $\{Pd_2(diphos)_2(dmb)^{2+}\}_n$ polymers

Compounds	ACN / 293K		PrCN / 293K		PrCN / 77K	
	λ_{max} (nm)	ε ($M^{-1}cm^{-1}$)	λ_{max} (nm)	FWHM (cm^{-1})	λ_{max} (nm)	FWHM (cm^{-1})
$[Pd_2(dppe)_2(CN\text{-}t\text{-}Bu)_2](ClO_4)_2$	420	28600	422	2200	416	1800
$[Pd_2(dppp)_2(CN\text{-}t\text{-}Bu)_2](ClO_4)_2$	416	26000	418	2100	410	1900
$\{[Pd_2(dppe)_2(dmb)](ClO_4)_2\}_n$	418	28000	420	2700	424	2500
$\{[Pd_2(dppp)_2(dmb)](ClO_4)_2\}_n$	414	26100	416	2500	406	2300

Table 5. Solid state emission data for the M(diphos) $(CN\text{-}t\text{-}Bu)_2^+$ model compounds and $\{M(diphos)(dmb)^+\}_n$ polymers

Compounds	λ_{max} emission / nm	τ_e / μs
$[Cu(dppe)(CN\text{-}t\text{-}Bu)_2](BF_4)$	540	42 ±4
$[Ag(dppe)(CN\text{-}t\text{-}Bu)_2](BF_4)$	515	21 ±4
$[Cu(dppp)(CN\text{-}t\text{-}Bu)_2](BF_4)$	478	18 ±3
$\{[Cu(dppe)(dmb)](BF_4)\}_n$	480	38 ±5
$\{[Ag(dppe)(dmb)](BF_4)\}_n$	548	27 ±2
$\{[Cu(dppp)(dmb)](BF_4)\}_n$	500	22 ±4
$\{[Ag(dppp)(dmb)](BF_4)\}_n$	480	48 ±4

Figure Captions

1. ORTEP drawing for $[Cu(dppe)(CN\text{-}t\text{-}Bu)_2]BF_4$. The ellipsoids are shown at 30% probability. The H-atoms and BF_4^- ion are not shown for clarity. The compound is isostructural to $[Ag(dppe)(CN\text{-}t\text{-}Bu)_2]BF_4$ (see Supproting Information).
2. ORTEP drawing for $[Cu(dppp)(CN\text{-}t\text{-}Bu)_2]BF_4$. The ellipsoids are shown at 30% probability. The H-atoms and the BF_4^- ion are not shown for clarity.
3. XRD patterns for the $\{[Ag(diphos)(dmb)]BF_4\}_n$ polymers (diphos = dppe, dppp). The other polymers are also amorphous.
4. TGA traces for $[Ag(dppp)(CN\text{-}t\text{-}Bu)_2]BF_4$ (up) and $\{[Ag(dppp)(dmb)]BF_4\}_n$ (down). The broken line is the first derivative of the TGA traces.
5. Computer model for $Pd_2(dppp)_2(CN\text{-}t\text{-}Bu)_2^{2+}$.
6. Computer model for a fragment of the $\{Pd_2(dppp)_2(dmb)^{2+}\}_n$ polymer. This is one possible conformation, and one pair of the same enantiomer. Other combinations exist.
7. UV-vis spectra (left hand side) for $\{[Ag(dppe)(dmb)]BF_4\}_n$ and in acetonitrile at 298K. Solid state emission spectra (right hand side) for the same materials at 298K.
8. Comparison of the UV-vis spectra of $\{[Pd_2(dppe)_2(dmb)](ClO_4)_2\}_n$ in PrCN at 298 (—) and 77 K (---).

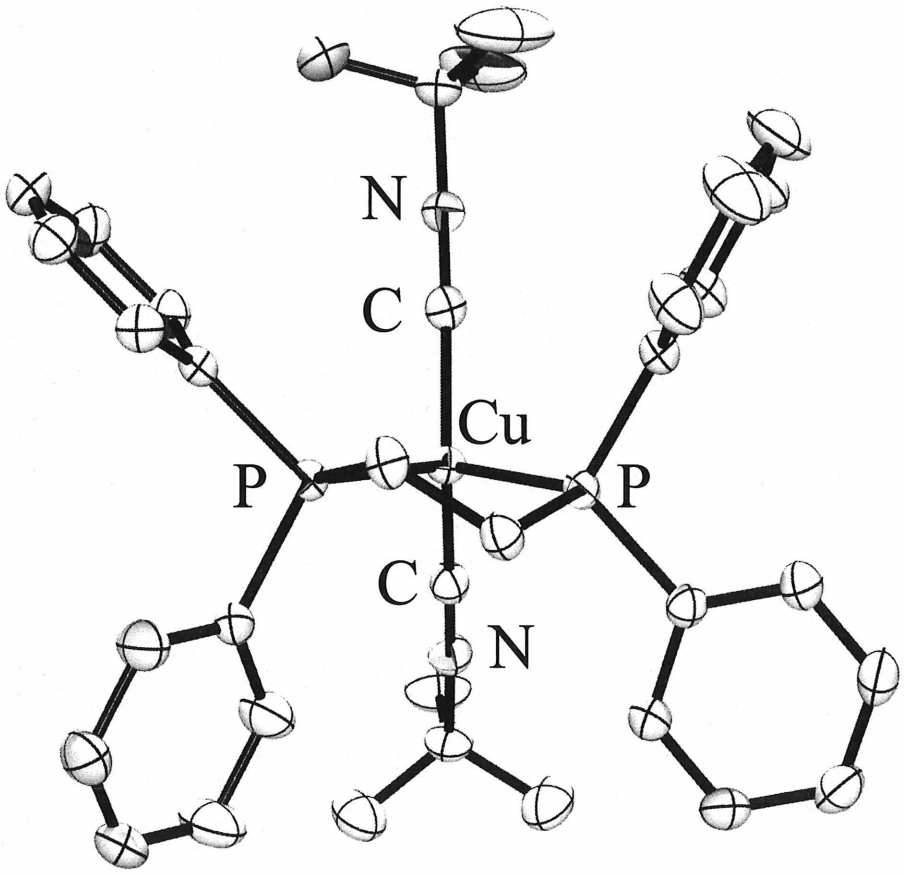

Fig. 1

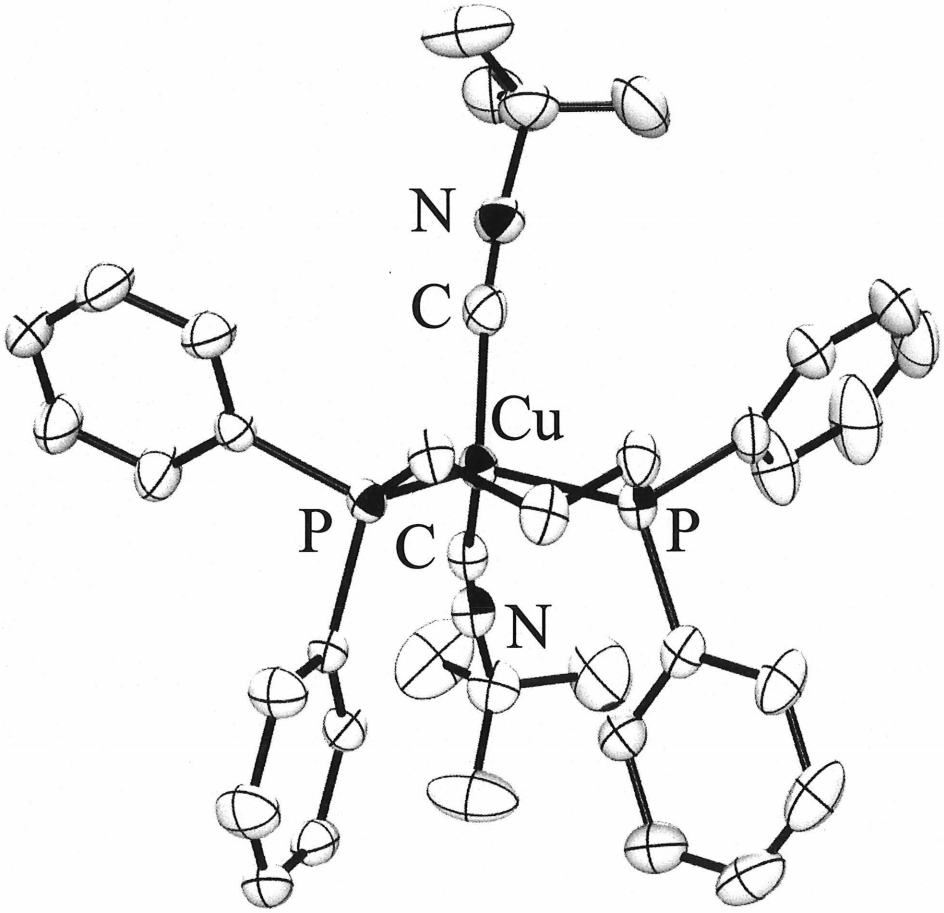

Fig.2

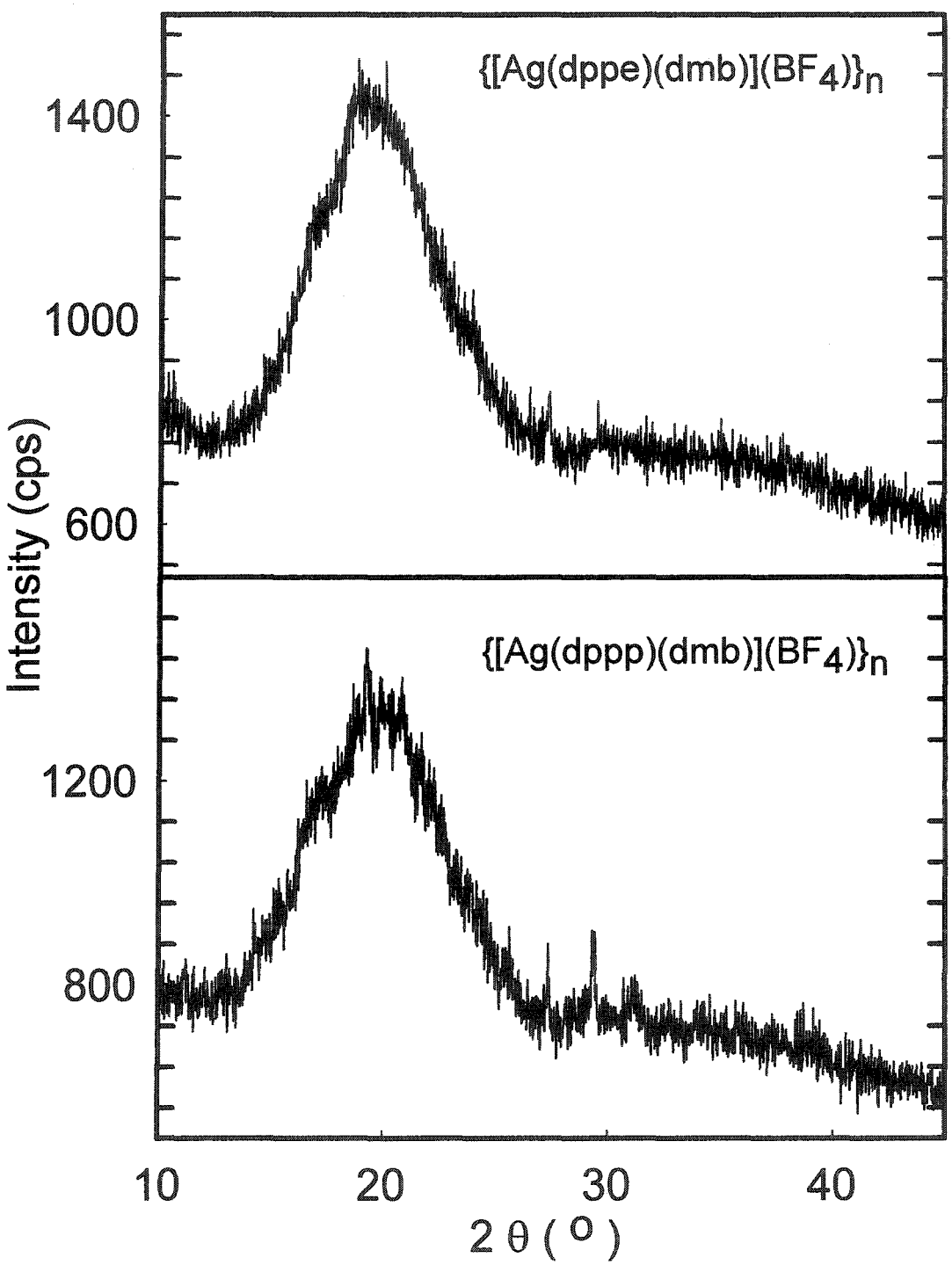
{[Ag(dppe)(dmb)](BF4)}n
{[Ag(dppp)(dmb)](BF4)}n
Intensity (cps)
1400
1000
600
1200
800
10
20
30
40
2θ(°)

Fig. 3

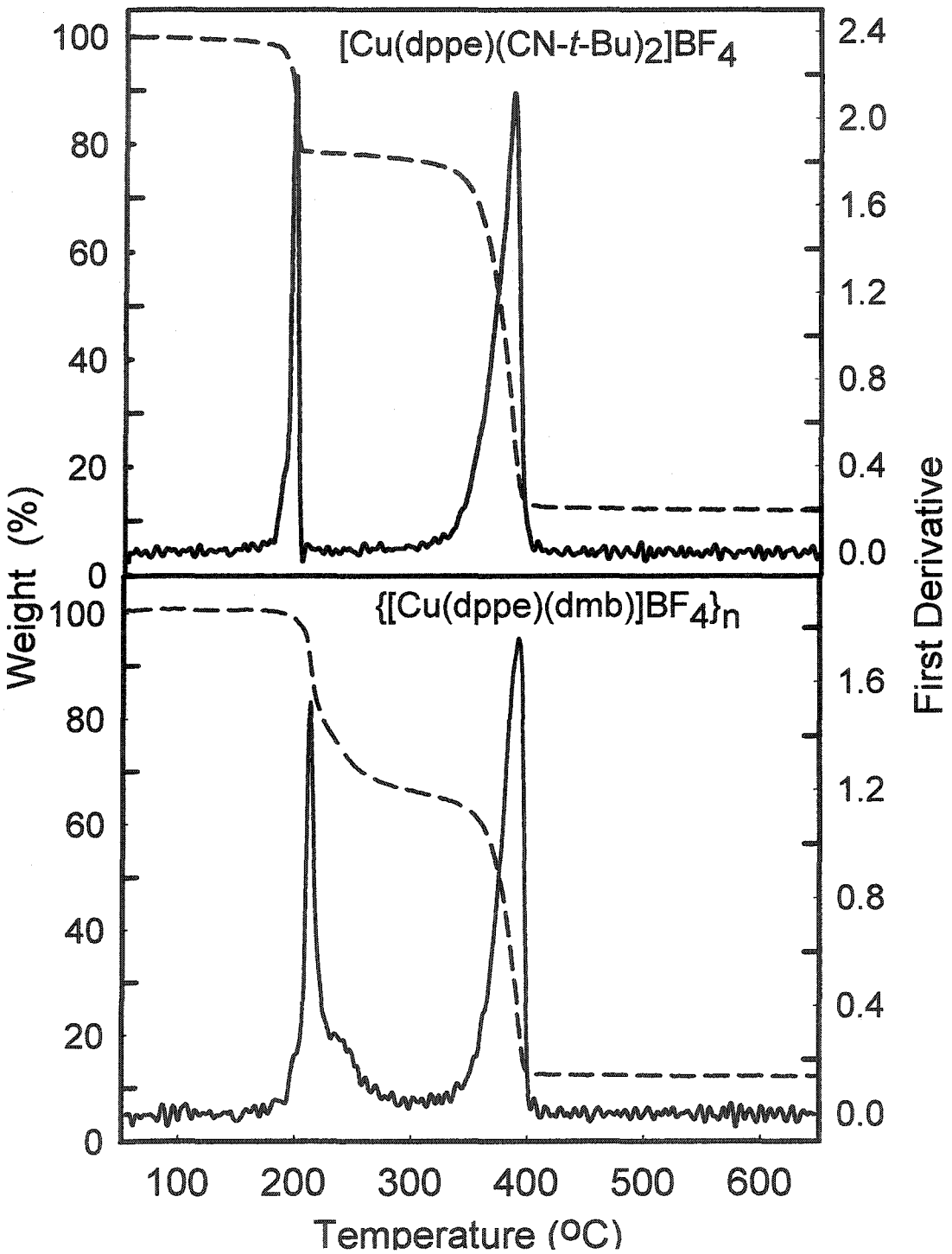
[Cu(dppe)(CN-t-Bu)2]BF4
{[Cu(dppe)(dmb)]BF4}n
Weight (%)
First Derivative
Temperature (°C)
100
80
60
40
20
0
2.4
2.0
1.6
1.2
0.8
0.4
0.0
100
200
300
400
500
600

Fig. 4

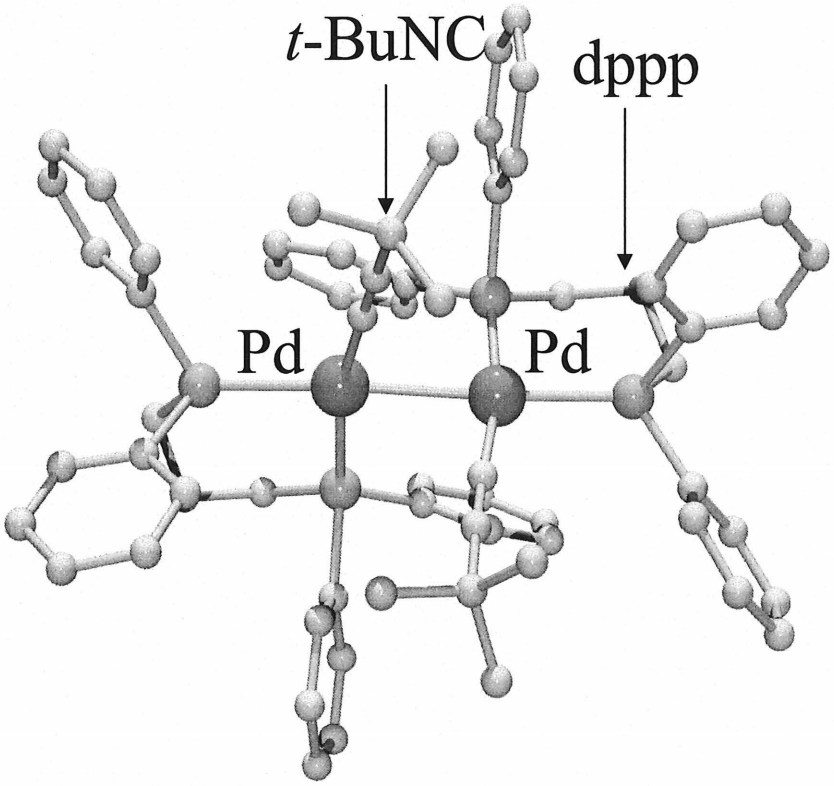

Fig. 5

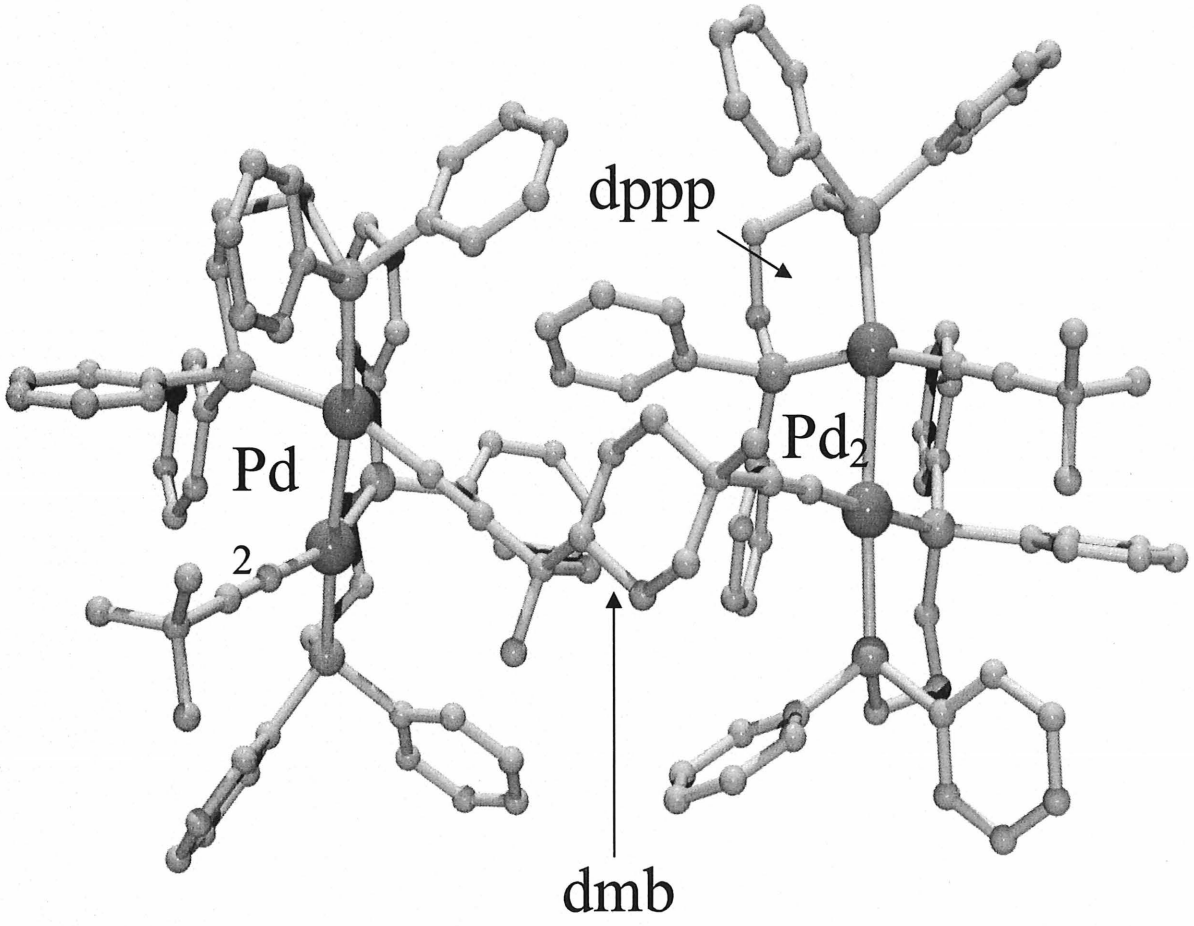

Fig. 6

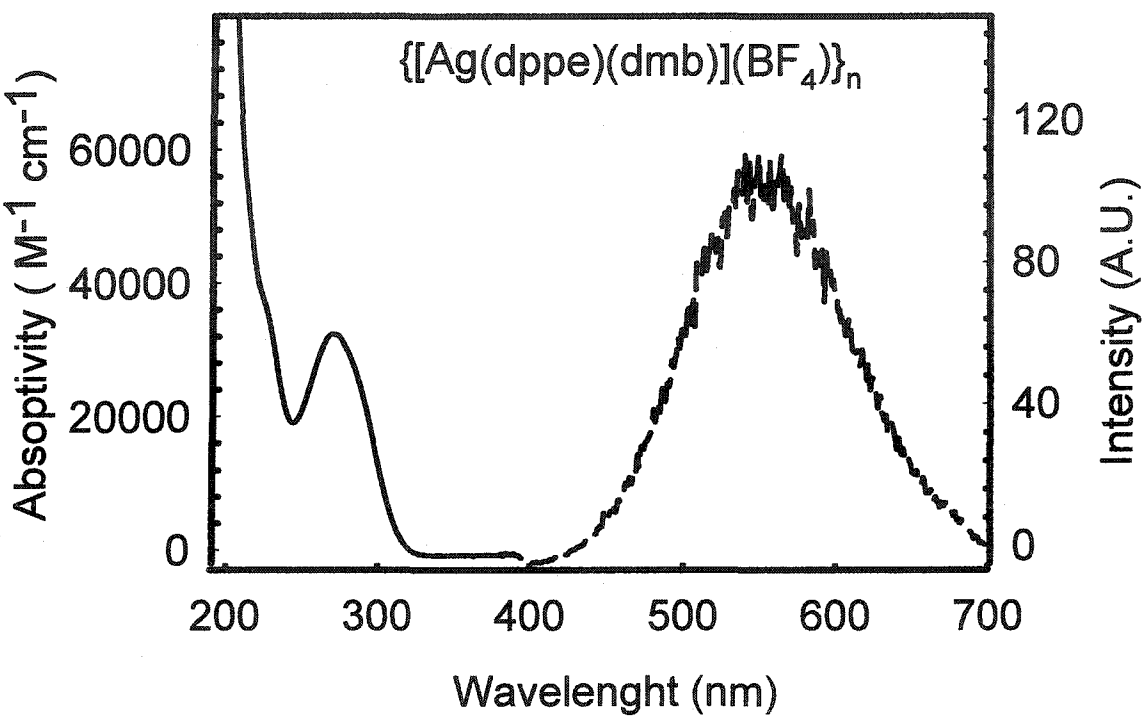
{[Ag(dppe)(dmb)](BF4)}n
Absoptivity (M-1 cm-1)
60000
40000
20000
0
120
80
40
0
Intensity (A.U.)
200
300
400
500
600
700
Wavelenght (nm)

Fig. 7

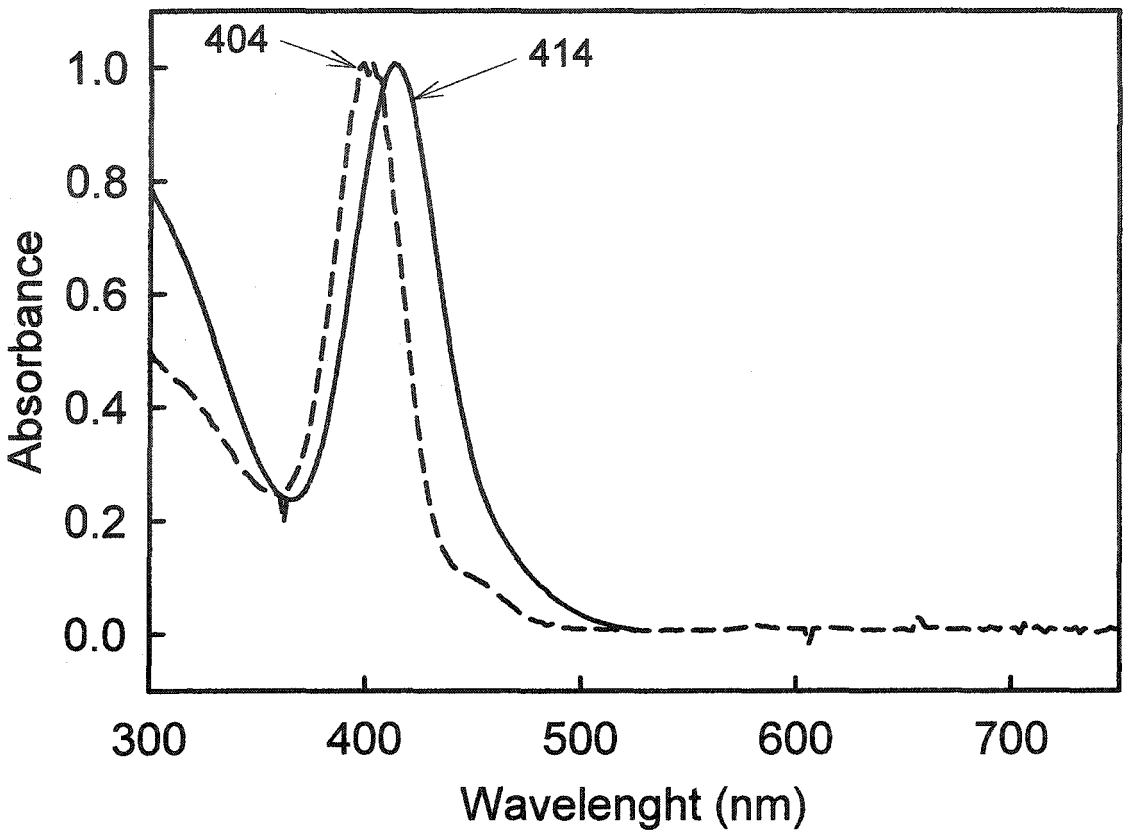
404
414
1.0
0.8
0.6
0.4
0.2
0.0
Absorbance
300
400
500
600
700
Wavelenght (nm)

Fig. 8

Organometallic Polymers Based on 1,8-Diisocyano-*p*-menthane (dmb); Syntheses and Characterization of the $\{[M(diphos)(dmb)]BF_4\}_n$ and $\{[Pd_2(diphos)_2(dmb)](ClO_4)_2\}_n$ Materials (M = Cu, Ag; diphos = dppe, dppp)

Eric Fournier, Stéphanie Sicard and Pierre D. Harvey*

Supporting Information

Table of contents

Table S1. Crystal data and structure refinement for $[Cu(dppe)(CN\text{-}t\text{-}Bu)_2](BF_4)$.

Empirical formula	C36 H42 B Cu F4 N2 P2	
Formula weight	715.01	
Temperature	198(1) K	
Wavelength	0.71073 Å	
Diffractometer used	Bruker AXS P4/SMART 1000	
Detector distance	5 cm	
Monochrometer used	Graphite	
Crystal size	0.275 x 0.45 x 0.5 mm^3	
Colour and habit	Colourless, parallelepiped	
Crystal system	Monoclinic	
Space group	P2(1)/n	
Unit cell dimensions	a = 14.0252(15) Å	α = 90°
	b = 10.2034(11) Å	β = 103.765(2)°
	c = 25.515(2) Å	γ = 90°
Volume	3546.4(6) $Å^3$	
Z	4	
Density (calculated)	1.339 Mg/m^3	
Absorption coefficient	0.755 mm^{-1}	
F(000)	1488	
Theta range for data collection	1.52 to 24.99°	
Completeness to theta = 24.99°	97.7 %	
Scan type	ω and ϕ	
Scan range	0.3°	
Exposure time	30s	

Index ranges	$-16 \leq h \leq 16, -12 \leq k \leq 11, -30 \leq l \leq 28$
Standard reflections	50 frames at beginning and end of data
collection	
Crystal stability	no decay
Reflections collected	17663
Independent reflections	6101 [R(int) = 0.0177]
System used	SHELXL 5.1
Solution	Direct methods
Hydrogen atoms	mixed
Absorption correction	SADABS
Min./Max. transmission ratio	0.924
Refinement method	Full-matrix least-squares on F^2
Data / restraints / parameters	6101 / 0 / 577
Goodness-of-fit on F^2	1.042
Final R indices [I>2sigma(I)]	R1 = 0.0289, wR2 = 0.0785
R indices (all data)	R1 = 0.0305, wR2 = 0.0793
Largest/mean shift/esd	0.001/0.000
Largest diff. peak and hole	0.427 and -0.170 e.$Å^{-3}$

$wR2 = (\Sigma [w(F_o^2 - F_c^2)^2] / \Sigma [F_o^4])^{1/2}$

$R1 = \Sigma \, | \, |F_o| - |F_c| \, | \, / \Sigma \, |F_o|$

$Weight = 1 / [\sigma^2(F_o^2) + (0.0463 * P)^2 + (1.7267 * P)]$

where $P = (\max (F_o^2, 0) + 2 * F_c^2)/3$

Figure S1 Numbering scheme for $[Cu(dppe)(CN\text{-}t\text{-}Bu)_2](BF_4)$

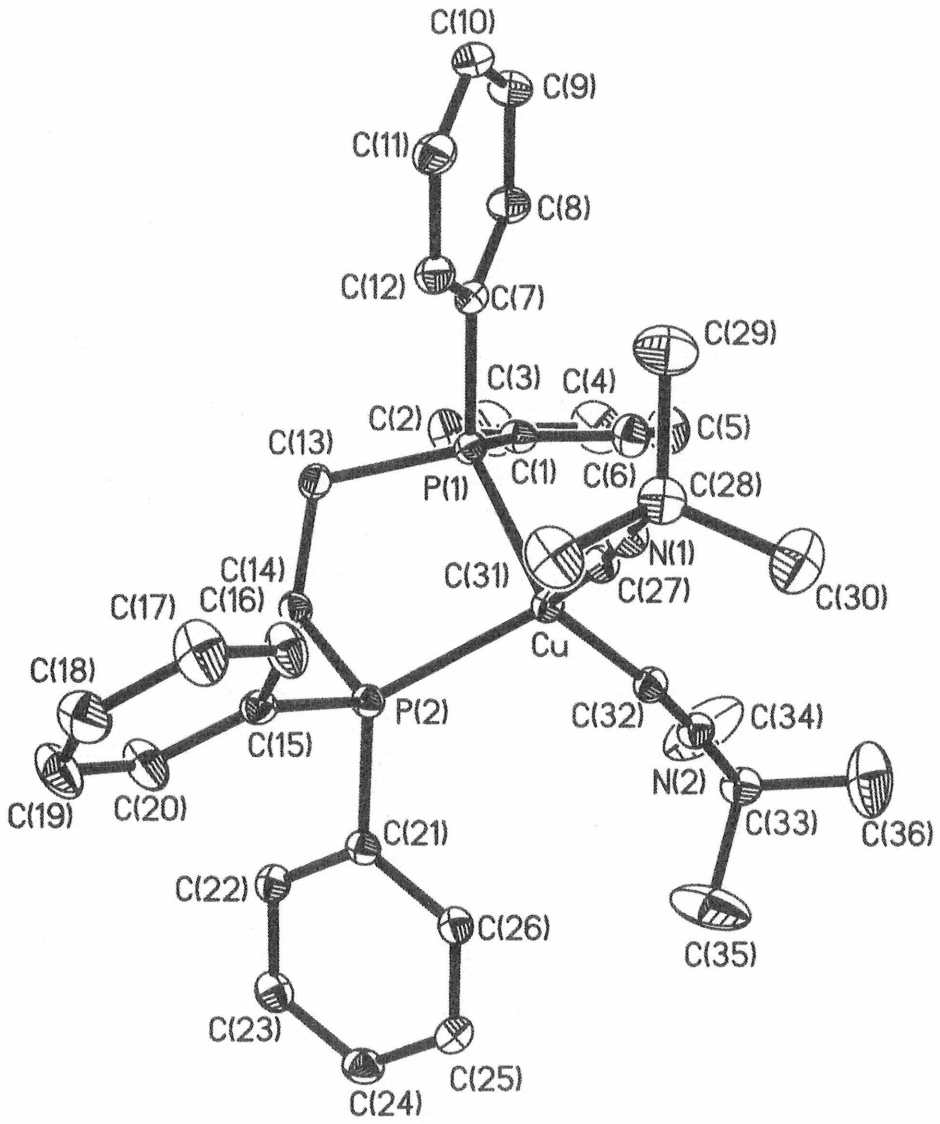

Table S2. Atomic coordinates (x 10^4) and equivalent isotropic displacement parameters ($Å^2$x 10^3) for Table S1. Crystal data and structure refinement for [Cu(dppe)(CN-t-Bu)$_2$](BF_4). U(eq) is defined as one third of the trace of the orthogonalized U^{ij} tensor.

	x	y	z	U(eq)
Cu	4450(1)	3289(1)	1091(1)	23(1)
P(1)	4772(1)	2734(1)	1988(1)	23(1)
P(2)	3875(1)	5290(1)	1300(1)	23(1)
C(1)	6058(1)	2760(2)	2341(1)	28(1)
C(2)	6425(2)	3469(2)	2808(1)	42(1)
C(3)	7423(2)	3468(3)	3037(1)	60(1)
C(4)	8049(2)	2760(3)	2813(1)	60(1)
C(5)	7697(2)	2041(3)	2355(1)	51(1)
C(6)	6704(1)	2052(2)	2117(1)	38(1)
C(7)	4279(1)	1256(2)	2222(1)	26(1)
C(8)	4844(1)	382(2)	2581(1)	34(1)
C(9)	4428(2)	-736(2)	2736(1)	39(1)
C(10)	3444(2)	-988(2)	2537(1)	38(1)
C(11)	2876(2)	-130(2)	2174(1)	38(1)
C(12)	3290(1)	982(2)	2015(1)	32(1)
C(13)	4175(1)	4042(2)	2284(1)	28(1)
C(14)	4310(1)	5371(2)	2041(1)	28(1)
C(15)	2552(1)	5534(2)	1181(1)	28(1)
C(16)	1933(2)	4515(2)	976(1)	45(1)
C(17)	928(2)	4665(3)	873(1)	58(1)
C(18)	538(2)	5839(2)	970(1)	54(1)
C(19)	1142(2)	6851(2)	1186(1)	59(1)

C(20)	2143(2)	6700(2)	1292(1)	48(1)
C(21)	4333(1)	6804(2)	1070(1)	25(1)
C(22)	4424(1)	7966(2)	1363(1)	30(1)
C(23)	4765(1)	9091(2)	1166(1)	35(1)
C(24)	5023(1)	9068(2)	678(1)	36(1)
C(25)	4944(2)	7926(2)	388(1)	37(1)
C(26)	4605(1)	6799(2)	581(1)	30(1)
C(27)	3507(1)	2137(2)	646(1)	28(1)
N(1)	2903(1)	1477(2)	401(1)	31(1)
C(28)	2122(1)	651(2)	79(1)	34(1)
C(29)	2012(2)	-538(3)	413(1)	53(1)
C(30)	2442(2)	284(3)	-426(1)	53(1)
C(31)	1188(2)	1458(3)	-44(1)	51(1)
C(32)	5682(1)	3651(2)	907(1)	28(1)
N(2)	6431(1)	3994(2)	854(1)	30(1)
C(33)	7388(1)	4513(2)	827(1)	35(1)
C(34)	8016(3)	4598(7)	1374(2)	101(2)
C(35)	7196(3)	5761(5)	520(3)	95(2)
C(36)	7819(3)	3540(5)	481(2)	84(1)
C(34A)	7439(9)	4809(18)	285(5)	78(4)
C(35A)	8143(7)	3561(12)	1095(7)	76(4)
C(36A)	7479(7)	5844(12)	1184(7)	76(4)
B(1)	75(2)	1033(2)	1358(1)	35(1)
F(1)	977(1)	1570(2)	1563(1)	82(1)
F(2)	-534(1)	1344(2)	1688(1)	76(1)
F(3)	143(1)	-308(1)	1338(1)	69(1)
F(4)	-304(1)	1508(1)	850(1)	60(1)

Table S3. Bond lengths [Å] and angles [°] for $[Cu(dppe)(CN\text{-}t\text{-}Bu)_2](BF_4)$.

Cu-C(27)	1.9245(18)	Cu-C(32)	1.9306(18)
Cu-P(1)	2.2979(5)	Cu-P(2)	2.3038(5)
P(1)-C(1)	1.8141(17)	P(1)-C(7)	1.8172(18)
P(1)-C(13)	1.8313(18)	P(2)-C(21)	1.8229(17)
P(2)-C(15)	1.8247(17)	P(2)-C(14)	1.8443(17)
C(1)-C(2)	1.383(3)	C(1)-C(6)	1.384(3)
C(2)-C(3)	1.382(3)	C(2)-H(16)	0.84(2)
C(3)-C(4)	1.364(4)	C(3)-H(33)	0.88(3)
C(4)-C(5)	1.369(4)	C(4)-H(27)	0.90(3)
C(5)-C(6)	1.381(3)	C(5)-H(15)	0.87(3)
C(6)-H(14)	0.93(2)	C(7)-C(8)	1.384(3)
C(7)-C(12)	1.390(2)	C(8)-C(9)	1.381(3)
C(8)-H(12)	0.94(2)	C(9)-C(10)	1.377(3)
C(9)-H(11)	0.95(2)	C(10)-C(11)	1.382(3)
C(10)-H(10)	0.96(2)	C(11)-C(12)	1.379(3)
C(11)-H(9)	0.89(2)	C(12)-H(5)	0.90(2)
C(13)-C(14)	1.522(2)	C(13)-H(2)	0.95(2)
C(13)-H(7)	0.95(2)	C(14)-H(1)	0.94(2)
C(14)-H(3)	0.92(2)	C(15)-C(16)	1.375(3)
C(15)-C(20)	1.379(3)	C(16)-C(17)	1.380(3)
C(16)-H(25)	0.91(2)	C(17)-C(18)	1.364(4)
C(17)-H(32)	0.96(3)	C(18)-C(19)	1.366(4)
C(18)-H(19)	0.98(3)	C(19)-C(20)	1.374(3)
C(19)-H(24)	0.91(3)	C(20)-H(20)	0.88(3)
C(21)-C(26)	1.389(2)	C(21)-C(22)	1.390(3)
C(22)-C(23)	1.383(3)	C(22)-H(4)	0.87(2)
C(23)-C(24)	1.375(3)	C(23)-H(8)	0.89(2)

C(24)-C(25)	1.372(3)	C(24)-H(17)	0.90(2)
C(25)-C(26)	1.380(3)	C(25)-H(13)	0.83(3)
C(26)-H(6)	0.91(2)	C(27)-N(1)	1.144(2)
N(1)-C(28)	1.468(2)	C(28)-C(30)	1.509(3)
C(28)-C(29)	1.511(3)	C(28)-C(31)	1.515(3)
C(29)-H(18)	0.94(3)	C(29)-H(22)	1.02(3)
C(29)-H(23)	0.92(3)	C(30)-H(28)	0.98(3)
C(30)-H(29)	0.93(3)	C(30)-H(31)	0.96(3)
C(31)-H(21)	0.97(3)	C(31)-H(26)	0.95(3)
C(31)-H(30)	0.95(3)	C(32)-N(2)	1.145(2)
N(2)-C(33)	1.459(2)	C(33)-C(34A)	1.435(11)
C(33)-C(34)	1.465(4)	C(33)-C(35A)	1.479(10)
C(33)-C(35)	1.486(4)	C(33)-C(36)	1.545(4)
C(33)-C(36A)	1.623(10)	C(34)-H(34A)	0.9600
C(34)-H(34B)	0.9600	C(34)-H(34C)	0.9600
C(35)-H(35A)	0.9600	C(35)-H(35B)	0.9600
C(35)-H(35C)	0.9600	C(36)-H(36A)	0.9600
C(36)-H(36B)	0.9600	C(36)-H(36C)	0.9600
B(1)-F(1)	1.363(3)	B(1)-F(4)	1.367(3)
B(1)-F(2)	1.371(3)	B(1)-F(3)	1.373(3)

C(27)-Cu-C(32)	120.19(7)	C(27)-Cu-P(1)	112.39(5)
C(32)-Cu-P(1)	108.35(5)	C(27)-Cu-P(2)	116.61(5)
C(32)-Cu-P(2)	105.69(5)	P(1)-Cu-P(2)	89.088(17)
C(1)-P(1)-C(7)	105.10(8)	C(1)-P(1)-C(13)	106.45(8)
C(7)-P(1)-C(13)	102.89(8)	C(1)-P(1)-Cu	115.28(6)
C(7)-P(1)-Cu	122.12(6)	C(13)-P(1)-Cu	103.30(6)
C(21)-P(2)-C(15)	104.63(8)	C(21)-P(2)-C(14)	103.59(8)
C(15)-P(2)-C(14)	103.90(8)	C(21)-P(2)-Cu	120.46(6)

C(15)-P(2)-Cu	118.76(6)	C(14)-P(2)-Cu	103.20(6)
C(2)-C(1)-C(6)	118.81(18)	C(2)-C(1)-P(1)	123.88(15)
C(6)-C(1)-P(1)	117.28(14)	C(3)-C(2)-C(1)	119.7(2)
C(3)-C(2)-H(16)	121.6(16)	C(1)-C(2)-H(16)	118.5(16)
C(4)-C(3)-C(2)	120.7(2)	C(4)-C(3)-H(33)	118.8(19)
C(2)-C(3)-H(33)	120.5(19)	C(3)-C(4)-C(5)	120.3(2)
C(3)-C(4)-H(27)	118.0(19)	C(5)-C(4)-H(27)	121.7(19)
C(4)-C(5)-C(6)	119.5(2)	C(4)-C(5)-H(15)	122.1(16)
C(6)-C(5)-H(15)	118.5(17)	C(5)-C(6)-C(1)	120.9(2)
C(5)-C(6)-H(14)	122.2(15)	C(1)-C(6)-H(14)	116.8(14)
C(8)-C(7)-C(12)	118.97(17)	C(8)-C(7)-P(1)	123.29(14)
C(12)-C(7)-P(1)	117.71(13)	C(9)-C(8)-C(7)	120.54(18)
C(9)-C(8)-H(12)	119.0(13)	C(7)-C(8)-H(12)	120.4(13)
C(10)-C(9)-C(8)	120.15(19)	C(10)-C(9)-H(11)	120.5(14)
C(8)-C(9)-H(11)	119.4(14)	C(9)-C(10)-C(11)	119.79(18)
C(9)-C(10)-H(10)	119.5(13)	C(11)-C(10)-H(10)	120.7(13)
C(12)-C(11)-C(10)	120.17(19)	C(12)-C(11)-H(9)	116.9(14)
C(10)-C(11)-H(9)	122.9(14)	C(11)-C(12)-C(7)	120.37(18)
C(11)-C(12)-H(5)	120.7(13)	C(7)-C(12)-H(5)	119.0(13)
C(14)-C(13)-P(1)	111.56(12)	C(14)-C(13)-H(2)	110.0(11)
P(1)-C(13)-H(2)	103.9(11)	C(14)-C(13)-H(7)	112.1(12)
P(1)-C(13)-H(7)	110.6(12)	H(2)-C(13)-H(7)	108.3(16)
C(13)-C(14)-P(2)	109.57(12)	C(13)-C(14)-H(1)	111.3(13)
P(2)-C(14)-H(1)	106.1(13)	C(13)-C(14)-H(3)	111.0(13)
P(2)-C(14)-H(3)	110.1(13)	H(1)-C(14)-H(3)	108.6(18)
C(16)-C(15)-C(20)	118.35(18)	C(16)-C(15)-P(2)	118.97(14)
C(20)-C(15)-P(2)	122.69(15)	C(15)-C(16)-C(17)	120.8(2)
C(15)-C(16)-H(25)	119.6(15)	C(17)-C(16)-H(25)	119.6(15)
C(18)-C(17)-C(16)	119.9(2)	C(18)-C(17)-H(32)	120.9(18)

C(16)-C(17)-H(32)	119.1(18)	C(17)-C(18)-C(19)	120.0(2)
C(17)-C(18)-H(19)	118.3(15)	C(19)-C(18)-H(19)	121.6(15)
C(18)-C(19)-C(20)	120.1(2)	C(18)-C(19)-H(24)	123.6(17)
C(20)-C(19)-H(24)	116.3(17)	C(19)-C(20)-C(15)	120.8(2)
C(19)-C(20)-H(20)	119.0(16)	C(15)-C(20)-H(20)	120.2(16)
C(26)-C(21)-C(22)	118.37(16)	C(26)-C(21)-P(2)	118.60(13)
C(22)-C(21)-P(2)	123.03(13)	C(23)-C(22)-C(21)	120.51(17)
C(23)-C(22)-H(4)	119.6(13)	C(21)-C(22)-H(4)	119.9(13)
C(24)-C(23)-C(22)	120.20(18)	C(24)-C(23)-H(8)	119.4(14)
C(22)-C(23)-H(8)	120.3(14)	C(25)-C(24)-C(23)	119.91(18)
C(25)-C(24)-H(17)	121.7(14)	C(23)-C(24)-H(17)	118.4(14)
C(24)-C(25)-C(26)	120.31(19)	C(24)-C(25)-H(13)	122.8(17)
C(26)-C(25)-H(13)	116.9(17)	C(25)-C(26)-C(21)	120.69(18)
C(25)-C(26)-H(6)	121.5(13)	C(21)-C(26)-H(6)	117.8(13)
N(1)-C(27)-Cu	175.55(16)	C(27)-N(1)-C(28)	178.9(2)
N(1)-C(28)-C(30)	106.62(16)	N(1)-C(28)-C(29)	108.01(16)
C(30)-C(28)-C(29)	111.9(2)	N(1)-C(28)-C(31)	107.31(17)
C(30)-C(28)-C(31)	112.0(2)	C(29)-C(28)-C(31)	110.7(2)
C(28)-C(29)-H(18)	109.1(18)	C(28)-C(29)-H(22)	106.9(16)
H(18)-C(29)-H(22)	111(2)	C(28)-C(29)-H(23)	109.1(16)
H(18)-C(29)-H(23)	110(2)	H(22)-C(29)-H(23)	111(2)
C(28)-C(30)-H(28)	111.7(18)	C(28)-C(30)-H(29)	107.6(16)
H(28)-C(30)-H(29)	108(2)	C(28)-C(30)-H(31)	111.1(17)
H(28)-C(30)-H(31)	109(2)	H(29)-C(30)-H(31)	110(2)
C(28)-C(31)-H(21)	107.5(15)	C(28)-C(31)-H(26)	108.3(17)
H(21)-C(31)-H(26)	113(2)	C(28)-C(31)-H(30)	110.6(17)
H(21)-C(31)-H(30)	107(2)	H(26)-C(31)-H(30)	110(2)
N(2)-C(32)-Cu	170.33(16)	C(32)-N(2)-C(33)	174.86(18)
C(34A)-C(33)-N(2)	112.3(4)	C(34A)-C(33)-C(34)	138.6(5)

N(2)-C(33)-C(34)	109.1(2)	C(34A)-C(33)-C(35A)	112.9(10)
N(2)-C(33)-C(35A)	107.8(4)	C(34)-C(33)-C(35A)	52.9(7)
C(34A)-C(33)-C(35)	49.9(7)	N(2)-C(33)-C(35)	106.4(2)
C(34)-C(33)-C(35)	116.4(4)	C(35A)-C(33)-C(35)	145.7(4)
C(34A)-C(33)-C(36)	57.8(8)	N(2)-C(33)-C(36)	106.4(2)
C(34)-C(33)-C(36)	110.7(4)	C(35A)-C(33)-C(36)	60.5(7)
C(35)-C(33)-C(36)	107.2(4)	C(34A)-C(33)-C(36A)	110.5(9)
N(2)-C(33)-C(36A)	103.2(4)	C(34)-C(33)-C(36A)	57.8(6)
C(35A)-C(33)-C(36A)	109.8(9)	C(35)-C(33)-C(36A)	63.8(6)
C(36)-C(33)-C(36A)	150.4(4)	C(33)-C(34)-H(34A)	109.5
C(33)-C(34)-H(34B)	109.5	H(34A)-C(34)-H(34B)	109.5
C(33)-C(34)-H(34C)	109.5	H(34A)-C(34)-H(34C)	109.5
H(34B)-C(34)-H(34C)	109.5	C(33)-C(35)-H(35A)	109.5
C(33)-C(35)-H(35B)	109.5	H(35A)-C(35)-H(35B)	109.5
C(33)-C(35)-H(35C)	109.5	H(35A)-C(35)-H(35C)	109.5
H(35B)-C(35)-H(35C)	109.5	C(33)-C(36)-H(36A)	109.5
C(33)-C(36)-H(36B)	109.5	H(36A)-C(36)-H(36B)	109.5
C(33)-C(36)-H(36C)	109.5	H(36A)-C(36)-H(36C)	109.5
H(36B)-C(36)-H(36C)	109.5	F(1)-B(1)-F(4)	109.66(19)
F(1)-B(1)-F(2)	109.16(19)	F(4)-B(1)-F(2)	109.95(18)
F(1)-B(1)-F(3)	110.40(19)	F(4)-B(1)-F(3)	109.49(17)
F(2)-B(1)-F(3)	108.18(19)		

Symmetry transformations used to generate equivalent atoms:

Table S4. Anisotropic displacement parameters ($Å^2 x\ 10^3$) for [Cu(dppe)(CN-t-Bu)$_2$](BF$_4$). The anisotropic displacement factor exponent takes the form: $-2\pi^2[\ h^2 a^{*2} U^{11} + ... + 2\ h\ k\ a^*\ b^*\ U^{12}\ ]$

	U^{11}	U^{22}	U^{33}	U^{23}	U^{13}	U^{12}
Cu	21(1)	25(1)	23(1)	-1(1)	5(1)	-2(1)
P(1)	20(1)	26(1)	23(1)	2(1)	5(1)	1(1)
P(2)	22(1)	24(1)	25(1)	1(1)	5(1)	1(1)
C(1)	24(1)	29(1)	30(1)	4(1)	3(1)	0(1)
C(2)	36(1)	43(1)	43(1)	-8(1)	-1(1)	5(1)
C(3)	44(1)	62(2)	60(2)	-16(1)	-16(1)	-2(1)
C(4)	25(1)	67(2)	77(2)	0(1)	-9(1)	2(1)
C(5)	28(1)	61(2)	62(2)	5(1)	10(1)	13(1)
C(6)	29(1)	45(1)	39(1)	-1(1)	6(1)	5(1)
C(7)	27(1)	27(1)	25(1)	1(1)	10(1)	1(1)
C(8)	32(1)	35(1)	32(1)	6(1)	3(1)	-1(1)
C(9)	46(1)	34(1)	37(1)	10(1)	9(1)	4(1)
C(10)	44(1)	32(1)	45(1)	5(1)	22(1)	-3(1)
C(11)	28(1)	40(1)	47(1)	4(1)	14(1)	-3(1)
C(12)	26(1)	35(1)	35(1)	6(1)	9(1)	3(1)
C(13)	27(1)	32(1)	25(1)	2(1)	8(1)	5(1)
C(14)	31(1)	28(1)	26(1)	-2(1)	6(1)	4(1)
C(15)	24(1)	30(1)	31(1)	7(1)	9(1)	2(1)
C(16)	29(1)	38(1)	67(1)	-10(1)	13(1)	0(1)
C(17)	28(1)	55(2)	89(2)	-13(1)	11(1)	-7(1)
C(18)	24(1)	53(1)	86(2)	17(1)	16(1)	5(1)
C(19)	37(1)	36(1)	108(2)	9(1)	28(1)	11(1)

C(20)	33(1)	29(1)	83(2)	-2(1)	18(1)	1(1)
C(21)	19(1)	27(1)	28(1)	2(1)	3(1)	2(1)
C(22)	29(1)	31(1)	29(1)	-3(1)	8(1)	-2(1)
C(23)	33(1)	28(1)	42(1)	-5(1)	7(1)	-3(1)
C(24)	34(1)	30(1)	44(1)	7(1)	12(1)	-2(1)
C(25)	43(1)	38(1)	35(1)	4(1)	17(1)	1(1)
C(26)	32(1)	28(1)	31(1)	-2(1)	8(1)	2(1)
C(27)	28(1)	28(1)	28(1)	2(1)	8(1)	2(1)
N(1)	30(1)	30(1)	33(1)	-3(1)	4(1)	-4(1)
C(28)	27(1)	36(1)	37(1)	-6(1)	2(1)	-10(1)
C(29)	52(2)	44(1)	59(2)	3(1)	4(1)	-17(1)
C(30)	47(1)	64(2)	49(1)	-21(1)	13(1)	-21(1)
C(31)	34(1)	50(1)	64(2)	-6(1)	0(1)	-3(1)
C(32)	29(1)	29(1)	26(1)	-1(1)	7(1)	1(1)
N(2)	26(1)	33(1)	33(1)	2(1)	8(1)	-2(1)
C(33)	22(1)	39(1)	44(1)	6(1)	8(1)	-4(1)
C(34)	55(2)	188(6)	52(2)	9(3)	-3(2)	-65(3)
C(35)	40(2)	69(3)	172(5)	64(3)	20(3)	-6(2)
C(36)	41(2)	96(3)	126(4)	-39(3)	40(2)	-7(2)
C(34A)	46(6)	133(13)	53(6)	30(7)	9(5)	-37(8)
C(35A)	20(4)	63(7)	142(13)	39(8)	15(6)	3(4)
C(36A)	34(5)	57(6)	138(11)	-47(7)	21(6)	-19(5)
B(1)	36(1)	32(1)	34(1)	-3(1)	4(1)	3(1)
F(1)	44(1)	78(1)	107(1)	-18(1)	-17(1)	-4(1)
F(2)	96(1)	69(1)	81(1)	-6(1)	54(1)	8(1)
F(3)	111(1)	33(1)	62(1)	-4(1)	15(1)	13(1)
F(4)	60(1)	65(1)	50(1)	18(1)	1(1)	-1(1)

Table S5. Hydrogen coordinates (x 10^4) and isotropic displacement parameters ($Å^2$x 10^3) for $[Cu(dppe)(CN\text{-}t\text{-}Bu)_2](BF_4)$.

	x	y	z	U(eq)
H(34A)	8629	4999	1362	152
H(34B)	8135	3733	1524	152
H(34C)	7696	5116	1596	152
H(35A)	7796	6076	447	142
H(35B)	6946	6400	729	142
H(35C)	6722	5612	186	142
H(36A)	7352	3397	144	127
H(36B)	7960	2722	670	127
H(36C)	8413	3895	414	127
H(1)	4977(17)	5600(20)	2111(8)	39(6)
H(2)	3502(15)	3805(18)	2193(7)	25(5)
H(3)	3978(15)	6020(20)	2176(8)	38(6)
H(4)	4255(14)	7992(19)	1670(8)	27(5)
H(5)	2923(16)	1550(20)	1780(9)	35(5)
H(6)	4566(14)	6020(20)	398(8)	32(5)
H(7)	4397(14)	4040(20)	2667(9)	33(5)
H(8)	4799(15)	9840(20)	1347(9)	38(6)
H(9)	2237(17)	-250(20)	2034(8)	36(5)
H(10)	3165(16)	-1770(20)	2645(9)	38(6)
H(11)	4824(17)	-1310(20)	2989(10)	48(6)
H(12)	5525(17)	520(20)	2709(8)	40(6)
H(13)	5091(17)	7870(20)	91(10)	46(6)
H(14)	6438(17)	1610(20)	1798(10)	45(6)

H(15)	8080(19)	1570(20)	2206(10)	48(7)
H(16)	6035(17)	3930(20)	2933(9)	44(6)
H(17)	5230(17)	9820(20)	555(9)	45(6)
H(18)	2610(20)	-990(30)	502(12)	74(9)
H(19)	-179(19)	5930(20)	884(10)	59(7)
H(20)	2524(18)	7360(30)	1439(10)	55(7)
H(21)	670(20)	900(30)	-246(11)	62(7)
H(22)	1470(20)	-1100(30)	182(11)	70(8)
H(23)	1844(18)	-270(20)	723(11)	53(7)
H(24)	920(20)	7640(30)	1276(11)	66(8)
H(25)	2190(17)	3740(20)	895(9)	49(6)
H(26)	1300(20)	2220(30)	-235(11)	67(8)
H(27)	8690(20)	2810(30)	2966(11)	73(8)
H(28)	2550(20)	1060(30)	-630(12)	80(9)
H(29)	1940(20)	-200(30)	-642(11)	64(8)
H(30)	1020(20)	1710(30)	278(12)	65(8)
H(31)	3040(20)	-220(30)	-341(11)	71(9)
H(32)	510(20)	3940(30)	718(12)	82(9)
H(33)	7660(20)	3930(30)	3328(12)	75(9)

Table S6. Crystal data and structure refinement for $[Ag(dppe)(CN\text{-}t\text{-}Bu)_2](BF_4)$.

Empirical formula	C36 H42 Ag B F4 N2 P2	
Formula weight	759.34	
Temperature	173(1) K	
Wavelength	0.71073 Å	
Diffractometer used	Bruker AXS P4/SMART 1000	
Detector distance	5 cm	
Monochrometer used	Graphite	
Crystal size	0.40 x 0.45 x 0.45 mm^3	
Colour and habit	Colourless, parallelepiped	
Crystal system	Monoclinic	
Space group	P2(1)/n	
Unit cell dimensions	a = 14.1130(8) Å	α = 90°
	b = 10.2075(6) Å	β = 103.3810(10)°
	c = 25.8175(16) Å	γ = 90°
Volume	3618.3(4) $Å^3$	
Z	4	
Density (calculated)	1.394 Mg/m^3	
Absorption coefficient	0.693 mm^{-1}	
F(000)	1560	
Theta range for data collection	1.85 to 27.50°	
Completeness to theta = 27.50°	98.8 %	
Scan type	ω and ϕ	
Scan range	0.3°	
Exposure time	10s	
Index ranges	$-17 \leq h \leq 18, -11 \leq k \leq 13, -31 \leq l \leq 33$	

Standard reflections collection	50 frames at beginning and end of data
Crystal stability	no decay
Reflections collected	25093
Independent reflections	8217 [R(int) = 0.0216]
System used	SHELXL 5.1
Solution	Direct methods
Hydrogen atoms	Found, refined isotropically
Absorption correction	SADABS
Min./Max. transmission ratio	0.889
Refinement method	Full-matrix least-squares on F^2
Data / restraints / parameters	8217 / 0 / 556
Goodness-of-fit on F^2	1.077
Final R indices [I>2sigma(I)]	R1 = 0.0292, wR2 = 0.0828
R indices (all data)	R1 = 0.0324, wR2 = 0.0845
Largest/mean shift/esd	0.002/0.000
Largest diff. peak and hole	1.074 and -0.224 e.$Å^{-3}$

$wR2 = (\sum[w(F_o^2-F_c^2)^2]/\sum[F_o^4])^{1/2}$

$R1 = \sum | |F_o| - |F_c| | / \sum |F_o|$

$Weight = 1 / [\sigma^2(F_o^2) + (0.0498 * P)^2 + (1.9892 * P)]$

where $P = (\max(F_o^2, 0) + 2 * F_c^2)/3$

Figure S2. Numbering scheme for $[Ag(dppe)(CN\text{-}t\text{-}Bu)_2](BF_4)$

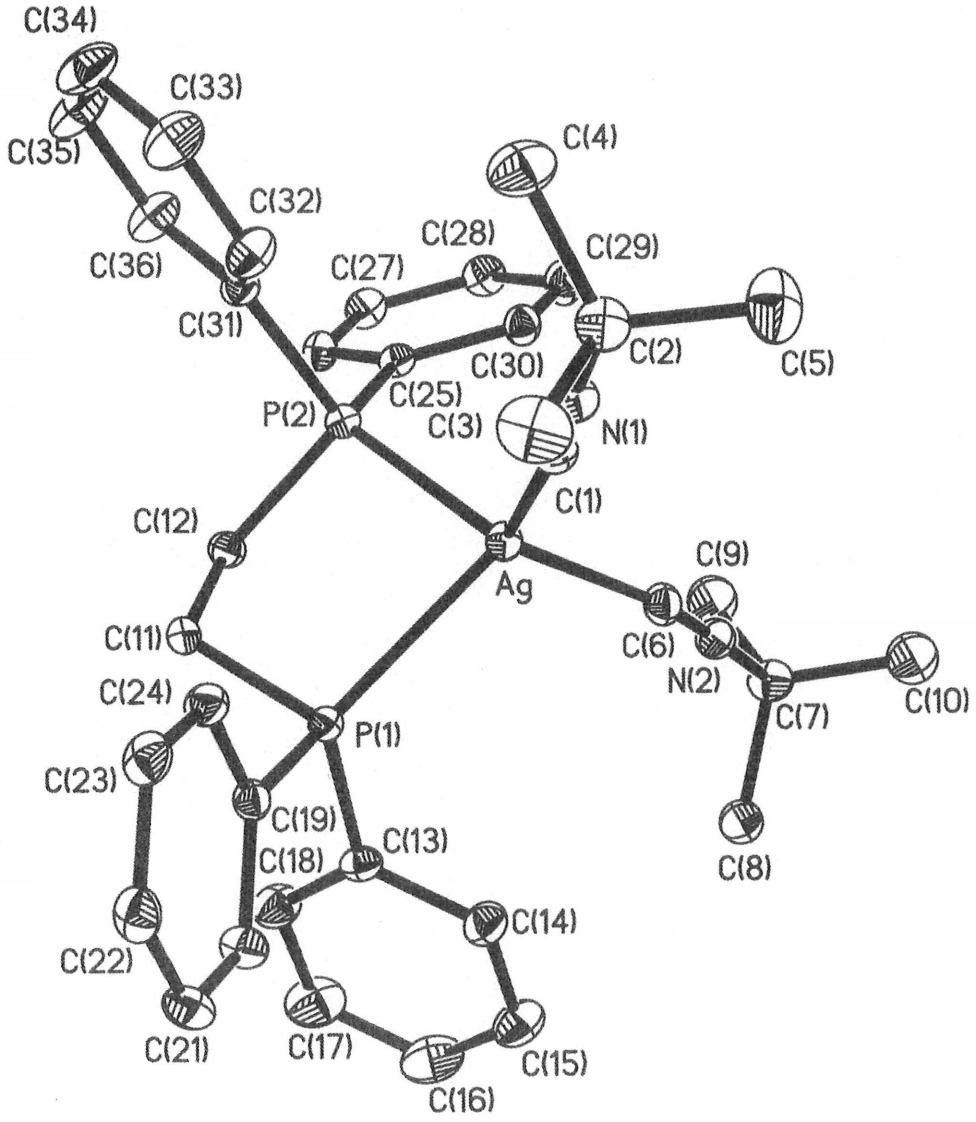

Table S7. Atomic coordinates (x 10^4) and equivalent isotropic displacement parameters ($Å^2$x 10^3) for [Ag(dppe)(CN-t-Bu)$_2$](BF$_4$). U(eq) is defined as one third of the trace of the orthogonalized U^{ij} tensor.

	x	y	z	U(eq)
Ag	9449(1)	6735(1)	1042(1)	24(1)
P(1)	9810(1)	7220(1)	2015(1)	21(1)
P(2)	8885(1)	4569(1)	1307(1)	22(1)
C(1)	8393(1)	8017(2)	565(1)	29(1)
N(1)	7787(1)	8675(2)	335(1)	31(1)
C(2)	7019(2)	9515(2)	29(1)	34(1)
C(3)	6905(2)	10658(3)	379(1)	53(1)
C(4)	6093(2)	8706(3)	-109(1)	49(1)
C(5)	7349(2)	9928(3)	-463(1)	53(1)
N(2)	11556(1)	5951(2)	795(1)	31(1)
C(6)	10814(1)	6359(2)	816(1)	31(1)
C(7)	12498(1)	5363(2)	801(1)	35(1)
C(8)	13228(5)	5935(9)	1288(4)	38(2)
C(9)	12353(7)	3874(9)	830(4)	53(2)
C(10)	12793(7)	5713(12)	281(4)	53(2)
C(8A)	13258(6)	6283(9)	1104(4)	46(2)
C(9A)	12512(6)	3989(8)	1112(4)	46(2)
C(10A)	12589(6)	5102(10)	246(3)	48(2)
C(8B)	13093(6)	5353(10)	1355(4)	50(2)
C(9B)	12262(7)	4089(9)	510(4)	56(2)
C(10B)	12967(6)	6302(9)	418(3)	44(2)
C(11)	9202(1)	5874(2)	2276(1)	25(1)

C(12)	9360(1)	4549(2)	2032(1)	26(1)
C(13)	11078(1)	7152(2)	2364(1)	26(1)
C(14)	11734(2)	7828(2)	2139(1)	36(1)
C(15)	12718(2)	7811(3)	2372(1)	48(1)
C(16)	13052(2)	7090(3)	2822(1)	54(1)
C(17)	12419(2)	6400(3)	3045(1)	54(1)
C(18)	11424(2)	6442(2)	2822(1)	39(1)
C(19)	9306(1)	8666(2)	2260(1)	25(1)
C(20)	9866(2)	9558(2)	2601(1)	31(1)
C(21)	9444(2)	10675(2)	2751(1)	35(1)
C(22)	8466(2)	10904(2)	2562(1)	35(1)
C(23)	7908(2)	10026(2)	2218(1)	35(1)
C(24)	8325(1)	8914(2)	2064(1)	30(1)
C(25)	9334(1)	3048(2)	1086(1)	23(1)
C(26)	9421(1)	1885(2)	1375(1)	27(1)
C(27)	9769(2)	766(2)	1182(1)	32(1)
C(28)	10042(2)	794(2)	705(1)	34(1)
C(29)	9965(2)	1938(2)	418(1)	36(1)
C(30)	9614(2)	3060(2)	608(1)	29(1)
C(31)	7580(1)	4344(2)	1218(1)	26(1)
C(32)	6974(2)	5366(2)	1010(1)	37(1)
C(33)	5974(2)	5241(3)	919(1)	50(1)
C(34)	5587(2)	4075(3)	1036(1)	51(1)
C(35)	6177(2)	3064(3)	1253(2)	53(1)
C(36)	7177(2)	3191(2)	1347(1)	41(1)
B	5130(2)	8886(2)	1381(1)	34(1)
F(1)	5178(2)	10230(2)	1352(1)	66(1)
F(2)	4794(1)	8377(2)	884(1)	54(1)
F(3)	6022(1)	8372(2)	1611(1)	80(1)

F(4)	4494(2)	8580(2)	1696(1)	68(1)

Table S8. Bond lengths [Å] and angles [°] for [Ag(dppe)(CN-t-Bu)$_2$](BF$_4$).

Ag-C(1)	2.145(2)	Ag-C(6)	2.1719(19)
Ag-P(1)	2.4939(5)	Ag-P(2)	2.4982(5)
P(1)-C(13)	1.8097(19)	P(1)-C(19)	1.8139(19)
P(1)-C(11)	1.8281(19)	P(2)-C(31)	1.8169(18)
P(2)-C(25)	1.8171(19)	P(2)-C(12)	1.8367(19)
C(1)-N(1)	1.141(3)	N(1)-C(2)	1.462(3)
C(2)-C(3)	1.507(4)	C(2)-C(5)	1.511(3)
C(2)-C(4)	1.517(3)	N(2)-C(6)	1.139(3)
N(2)-C(7)	1.455(2)	C(7)-C(8B)	1.481(9)
C(7)-C(10A)	1.492(9)	C(7)-C(9B)	1.500(10)
C(7)-C(8A)	1.503(9)	C(7)-C(10)	1.537(10)
C(7)-C(9)	1.537(10)	C(7)-C(8)	1.545(8)
C(7)-C(9A)	1.613(8)	C(7)-C(10B)	1.624(8)
C(8)-C(8A)	0.602(10)	C(8)-C(8B)	0.660(10)
C(9)-C(9A)	0.721(10)	C(9)-C(9B)	0.836(11)
C(10)-C(10A)	0.685(11)	C(10)-C(10B)	0.711(11)
C(10)-C(9B)	1.966(15)	C(8A)-C(8B)	1.202(13)
C(8A)-C(10B)	1.723(13)	C(9A)-C(9B)	1.516(12)
C(9A)-C(8B)	1.662(13)	C(10A)-C(10B)	1.368(12)
C(10A)-C(9B)	1.375(13)	C(11)-C(12)	1.530(3)
C(13)-C(18)	1.378(3)	C(13)-C(14)	1.385(3)
C(14)-C(15)	1.379(3)	C(15)-C(16)	1.364(4)
C(16)-C(17)	1.366(4)	C(17)-C(18)	1.390(3)
C(19)-C(20)	1.381(3)	C(19)-C(24)	1.383(3)
C(20)-C(21)	1.382(3)	C(21)-C(22)	1.373(3)
C(22)-C(23)	1.373(3)	C(23)-C(24)	1.379(3)
C(25)-C(30)	1.382(3)	C(25)-C(26)	1.391(3)

C(26)-C(27)	1.382(3)	C(27)-C(28)	1.372(3)
C(28)-C(29)	1.374(3)	C(29)-C(30)	1.381(3)
C(31)-C(32)	1.377(3)	C(31)-C(36)	1.380(3)
C(32)-C(33)	1.382(3)	C(33)-C(34)	1.372(4)
C(34)-C(35)	1.362(4)	C(35)-C(36)	1.382(3)
B-F(2)	1.363(3)	B-F(3)	1.366(3)
B-F(1)	1.377(3)	B-F(4)	1.378(3)

C(1)-Ag-C(6)	119.67(8)	C(1)-Ag-P(1)	114.21(6)
C(6)-Ag-P(1)	108.57(6)	C(1)-Ag-P(2)	118.28(5)
C(6)-Ag-P(2)	106.01(6)	P(1)-Ag-P(2)	84.504(16)
C(13)-P(1)-C(19)	106.26(9)	C(13)-P(1)-C(11)	106.39(9)
C(19)-P(1)-C(11)	103.17(8)	C(13)-P(1)-Ag	116.20(6)
C(19)-P(1)-Ag	120.47(6)	C(11)-P(1)-Ag	102.60(6)
C(31)-P(2)-C(25)	105.65(8)	C(31)-P(2)-C(12)	104.32(9)
C(25)-P(2)-C(12)	103.79(9)	C(31)-P(2)-Ag	117.09(7)
C(25)-P(2)-Ag	120.92(6)	C(12)-P(2)-Ag	102.93(6)
N(1)-C(1)-Ag	174.96(18)	(1)-N(1)-C(2)	178.7(2)
N(1)-C(2)-C(3)	107.38(19)	N(1)-C(2)-C(5)	106.49(18)
C(3)-C(2)-C(5)	112.6(2)	N(1)-C(2)-C(4)	107.35(19)
C(3)-C(2)-C(4)	110.8(2)	C(5)-C(2)-C(4)	111.8(2)
C(6)-N(2)-C(7)	175.6(2)	N(2)-C(6)-Ag	163.54(18)
N(2)-C(7)-C(8B)	109.0(4)	N(2)-C(7)-C(10A)	110.2(4)
C(8B)-C(7)-C(10A)	140.3(5)	N(2)-C(7)-C(9B)	104.9(4)
C(8B)-C(7)-C(9B)	119.2(6)	C(10A)-C(7)-C(9B)	54.7(5)
N(2)-C(7)-C(8A)	106.7(4)	C(8B)-C(7)-C(8A)	47.5(5)
C(10A)-C(7)-C(8A)	113.7(5)	C(9B)-C(7)-C(8A)	148.4(5)
N(2)-C(7)-C(10)	109.1(4)	C(8B)-C(7)-C(10)	129.6(6)
C(10A)-C(7)-C(10)	26.1(4)	C(9B)-C(7)-C(10)	80.7(6)

C(8A)-C(7)-C(10)	90.2(6)	N(2)-C(7)-C(9)	106.1(4)
C(8B)-C(7)-C(9)	89.9(6)	C(10A)-C(7)-C(9)	85.0(6)
C(9B)-C(7)-C(9)	31.9(4)	C(8A)-C(7)-C(9)	132.8(6)
C(10)-C(7)-C(9)	109.8(6)	N(2)-C(7)-C(8)	106.8(3)
C(8B)-C(7)-C(8)	25.1(4)	C(10A)-C(7)-C(8)	131.2(5)
C(9B)-C(7)-C(8)	139.9(5)	C(8A)-C(7)-C(8)	22.7(4)
C(10)-C(7)-C(8)	111.0(6)	C(9)-C(7)-C(8)	113.9(6)
N(2)-C(7)-C(9A)	105.6(3)	C(8B)-C(7)-C(9A)	64.8(5)
C(10A)-C(7)-C(9A)	109.2(5)	C(9B)-C(7)-C(9A)	58.1(5)
C(8A)-C(7)-C(9A)	111.0(5)	C(10)-C(7)-C(9A)	131.5(5)
C(9)-C(7)-C(9A)	26.3(4)	C(8)-C(7)-C(9A)	89.7(5)
N(2)-C(7)-C(10B)	104.5(3)	C(8B)-C(7)-C(10B)	111.8(5)
C(10A)-C(7)-C(10B)	51.9(4)	C(9B)-C(7)-C(10B)	106.3(5)
C(8A)-C(7)-C(10B)	66.8(5	C(10)-C(7)-C(10B)	25.8(4)
C(9)-C(7)-C(10B)	133.6(5)	C(8)-C(7)-C(10B)	89.0(5)
C(9A)-C(7)-C(10B)	148.9(4)	C(8A)-C(8)-C(8B)	145(2)
C(8A)-C(8)-C(7)	74.7(12)	C(8B)-C(8)-C(7)	72.1(11)
C(9A)-C(9)-C(9B)	153.8(18)	C(9A)-C(9)-C(7)	82.7(11)
C(9B)-C(9)-C(7)	71.6(10)	C(10A)-C(10)-C(10B)	157(2)
C(10A)-C(10)-C(7)	73.3(12)	C(10B)-C(10)-C(7)	84.0(11)
C(10A)-C(10)-C(9B)	24.9(10)	C(10B)-C(10)-C(9B)	132.4(13)
C(7)-C(10)-C(9B)	48.9(4)	C(8)-C(8A)-C(8B)	18.6(11)
C(8)-C(8A)-C(7)	82.6(13)	C(8B)-C(8A)-C(7)	65.3(6)
C(8)-C(8A)-C(10B)	140.7(15)	C(8B)-C(8A)-C(10B)	122.2(8)
C(7)-C(8A)-C(10B)	60.0(4)	C(9)-C(9A)-C(9B)	14.1(10)
C(9)-C(9A)-C(7)	71.0(11)	C(9B)-C(9A)-C(7)	57.2(5)
C(9)-C(9A)-C(8B)	121.9(13)	C(9B)-C(9A)-C(8B)	107.9(7)
C(7)-C(9A)-C(8B)	53.8(4)	C(10)-C(10A)-C(10B)	11.6(10)
C(10)-C(10A)-C(9B)	143.0(15)	C(10B)-C(10A)-C(9B)	131.5(8)

C(10)-C(10A)-C(7)	80.6(12)	C(10B)-C(10A)-C(7)	69.0(5)
C(9B)-C(10A)-C(7)	62.9(5)	C(8)-C(8B)-C(8A)	16.9(10)
C(8)-C(8B)-C(7)	82.9(12)	C(8A)-C(8B)-C(7)	67.2(6)
C(8)-C(8B)-C(9A)	143.5(14)	C(8A)-C(8B)-C(9A)	126.8(8)
C(7)-C(8B)-C(9A)	61.4(5)	C(9)-C(9B)-C(10A)	134.0(13)
C(9)-C(9B)-C(7)	76.5(10)	C(10A)-C(9B)-C(7)	62.3(5)
C(9)-C(9B)-C(9A)	12.1(8)	C(10A)-C(9B)-C(9A)	122.2(8)
C(7)-C(9B)-C(9A)	64.7(5)	C(9)-C(9B)-C(10)	122.4(11)
C(10A)-C(9B)-C(10)	12.1(5)	C(7)-C(9B)-C(10)	50.5(4)
C(9A)-C(9B)-C(10)	110.5(7)	C(10)-C(10B)-C(10A)	11.2(10)
C(10)-C(10B)-C(7)	70.2(11)	C(10A)-C(10B)-C(7)	59.1(5)
C(10)-C(10B)-C(8A)	118.3(12)	C(10A)-C(10B)-C(8A)	107.8(7)
C(7)-C(10B)-C(8A)	53.2(4)	C(12)-C(11)-P(1)	112.77(13)
C(11)-C(12)-P(2)	110.89(13)	C(18)-C(13)-C(14)	119.00(19)
C(18)-C(13)-P(1)	124.06(16)	C(14)-C(13)-P(1)	116.90(16)
C(15)-C(14)-C(13)	120.9(2)	C(16)-C(15)-C(14)	119.5(2)
C(15)-C(16)-C(17)	120.4(2)	C(16)-C(17)-C(18)	120.4(3)
C(13)-C(18)-C(17)	119.6(2)	C(20)-C(19)-C(24)	119.25(18)
C(20)-C(19)-P(1)	123.11(15)	C(24)-C(19)-P(1)	117.51(15)
C(19)-C(20)-C(21)	120.16(19)	C(22)-C(21)-C(20)	120.3(2)
C(21)-C(22)-C(23)	119.8(2)	C(22)-C(23)-C(24)	120.3(2)
C(23)-C(24)-C(19)	120.2(2)	C(30)-C(25)-C(26)	118.58(18)
C(30)-C(25)-P(2)	117.73(15)	C(26)-C(25)-P(2)	123.68(15)
C(27)-C(26)-C(25)	120.48(19)	C(28)-C(27)-C(26)	120.18(19)
C(27)-C(28)-C(29)	119.9(2)	C(28)-C(29)-C(30)	120.2(2)
C(29)-C(30)-C(25)	120.6(2)	C(32)-C(31)-C(36)	119.11(19)
C(32)-C(31)-P(2)	118.26(15)	C(36)-C(31)-P(2)	122.63(16)
C(31)-C(32)-C(33)	120.9(2)	C(34)-C(33)-C(32)	119.1(2)
C(35)-C(34)-C(33)	120.7(2)	C(34)-C(35)-C(36)	120.3(2)

C(31)-C(36)-C(35)	119.9(2)	F(2)-B-F(3)	110.3(2)
F(2)-B-F(1)	109.8(2)	F(3)-B-F(1)	110.7(2)
F(2)-B-F(4)	109.6(2)	F(3)-B-F(4)	108.5(2)
F(1)-B-F(4)	107.7(2)		

Symmetry transformations used to generate equivalent atoms:

Table S9. Anisotropic displacement parameters ($Å^2 x\ 10^3$) for [Ag(dppe)(CN-t-Bu)$_2$](BF$_4$). The anisotropic displacement factor exponent takes the form: $-2p^2[\ h^2 a^{*2} U^{11} + ... + 2\ h\ k\ a^*\ b^*\ U^{12}\ ]$

	U^{11}	U^{22}	U^{33}	U^{23}	U^{13}	U^{12}
Ag	22(1)	25(1)	23(1)	2(1)	6(1)	2(1)
P(1)	20(1)	23(1)	22(1)	-2(1)	5(1)	-1(1)
P(2)	21(1)	21(1)	23(1)	0(1)	5(1)	-1(1)
C(1)	27(1)	30(1)	31(1)	1(1)	5(1)	0(1)
N(1)	29(1)	30(1)	33(1)	2(1)	4(1)	3(1)
C(2)	27(1)	37(1)	37(1)	8(1)	3(1)	11(1)
C(3)	50(2)	45(2)	61(2)	-4(1)	6(1)	17(1)
C(4)	32(1)	51(2)	59(2)	5(1)	-1(1)	4(1)
C(5)	44(1)	65(2)	50(2)	25(1)	13(1)	19(1)
N(2)	26(1)	37(1)	31(1)	-2(1)	7(1)	1(1)
C(6)	28(1)	36(1)	28(1)	1(1)	9(1)	1(1)
C(7)	23(1)	39(1)	42(1)	-7(1)	8(1)	5(1)
C(11)	27(1)	28(1)	22(1)	-2(1)	9(1)	-4(1)
C(12)	30(1)	24(1)	23(1)	1(1)	4(1)	-3(1)
C(13)	21(1)	26(1)	30(1)	-4(1)	3(1)	0(1)
C(14)	27(1)	46(1)	36(1)	2(1)	7(1)	-5(1)
C(15)	26(1)	60(2)	57(2)	-3(1)	9(1)	-9(1)
C(16)	26(1)	62(2)	67(2)	-2(1)	-5(1)	1(1)
C(17)	39(1)	57(2)	56(2)	12(1)	-11(1)	4(1)
C(18)	33(1)	42(1)	39(1)	7(1)	0(1)	-4(1)
C(19)	26(1)	25(1)	24(1)	-1(1)	9(1)	0(1)
C(20)	29(1)	32(1)	30(1)	-4(1)	3(1)	2(1)

C(21)	42(1)	30(1)	31(1)	-9(1)	6(1)	-2(1)
C(22)	39(1)	29(1)	40(1)	-3(1)	19(1)	5(1)
C(23)	26(1)	38(1)	44(1)	-3(1)	14(1)	4(1)
C(24)	25(1)	32(1)	33(1)	-6(1)	9(1)	-2(1)
C(25)	20(1)	23(1)	26(1)	-1(1)	4(1)	-1(1)
C(26)	28(1)	27(1)	28(1)	3(1)	8(1)	1(1)
C(27)	33(1)	24(1)	39(1)	4(1)	8(1)	2(1)
C(28)	35(1)	28(1)	42(1)	-8(1)	12(1)	2(1)
C(29)	44(1)	35(1)	33(1)	-5(1)	18(1)	-2(1)
C(30)	35(1)	26(1)	29(1)	1(1)	10(1)	-2(1)
C(31)	22(1)	28(1)	29(1)	-6(1)	8(1)	-2(1)
C(32)	29(1)	35(1)	50(1)	4(1)	12(1)	1(1)
C(33)	28(1)	51(2)	72(2)	2(1)	12(1)	9(1)
C(34)	24(1)	51(2)	80(2)	-17(1)	17(1)	-5(1)
C(35)	35(1)	35(1)	94(2)	-12(1)	28(1)	-11(1)
C(36)	31(1)	30(1)	65(2)	-2(1)	16(1)	-3(1)
B	36(1)	29(1)	33(1)	4(1)	1(1)	-3(1)
F(1)	106(1)	29(1)	57(1)	4(1)	11(1)	-14(1)
F(2)	61(1)	54(1)	42(1)	-13(1)	2(1)	5(1)
F(3)	42(1)	78(1)	101(2)	23(1)	-20(1)	-2(1)
F(4)	86(1)	58(1)	73(1)	5(1)	46(1)	-7(1)

Table S10. Hydrogen coordinates (x 10^4) and isotropic displacement parameters ($Å^2$x 10^3) for [Ag(dppe)(CN-t-Bu)$_2$](BF$_4$).

	x	y	z	U(eq)
H(3A)	7510(30)	11100(30)	466(14)	68(10)
H(3B)	6730(20)	10330(30)	662(14)	58(9)
H(3C)	6380(20)	11190(30)	161(14)	64(9)
H(4A)	6140(30)	8000(40)	-319(15)	70(11)
H(4B)	5570(20)	9290(30)	-300(13)	58(8)
H(4C)	5860(20)	8390(30)	210(13)	50(8)
H(5A)	7400(30)	9110(40)	-689(17)	94(13)
H(5B)	7900(30)	10390(40)	-377(16)	80(12)
H(5C)	6860(20)	10500(30)	-669(13)	62(9)
H(11A)	9405(16)	5880(20)	2634(9)	23(5)
H(11B)	8513(16)	6090(20)	2171(8)	20(5)
H(12A)	10036(18)	4360(20)	2087(10)	31(6)
H(12B)	9079(18)	3880(30)	2182(10)	34(6)
H(14)	11510(20)	8250(20)	1834(12)	38(7)
H(15)	13280(30)	8310(40)	2219(17)	88(13)
H(16)	13730(30)	7160(40)	3021(17)	96(13)
H(17)	12670(30)	5930(30)	3394(14)	73(10)
H(18)	11010(20)	5960(30)	2966(11)	43(7)
H(20)	10507(19)	9450(20)	2716(10)	34(6)
H(21)	9800(20)	11220(30)	2983(12)	48(7)
H(22)	8196(19)	11630(20)	2640(11)	35(7)
H(23)	7340(20)	10160(30)	2096(11)	40(7)
H(24)	8006(18)	8350(20)	1839(10)	28(6)

H(26)	9236(19)	1820(20)	1685(11)	30(6)
H(27)	9769(19)	-10(30)	1364(11)	38(7)
H(28)	10250(20)	90(30)	591(12)	46(7)
H(29)	10120(20)	2060(30)	133(13)	57(9)
H(30)	9570(17)	3810(20)	415(10)	28(6)
H(32)	7220(20)	6130(30)	932(11)	43(7)
H(33)	5530(30)	5930(40)	725(15)	78(11)
H(34)	4930(30)	3970(30)	953(14)	68(10)
H(35)	5970(20)	2370(30)	1334(13)	57(9)
H(36)	7569(19)	2430(30)	1502(10)	40(7)

Table S11. Crystal data and structure refinement for $[Cu(dppp)(CN\text{-}t\text{-}Bu)_2](BF_4)$.

Empirical formula	C37 H44 B Cu F4 N2 P2	
Formula weight	729.03	
Temperature	173(1) K	
Wavelength	0.71073 Å	
Diffractometer used	Bruker AXS P4/SMART 1000	
Detector distance	5 cm	
Monochrometer used	Graphite	
Crystal size	0.25 x 0.3 x 0.4 mm^3	
Colour and habit	Colourless, irregular	
Crystal system	Monoclinic	
Space group	P2(1)/c	
Unit cell dimensions	a = 15.5433(9) Å	α = 90°
	b = 11.2094(6) Å	β = 92.4830(10)°
	c = 21.4362(12) Å	γ = 90°
Volume	3731.3(4) $Å^3$	
Z	4	
Density (calculated)	1.298 Mg/m^3	
Absorption coefficient	0.719 mm^{-1}	
F(000)	1520	
Theta range for data collection	1.90 to 27.50°	
Completeness to theta = 27.50°	98.9 %	
Scan type	ω and ϕ	
Scan range	0.3°	
Exposure time	10s	
Index ranges	$-19 \leq h \leq 20, -14 \leq k \leq 14, -27 \leq l \leq 27$	

Standard reflections collection	50 frames at beginning and end of data
Crystal stability	no decay
Reflections collected	26303
Independent reflections	8479 [R(int) = 0.0225]
System used	SHELXL 5.1
Solution	Direct methods
Hydrogen atoms atoms on C(6)	Found, refined isotropically. Hydrogen included in calculated positions, refined using a riding model
Absorption correction	SADABS
Min./Max. transmission ratio	0.902
Refinement method	Full-matrix least-squares on F^2
Data / restraints / parameters	8479 / 0 / 642
Goodness-of-fit on F^2	1.085
Final R indices [I>2sigma(I)]	R1 = 0.0327, wR2 = 0.0905
R indices (all data)	R1 = 0.0458, wR2 = 0.0976
Largest/mean shift/esd	0.001/0.000
Largest diff. peak and hole	0.387 and -0.293 e.Å^{-3}

$wR2 = (\Sigma [w(F_o^2-F_c^2)^2]/\Sigma [F_o^4])^{1/2}$

$R1 = \Sigma \, | \, |F_o| - |F_c| \, | \, / \Sigma \, |F_o|$

$Weight = 1 / [\sigma^2(F_o^2) + (0.0569 * P)^2 + (0.6494 * P)]$

where $P = (\max (F_o^2, 0) + 2 * F_c^2)/3$

Figure S3. Numbering scheme for $[Cu(dppp)(CN\text{-}t\text{-}Bu)_2](BF_4)$.

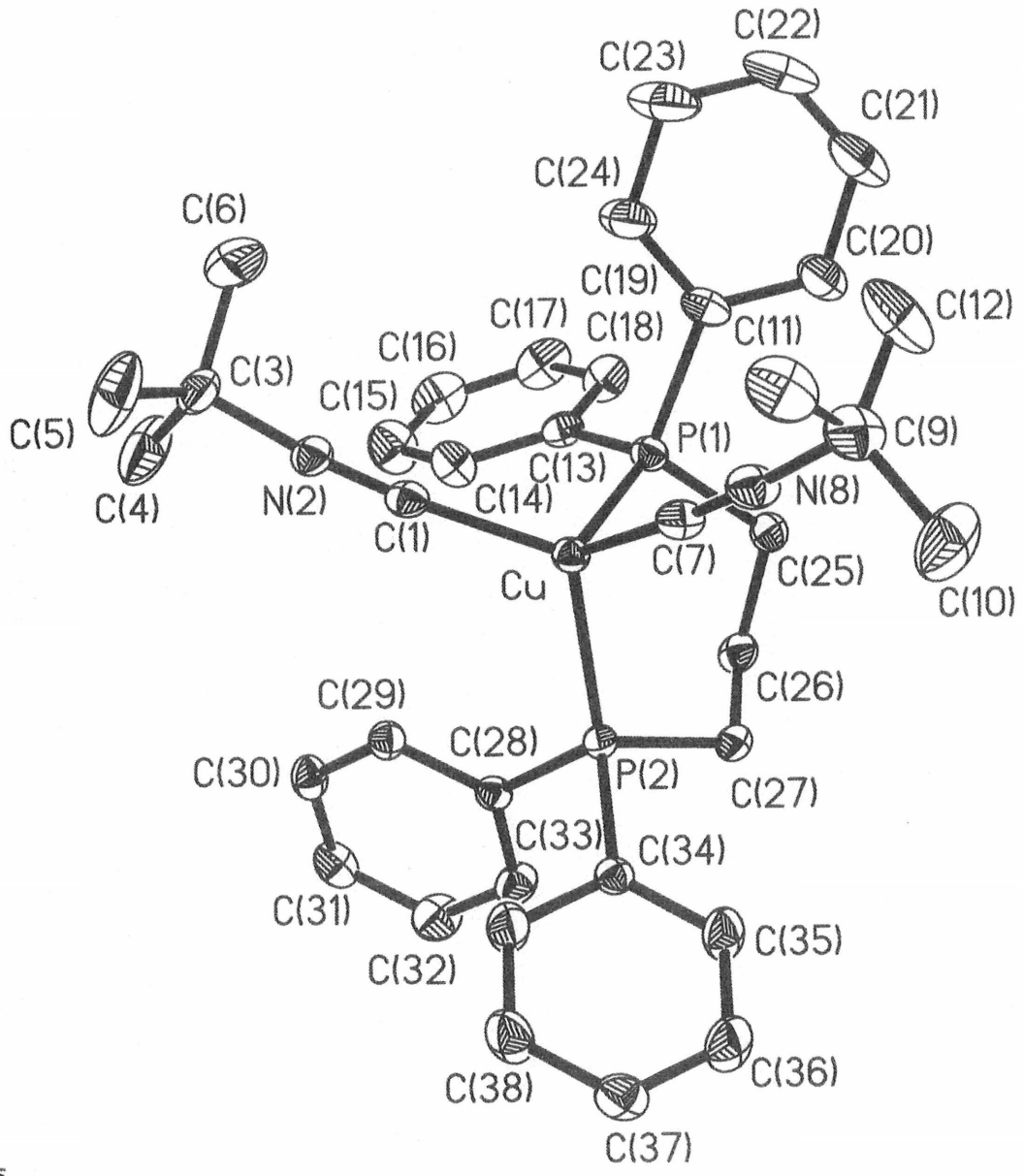

Table S12. Atomic coordinates (x 10^4) and equivalent isotropic displacement parameters ($Å^2$x 10^3) for [Cu(dppp)(CN-t-Bu)$_2$](BF$_4$). U(eq) is defined as one third of the trace of the orthogonalized U^{ij} tensor.

	x	y	z	U(eq)
Cu	2632(1)	7340(1)	2326(1)	29(1)
P(1)	2037(1)	5790(1)	2854(1)	31(1)
P(2)	3873(1)	6446(1)	2066(1)	27(1)
C(1)	2688(1)	8708(2)	2863(1)	33(1)
N(2)	2677(1)	9425(1)	3241(1)	36(1)
C(3)	2619(1)	10202(2)	3785(1)	45(1)
C(4)	3345(3)	9882(4)	4230(2)	87(1)
C(5)	2641(4)	11454(3)	3576(2)	95(1)
C(6)	1763(2)	9915(4)	4055(2)	96(1)
C(7)	1871(1)	7549(2)	1596(1)	40(1)
N(8)	1363(1)	7611(2)	1203(1)	47(1)
C(9)	655(2)	7612(2)	733(1)	60(1)
C(10)	1001(4)	7130(6)	156(2)	91(2)
C(11)	420(3)	8975(4)	621(2)	70(1)
C(12)	-55(3)	7033(6)	1028(3)	87(2)
C(10A)	-138(6)	7983(14)	984(6)	86(4)
C(11A)	455(5)	6111(8)	550(5)	60(2)
C(12A)	885(9)	8088(18)	151(6)	106(5)
C(13)	2355(1)	5551(2)	3670(1)	35(1)
C(14)	2924(1)	6307(2)	3974(1)	47(1)
C(15)	3176(2)	6123(3)	4593(1)	63(1)
C(16)	2857(2)	5191(3)	4910(1)	64(1)

C(17)	2284(2)	4426(2)	4618(1)	62(1)
C(18)	2035(2)	4599(2)	4002(1)	51(1)
C(19)	870(1)	5780(2)	2877(1)	42(1)
C(20)	353(2)	4941(3)	2578(1)	56(1)
C(21)	-535(2)	5005(3)	2629(1)	74(1)
C(22)	-900(2)	5878(3)	2960(2)	78(1)
C(23)	-394(2)	6721(3)	3248(2)	82(1)
C(24)	490(2)	6669(2)	3208(2)	63(1)
C(25)	2309(1)	4376(2)	2493(1)	38(1)
C(26)	3272(1)	4196(2)	2444(1)	38(1)
C(27)	3674(1)	4868(2)	1914(1)	34(1)
C(28)	4751(1)	6432(1)	2655(1)	28(1)
C(29)	4736(1)	7217(2)	3152(1)	33(1)
C(30)	5401(1)	7239(2)	3602(1)	39(1)
C(31)	6085(1)	6483(2)	3561(1)	44(1)
C(32)	6111(1)	5709(2)	3072(1)	53(1)
C(33)	5454(1)	5682(2)	2619(1)	43(1)
C(34)	4429(1)	6939(2)	1383(1)	30(1)
C(35)	4403(2)	6343(2)	823(1)	47(1)
C(36)	4855(2)	6767(2)	331(1)	56(1)
C(37)	5327(1)	7793(2)	385(1)	49(1)
C(38)	5346(2)	8399(2)	933(1)	59(1)
C(39)	4904(2)	7978(2)	1429(1)	52(1)
B	2094(2)	3435(3)	675(1)	59(1)
F(1)	2074(3)	4625(3)	797(2)	118(2)
F(2)	2878(2)	3219(3)	395(2)	89(1)
F(3)	2122(2)	2824(3)	1220(1)	58(1)
F(4)	1470(1)	3115(2)	247(1)	86(1)
F(1A)	2052(6)	2321(9)	1014(5)	76(3)

F(2A)	1498(9)	4144(10)	1026(5)	131(4)
F(3A)	2705(12)	3951(18)	579(5)	165(9)

Table S13. Bond lengths [Å] and angles [°] for $[Cu(dppp)(CN\text{-}t\text{-}Bu)_2](BF_4)$.

Cu-C(1)	1.9176(18)	Cu-C(7)	1.935(2)
Cu-P(2)	2.2636(4)	Cu-P(1)	2.2898(5)
P(1)-C(19)	1.8173(18)	P(1)-C(13)	1.8181(18)
P(1)-C(25)	1.8209(19)	P(2)-C(34)	1.8195(17)
P(2)-C(28)	1.8194(16)	P(2)-C(27)	1.8229(17)
C(1)-N(2)	1.142(2)	N(2)-C(3)	1.461(2)
C(3)-C(5)	1.474(4)	C(3)-C(4)	1.488(3)
C(3)-C(6)	1.509(4)	C(7)-N(8)	1.132(3)
N(8)-C(9)	1.459(3)	C(9)-C(12A)	1.417(12)
C(9)-C(10A)	1.428(10)	C(9)-C(12)	1.449(5)
C(9)-C(10)	1.473(6)	C(9)-C(11)	1.587(5)
C(9)-C(11A)	1.752(9)	C(10)-C(12A)	1.089(19)
C(10)-C(11A)	1.674(13)	C(11)-C(12A)	1.61(2)
C(11)-C(10A)	1.629(17)	C(12)-C(10A)	1.077(15)
C(12)-C(11A)	1.678(12)	C(13)-C(14)	1.368(3)
C(13)-C(18)	1.386(3)	C(14)-C(15)	1.384(3)
C(15)-C(16)	1.352(4)	C(16)-C(17)	1.368(4)
C(17)-C(18)	1.373(3)	C(19)-C(24)	1.372(3)
C(19)-C(20)	1.377(3)	C(20)-C(21)	1.390(4)
C(21)-C(22)	1.350(5)	C(22)-C(23)	1.360(5)
C(23)-C(24)	1.381(3)	C(25)-C(26)	1.519(3)
C(26)-C(27)	1.519(3)	C(28)-C(29)	1.382(2)
C(28)-C(33)	1.383(2)	C(29)-C(30)	1.383(3)
C(30)-C(31)	1.365(3)	C(31)-C(32)	1.363(3)
C(32)-C(33)	1.378(3)	C(34)-C(35)	1.373(3)
C(34)-C(39)	1.380(3)	C(35)-C(36)	1.376(3)
C(36)-C(37)	1.366(3)	C(37)-C(38)	1.357(3)

C(38)-C(39)	1.373(3)	B-F(3A)	1.138(10)
B-F(4)	1.354(3)	B-F(3)	1.354(4)
B-F(1)	1.360(4)	B-F(2)	1.402(5)
B-F(1A)	1.448(10)	B-F(2A)	1.455(12)
F(1)-F(2A)	1.171(11)	F(1)-F(3A)	1.34(2)
F(2)-F(3A)	0.95(2)	F(3)-F(1A)	0.721(10)

C(1)-Cu-C(7)	113.54(8)	C(1)-Cu-P(2)	118.98(5)
C(7)-Cu-P(2)	110.63(6)	C(1)-Cu-P(1)	108.61(5)
C(7)-Cu-P(1)	104.22(6)	P(2)-Cu-P(1)	98.737(17)
C(19)-P(1)-C(13)	101.67(9)	C(19)-P(1)-C(25)	104.85(9)
C(13)-P(1)-C(25)	102.80(9)	C(19)-P(1)-Cu	116.34(6)
C(13)-P(1)-Cu	119.26(6)	C(25)-P(1)-Cu	110.17(6)
C(34)-P(2)-C(28)	101.11(7)	C(34)-P(2)-C(27)	103.51(8)
C(28)-P(2)-C(27)	103.41(8)	C(34)-P(2)-Cu	120.22(5)
C(28)-P(2)-Cu	117.07(5)	C(27)-P(2)-Cu	109.51(6)
N(2)-C(1)-Cu	170.86(15)	C(1)-N(2)-C(3)	171.50(18)
N(2)-C(3)-C(5)	108.8(2)	N(2)-C(3)-C(4)	107.23(18)
C(5)-C(3)-C(4)	113.4(3)	N(2)-C(3)-C(6)	105.34(18)
C(5)-C(3)-C(6)	110.6(3)	C(4)-C(3)-C(6)	111.1(3)
N(8)-C(7)-Cu	172.85(18)	C(7)-N(8)-C(9)	174.2(2)
C(12A)-C(9)-C(10A)	118.4(9)	C(12A)-C(9)-C(12)	141.2(5)
C(10A)-C(9)-C(12)	44.0(7)	C(12A)-C(9)-N(8)	113.4(5)
C(10A)-C(9)-N(8)	112.2(4)	C(12)-C(9)-N(8)	105.3(2)
C(12A)-C(9)-C(10)	44.2(8)	C(10A)-C(9)-C(10)	140.9(5)
C(12)-C(9)-C(10)	121.0(5)	N(8)-C(9)-C(10)	106.7(3)
C(12A)-C(9)-C(11)	64.5(9)	C(10A)-C(9)-C(11)	65.1(7)
C(12)-C(9)-C(11)	108.8(4)	N(8)-C(9)-C(11)	105.4(2)
C(10)-C(9)-C(11)	108.4(4)	C(12A)-C(9)-C(11A)	102.3(9)

C(10A)-C(9)-C(11A)	102.5(7)	C(12)-C(9)-C(11A)	62.4(5)
N(8)-C(9)-C(11A)	106.0(3)	C(10)-C(9)-C(11A)	61.8(5)
C(11)-C(9)-C(11A)	148.6(4)	C(12A)-C(10)-C(9)	65.2(8)
C(12A)-C(10)-C(11A)	126.2(10)	C(9)-C(10)-C(11A)	67.3(4)
C(9)-C(11)-C(12A)	52.6(5)	C(9)-C(11)-C(10A)	52.7(4)
C(12A)-C(11)-C(10A)	98.0(7)	C(10A)-C(12)-C(9)	67.0(7)
C(10A)-C(12)-C(11A)	127.8(9)	C(9)-C(12)-C(11A)	67.7(4)
C(12)-C(10A)-C(9)	69.0(6)	C(12)-C(10A)-C(11)	130.8(9)
C(9)-C(10A)-C(11)	62.2(6)	C(10)-C(11A)-C(12)	98.7(5)
C(10)-C(11A)-C(9)	50.9(3)	C(12)-C(11A)-C(9)	49.9(3)
C(10)-C(12A)-C(9)	70.6(8)	C(10)-C(12A)-C(11)	133.0(11)
C(9)-C(12A)-C(11)	62.9(7)	C(14)-C(13)-C(18)	118.13(19)
C(14)-C(13)-P(1)	120.61(14)	C(18)-C(13)-P(1)	121.26(16)
C(13)-C(14)-C(15)	121.0(2)	C(16)-C(15)-C(14)	120.1(3)
C(15)-C(16)-C(17)	120.1(2)	C(16)-C(17)-C(18)	120.1(2)
C(17)-C(18)-C(13)	120.6(2)	C(24)-C(19)-C(20)	118.7(2)
C(24)-C(19)-P(1)	117.56(16)	C(20)-C(19)-P(1)	123.70(17)
C(19)-C(20)-C(21)	119.3(3)	C(22)-C(21)-C(20)	121.4(3)
C(21)-C(22)-C(23)	119.6(2)	C(22)-C(23)-C(24)	120.0(3)
C(19)-C(24)-C(23)	121.0(3)	C(26)-C(25)-P(1)	113.10(13)
C(25)-C(26)-C(27)	115.05(16)	C(26)-C(27)-P(2)	114.78(12)
C(29)-C(28)-C(33)	118.04(16)	C(29)-C(28)-P(2)	119.45(13)
C(33)-C(28)-P(2)	122.49(13)	C(28)-C(29)-C(30)	120.79(17)
C(31)-C(30)-C(29)	120.28(18)	C(32)-C(31)-C(30)	119.55(18)
C(31)-C(32)-C(33)	120.70(19)	C(32)-C(33)-C(28)	120.63(19)
C(35)-C(34)-C(39)	117.91(17)	C(35)-C(34)-P(2)	124.02(14)
C(39)-C(34)-P(2)	118.07(14)	C(34)-C(35)-C(36)	120.3(2)
C(37)-C(36)-C(35)	121.0(2)	C(38)-C(37)-C(36)	119.1(2)
C(37)-C(38)-C(39)	120.3(2)	C(38)-C(39)-C(34)	121.3(2)

F(3A)-B-F(4)	126.3(6)	F(3A)-B-F(3)	114.6(8)
F(4)-B-F(3)	116.5(3)	F(3A)-B-F(1)	64.0(11)
F(4)-B-F(1)	111.6(2)	F(3)-B-F(1)	109.3(3)
F(3A)-B-F(2)	42.6(11)	F(4)-B-F(2)	105.9(3)
F(3)-B-F(2)	106.6(3)	F(1)-B-F(2)	106.2(4)
F(3A)-B-F(1A)	125.8(12)	F(4)-B-F(1A)	93.8(4)
F(3)-B-F(1A)	29.6(4)	F(1)-B-F(1A)	138.4(5)
F(2)-B-F(1A)	97.2(4)	F(3A)-B-F(2A)	111.7(11)
F(4)-B-F(2A)	92.4(5)	F(3)-B-F(2A)	80.0(5)
F(1)-B-F(2A)	49.0(4)	F(2)-B-F(2A)	154.1(6)
F(1A)-B-F(2A)	99.6(6)	F(2A)-F(1)-F(3A)	118.2(8)
F(2A)-F(1)-B	69.7(6)	F(3A)-F(1)-B	49.9(4)
F(3A)-F(2)-B	53.8(7)	F(1A)-F(3)-B	82.4(9)
F(3)-F(1A)-B	68.0(9)	F(1)-F(2A)-B	61.3(6)
F(2)-F(3A)-B	83.6(9)	F(2)-F(3A)-F(1)	148.5(10)
B-F(3A)-F(1)	66.1(10)		

Symmetry transformations used to generate equivalent atoms:

Table S14. Anisotropic displacement parameters ($Å^2 x\ 10^3$) for [Cu(dppp)(CN-t-Bu)$_2$](BF$_4$). The anisotropic displacement factor exponent takes the form: $-2p^2[\ h^2\ a^{*2}U^{11} + ... + 2\ h\ k\ a^*\ b^*\ U^{12}\ ]$

	U^{11}	U^{22}	U^{33}	U^{23}	U^{13}	U^{12}
Cu	25(1)	28(1)	33(1)	0(1)	2(1)	2(1)
P(1)	28(1)	30(1)	36(1)	2(1)	5(1)	-2(1)
P(2)	25(1)	27(1)	28(1)	-3(1)	1(1)	1(1)
C(1)	29(1)	29(1)	41(1)	4(1)	5(1)	4(1)
N(2)	35(1)	29(1)	42(1)	-1(1)	5(1)	4(1)
C(3)	50(1)	39(1)	47(1)	-12(1)	4(1)	9(1)
C(4)	95(2)	91(2)	72(2)	-43(2)	-33(2)	38(2)
C(5)	170(4)	36(1)	80(2)	-15(1)	18(3)	2(2)
C(6)	76(2)	138(3)	77(2)	-47(2)	32(2)	-7(2)
C(7)	33(1)	45(1)	41(1)	3(1)	5(1)	6(1)
N(8)	35(1)	68(1)	37(1)	5(1)	-1(1)	8(1)
C(9)	45(1)	92(2)	42(1)	7(1)	-12(1)	11(1)
C(10)	105(4)	118(5)	48(2)	-18(3)	-24(3)	39(4)
C(11)	57(2)	79(3)	73(3)	23(2)	-13(2)	10(2)
C(12)	55(2)	111(4)	93(4)	37(3)	-30(3)	-30(3)
C(10A)	42(5)	131(10)	84(8)	-46(8)	-25(5)	30(6)
C(11A)	43(4)	66(5)	70(6)	-28(4)	-11(4)	6(3)
C(12A)	87(8)	158(14)	68(7)	54(9)	-36(6)	-22(9)
C(13)	36(1)	33(1)	36(1)	4(1)	8(1)	7(1)
C(14)	46(1)	53(1)	42(1)	11(1)	-3(1)	-7(1)
C(15)	65(2)	77(2)	48(1)	8(1)	-13(1)	-5(1)
C(16)	78(2)	72(2)	41(1)	14(1)	-2(1)	21(1)

C(17)	89(2)	48(1)	51(1)	17(1)	17(1)	11(1)
C(18)	71(2)	37(1)	46(1)	6(1)	15(1)	-2(1)
C(19)	30(1)	48(1)	48(1)	13(1)	6(1)	-4(1)
C(20)	38(1)	81(2)	48(1)	3(1)	0(1)	-12(1)
C(21)	39(1)	114(2)	68(2)	19(2)	-9(1)	-25(2)
C(22)	30(1)	112(2)	92(2)	38(2)	9(1)	2(1)
C(23)	40(1)	81(2)	128(3)	14(2)	28(2)	14(1)
C(24)	37(1)	55(1)	97(2)	-1(1)	17(1)	3(1)
C(25)	40(1)	31(1)	42(1)	-3(1)	8(1)	-8(1)
C(26)	45(1)	25(1)	44(1)	-2(1)	9(1)	2(1)
C(27)	35(1)	29(1)	39(1)	-7(1)	7(1)	0(1)
C(28)	27(1)	31(1)	28(1)	3(1)	1(1)	-1(1)
C(29)	35(1)	32(1)	33(1)	-1(1)	2(1)	-2(1)
C(30)	49(1)	39(1)	30(1)	1(1)	-2(1)	-10(1)
C(31)	41(1)	55(1)	37(1)	13(1)	-10(1)	-6(1)
C(32)	42(1)	64(1)	51(1)	0(1)	-9(1)	18(1)
C(33)	40(1)	48(1)	40(1)	-7(1)	-3(1)	12(1)
C(34)	25(1)	35(1)	30(1)	0(1)	-1(1)	3(1)
C(35)	59(1)	50(1)	30(1)	-2(1)	-2(1)	-12(1)
C(36)	76(2)	67(1)	26(1)	-2(1)	3(1)	-15(1)
C(37)	46(1)	70(1)	31(1)	11(1)	3(1)	-9(1)
C(38)	67(2)	67(2)	42(1)	2(1)	8(1)	-32(1)
C(39)	63(1)	56(1)	39(1)	-9(1)	12(1)	-23(1)
B	81(2)	55(2)	40(1)	0(1)	-18(1)	7(1)
F(1)	182(4)	53(2)	112(3)	-20(2)	-73(3)	26(2)
F(2)	70(2)	130(3)	68(2)	37(2)	21(1)	6(2)
F(3)	53(1)	77(2)	45(1)	8(1)	0(1)	-2(1)
F(4)	87(1)	85(1)	83(1)	-14(1)	-43(1)	5(1)
F(1A)	42(3)	104(8)	81(7)	51(5)	0(4)	5(5)

F(2A)	215(13)	90(7)	90(6)	-36(5)	11(7)	-20(7)
F(3A)	202(16)	234(18)	58(6)	23(9)	-12(8)	-186(16)

Table S15. Hydrogen coordinates (x 10^4) and isotropic displacement parameters ($Å^2$x 10^3) for [Cu(dppp)(CN-t-Bu)$_2$](BF$_4$).

	x	y	z	U(eq)
H(6A)	1364	10102	3797	144
H(6B)	1739	9076	4141	144
H(6C)	1705	10354	4435	144
H(4A)	3190(30)	9040(40)	4330(20)	144(17)
H(4B)	3311(19)	10350(30)	4574(15)	82(9)
H(4C)	3870(30)	9840(40)	4077(17)	112(14)
H(5A)	3167(15)	11587(19)	3416(11)	36(6)
H(5B)	2570(20)	11970(30)	3952(16)	93(10)
H(5C)	2340(30)	11630(40)	3230(20)	138(18)
H(10A)	1050(30)	6170(40)	294(19)	75(12)
H(10B)	1510(40)	7560(40)	0(20)	86(16)
H(10C)	460(40)	7160(60)	-170(30)	150(20)
H(11A)	930(30)	9300(40)	440(20)	91(15)
H(11B)	50(50)	8880(70)	290(30)	170(30)
H(11C)	180(30)	9270(40)	1040(20)	93(15)
H(12A)	260(20)	6100(30)	920(17)	44(9)
H(12B)	-230(30)	7480(30)	1390(20)	53(12)
H(12C)	-560(40)	7180(50)	740(30)	123(19)
H(14)	3146(18)	6950(30)	3770(13)	72(8)
H(15)	3540(18)	6630(30)	4794(13)	71(8)
H(16)	3025(18)	5140(30)	5319(14)	76(8)
H(17)	2031(17)	3780(20)	4804(12)	68(8)
H(18)	1649(17)	4090(20)	3804(12)	65(8)

H(20)	583(18)	4370(20)	2351(13)	69(8)
H(21)	-810(20)	4480(30)	2428(14)	82(10)
H(22)	-1532(19)	5940(20)	2997(13)	76(8)
H(23)	-610(20)	7330(30)	3452(15)	80(9)
H(24)	820(30)	7210(30)	3423(17)	104(12)
H(25A)	2027(13)	4340(18)	2079(10)	42(5)
H(25B)	2075(14)	3760(20)	2727(10)	44(5)
H(26A)	3398(13)	3362(19)	2381(9)	39(5)
H(26B)	3535(13)	4379(17)	2831(10)	35(5)
H(27A)	3295(13)	4831(18)	1554(10)	37(5)
H(27B)	4174(13)	4526(17)	1807(9)	31(5)
H(28)	4246(15)	7737(18)	3167(10)	41(5)
H(29)	5407(15)	7810(20)	3909(11)	48(6)
H(30)	6529(15)	6500(20)	3853(10)	51(6)
H(31)	6583(17)	5200(20)	3025(12)	64(7)
H(32)	5448(14)	5120(20)	2301(11)	51(6)
H(35)	4103(16)	5650(20)	789(11)	56(7)
H(36)	4846(18)	6370(20)	-27(13)	73(8)
H(37)	5629(16)	8050(20)	63(11)	55(6)
H(38)	5640(20)	9090(30)	972(14)	86(9)
H(39)	4921(15)	8400(20)	1810(11)	56(7)

Table S16. Crystal data and structure refinement for $[Ag_2(dppp)_2](BF_4)_2$.

Empirical formula	C54 H52 Ag2 B2 F8 P4	
Formula weight	1214.20	
Temperature	173(1) K	
Wavelength	0.71073 Å	
Diffractometer used	Bruker AXS P4/SMART 1000	
Detector distance	5 cm	
Monochrometer used	Graphite	
Crystal size	0.15 x 0.30 x 0.575 mm^3	
Colour and habit	Colourless, parallelepiped	
Crystal system	Triclinic	
Space group	P-1	
Unit cell dimensions	a = 10.6110(6) Å	α = 90.9480(10)°
	b = 11.3248(7) Å	β = 114.1240(10)°
	c = 12.8341(7) Å	γ = 112.6470(10)°
Volume	1271.02(13) $Å^3$	
Z	1	
Density (calculated)	1.586 Mg/m^3	
Absorption coefficient	0.963 mm^{-1}	
F(000)	612	
Theta range for data collection	1.78 to 27.50°	
Completeness to theta = 27.50°	96.7 %	
Scan type	ω and ϕ	
Scan range	0.3°	
Exposure time	25s	
Index ranges	$-12 \leq h \leq 13, -13 \leq k \leq 14, -15 \leq l \leq 16$	

Standard reflections collection	50 frames at beginning and end of data
Crystal stability	no decay
Reflections collected	9111
Independent reflections	5652 [R(int) = 0.0167]
System used	SHELXL 5.1
Solution	Direct methods
Hydrogen atoms	Found, refined isotropically
Absorption correction	SADABS
Min./Max. transmission ratio	0.846
Refinement method	Full-matrix least-squares on F^2
Data / restraints / parameters	5652 / 0 / 449
Goodness-of-fit on F^2	1.069
Final R indices [I>2sigma(I)]	R1 = 0.0258, wR2 = 0.0681
R indices (all data)	R1 = 0.0271, wR2 = 0.0689
Largest/mean shift/esd	0.001/0.000
Largest diff. peak and hole	0.761 and -0.398 e.Å^{-3}

$wR2 = (\Sigma[w(F_o^2-F_c^2)^2]/\Sigma[F_o^4])^{1/2}$

$R1 = \Sigma \, | \, |F_o| - |F_c| \, | \, / \Sigma \, |F_o|$

$Weight = 1 / [\sigma^2(F_o^2) + (0.0427 * P)^2 + (0.4145 * P)]$

where $P = (\max(F_o^2, 0) + 2 * F_c^2)/3$

Figure S4: Numbering scheme for $[Ag_2(dppp)_2](BF_4)$

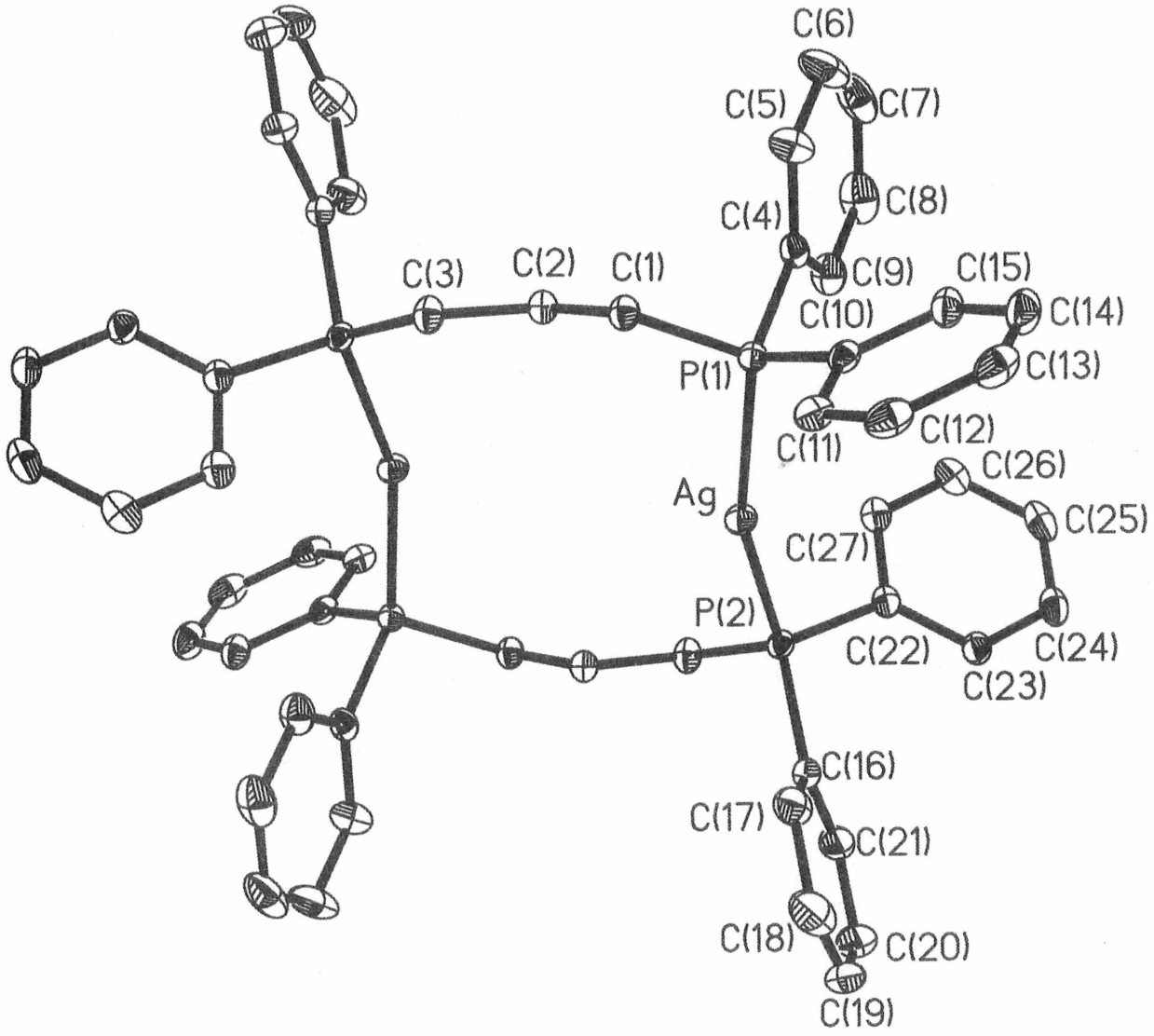

Table S17. Atomic coordinates (x 10^4) and equivalent isotropic displacement parameters ($Å^2$x 10^3) for $[Ag_2(dppp)_2](BF_4)_2$. U(eq) is defined as one third of the trace of the orthogonalized U^{ij} tensor.

	x	y	z	U(eq)
Ag	8988(1)	3859(1)	2993(1)	29(1)
P(1)	6462(1)	2604(1)	2766(1)	23(1)
P(2)	11394(1)	4342(1)	3023(1)	24(1)
C(1)	5911(2)	3437(2)	3609(2)	27(1)
C(2)	7042(2)	3820(2)	4902(1)	27(1)
C(3)	6997(2)	4943(2)	5525(2)	30(1)
C(4)	6205(2)	1069(2)	3220(1)	29(1)
C(5)	4899(3)	304(2)	3317(2)	45(1)
C(6)	4729(3)	-873(2)	3668(2)	61(1)
C(7)	5858(4)	-1282(2)	3922(2)	62(1)
C(8)	7152(4)	-540(3)	3830(2)	57(1)
C(9)	7338(3)	644(2)	3484(2)	40(1)
C(10)	4963(2)	2207(2)	1289(1)	27(1)
C(11)	4584(2)	3189(2)	827(2)	33(1)
C(12)	3466(2)	2922(2)	-308(2)	42(1)
C(13)	2755(2)	1697(3)	-990(2)	46(1)
C(14)	3138(3)	725(2)	-546(2)	45(1)
C(15)	4240(2)	968(2)	595(2)	35(1)
C(16)	11949(2)	5400(2)	2106(2)	33(1)
C(17)	11078(3)	6028(2)	1513(2)	45(1)
C(18)	11552(5)	6866(3)	823(2)	74(1)
C(19)	12845(5)	7043(3)	736(3)	88(1)

C(20)	13711(5)	6432(3)	1331(4)	81(1)
C(21)	13291(3)	5630(2)	2022(3)	53(1)
C(22)	11430(2)	2812(2)	2629(2)	28(1)
C(23)	11475(2)	2463(2)	1611(2)	33(1)
C(24)	11361(2)	1225(2)	1317(2)	40(1)
C(25)	11199(2)	352(2)	2027(2)	43(1)
C(26)	11170(2)	695(2)	3050(2)	41(1)
C(27)	11282(2)	1918(2)	3348(2)	35(1)
B	8816(3)	6725(2)	3529(2)	45(1)
F(1)	9458(2)	6141(1)	4419(1)	52(1)
F(2)	7394(3)	6602(3)	3468(3)	86(1)
F(3)	8358(5)	5959(4)	2520(3)	92(2)
F(4)	9629(4)	7952(3)	3642(4)	122(2)
F(2A)	10246(13)	7457(9)	3314(9)	97(3)
F(3A)	8730(20)	7601(13)	3977(9)	116(5)
F(4A)	7922(13)	5898(8)	2562(10)	124(7)

Table S18. Bond lengths [Å] and angles [°] for $[Ag_2(dppp)_2](BF_4)_2$.

Ag-P(2)	2.3797(4)	Ag-P(1)	2.3890(4)
P(1)-C(4)	1.7986(17)	P(1)-C(10)	1.8114(17)
P(1)-C(1)	1.8195(17)	P(2)-C(16)	1.7993(19)
P(2)-C(22)	1.8153(17)	P(2)-C(3)#1	1.8239(18)
C(1)-C(2)	1.526(2)	C(2)-C(3)	1.518(2)
C(3)-P(2)#1	1.8239(17)	C(4)-C(5)	1.381(3)
C(4)-C(9)	1.381(3)	C(5)-C(6)	1.383(3)
C(6)-C(7)	1.367(5)	C(7)-C(8)	1.361(5)
C(8)-C(9)	1.386(3)	C(10)-C(15)	1.386(3)
C(10)-C(11)	1.387(3)	C(11)-C(12)	1.385(3)
C(12)-C(13)	1.369(3)	C(13)-C(14)	1.370(4)
C(14)-C(15)	1.388(3)	C(16)-C(17)	1.374(3)
C(16)-C(21)	1.396(3)	C(17)-C(18)	1.402(4)
C(18)-C(19)	1.360(6)	C(19)-C(20)	1.356(6)
C(20)-C(21)	1.359(4)	C(22)-C(23)	1.384(2)
C(22)-C(27)	1.388(3)	C(23)-C(24)	1.391(3)
C(24)-C(25)	1.366(3)	C(25)-C(26)	1.379(3)
C(26)-C(27)	1.377(3)	B-F(3A)	1.193(7)
B-F(4A)	1.278(11)	B-F(4)	1.290(3)
B-F(3)	1.337(4)	B-F(1)	1.394(3)
B-F(2)	1.430(4)	B-F(2A)	1.564(9)
F(2)-F(3A)	1.302(17)	F(2)-F(4A)	1.775(18)
F(4)-F(3A)	1.145(12)	F(4)-F(2A)	1.192(9)
P(2)-Ag-P(1)	159.409(16)	C(4)-P(1)-C(10)	105.77(8)
C(4)-P(1)-C(1)	105.26(8)	C(10)-P(1)-C(1)	103.71(8)
C(4)-P(1)-Ag	113.30(6)	C(10)-P(1)-Ag	114.65(5)

C(1)-P(1)-Ag	113.18(6)	C(16)-P(2)-C(22)	107.24(8)
C(16)-P(2)-C(3)#1	104.79(9)	C(22)-P(2)-C(3)#1	103.44(8)
C(16)-P(2)-Ag	118.43(7)	C(22)-P(2)-Ag	108.31(5)
C(3)#1-P(2)-Ag	113.48(6)	C(2)-C(1)-P(1)	111.02(11)
C(3)-C(2)-C(1)	111.28(14)	C(2)-C(3)-P(2)#1	112.18(12)
C(5)-C(4)-C(9)	119.08(19)	C(5)-C(4)-P(1)	121.36(15)
C(9)-C(4)-P(1)	119.56(15)	C(4)-C(5)-C(6)	120.3(2)
C(7)-C(6)-C(5)	119.9(3)	C(8)-C(7)-C(6)	120.5(2)
C(7)-C(8)-C(9)	120.1(2)	C(4)-C(9)-C(8)	120.1(2)
C(15)-C(10)-C(11)	119.31(17)	C(15)-C(10)-P(1)	121.83(14)
C(11)-C(10)-P(1)	118.79(14)	C(12)-C(11)-C(10)	120.1(2)
C(13)-C(12)-C(11)	120.3(2)	C(12)-C(13)-C(14)	120.03(19)
C(13)-C(14)-C(15)	120.5(2)	C(10)-C(15)-C(14)	119.7(2)
C(17)-C(16)-C(21)	119.4(2)	C(17)-C(16)-P(2)	119.99(16)
C(21)-C(16)-P(2)	120.61(18)	C(16)-C(17)-C(18)	118.8(3)
C(19)-C(18)-C(17)	120.3(3)	C(20)-C(19)-C(18)	120.7(3)
C(19)-C(20)-C(21)	120.2(3)	C(20)-C(21)-C(16)	120.6(3)
C(23)-C(22)-C(27)	119.11(17)	C(23)-C(22)-P(2)	123.19(14)
C(27)-C(22)-P(2)	117.50(13)	C(22)-C(23)-C(24)	119.92(19)
C(25)-C(24)-C(23)	120.26(19)	C(24)-C(25)-C(26)	120.32(19)
C(27)-C(26)-C(25)	119.8(2)	C(26)-C(27)-C(22)	120.64(19)
F(3A)-B-F(4A)	132.1(10)	F(3A)-B-F(4)	54.8(7)
F(4A)-B-F(4)	125.5(5)	F(3A)-B-F(3)	145.3(6)
F(4A)-B-F(3)	20.4(8)	F(4)-B-F(3)	115.7(4)
F(3A)-B-F(1)	106.6(4)	F(4A)-B-F(1)	111.3(5)
F(4)-B-F(1)	115.7(2)	F(3)-B-F(1)	106.9(2)
F(3A)-B-F(2)	58.7(8)	F(4A)-B-F(2)	81.7(8)
F(4)-B-F(2)	106.9(3)	F(3)-B-F(2)	101.9(3)
F(1)-B-F(2)	108.9(2)	F(3A)-B-F(2A)	102.4(8)

F(4A)-B-F(2A)	100.0(8)	F(4)-B-F(2A)	48.2(4)
F(3)-B-F(2A)	81.1(5)	F(1)-B-F(2A)	98.2(4)
F(2)-B-F(2A)	150.3(4)	F(3A)-F(2)-B	51.5(3)
F(3A)-F(2)-F(4A)	93.2(4)	B-F(2)-F(4A)	45.4(3)
F(3A)-F(4)-F(2A)	135.4(6)	F(3A)-F(4)-B	58.3(5)
F(2A)-F(4)-B	78.0(5)	F(4)-F(2A)-B	53.8(4)
F(4)-F(3A)-B	66.9(5)	F(4)-F(3A)-F(2)	126.5(8)
B-F(3A)-F(2)	69.8(7)	B-F(4A)-F(2)	52.9(6)

Symmetry transformations used to generate equivalent atoms:

#1 -x+2,-y+1,-z+1

Table S19. Anisotropic displacement parameters ($Å^2 x\ 10^3$) for $[Ag_2(dppp)_2](BF_4)_2$. The anisotropic displacement factor exponent takes the form: $-2p^2[\ h^2\ a^{*2}U^{11} + ... + 2\ h\ k\ a^*\ b^*\ U^{12}\ ]$

	U^{11}	U^{22}	U^{33}	U^{23}	U^{13}	U^{12}
Ag	21(1)	33(1)	32(1)	5(1)	14(1)	11(1)
P(1)	20(1)	25(1)	23(1)	3(1)	9(1)	9(1)
P(2)	21(1)	28(1)	24(1)	2(1)	12(1)	10(1)
C(1)	24(1)	30(1)	27(1)	1(1)	10(1)	13(1)
C(2)	28(1)	28(1)	25(1)	3(1)	10(1)	13(1)
C(3)	25(1)	35(1)	27(1)	-1(1)	8(1)	15(1)
C(4)	31(1)	26(1)	24(1)	3(1)	9(1)	11(1)
C(5)	38(1)	37(1)	52(1)	16(1)	18(1)	11(1)
C(6)	58(2)	37(1)	59(2)	19(1)	18(1)	1(1)
C(7)	85(2)	29(1)	45(1)	10(1)	10(1)	19(1)
C(8)	77(2)	47(1)	51(1)	13(1)	17(1)	43(1)
C(9)	47(1)	40(1)	39(1)	8(1)	16(1)	26(1)
C(10)	22(1)	36(1)	23(1)	4(1)	11(1)	11(1)
C(11)	30(1)	40(1)	31(1)	11(1)	15(1)	14(1)
C(12)	34(1)	59(1)	33(1)	20(1)	16(1)	21(1)
C(13)	30(1)	71(2)	24(1)	9(1)	9(1)	15(1)
C(14)	38(1)	55(1)	28(1)	-6(1)	11(1)	11(1)
C(15)	32(1)	40(1)	29(1)	-1(1)	12(1)	14(1)
C(16)	38(1)	28(1)	30(1)	0(1)	19(1)	6(1)
C(17)	46(1)	39(1)	33(1)	7(1)	9(1)	9(1)
C(18)	97(2)	43(1)	38(1)	10(1)	8(2)	10(2)
C(19)	124(3)	50(2)	58(2)	0(1)	63(2)	-16(2)

C(20)	110(3)	49(2)	98(2)	4(2)	87(2)	3(2)
C(21)	55(1)	39(1)	71(2)	-1(1)	47(1)	5(1)
C(22)	20(1)	29(1)	31(1)	0(1)	10(1)	10(1)
C(23)	27(1)	34(1)	35(1)	-2(1)	16(1)	9(1)
C(24)	29(1)	39(1)	45(1)	-12(1)	16(1)	9(1)
C(25)	30(1)	31(1)	55(1)	-8(1)	11(1)	12(1)
C(26)	36(1)	32(1)	45(1)	5(1)	10(1)	15(1)
C(27)	34(1)	35(1)	33(1)	3(1)	13(1)	15(1)
B	65(2)	33(1)	42(1)	17(1)	23(1)	26(1)
F(1)	54(1)	50(1)	49(1)	24(1)	18(1)	25(1)
F(2)	81(2)	90(2)	136(3)	69(2)	66(2)	65(2)
F(3)	164(4)	115(3)	47(2)	26(2)	42(2)	115(3)
F(4)	82(2)	44(1)	142(3)	51(2)	-5(2)	-8(1)
F(2A)	157(9)	84(6)	138(8)	81(6)	123(8)	72(6)
F(3A)	265(15)	127(8)	108(7)	83(7)	133(9)	176(11)
F(4A)	84(6)	40(4)	82(7)	34(4)	-48(5)	-43(5)

Table S20. Hydrogen coordinates (x 10^4) and isotropic displacement parameters ($Å^2$x 10^3) for $[Ag_2(dppp)_2](BF_4)_2$.

	x	y	z	U(eq)
H(1A)	4880(20)	2840(20)	3499(18)	25(5)
H(2A)	6830(30)	3080(20)	5280(20)	36(6)
H(3A)	6060(30)	4650(20)	5610(19)	33(5)
H(1B)	5920(30)	4160(20)	3292(19)	33(5)
H(2B)	8040(30)	4070(20)	4998(18)	29(5)
H(3B)	7090(30)	5640(20)	5130(20)	34(6)
H(5)	4200(30)	600(30)	3200(20)	57(8)
H(6)	3890(40)	-1280(30)	3770(30)	70(9)
H(7)	5720(40)	-2080(40)	4150(30)	94(12)
H(8)	7830(40)	-810(30)	3960(30)	72(10)
H(9)	8260(30)	1190(30)	3490(20)	47(7)
H(11)	5060(30)	4000(20)	1260(20)	38(6)
H(12)	3200(30)	3530(30)	-590(20)	50(7)
H(13)	2120(30)	1590(30)	-1720(20)	53(7)
H(14)	2730(30)	-110(30)	-980(20)	52(7)
H(15)	4510(30)	320(30)	930(20)	46(7)
H(17)	10350(30)	5930(20)	1623(18)	24(5)
H(18)	10970(40)	7180(40)	540(30)	75(11)
H(19)	13120(50)	7510(40)	330(40)	111(14)
H(20)	14640(50)	6640(40)	1280(30)	98(12)
H(21)	13810(50)	5110(40)	2370(40)	106(14)
H(23)	11600(30)	3070(20)	1130(20)	33(5)
H(24)	11310(30)	1000(20)	550(20)	39(6)
H(25)	11140(30)	-470(30)	1840(20)	55(7)

H(26)	11060(30)	120(30)	3550(20)	54(7)
H(27)	11200(30)	2100(20)	4000(20)	41(6)

Table S21. TGA data for the $[M(diphos)(CN\text{-}t\text{-}Bu)_2](BF_4)$, $\{[M(diphos)(dmb)](BF_4)\}_n$, $[Pd_2(diphos)_2(CN\text{-}t\text{-}Bu)_2](ClO_4)_2$ and $\{[Pd_2(diphos)_2(dmb)](ClO_4)_2\}_n$ compounds (M = Cu, Ag; diphos = dppe, dppp).[a,b]

Compounds	Weight loss 1			Weight Loss 2			Residue	
	Temp. Range(°C)	Exp. %	Theor. %	Temp. Range(°C)	Exp. %	Theor. %	Exp. %	Theor. %
$[Cu(dppe)(CN\text{-}t\text{-}Bu)_2](BF_4)$	160-224	22	23	300-427	66	68	12	9
$[Ag(dppe)(CN\text{-}t\text{-}Bu)_2](BF_4)$	138-209	23	23	298-406	63	63	14	14
$[Cu(dppp)(CN\text{-}t\text{-}Bu)_2](BF_4)$	169-272	19	22	309-407	74	68	7	9
$\{[Cu(dppe)(dmb)](BF_4)\}_n$	178-334	36	37	334-427	52	54	12	9
$\{[Ag(dppe)(dmb)](BF_4)\}_n$	144-200	21	24	277-369	65	62	14	14
$\{[Cu(dppp)(dmb)](BF_4)\}_n$	209-268	35	37	312-442	54	55	11	8
$\{[Ag(dppp)(dmb)](BF_4)\}_n$	168-226	27	24	296-402	60	63	13	13
$[Pd_2(dppe)_2(CN\text{-}t\text{-}Bu)_2](ClO_4)_2$	120-198	14	12	198-280	69	72	17	15
$[Pd_2(dppp)_2(CN\text{-}t\text{-}Bu)_2](ClO_4)_2$	128-197	14	12	197-269	69	73	17	15
$\{[Pd_2(dppp)_2(dmb)](ClO_4)_2\}_n$	160-216	14	13	288-450	70	72	16	15

[a] The uncertainty is estimated to be ± 3 % because of a small drift in the baseline. [b] All investigated materials exhibit two well defined thermal events corresponding to the losses of the isocyanide (lower temperature) and the diphosphine ligands (higher temperature). The weight loss of the counter ion is not well defined in the TGA traces. In most cases, the weight loss 2 includes both the diphosphine and the counter-anion for both the experimental and theoretical values, except for two cases $\{[Cu(dppe)(dmb)]\text{-}(BF_4)\}_n$ and $\{[Cu(dppp)(dmb)](BF_4)\}_n$ (see Figure 4 as an example), for which the loss of the counter-ion is observed at a lower temperature. So, the calculated and experimental weight losses 1 include both the isocyanide and counter ion for these two materials.

Figure S5. Computer modeling of a fictive dimer $Pd_2(dppe)_2(dmb)^{2+}$.

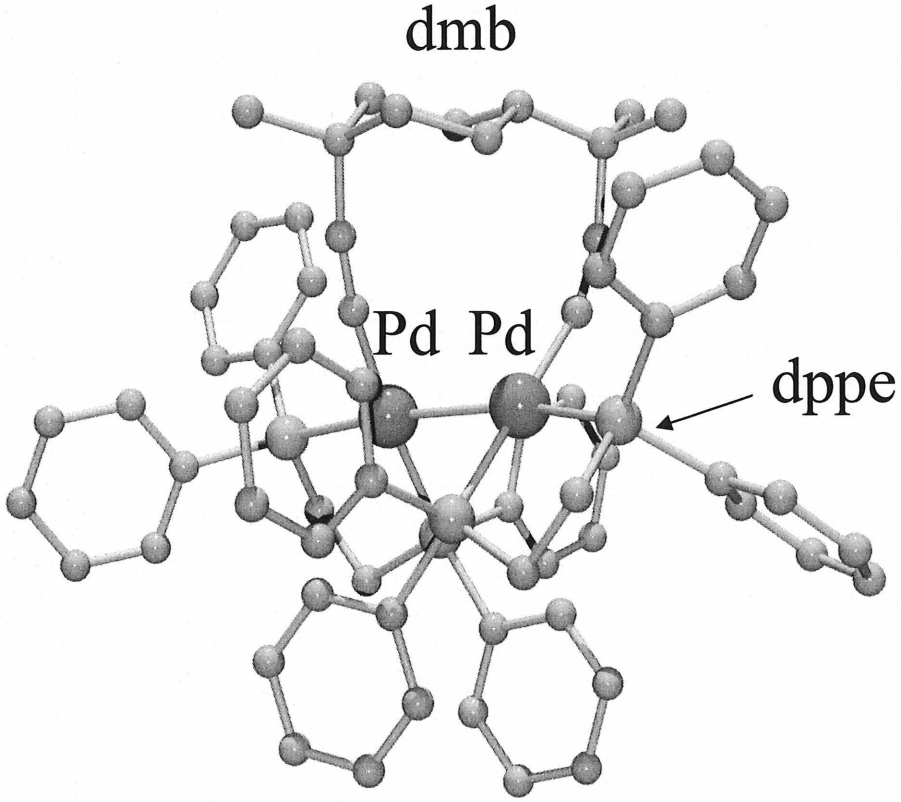

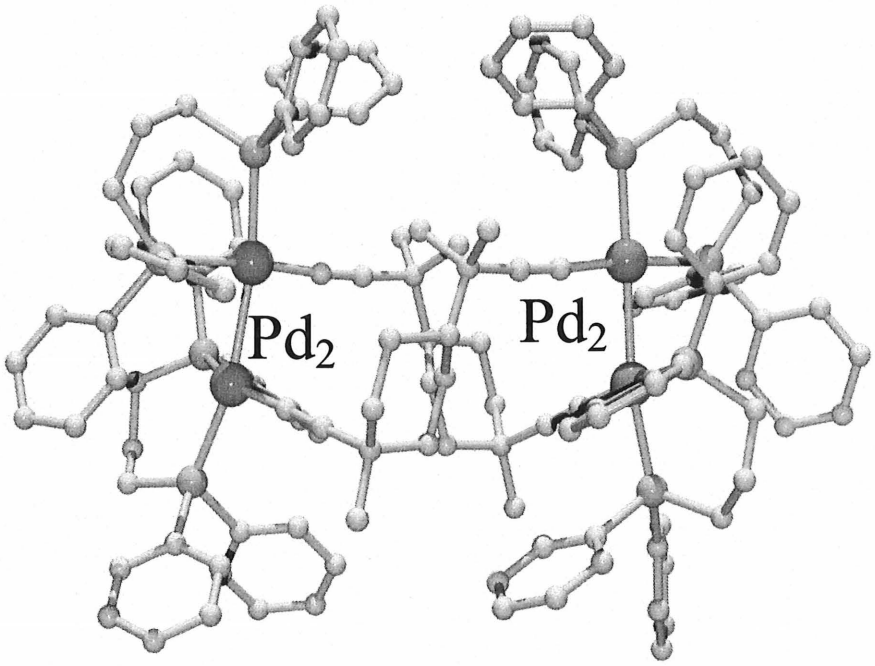

Z-dmb dppp

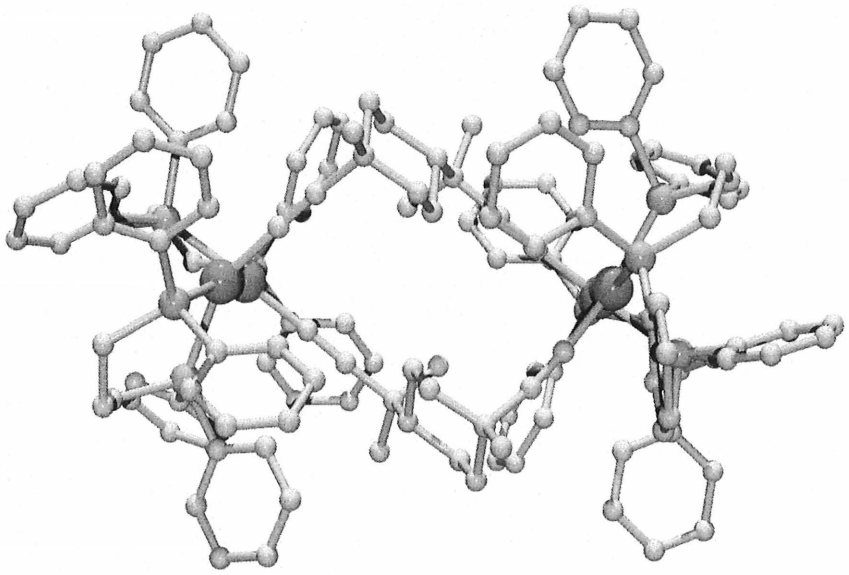

Figure S7. Space filling model for the fictive $[Pd_2(diphos)_2(dmb)]_2^{4+}$ complex showing the steric environment of the dmb ligand.

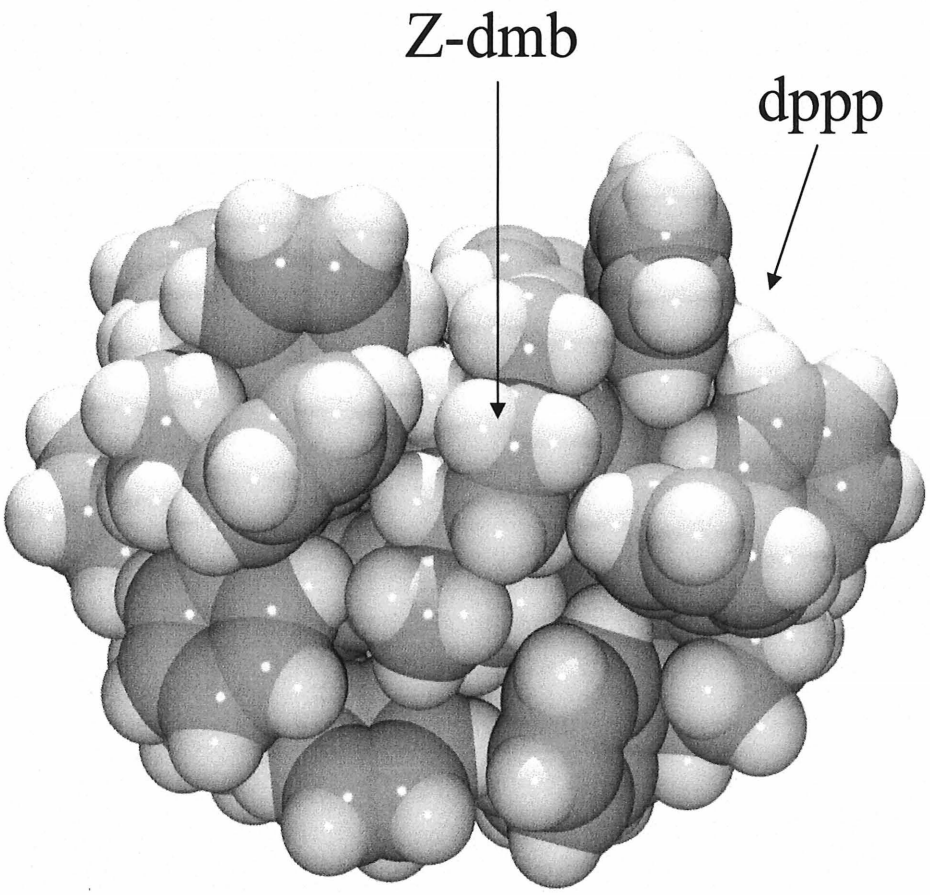

Figure S8. Computer model for the fictive $Cu_2(dppp)_2(dmb)_2^{2+}$ complex.

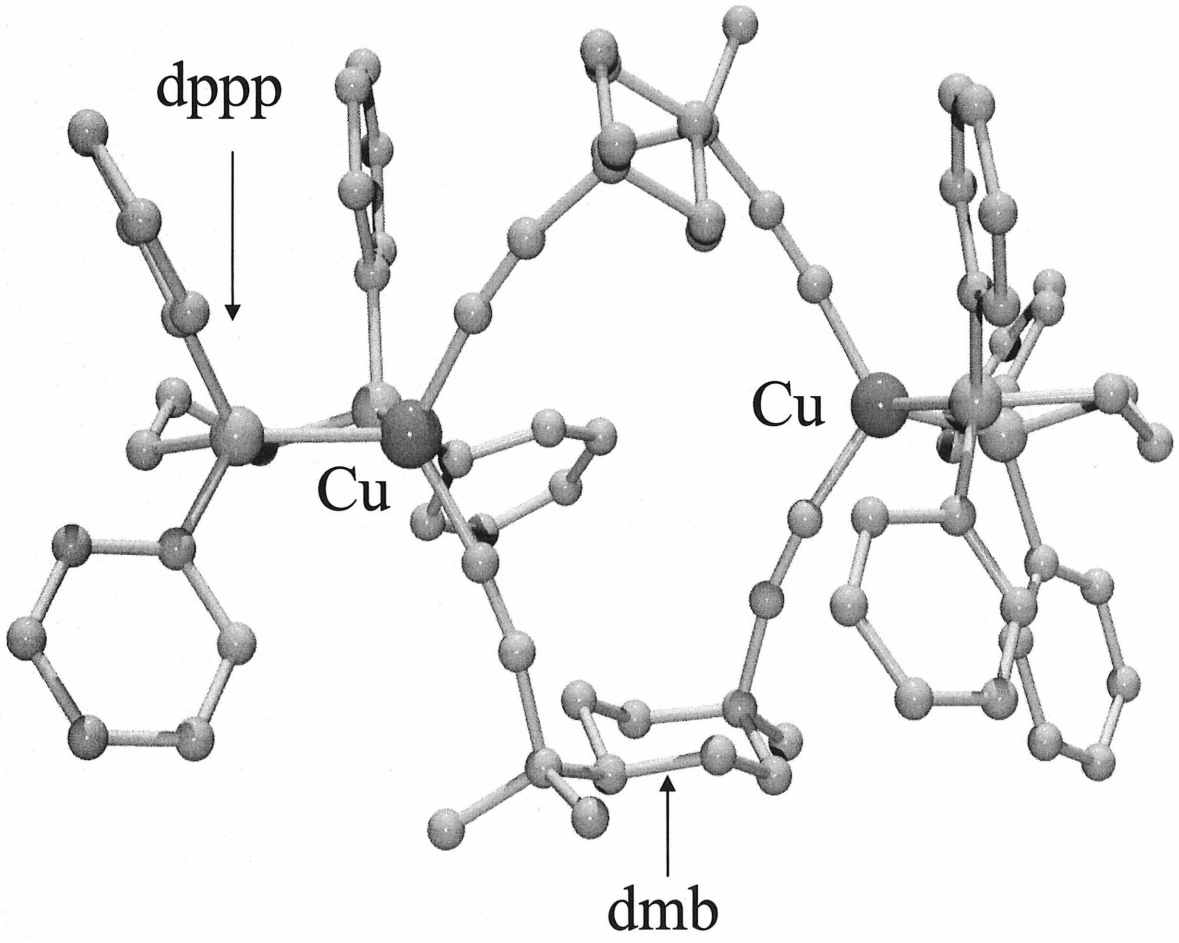

CHAPITRE 4

DISCUSSION GÉNÉRALE

Ce chapitre comporte trois sections qui respectent l'ordre des trois chapitres précédents. Chaque section résume les résultats rapportés dans l'article correspondant et met en évidence les points importants.

4.1. Ligand dmpm

Les complexes binucléaires $M_2(dmpm)_3^{2+}$ (M = Cu, Ag) et $Ag_2(dmpm)_2^{2+}$ sont synthétisés par réaction directe entre le dmpm et le métal cationique.

$$2\ [Cu(NCMe)_4]BF_4 + 3\ dmpm \rightarrow [Cu_2(dmpm)_3](BF_4)_2 \qquad [4.1]$$

$$2\ AgBF_4 + 3\ dmpm \rightarrow [Ag_2(dmpm)_3](BF_4)_2 \qquad [4.2]$$

$$2\ AgBF_4 + 2\ dmpm \rightarrow [Ag_2(dmpm)_2)](BF_4)_2 \qquad [4.3]$$

Les structures cristallographiques de $[Cu_2(dmpm)_3](BF_4)_2$ et $[Ag_2(dmpm)_3](BF_4)_2$ nous montrent que les métaux sont placés face-à-face, adoptent une géométrie triangle plan et sont séparés par 2,9265(3) et 2,9893(2)Å dans les complexes de cuivre et d'argent, respectivement. Ces distances sont plus courtes lorsqu'on les compare à l'analogue isostructural $[Au_2(dmpm)_3]^{2+}$ (3,040 et 3,050 Å) (49) mais elles suivent la tendance de leur rayon atomique respectif (Cu(I), 0,91Å ; Ag(I), 1,29Å ; Au(I), 1,51Å) (50). La distance inter-métallique du complexe Cu_2 est plus grande que la somme des rayons de

van der Waals alors que celle des complexes d'Ag_2 et d'Au_2 sont plus petites. La moyenne des angles PCuCu (91,7°) suggère la présence d'une faible interaction métal-métal. La distance d(Ag_2) du $[Ag_2(dmpm)_2)](PF_6)_2$ (3,041(1)Å) (51) est plus longue que celle trouvée dans $[Ag_2(dmpm)_3](BF_4)_2$ ce qui indique que le troisième ligand dmpm applique une force supplémentaire, rapprochant les métaux.

Le composé modèle $Cu_2(dmpm)_3(CN\text{-}t\text{-}Bu)_2^{2+}$ est préparé par la réaction directe entre $[Cu_2(dmpm)_3](BF_4)_2$ et deux équivalents de *t*-BuNC.

$$Cu_2(dmpm)_3^{2+} + 2\ t\text{-BuNC} \rightarrow Cu_2(dmpm)_3(CN\text{-}t\text{-}Bu)_2^{2+} \qquad [4.4]$$

L'identité de ce composé est déduite des spectres RMN ^1H et ^{31}P. La structure cristallographique de ce composé à été résolue partiellement et les résultats préliminaires sont disponibles en annexe de cet ouvrage. Le désordre qui fait en sorte que la structure n'est pas publiable provient des *t*-BuNC. Pour ce qui est des composés modèles d'argent, le $Ag_2(dmpm)_2(CN\text{-}t\text{-}Bu)_2^{2+}$ ne fût pas synthétisé car un analogue $Ag_2(dppm)_2(CN\text{-}t\text{-}Bu)_2^{2+}$ était déjà connu (52). Le dimère $Ag_2(dmpm)_3(CN\text{-}t\text{-}Bu)_2^{2+}$ n'a pu être obtenu ce qui est probablement dû à la labilité du *t*-BuCN sur l'argent. La synthèse des oligomères a été réalisée de la même façon que pour les composés modèles en ajoutant un équivalent de dmb au lieu de deux équivalents de *t*-BuNC. Le nombre d'unités dimériques dans les complexes $[Cu_6(dmpm)_9(dmb)_4](BF_4)_6$ ou $\{[Cu_2(dmpm)_3(dmb)_{1.33}](BF_4)_2\}_2$ a été déterminé en se basant sur l'analyse élémentaire et la RMN ^1H (intégration de dmpm vs dmb). De plus, l'ATG et l'approximation de l'intensité des bandes infra-rouge des (C≡N) libre versus (C≡N) liés corrobore cette estimé. Le complexe oligomérique d'argent donne les mêmes résultats avec cette batterie d'analyses et peut être nommé $[Ag_6(dmpm)_6(dmb)_4](BF_4)_6$ ou $\{[Ag_2(dmpm)_2(dmb)_{1.33}](BF_4)_2\}_3$. Il est important de remarquer que ces oligomères ont 6 atomes métalliques et sont plus petits que les polymères $\{[Ag(dmb)_2]BF_4\}_n$ en solution (n = 7-8). Cette dernière valeur a été déterminée par la technique RMN T_1/NOE (28).

Les deux oligomères ne montrent pas de transitions vitreuses, ce qui est en accord avec leur caractère cristallin. Les spectres d'absorption des composés $[Cu_2(dmpm)_3](BF_4)_2$ et $[Ag_2(dmpm)_3](BF_4)_2$ montrent une bande aux alentours de 250 nm. Ces bandes non-résolues proviennent d'une transition $d\sigma^* \rightarrow p\sigma$. Pour prouver cette affirmation, le spectre d'absorption a été mesuré à 77K dans un tube de quartz en utilisant le butyronitrile comme solvant. À cette température, la largeur de la bande d'absorption diminue et ce phénomène est bien documenté (53-60). Pour ce qui est des spectres d'absorption du $Cu_2(dmpm)_3(CN\text{-}t\text{-}Bu)_2^{2+}$ et $\{[Cu_2(dmpm)_3(dmb)_{1.33}](BF_4)_2\}_3$, ils sont quasi identiques entre eux mais diffèrent du dimère $[Cu_2(dmpm)_3](BF_4)_2$ correspondant par la bande de transition $d\sigma^* \rightarrow p\sigma$ qui ne peut être observée pour ces complexes. En effet, lorsque le métal passe de l'hybridation sp^2 à sp^3, il ne reste plus d'orbitale "p" vide pour y promouvoir l'électron. Il est bien de noter que cette bande d'absorption ($d\sigma^* \rightarrow p\sigma$) est toujours observable pour $\{[Ag_2(dmpm)_2(dmb)_{1.33}](BF_4)_2\}_3$.

Tous ces composés sont luminescents en solution, à 298 et 77K ainsi qu'à l'état solide. Cette émission est due à une phosphorescence et la durée de vie est en accord avec cette affirmation. Les données de τ_e montrent deux tendances. La première est que le τ_e augmente avec la rigidité du médium et diminue lorsqu'on augmente la température. Deuxièmement, le τ_e et le Φ_e diminuent quand la grosseur de la molécule augmente. Pour ce qui est du processus excitonique, si l'on accepte que le transfert d'énergie (K_{ET}) varie comme suit : $K_{ET} \propto 1/r^6$ (r = distance interchromophore) pour un mécanisme de Föster (32), on peut dire que la contribution du processus intermoléculaire est négligeable. Les composés oligomériques ont des spectres d'émission dépendant du temps. En effet, peu de temps après le pulse de lumière, la bande d'émission ressemble beaucoup à celle du monomère métallique et en fonction du temps elle se déplace vers le rouge. Ce déplacement est essentiellement dû à la délocalisation de l'exciton qui ne peut être observé avec un monomère. Ce phénomène est observable même pour des petites molécules comme les dimères et les oligomères et plafonne rapidement.

4.2. Les "diphos" pontantes

Les "diphos" pontantes sont la bis(diphénylphosphino)méthane (dppm), la 1,4-bis(diphénylphosphino)butane (dppb), la 1,5-bis(diphénylphosphino) pentane (dpppen) et la 1,6-bis(diphénylphosphino)hexane (dpph). Combinée avec le *t*-BuNC et le dmb en utiliseant le cuivre(I) ou l'argent(I) comme métaux, cette famille de polymères montrent des propriétés intéressantes. Ces nouveaux polymères sont obtenus à partir de $[M_2(diphos)_2](BF_4)_2$ (M = Cu(I), Ag(I)) et du *t*-BuNC ou du dmb. Premièrement, les dimères $Ag_2(dppm)_2^{2+}$ et $Cu_2(dppm)_2(NCMe)_4^{2+}$ réagissent avec deux équivalents de dmb pour former les polymères de type $\{[M_2(dppm)_2(dmb)_2](BF_4)_2\}_n$. Cette réaction étant déjà connue dans le laboratoire du Pr Harvey (52), elle ne sera pas discutée ici.

Pour ce qui est des autres diphos (dppb, dpppen et dpph), le *t*-BuNC a été utilisé pour imiter l'encombrement stérique du dmb autour du métal et pour augmenter la probabilité d'obtenir des monocristaux pour ces composés modèles aptes à l'analyse cristallographique. En effet, la structure du polymère $\{[Ag(dpppen)(CN\text{-}t\text{-}Bu)_2]BF_4\}_n$ a été obtenue (Figure 2, Chapitre 2). La particularité de cette structure réside dans l'obtention d'un polymère à base de *t*-BuNC au lieu d'un dimère doublement ponté comme espéré. Même si le *t*-BuNC imite stériquement le dmb, celui-ci n'est pas reconnu comme un ligand chélatant et la modélisation indique que le dmb pontera une autre chaîne polymérique. Cette réticulation de la matrice provoque et explique certains phénomènes macroscopiques observés (précipitation de la matrice polymérique, gonflement de la poudre). De plus, deux de ces polymères ont des températures de transition vitreuse observables en DSC. La formation de films a aussi été pratiquée dans le but de démontrer la présence de polymères (Figure 13).

Les propriétés de luminescence à l'état solide ont été étudiées à 293K. Les résultats montrent des bandes d'émissions et des τ_e similaires entre eux, ce qui indique que la

nature de l'espèce excitée est la même pour tous les polymères. Le chromophore serait le $MP_2(CNR)_2$ pour tous les produits et l'état excité responsable de la luminescence serait du type "transfert-de-charge-métal-ligand" (MLCT).

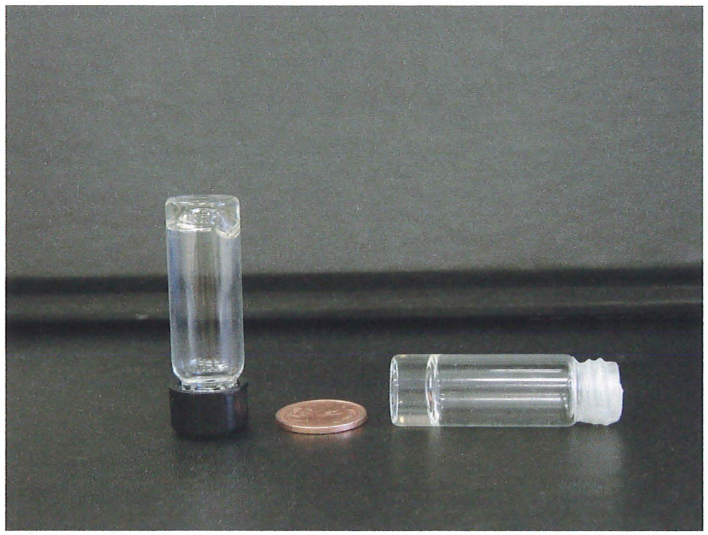

Figure 13 : Évidence d'un polymère ; à gauche : essai de solubilité, à droite : essai de cristaux.

4.2. Les "diphos" chélates

Le ligand dppe (61-63) et la dppp (64-66) peuvent agir comme chélates ou pontants sur le Cu(I) et l'Ag(I). Étant donné qu'aucune structure cristallographique n'a été obtenue pour les quatre polymères correspondants, l'utilisation d'un ligand qui imite l'encombrement stérique du dmb fût nécessaire ; il s'agit du *t*-BuNC. Avec cette méthode, nous avons obtenu des cristaux analysables par rayons-X pour trois des composés modèles et les structures démontrent clairement que ces "diphos" sont préférentiellement chélates dans l'environnement étudié. Ces cycles à 5 et 6 unités sont naturellement favorisés. La différence entre le ligand chélate et pontant est visible par le déplacement chimique en ^1H RMN des deux protons en α du phosphore présent sur la "diphos". En comparant le

déplacement de ces protons pour les polymères et les composés modèles, nous avons déduit que les polymères ont aussi un environnement chélate.

En se basant sur les résultats obtenus en DRX de poudre de ces polymères nous pouvons affirmer qu'ils sont tous très amorphes. En utilisant des méthodes comme le "spin-coating" ou l'évaporation lente, ces polymères forment des films homogènes. Il est bien de remarquer que les polymères d'argent sont beaucoup plus friables que les analogues de cuivre. Une transition vitreuse a été observée pour le polymère $\{[Cu(dppe)(dmb)]BF_4\}_n$ $T_g = 81.5^oC$ ($\Delta C_p = 0.43$ J/g^o). Par mesure de leurviscosité intrinsèque, il a été démontré que les polymères gardaient une nature oligomérique en solution (8-9 unités).

CONCLUSION

La série de composés synthétisés et caractérisés a permis d'augmenter et de diversifier la famille des polymères organométalliques de Cu(I) et d'Ag(I). La réactivité des diphosphines et le comportement des métaux ont été un peu plus étudiés. Les multiples structures cristallographiques et une caractérisation exhaustive contenues dans ce mémoire aideront les futurs étudiants dans leurs projets dans le domaine des polymères organométalliques. Dans le cadre de cet ouvrage la série de co-polymères diphénylphosphine/dmb a été étudiée ainsi que les oligomères diméthylphosphine/dmb.

Pour ce qui est des polymères construits à partir de diphénylphosphine, les polymères d'Ag(I) sont de plus petites dimensions en solution, plus cristallins et certainement plus propices à l'obtention de monocristaux dans le but de résoudre leur structure cristallogarphique. Cette propriété est essentiellement due à la labilité des ligands sur l'Ag(I). Pour ce qui est des polymères de Cu(I), le caractère amorphe de ces polymères a été prouvé. L'obtention de monocristaux dans ces cas devient une tâche impossible. Toutefois les propriétés de ces polymères sont très intéressantes. L'observation de patron de diffraction des rayons-X halo-diffus, la mesure de température de transition vitreuse et surtout la formation de films polymériques (Figure 13 chapitre 4) sont en accord avec la présence d'un polymère.

La labilité des ligands en solution et les réarrangements résultants de cette propriété peuvent causer certains problèmes de caractérisation et peuvent aussi montrer des résultats inattendus au niveau structural de ces polymères. Tous les résultats émergeant de ces réarrangements feront l'objet d'une autre publication qui n'est pas mentionnée dans cet ouvrage. Les résultats sont encourageants et seront présentés brièvement : deux produits, $\{[Ag_2(dppb)_3(t\text{-BuNC})_2]BF_4\}_n$ et $\{[Ag(dpppen)(t\text{-BuNC})]\ BF_4\}_n$ ont donné des cristaux uniques très intéressants. Ces cristaux proviennent d'un réarrangement survenu

sur une période de plus de huit mois en solution (essai de cristaux). Les images qui représentent les deux structures qui ont été résolues sont en annexe de cet ouvrage. L'étude photophysique de ces cristaux devrait certainement faire l'objet d'une attention particulière dans le futur.

Par ailleurs, il a été démontré que tous ces polymères sont luminescents sous leur forme solide à 293K. Les films de ses polymères ont le même comportement photophysique que sous la forme de poudre (forme étudiée).

Pour ce qui est des complexes à base de ligands dmpm/dmb, nous avons réussi à démontrer qu'en changeant la nature des unités de base, on peut contrôler la grandeur de l'oligomère, ce qui n'avait jamais été tenté. Cette méthode permet de changer (et éventuellement, contrôler) les propriétés photophysiques de ces matériaux. De plus, l'étude portant sur la quantification du phénomène de l'exciton intra-chaîne nous a permis de découvrir que ce processus est détectable même pour des chaînes courtes. En fonction du nombre d'unités chromophoriques, le phénomène s'intensifie et l'ampleur du processus atteint son maximum très rapidement. La compréhension de l'assemblage et les propriétés fondamentales de ces matériaux ont un lien direct avec le contrôle des matériaux conducteurs.

ANNEXE

Polymère 2-D : $\{[Ag_2(dppb)_3(t\text{-}BuNC)_2]BF_4\}_n$

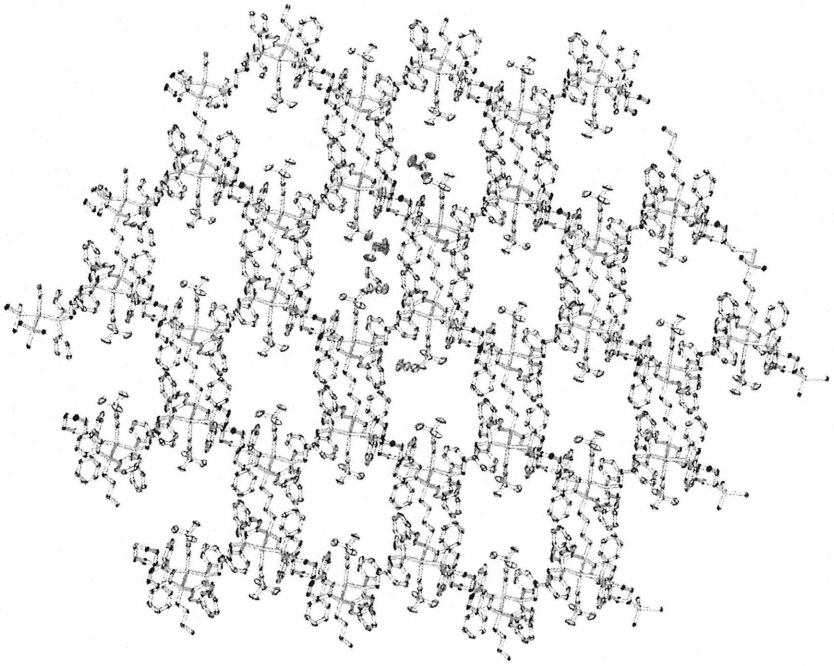

Représentation de la structure de : $\{[Ag(dpppen)(t\text{-BuNC})]\ BF_4\}_n$

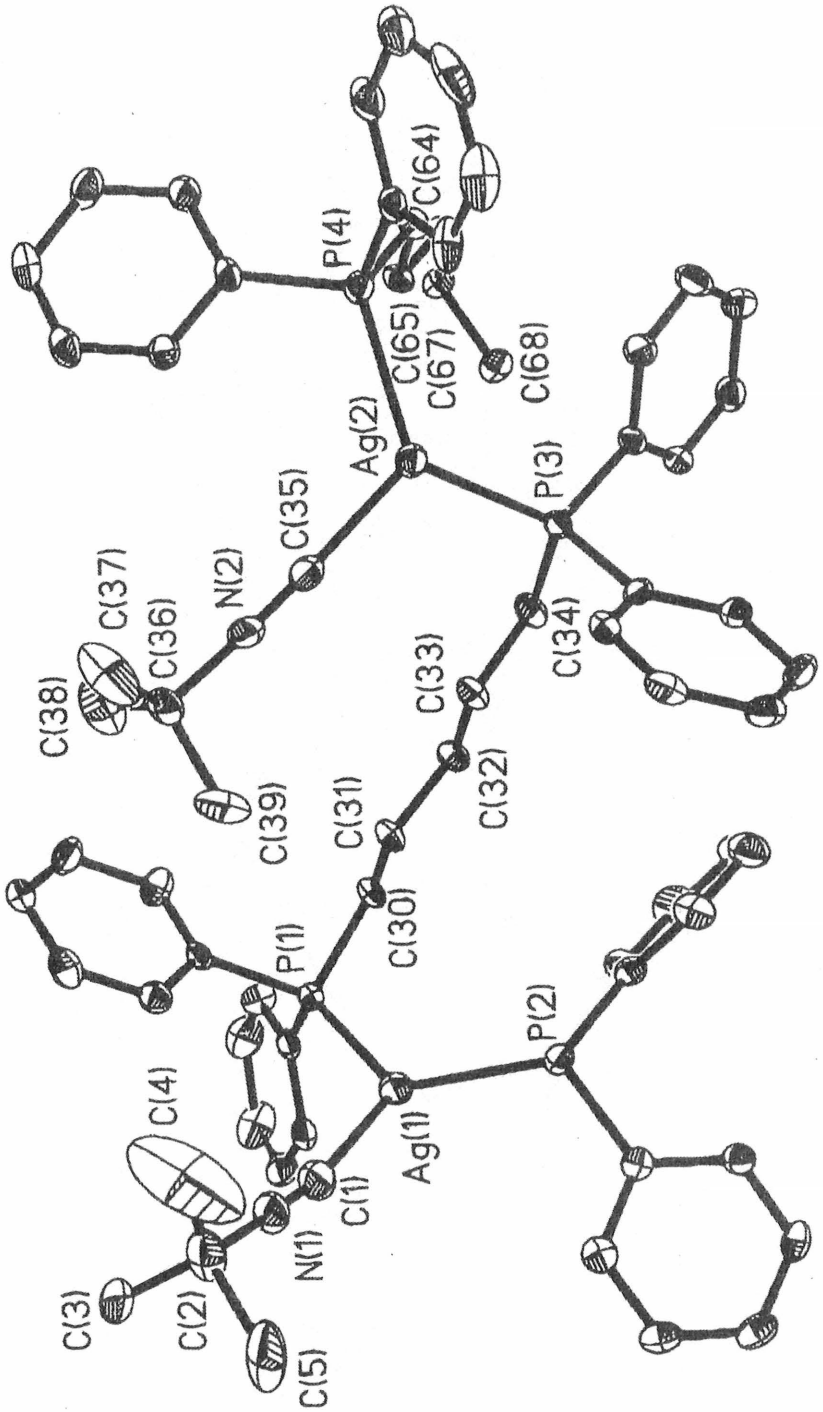

Numérotation pour le $[Cu_2(dmpm)_3(CN\text{-}t\text{-}Bu)_2](BF_4)_2$

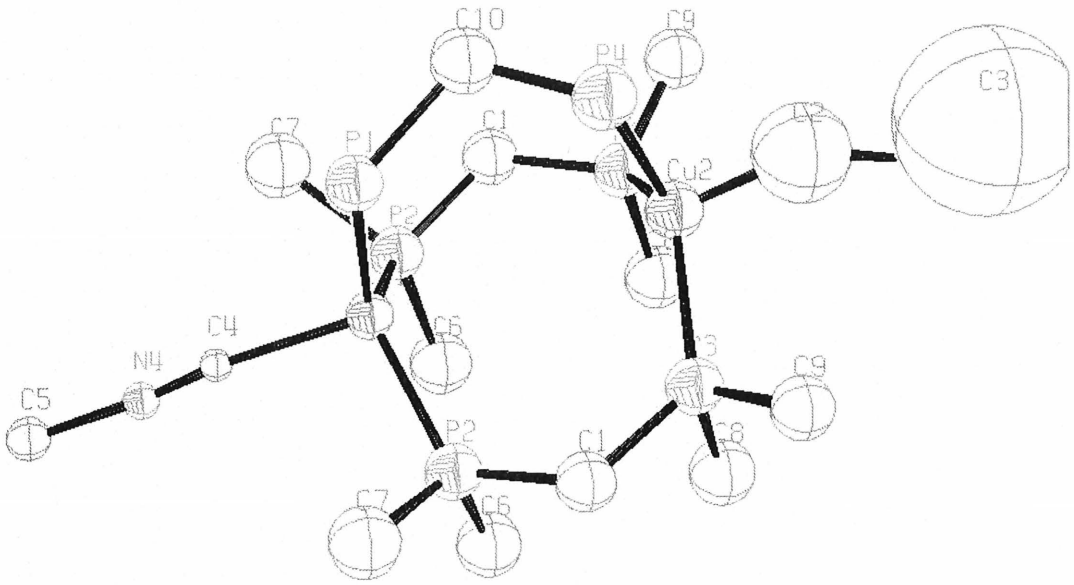

Table A1. Crystal data and structure refinement for $[Cu_2(dmpm)_3(CN\text{-}t\text{-}Bu)_2](BF_4)_2$.

Empirical formula	C15.50 H37 B2 Cu2 F8 N1.50 P6
Formula weight	730.99
Temperature	198(2) K
Wavelength	0.71073 Å
Unit cell dimensions	a = 24.935(4) Å $\alpha = 90°$.
	b = 10.5070(15) Å $\beta = 111.034(2)°$.
	c = 19.266(3) Å $\gamma = 90°$.
Volume	4711.2(12) $Å^3$
Z, Calculated density	8, 2.061 Mg/m^3
Absorption coefficient	2.288 mm^{-1}
F(000)	2964
Theta range for data collection	1.71 to 25.82°.
Limiting indices	-29<=h<=30, -12<=k<=12, -22<=l<=23
Reflections collected / unique	11822 / 7101 [R(int) = 0.0333]
Completeness to theta = 25.82	89.8 %
Refinement method	Full-matrix least-squares on F^2
Data / restraints / parameters	7101 / 2 / 117
Goodness-of-fit on F^2	2.603
Final R indices [I>2sigma(I)]	R1 = 0.2163, wR2 = 0.5370
R indices (all data)	R1 = 0.2268, wR2 = 0.5517
Absolute structure parameter	0.47(7)
Largest diff. peak and hole	3.295 and -1.798 e. $Å^{-3}$

Table A2. Atomic coordinates (x 10^4) and equivalent isotropic displacement parameters ($Å^2$ x 10^3) for $[Cu_2(dmpm)_3(CN\text{-}t\text{-}Bu)_2](BF_4)_2$. U(eq) is defined as one third of the trace of the orthogonalized Uij tensor.

	x	y	z	U(eq)
Cu(1)	4517(1)	0	1919(2)	37(1)
Cu(2)	3232(2)	0	2708(2)	55(1)
P(3)	3091(3)	1851(6)	2089(4)	54(2)
P(4)	3988(5)	0	3791(6)	64(3)
P(2)	4078(3)	1835(6)	1436(3)	52(2)
P(1)	5002(4)	0	3180(5)	49(2)
N(2)	2057(10)	0	3016(13)	38(5)
N(4)	5469(8)	0	1258(10)	22(4)
C(4)	5178(9)	0	1550(11)	17(4)
C(5)	5952(11)	0	969(14)	31(5)
C(2)	2750(40)	0	3160(50)	160(30)
C(3)	1850(130)	0	3330(180)	580(160)
C(1)	3629(12)	2750(20	1821(14)	56(6)
Cu(4)	525(1)	0	7667(2)	34(1)
Cu(3)	1933(2)	0	7098(2)	57(1)
P(7)	129(4)	0	6426(5)	52(2)
P(8)	991(3)	1812(7)	8194(4)	56(2)
P(5)	2063(3)	1825(7)	7750(4)	62(2)
P(6)	1214(6)	0	5989(7)	77(3)
N(21)	2890(60)	0	6700(70)	280(60)
C(24)	1478(13)	2690(30)	7831(16)	64(7)
C(21)	2614(18)	0	6820(20)	61(9)
C(6)	3521(13)	1540(30)	416(17)	72(7)

C(8)	2535(13)	1690(30)	1060(18)	74(8)
C(22)	2720(20)	1840(40)	8570(30)	113(13)
C(28)	1310(20)	1950(40)	9110(30)	116(13)
C(9)	2849(12)	3010(20)	2529(15)	63(6)
C(10)	4614(12)	770(20)	3794(15)	66(6)
C(25)	522(17)	3010(30)	8310(20)	97(10)
C(23)	1940(20)	3310(50)	6870(30)	150(20)
C(27)	-506(17)	-1210(40)	6140(20)	100(11)
C(7)	4699(15)	3130(30)	1684(18)	78(8)
C(26)	1110(20)	1330(50)	5360(30)	126(14)

Table A3. Bond lengths [Å] and angles [°] for $[Cu_2(dmpm)_3(CN\text{-}t\text{-}Bu)_2](BF_4)_2$.

Cu(1)-C(4)	2.02(2)	Cu(1)-P(2)#1	2.248(7)
Cu(1)-P(2)	2.248(7)	Cu(1)-P(1)	2.293(9)
Cu(2)-C(2)	1.72(10)	Cu(2)-P(3)#1	2.243(7)
Cu(2)-P(3)	2.243(7)	Cu(2)-P(4)	2.255(11)
P(3)-C(9)	1.71(3)	P(3)-C(1)	1.86(3)
P(3)-C(8)	1.98(3)	P(4)-C(10)	1.75(3)
P(4)-C(10)#1	1.75(3)	P(2)-C(1)	1.82(3)
P(2)-C(6)	1.98(3)	P(2)-C(7)	1.99(3)
P(1)-C(10)#1	1.95(3)	P(1)-C(10)	1.95(3)
N(2)-C(3)	0.9(3)	N(2)-C(2)	1.65(10)
N(4)-C(4)	1.06(3)	N(4)-C(5)	1.50(3)
Cu(4)-P(7)	2.234(10)	Cu(4)-P(8)	2.272(7)
Cu(4)-P(8)#1	2.272(7)	Cu(3)-C(21)	1.96(4)
Cu(3)-P(6)	2.242(13)	Cu(3)-P(5)	2.251(8)
Cu(3)-P(5)#1	2.251(8)	P(7)-C(27)	1.95(4)
P(7)-C(27)#1	1.95(4)	P(8)-C(28)	1.65(5)
P(8)-C(25)	1.79(4)	P(8)-C(24)	1.85(3)
P(5)-C(24)	1.77(3)	P(5)-C(22)	1.83(5)
P(5)-C(23)	2.25(6)	P(6)-C(26)#1	1.80(5)
P(6)-C(26)	1.80(5)	N(21)-C(21)	0.81(14)
C(10)-C(10)#1	1.61(5)		
C(4)-Cu(1)-P(2)#1	101.1(3)	C(4)-Cu(1)-P(2)	101.1(3)
P(2)#1-Cu(1)-P(2)	118.2(4)	C(4)-Cu(1)-P(1)	100.8(6)
P(2)#1-Cu(1)-P(1)	115.6(2)	P(2)-Cu(1)-P(1)	115.6(2)
C(2)-Cu(2)-P(3)#1	105.3(14)	C(2)-Cu(2)-P(3)	105.3(14)

P(3)#1-Cu(2)-P(3)	120.3(4)	C(2)-Cu(2)-P(4)	92(3)
P(3)#1-Cu(2)-P(4)	114.3(2)	P(3)-Cu(2)-P(4)	114.3(2)
C(9)-P(3)-C(1)	101.1(13)	C(9)-P(3)-C(8)	108.2(13)
C(1)-P(3)-C(8)	94.6(12)	C(9)-P(3)-Cu(2)	111.7(10)
C(1)-P(3)-Cu(2)	126.7(9)	C(8)-P(3)-Cu(2)	112.3(9)
C(10)-P(4)-C(10)#1	54.6(18)	C(10)-P(4)-Cu(2)	116.8(10)
C(10)#1-P(4)-Cu(2)	116.8(10)	C(1)-P(2)-C(6)	99.9(12)
C(1)-P(2)-C(7)	94.5(13)	C(6)-P(2)-C(7)	123.7(13)
C(1)-P(2)-Cu(1)	124.3(9)	C(6)-P(2)-Cu(1)	109.8(9)
C(7)-P(2)-Cu(1)	105.5(10)	C(10)#1-P(1)-C(10)	48.7(15)
C(10)#1-P(1)-Cu(1)	117.0(9)	C(10)-P(1)-Cu(1)	117.0(9)
C(3)-N(2)-C(2)	133(10)	C(4)-N(4)-C(5)	171(2)
N(4)-C(4)-Cu(1)	169.7(19)	N(2)-C(2)-Cu(2)	143(6)
P(2)-C(1)-P(3)	117.0(13)	P(7)-Cu(4)-P(8)	115.9(2)
P(7)-Cu(4)-P(8)#1	115.9(2)	P(8)-Cu(4)-P(8)#1	113.9(4)
C(21)-Cu(3)-P(6)	102.4(12)	C(21)-Cu(3)-P(5)	100.8(6)
P(6)-Cu(3)-P(5)	115.9(2)	C(21)-Cu(3)-P(5)#1	100.8(6)
P(6)-Cu(3)-P(5)#1	115.9(2)	P(5)-Cu(3)-P(5)#1	116.9(4)
C(27)-P(7)-C(27)#1	82(2)	C(27)-P(7)-Cu(4)	107.8(12)
C(27)#1-P(7)-Cu(4)	107.8(12)	C(28)-P(8)-C(25)	84(2)
C(28)-P(8)-C(24)	103.4(19)	C(25)-P(8)-C(24)	104.0(16)
C(28)-P(8)-Cu(4)	121.4(16)	C(25)-P(8)-Cu(4)	113.2(13)
C(24)-P(8)-Cu(4)	123.2(10)	C(24)-P(5)-C(22)	115.8(18)
C(24)-P(5)-C(23)	79.8(18)	C(22)-P(5)-C(23)	119(2)
C(24)-P(5)-Cu(3)	121.7(10)	C(22)-P(5)-Cu(3)	113.1(15)
C(23)-P(5)-Cu(3)	102.6(15)	C(26)#1-P(6)-C(26)	102(3)
C(26)#1-P(6)-Cu(3)	120.9(16)	C(26)-P(6)-Cu(3)	120.8(16)
P(5)-C(24)-P(8)	117.0(16)	N(21)-C(21)-Cu(3)	179(10)
C(10)#1-C(10)-P(4)	62.7(9)	C(10)#1-C(10)-P(1)	65.7(8)

P(4)-C(10)-P(1)	116.3(14)

Symmetry transformations used to generate equivalent atoms:

#1 x,-y,z

Numérotation pour $\{[Ag_2(dppb)_3(t\text{-}BuNC)_2](BF_4)\}_n$

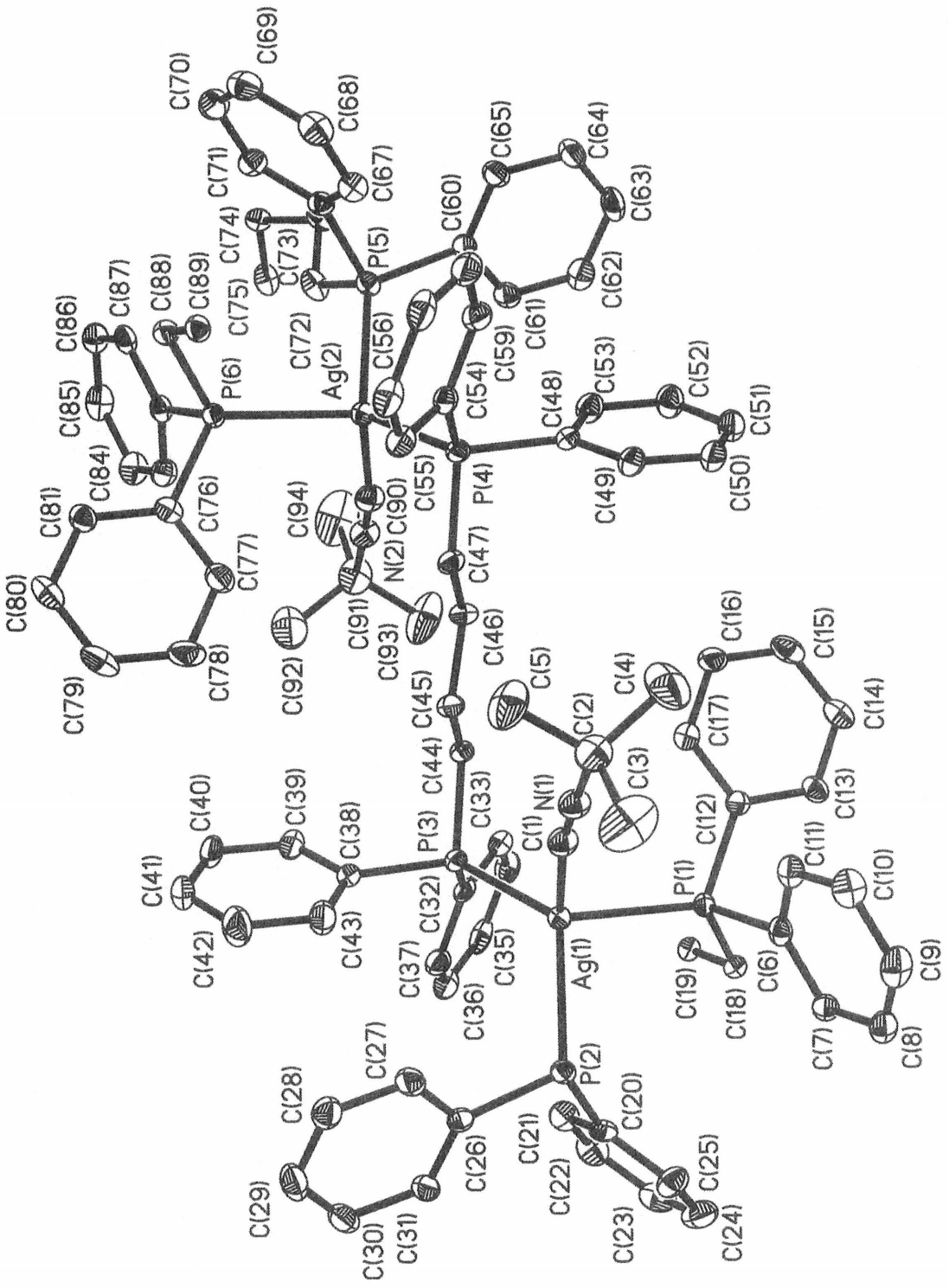

Table A4. Crystal data and structure refinement for $\{[Ag_2(dppb)_3(t\text{-}BuNC)_2](BF_4)\}_n$.

Empirical formula	C98 H108 Ag2 B2 F8 N4 P6	
Molecular formula	$[(Ph_2PC_4H_8PPh_2)_3Ag_2(CN\text{-}t\text{-}Bu)_2][BF_4]_2 \bullet 2$ MeCN	
Formula weight	1917.06	
Temperature	173(1) K	
Wavelength	0.71073 Å	
Diffractometer used	Bruker AXS P4/SMART 1000	
Detector distance	5 cm	
Monochrometer used	Graphite	
Crystal size	0.2 x 0.3 x 0.35 mm^3	
Colour and habit	Colourless, irregular	
Crystal system	Triclinic	
Space group	P-1	
Unit cell dimensions	a = 11.4175(12) Å	α = 90.565(2)°
	b = 17.7558(19) Å	β = 92.498(2)°
	c = 23.465(3) Å	γ = 94.076(2)°
Volume	4740.0(9) $Å^3$	
Z	2	
Density (calculated)	1.343 Mg/m^3	
Absorption coefficient	0.577 mm^{-1}	
F(000)	1980	
Theta range for data collection	0.87 to 27.50°	
Completeness to theta = 27.50°	92.8 %	
Scan type	ω and ϕ	
Scan range	0.3°	
Exposure time	25s	

Index ranges	$-14 \leq h \leq 13, -23 \leq k \leq 22, -29 \leq l \leq 30$
Standard reflections	50 frames at beginning and end of data
collection	
Crystal stability	no decay
Reflections collected	31368
Independent reflections	20217 [R(int) = 0.0273]
System used	SHELXL 5.1
Solution	Direct methods
Hydrogen atoms	Calculated, riding model,
	solvent molecule hydrogen atoms omitted
Absorption correction	SADABS
Min./Max. transmission ratio	0.855
Refinement method	Full-matrix least-squares on F^2
Data / restraints / parameters	20217 / 0 / 1117
Goodness-of-fit on F^2	1.056
Final R indices [I>2sigma(I)]	R1 = 0.0582, wR2 = 0.1901
R indices (all data)	R1 = 0.0879, wR2 = 0.2092
Largest/mean shift/esd	0.001/0.000
Largest diff. peak and hole	2.983 and -1.170 e.$Å^{-3}$

$wR2 = (\Sigma[w(F_o^2-F_c^2)^2]/\Sigma[F_o^4])^{1/2}$

$R1 = \Sigma \, | \, |F_o| - |F_c| \, | \, / \Sigma \, |F_o|$

$Weight = 1 / [\sigma^2(F_o^2) + (0.1342 * P)^2]$

where $P = (\max(F_o^2, 0) + 2 * F_c^2)/3$

Table A5. Atomic coordinates (x 10^4) and equivalent isotropic displacement parameters ($Å^2$x 10^3) for $\{[Ag_2(dppb)_3(t\text{-}BuNC)_2](BF_4)\}_n$. U(eq) is defined as one third of the trace of the orthogonalized U^{ij} tensor.

	x	y	z	U(eq)
Ag(1)	1414(1)	5007(1)	2024(1)	27(1)
Ag(2)	3619(1)	9802(1)	2995(1)	28(1)
P(1)	2232(1)	4857(1)	1053(1)	24(1)
P(2)	579(1)	3682(1)	2152(1)	26(1)
P(3)	245(1)	6123(1)	2118(1)	26(1)
P(4)	4827(1)	8706(1)	2954(1)	26(1)
P(5)	4409(1)	11121(1)	2801(1)	27(1)
P(6)	2758(1)	10014(1)	3946(1)	25(1)
C(1)	3032(4)	5134(3)	2603(2)	36(1)
N(1)	3912(3)	5144(2)	2858(2)	37(1)
C(2)	5062(4)	5149(3)	3164(3)	49(1)
C(3)	5271(7)	4327(4)	3283(4)	94(3)
C(4)	5954(6)	5493(6)	2766(3)	91(3)
C(5)	5016(6)	5616(4)	3690(3)	73(2)
C(6)	3301(4)	4132(3)	1104(2)	30(1)
C(7)	3083(4)	3405(2)	889(2)	33(1)
C(8)	3926(4)	2883(3)	976(2)	43(1)
C(9)	4980(5)	3088(3)	1276(2)	48(1)
C(10)	5184(5)	3806(3)	1488(2)	46(1)
C(11)	4353(4)	4332(3)	1404(2)	36(1)
C(12)	3159(3)	5640(2)	797(2)	27(1)
C(13)	3713(4)	5599(3)	281(2)	33(1)

C(14)	4426(4)	6194(3)	96(2)	40(1)
C(15)	4620(4)	6837(3)	429(2)	44(1)
C(16)	4112(4)	6882(3)	948(3)	43(1)
C(17)	3386(4)	6290(3)	1132(2)	38(1)
C(18)	1268(3)	4561(2)	436(2)	28(1)
C(19)	369(3)	5126(2)	270(2)	28(1)
C(20)	-332(4)	3377(2)	1522(2)	29(1)
C(21)	-1214(4)	3844(3)	1349(2)	40(1)
C(22)	-1880(4)	3695(3)	858(2)	46(1)
C(23)	-1703(5)	3088(3)	525(2)	51(1)
C(24)	-839(5)	2619(3)	679(3)	53(1)
C(25)	-166(5)	2760(3)	1183(2)	43(1)
C(26)	-351(4)	3539(2)	2753(2)	27(1)
C(27)	135(4)	3762(3)	3291(2)	39(1)
C(28)	-521(5)	3698(3)	3767(2)	43(1)
C(29)	-1683(5)	3414(3)	3716(3)	54(2)
C(30)	-2181(4)	3191(3)	3197(2)	44(1)
C(31)	-1527(4)	3251(3)	2710(2)	37(1)
C(32)	-868(3)	6268(2)	1558(2)	29(1)
C(33)	-652(4)	6763(3)	1113(2)	34(1)
C(34)	-1496(4)	6845(3)	681(2)	43(1)
C(35)	-2547(4)	6427(3)	689(2)	48(1)
C(36)	-2786(4)	5931(3)	1123(2)	44(1)
C(37)	-1935(4)	5853(3)	1552(2)	38(1)
C(38)	-534(4)	6240(2)	2768(2)	29(1)
C(39)	-1177(4)	6859(3)	2858(2)	38(1)
C(40)	-1688(4)	6959(3)	3369(2)	46(1)
C(41)	-1606(5)	6433(3)	3791(3)	53(2)
C(42)	-996(6)	5822(4)	3704(3)	66(2)

C(43)	-455(5)	5717(3)	3194(2)	49(1)
C(44)	1163(3)	7005(2)	2105(2)	28(1)
C(45)	2141(4)	7048(2)	2569(2)	30(1)
C(46)	2950(4)	7760(2)	2512(2)	31(1)
C(47)	3930(4)	7818(2)	2981(2)	29(1)
C(48)	5628(3)	8582(2)	2311(2)	28(1)
C(49)	6290(4)	7966(3)	2236(2)	36(1)
C(50)	6826(4)	7859(3)	1738(2)	43(1)
C(51)	6745(4)	8376(3)	1303(2)	44(1)
C(52)	6132(4)	8995(3)	1381(2)	44(1)
C(53)	5562(4)	9099(3)	1879(2)	38(1)
C(54)	5940(4)	8589(2)	3528(2)	30(1)
C(55)	5718(4)	8119(3)	3985(2)	38(1)
C(56)	6566(4)	8060(3)	4418(2)	45(1)
C(57)	7622(4)	8473(3)	4401(2)	49(1)
C(58)	7856(4)	8951(3)	3954(3)	50(1)
C(59)	7013(4)	9004(3)	3520(2)	39(1)
C(60)	5348(4)	11263(2)	2197(2)	29(1)
C(61)	4862(4)	11042(3)	1669(2)	35(1)
C(62)	5533(5)	11085(3)	1188(2)	44(1)
C(63)	6704(5)	11353(3)	1247(2)	48(1)
C(64)	7187(4)	11587(3)	1763(2)	45(1)
C(65)	6520(4)	11541(3)	2250(2)	37(1)
C(66)	5281(4)	11480(2)	3427(2)	29(1)
C(67)	6220(4)	11062(3)	3610(2)	37(1)
C(68)	6864(4)	11256(3)	4098(2)	46(1)
C(69)	6595(5)	11865(3)	4418(2)	48(1)
C(70)	5673(5)	12270(3)	4256(2)	47(1)
C(71)	5018(4)	12082(3)	3753(2)	36(1)

C(72)	3283(4)	11790(3)	2686(2)	39(1)
C(73)	3629(5)	12549(3)	2531(3)	25(1)
C(74)	2665(5)	13099(4)	2605(3)	28(1)
C(73A)	2285(13)	11712(9)	2291(8)	56(4)
C(74A)	1304(11)	12267(8)	2345(6)	39(3)
C(75)	1648(4)	12950(3)	2225(2)	39(1)
C(76)	1854(3)	9245(2)	4246(2)	30(1)
C(77)	1708(4)	8551(3)	3962(3)	45(1)
C(78)	1003(5)	7970(3)	4177(3)	56(2)
C(79)	461(4)	8066(3)	4687(3)	49(1)
C(80)	590(4)	8753(3)	4963(2)	43(1)
C(81)	1272(4)	9341(3)	4746(2)	34(1)
C(82)	1667(4)	10709(2)	3851(2)	29(1)
C(83)	627(4)	10495(3)	3552(2)	36(1)
C(84)	-196(4)	11004(3)	3425(2)	45(1)
C(85)	7(5)	11751(3)	3595(2)	46(1)
C(86)	1044(4)	11978(3)	3892(2)	39(1)
C(87)	1875(4)	11461(3)	4020(2)	34(1)
C(88)	3710(3)	10376(2)	4553(2)	30(1)
C(89)	4639(3)	9850(2)	4739(2)	29(1)
C(90)	2023(4)	9683(3)	2391(2)	39(1)
N(2)	1177(3)	9701(2)	2125(2)	39(1)
C(91)	61(5)	9753(4)	1796(3)	59(2)
C(92)	-898(6)	9475(6)	2181(3)	101(3)
C(93)	73(6)	9276(5)	1276(3)	103(3)
C(94)	-24(8)	10601(5)	1676(4)	111(3)
B(1)	7587(11)	8894(6)	9724(5)	105(4)
B(2)	7253(10)	6244(5)	5439(5)	81(3)
F(1)	7442(5)	9174(4)	9218(2)	122(2)

F(2)	8161(6)	8257(4)	9741(4)	195(4)
F(3)	6470(6)	8700(5)	9918(3)	153(3)
F(4)	8193(8)	9386(4)	10066(3)	211(4)
F(5)	6763(6)	6849(4)	5645(4)	188(4)
F(6)	7504(5)	5770(3)	5860(2)	123(2)
F(7)	6537(7)	5901(5)	5049(3)	186(4)
F(8)	8302(6)	6505(4)	5228(2)	145(2)
N(3)	1973(7)	8027(5)	860(4)	126(3)
C(95)	2605(8)	8481(5)	680(4)	87(3)
C(96)	3427(8)	9068(6)	449(4)	108(3)
N(4)	3219(8)	6855(5)	4324(4)	109(3)
C(97)	2502(18)	6404(11)	4443(10)	86(5)
C(98)	1601(19)	5815(11)	4666(10)	123(8)
C(97A)	3289(18)	6386(11)	4651(7)	80(5)
C(98A)	3330(18)	5706(10)	5057(9)	115(7)

Table A6. Bond lengths [Å] and angles [°] for $\{[Ag_2(dppb)_3(t\text{-}BuNC)_2](BF_4)\}_n$.

Ag(1)-C(1)	2.243(5)	Ag(1)-P(3)	2.4814(11)
Ag(1)-P(2)	2.5000(11)	Ag(1)-P(1)	2.5190(11)
Ag(2)-C(90)	2.255(5)	Ag(2)-P(4)	2.4670(11)
Ag(2)-P(5)	2.5022(11)	Ag(2)-P(6)	2.5141(12)
P(1)-C(12)	1.810(4)	P(1)-C(6)	1.837(4)
P(1)-C(18)	1.829(4)	P(2)-C(26)	1.810(4)
P(2)-C(20)	1.824(5)	P(2)-C(75)#1	1.850(4)
P(3)-C(32)	1.820(4)	P(3)-C(38)	1.817(5)
P(3)-C(44)	1.823(4)	P(4)-C(48)	1.817(5)
P(4)-C(47)	1.821(4)	P(4)-C(54)	1.835(5)
P(5)-C(66)	1.821(5)	P(5)-C(60)	1.823(4)
P(5)-C(72)	1.824(4)	P(6)-C(76)	1.817(4)
P(6)-C(82)	1.823(4)	P(6)-C(88)	1.836(4)
C(1)-N(1)	1.144(6)	N(1)-C(2)	1.469(6)
C(2)-C(5)	1.484(8)	C(2)-C(4)	1.511(9)
C(2)-C(3)	1.523(9)	C(6)-C(7)	1.383(6)
C(6)-C(11)	1.387(6)	C(7)-C(8)	1.393(6)
C(8)-C(9)	1.391(8)	C(9)-C(10)	1.365(8)
C(10)-C(11)	1.387(6)	C(12)-C(17)	1.394(6)
C(12)-C(13)	1.393(6)	C(13)-C(14)	1.372(6)
C(14)-C(15)	1.375(8)	C(15)-C(16)	1.376(8)
C(16)-C(17)	1.377(7)	C(18)-C(19)	1.527(5)
C(19)-C(19)#2	1.534(8)	C(20)-C(25)	1.377(7)
C(20)-C(21)	1.399(6)	C(21)-C(22)	1.366(7)
C(22)-C(23)	1.357(8)	C(23)-C(24)	1.374(8)
C(24)-C(25)	1.392(8)	C(26)-C(27)	1.401(7)
C(26)-C(31)	1.401(6)	C(27)-C(28)	1.372(7)

C(28)-C(29)	1.385(8)	C(29)-C(30)	1.365(8)
C(30)-C(31)	1.393(7)	C(32)-C(37)	1.378(6)
C(32)-C(33)	1.390(6)	C(33)-C(34)	1.385(6)
C(34)-C(35)	1.366(8)	C(35)-C(36)	1.375(8)
C(36)-C(37)	1.384(7)	C(38)-C(43)	1.374(7)
C(38)-C(39)	1.383(6)	C(39)-C(40)	1.372(7)
C(40)-C(41)	1.372(8)	C(41)-C(42)	1.348(8)
C(42)-C(43)	1.389(7)	C(44)-C(45)	1.522(6)
C(45)-C(46)	1.522(6)	C(46)-C(47)	1.532(6)
C(48)-C(53)	1.377(6)	C(48)-C(49)	1.388(6)
C(49)-C(50)	1.361(7)	C(50)-C(51)	1.383(7)
C(51)-C(52)	1.359(7)	C(52)-C(53)	1.380(7)
C(54)-C(55)	1.385(7)	C(54)-C(59)	1.385(6)
C(55)-C(56)	1.384(7)	C(56)-C(57)	1.368(8)
C(57)-C(58)	1.379(8)	C(58)-C(59)	1.380(7)
C(60)-C(61)	1.379(7)	C(60)-C(65)	1.393(6)
C(61)-C(62)	1.390(7)	C(62)-C(63)	1.389(7)
C(63)-C(64)	1.356(8)	C(64)-C(65)	1.400(7)
C(66)-C(71)	1.367(7)	C(66)-C(67)	1.402(6)
C(67)-C(68)	1.361(7)	C(68)-C(69)	1.371(8)
C(69)-C(70)	1.360(7)	C(70)-C(71)	1.394(7)
C(72)-C(73)	1.433(7)	C(73)-C(74)	1.537(8)
C(74)-C(75)	1.440(8)	C(73A)-C(74A)	1.553(19)
C(74A)-C(75)	1.286(14)	C(75)-P(2)#3	1.850(4)
C(76)-C(77)	1.391(7)	C(76)-C(81)	1.388(6)
C(77)-C(78)	1.377(7)	C(78)-C(79)	1.386(8)
C(79)-C(80)	1.371(8)	C(80)-C(81)	1.373(7)
C(82)-C(83)	1.379(6)	C(82)-C(87)	1.391(6)
C(83)-C(84)	1.375(6)	C(84)-C(85)	1.382(8)

C(85)-C(86)	1.380(7)	C(86)-C(87)	1.392(6)
C(88)-C(89)	1.515(5)	C(89)-C(89)#4	1.517(9)
C(90)-N(2)	1.130(6)	N(2)-C(91)	1.469(6)
C(91)-C(93)	1.482(9)	C(91)-C(92)	1.509(10)
C(91)-C(94)	1.543(11)	B(1)-F(1)	1.302(11)
B(1)-F(4)	1.317(11)	B(1)-F(2)	1.347(13)
B(1)-F(3)	1.395(14)	B(2)-F(7)	1.316(10)
B(2)-F(6)	1.338(10)	B(2)-F(5)	1.342(12)
B(2)-F(8)	1.368(11)	N(3)-C(95)	1.140(11)
C(95)-C(96)	1.474(13)	N(4)-C(97)	1.15(2)
N(4)-C(97A)	1.14(2)	C(97)-C(97A)	1.01(2)
C(97)-C(98)	1.53(3)	C(97A)-C(98A)	1.55(3)

C(1)-Ag(1)-P(3)	110.20(12)	C(1)-Ag(1)-P(2)	105.51(12)
P(3)-Ag(1)-P(2)	123.07(4)	C(1)-Ag(1)-P(1)	103.09(13)
P(3)-Ag(1)-P(1)	113.87(4)	P(2)-Ag(1)-P(1)	98.88(4)
C(90)-Ag(2)-P(4)	112.69(12)	C(90)-Ag(2)-P(5)	101.51(12)
P(4)-Ag(2)-P(5)	122.89(4)	C(90)-Ag(2)-P(6)	103.14(13)
P(4)-Ag(2)-P(6)	114.48(4)	P(5)-Ag(2)-P(6)	99.49(4)
C(12)-P(1)-C(6)	99.94(19)	C(12)-P(1)-C(18)	104.4(2)
C(6)-P(1)-C(18)	104.3(2)	C(12)-P(1)-Ag(1)	117.08(15)
C(6)-P(1)-Ag(1)	107.64(14)	C(18)-P(1)-Ag(1)	120.81(14)
C(26)-P(2)-C(20)	105.8(2)	C(26)-P(2)-C(75)#1	104.7(2)
C(20)-P(2)-C(75)#1	103.7(2)	C(26)-P(2)-Ag(1)	115.46(14)
C(20)-P(2)-Ag(1)	109.65(14)	C(75)#1-P(2)-Ag(1)	116.41(16)
C(32)-P(3)-C(38)	103.21(19)	C(32)-P(3)-C(44)	102.0(2)
C(38)-P(3)-C(44)	101.6(2)	C(32)-P(3)-Ag(1)	117.39(14)
C(38)-P(3)-Ag(1)	118.45(15)	C(44)-P(3)-Ag(1)	111.83(13)
C(48)-P(4)-C(47)	102.1(2)	C(48)-P(4)-C(54)	103.16(19)

C(47)-P(4)-C(54)	101.8(2)	C(48)-P(4)-Ag(2)	117.16(14)
C(47)-P(4)-Ag(2)	111.63(14)	C(54)-P(4)-Ag(2)	118.70(14)
C(66)-P(5)-C(60)	106.0(2)	C(66)-P(5)-C(72)	105.2(2)
C(60)-P(5)-C(72)	104.1(2)	C(66)-P(5)-Ag(2)	108.55(14)
C(60)-P(5)-Ag(2)	117.67(15)	C(72)-P(5)-Ag(2)	114.32(16)
C(76)-P(6)-C(82)	99.91(19)	C(76)-P(6)-C(88)	103.9(2)
C(82)-P(6)-C(88)	104.7(2)	C(76)-P(6)-Ag(2)	118.25(16)
C(82)-P(6)-Ag(2)	107.70(14)	C(88)-P(6)-Ag(2)	119.89(14)
N(1)-C(1)-Ag(1)	172.2(4)	C(1)-N(1)-C(2)	177.9(5)
N(1)-C(2)-C(5)	108.0(4)	N(1)-C(2)-C(4)	106.5(5)
C(5)-C(2)-C(4)	111.2(6)	N(1)-C(2)-C(3)	106.1(5)
C(5)-C(2)-C(3)	113.4(6)	C(4)-C(2)-C(3)	111.2(6)
C(7)-C(6)-C(11)	119.6(4)	C(7)-C(6)-P(1)	123.7(3)
C(11)-C(6)-P(1)	116.6(4)	C(6)-C(7)-C(8)	119.5(5)
C(9)-C(8)-C(7)	120.5(5)	C(8)-C(9)-C(10)	119.5(4)
C(9)-C(10)-C(11)	120.5(5)	C(10)-C(11)-C(6)	120.3(5)
C(17)-C(12)-C(13)	118.2(4)	C(17)-C(12)-P(1)	120.0(3)
C(13)-C(12)-P(1)	121.7(3)	C(14)-C(13)-C(12)	121.0(5)
C(15)-C(14)-C(13)	119.9(5)	C(14)-C(15)-C(16)	120.2(5)
C(15)-C(16)-C(17)	120.1(5)	C(12)-C(17)-C(16)	120.5(5)
C(19)-C(18)-P(1)	114.0(3)	C(19)#2-C(19)-C(18)	112.0(4)
C(25)-C(20)-C(21)	117.6(4)	C(25)-C(20)-P(2)	125.5(4)
C(21)-C(20)-P(2)	116.7(4)	C(22)-C(21)-C(20)	121.1(5)
C(21)-C(22)-C(23)	120.7(5)	C(24)-C(23)-C(22)	119.9(5)
C(23)-C(24)-C(25)	119.8(5)	C(20)-C(25)-C(24)	120.8(5)
C(27)-C(26)-C(31)	118.4(4)	C(27)-C(26)-P(2)	117.1(3)
C(31)-C(26)-P(2)	124.5(4)	C(28)-C(27)-C(26)	120.9(5)
C(27)-C(28)-C(29)	119.9(5)	C(30)-C(29)-C(28)	120.6(5)
C(29)-C(30)-C(31)	120.3(5)	C(30)-C(31)-C(26)	120.0(5)

C(37)-C(32)-C(33)	118.3(4)	C(37)-C(32)-P(3)	120.0(4)
C(33)-C(32)-P(3)	121.7(3)	C(32)-C(33)-C(34)	120.7(4)
C(35)-C(34)-C(33)	119.5(5)	C(34)-C(35)-C(36)	121.1(5)
C(35)-C(36)-C(37)	118.9(5)	C(36)-C(37)-C(32)	121.4(5)
C(43)-C(38)-C(39)	118.6(5)	C(43)-C(38)-P(3)	119.6(4)
C(39)-C(38)-P(3)	121.7(4)	C(40)-C(39)-C(38)	120.4(5)
C(41)-C(40)-C(39)	120.6(5)	C(42)-C(41)-C(40)	119.5(5)
C(41)-C(42)-C(43)	120.9(6)	C(38)-C(43)-C(42)	120.1(5)
C(45)-C(44)-P(3)	112.5(3)	C(46)-C(45)-C(44)	110.9(4)
C(45)-C(46)-C(47)	111.6(4)	C(46)-C(47)-P(4)	112.0(3)
C(53)-C(48)-C(49)	118.5(4)	C(53)-C(48)-P(4)	119.8(3)
C(49)-C(48)-P(4)	121.6(4)	C(50)-C(49)-C(48)	120.7(5)
C(49)-C(50)-C(51)	120.4(5)	C(52)-C(51)-C(50)	119.3(5)
C(51)-C(52)-C(53)	120.7(5)	C(52)-C(53)-C(48)	120.3(4)
C(55)-C(54)-C(59)	118.8(4)	C(55)-C(54)-P(4)	121.7(3)
C(59)-C(54)-P(4)	119.4(4)	C(54)-C(55)-C(56)	120.2(5)
C(57)-C(56)-C(55)	120.1(5)	C(56)-C(57)-C(58)	120.7(5)
C(59)-C(58)-C(57)	119.1(5)	C(58)-C(59)-C(54)	121.1(5)
C(61)-C(60)-C(65)	119.6(4)	C(61)-C(60)-P(5)	116.6(3)
C(65)-C(60)-P(5)	123.7(4)	C(60)-C(61)-C(62)	120.8(4)
C(63)-C(62)-C(61)	119.0(5)	C(64)-C(63)-C(62)	120.8(5)
C(63)-C(64)-C(65)	120.5(5)	C(64)-C(65)-C(60)	119.3(5)
C(71)-C(66)-C(67)	118.4(4)	C(71)-C(66)-P(5)	124.5(3)
C(67)-C(66)-P(5)	116.8(4)	C(68)-C(67)-C(66)	120.8(5)
C(67)-C(68)-C(69)	120.1(5)	C(70)-C(69)-C(68)	120.2(5)
C(69)-C(70)-C(71)	120.1(5)	C(66)-C(71)-C(70)	120.3(5)
C(73)-C(72)-P(5)	119.1(4)	C(72)-C(73)-C(74)	113.5(5)
C(75)-C(74)-C(73)	114.0(6)	C(75)-C(74A)-C(73A)	112.8(10)
C(74A)-C(75)-C(74)	102.7(7)	C(74A)-C(75)-P(2)#3	120.5(7)

C(74)-C(75)-P(2)#3	118.4(4)	C(77)-C(76)-C(81)	118.9(4)
C(77)-C(76)-P(6)	119.7(4)	C(81)-C(76)-P(6)	121.4(4)
C(78)-C(77)-C(76)	120.3(5)	C(77)-C(78)-C(79)	120.1(5)
C(80)-C(79)-C(78)	119.6(5)	C(79)-C(80)-C(81)	120.6(5)
C(80)-C(81)-C(76)	120.4(5)	C(83)-C(82)-C(87)	118.3(4)
C(83)-C(82)-P(6)	118.4(3)	C(87)-C(82)-P(6)	123.0(3)
C(82)-C(83)-C(84)	121.7(5)	C(83)-C(84)-C(85)	120.1(5)
C(86)-C(85)-C(84)	119.2(5)	C(85)-C(86)-C(87)	120.5(5)
C(82)-C(87)-C(86)	120.2(5)	C(89)-C(88)-P(6)	113.8(3)
C(88)-C(89)-C(89)#4	112.1(4)	N(2)-C(90)-Ag(2)	171.1(4)
C(90)-N(2)-C(91)	177.4(5)	N(2)-C(91)-C(93)	108.7(5)
N(2)-C(91)-C(92)	106.3(5)	C(93)-C(91)-C(92)	111.6(7)
N(2)-C(91)-C(94)	105.6(6)	C(93)-C(91)-C(94)	114.0(7)
C(92)-C(91)-C(94)	110.2(6)	F(1)-B(1)-F(4)	110.4(9)
F(1)-B(1)-F(2)	114.8(13)	F(4)-B(1)-F(2)	106.5(9)
F(1)-B(1)-F(3)	106.9(8)	F(4)-B(1)-F(3)	112.2(13)
F(2)-B(1)-F(3)	106.1(9)	F(7)-B(2)-F(6)	110.5(8)
F(7)-B(2)-F(5)	109.6(9)	F(6)-B(2)-F(5)	110.7(10)
F(7)-B(2)-F(8)	112.7(9)	F(6)-B(2)-F(8)	106.8(8)
F(5)-B(2)-F(8)	106.4(8)	N(3)-C(95)-C(96)	179.8(12)
C(97)-N(4)-C(97A)	52.1(12)	C(97A)-C(97)-N(4)	63.6(18)
C(97A)-C(97)-C(98)	112(3)	N(4)-C(97)-C(98)	174(3)
C(97)-C(97A)-N(4)	64.3(18)	C(97)-C(97A)-C(98A)	112(3)
N(4)-C(97A)-C(98A)	175.4(19)		

Symmetry transformations used to generate equivalent atoms:

#1 x,y-1,z #2 -x,-y+1,-z #3 x,y+1,z #4 -x+1,-y+2,-z+1

Table A7. Anisotropic displacement parameters ($Å^2$x 10^3) for{[Ag_2(dppb)$_3$(*t*-BuNC)$_2$](BF_4)}$_n$. The anisotropic displacement factor exponent takes the form: $-2\pi^2[\ h^2 a^{*2}U^{11} + ... + 2\ h\ k\ a^*\ b^*\ U^{12}\ ]$

	U^{11}	U^{22}	U^{33}	U^{23}	U^{13}	U^{12}
Ag(1)	27(1)	23(1)	30(1)	-1(1)	6(1)	1(1)
Ag(2)	27(1)	24(1)	32(1)	-2(1)	5(1)	2(1)
P(1)	26(1)	23(1)	25(1)	1(1)	5(1)	3(1)
P(2)	26(1)	20(1)	32(1)	4(1)	4(1)	4(1)
P(3)	25(1)	22(1)	31(1)	-3(1)	4(1)	2(1)
P(4)	24(1)	21(1)	33(1)	-3(1)	2(1)	2(1)
P(5)	25(1)	24(1)	31(1)	5(1)	4(1)	3(1)
P(6)	26(1)	23(1)	27(1)	2(1)	5(1)	3(1)
C(1)	41(2)	29(2)	40(3)	2(2)	2(2)	6(2)
N(1)	35(2)	35(2)	41(2)	-1(2)	-3(2)	2(2)
C(2)	33(2)	56(3)	57(4)	-7(3)	-10(2)	8(2)
C(3)	89(5)	81(5)	111(7)	-6(5)	-46(5)	44(4)
C(4)	49(4)	153(9)	65(5)	-19(5)	-2(3)	-28(4)
C(5)	67(4)	96(6)	54(4)	-31(4)	-19(3)	16(4)
C(6)	36(2)	31(2)	24(2)	6(2)	8(2)	9(2)
C(7)	41(2)	24(2)	35(3)	8(2)	11(2)	4(2)
C(8)	58(3)	27(2)	47(3)	12(2)	20(3)	13(2)
C(9)	61(3)	41(3)	47(3)	16(3)	9(3)	28(3)
C(10)	46(3)	50(3)	42(3)	10(3)	-2(2)	15(2)
C(11)	39(2)	37(3)	33(3)	4(2)	7(2)	10(2)
C(12)	23(2)	25(2)	32(2)	2(2)	0(2)	5(2)
C(13)	32(2)	40(3)	27(2)	4(2)	4(2)	-2(2)

C(14)	32(2)	49(3)	38(3)	12(2)	3(2)	-3(2)
C(15)	31(2)	36(3)	64(4)	20(3)	5(2)	3(2)
C(16)	36(2)	25(2)	69(4)	-4(2)	10(2)	-1(2)
C(17)	38(2)	35(3)	41(3)	-5(2)	9(2)	2(2)
C(18)	28(2)	26(2)	28(2)	-4(2)	3(2)	-1(2)
C(19)	29(2)	27(2)	27(2)	-3(2)	3(2)	2(2)
C(20)	31(2)	22(2)	33(2)	6(2)	1(2)	-1(2)
C(21)	38(2)	38(3)	44(3)	7(2)	2(2)	8(2)
C(22)	33(2)	61(4)	44(3)	8(3)	-5(2)	4(2)
C(23)	52(3)	60(4)	37(3)	6(3)	-10(2)	-16(3)
C(24)	71(4)	39(3)	46(3)	-4(3)	-1(3)	-9(3)
C(25)	58(3)	30(3)	41(3)	1(2)	-1(2)	11(2)
C(26)	32(2)	19(2)	32(2)	3(2)	3(2)	4(2)
C(27)	43(2)	26(2)	48(3)	8(2)	13(2)	4(2)
C(28)	60(3)	33(3)	38(3)	2(2)	10(2)	6(2)
C(29)	69(4)	45(3)	52(4)	13(3)	34(3)	14(3)
C(30)	36(2)	38(3)	58(4)	8(3)	16(2)	1(2)
C(31)	35(2)	29(2)	46(3)	3(2)	10(2)	1(2)
C(32)	27(2)	25(2)	35(3)	-10(2)	1(2)	6(2)
C(33)	38(2)	32(2)	33(3)	-5(2)	2(2)	4(2)
C(34)	44(3)	46(3)	40(3)	-5(2)	0(2)	17(2)
C(35)	43(3)	59(4)	46(3)	-23(3)	-4(2)	24(3)
C(36)	27(2)	56(3)	50(3)	-21(3)	-2(2)	4(2)
C(37)	32(2)	35(3)	48(3)	-11(2)	3(2)	3(2)
C(38)	29(2)	27(2)	32(2)	-6(2)	6(2)	-2(2)
C(39)	41(2)	40(3)	34(3)	-7(2)	5(2)	6(2)
C(40)	42(3)	52(3)	44(3)	-18(3)	13(2)	5(2)
C(41)	52(3)	62(4)	45(3)	-16(3)	21(3)	-4(3)
C(42)	97(5)	56(4)	48(4)	10(3)	32(4)	10(3)

C(43)	68(3)	38(3)	44(3)	2(2)	22(3)	9(3)
C(44)	29(2)	19(2)	36(3)	-2(2)	6(2)	1(2)
C(45)	32(2)	25(2)	32(2)	-1(2)	-1(2)	-4(2)
C(46)	30(2)	23(2)	37(3)	0(2)	-2(2)	-3(2)
C(47)	31(2)	22(2)	34(3)	-3(2)	0(2)	2(2)
C(48)	29(2)	23(2)	32(2)	-5(2)	4(2)	0(2)
C(49)	37(2)	29(2)	43(3)	-4(2)	5(2)	8(2)
C(50)	39(2)	42(3)	48(3)	-12(2)	7(2)	8(2)
C(51)	39(2)	54(3)	39(3)	-9(2)	7(2)	1(2)
C(52)	53(3)	46(3)	36(3)	3(2)	8(2)	7(2)
C(53)	45(3)	32(3)	39(3)	-1(2)	4(2)	7(2)
C(54)	28(2)	26(2)	37(3)	-5(2)	4(2)	8(2)
C(55)	36(2)	39(3)	38(3)	-7(2)	-2(2)	7(2)
C(56)	47(3)	54(3)	35(3)	-9(2)	-2(2)	16(2)
C(57)	37(3)	72(4)	38(3)	-21(3)	-7(2)	19(3)
C(58)	31(2)	63(4)	55(4)	-26(3)	-1(2)	4(2)
C(59)	33(2)	41(3)	42(3)	-10(2)	-1(2)	1(2)
C(60)	34(2)	23(2)	30(2)	4(2)	5(2)	3(2)
C(61)	40(2)	26(2)	40(3)	6(2)	8(2)	0(2)
C(62)	57(3)	38(3)	37(3)	5(2)	8(2)	9(2)
C(63)	56(3)	44(3)	48(3)	10(3)	29(3)	8(2)
C(64)	32(2)	48(3)	55(4)	0(3)	13(2)	1(2)
C(65)	31(2)	35(3)	46(3)	2(2)	7(2)	1(2)
C(66)	31(2)	27(2)	29(2)	4(2)	2(2)	-3(2)
C(67)	37(2)	37(3)	38(3)	3(2)	1(2)	4(2)
C(68)	35(2)	59(4)	43(3)	11(3)	-6(2)	6(2)
C(69)	48(3)	60(4)	33(3)	7(3)	-6(2)	-15(3)
C(70)	53(3)	45(3)	41(3)	0(2)	7(3)	-5(2)
C(71)	41(2)	29(2)	38(3)	3(2)	1(2)	3(2)

C(72)	31(2)	48(3)	40(3)	16(2)	5(2)	12(2)
C(73)	20(3)	21(3)	34(4)	14(3)	4(3)	2(2)
C(74)	31(3)	19(3)	35(4)	7(3)	-2(3)	5(2)
C(73A)	52(9)	29(8)	86(14)	2(8)	-5(9)	6(7)
C(74A)	31(6)	41(8)	45(9)	12(7)	13(6)	-2(6)
C(75)	38(2)	41(3)	41(3)	12(2)	7(2)	19(2)
C(76)	24(2)	26(2)	40(3)	8(2)	3(2)	5(2)
C(77)	40(3)	34(3)	63(4)	1(2)	19(3)	2(2)
C(78)	46(3)	25(3)	98(5)	-4(3)	16(3)	-3(2)
C(79)	32(2)	42(3)	73(4)	24(3)	11(3)	1(2)
C(80)	30(2)	59(4)	38(3)	17(3)	5(2)	-2(2)
C(81)	33(2)	41(3)	28(2)	4(2)	1(2)	-2(2)
C(82)	32(2)	29(2)	27(2)	5(2)	8(2)	7(2)
C(83)	37(2)	33(3)	39(3)	0(2)	2(2)	8(2)
C(84)	43(3)	51(3)	44(3)	2(3)	0(2)	16(2)
C(85)	59(3)	45(3)	38(3)	11(2)	5(2)	25(3)
C(86)	50(3)	29(2)	38(3)	6(2)	10(2)	10(2)
C(87)	39(2)	30(2)	34(3)	7(2)	16(2)	7(2)
C(88)	30(2)	27(2)	33(2)	0(2)	4(2)	1(2)
C(89)	28(2)	28(2)	32(2)	0(2)	5(2)	4(2)
C(90)	42(2)	29(2)	46(3)	2(2)	1(2)	6(2)
N(2)	38(2)	40(2)	40(2)	0(2)	-7(2)	7(2)
C(91)	39(3)	79(5)	60(4)	-6(3)	-15(3)	22(3)
C(92)	47(4)	172(10)	78(6)	-45(6)	-5(4)	-15(4)
C(93)	77(5)	156(9)	77(5)	-60(6)	-41(4)	53(5)
C(94)	121(7)	125(8)	94(7)	9(6)	-24(5)	79(6)
B(1)	121(9)	68(6)	116(9)	26(6)	-63(8)	-29(6)
B(2)	99(7)	56(5)	84(7)	1(5)	-19(6)	-14(5)
F(1)	116(4)	152(5)	92(4)	48(4)	-31(3)	-17(4)

F(2)	165(6)	122(6)	295(11)	63(6)	-57(6)	29(5)
F(3)	136(5)	225(8)	91(4)	1(5)	-16(4)	-26(5)
F(4)	271(9)	158(7)	175(7)	20(5)	-155(7)	-76(6)
F(5)	131(5)	96(5)	338(12)	-25(6)	31(6)	21(4)
F(6)	151(5)	104(4)	109(4)	35(3)	-51(4)	-6(4)
F(7)	194(6)	209(8)	134(6)	11(5)	-97(5)	-78(6)
F(8)	136(5)	203(7)	88(4)	-13(4)	-3(4)	-44(5)
N(3)	113(6)	91(6)	184(9)	53(6)	53(6)	44(5)
C(95)	97(6)	88(6)	84(6)	18(5)	24(5)	48(5)
C(96)	100(6)	106(8)	116(8)	28(6)	-14(6)	-2(6)
N(4)	106(6)	83(6)	146(8)	10(6)	28(6)	33(5)
C(97)	92(12)	75(13)	96(15)	-9(10)	25(12)	25(11)
C(98)	131(16)	78(13)	160(20)	-15(13)	-33(15)	6(12)
C(97A)	92(12)	79(13)	67(11)	-39(10)	15(10)	-2(10)
C(98A)	170(18)	60(10)	120(16)	4(10)	54(14)	11(11)

Table A8. Hydrogen coordinates (x 10^4) and isotropic displacement parameters ($Å^2$x 10 ^{3}) for $\{[Ag_2(dppb)_3(t\text{-BuNC})_2](BF_4)\}_n$.

	x	y	z	U(eq)
H(3A)	4684	4119	3542	141
H(3B)	6059	4295	3459	141
H(3C)	5203	4037	2924	141
H(4A)	5799	6021	2697	136
H(4B)	5894	5211	2404	136
H(4C)	6746	5469	2941	136
H(5A)	4439	5377	3941	109
H(5B)	4786	6120	3588	109
H(5C)	5792	5659	3887	109
H(7A)	2365	3263	684	40
H(8A)	3779	2383	830	51
H(9A)	5555	2731	1332	58
H(10A)	5900	3947	1696	55
H(11A)	4505	4830	1552	43
H(13A)	3595	5152	53	39
H(14A)	4785	6161	-260	48
H(15A)	5107	7251	299	52
H(16A)	4263	7323	1179	52
H(17A)	3037	6326	1491	45
H(18A)	1758	4480	106	33
H(18B)	845	4072	521	33
H(19A)	-159	5184	589	41
H(19B)	784	5624	204	41
H(21A)	-1351	4271	1576	47

H(22A)	-2474	4020	748	55
H(23A)	-2176	2987	186	61
H(24A)	-701	2200	442	64
H(25A)	415	2426	1294	51
H(27A)	930	3961	3328	46
H(28A)	-179	3849	4130	52
H(29A)	-2137	3373	4045	65
H(30A)	-2977	2994	3167	53
H(31A)	-1877	3097	2349	44
H(33A)	83	7048	1106	41
H(34A)	-1346	7189	381	51
H(35A)	-3123	6480	391	58
H(36A)	-3523	5647	1127	53
H(37A)	-2091	5505	1849	46
H(39A)	-1264	7217	2564	46
H(40A)	-2103	7395	3431	55
H(41A)	-1975	6499	4141	64
H(42A)	-936	5459	3997	79
H(43A)	-30	5283	3138	59
H(44A)	1516	7054	1728	34
H(44B)	666	7433	2155	34
H(45A)	1793	7048	2948	36
H(45B)	2602	6599	2541	36
H(46A)	2485	8208	2533	37
H(46B)	3304	7756	2134	37
H(47A)	4437	7393	2937	35
H(47B)	3577	7775	3358	35
H(49A)	6371	7615	2536	43
H(50A)	7259	7428	1688	51

H(51A)	7113	8299	954	53
H(52A)	6095	9360	1088	53
H(53A)	5122	9528	1924	46
H(55A)	4981	7837	4000	45
H(56A)	6415	7732	4728	54
H(57A)	8201	8429	4700	58
H(58A)	8588	9239	3945	60
H(59A)	7170	9331	3210	47
H(61A)	4061	10858	1632	42
H(62A)	5194	10933	824	52
H(63A)	7174	11374	923	58
H(64A)	7983	11784	1794	54
H(65A)	6863	11697	2612	45
H(67A)	6410	10638	3391	45
H(68A)	7501	10970	4216	55
H(69A)	7053	12003	4756	58
H(70A)	5475	12682	4485	56
H(71A)	4386	12373	3637	43
H(72A)	2720	11575	2384	46
H(72B)	2847	11815	3041	46
H(73A)	3849	12551	2127	30
H(73B)	4334	12729	2767	30
H(74A)	2414	13074	3003	34
H(74B)	3002	13619	2541	34
H(73C)	1945	11206	2329	67
H(73D)	2580	11751	1915	67
H(74C)	1024	12257	2725	47
H(74D)	661	12095	2088	47
H(75B)	1035	13301	2300	59

H(75C)	1859	12993	1821	59
H(77A)	2097	8478	3618	54
H(78A)	888	7502	3976	68
H(79A)	3	7659	4845	58
H(80A)	203	8824	5308	51
H(81A)	1347	9815	4939	41
H(83A)	476	9984	3432	43
H(84A)	-906	10842	3219	54
H(85A)	-561	12104	3510	55
H(86A)	1193	12490	4009	46
H(87A)	2587	11622	4224	41
H(88A)	4104	10867	4448	36
H(88B)	3216	10467	4879	36
H(89A)	5168	9782	4422	43
H(89B)	4253	9350	4825	43
H(92A)	-839	8936	2252	151
H(92B)	-1666	9552	1997	151
H(92C)	-811	9755	2544	151
H(93A)	110	8746	1384	154
H(93B)	762	9433	1059	154
H(93C)	-644	9332	1040	154
H(94A)	598	10774	1423	166
H(94B)	68	10888	2036	166
H(94C)	-793	10678	1492	166

RMN ^{1}H de $[Cu(dppe)(CN\text{-}t\text{-}Bu)_2]BF_4$.

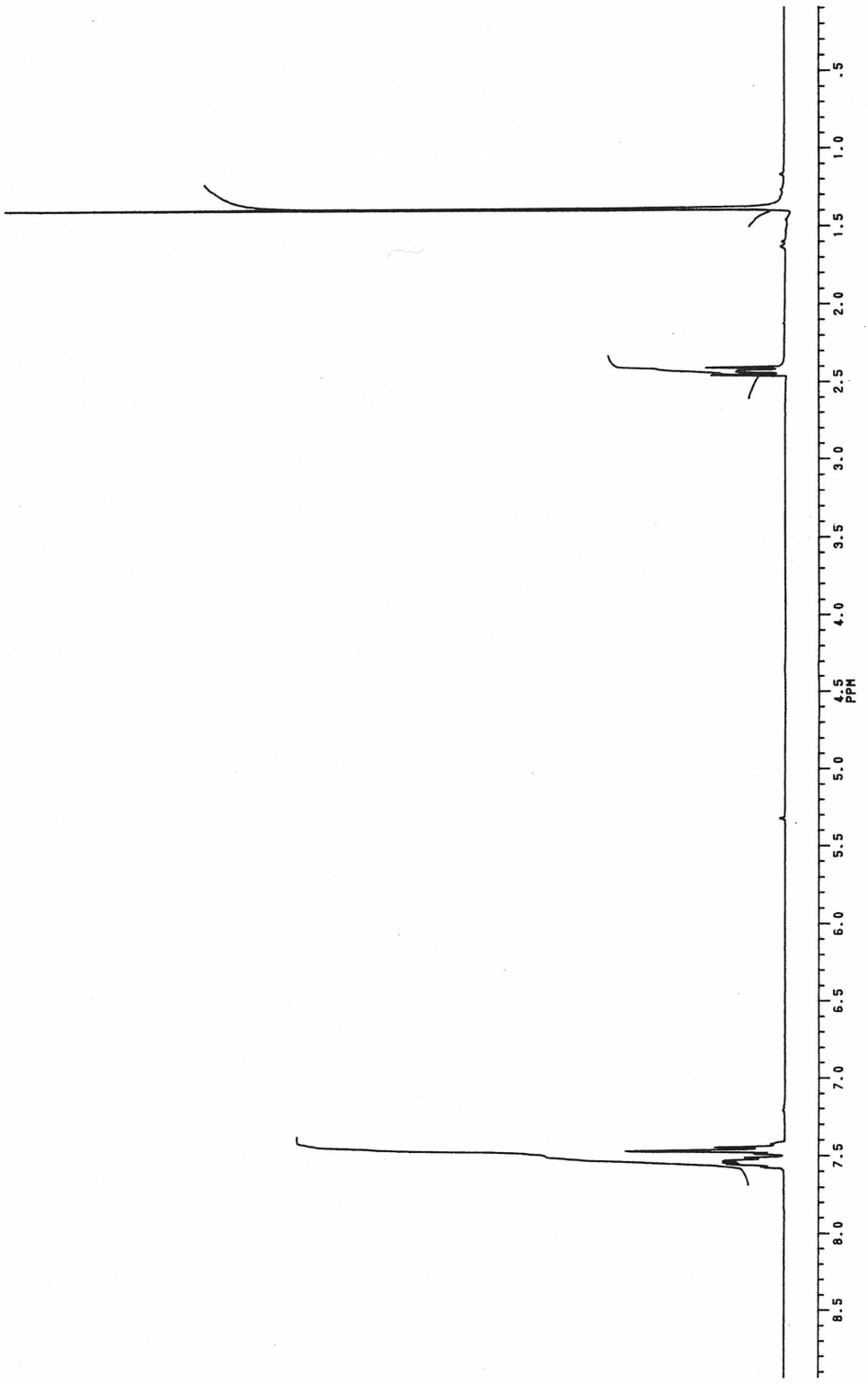

RMN ^{31}P de $[Cu(dppe)(CN\text{-}t\text{-}Bu)_2]BF_4$.

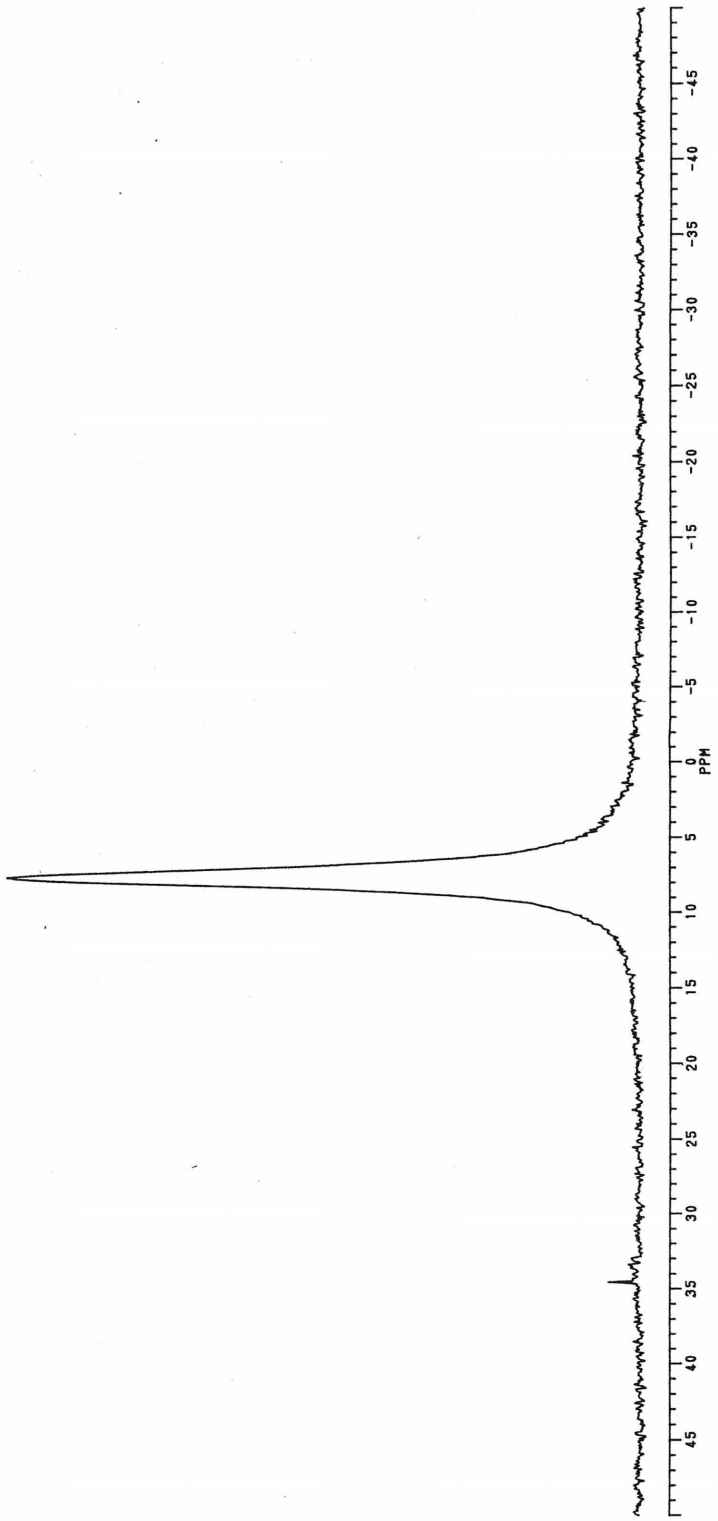

RMN ^{13}C de $[Cu(dppe)(CN\text{-}t\text{-}Bu)_2]BF_4$.

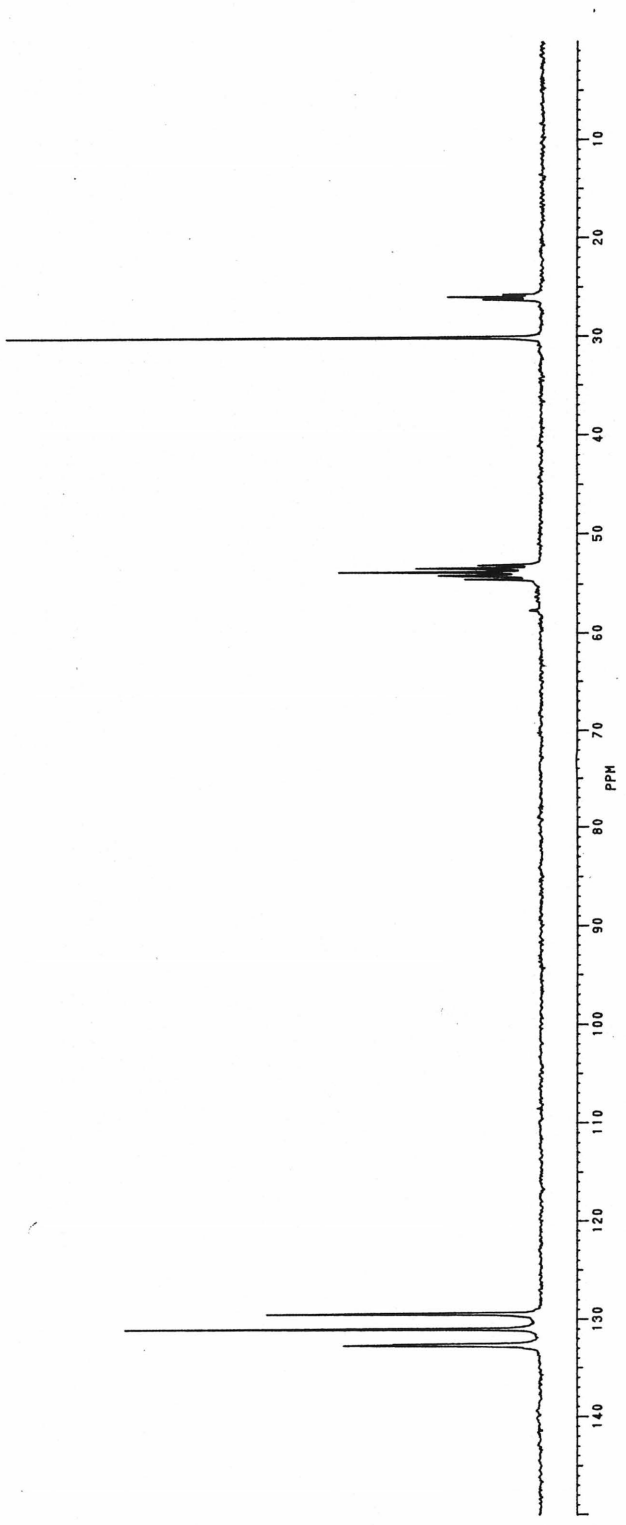

RMN ^{1}H de $[Cu(dppp)(CN\text{-}t\text{-}Bu)_2]BF_4$.

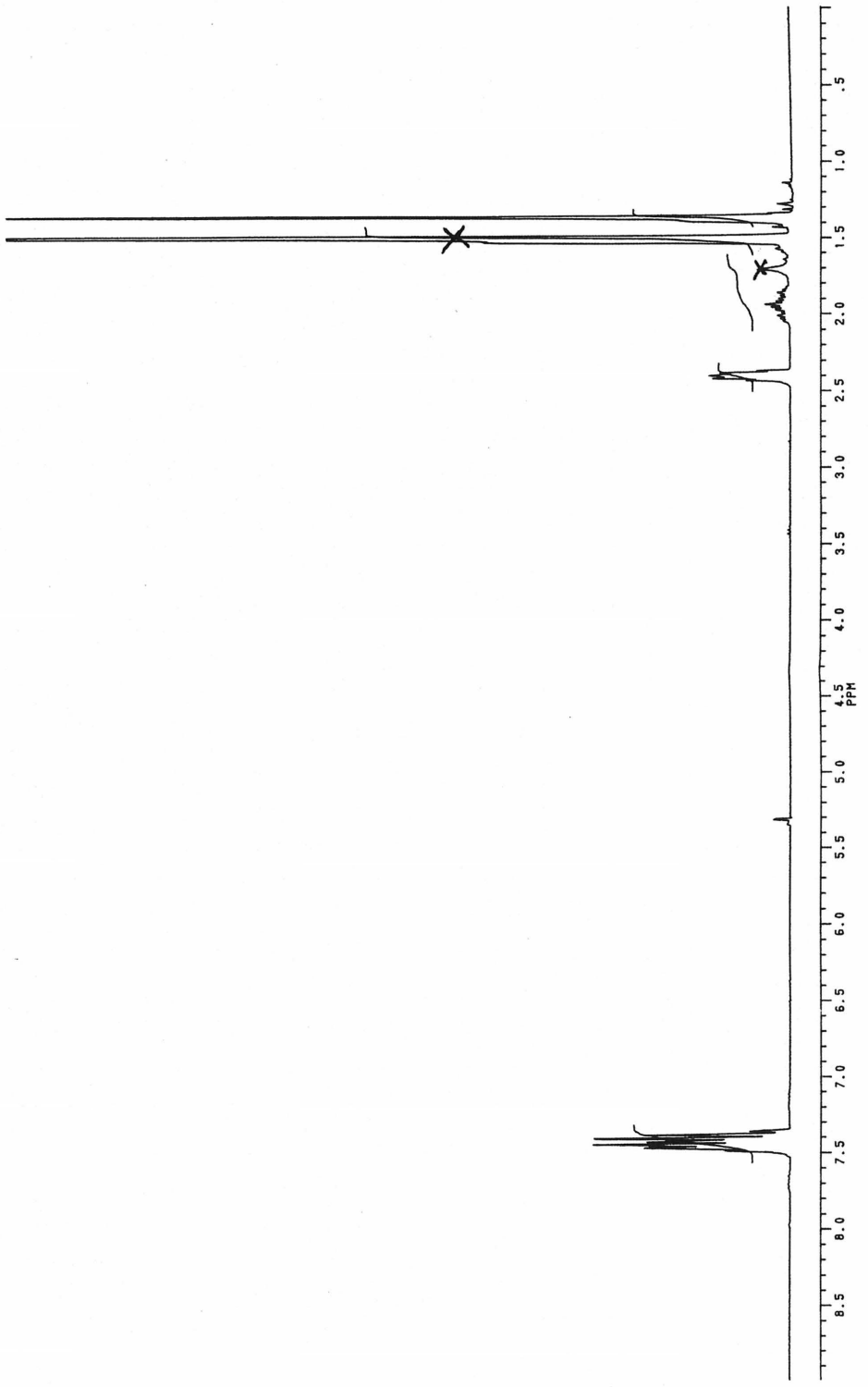

RMN ^{31}P de $[Cu(dppp)(CN\text{-}t\text{-}Bu)_2]BF_4$.

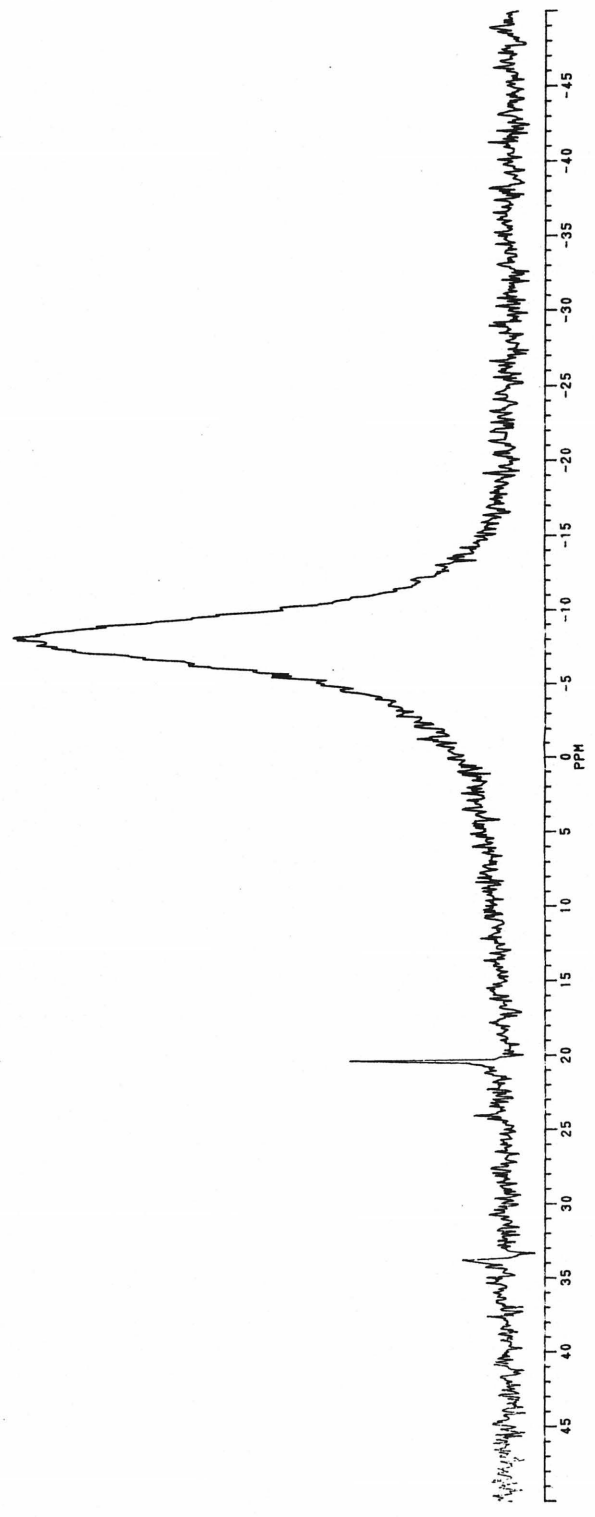

RMN ^{13}C de $[Cu(dppp)(CN\text{-}t\text{-}Bu)_2]BF_4$.

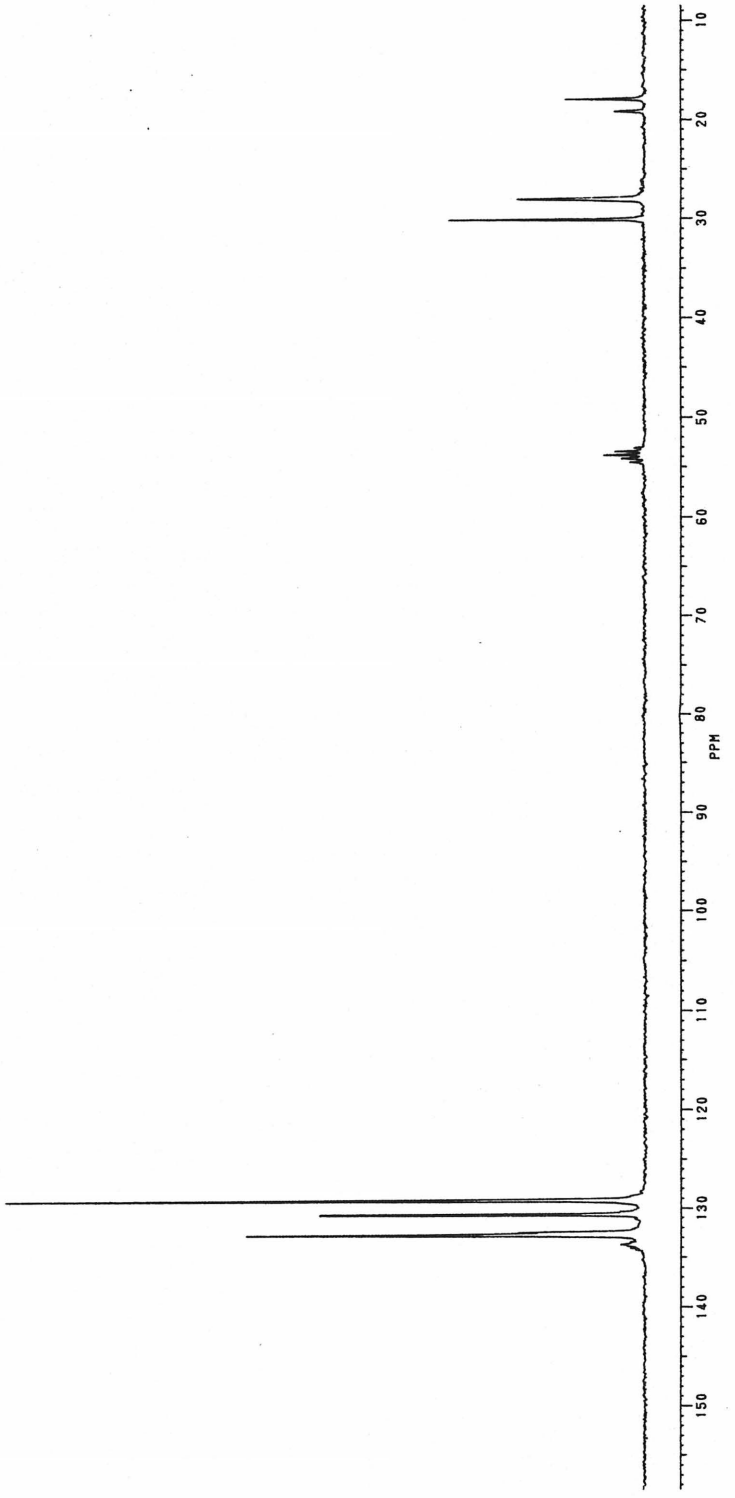

RMN ^{1}H de $\{[Cu(dppb)(CN\text{-}t\text{-}Bu)_2]BF_4\}_n$.

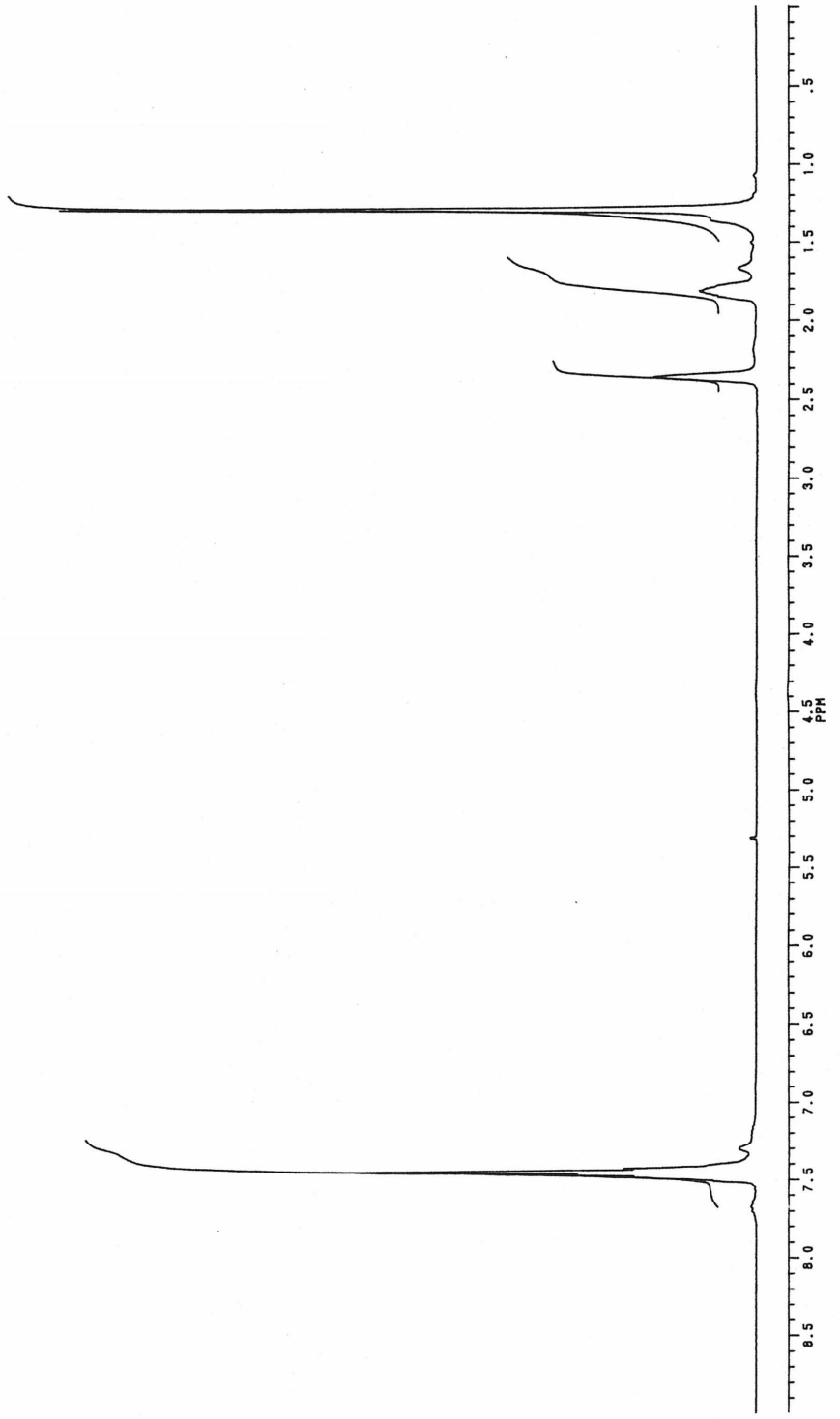

RMN ^{31}P de $\{[Cu(dppb)(CN\text{-}t\text{-}Bu)_2]BF_4\}_n$.

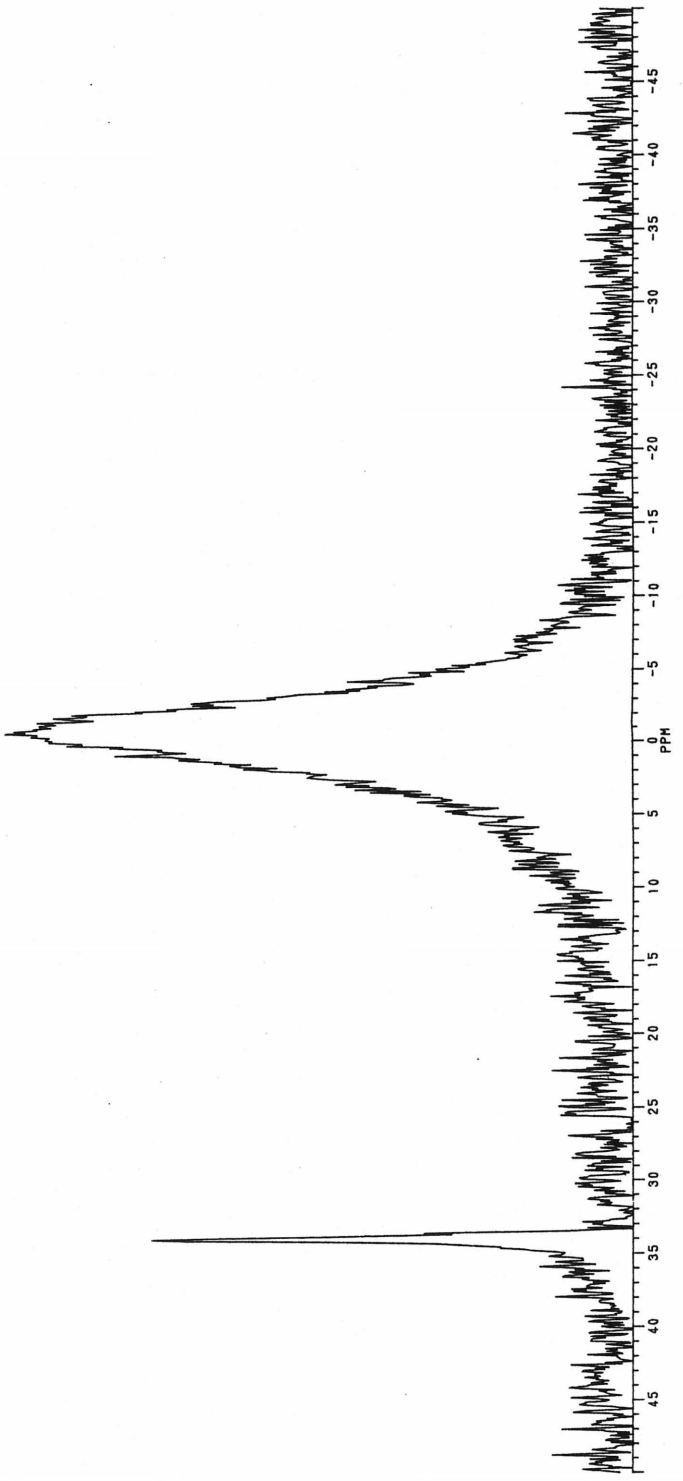

RMN ^{13}C de $\{[Cu(dppb)(CN\text{-}t\text{-}Bu)_2]BF_4\}_n$.

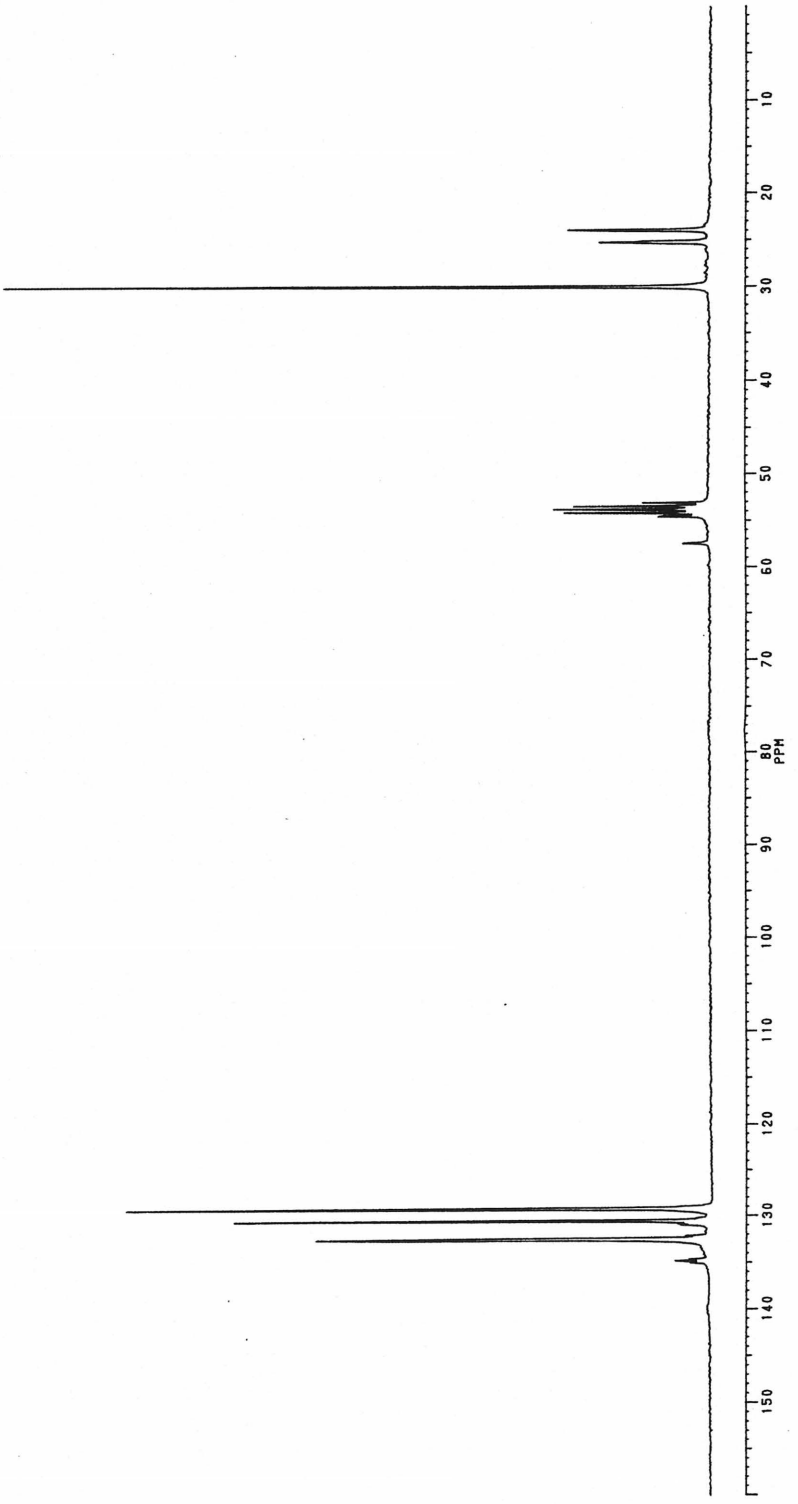

RMN ^{1}H de $\{[Cu(dpppen)(CN\text{-}t\text{-}Bu)_2]BF_4\}_n$.

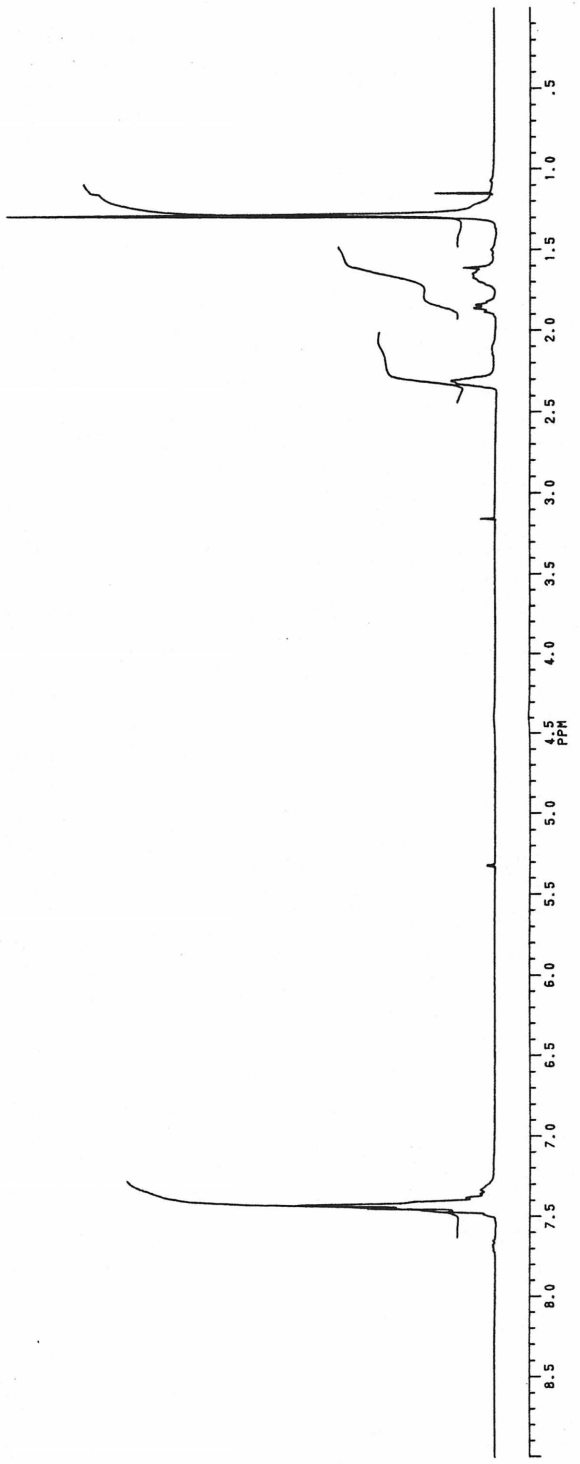

RMN ^{31}P de $\{[Cu(dpppen)(CN\text{-}t\text{-}Bu)_2]BF_4\}_n$.

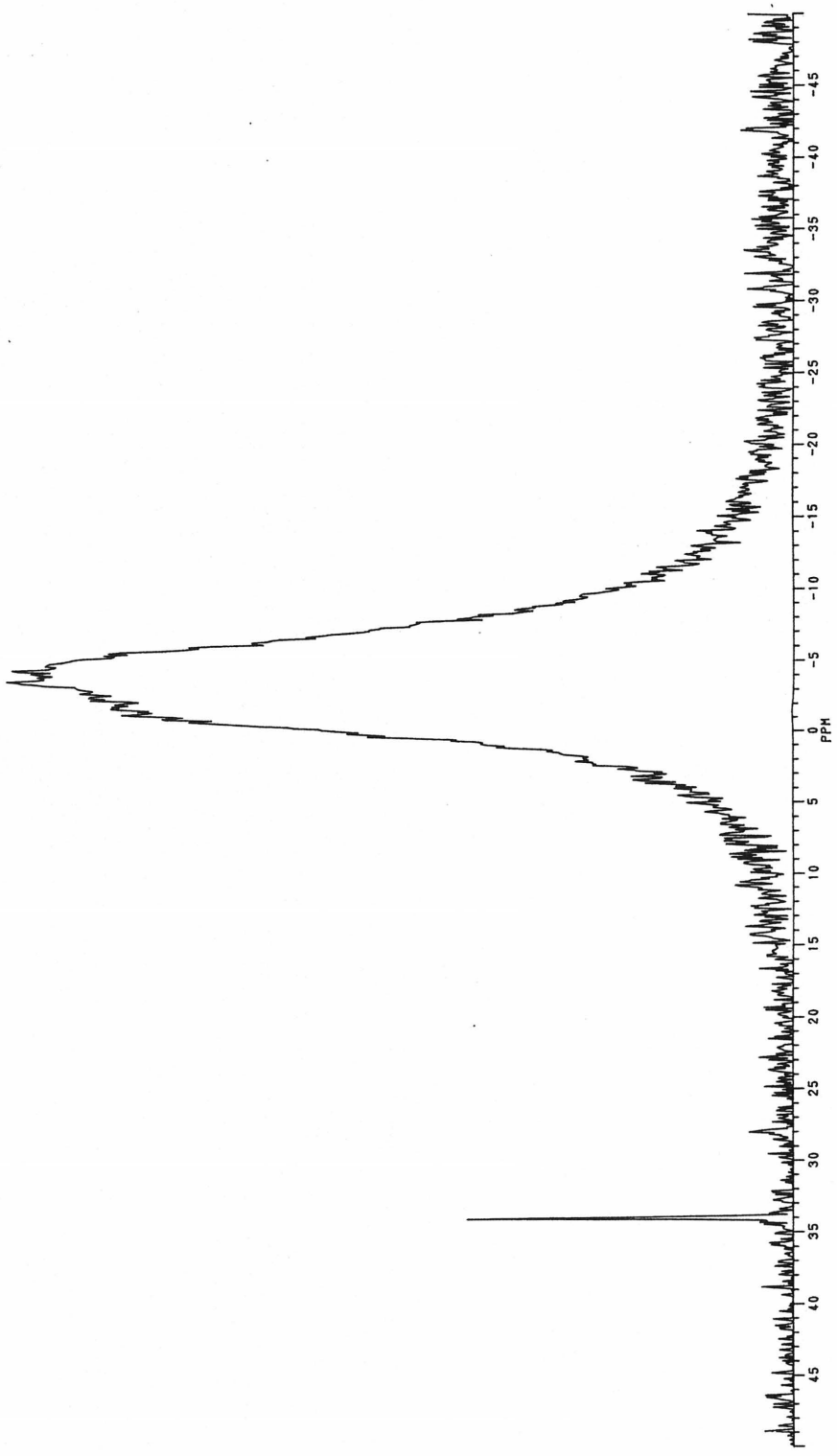

RMN ^{13}C de $\{[Cu(dpppen)(CN\text{-}t\text{-}Bu)_2]BF_4\}_n$.

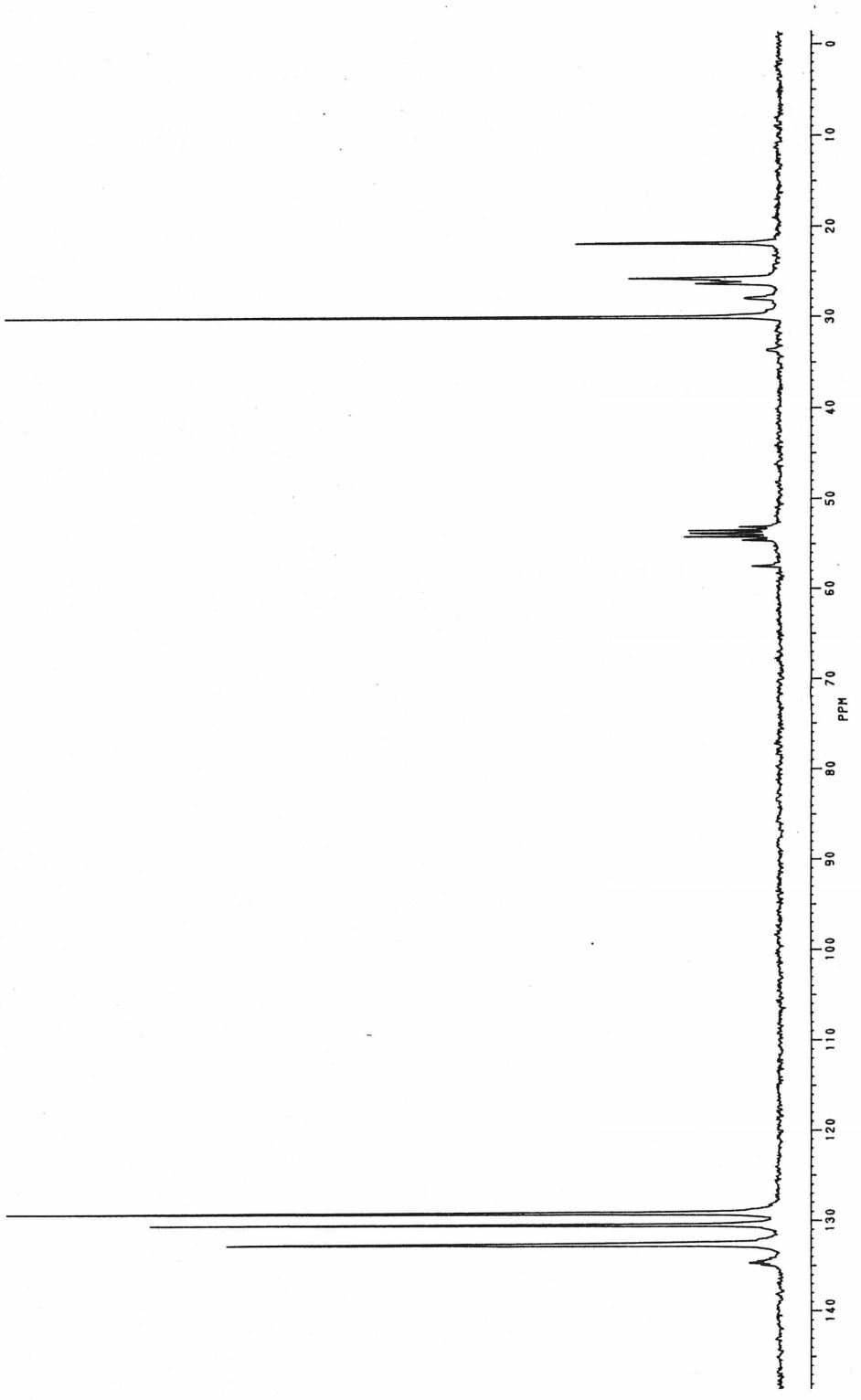

RMN ^{1}H de $\{[Cu(dpph)(CN\text{-}t\text{-}Bu)_2]BF_4\}_n$.

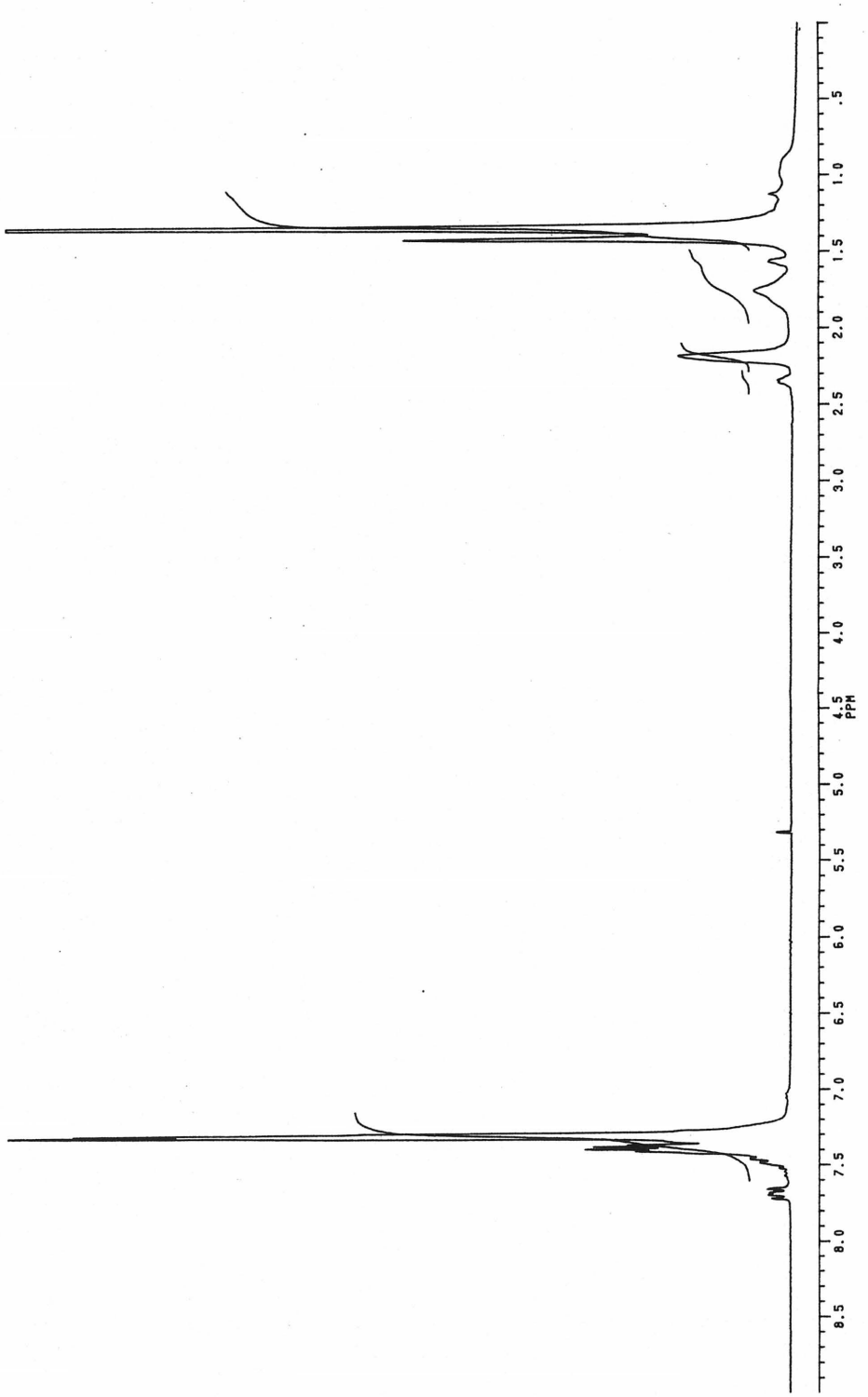

RMN ^{31}P de $\{[Cu(dpph)(CN\text{-}t\text{-}Bu)_2]BF_4\}_n$.

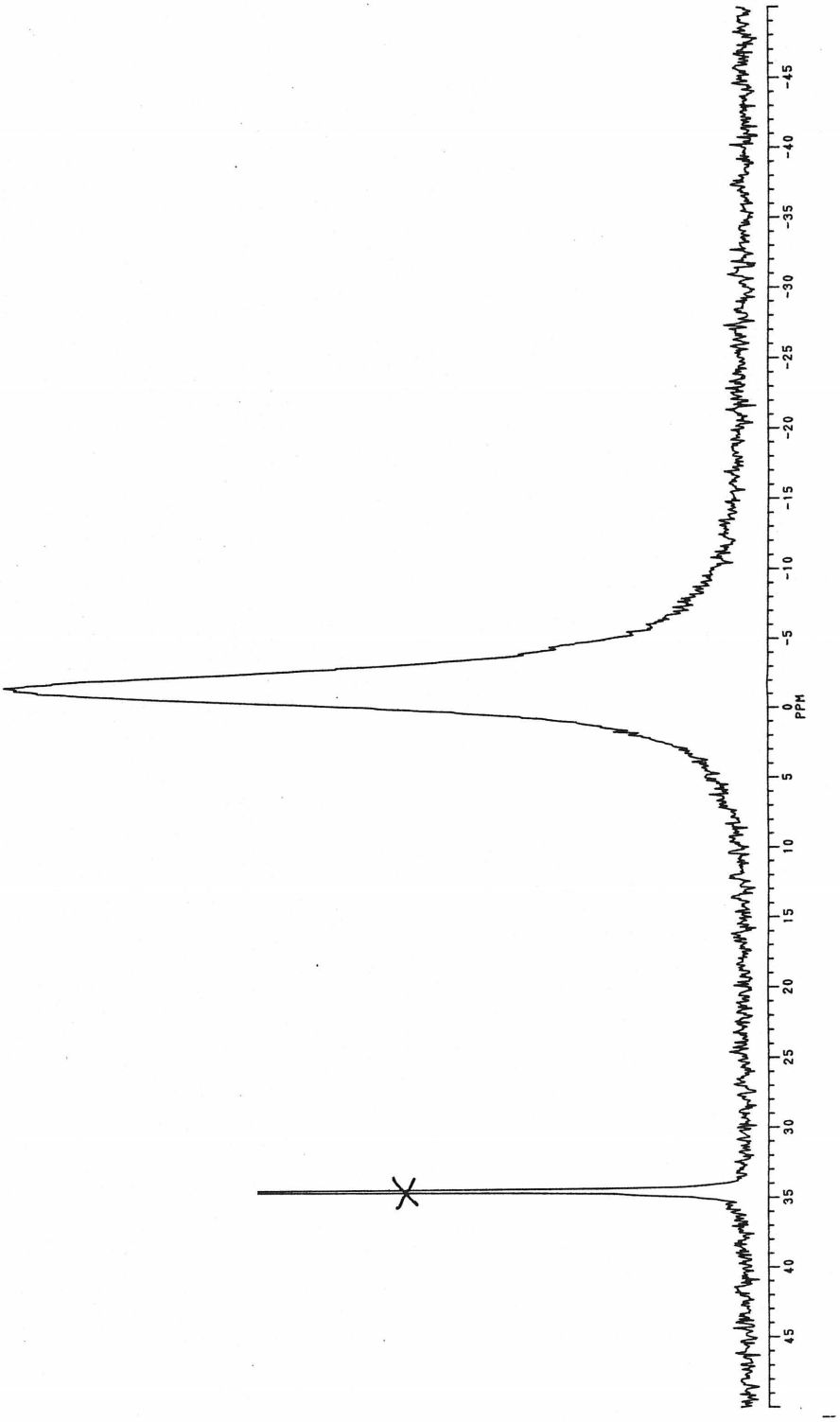

RMN ^{13}C de $\{[Cu(dpph)(CN\text{-}t\text{-}Bu)_2]BF_4\}_n$.

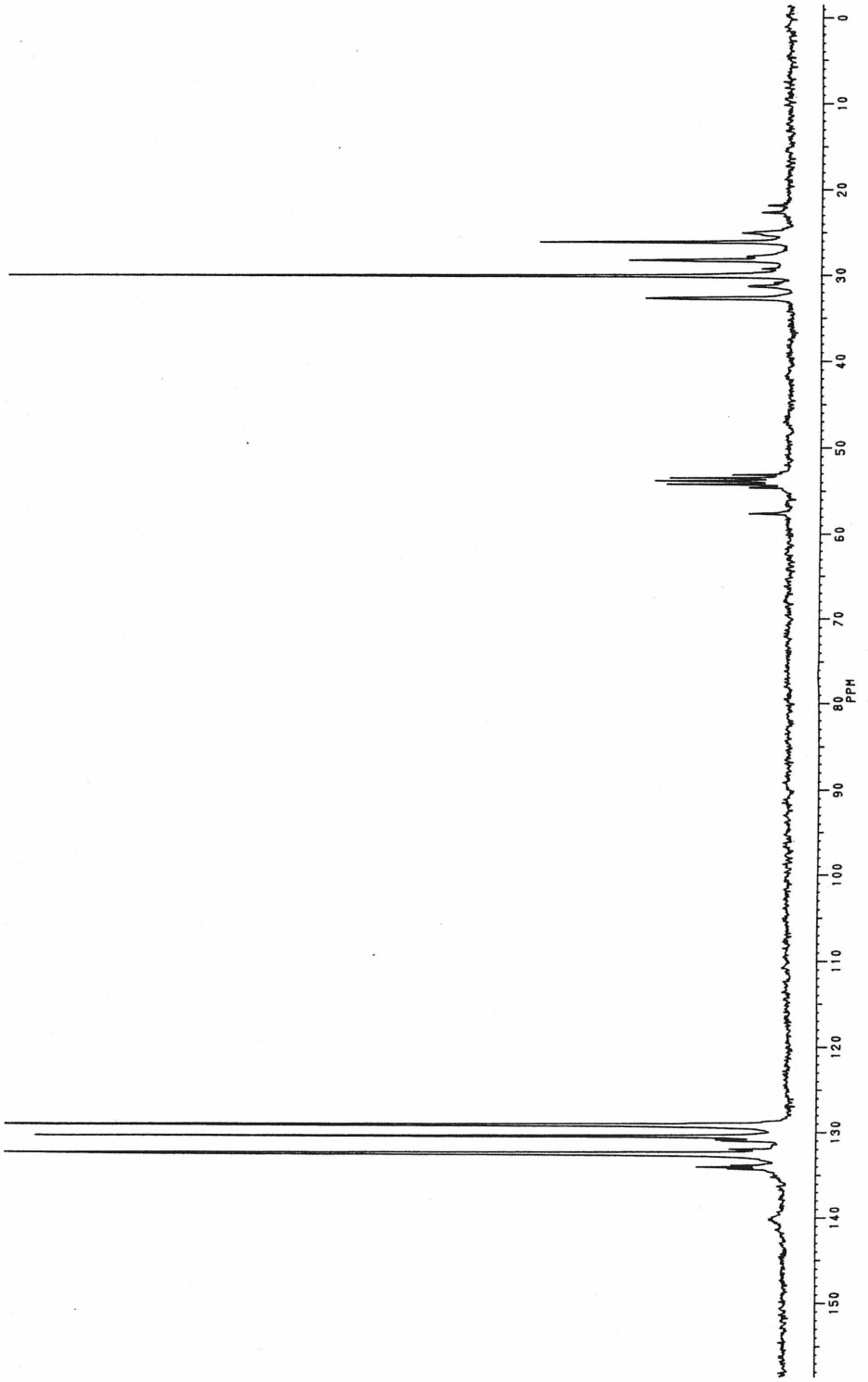

RMN ^{1}H de $\{[Cu_2(dppm)_2(dmb)_2](BF_4)_2\}_n$.

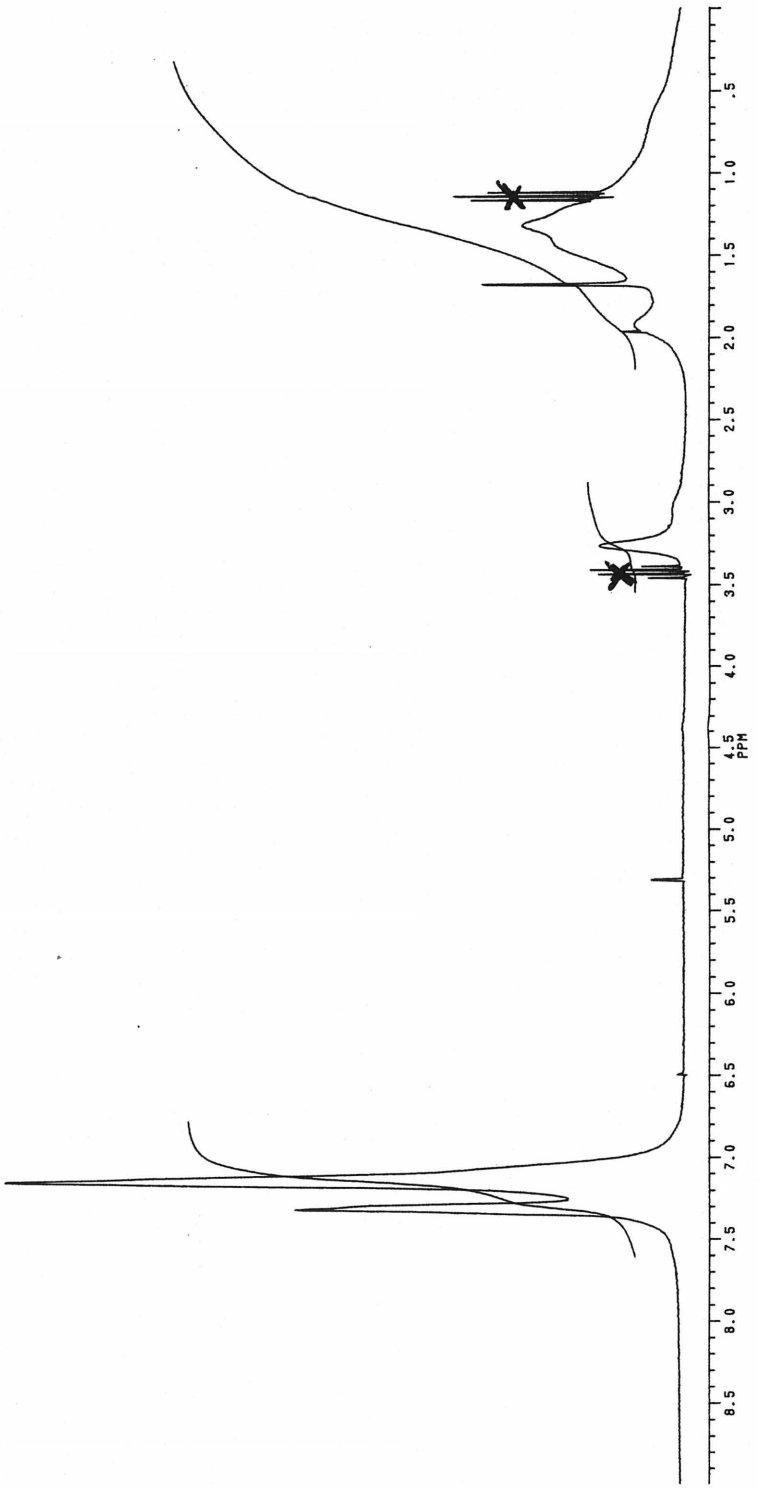

RMN ^{31}P de $\{[Cu_2(dppm)_2(dmb)_2](BF_4)_2\}_n$.

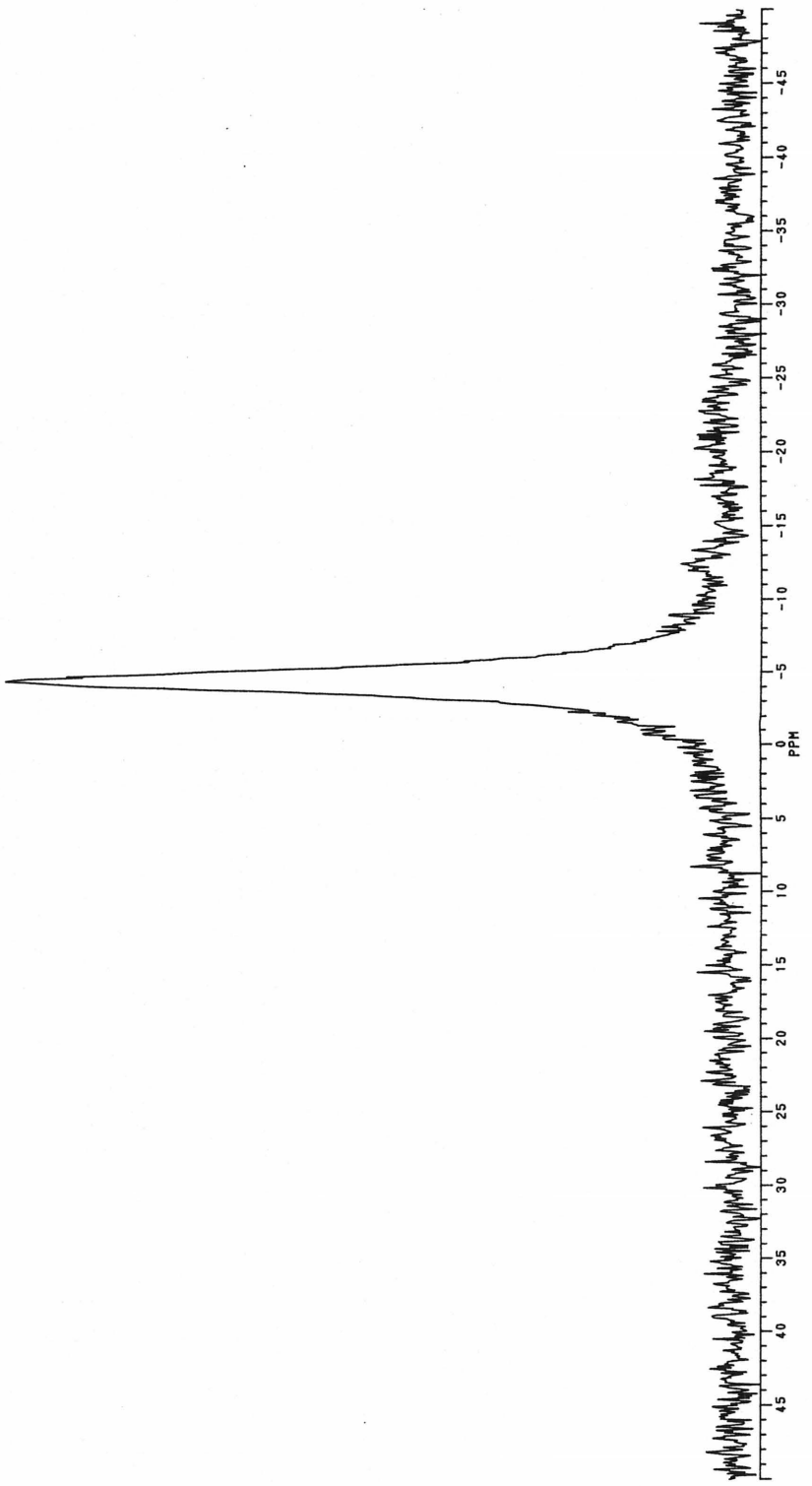

RMN ^{13}C de $\{[Cu_2(dppm)_2(dmb)_2](BF_4)_2\}_n$.

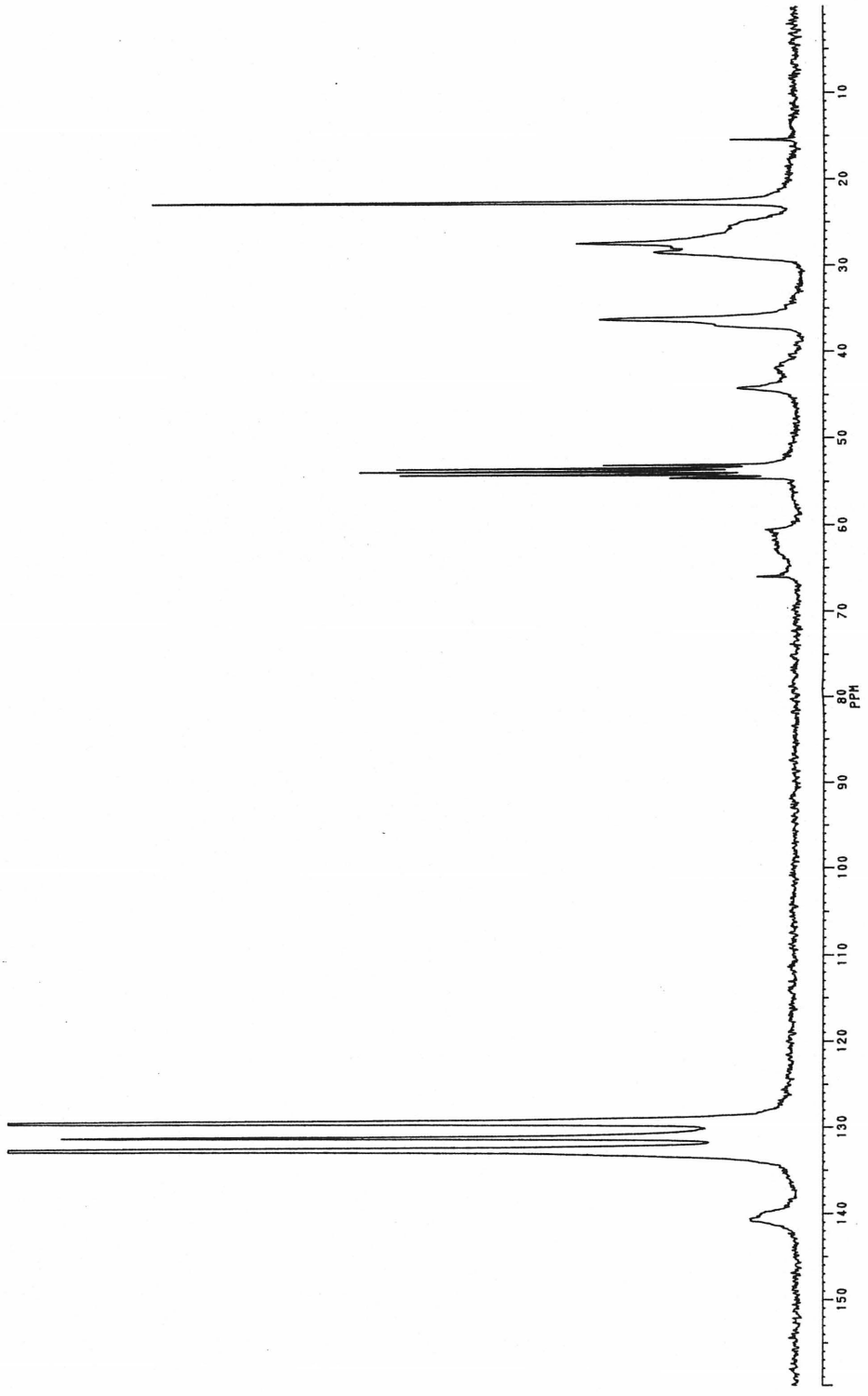

RMN ^{1}H de $\{[Cu(dppe)(dmb)]BF_4\}_n$.

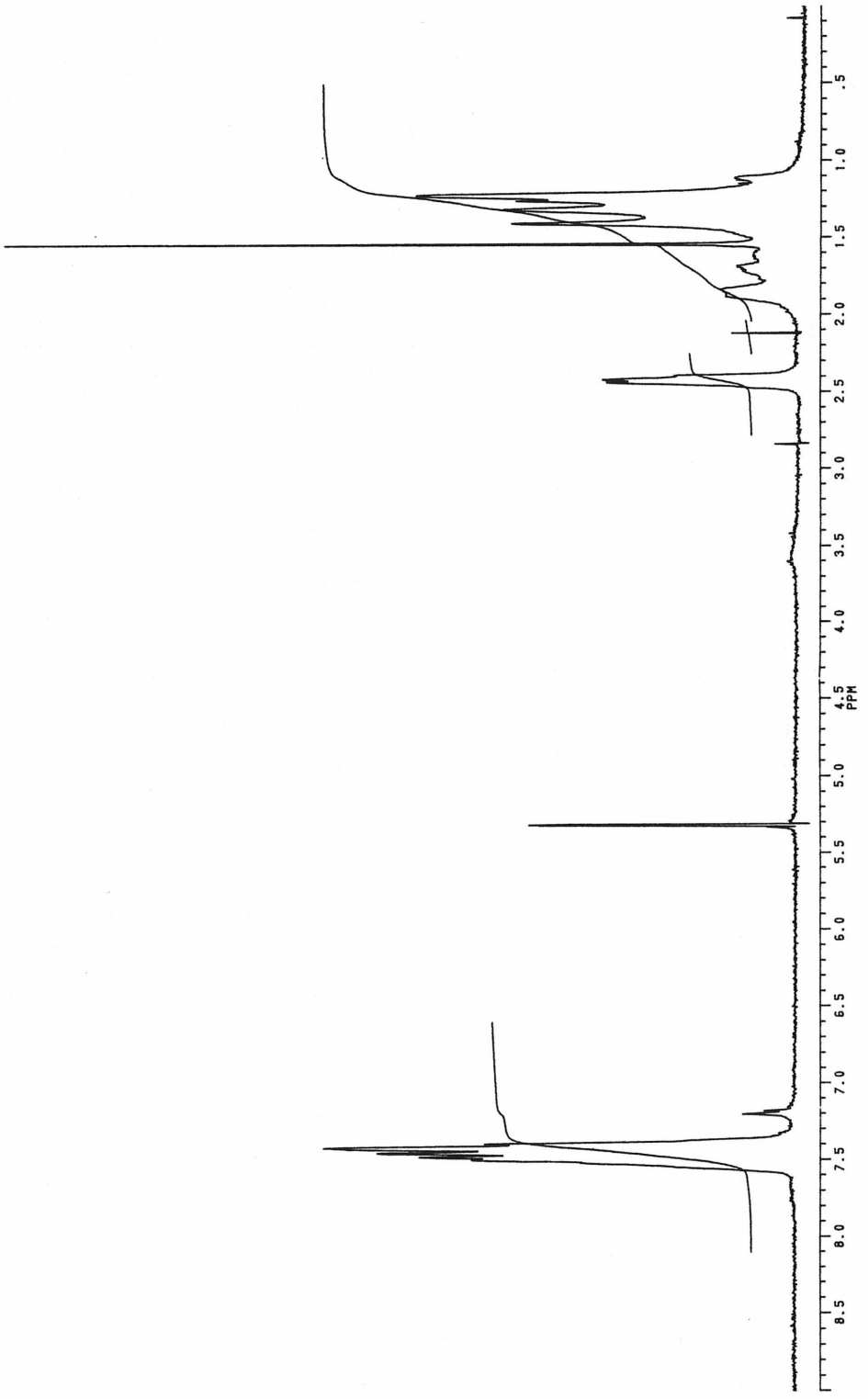

RMN ^{31}P de $\{[Cu(dppe)(dmb)]BF_4\}_n$.

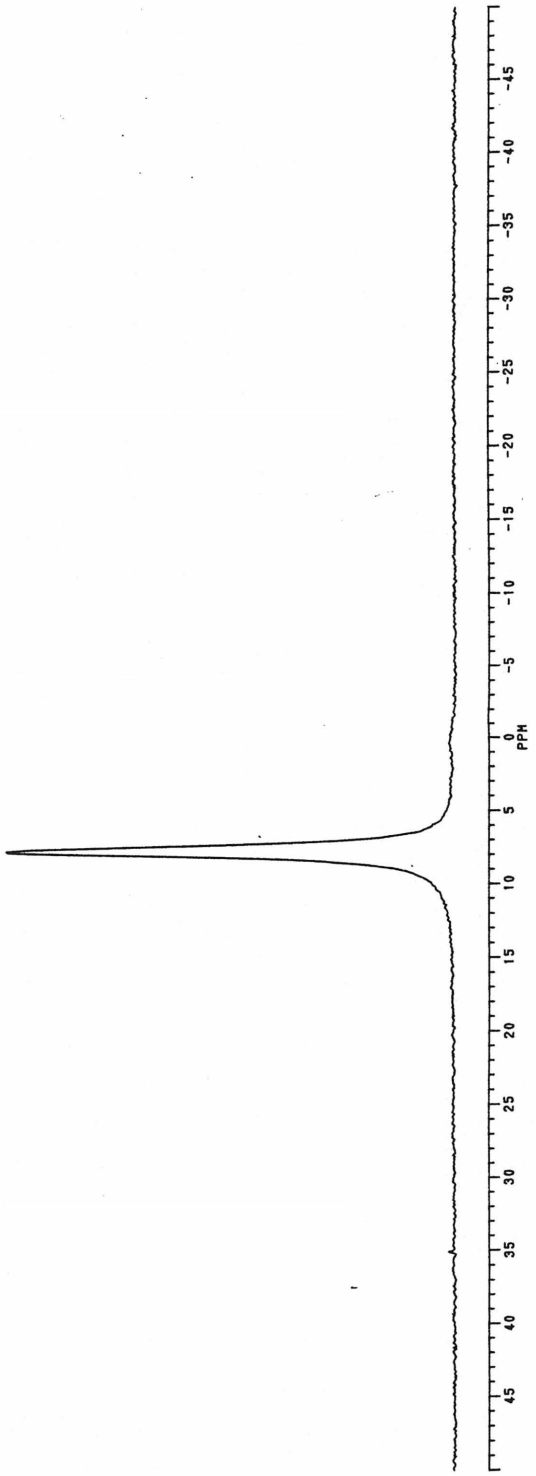

RMN ^{13}C de $\{[Cu(dppe)(dmb)]BF_4\}_n$.

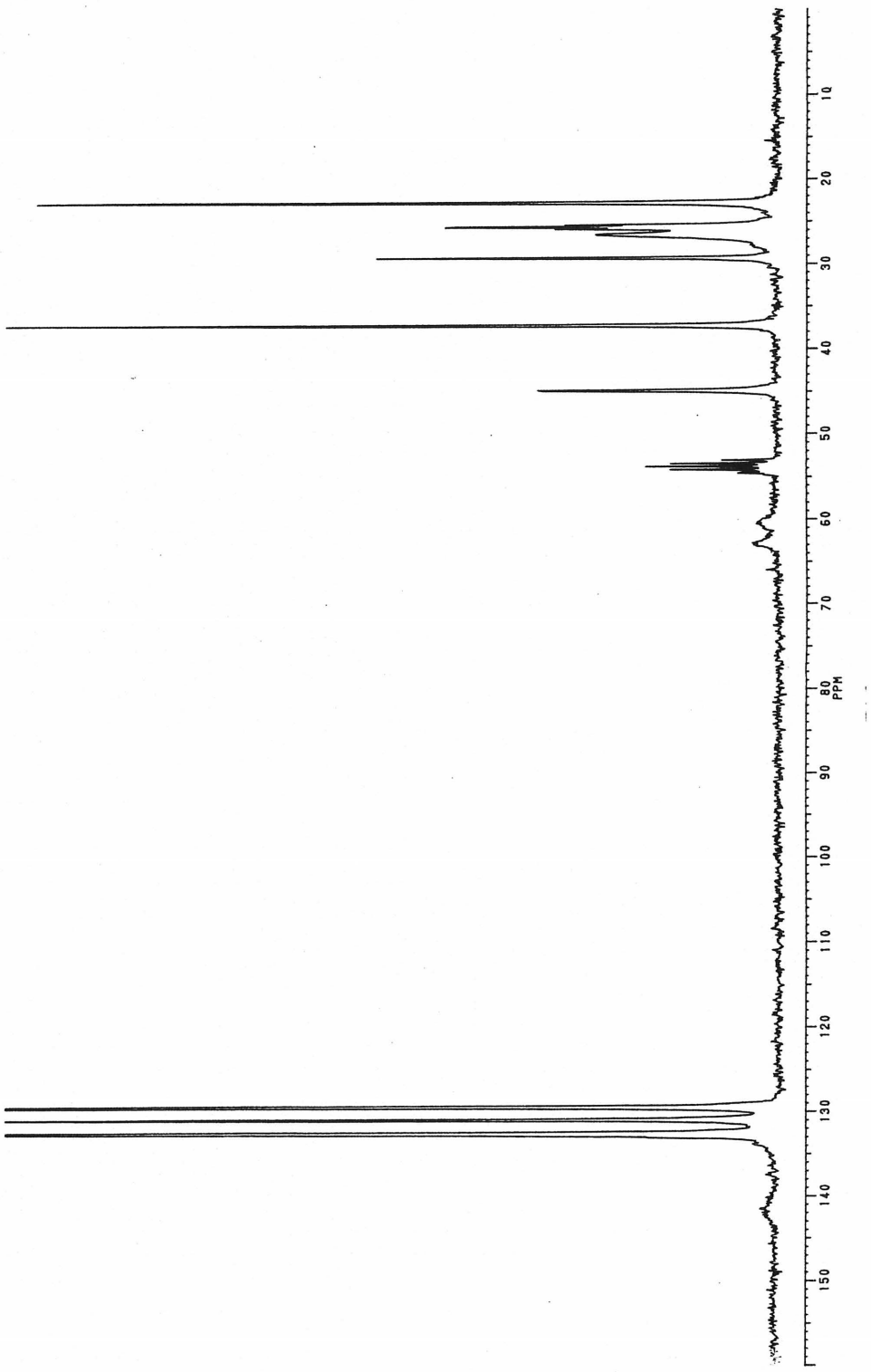

RMN ^{1}H de $\{[Cu(dppp)(dmb)]BF_4\}_n$.

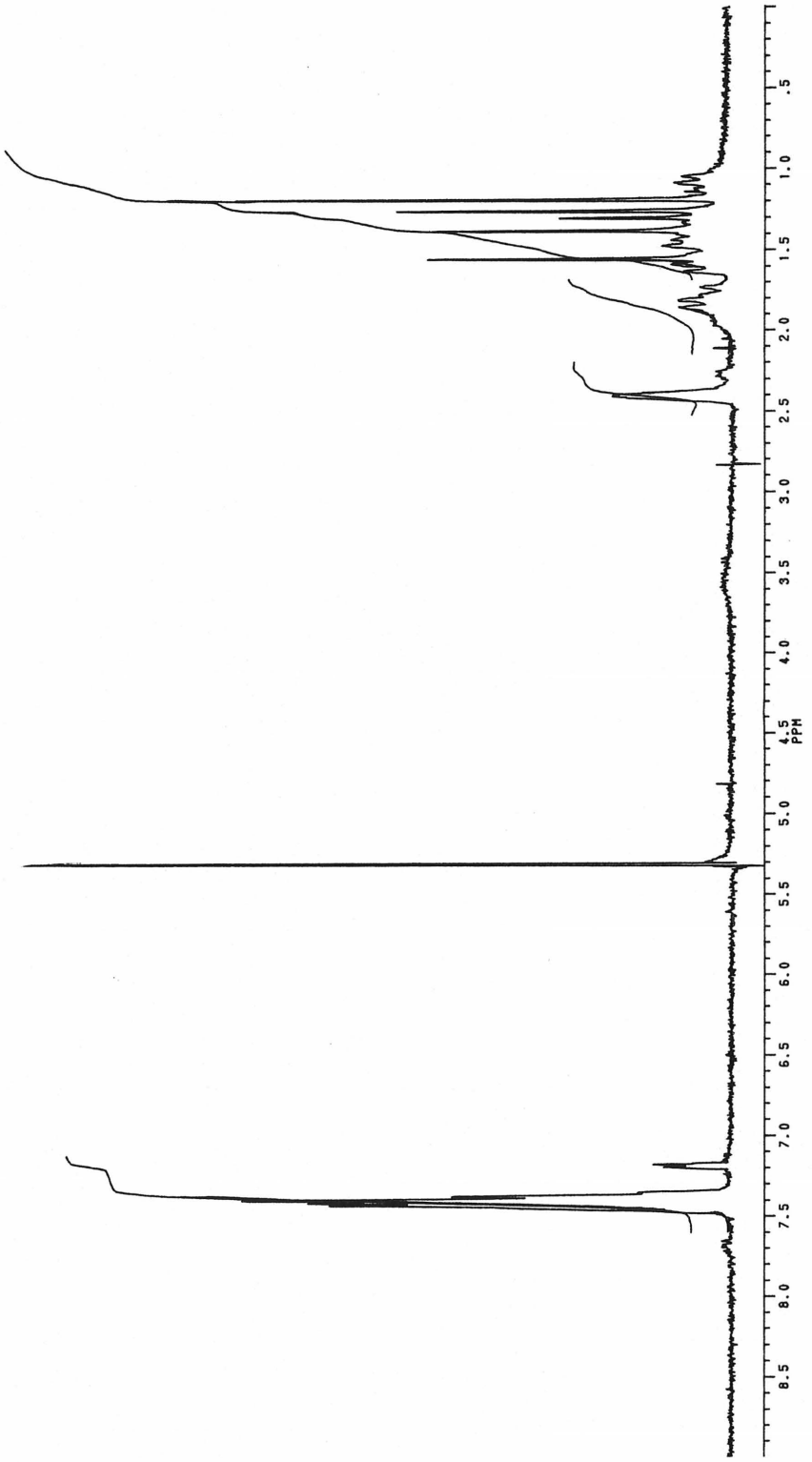

RMN ^{31}P de $\{[Cu(dppp)(dmb)]BF_4\}_n$.

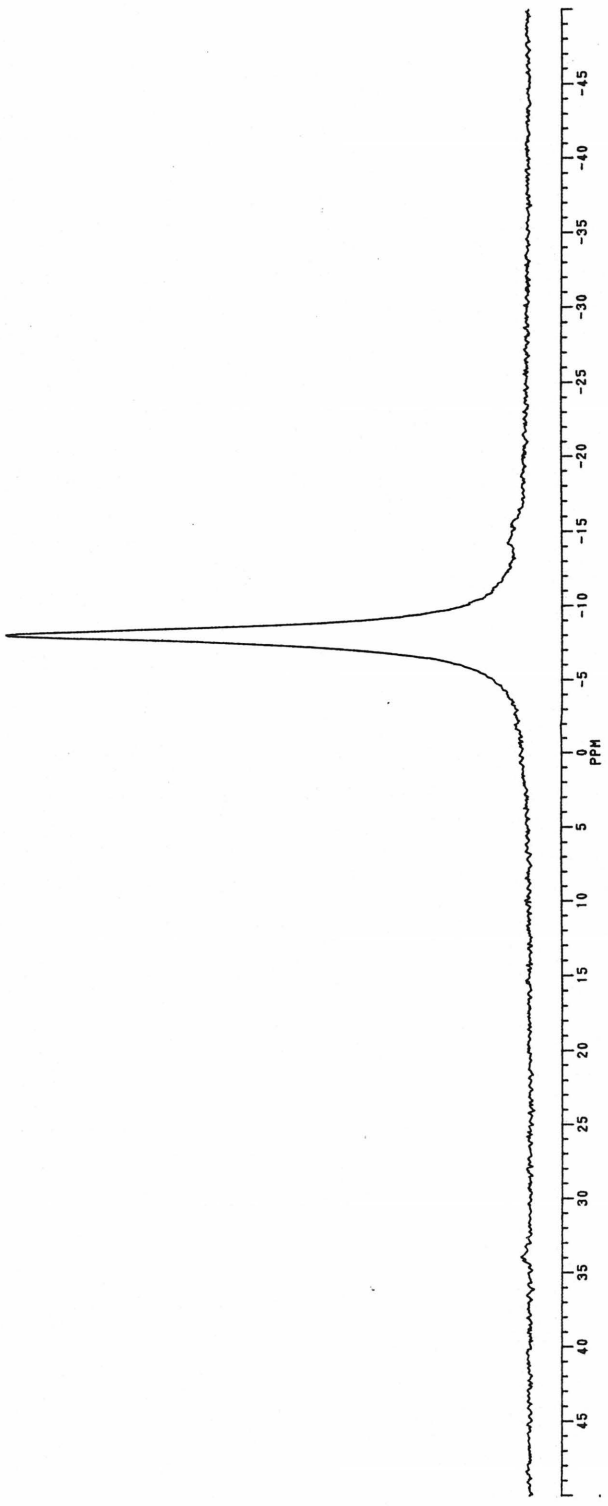

RMN ^{13}C de $\{[Cu(dppp)(dmb)]BF_4\}_n$.

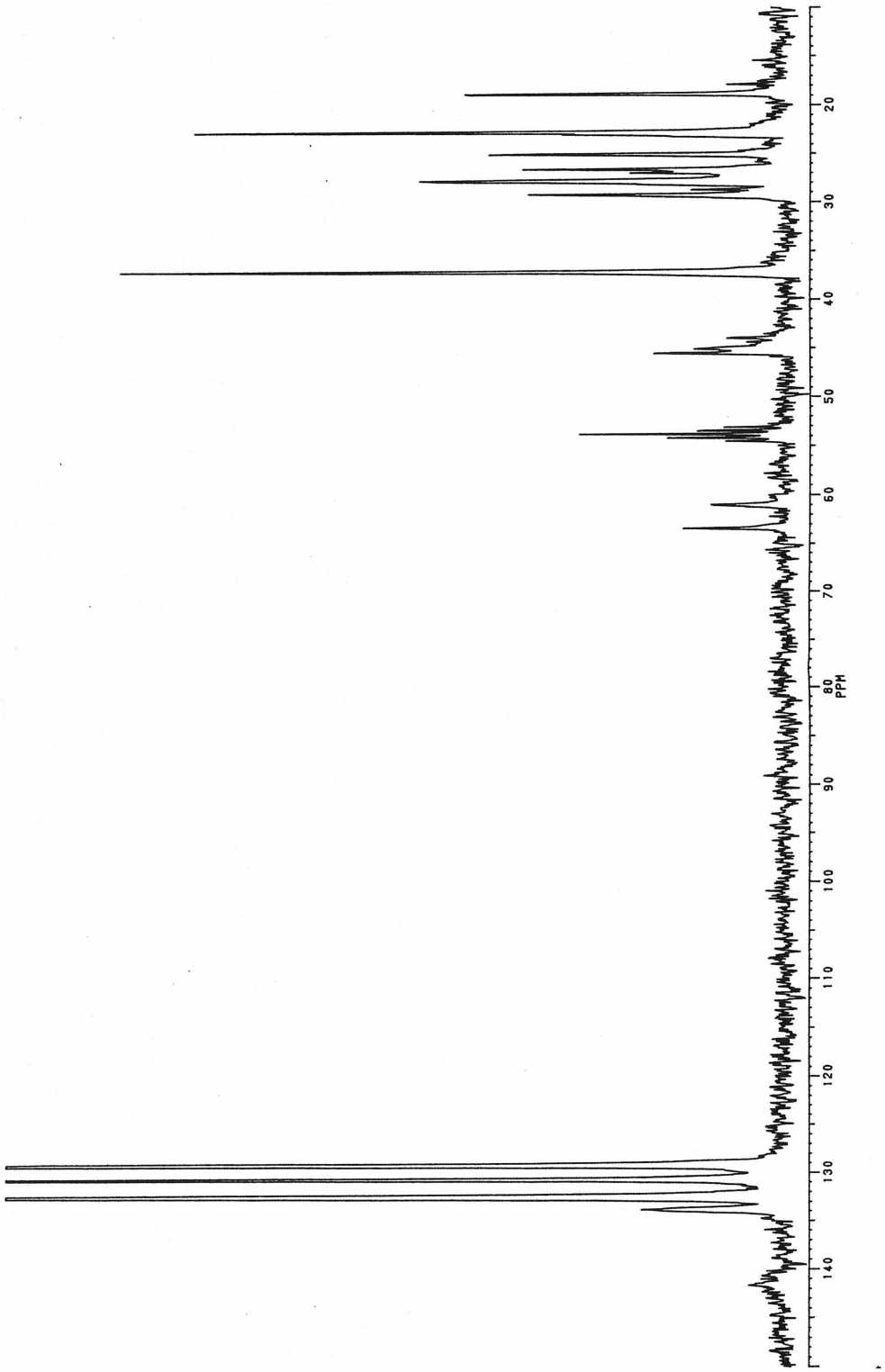

RMN ^{1}H de $\{[Cu(dppb)(dmb)]BF_4\}_n$.

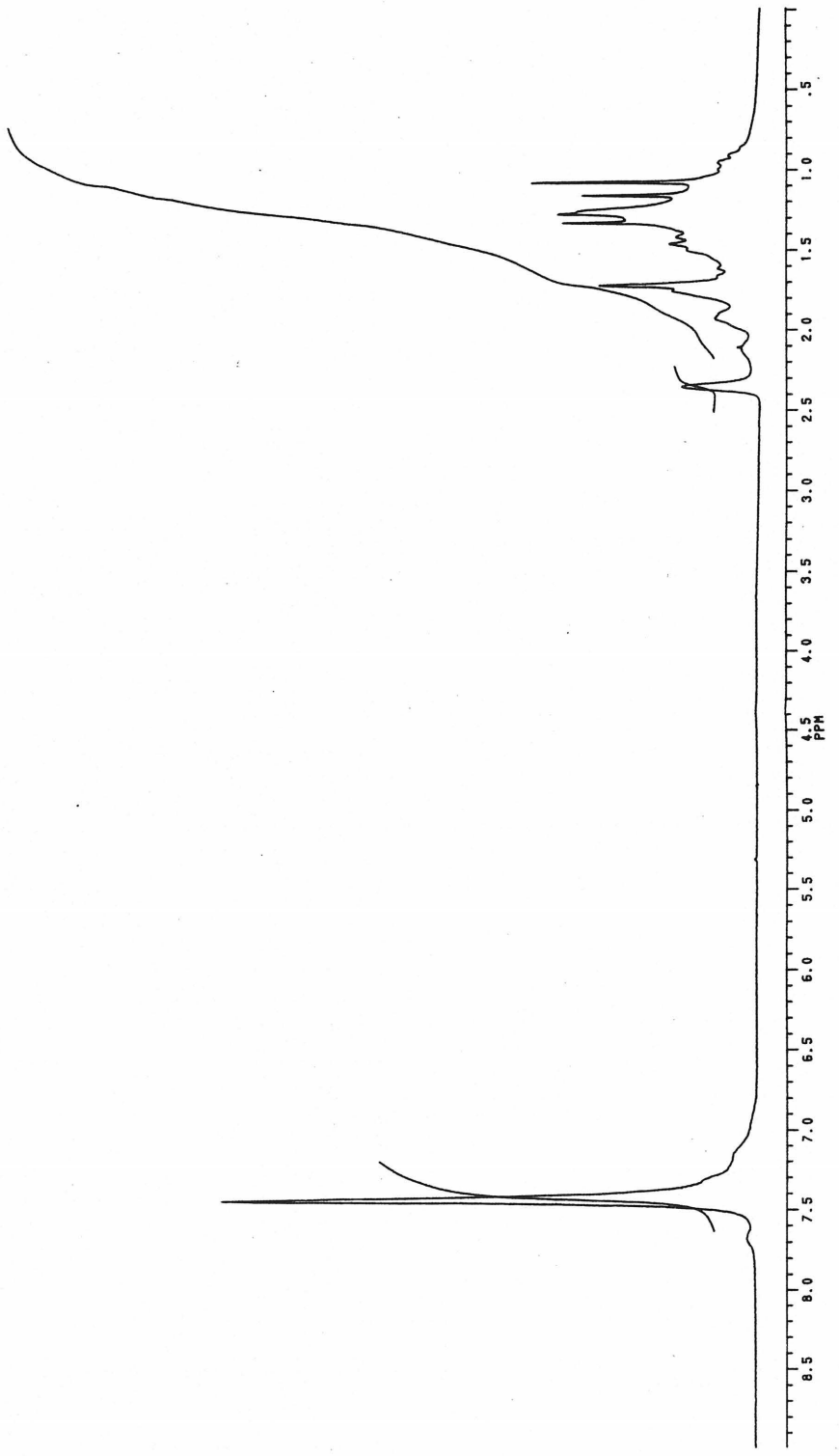

RMN ^{31}P de $\{[Cu(dppb)(dmb)]BF_4\}_n$.

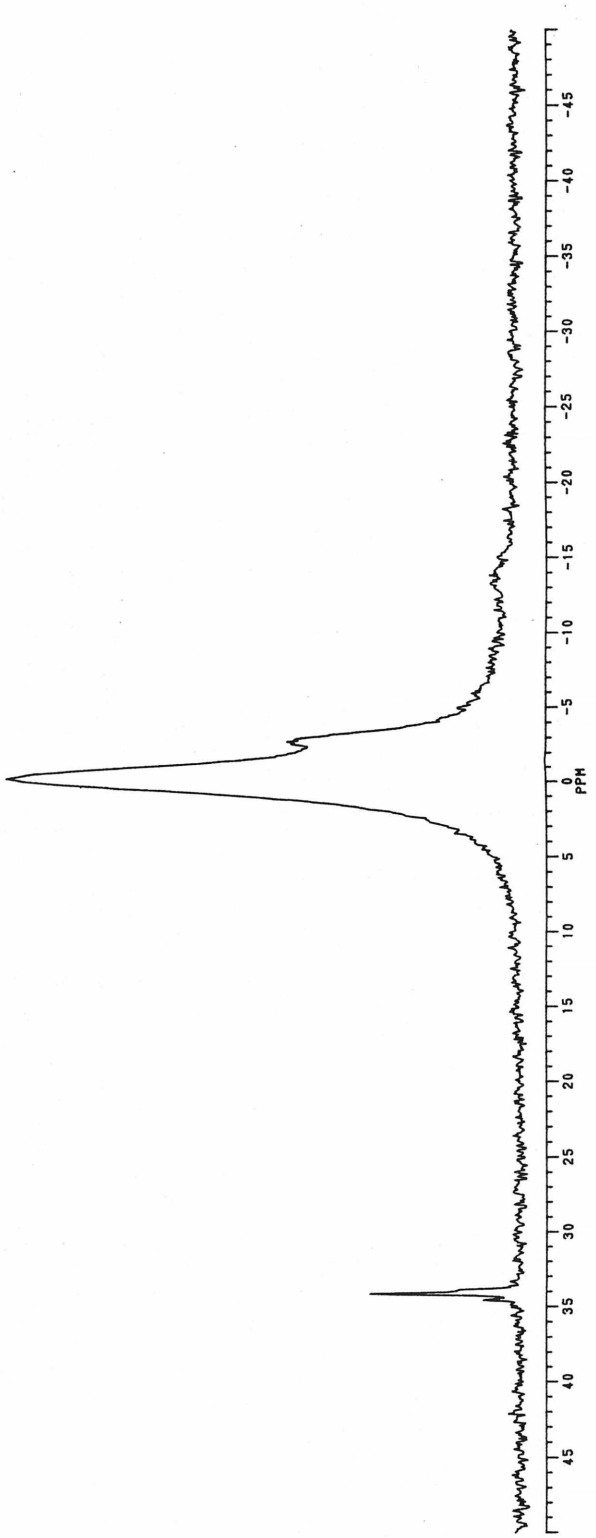

RMN ^{13}C de $\{[Cu(dppb)(dmb)]BF_4\}_n$.

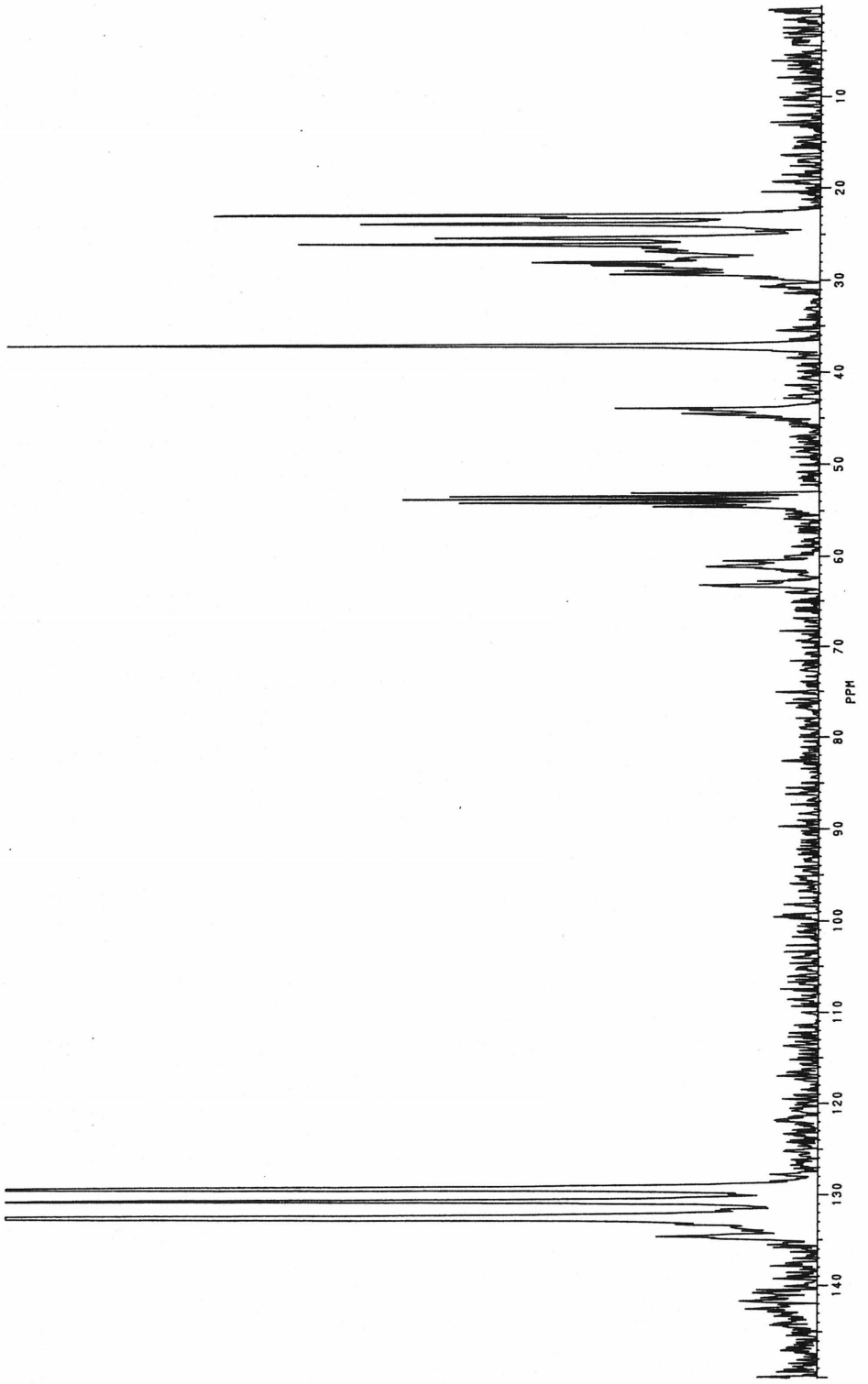

RMN ^{1}H de $[Cu_2(dmpm)_3](BF_4)_2$.

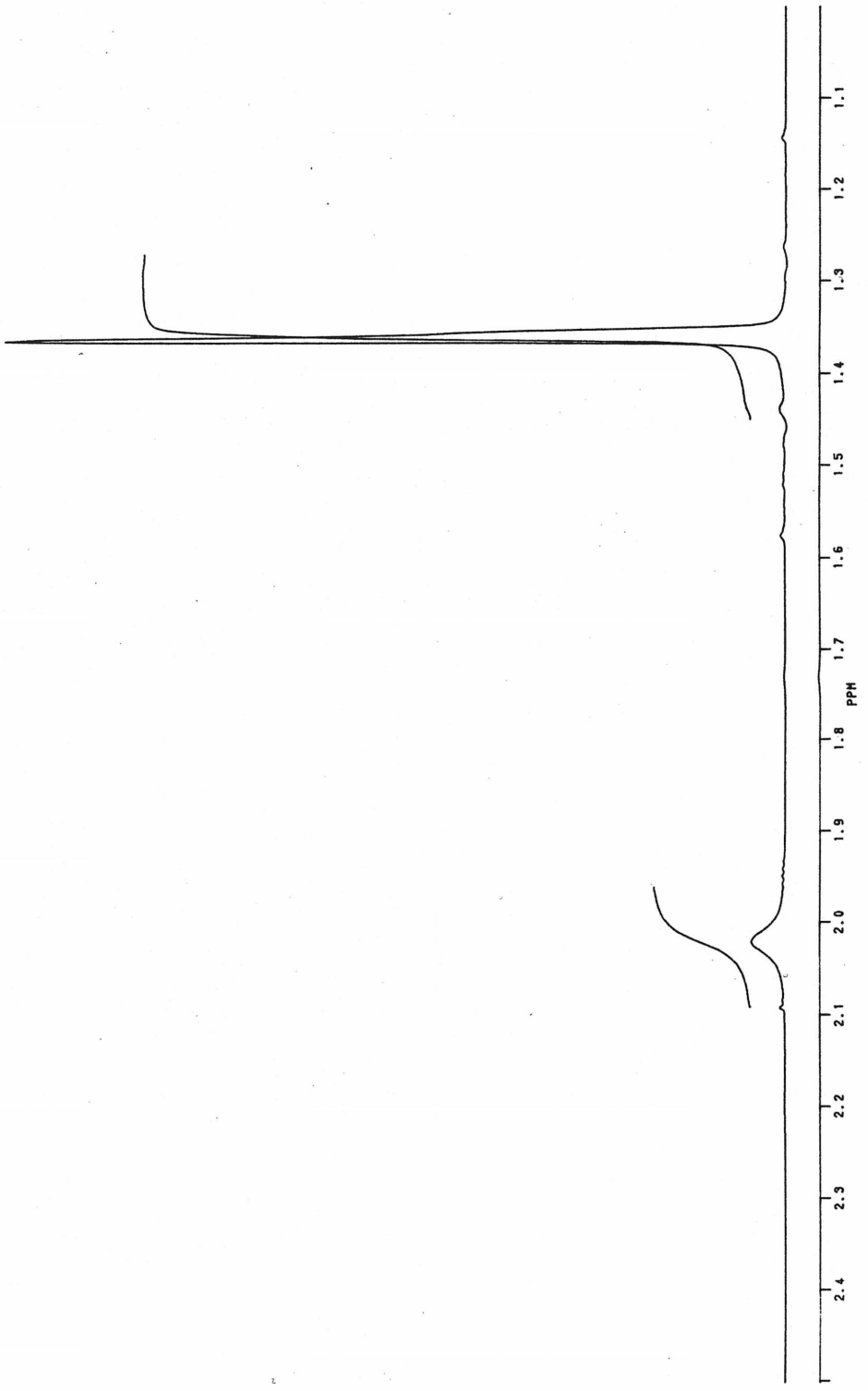

RMN ^{31}P de $[Cu_2(dmpm)_3](BF_4)_2$.

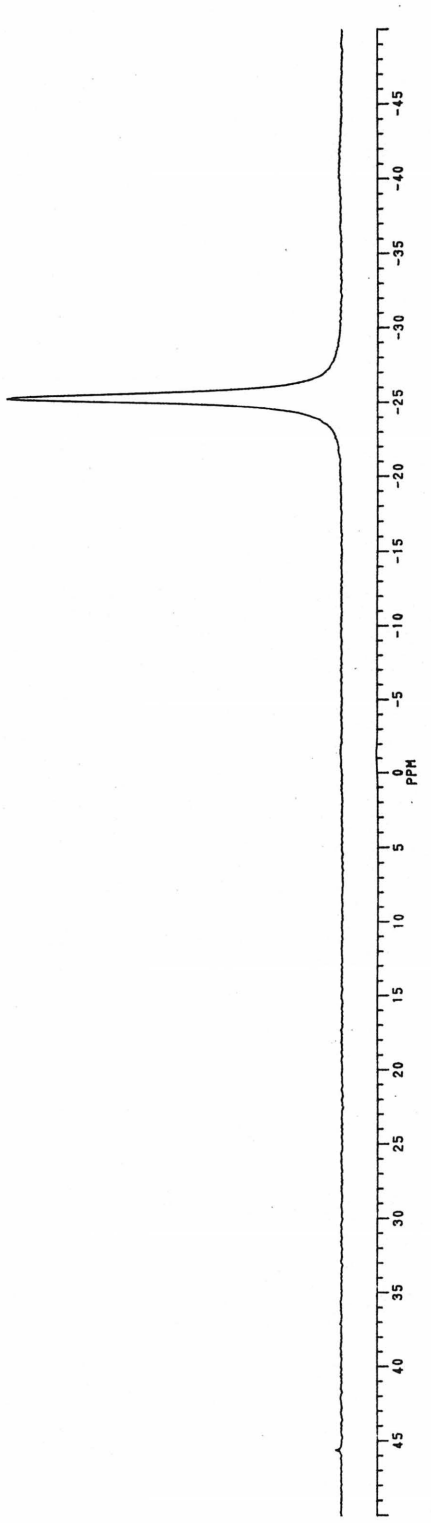

RMN ^{13}C de $[Cu_2(dmpm)_3](BF_4)_2$.

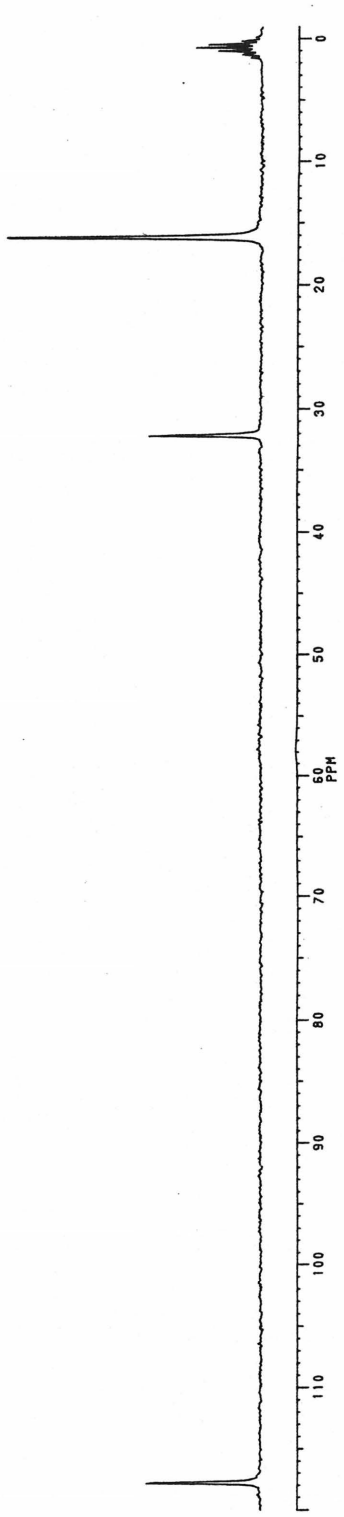

RMN ^{1}H de $[Cu_2(dmpm)_3(CN\text{-}t\text{-}Bu)_2](BF_4)_2$.

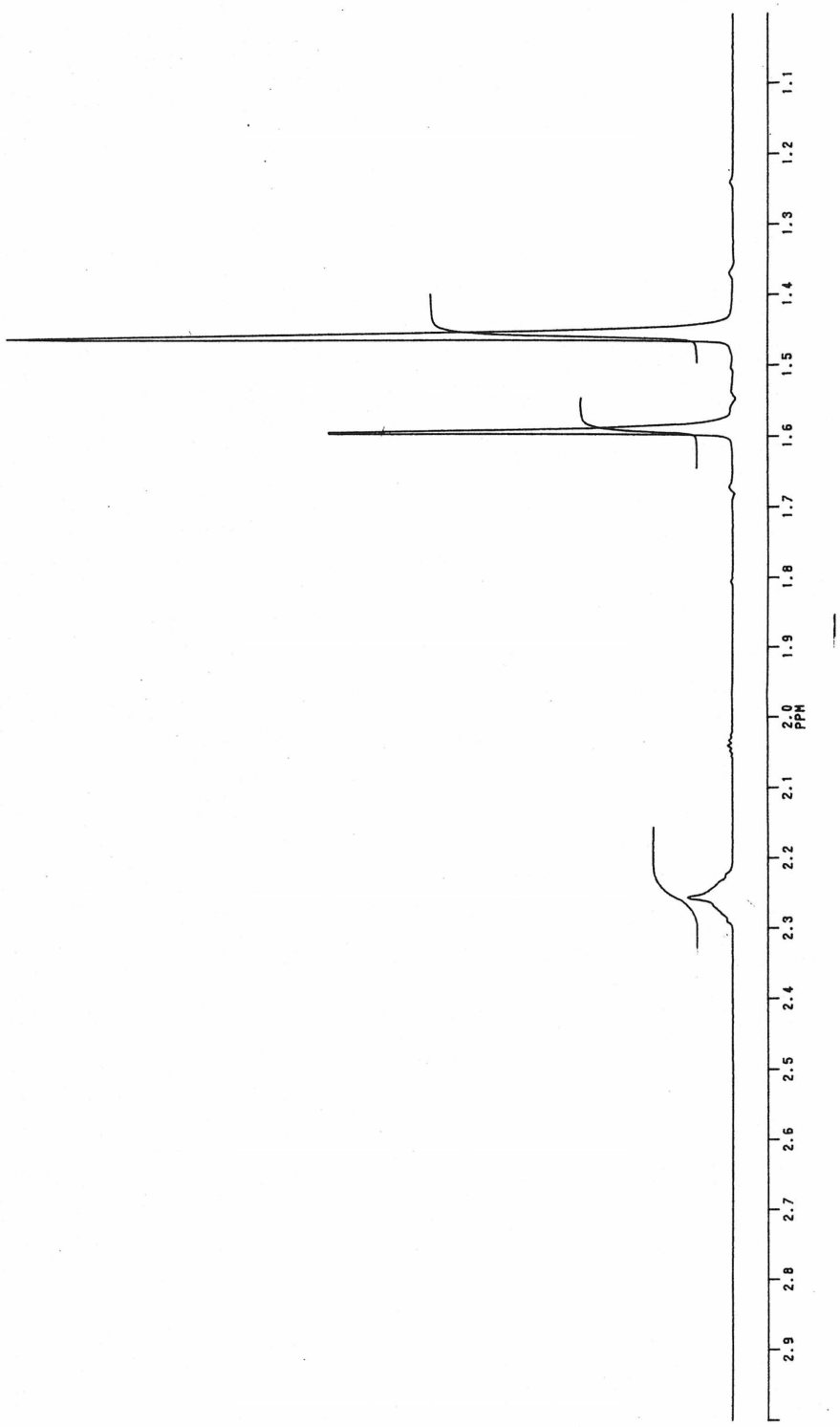

RMN ^{31}P de $[Cu_2(dmpm)_3(CN\text{-}t\text{-}Bu)_2](BF_4)_2$.

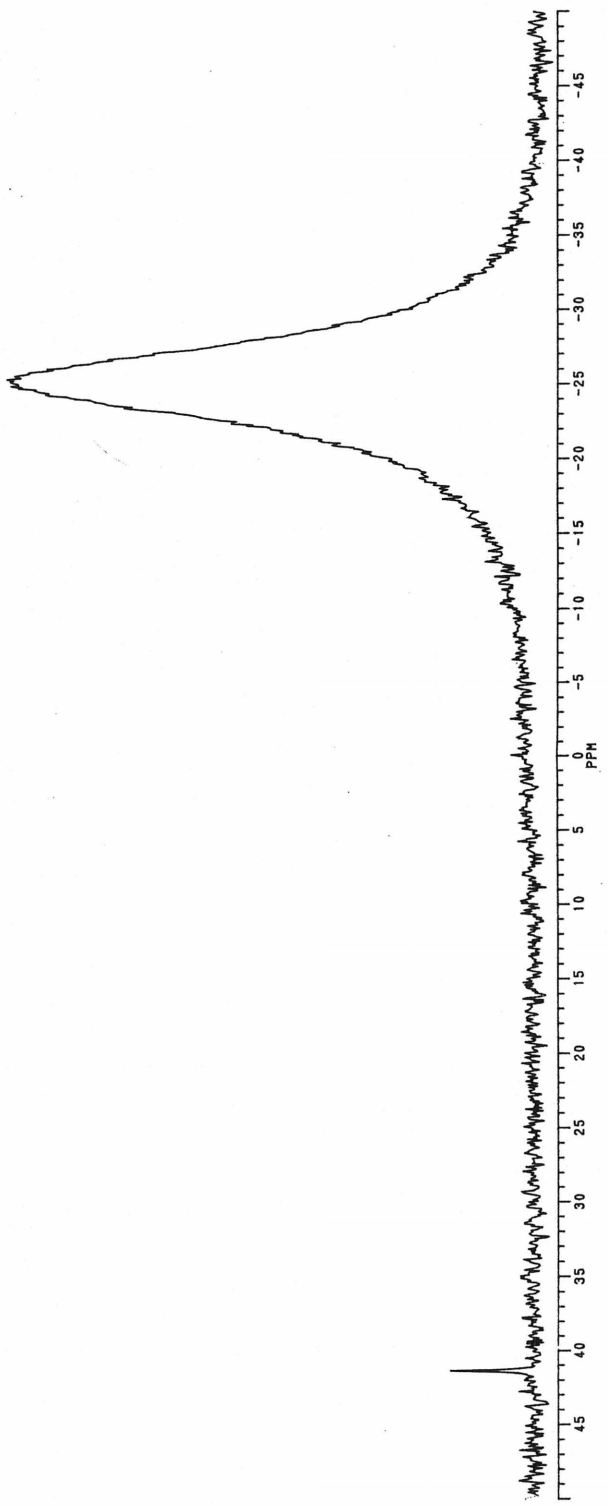

RMN ^{13}C de $[Cu_2(dmpm)_3(CN\text{-}t\text{-}Bu)_2](BF_4)_2$.

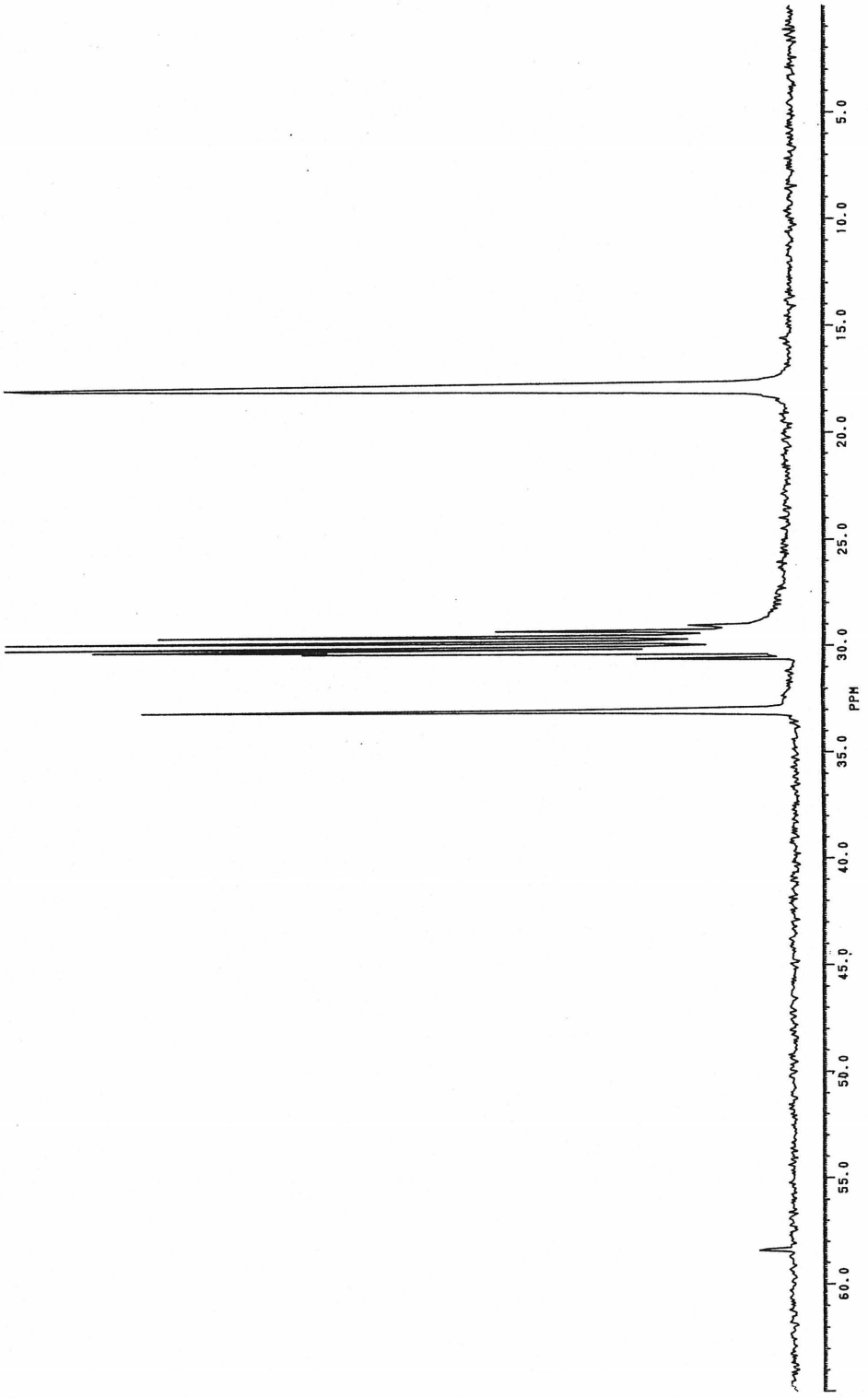

RMN ^{1}H de $\{[Cu_2(dmpm)_3(dmb)_{1.33}](BF_4)_2\}_3$.

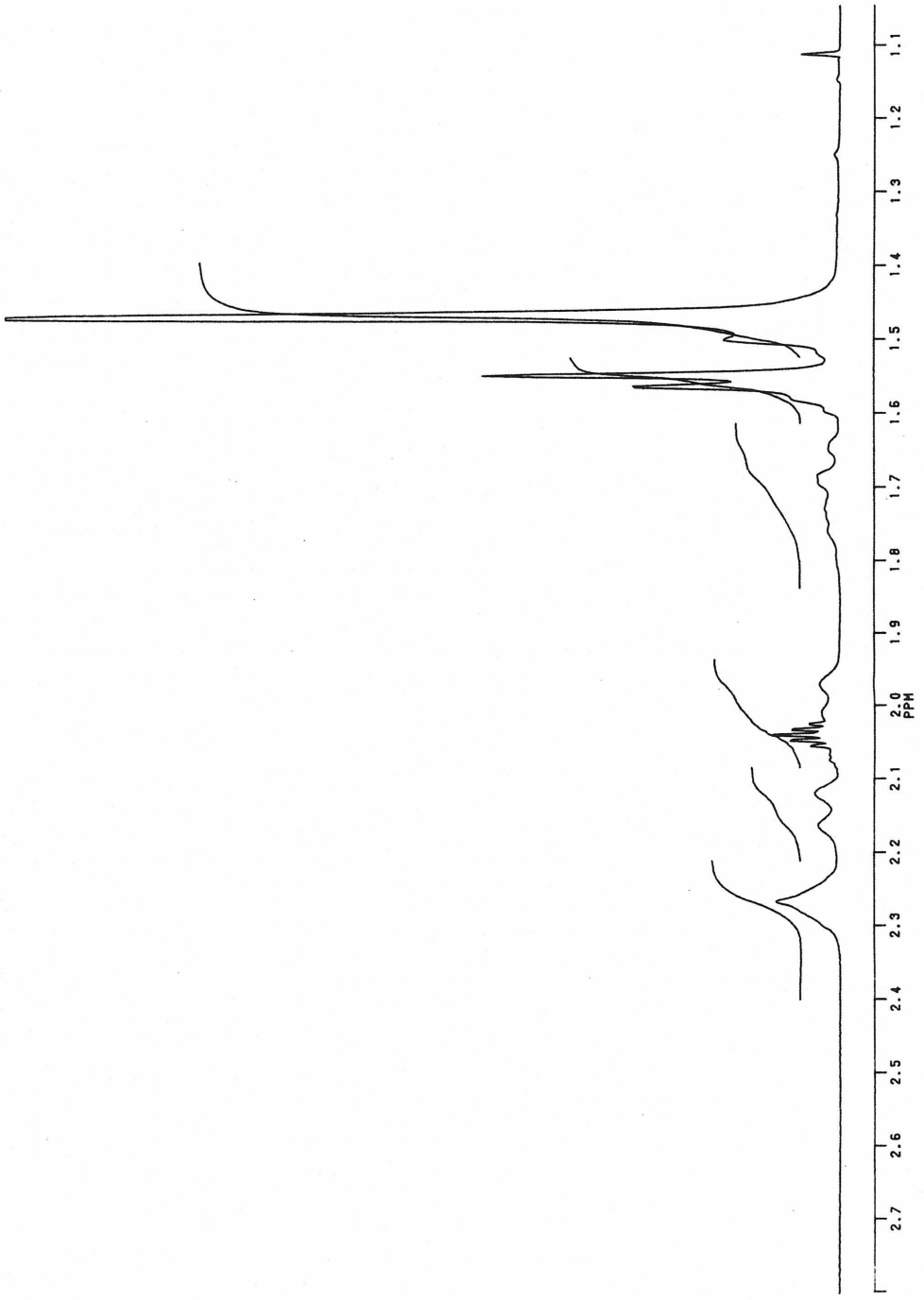

RMN ^{31}P de $\{[Cu_2(dmpm)_3(dmb)_{1.33}](BF_4)_2\}_3$.

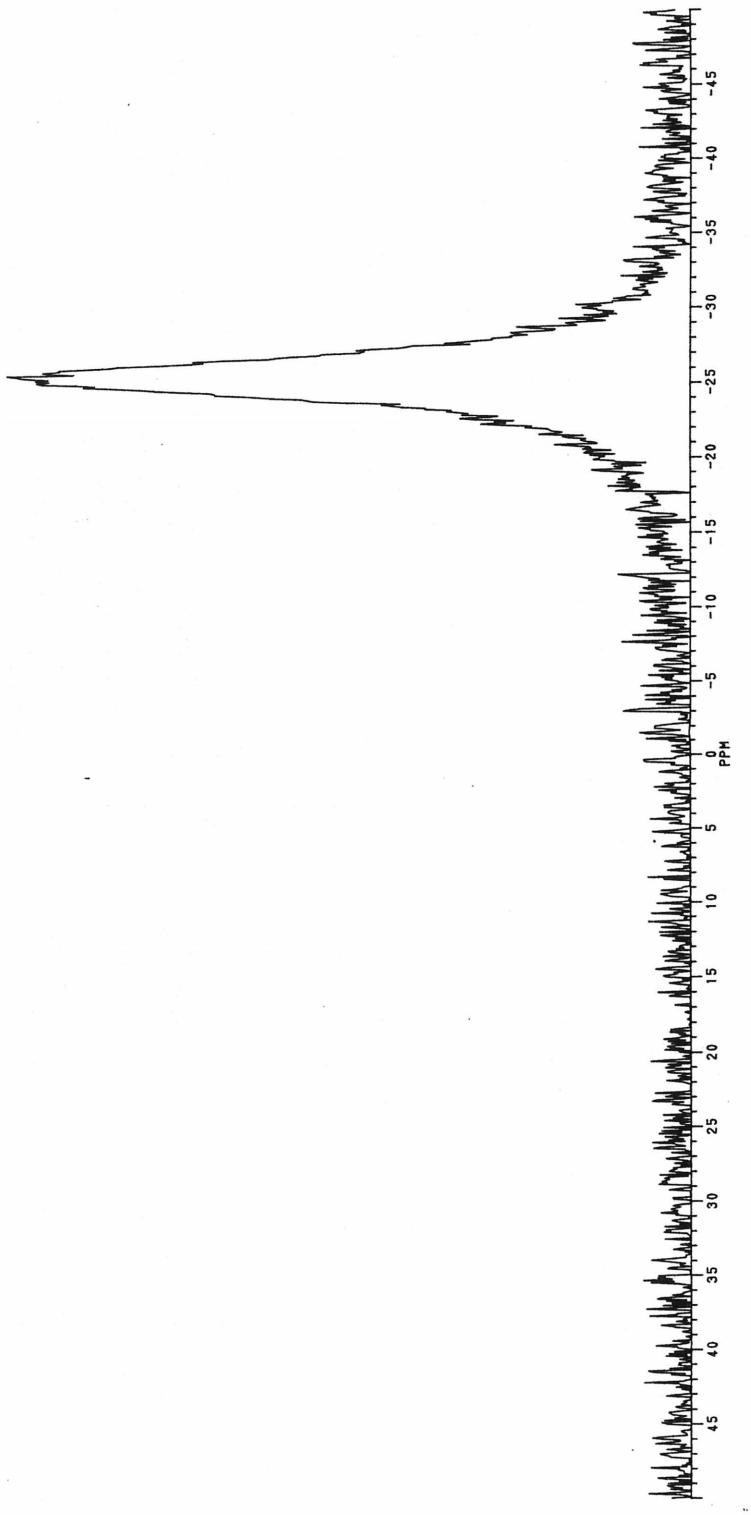

RMN ^{13}C de $\{[Cu_2(dmpm)_3(dmb)_{1.33}](BF_4)_2\}_3$.

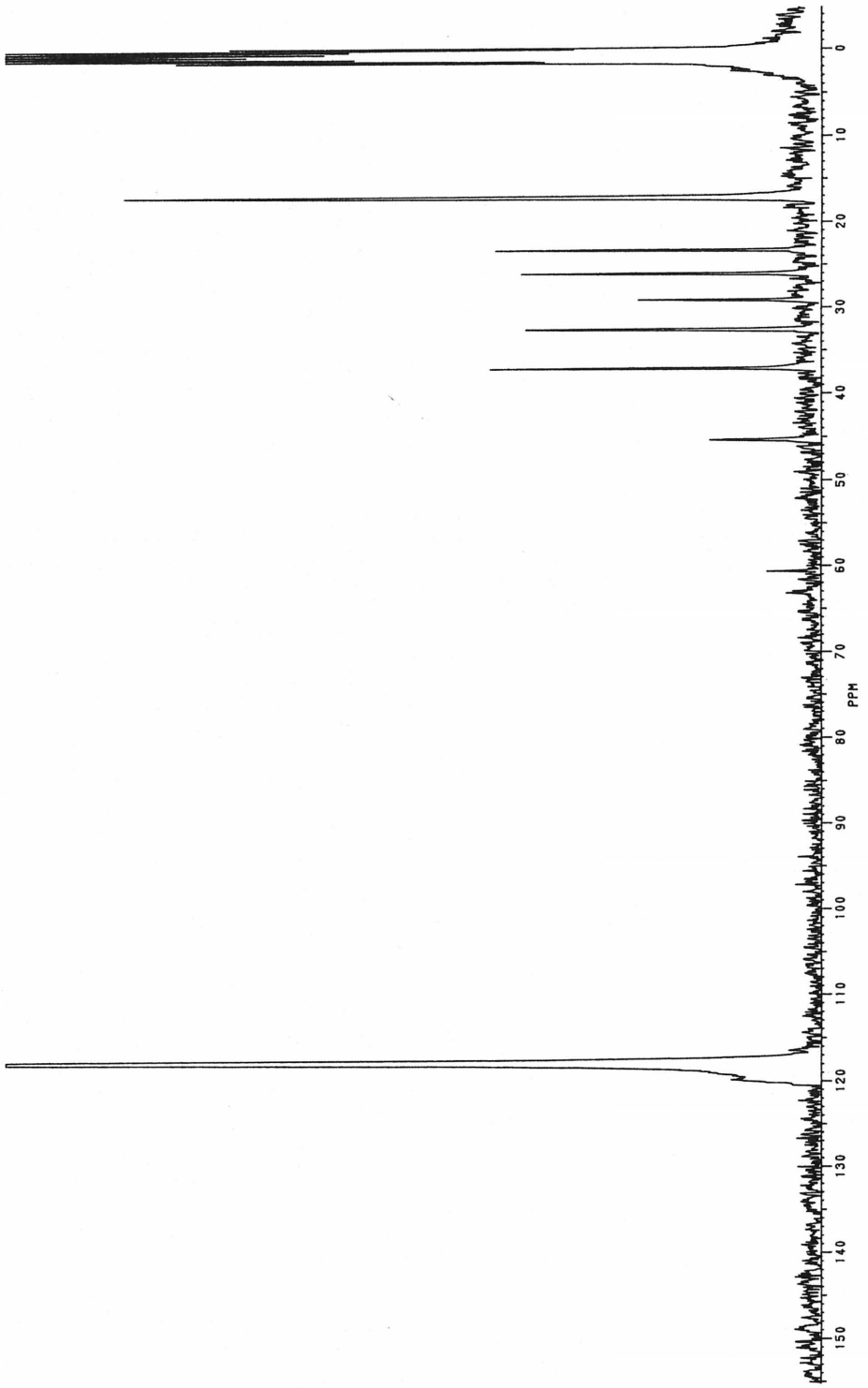

RMN ^{1}H de $[Ag_2(dmpm)_2](BF_4)_2$.

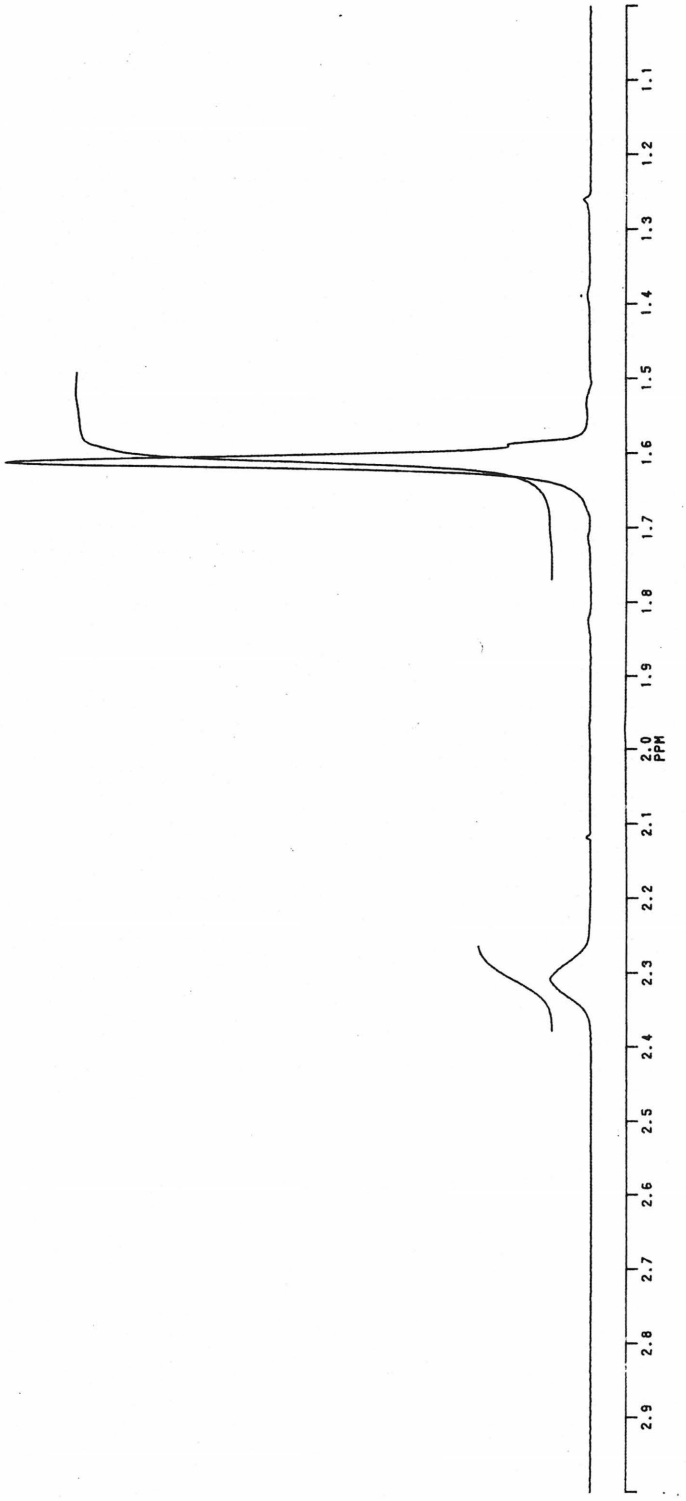

RMN ^{31}P de $[Ag_2(dmpm)_2](BF_4)_2$.

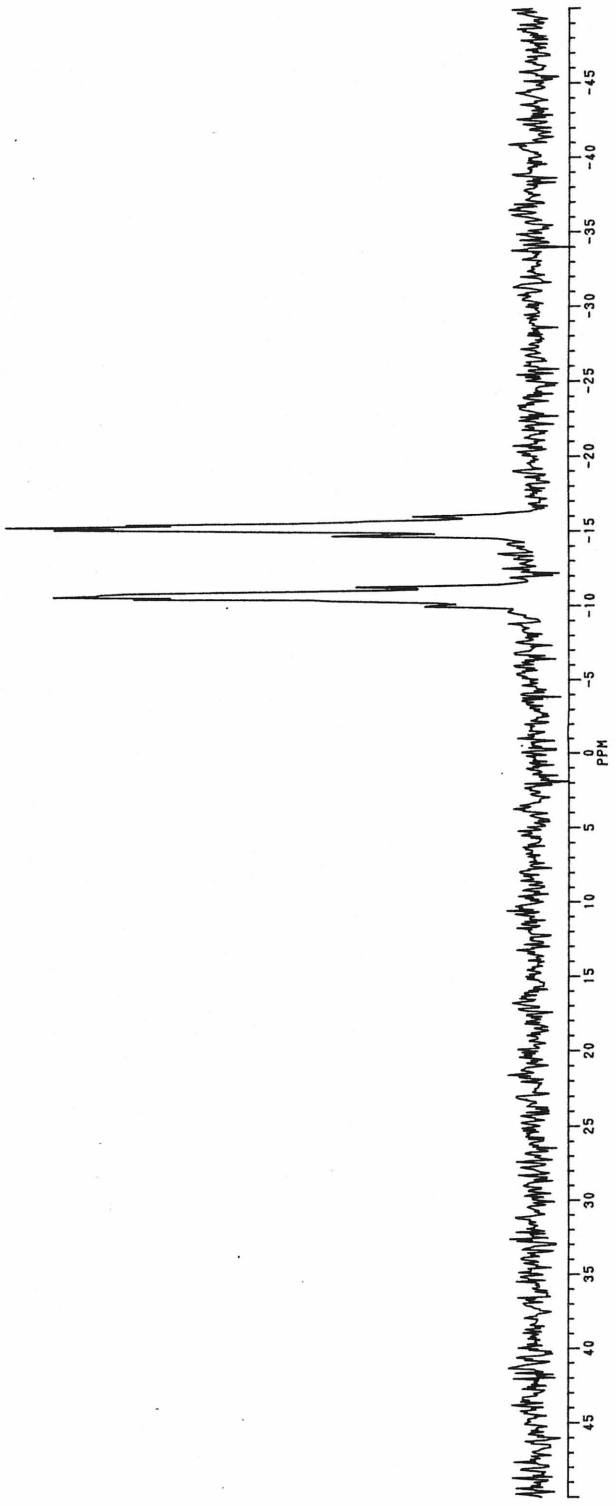

RMN ^{13}C de $[Ag_2(dmpm)_2](BF_4)_2$.

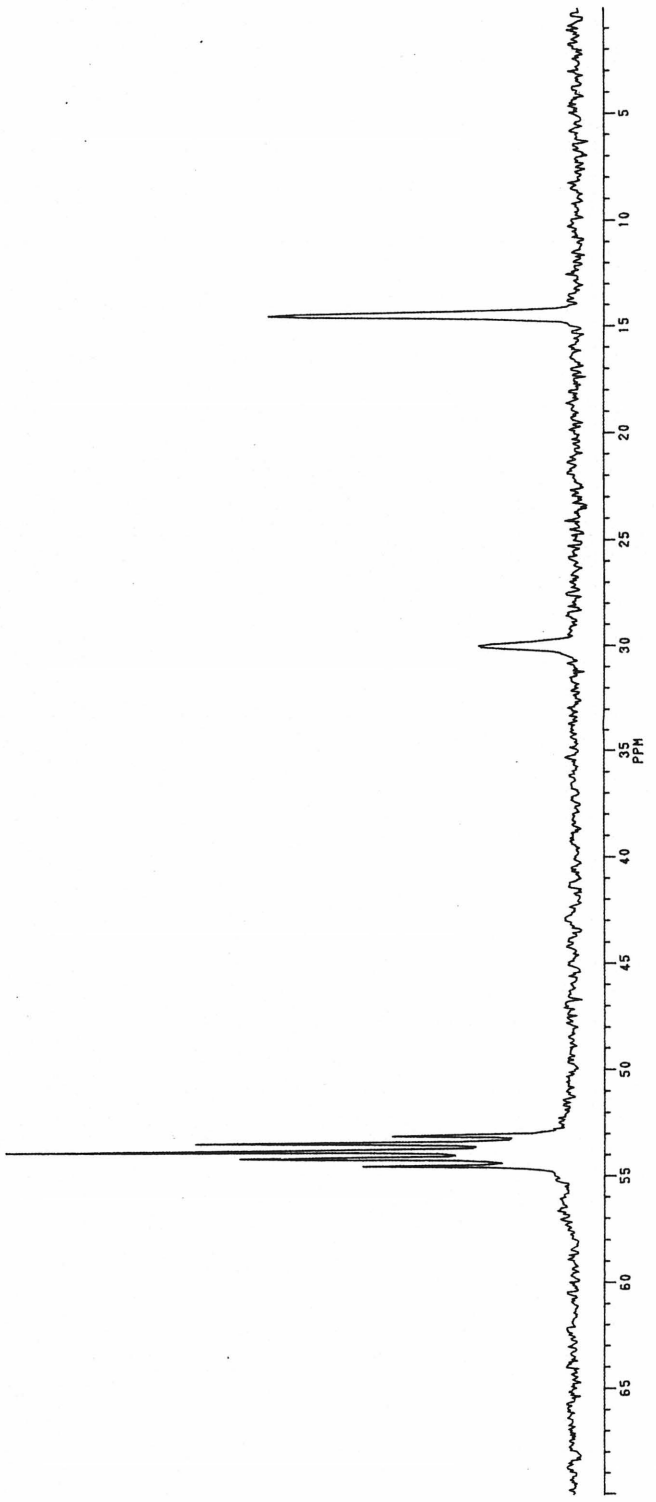

RMN ^{1}H de $[Ag_2(dmpm)_3](BF_4)_2$.

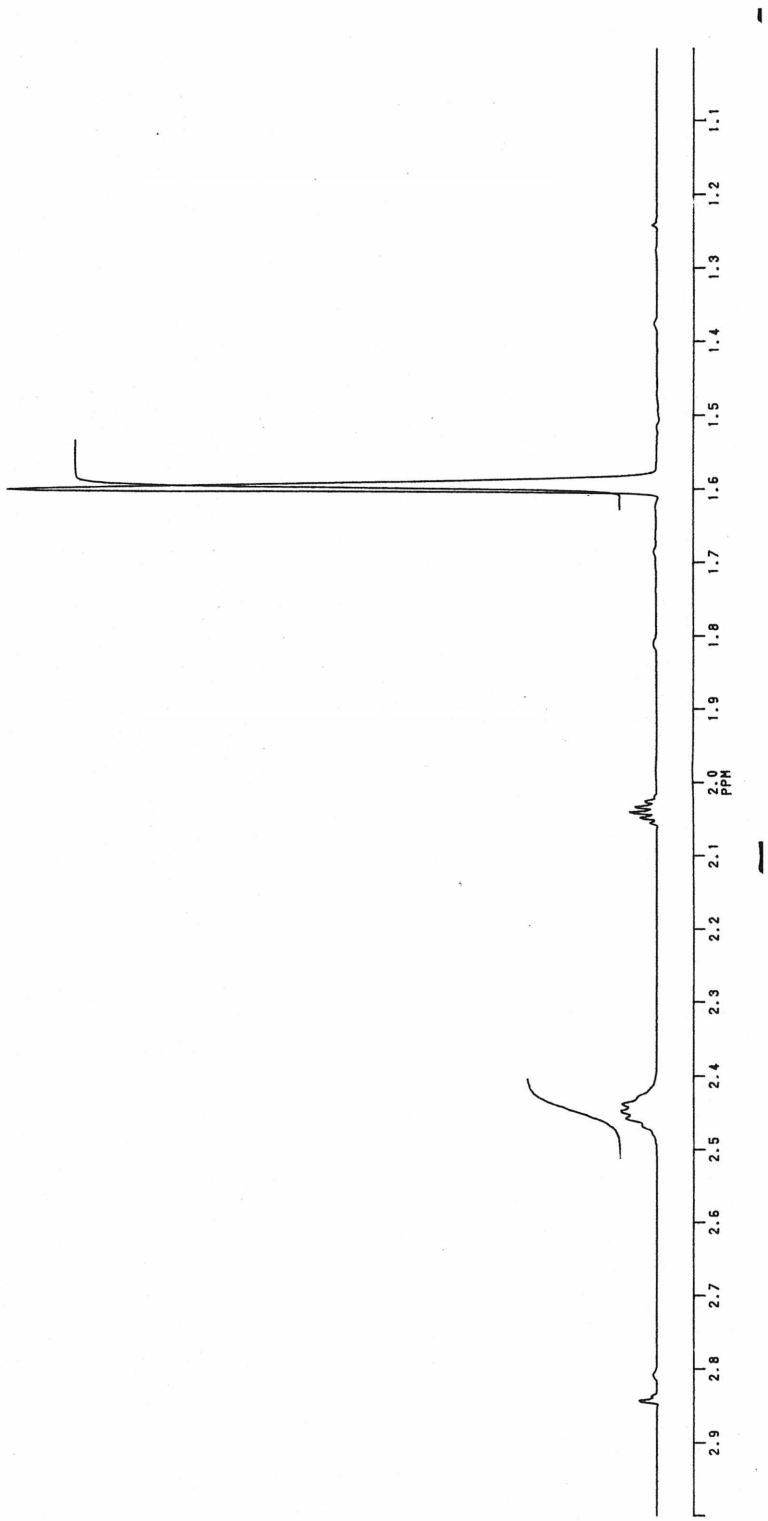

RMN ^{31}P de $[Ag_2(dmpm)_3](BF_4)_2$.

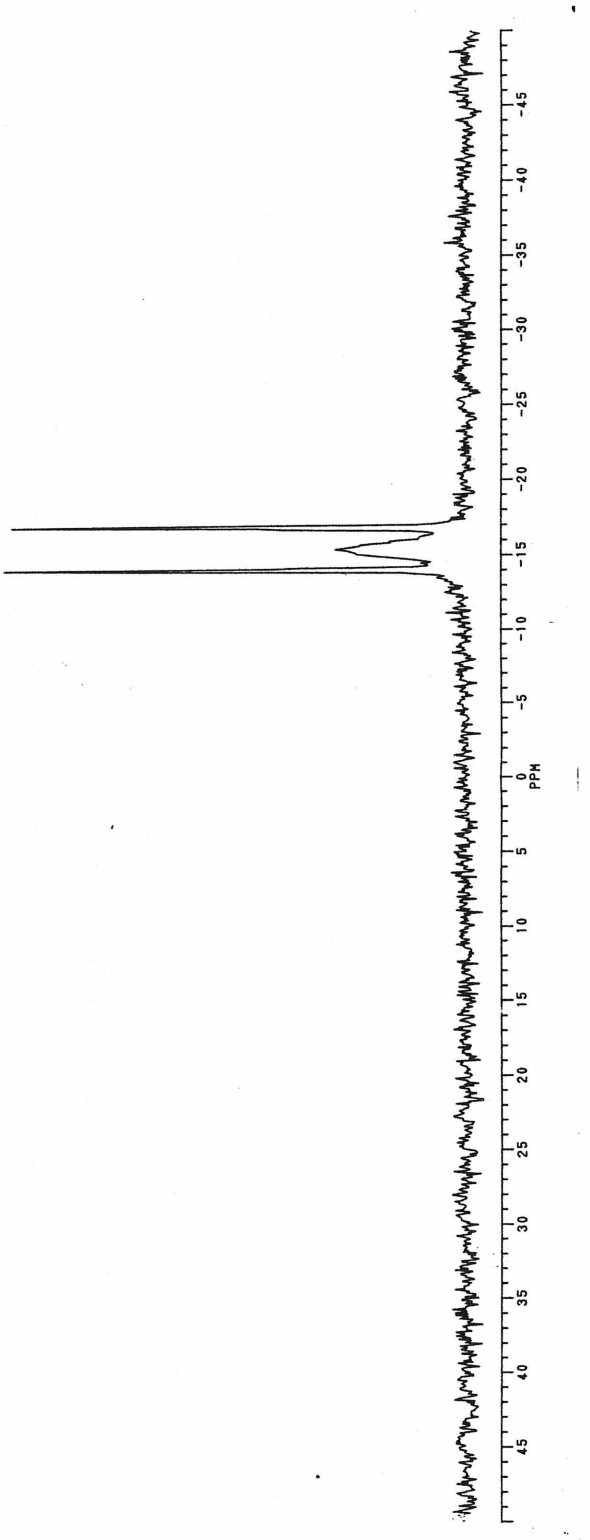

RMN ^{13}C de $[Ag_2(dmpm)_3](BF_4)_2$.

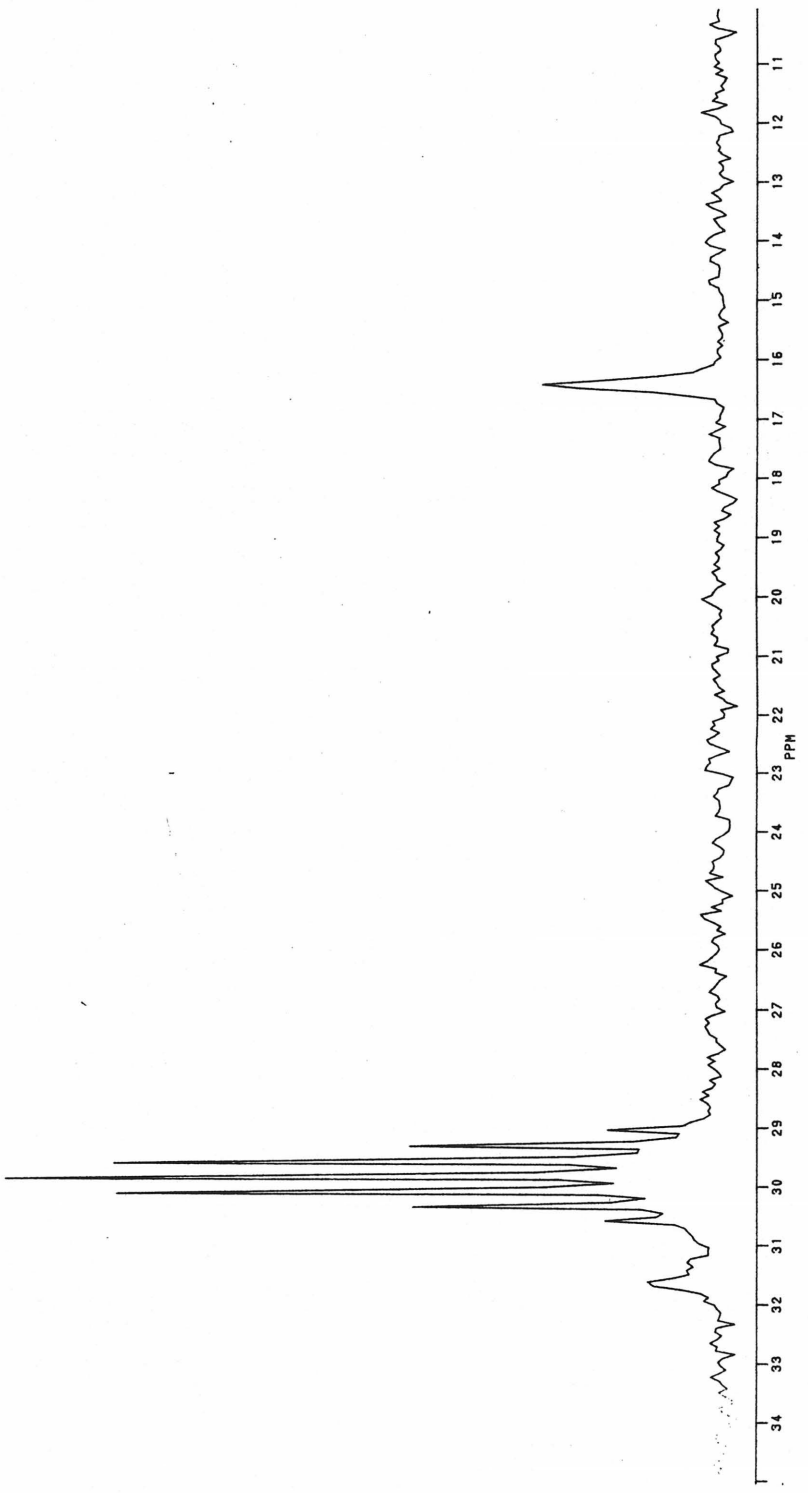

RMN ^{1}H de $\{[Ag_2(dmpm)_2(dmb)_{1.33}](BF_4)_2\}_3$.

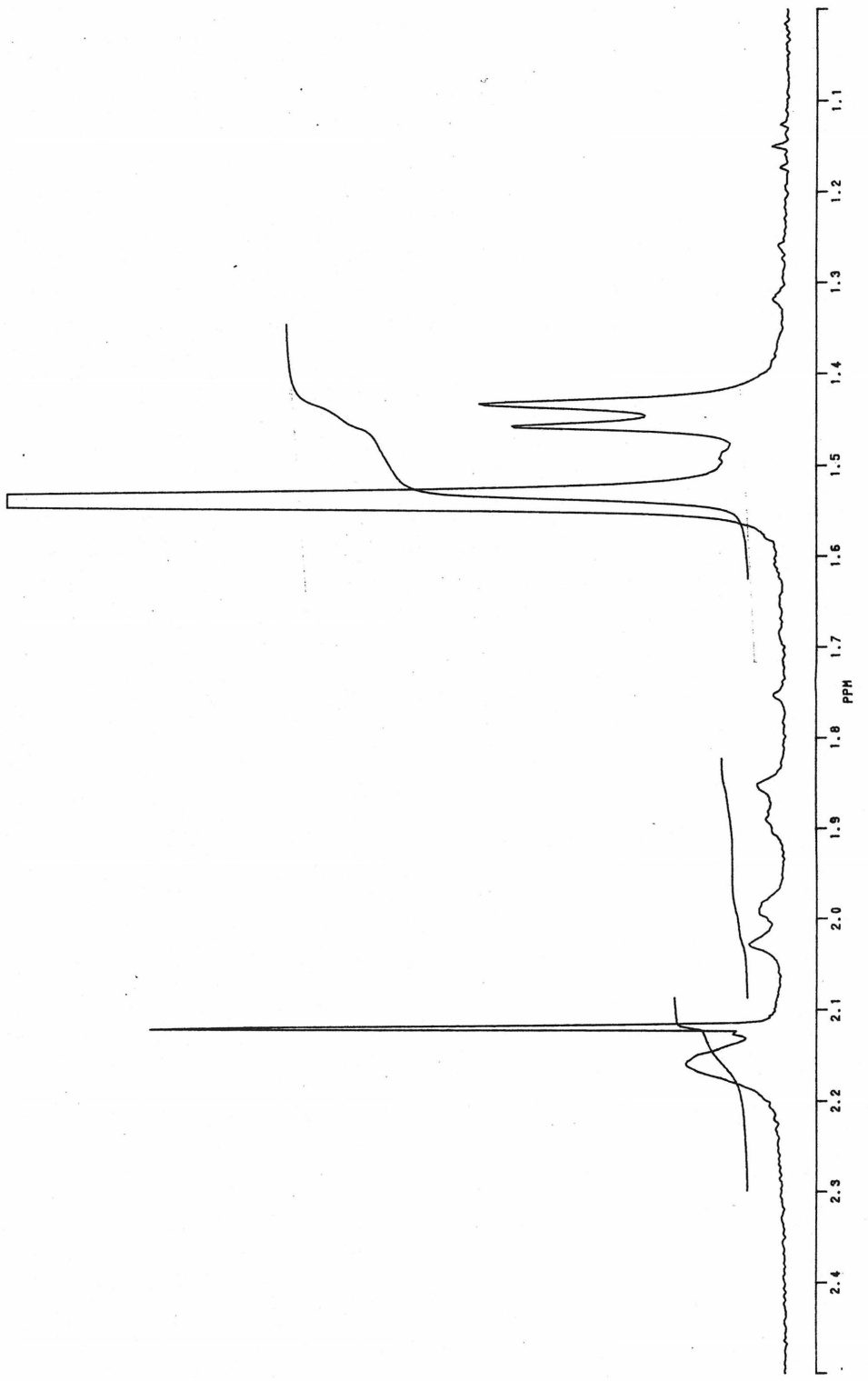

RMN ^{31}P de $\{[Ag_2(dmpm)_2(dmb)_{1.33}](BF_4)_2\}_3$.

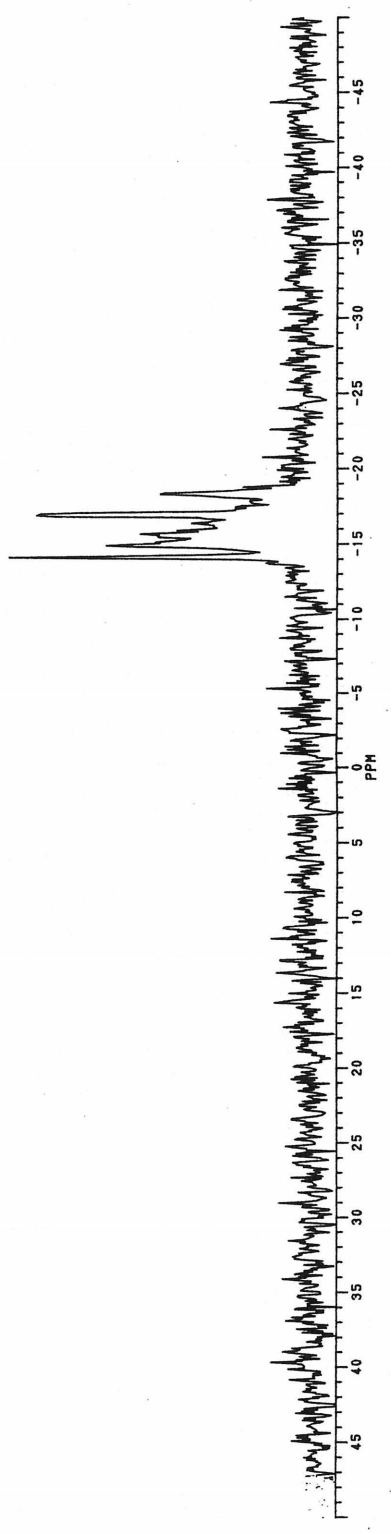

RMN ^{13}C de $\{[Ag_2(dmpm)_2(dmb)_{1.33}](BF_4)_2\}_3$.

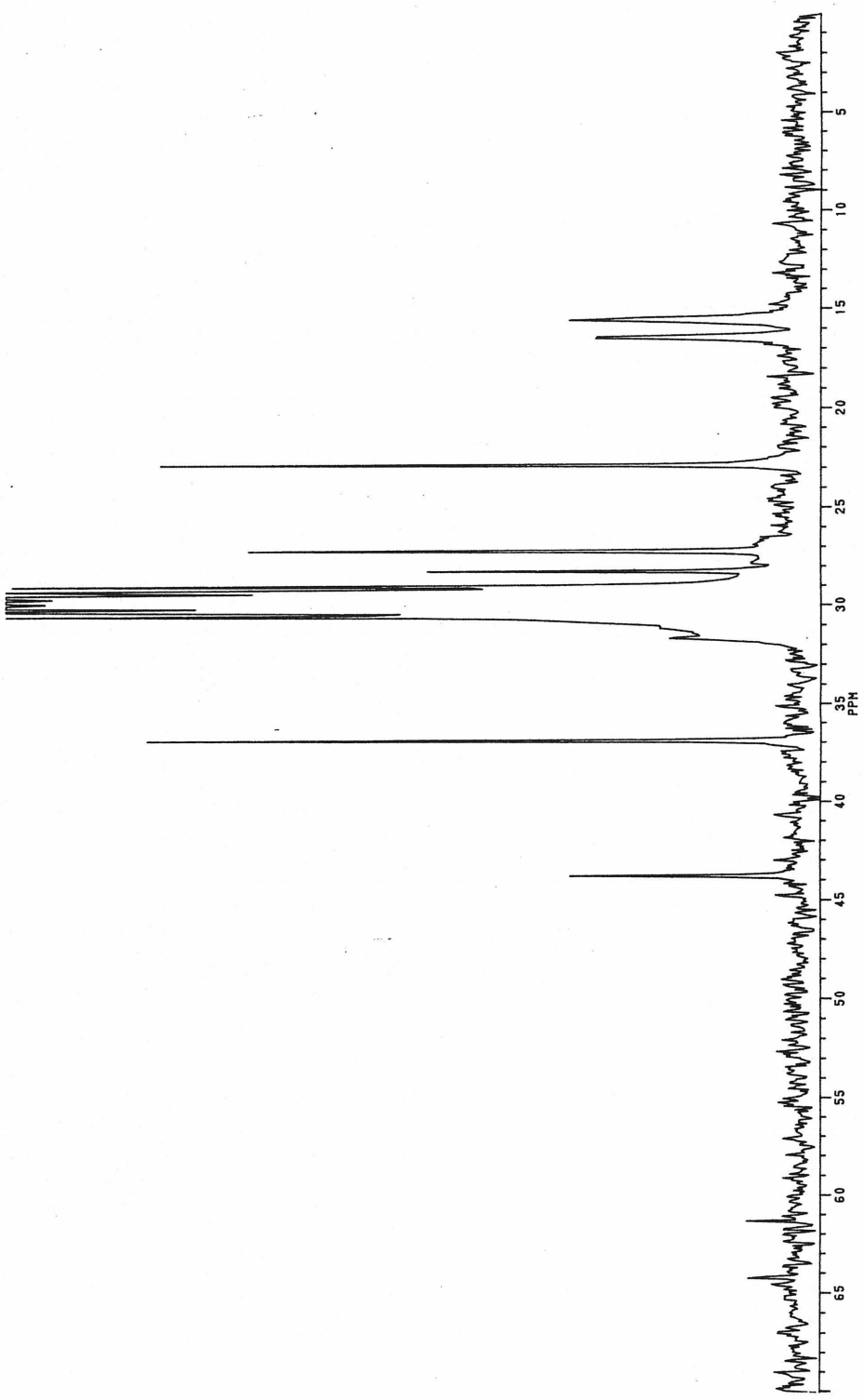

RMN ^{1}H et ^{13}C de $[Ag(dppe)(CN\text{-}t\text{-}Bu)_2]BF_4$.

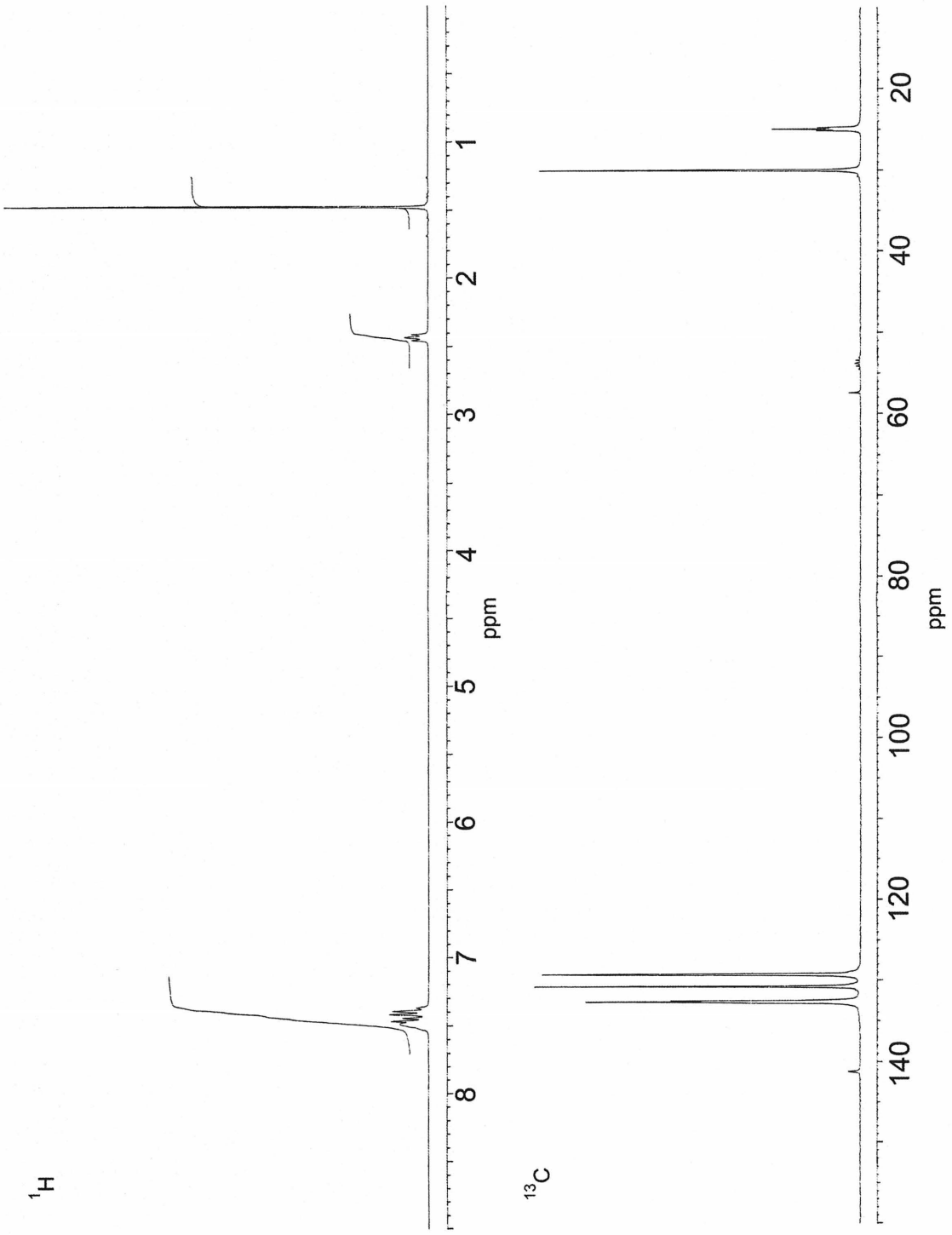

RMN ^{31}P de $[Ag(dppe)(CN\text{-}t\text{-}Bu)_2]BF_4$.

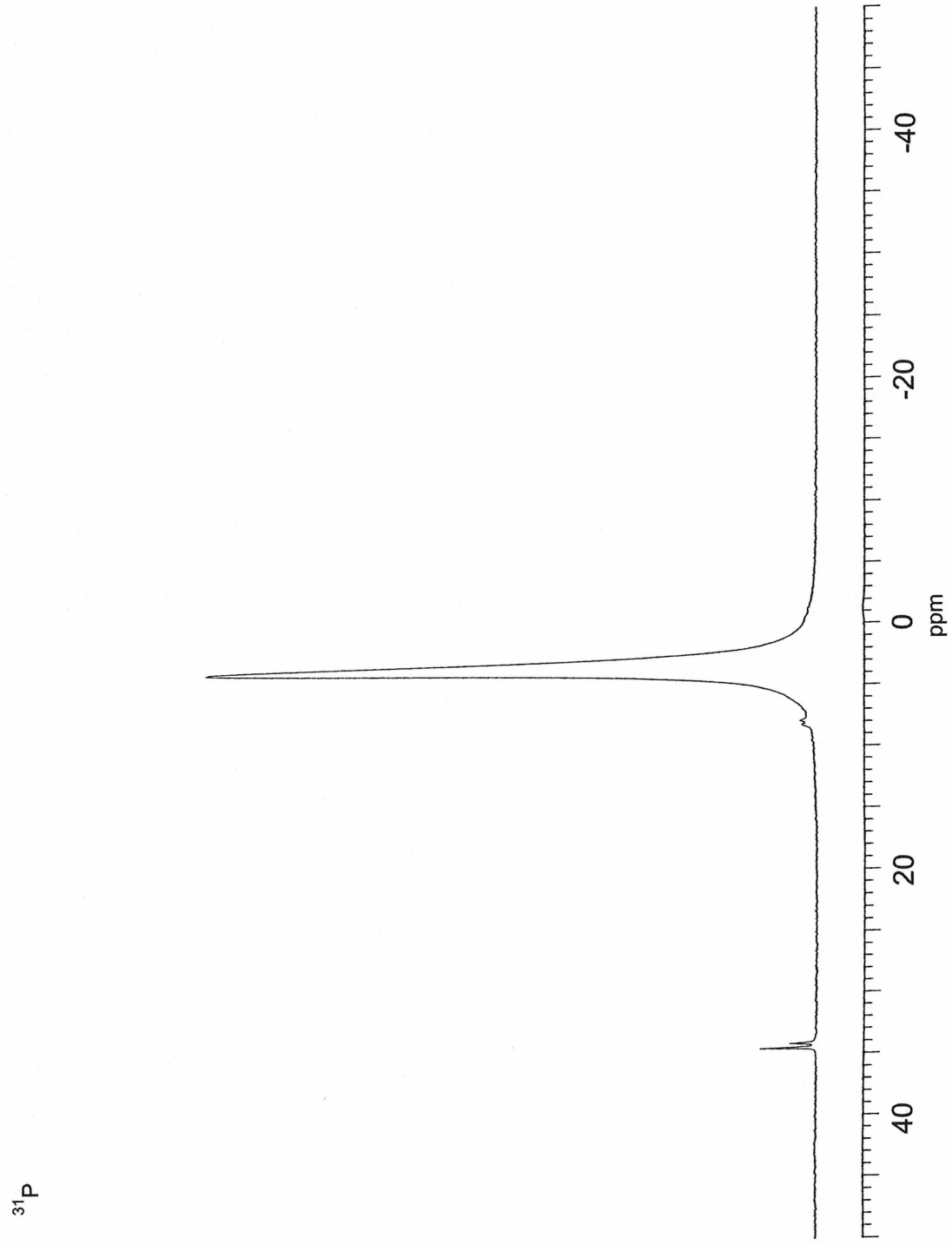

RMN ^{1}H et ^{13}C de $\{[Ag(dppb)(CN\text{-}t\text{-}Bu)_2]BF_4\}_n$.

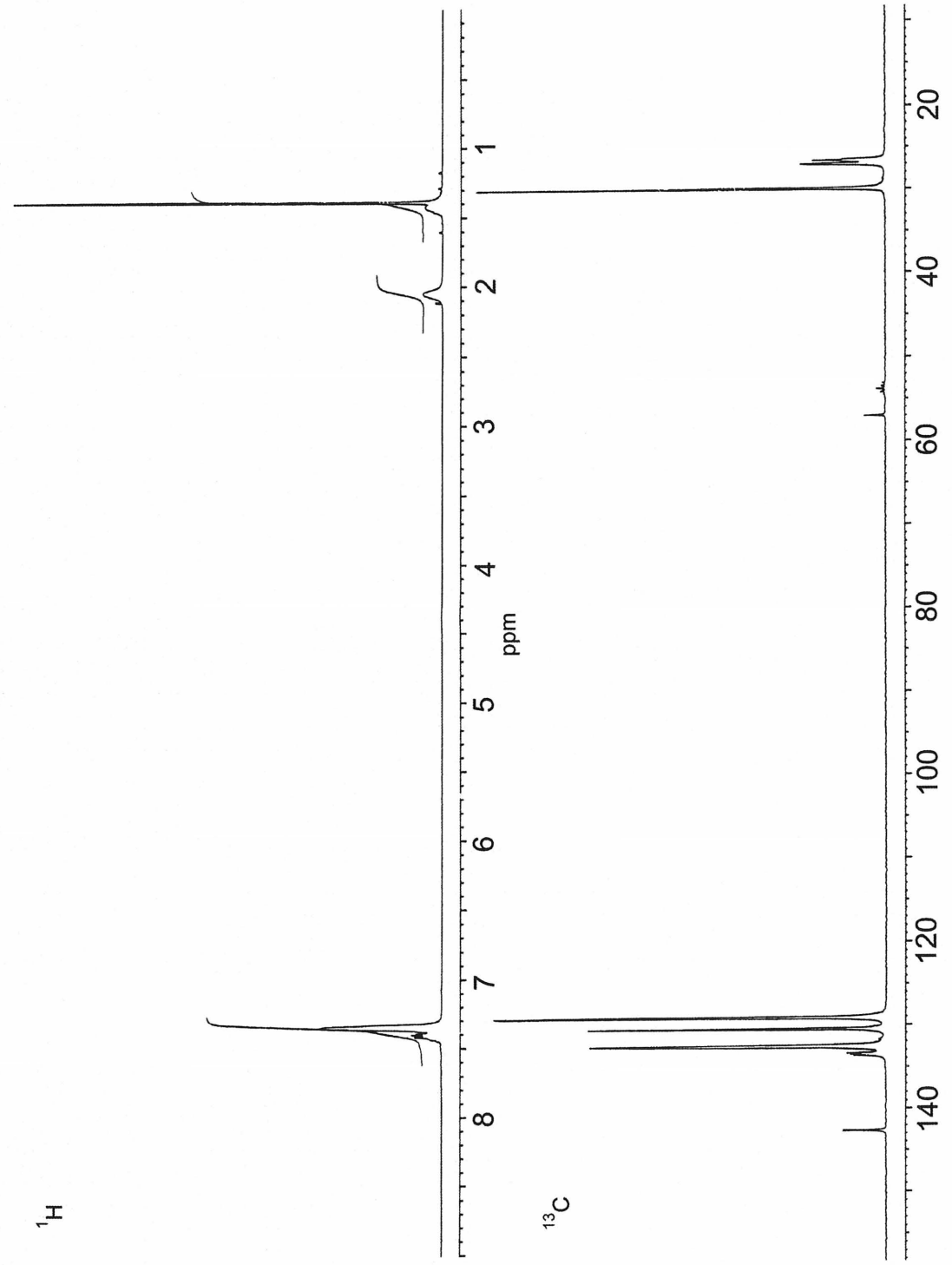

RMN ^{31}P de $\{[Ag(dppb)(CN\text{-}t\text{-}Bu)_2]BF_4\}_n$.

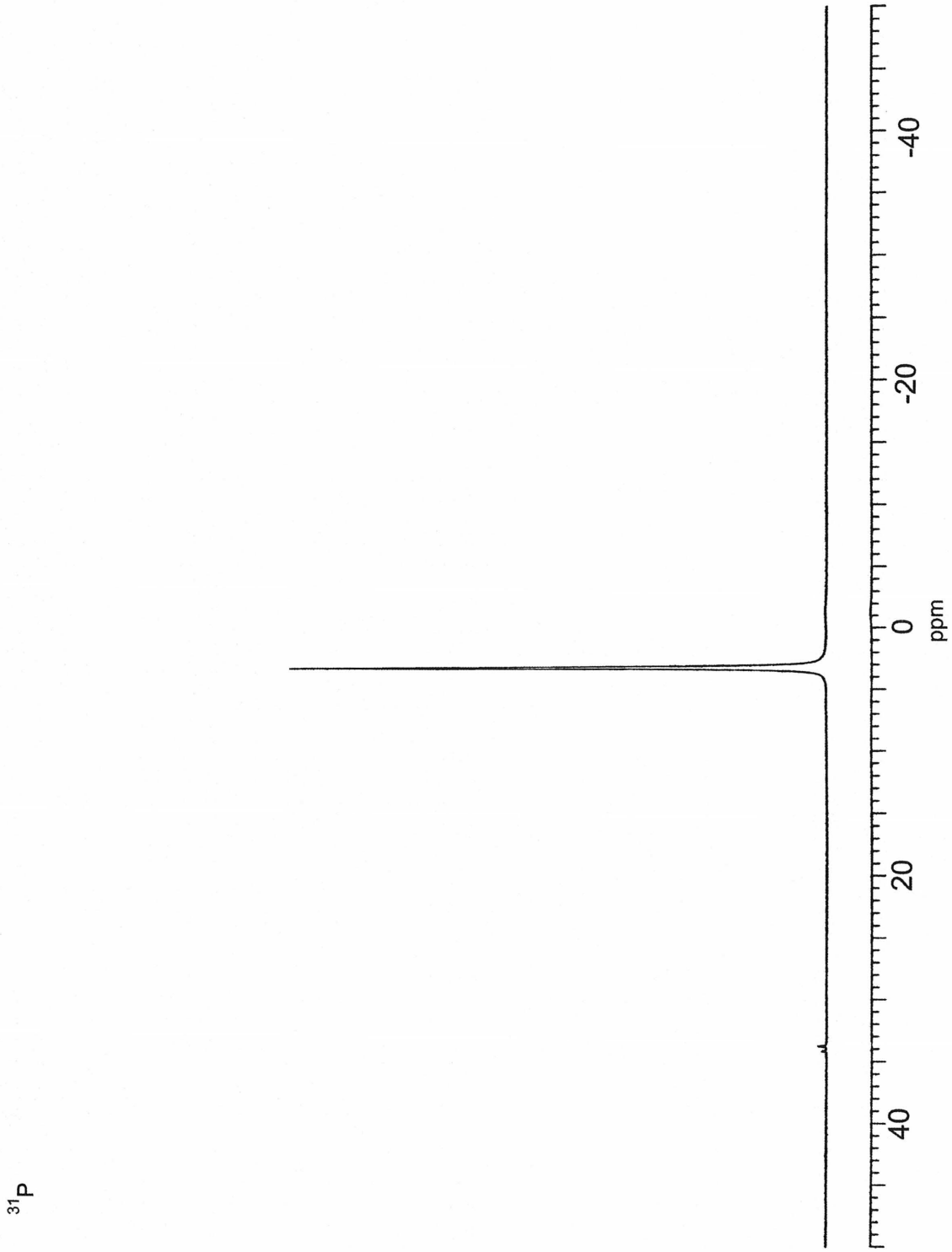

RMN ^{1}H et ^{13}C de $\{[Ag(dpppen)(CN\text{-}t\text{-}Bu)_2]BF_4\}_n$.

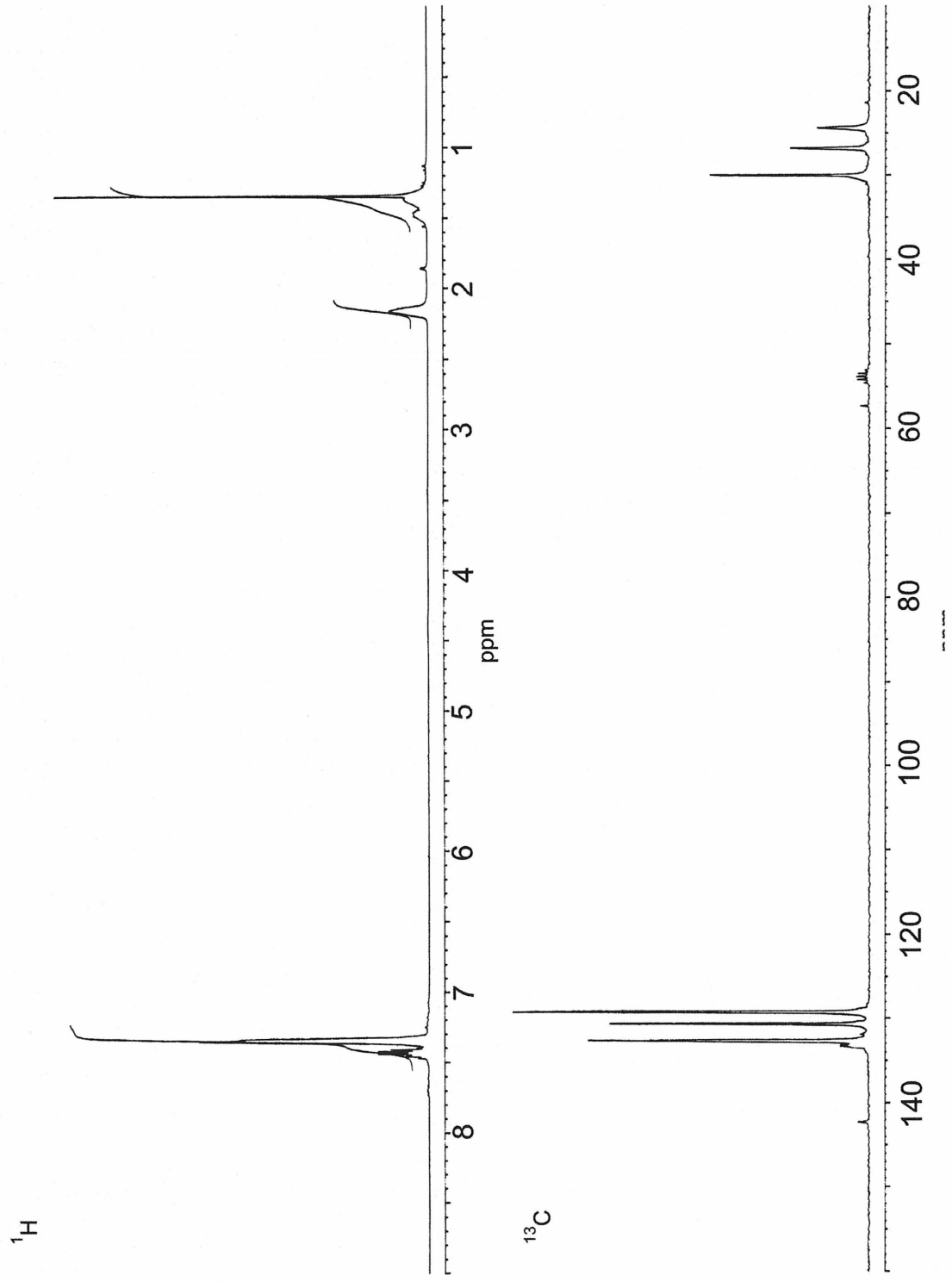

RMN ^{31}P de $\{[Ag(dpppen)(CN\text{-}t\text{-}Bu)_2]BF_4\}_n$.

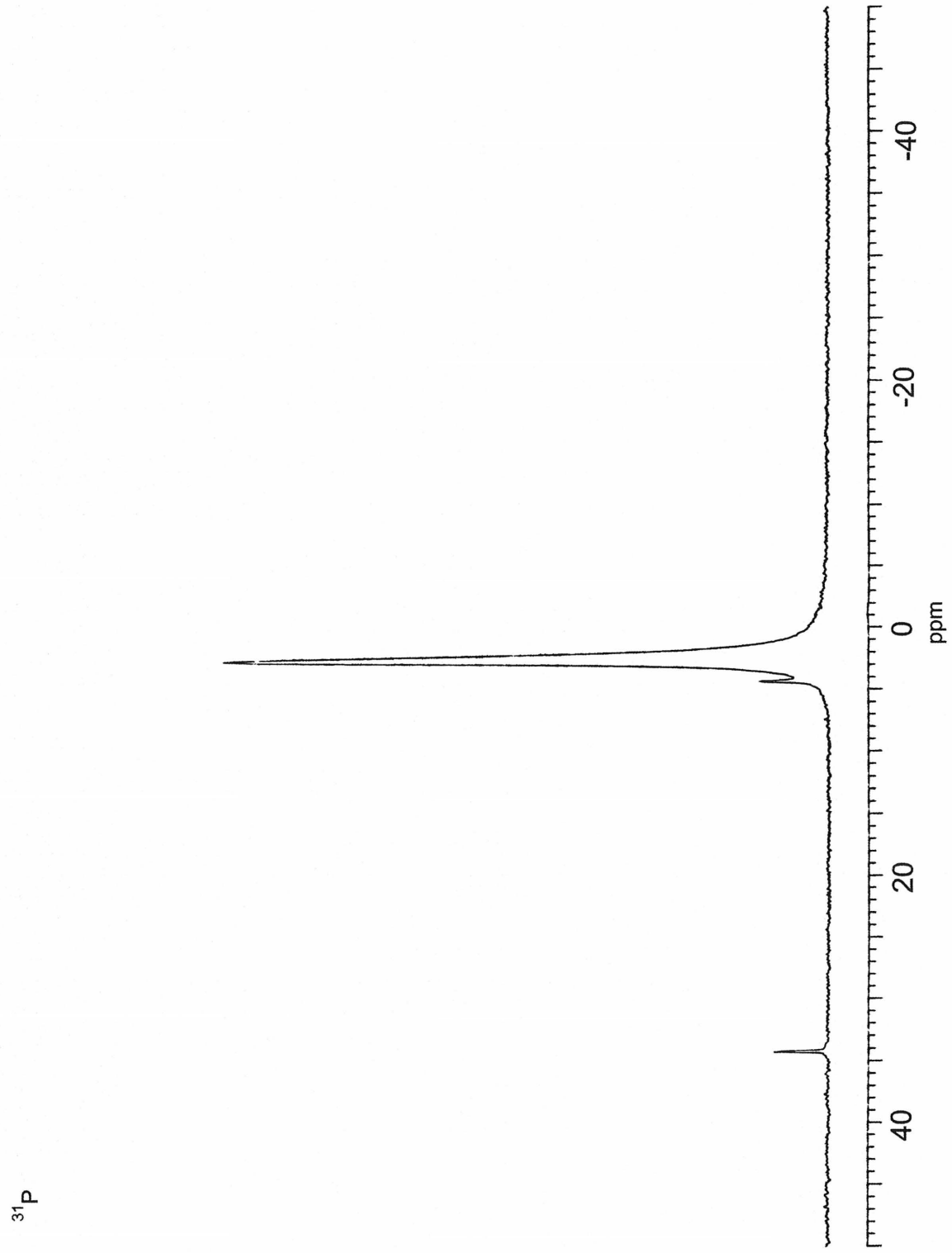

RMN ^{1}H et ^{13}C de $\{[Ag(dpph)(CN\text{-}t\text{-}Bu)_2]BF_4\}_n$.

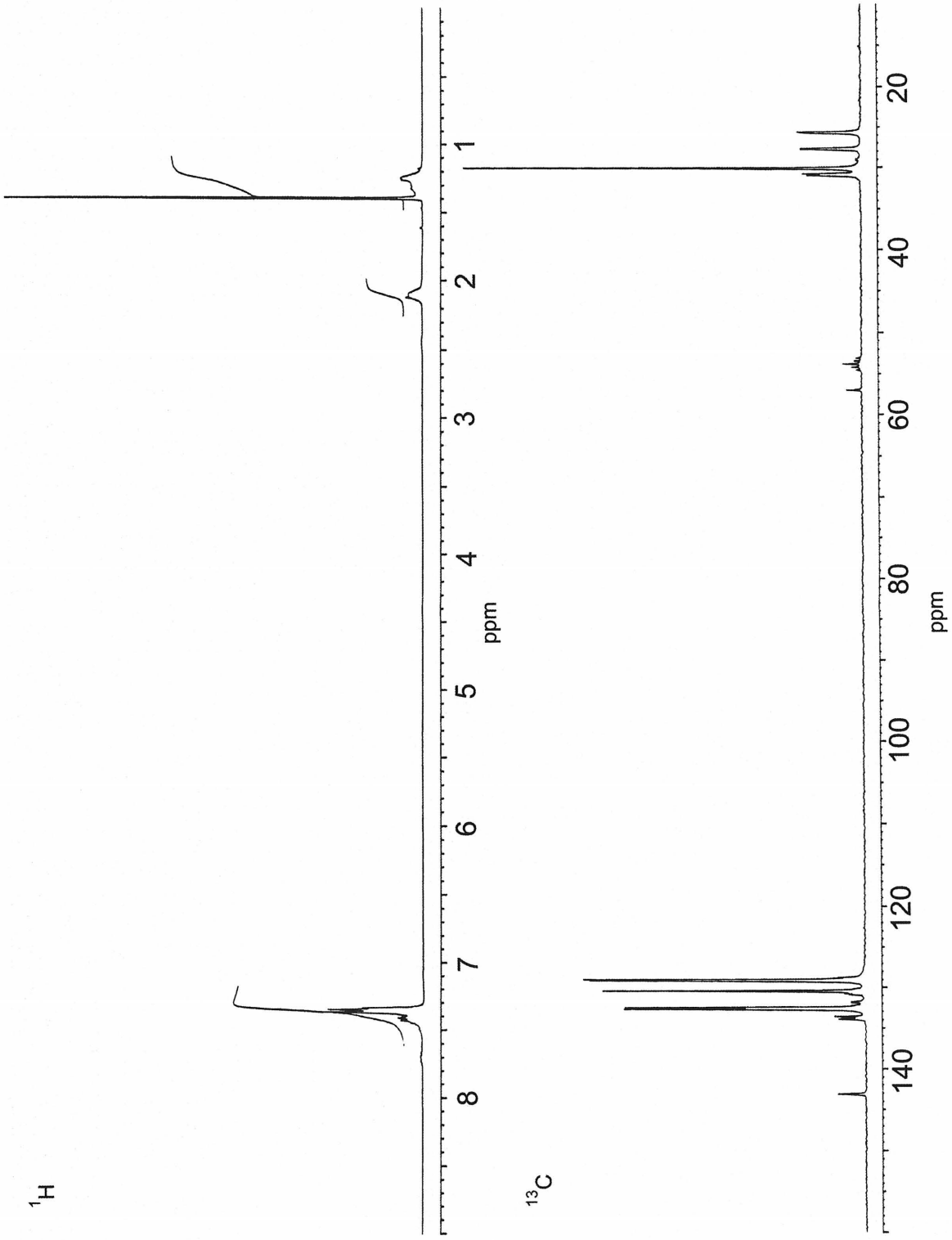

RMN ^{31}P de $\{[Ag(dpppen)(CN\text{-}t\text{-}Bu)_2]BF_4\}_n$.

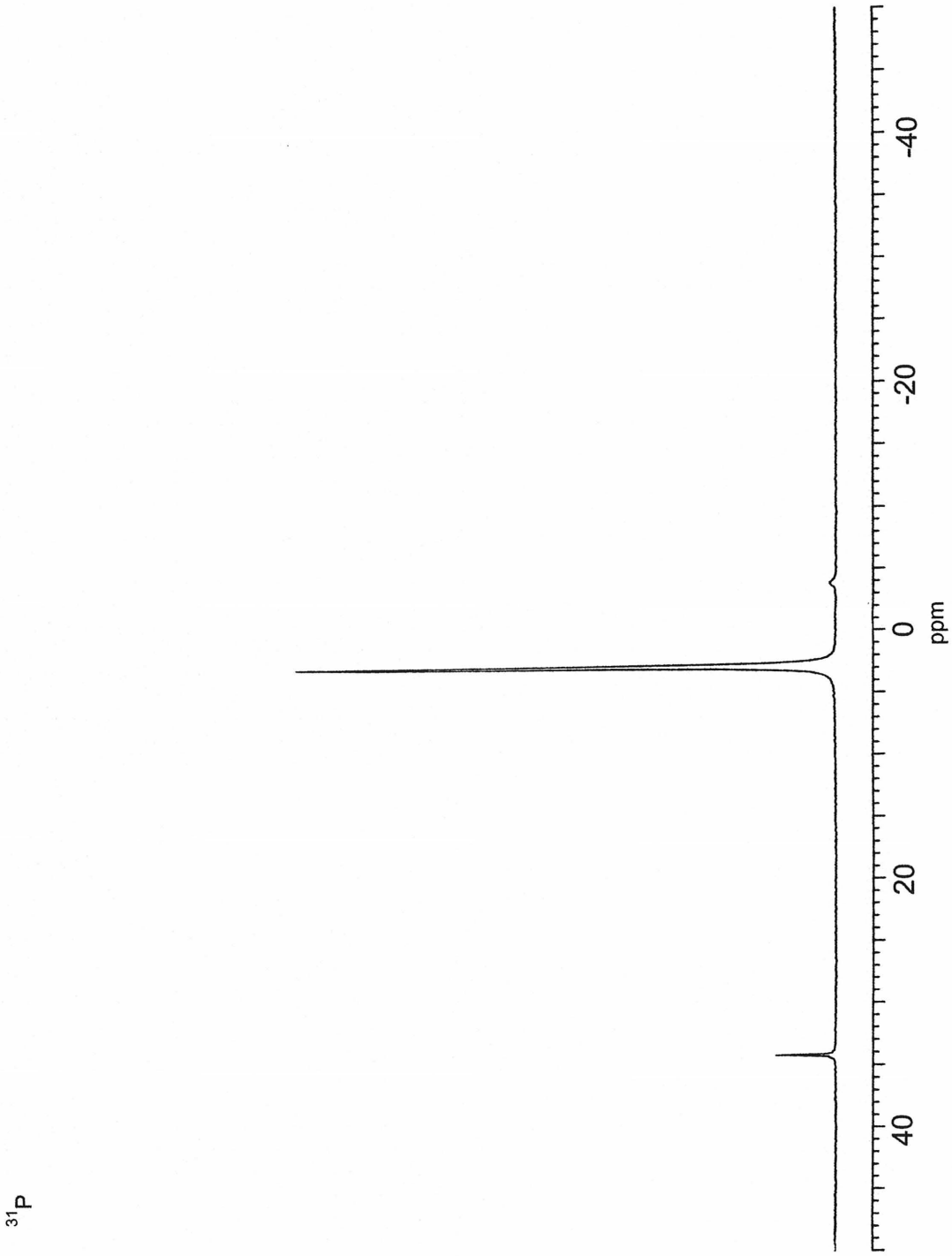

RMN ^{1}H et ^{13}C de $\{[Ag_2(dppm)_2(dmb)_2](BF_4)_2\}_n$.

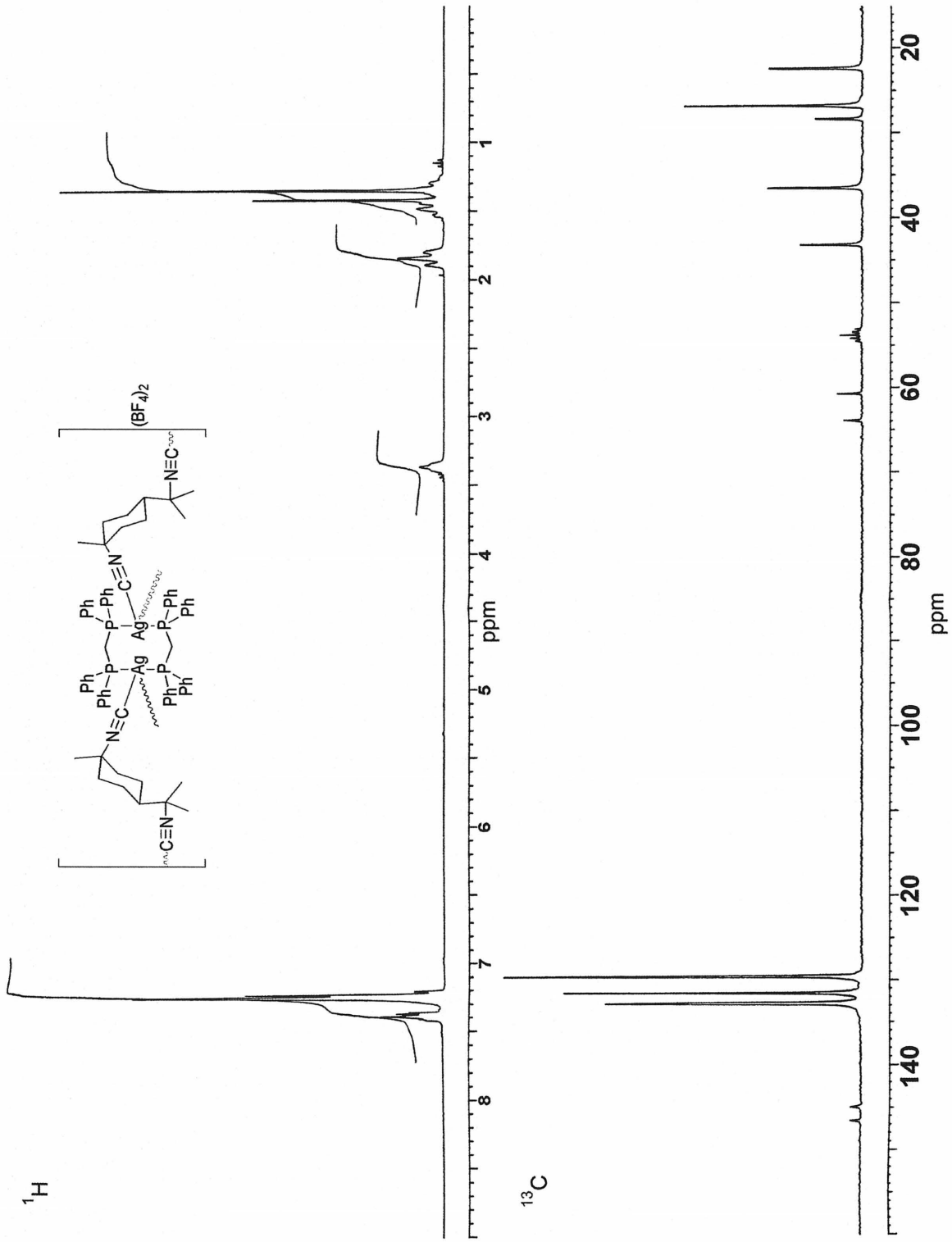

RMN ^{31}P de $\{[Ag_2(dppm)_2(dmb)_2](BF_4)_2\}_n$.

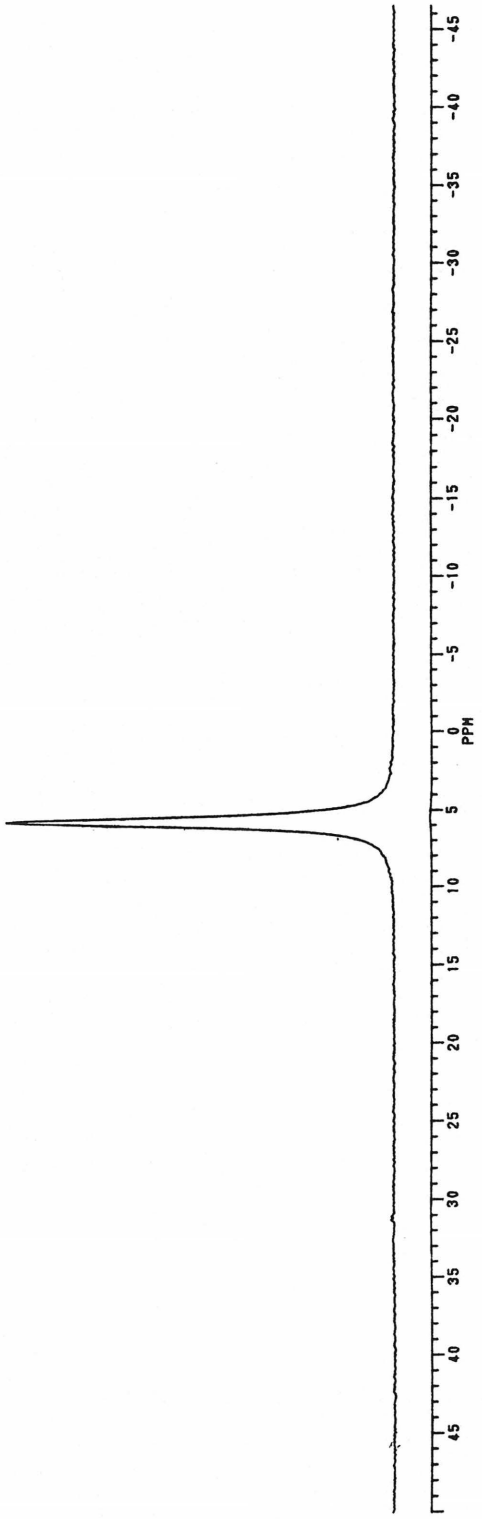

RMN ^{1}H et ^{13}C de $\{[Ag(dppe)(dmb)]BF_4\}_n$.

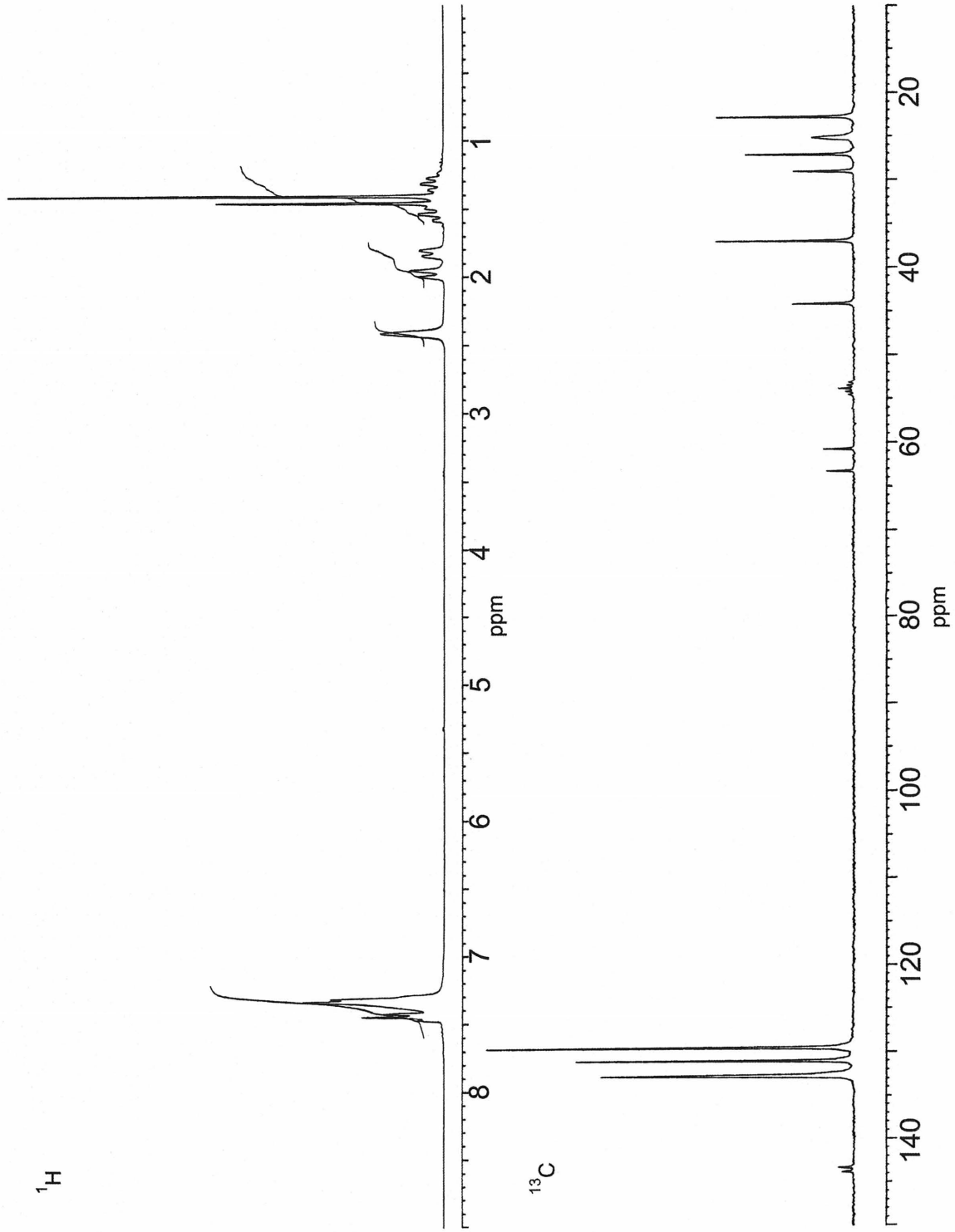

RMN ^{31}P de $\{[Ag(dppe)(dmb)]BF_4\}_n$.

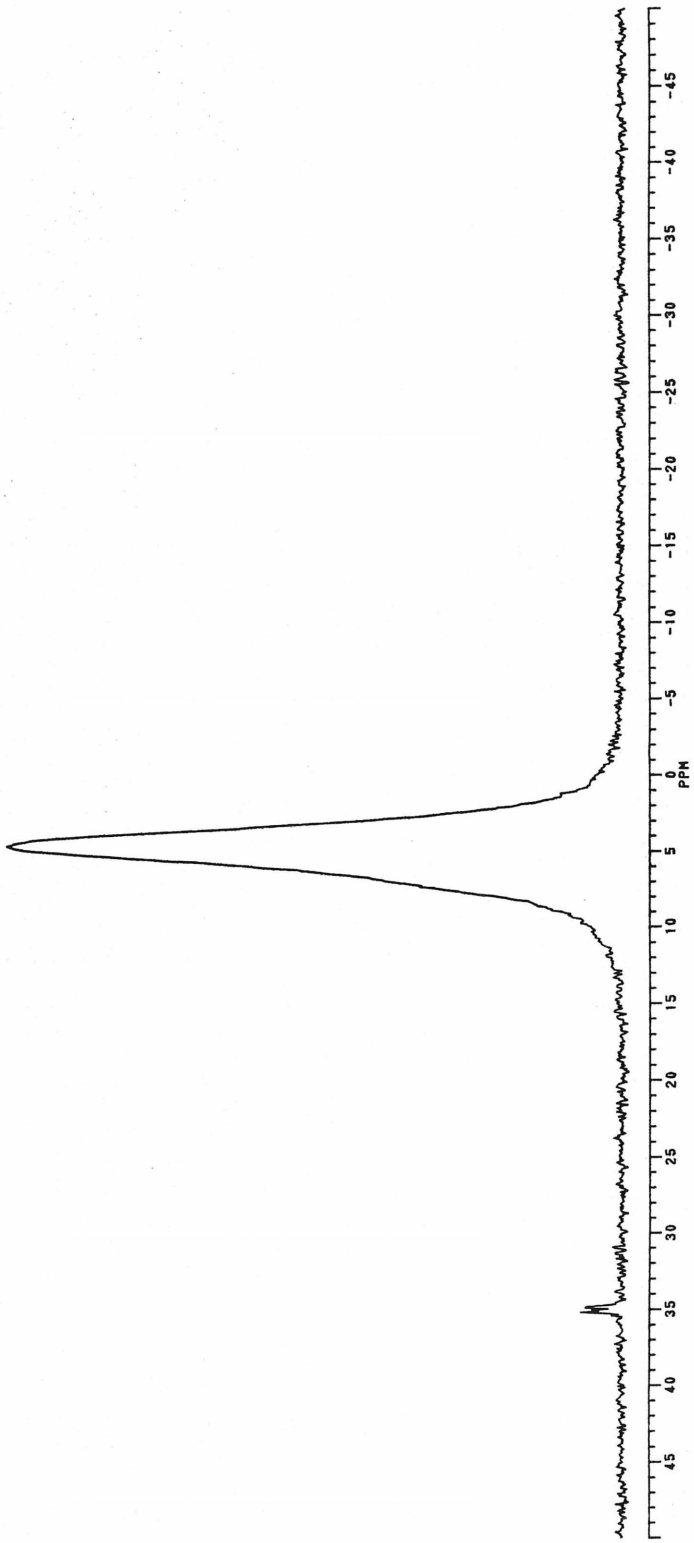

RMN ^{1}H et ^{13}C de $\{[Ag(dppp)(dmb)]BF_4\}_n$.

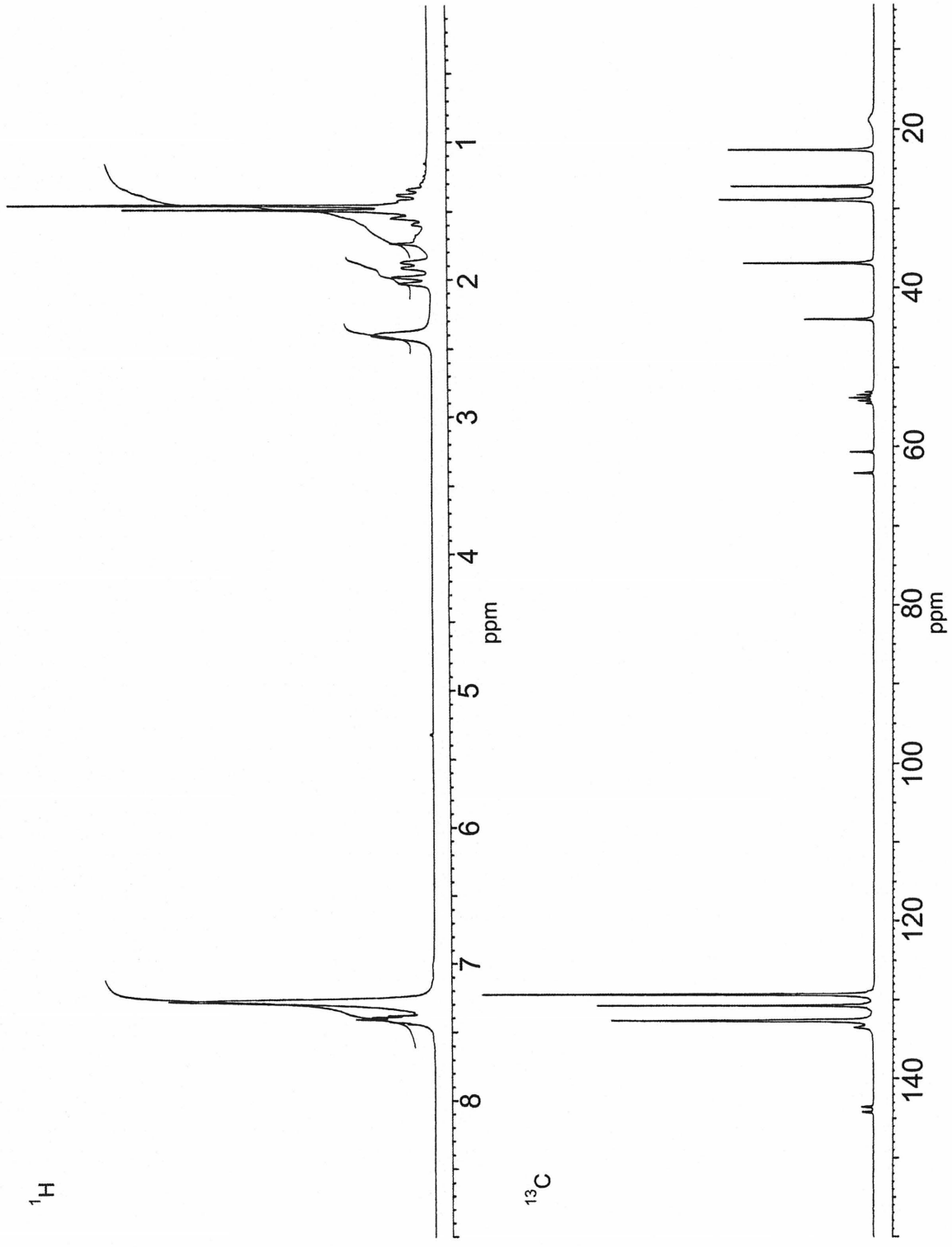

RMN ^{31}P de $\{[Ag(dppp)(dmb)]BF_4\}_n$.

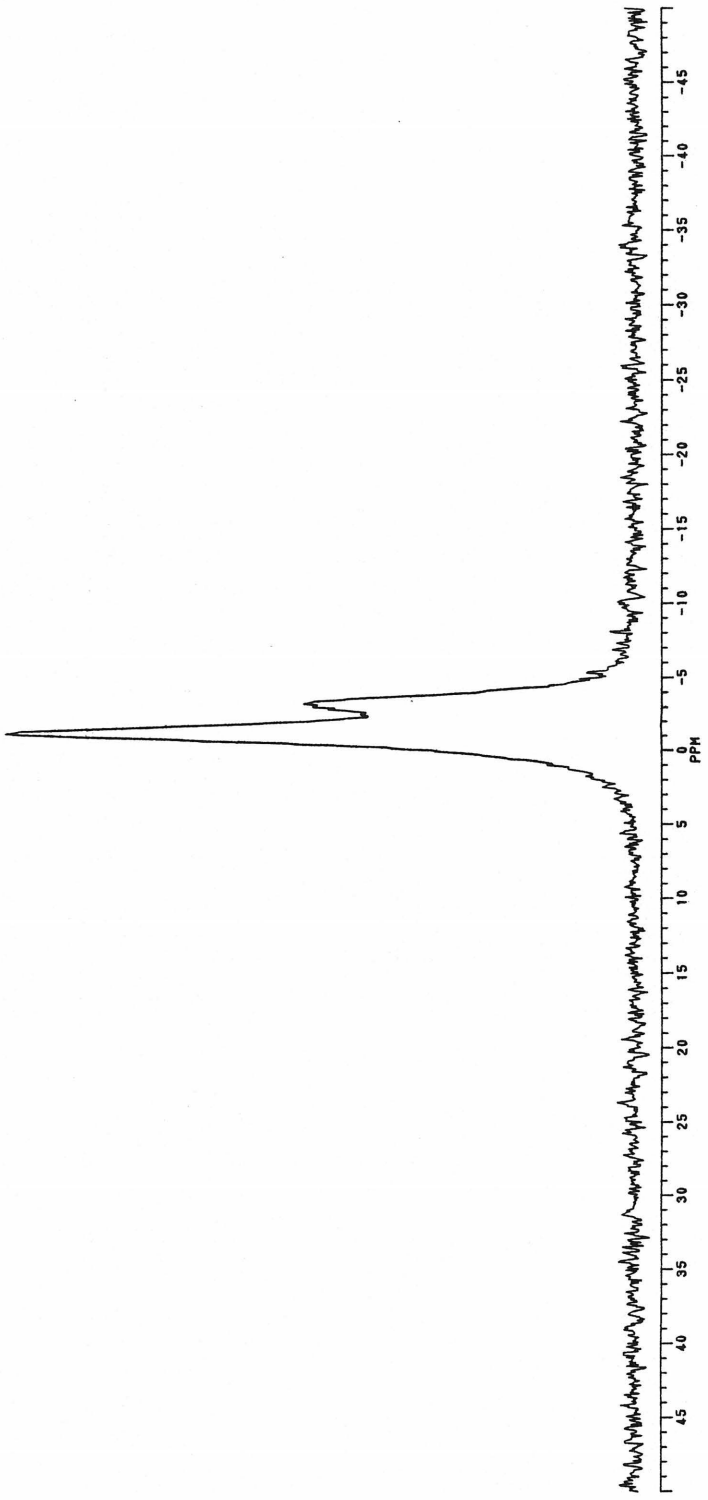

RMN ^{1}H et ^{13}C de $\{[Ag(dppb)(dmb)]BF_4\}_n$.

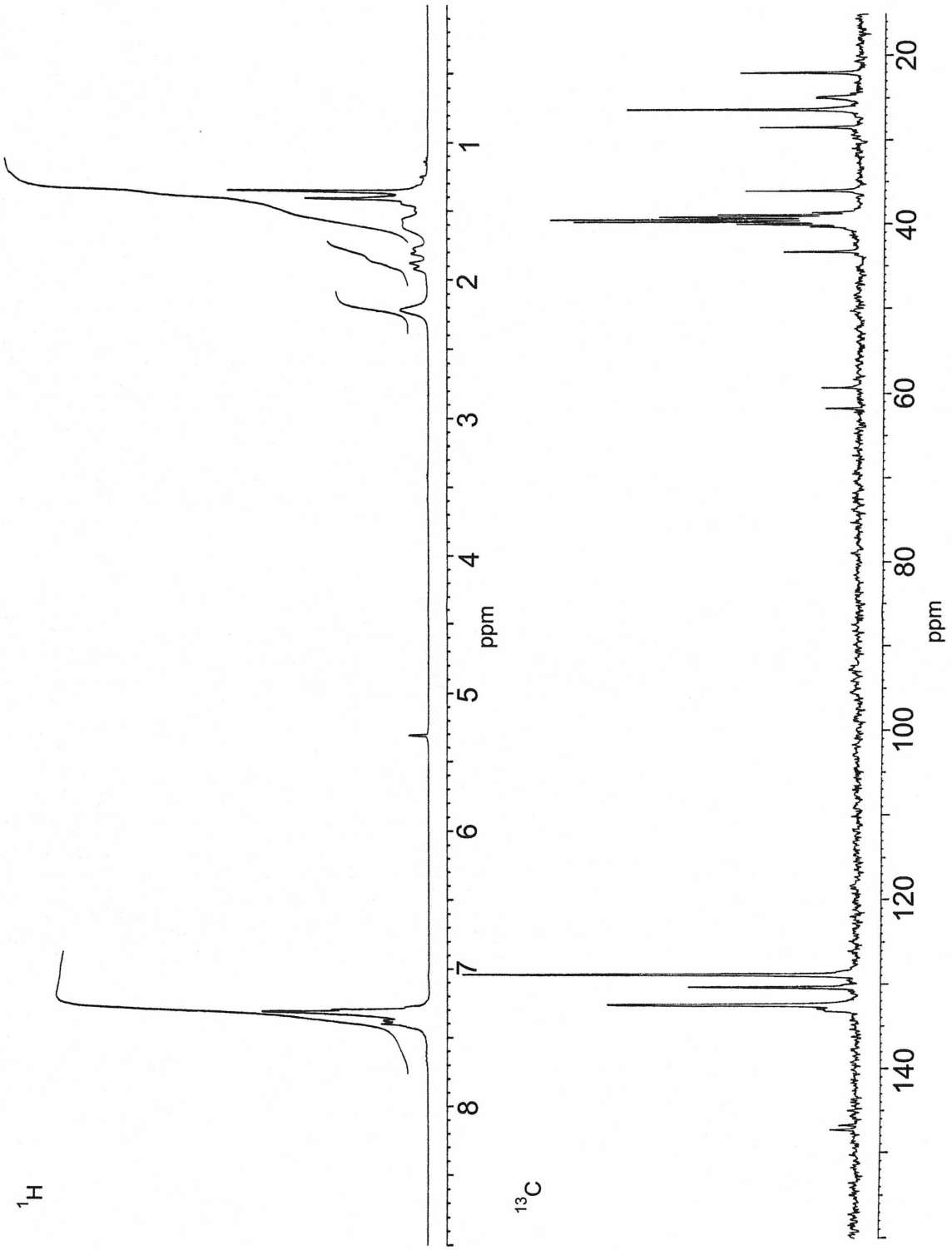

RMN ^{31}P de $\{[Ag(dppb)(dmb)]BF_4\}_n$.

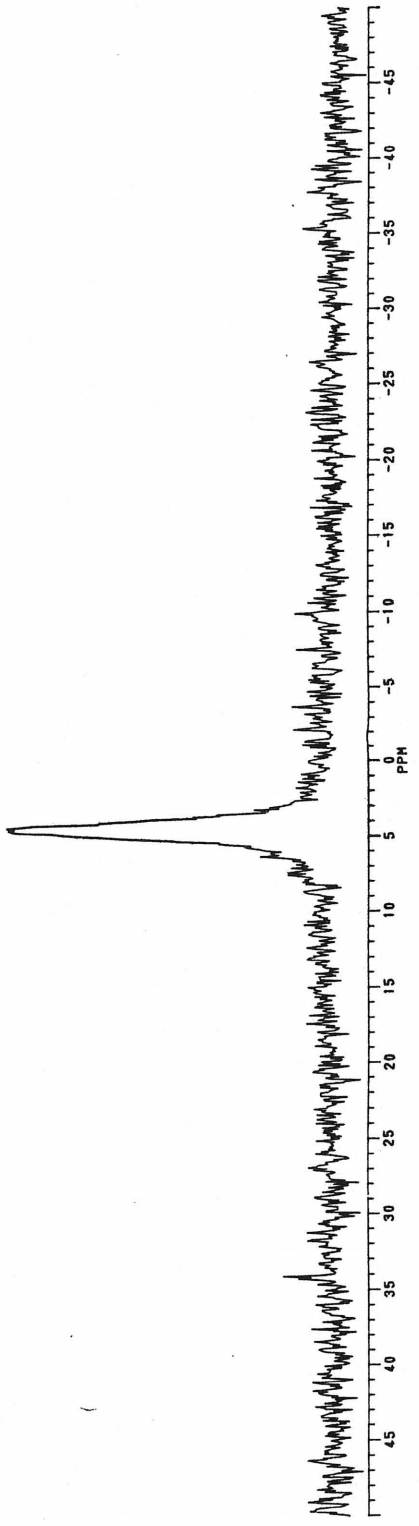

RMN ^{1}H et ^{13}C de $\{[Ag(dpph)(dmb)]BF_4\}_n$.

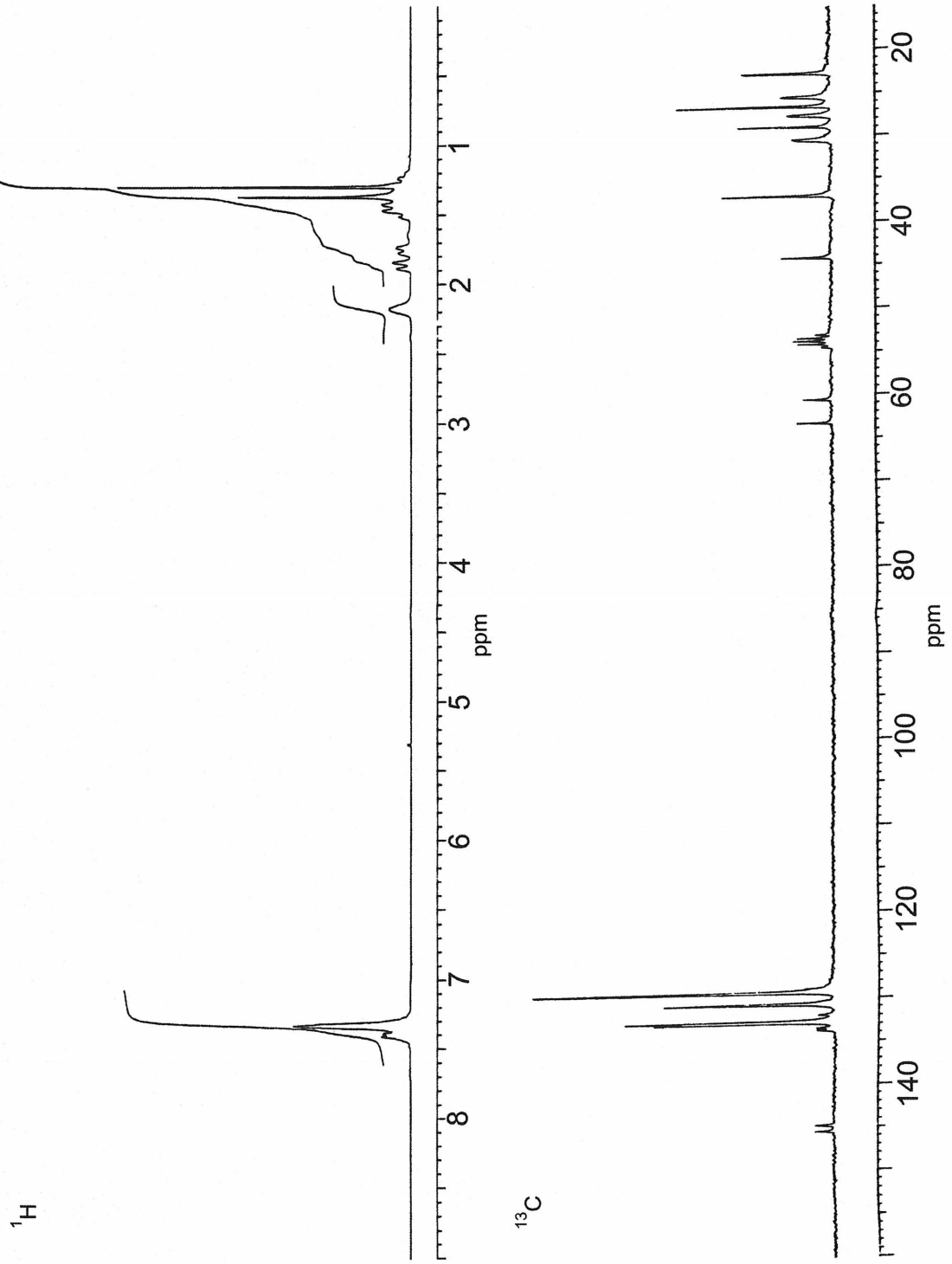

RMN ^{31}P de $\{[Ag(dpph)(dmb)]BF_4\}_n$.

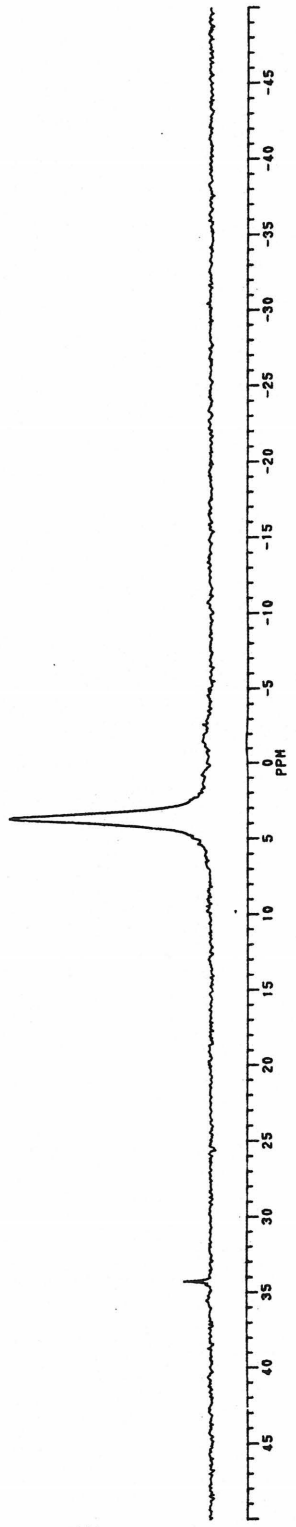

BIBLIOGRAPHIE

1. S. PAGLIARA, F. PARMIGIANI, P. GALINETTO, A. REVCOLEVSCHI, G. SAMOGGIA, Phys. Rev. B.; Cond. Mat. Mat. Phys., 66, 24518/1, (2002).

2. A. JALK, M. JORGER, C. KLINGSHIRN, Phys. Rev. B.; Cond. Mat. Mat. Phys., 65, 245209/1, (2002).

3. K. WAKITA, K. NISHI, Y. OHTA, N. NAOJI, Applied Phys. Let., 80, 3316, (2002).

4. F. DUBIN, J. BERREHAR, R. GROUSSON, T. GUILLET, C. LAPERSONNE-MEYER, M. SCHOTT, V. VOLIOTIS, Cond. Matter., 1-8, 0209199, (2002).

5. M. WOHLGENANNT, X.M. JIANG, Z.V. VARDENY, R.A. JANSSEN, J. Phys. Rev. Lett., 88, 197401/1, (2002).
6. M. WOHLGENANNT, Z.V. VARDENY, J. Phys.: Cond. Matter., 15, R83, (2003).

7. C.F. WANG, J.D. WHITE, T.L. LIM, J.H. HSU, S.C. YANG, W.S. FANN, K.Y. PENG, S.A. CHEN, Phys. Rev. B: Cond. Matt. Mat. Phys., 67, 0352002/1, (2003).

8. E.J.W. LIST, U. SCHERF, K. MULLEN, W. GRAUPNER, C.-H. KIM, J. SHINAR, Phys. Rev. B, 66, 235203/1, (2002).

9. A. CHARAS, J. MORGADO, J.M.G. MARTINHO, A. FEDOROV, L. ALCACER, F. CACIALLI, J. Mat. Chem., 12, 3523, (2002).

10. F. MEINARDI, M. CERMINANA, A. SASSELLA, A. BORGHESI, P. SPEARMAN, G. BONGIOVANNI, A. MURA, R. TUBINO, Phys, Rev. Let., 89, 157403/1, (2002).

11. D.-M. CHEN, Y.-H. ZHANG, T.-J. HE, F.-C. LIU, Spectrochim. Acta, 58A, 2291, (2002).

12. N.M. SPEIRS, W.J. EHENEZER, A.C. JONE, Photochem. Photobio., 76, 247, (2002).

13. J. LEWIS, L.J. ROTHBERG A.J. LOVINGER, J. Mater. Res., 11, No. 12, 3174, (1996).

14. R.A.J. JANSSEN, M.P.T. CHRISTIAANS, C. HARE, N. MARTIN, N.S. SARICIFTI, A.J. HEEGER, F. WUDL, J. Chem. Phys., 103, No. 20, 8840, (1995).

15. N.C. GREENHAM, S.C. MORATTI, D.D.C. BRADLEY, R.H. FRIEND, A.S. HOLMES, Nature, 365, 628, (1993).

16. A.L. BALCH, J.W. LEE, B.C. NOOL, M.M. OLMSTEAD, Inorg. Chem., 32, No. 17, 3577, (1993).

17. J.J. HICKMAN, C. ZOU, D. OFER, P.D. HARVEY, M.S. WRIGHTON, P.E. LABINIS, C.D. NAIN, G.M. WHITESIDES, J. Am. Chem. Soc., 111, 7271, (1989).

18. A. EFFRATY, I. FREINSTEN, Inorg. Chem., 21, 3115, (1982).

19. J.S. MILLER, A.J. EPSTEIN, Synthesis and Properties of Low-Dimensional Materials, Joel S. Miller, Arthur J. Epstein, Annals of the Ney York Academy of Science, Vol. 313, New York, New York 10021, (1978).

20. E.L. MUETTERTIES, Science, 196, No. 4292, 839, (1977).

21. Physics of Semiconductor Devices 3 ed. De S.M. Sze.

22. T. ZHANG, M. DROUIN, P.D. HARVEY, Inorg. Chem., 38, 1305, (1999).

23. D. PICHÉ, P.D. HARVEY, Can. J. Chem., 72, 705, (1994).

24. D. PERREAULT, M. DROUIN, A. MICHEL, P.D. HARVEY, Inorg. Chem., 31, 3688, (1992).

25. D. FORTIN, M. DROUIN, M. TURCOTTE, P.D. HARVEY, J. Am. Chem. Soc., 119, 531, (1997).

26. D. FORTIN, M. DROUIN, P.D. HARVEY, J. Am. Chem. Soc., 120, 5351, (1998).

27. D. FORTIN, M. DROUIN, P.D. HARVEY, Inorg. Chem., 39, 2758, (2000).

28. M. TURCOTTE, P.D. HARVEY, Inorg. Chem., 41, 1739, (2002).

29. T. ZHANG, M. DROUIN, P.D. HARVEY, Inorg. Chem., 38, 957, (1999).

30. J. DIEZ, M.P. GAMASA, J. GIMENO, A. TIRIPICCHIO, M.T. CAMELLINI, J. Chem. Soc. Dalton trans., 1275, (1987).

31. A.F.M.J. VAN DER PLOEG, G. VAN KOTEN, Inorg. Chim. Acta., 51, 225, (1981).

32. N.J. TURRO. Modern Molecular Photochemistry. The Benjamin / Cummings Publishing Compagny inc. Menl. Park, Californie 94025, 1978.

33. A. SIEMIARCZUK, B.D. WAGNER, W.R. WARE, J. Phys. Chem. 94, 1661, (1990).

34. A. SIEMIARCZUK, W.R. WARE, Chem. Phys. Lett. 160, 285, (1989).

35. J.I. FRENKEL, Phys. Rev., 37, 1276, (1931).

36. N. ARATANI, A. OSUKA, H.S. CHO, D. KIM, J. Photochem. Photobio. C: Photochem. Rev., 3, 25, (2002).

37. P.D. HARVEY. The Porphirin Handbook II Kadish, K.M.; Smith, K.M.; Guilard, R., Eds.; Academic Press, Amsterdam, Vol. 18, pp. 63-250 (2003).

38. J. ZHANG, R.-G. XIONG, X.-T. CHEN, C.-M. CHE, Z. XUE, X.-Z. YOU, Organometallics, 20, 41,18, (2001).

39. Q.-X. LIU, F.-B. XU, Q.-S. LI, X.-S. ZANG, X.-B. LENG, Y. L. CHOU, Z.-Z. ZHANG, Organometallics, 22, 309, (2003).

40. J. ZHANG, R.-G. XIONG, X.-T. CHEN, Z. XUE, S.-M. PENG, X.-Z. YOU, Organometallics, 21, 235, (2002).

41. D. SUN, R. CAO, J. WENG, M. HONG, Y. LIANG, Dalton, 291, (2002).

42. M.-L. TONG, J.-X. SHI, X.-M. CHEN, New. J. Chem., 26, 814, (2002).

43. S.-L. ZHENG, M.-L. TONG, S.-D. TAN, Y. WANG, J.-X. SHI, Y.-X. TONG, H. K. LEE, X.-M. CHEN, Organometallics, 20, 5319, (2001).

44. M. HENARY, J. L. WOOTTON, S. I. KHAN, J. I. ZINK, Inorg. Chem., 36, 796, (1997).

45. M.-C. BRANDYS, R. J. PUDDEPHATT, Chem. Commun., 1508, (2001).

46. M.-C. BRANDYS, R. J. PUDDEPHATT, J. Am. of Chem. Soc, 123, 4839, (2001).

47. M.-C. BRANDYS, R. J. PUDDEPHATT, Chem. Commun., 1280, (2001).

48. P.D. HARVEY, Coord. Chem. Rev., 219, 17, (2001).

49. W. BENSCH, M. PRELATI, W. LUDWIG, J. Chem. Soc., Chem. Commun., 1162, (1986).

50. F.A. COTTON, G. WILKINSON, P. GAUS, Basic Inorganic Chemistry Wiley, New York 1995 p.61.

51. H.H. KARSCH, U.Z. SCHUBERT, Naturforsch., 37b, 186, (1982).

52. F. LEBRUN. Mémoire de maîtrise, Faculté des sciences, Université de Sherbrooke, Sherbrooke, Québec, Canada (2001).

53. V.M. MISKOWSKI, T.P. SMITH, T.M. LOEHR, H.B. GRAY, J. Am. Chem. Soc., 107, 7925, (1985).

54. R.A. LEVENSON, H.B. GRAY, J. Am. Chem. Soc., 97, 6042, (1975).

55. M.S. WRIGHTON, D.S. GINLEY, J. Am. Chem. Soc., 97, 4246, (1975).

56. H.B. ABRAHAMSON, C.C. FRAZIER, D.S. GINLEY, H.B. GRAY, J. LILIENTHAL, D.R. TYLER, M.S. WRIGHTON Inorg. Chem., 16, 1554, (1977).

57. D.R. TYLER, R.A. LEVENSON, H.B. GRAY, J. Am. Chem. Soc., 100, 7888, (1978).

58. J. MARKHAM, J. Rev. Mod. Phys., 31, 956, (1959).

59. C. BALLHAUSEN, J. Molecular Electronic Structures of Transition Metal Complexes; McGraw-Hill: New York, 1979: pp 132-135.

60. P.D. HARVEY, Z. MURTAZA, Inorg. Chem., 32, 4721, (1993).

61. V.C. ALBANO, P.L. BELLON, G. CIANI, J. Chem. Soc., Dalton Trans., 1938, (1972).

62. L. CHI-CHANG, L. YONG-SHOU, L. LI, Jiegou Huaxue, *12*, 286, (1993).

63. D. SARAVANABHARATHI MONIKA, P. VENUGOPALAN, A.G. SAMUELSON, Polyhedron, 21, 2433, (2002).

64. S. KITAGAWA, M. KONDO, S. KATAWA, S. WADA, M. MACKAWA, M. MUNAKATA, Inorg. Chem., 34, 1455, (1995).

65. T.R.E. TIEKINK, Acta Cryst. 46c, 1933 (1990).

66. D. AFFANDI, S.J. BERNERS-PRICE, S. EFFENDY, P.J. HARVEY, P.C. HEALY, B.E. RUCH, A.H. WHITE, J. Chem. Soc., Dalton Trans., 1411, (1997).